Metagenomics: Screening of Organisms and Functional Profiles Associated with Polycyclic Aromatic Hydrocarbon Bioremediation in Contaminated Soils.

Samuel Aleer

Submitted in fulfilment of the requirements for the degree of

Doctor of Philosophy

Future Industries Institute, Division of Information

Technology, Engineering and the Environment



University of
South Australia

March 2016

Contents

List of figures ..... **ix**
List of tables ..... **xvi**
Glossary and abbreviations ..... **xviii**
Abstract ..... **xx**
Declaration ..... **xxiii**
Acknowledgements ..... **xxiv**
Chapter 1 ..... **1**
Literature review of microbial biodegradation of PAHs **1**
1.1 Introduction **1**
1.2 Polycyclic aromatic hydrocarbons (PAHs) **2**
1.2.1 PAH structures 2
1.2.2 Physio-chemical properties 4
1.2.3 Occurrence/formation of PAHs 5
1.2.4 Toxicity of PAHs 6
1.2.5 Environmental PAH contamination 10
1.2.5.1 Sources 10
1.2.5.2 Fate of PAH in the environment 11
1.2.6 Biodegradation of PAH 12
1.2.6.1 Bacteria degradation of PAHs 12
1.2.6.2 Fungal degradation of PAHs 13
1.2.6.3 Phenanthrene degradation 19
1.2.6.4 Pyrene degradation 19
1.2.6.5 Benzo(a)pyrene degradation 21
1.3 Bioremediation of PAHs **23**
1.3.1 Natural attenuation 24
1.3.2 Enhanced natural attenuation 26
1.3.3 Bioaugmentation 26
1.3.4 Factors influence bioremediation 27
1.4 Bioavailability **28**
1.5 Molecular tools **29**
1.5.1 Culture-dependent technique 30
1.5.2 16S rDNA/RNA strategy 30
1.5.3 Next generation sequencing 34
1.5.4 Sequencing technologies 35

1.5.5 Metagenomics 36
1.6 Advantages and disadvantages of NGS platforms 37
1.7 Current gap in knowledge of PAH microbial biodegradation 40
1.8 Summary 42
1.9 Aims and significance of this project 42
1.9.1 Specific aims 42
1.10 Hypotheses 43
Chapter 2 45
Materials and Methods 45
2.1 Ethics statement 45
2.2 Chemicals and reagents 45
2.3 Stock solutions 45
2.4 Media composition 47
2.4.1 Basal salts medium (BSM) 47
2.4.2 Tryptone soya broth (TSB) 47
2.4.3 Nutrient broth 47
2.5 Methods 47
2.5.1 General laboratory equipment 47
2.5.2 Microbiological methods 48
2.5.2.1 Soil processing 48
2.5.2.2 Soil physiochemical properties 48
2.5.2.3 Soil pH 49
2.5.2.4 Water holding capacity (% WHC) 49
2.5.2.5 Soil moisture content (MC %) 49
2.5.2.6 Soil organic matter (%) 49
2.6 Inoculum preparation 50
2.6.1 Mycobacterium cells harvesting 50
2.7 Bioavailability assessment 50
2.8 Soil microcosms 51
2.8.1 Summary of microcosm design 51
2.9 Sampling 53
2.10 Enumeration of PAH-degrading bacteria 53
2.11 Chemical analyses 56
2.11.1 PAH extraction 56
2.11.2 Gas chromatography (GC) 56

2.12 Molecular analyses **57**
2.12.1 DNA extraction 57
2.12.2 Agarose gel electrophoresis 57
2.12.3 Polymerase chain reaction (PCR) 58
2.12.3.1 Bacterial universal amplification 58
2.13 Denaturing gradient gel electrophoresis (DGGE) **59**
2.13.1 DGGE analysis of bacterial community 59
2.13.2 DGGE analysis of fungal communities 59
2.13.3 DGGE staining 60
2.13.4 Analysis of DGGE banding patterns 60
2.13.5 Similarity and diversity analyses 60
2.14 Metagenomics analyses **61**
2.14.1 Whole genome amplification (WGA) 61
2.14.2 Preparation of sequencing libraries 61
2.14.3 Template preparation (Ion PI™ Template OT2 200 Kit V3) 62
2.14.4 Ion PI sequencing preparation (Sequencing 200 kit V3) 62
2.14.5 Data annotation and bioinformatics analyses 62
2.15 Statistical analyses **63**
Chapter 3 ..... **65**
Treatability studies to assess bioremediation performance in three PAH impacted soils **65**
3.1. Introduction **65**
3.2. Assessment of PAH-contaminated soil using different bioremediation strategies **66**
3.3. Aim of the treatability study **67**
3.4 Hypothesis **67**
3.5 Soils characterisation **67**
3.6 Assessment of PAH biodegradation in soil microcosms **70**
3.6.1 Creo microcosms 70
3.6.2 Comparison of phenanthrene, pyrene, and B(a)P degradation in Creo microcosms 71
3.6.3 Enumeration of PAH degrading population in Creo microcosms 74
3.6.4 TB microcosms 75
3.6.5 Comparison of phenanthrene, pyrene and B(a)P degradation in TB microcosms 76
3.6.6 Estimation of PAH-degrading bacteria in TB soil using MPN 79
3.6.7 AP microcosms 80
3.6.8 Comparison of phenanthrene, pyrene, and B(a)P degradation in AP microcosms 80
3.6.9 Estimation of PAH-degrading population in AP soil using MPN 82

3.7 Discussion **83**
3.8 Conclusion **88**
Chapter 4 ..... **90**
Assessment of PAH-degrading microorganisms in three aged PAH contaminated soils using community profiling analysis **90**
4.1 Introduction **90**
4.2 Aim **92**
4.3 Hypothesis **92**
4.4 Assessment of microbial communities in Creo soil microcosms **92**
4.4.1 Bacterial community in Creo microcosms 92
4.4.2 Effect of incubation time and amendments on bacterial communities 93
4.4.3 Bacterial community profile analysis 96
4.4.4 Assessment of supplemented PAH-degrading organisms in Creo microcosms 100
4.4.5 Effect of incubation time and amendments on Mycobacterium communities 101
4.4.6 *Mycobacterium* community profile analysis 103
4.5 Assessment of microbial communities in TB soil microcosms **107**
4.5.1 Bacterial community profile analysis in TB soil microcosms 107
4.5.2 Effect of incubation time and amendments on bacterial communities 108
4.5.3 Bacterial community profile analysis 109
4.5.4 Assessment of supplemented PAH-degrading organisms in TB microcosms 114
4.5.5 Effect of incubation time and amendments on *Mycobacterium* communities 115
4.5.6 *Mycobacterium* community profile analysis 118
4.6 Assessment of microbial communities in AP soil microcosms **121**
4.6.1 Bacterial community in AP microcosms 121
4.6.2 Effect of incubation time and amendment on bacterial communities 123
4.6.3 Bacterial community profile analysis 124
4.7 Bacterial communitity in composite gel (All three soils) **128**
4.7.1 Effect of incubation time and amendments on bacterial communities 130
4.7.2 Assessment of PAH-degrading organisms in composite gel (AP, TB and Creo) of three treated microcosms 131
4.7.3. Effect of incubation time and amendments on Mycobacterium communities in composite gel (AP, TB and Creo) 132
4.8 Discussion **136**
4.8.1 Comparison of bacterial community profiles in unamended (NA) and amended (ENA and Combined) microcosms (Creo, TB and AP soils) 136
4.8.2 Overall comparison of bacterial community profiles in composite gels (Creo, TB and AP) 139

4.8.3 Comparison of Mycobacterium community profiles in unamended (NA) and amended (ENA and Combined) microcosms (Creo, TB and AP soils) 140
4.8.4 Overall comparison of *Mycobacterium* community profiles in composite gels (Creo, TB and AP) 142
4.9 Conclusion 143
Chapter 5 144
Assessment of PAH-degrading microorganisms using next generation sequencing technology (NGS) 144
5.1 Introduction 144
5.2 Objective 146
5.3 Hypothesis 147
5.4 Results 147
5.4.1 Assessment of microbial communities in Creo soil microcosms 147
5.4.2 Taxonomic analysis at domain level in NA Creo microcosms 147
5.4.3 Taxonomic analysis at domain level in ENA and Comb Creo microcosms 148
5.4.4 Taxonomic analysis at phylum level in NA Creo microcosms 148
5.4.5 Taxonomic analysis at phylum level in ENA and Comb Creo microcosms 152
5.4.6 Taxonomic analysis at order level in NA Creo microcosms 152
5.4.7 Taxonomic analysis at order level in ENA and Comb Creo microcosms 153
5.5 Assessment of microbial communities in TB soil microcosms 160
5.5.1 Taxonomic analysis at domain level in NA TB microcosms 160
5.5.2 Taxonomic analysis at domain level in ENA and Comb TB microcosms 160
5.5.3 Taxonomic analysis at phylum level in NA TB microcosms 161
5.5.4 Taxonomic analysis at phylum level in ENA and Comb TB microcosms 165
5.5.5 Taxonomic analysis at order level in NA TB microcosms 166
5.5.6 Taxonomic analysis at order level in ENA and Comb TB microcosms 167
5.6 Assessment of bacterial communities in the AP soil microcosms 174
5.6.1 Taxonomic analysis at domain level in NA AP microcosms 174
5.6.2 Taxonomic analysis at domain level in ENA and Comb AP microcosms 176
5.6.3 Taxonomic analysis at phylum level in NA AP microcosms 176
5.6.4 Taxonomic analysis at phylum level in ENA and Comb AP microcosms 179
5.6.5 Taxonomic analysis at order level in NA AP microcosms 179
5.6.6 Taxonomic analysis at the order level in ENA and Comb AP microcosms 180
5.7 MG-RAST analysis of functional profiles 185
5.7.1 Comparison of metabolic profiles in Creo metagenomes 185
5.7.2 Comparison of metabolic profiles in TB metagenomes 194

5.7.3 Comparison of metabolic profiles in AP metagenomes 201
5.8 Analysis of enzymes for PAH metabolism 206
5.8.1 Naphthalene metabolism in unamended and amended Creo microcosms 207
5.8.2 Benzo(a)pyrene metabolism in unamended and amended Creo microcosms.....209
5.8.3 Analysis of enzymes required for metabolism of PAHs in TB microcosms 212
5.8.4 Naphthalene metabolism in unamended and amended TB microcosms 212
5.8.5 Benzo(a)pyrene metabolism in unamended and amended microcosms 213
5.8.6 Analysis of enzymes for PAHs metabolism 214
5.8.7 Naphthalene metabolism in unamended and amended microcosms 215
5.8.8 Benzo(a)pyrene metabolism in unamended and amended microcosms 216
5.9 Discussion 218
5.10 Conclusion 227
Chapter 6 228
Application of bioavailability assessment tools to predict PAH bioremediation endpoints in 3 PAH-contaminated soils. 228
6.1 Introduction 228
6.2 Aim 229
6.3 Hypothesis 229
6.4 Results 229
6.4.1 Three-ring compound bioavailability 230
6.4.2 Four-ring compound 230
6.4.3 Five-ring compound 234
6.5 Discussion 235
6.6 Conclusion 240
Chapter 7 241
Effect of the addition of surfactant, carbon source and chemical oxidation on the bioremediation of PAHs in contaminated soil. 241
7.1 Introduction 241
7.2 Aims 244
7.3 PAH remediation in Creo soil microcosms 245
7.4 Assessment of PAH-degrading microorganisms using next generation sequencing technology (NGS) in alternative Creo soil microcosms 248
7.4.1 Taxonomic analysis at the domain level in unamended microcosms (NA).....248
7.4.2 Taxonomic analysis at the phylum level 251
7.4.3 Taxonomic analysis at order level 256

7.5 MG-RAST analysis of functional profiles 263
7.5.1 Comparison of metabolic profiles in unamended and amended microcosms 263
7.5.2 Analysis of enzymes required for metabolism of PAHs 271
7.5.3 Analysis of PAH metabolism in unamended and amended microcosms 271
7.6 Discussion 274
7.7 Conclusion 284
Chapter 8 285
Conclusions and future research work recommendations 285
8.1 Conclusions 285
8.2 Future research work recommendations 288
8.2.1 Characterisation of other potential co-contaminants and assessment of their impact on biodegradation processes. 288
8.2.2 Bioaugmentation of PAH-degrading organisms isolated from target clean up soil and determination of their degradative capacity 289
8.2.3 Identification of PAH metabolites 290
8.2.4 Identification of active PAH-degrading organisms and specific genes involve in the metabolism of PAHs 290
Reference 292
Appendix 320
Appendix 1: Media and solutions used in this study (Chapter 2) 320
1.1 DGGE SOLUTIONS 320
Appendix 2: Treatability studies to assess bioremediation performance in three PAH impacted soils (Chapter 3) 329
Appendix 3: Assessment of PAH-degrading microorganisms in three aged hydrocarbons contaminated soils using community profiling analysis (Chapter 4) 332
Appendix 4: Analysis of enzymes associated with PAH metabolism (Chapter 5) 341
Appendix 5: MG-RAST analysis of metabolic functional profiles (Chapter 7) 347

List of figures

Figure		Page
1.1	Chemical structures of the 16 PAHs identified as priority pollutants by US EPA.	4
1.2	Pathways showing B(a)P activation and detoxification……	9
1.3	A simple schematic diagram demonstrating environmental fate of PAHs.	12
1.4	The main pathway for PAHs degradation by bacteria…….	14
1.5	The main pathway for PAHs degradation by fungi…….	18
1.6	Proposed pathway for the degradation of phenanthrene by bacteria……	20
1.7	Proposed catabolic pathways of pyrene degradation by bacteria ……	21
1.8	Proposed catabolic pathways of B(a)P degradation by bacteria …….	22
1.9	Evolution of increasingly sophisticated studies of pure cultures and their application to the study of microbial communities ……	31
1.10	Ion Proton workflow system showing all four major steps when using Ion Express library kit…….	36
3.1	Change in total PAH concentration in Creo soil microcosms following 42 weeks incubation under natural attenuation (NA), enhanced natural attenuation (ENA), bioaugmentation (BioA), and combined treatment (Comb)…….....	71
3.2	Change in phenanthrene concentration in Creo soil microcosms following 42 weeks of incubation under natural attenuation (NA), enhanced natural attenuation (ENA), bioaugmentation (BioA) and combined treatment (Comb) strategies …….	72
3.3	Change in pyrene concentration in Creo soil microcosm weeks of incubation under natural attenuation (NA), enhanced natural attenuation (ENA), bioaugmentation (BioA) and combined treatment (Comb) strategies…….	73
3.4	Change in B(a)P concentration in Creo soil following 42 weeks of incubation under natural attenuation (NA), enhanced natural attenuation (ENA), bioaugmentation (BioA) and combine treatment (Comb) strategies …….	74
3.5	Determination of microbial populations in Creo soil microcosms using a most probable number technique (nutrient broth media) …….	75
3.6	Change in total PAH concentration in TB soil microcosms following 42 weeks incubation under natural attenuation (NA), enhanced natural attenuation (ENA), bioaugmentation (BioA) and combined treatment (Comb) strategies.…….	76
3.7	Change in phenanthrene concentration in TB soil microcosms following 42 weeks incubation under natural attenuation (NA), enhanced natural attenuation (ENA), bioaugmentation (BioA) and combined treatment (Comb) strategies…….	77
3.8	Change in pyrene concentration in TB soil microcosms following 42 weeks incubation under natural attenuation (NA), enhanced natural attenuation (ENA), bioaugmentation (BioA) and combined treatment (Comb) strategies.…….	78
3.9	Change in B(a)P concentration in TB soil microcosms following 42 weeks incubation under natural attenuation (NA), enhanced natural attenuation (ENA), bioaugmentation (BioA) and combined treatment (Comb) strategies…….	78
3.10	Determination of microbial populations in TB soil microcosms using most probable number technique (nutrient broth media)…….	79
3.11	Change in total PAH concentration in AP soil microcosms following weeks incubation under natural attenuation (NA), enhanced natural attenuation (ENA), bioaugmentation (BioA) and combined treatment (Comb) strategies……..	80
3.12	Change in phenanthrene concentration in AP soil microcosms following 42 weeks incubation under natural attenuation (NA), enhanced natural attenuation (ENA), bioaugmentation (BioA) and combined treatment (Comb) strategies.……	81

3.13	Change in pyrene concentration in AP soil microcosms following 42 weeks incubation under natural attenuation (NA), enhanced natural attenuation (ENA), bioaugmentation (BioA) and combined treatment (Comb) strategies.……	81
3.14	Change in B(a)P concentration in AP soil microcosms following 42 weeks incubation under natural attenuation (NA), enhanced natural attenuation (ENA), bioaugmentation (BioA) and combined treatment (Comb) strategies …….	82
3.15	Determination of microbial populations in AP soil using a most probable…….	83
4.1	Bacterial community profiles generated using 16S rDNA from samples taken at four different time points following 42 weeks of bioremediation of Creo contaminated soil. ……	94
4.2	UPGMA dendrogram constructed using the similarity matching produced from Creo bacterial DGGE community profiles of the 16S rDNA fragments, amplified from all treatments across sampling time points……..	97
4.3	Comparison of bacterial community diversity expressed as Shannon Weaver diversity index (H') from DGGE analysis of 16S rDNA fragments in Creo soil microcosms.……..	98
4.4	Comparison of bacterial community diversity expressed as Shannon Weaver equitability index (J) from DGGE analysis of 16S rDNA fragments in Creo soil microcosms.……..	100
4.5	Comparison of Mycobacterium community profiles in Creo-contaminated soil generated using NidA genes following 42 weeks incubation……..	103
4.6	UPGMA dendrogram constructed from the similarity matching produced from Creo NidA DGGE community profiles of the 16S rDNA fragments, amplified from all treatments across sampling time point……..	105
4.7	Comparison of Mycobacterium community expressed as Shannon Weaver diversity index (H') from DGGE analysis of 16S rDNA fragments in Creo soil microcosms incubated for 42 weeks…….	106
4.8	Comparison of Mycobacterium communities expressed as Shannon Weaver equitability index (J) from DGGE analysis of 16S rDNA fragments in Creo soil microcosms incubated for 42 weeks.……	106
4.9	Bacterial community profiles generated using 16S rDNA from samples taken at four different time points following 42 weeks of bioremediation of TB-contaminated soil.…….	110
4.10	UPGMA dendrogram constructed using the similarity matching produced from TB bacterial DGGE community profiles of the 16S rDNA fragments, amplified from all treatments across sampling time point ……	111
4.11	Comparison of bacterial community expressed as Shannon Weaver diversity index (H') from DGGE analysis of 16S rDNA fragments in TB soil microcosms incubated for 42 weeks over selected time points ……..	113
4.12	Comparison of bacterial community expressed as Shannon Weaver equitability index (J) from DGGE analysis of 16S rDNA fragments in TB soil microcosms incubated for 42 weeks.……..	113
4.13	Comparison of Mycobacterium community profiles in TB-contaminated soil generated using NidA genes following 42 weeks incubation……..	117
4.14	UPGMA dendrogram constructed from the similarity matching produced from TB NidA DGGE community profiles of the 16S rDNA fragments, amplified from all treatments across sampling time point……..	119

4.15 Comparison of Mycobacterium community expressed as Shannon Weaver diversity index (H') from DGGE analysis of 16S rDNA fragments in TB-contaminated soil microcosms incubated for 42 weeks over selected time points..... 120

4.16 Comparison of Mycobacterium community expressed as Shannon Weaver equitability index (J) from DGGE analysis of 16S rDNA fragments in TB soil microcosms incubated for 42 weeks……. 120

4.17 Comparison of bacterial community profiles in AP-contaminated soil generated using 16S rDNA following 42 weeks incubation.…… 122

4.18 UPGMA dendrogram constructed from the similarity matching produced from AP bacterial DGGE community profiles of the 16S rDNA fragments, amplified from all treatments across sampling time points ……... 125

4.19 Comparison of bacterial community expressed as Shannon Weaver diversity index (H') from DGGE analysis of 16S rDNA fragments in AP soil microcosms incubated for 42 weeks over selected time points…… 127

4.20 Comparison of bacterial community expressed as Shannon Weaver equitability index (J) from DGGE analysis of 16S rDNA fragments in AP soil microcosms incubated for 42 weeks……. 127

4.21 Comparison of bacterial community profiles in composite gel generated using 16S rDNA from samples taken at four different time points following 42 weeks of incubation (all soils)……. 129

4.22 UPGMA dendrogram constructed from the similarity matching produced from composite bacterial DGGE community profiles of the 16S rDNA fragments. Amplified PCR products of DNA extracted from samples collected on day 0, weeks 6, 18 and 42 from all microcosms…… 132

4.23 Comparison of Mycobacterium community profiles in three PAH-contaminated soils (AP, TB and Creo) generated using NidA genes following 42 weeks incubation…….. 134

4.24 UPGMA dendrogram constructed from the similarity matching produced from composite NidA DGGE community profiles of the 16S rDNA fragments, amplified PCR products of DNA extracted from samples collected on day 0, weeks 6, 18 and 42 from all microcosms……... 135

5.1 Distribution of taxonomic domain determined in sequences obtained from (i) NA0, (ii) NA18, (iii) NA42, (iv) ENA18, (v) ENA42, (vi) Comb18, and (vii) Comb42 metagenomes sampled from the Creo soil following 42 week incubation period.……. 150

5.2 Distribution of taxonomic phylogenetic groups determined in sequences obtained from (i) NA0, (ii) NA18, (iii) NA42, (iv) ENA18, (v) ENA42, (vi) Comb18, and (vii) Comb42 metagenomes sampled from the Creo soil following 42 weeks of incubation.…….. 151

5.3 Distribution of organisms at Order level determined in sequences obtained from (i) NA0, (ii) NA18, and (iii) NA42 metagenomes sampled from the Creo soil following 42 week incubation period under natural attenuation conditions (NA)….. 157

5.4 Distribution of organisms at Order level determined in sequences obtained from (i) ENA0, (ii) ENA18, and (iii) ENA42 metagenomes sampled from the Creo soil following 42 week incubation period under enhanced natural attenuation (ENA) conditions…….. 158

5.5 Distribution of organisms at order level determined in sequences obtained from (i) Comb0, (ii) Comb18, and (iii) Comb42 metagenomes sampled from the Creo soil following 42 week incubation period under combined (Comb) conditions.…… 159
5.6 Distribution of taxonomic domain determined in sequences obtained from (i) NA0, (ii) NA18, (iii) NA42, (iv) ENA18, (v) ENA42, (vi) Comb18, and (vii) Comb42 metagenomes sampled from the TB soil following 42 week incubation period.……. 163
5.7 Distribution of taxonomic phylogenetic groups determined in sequences from (i) NA0, (ii) NA18, (iii) NA42, (iv) ENA18, (v) ENA42, (vi) Comb18, and (vii) Comb42 metagenomes sampled from TB microcosm after 42-week incubation.…… 164
5.8 Distribution of organisms at order level determined in sequences obtained from (i) NA0, (ii) NA18, and (iii) NA42 metagenomes sampled from TB soil following 42 weeks of incubation under natural attenuation (NA) conditions.……..... 170
5.9 Distribution of organisms at order level determined in sequences obtained from (i) ENA0, (ii) ENA18, and (iii) ENA42 metagenomes sampled from TB soil following 42 weeks of incubation under enhanced natural attenuation (ENA) conditions.…….. 171
5.10 Distribution of organisms at order level determined in sequences obtained from (i) Comb0, (ii) Comb18, and (iii) Comb42 metagenomes sampled from TB soil following 42 weeks of incubation under combined conditions (Comb).…….. 175
5.11 Distribution of taxonomic domain determined in sequences obtained from (i) NA0, (ii) NA18, (iii) NA42, (iv) ENA18, (v) ENA42, (vi) Comb18, and (vii) Comb42 metagenomes sampled from AP soil following 42 weeks of incubation.……... 178
5.12 Distribution of taxonomic phylogenetic groups determined in sequences obtained from (i) NA0, (ii) NA18, (iii) NA42, (iv) ENA18, (v) ENA42, (vi) Comb18, and (vii) Comb42 metagenomes sampled from AP soil following 42 weeks of incubation……. 187
5.13 Distribution of organisms at Order level determined in sequences obtained from (i) NA0, (ii) NA18, and (iii) NA42 metagenomes sampled from AP soil following 42 weeks of incubation under natural attenuation conditions (NA)……. 182
5.14 Distribution of organisms at order level determined in sequences obtained from (i) ENA0, (ii) ENA18, and (iii) ENA42 metagenomes sampled from AP soil following 42 weeks of incubation under enhanced natural attenuation conditions (ENA).…….. 183
5.15 Distribution of organisms at order level determined in sequences obtained from (i) Comb0, (ii) Comb18, and (iii) Comb42 metagenomes sampled from AP soil following 42 weeks of incubation under combined conditions (Comb).……. 184
5.16 Comparison of metagenome functional profiles from Creo microcosms incubated under NA conditions …… 189
5.17 Comparison of metagenome functional profiles from Creo microcosms incubated under NA conditions …… 190
5.18 Comparison of metagenome functional profiles from Creo microcosms incubated under ENA conditions.……. 191
5.19 Comparison of metagenome functional profiles from Creo microcosms incubated under ENA conditions.……. 192
5.20 Comparison of metagenome functional profiles from Creo microcosms incubated under combined (Comb) conditions …… 193
5.21 Comparison of metagenome functional profiles from Creo microcosms incubated under combined (Comb) conditions …… 194
5.22 Comparison of metagenome functional profiles from TB microcosms incubated under NA conditions.…… 196
5.23 Comparison of metagenome functional profiles from TB microcosms incubated under NA conditions.…… 197

5.24 Comparison of metagenome functional profiles from TB microcosms incubated under ENA conditions.…… 198
5.25 Comparison of metagenome functional profiles from TB microcosms incubated under ENA conditions.…… 199
5.26 Comparison of metagenome functional profiles from TB microcosms incubated under combined (Comb) conditions.…… 200
5.27 Comparison of metagenome functional profiles from TB microcosms incubated under combined (Comb) conditions.…… 200
5.28 Comparison of metagenome functional profiles from AP microcosms incubated under NA conditions. ……... 202
5.29 Comparison of metagenome functional profiles from AP microcosms incubated under NA conditions. ……... 202
5.30 Comparison of metagenome functional profiles from AP microcosms incubated under ENA conditions.…… 203
5.31 Comparison of metagenome functional profiles from AP microcosms incubated under ENA conditions.…… 204
5.32 Comparison of metagenome functional profiles from AP microcosms incubated under combined (Comb) conditions.…… 205
5.33 Comparison of metagenome functional profiles from AP microcosms incubated under combined (Comb) conditions.…… 206
5.34 KEGG pathway analysis of metagenomes from Creo microcosms incubated under NA conditions displaying enzymes required for the metabolism of naphthalene.…... 209
5.35 KEGG pathway analysis of metagenomes from Creo microcosms incubated under NA conditions displaying enzymes required for the metabolism of B(a)P..... 210
5.36 KEGG pathway analysis of metagenomes from TB microcosms incubated under NA conditions displaying enzymes required for the metabolism of naphthalene.…... 214
5.37 KEGG pathway analysis of metagenomes from TB microcosms incubated under NA conditions displaying enzymes required for the metabolism of B(a)P. …… 214
5.38 KEGG pathway analysis of metagenomes from AP microcosms incubated under NA conditions displaying enzymes required for the metabolism of naphthalene.…... 217
5.39 KEGG pathway analysis of metagenomes from AP microcosms incubated under NA conditions displaying enzymes required for the metabolism of B(a)P. …… 217

6.1 Comparison of the predicted residual phenanthrene concentration (determined using HP-β-CD extraction) and measured residual phenanthrene concentration (following 42 weeks ENA) in Creo, TB and AP soils.…….. 232
6.2 Comparison of the predicted residual pyrene concentration (determined using HP-β-CD extraction) and measured residual pyrene concentration (following 42 weeks ENA) in Creo, TB and AP soils. …….. 232
6.3 Comparison of the predicted residual B(a)P concentration (determined using HP-β-CD extraction) and measured residual B(a)P concentration (following 42 weeks ENA) in Creo, TB and AP soils.……... 234

7.1 Change in total PAH concentration in Creo contaminated soil following28 days incubation using natural attenuation (NA), enhanced natural attenuation (ENA), sodium succinate (SS), hydrogen peroxide (H2O2) and Tween20 treatments (T20). 246
7.2 Change in phenanthrene concentration in Creo soil following 28 days incubation using natural attenuation (NA), enhanced natural attenuation (ENA), sodium succinate (SS), hydrogen peroxide (H2O2) and Tween20 treatments (T20). 246

7.3	Change in pyrene concentration in Creo soil following 28 days incubation using natural attenuation (NA), enhanced natural attenuation (ENA), sodium succinate (SS), hydrogen peroxide (H2O2) and Tween20 treatments (T20).	247
7.4	Change in B(a)P concentration in Creo soil following28 days incubation using natural attenuation (NA), enhanced natural attenuation (ENA), sodium succinate (SS), hydrogen peroxide (H2O2) and Tween20 treatments (T20).	247
7.5	Distribution of taxonomic domain determined in sequences obtained from (i) NA0, (ii) NA14, (iii) NA28, (iv) ENA14, (v) ENA28, (vi) H2O2-14, (vii) H2O2-28, (viii) SS-14, (ix) SS-28 and (x) T20 metagenomes sampled from Creo alternative soil microcosms following 28 day incubation period. ……	250
7.6	Distribution of taxonomic phylogenetic groups determined in sequences obtained from (i) NA0, (ii) NA14, (iii) NA28, (iv) ENA14, (v) ENA28, (vi) H2O2, and (vii) H2O2 metagenomes sampled from the Creo soil microcosms following 28 day incubation period.…….....	253
7.7	Distribution of taxonomic phylogenetic groups determined in sequences obtained from (i) day zero, (ii) NA14, (iii) NA28, (iv) SS-14, (v) SS-28, and (vi) T20 metagenomes sampled from Creo soil microcosms following 28 days of incubation.	254
7.8	Distribution of taxonomic phylogenetic groups determined in sequences obtained from (i) day zero, (ii) day 14 and (ii) day 28 metagenomes sampled from the Creo soil microcosms following 28-day incubation using natural attenuation conditions (NA)……..	257
7.9	Distribution of organisms at order level determined in sequences obtained from (i) day zero, (ii) day 14 and (ii) day 28 metagenomes sampled from the Creo soil microcosms following 28-day incubation under enhanced natural attenuation conditions (ENA).…….	258
7.10	Distribution of organisms at order level determined in sequences obtained from (i) day zero metagenomes, (ii) day 14 metagenomes and (ii) day 28 metagenomes sampled from the Creo soil microcosms following 28-day incubation in microcosms treated with hydrogen peroxide (H2O2).……..	260
7.11	Distribution of organisms at order level determined in sequences obtained from (i) day zero, (ii) day 14 and (ii) day 28 metagenomes sampled from the Creo soil microcosms following 28-day incubation in microcosms amended with sodium succinate (SS).……..	261
7.12	Distribution of organisms at order level determined in sequences obtained from (i) day zero, (ii) day 14, and (ii) day 28 metagenomes sampled from the Creo soil microcosms following 28-day incubation in microcosms amended with Tween 20 (T20)…….	262
7.13	Comparison of metagenome functional profiles from Creo soil incubated under chemical oxidation (H2O2) conditions.……	267
7.14	Comparison of metagenome functional profiles from Creo soil incubated under chemical oxidation (H2O2) conditions. ……...	268
7.15	Comparison of metagenome functional profiles from Creo soil incubated in microcosms treated with sodium succinate (SS). ……	269
7.16	Comparison of metagenome functional profiles from Creo soil incubated in microcosms treated with sodium succinate (SS). ……	270
7.17	Comparison of metagenome functional profiles from Creo soil incubated in microcosms treated with Tween 20 (T20)……	271
7.18	KEGG pathway analysis of metagenomes from Creo soil incubated under natural attenuation conditions (NA), displaying enzymes required for the metabolism of naphthalene.……..	273

7.19 KEGG pathway analysis of metagenomes from Creo soil incubated under natural attenuation conditions (NA), displaying enzymes required for the metabolism of B(a)P……. 273

List of tables

Table		Page
1.1	Selected physical-chemical properties of the USEPA defined 16 priority PAHs (Dabestani & Ivanov 1999; Mackay, Shiu & Ma 1997).	3
1.2	Carcinogenic classification of PAH compounds by specific agencies.	8
1.3	Pyrogenic and Petrogenic sources of PAHs (Maliszewska-Kordybach 1999).	11
1.4	Polycyclic aromatic hydrocarbons oxidised by difference species of bacteria adapted from Juhasz and Naidu (2000).	15
1.5	Polycyclic aromatic hydrocarbons oxidized by difference species of fungi adapted from Juhasz and Naidu (2000).	17
1.6	Summary of the advantages and disadvantages of bioremediation technologies (Vidali 2001).	25
1.7	Factors influencing the bioremediation of PAHs in contaminated soils.	28
1.8	Platforms currently available in the market alongside sequencing technologies they used.	39
1.9	Key advantages and drawbacks of five selected NGS platforms alongside Sanger sequencer.	41
2.1	Experimental set up for PAH biodegradation microcosms of the amended and unamended using three historical PAH-contaminated soils (Creo, TB, and AP).	54
2.2	Primer pairs used for PCR amplification of bacterial and fungal genes in this study.	55
2.3	Experimental set up for PAH biodegradation microcosms using Creo soil amended with sodium succinate, hydrogen peroxide and Tween 20.	55
2.4	Primer pairs used for PCR amplification of bacterial genes in this study……..	59
3.1	Individual PAH concentration in 3 contaminated soils used Table 3.1: Individual PAH concentration in 3 contaminated soils used in this project prior to the preparation of microcosm experiments.	69
3.2	Summary of selected soil properties for PAH-contaminated soils utilised in this study.	69
5.1	Taxonomic bacterial composition at phylum level in Creo soil metagenomes obtained from unamended and amended microcosms following 42 weeks incubation……	149
5.2	Taxonomic bacterial composition at order level in Creo soil metagenomes obtained from unamended and amended microcosms following 42 weeks of incubation…...	154
5.3	Taxonomic bacterial composition at phylum level in the TB soil metagenomes obtained from unamended and amended microcosms following 42 weeks of incubation…….	162
5.4	Taxonomic bacterial composition at order level in TB soil metagenomes obtained from unamended and amended microcosms following 42 weeks incubation……	168

5.5	Taxonomic bacterial composition at phylum level in AP soil metagenomes obtained from unamended and amended microcosms following 42 weeks incubation……	177
5.6	Taxonomic bacterial composition at order level in AP soil metagenomes obtained from unamended and amended microcosms following 42 weeks of incubation…...	186
5.7	Summary of hits matching three enzymes associated with PAH degradation specific functions in KEGG pathways analysis of metagenomes sampled from three soil microcosms (Creo, TB and AP) over the 42 week incubation period.	211
6.1	Summary of linear regression models used in this study for predicting residual PAH fractions in Creo, TB and AP soils.	231
6.2	Comparison of predicted residual PAH fractions and measured residual PAH fractions following biodegradability (42 weeks) in 3 contaminated soils.	233
7.1	Taxonomic bacterial composition at the phylum level in Creo soil metagenomes obtained from microcosms following 28-day incubation under natural attenuation (NA), enhanced natural attenuation (ENA), sodium succinate (SS), hydrogen peroxide (H2O2) and tween 20 treatments (T20)…….	255
7.2	Taxonomic bacterial composition at order level in Creo soil metagenomes obtained from experimental microcosms following 28 days of incubation……..	264
7.3	Summary of hits matching each of the three enzymes associated with PAH degradation specific functions in KEGG pathways analysis of metagenomes sampled from alternative Creo soil microcosms over the 28-day incubation period.	274

Glossary and abbreviations

Term	Definition
%	percent
Acryl	acrylamide
APS	ammonium persulfate
AP	soil collected from a former manufacturing gas plant in Albert Park in Victoria
ASE	accelerated solvent extraction
ATSDR	Agency for Toxic Substances and Disease Registry
TP	Adenosine-5'-triphosphate
B(a)P	benzo(a)pyrene
BioA	bioaugmentation
BLAST	basic local alignment search tool
bp	base pairs
^{o}C	degree Celsius
Comb	enhanced natural attenuation and bioaugmentation
Creo	soil collected from a former wood treatment site (Creosote)
C: N	carbon to nitrogen ratio
d	day
DCM	dichloromethane
ddH_2O	deionised water
DGGE	denaturant gradient gel electrophoresis
DM	dry matter
DNA	deoxyribonucleic acid
dNTP	deoxynucleotide triphosphate
EDTA	ethylenediaminetetra-acetic acid
ENA	enhanced natural attenuation
EPA	Environment Protection Authority (Australia)
FID	flame ionisation detector
g	gram
GC	gas chromatography
GC-FID	gas chromatography equipped with flame ionisation detection
H_2O	water
h	hour
HMW	high molecular weight
HPCD	hydroxypropyl-β-cyclodextrin
ITS	internal transcribed spacer region
K_{ow}	octanol/water partition coefficient
kg	kilogram
l	litre
LMW	low molecular weight
LiP	lignin peroxidase

M	molar
MC	moisture content
$MgCl_2$	magnesium chloride
MG-RAST	metagenomics rapid annotation using subsystem technology
min	minute
MnP	manganese peroxidase
MGP	manufacturing gas plant
MW	molecular weight
µm	micrometre
µmols/mL	micromoles per milliliter
µg	microgram
mg	milligram
mM	millimolar
ml	millilitre
MPN	most probable number
NA	nutrient agar
NA	natural attenuation
NB	nutrient broth
NCBI	National Centre for Biotechnology Information
NEPM	National Environment Protection Measures
OM	organic matter
PAHs	polycyclic aromatic hydrocarbons
PBS	phosphate buffered saline
PCR	polymerase chain reaction
PHE	phenanthrene
PYR	pyrene
pH	hydrogen ion concentration (-$[\log]_{10}$ hydrogen ions)
rpm	revolutions per minute
rDNA	ribosomal deoxynucleic acid
rRNA	ribosomal deoxynucleic acid
SOM	soil organic matter
TAE	tris-acetic EDTA
TB	soil collected from a former tram maintenance yard
TEMED	tetramethylethylenediamine
TOC	total organic carbon
TSB	tryptone soya broth
USEPA	United States Environment Protection Authority
UV	ultraviolet
v/v	volume per volume
w/v	weight per volume
V	voltage
WHC	water holding capacity
Xg	times gravity

Abstract

Polycyclic aromatic hydrocarbons (PAHs) may be released into the environment as a result of anthropogenic activities. Due to their persistence, ubiquity, toxicity and carcinogenicity, there is great concern regarding the presence of PAH in the environment. However, a potential strategy for reducing the environmental impact of PAH contamination is the application of bioremediation; a technology which is considered cost effective and environmentally friendly. This thesis investigated the influence of bioremediation strategies on PAH removal efficacy in PAH-contaminated soils collected from former wood treatment (Creo), manufacturing gas plant (AP) and tram maintenance (TB) sites. Shotgun pyrosequencing (Ion Proton) was also utilised to characterise the impact of bioremediation strategy on the composition and metabolic potential of soil microbial communities.

Bioremediation efficacy was assessed using natural attenuation (NA), enhanced natural attenuation (ENA), bioaugmentation (BioA) and a combined BioA-ENA strategy (Comb) over a 42 week period. In all soils, total PAH removal was limited using NA (<12%) presumably due to the lack of nutrients to sustain microbial growth, the lack of PAH degraders and/or limited PAH bioavailability. Amending soils with nitrogen and phosphorus resulted in a small but significant increase in bioremediation efficacy in TB and Creo soil although total PAH removal did not exceed 16%. Similarly, in microcosms augmented with *Mycobacterium gilvum* (BioA and Combined) a small increase in PAH removal was observed in Creo soil compared to the NA treatment. Although amendment strategies had minimal impact on enhancing PAH degradation, analyses of microbial communities using a MPN method determined a positive effect on microbial numbers (by up to 2 orders of magnitude). In addition, analysis of soil microbial and *Mycobacterium* community profiles using 16S rDNA, specific NidA genes and denaturing gradient gel electrophoresis (DGGE) determined shifts in bacterial banding profiles as a result of incubation time rather than bioremediation strategy.

In order to gain a greater insight into potential changes in microbial community structure as a consequence of bioremediation strategies, Creo, TB and AP soil metagenomes were analysed using shotgun pyrosequencing (Ion Proton platform). In all soils and treatments, the bacterial domain was dominant comprising 88.8 to 99.0% of hits. According to the MG-RAST annotation systems, Proteobacteria (35.4 to 82.5% of total organisms) dominated bacterial taxa distribution in all metagenomes, however, the proportion of sequences decreased over the 42 week incubation period as the relative abundance of the other phyla including

Acidobacteria, Actinobacteria, Firmicutes, Bacteroidetes, Verrucomicrobia and Planctomycete increased resulting in more diverse microbial assemblages. Of note was the 2-fold increase in the relative abundance of the order Acidobacteriales in NA microcosms presumably due to their ability to proliferate under low nutrient conditions. Under ENA and combined conditions, the relative abundance of the orders Cytophagales and Rhizobiales rapidly increased (up to 50-fold) presumably due to their ability to compete for available nutrients.

Functional profile analysis showed significant metabolic potential in sequences related to PAH bioremediation in all soils. A relative overrepresentation of genes affiliated with activities such as metabolism of aromatic compounds, clustering-based subsystems, central carbohydrate metabolism and associated pathways were detected. For instance, a reduction in activities related to central carbohydrate metabolism was observed among NA metagenomes over time. However, following the addition of nutrients to ENA microcosms, metabolic processes were enhanced. These results suggest the significance of amending nutrients to soil in order to stimulate the growth of key microorganisms. Furthermore, three key enzymes involved in the metabolism of naphthalene, pyrene and B(a)P were detected based on KEGG pathways analysis. The prevalence of xenobiotic monooxygenase, glutathione transferase and benzo(a)-4,5-epoxide hydrolase was indicative of the biodegradability capacity in these soils. Although metagenomics analysis demonstrated diverse bacterial communities and functionality in the three soils, there was no relationship between PAH degradative potential and actual PAH removal.

In order to determine if PAH bioavailability limited PAH biodegradation in Creo, TB and AP soil, hydroxypropyl-β-cyclodextrin (HP-β-CD) extraction was utilised to predict biodegradation endpoints. A comparison of predicted biodegradation endpoints to measured residual PAH concentrations after 42 weeks in amended microcosms resulted in values which were either similar or higher than actual biodegradation endpoints (i.e. under-prediction of biodegradation). Regardless of the variation observed in predicted residual biodegradation endpoints, PAH bioavailability was determined to be low in Creo, TB and AP soil which limited PAH biodegradation and bioremediation efficacy.

In an attempt to overcome the observed PAH bioavailability limitations, additional microcosm experiments were conducted with Creo soil to investigate whether the addition of an alternative carbon source (sodium succinate), a surfactant (Tween 20) or pre-treatment using

chemical oxidation (hydrogen peroxide) would increase PAH bioavailability and hence bioremediation efficacy. Sodium succinate or Tween 20 addition failed to enhance microbial biodegradation of PAHs over a 28 day incubation period, however, treatment of soil with hydrogen peroxide resulted in a rapid reduction in total PAH concentration (72.3%) after 90 min. The rapid decrease in PAH concentration occurred through the interaction of hydroxyl radicals with PAHs and soil organic matter. However, further incubation did not result in a further decrease in PAH concentration. Analysis of metagenomes sampled from additional Creo microcosms was also undertaken to determine whether supplementation of sodium succinate, Tween 20 or chemical oxidation influenced soil microbial diversity and functional profiles.

Using the MG-RAST interface, Acidobacteria, Actinobacteria, Firmicutes, Bacteroidetes, Verrucomicrobia and Proteobacteria were the most dominant phylum (relative abundance ranging from 76.1-90.9% of the total organisms) in all treatments. In addition, analysis of metabolic functional profiles showed an abundance of generic genes affiliated with the metabolism of aromatic compounds, central carbohydrate and clustering-based subsystems regardless of treatments. Three key enzymes including xenobiotic monooxygenase, glutathione transferase and benzo(a)-4,5-epoxide hydrolase associated with the metabolism of naphthalene, pyrene and B(a)P partial pathways were also prevalent both augmented and hydrogen peroxide treated soil. The prevalence of these enzymes highlight the robustness, resilience and biodegradation potential of the microbial community in Creo soil. The results reported in this thesis illustrate that contaminant bioavailability is a key parameter for bioremediation success and that next generation sequencing technologies provide an approach for profiling microbial community structure and functionality with potential application for PAH bioremediation

Declaration

This thesis presents work carried out by myself and does not incorporate without acknowledgment any material previously submitted for a degree or diploma in any university; to the best of my knowledge it does not contain any materials previously published or written by another person except where due reference is made in the text; and all substantive contributions by others to the work presented, including jointly authored publications, are clearly acknowledged.

Samuel Aleer

Signature Date

Acknowledgements

I would like to express my gratitude to my principal supervisor, Associate Research Professor Albert Juhasz whose expertise, understanding, encouragement, and patient considerably added to my experience. I would like to acknowledge your dedication and support you have provided to me throughout my candidature by supplying PAH contaminated soils and a well maintained *Mycobacterium* gilvum cultures for a smooth start of my experiments. The research themes addressed in this thesis was possible because of your unreserved support and assistant I have received during my candidature from you at UNISA. You always know how to encourage a person to breakdown complex problems into a manageable form.

To my C-supervisor Dr. Euan Smith (UNISA), thanks for being instrumental during my write up time, by providing never-ending advice and suggestions to pay attention to some silly errors by being consistent.

To Prof. Andy Ball, my associate supervisor, your assistant with all microbiological and molecular analysis was incredible. You provided me with a lab bench space and free access to most of lab consumables and sequencing facility (Ion Proton platform) during my time at RMIT University.

A very special thanks goes out to Dr. Akin Adetutu, for his unwavering endless motivation, encouragement, constructive advice, support and for the assistant he provided at all levels of metagenomics and molecular analyses. He provided me with direction, technical support and became more of a mentor and friend, by spending a huge amount of his time helping genomic DNA down streaming including library construction, template preparation, sequencing and part of data analysis than I would imagine. Dr. Adetutu is the real handyman when it comes to handling of DNA, who he introduced me to the idea of using next generation sequencing technology.

I would also like to give special thanks to Fabrice Odefren (Life Technology Australia) for your timely helped with Ion Proton training and product knowledge. You gave us invaluable hands-on experience to be able to use the sequencer with confidence. My sincere gratitude to Vijay whom we shared sequencing lab and working bench space during my time at RMIT university. I would like to extend my grateful to all CERARians (Current FII) and Ball lab staff members and my postgraduate colleagues working in these two laboratories particularly Sayali, Tanvi, Shahsavari, Mohammed, Aida, Kavitha, Weighong, Naser, and Thavamani. It has been a wonderful experience sharing the same environment with you and I appreciated all

of you for your technical support. I must also acknowledge Ray Corrrell and Sotirios Vasileiadis for your assistant with statistical and bioinformative analysis.

I would like to give my special thanks to my parents (Dad and Mum), as no words can express their incredible love, support, encouragement, motivation and patience to allow me pursue my dreams at a time when I should be taking care of you. I have the fortune of having lovely siblings with whom I have shared many difficult and memorable times, particularly Priscilla, Tabitha and Mayen Deng (brother-in-law). I'm also thankful for my cousin David Chan and his family, who have provided me with eight months free accommodation during the time I was doing my sequencing at RMIT University in Melbourne. I would like to express my sincere thank and gratitude to Aluel Mawut and Aweng Ajak, for being supportive in the absence and presence of my cousin (David Chan), through whom I had a chance to know you. I wouldn't have completed major components of my thesis, I undertaken in Melbourne without your hospitality.

I'm grateful to the University of South Australia and in particular to the Centre of Environmental Risk Assessment and Remediation (CERAR), Division of the Information Technology, Engineering and the Environment for giving me this opportunity to pursue my dreams by awarding me a scholarship that financially supported me throughout my candidature. I many thanks goes to the Cooperative Research Centre for Contamination Assessment and Remediation (CRC-CARE) for awarding me a top up scholarship for my living allowances and laboratory consumables expenses.

Above all, I would like to thank God for helping me through difficult times of my candidature.

Chapter 1

Literature review of microbial biodegradation of PAHs

1.1 Introduction

Pollution is one of the challenges currently affecting environmental quality and natural resource around the world. A large number of these pollutants have been generated through industrial, agricultural and medical associated activities. The impact of these environmental pollutants constitute major environmental and public health risks mostly in some industrialised countries (Gateuille et al. 2014; Sun, L et al. 2014). There are a number of contaminant sources through which a wide range of organic and inorganic chemicals are released into the air, water, and sediments/soil (Cai et al. 2014; Gateuille et al. 2014). One of the leading sources of environmental contamination in industrialized countries is via anthropogenic activity. For example, Zhang et al. (2014) investigated distribution and sources of polycyclic aromatic hydrocarbon (PAH) in wetlands in Northeast China. In this study, they detected high concentration of PAHs in groundwater, surface water, sediments, and soils due to the discharge of industrial wastewater into the wetland. They also showed that premium gasoline was one of the major contributors of PAH pollution in surface water, groundwater, and sediments (Zhang et al. 2014).

A large area of fertile land is considered to be chemically contaminated with agro-chemicals and from various resource activities such as oil and gas drilling (Sinha et al. 2010). Numerous sites are known or suspected to be contaminated with several toxic chemicals. For example, in Australia, there are approximately over 80,000 contaminated sites with various hazardous chemicals according to the National Environmental Protect Council as reported by (Sinha et al. 2010). A total of 75% of these sites are located in NSW and Queensland (30,000 in each state), 12.5% in Victoria (10,000), 5% in South Australia and Western Australia (4,000 in each state), and less than 1% in Tasmania and Northern Territory (500 in each state). However, most recent data from the Australia Broadcasting Corporation (broadcast on 16 Sep. 2013 and access on 30/01/2015) has estimated the number of contaminated to be over 150, 000 in Australia. According to this report, less than 1 per cent of these sites have been remediated. Moreover, at the global scale, there are in excess of 3 million potentially contaminated sites(EPA 2004). While the cost associated with site assessment, management and possible clean-up is estimated to be in excess of $200 billion annually over the next 30 years (EPA 2004).

This literature review aims to highlight common sources of PAH contamination in the environment, their structural behaviour, physio-chemical properties, and bioremediation strategies for the remediation of PAHs and PAH impact on microbial community structure and functionality.

1.2 Polycyclic aromatic hydrocarbons (PAHs)

1.2.1 PAH structures

Polycyclic aromatic hydrocarbons are a group of organic pollutants that are ubiquitous in the environment (Lladó, S. et al. 2013). PAHs are composed of fused benzene rings arranged in a linear, angular or clustered structural manner (Hadibarata & Tachibana 2009). There are well over one hundred PAH compounds known to be present in environment soil matrices, sediment, water and air. Of these compounds, 16 PAHs have been classified by the US Environmental Protection Agency (USEPA) as priority pollutants based on their physio-chemical and toxicological properties (Table 1.1). The phase "priority pollutants" refers to the set of chemical compounds regulated by the USEPA with developed analytical test methods (USEPA). In 1978, the USEPA developed the first list of priority pollutants containing 129 compounds (Chemicals 2001). The criteria to include individual compound on this list was based on the following four merits; (I) the pollutant must be specifically named on the list of toxic pollutants, (II) there must be a chemical testing standard available for the pollutant, (III) the pollutant had to have been reported as frequently found in water with 2.5% minimal detection level, (IV) the pollutant must have been produced in significant quantities to match the similar mass chemical productions as reported in the 1976 Directory of Chemical Producers, USA (Chemicals 2001). PAHs are considered priority pollutants due to their toxicity, high frequency of occurrence, and their ability to persist in the environment. PAHs fulfil these criteria and the US EPA included 16 PAHs in the list of Consent Decree Priority Pollutants according to Keith and Telliard, 1979 (Table 1.1). Currently, the 16 EPA priority PAHs are used by regulatory authorities to assess and identify suspected and contaminated sites with petroleum hydrocarbons. More commonly, they are being used as standard compounds in most research involving remediation of environment contaminated with PAHs.

Among the compounds, naphthalene is the simplest compound with a structure consists of 2 rings (Figure 1.1). Whereas the more complex compounds are characterised by 6 or more rings including some of the alkyl groups.

Table 1.1. Selected physical-chemical properties of the US EPA defined 16 priority PAHs (Dabestani & Ivanov 1999; Mackay, Shiu & Ma 1997)

Compound	Number of rings	Molecular Weight[a]	Melting point (°C)[b]	Boiling point(°C)[b]	Vapour Pressure (pa at 25 °C)[b]	Aqueous Solubility (mg/l)[a]	n-Octanol-: water partition Coefficient ($logK_{ow}$)[b]	Henry's Law Constant at 25 °C (kpa)[b]	Density[b]
Naphthalene	2	128	81	217.9	10.4	31	3.4	$4.89x10^{-2}$	1.154
Acenaphthylene	3	152	92-93	279	$8.9x10^{-1}$	16	4.07	$1.14x10^{-3}$	0.899
Acenaphthene	3	154	95	279	$2.9x10^{-1}$	3.8	3.92	$1.48x10^{-2}$	1.024
Fluorene	3	156	115-116	295	$8.0x10^{-2}$	1.8	4.18	$1.01x10^{-2}$	1.203
Anthracene	3	178	216.4	342	$8.0x10^{-4}$	1.1	4.5	$7.3x10^{-2}$	1.283
Phenanthrene	3	178	100.5	340	$1.6x10^{-2}$	0.045	4.6	$3.98x10^{-3}$	0.98
Fluoranthene	4	202	108.8	375	$1.2x10^{-3}$	0.13	5.22	$6.5x10^{-4}$	1.252
Pyrene	4	202	150.4	393	$6.0x10^{-4}$	0.246	5.18	$1.1x10^{-3}$	1.271
Benzo(a)anthracene	4	228	160.7	400	$2.8x10^{-5}$	0.011	5.61	Na	1.226
Chrysene	4	228	253.8	448	$8.4x10^{-5}$	0.006	5.91	Na	1.274
Benz(b)fluoranthene	5	252	168.3	481	$6.7x10^{-5}$	0.0015	6.12	$5.1x10^{-5}$	Na
Benzo(k)fluoranthene	5	252	215.7	480	$1.3x10^{-8}$	0.0008	6.84	$4.4x10^{-5}$	Na
Benzo(a)pyrene	5	252	178.1	496	$7.3x10^{-7}$	0.0038	6.5	$3.54x10^{-5}$	1.351
Benzo(a, h)anthracene	5	278	266.6	524	$1.3x10^{-8}$	0.00006	6.5	$7.0x10^{-6}$	1.282
Indeno(1, 2, 3-cd)pyrene	6	278	163.6	536	$1.3x10^{-8}$	0.000019	6.58	$2.9x10^{-5}$ C	Na
Benzo(g, h, i)perylene	6	276	278.3	545	$1.4x10^{-8}$	0.00026	7.1	$2.7x10^{-5}$	1.329

Na no values available for this parameter

[a] data obtained from Mackay et al., (1992)

[b] data obtained from Debestani and Ivanov (1999) and data obtained at 25°C.

Although PAH compounds merely contain C and H atoms, it is also possible for the benzene ring to be substituted with nitrogen, sulfur, and oxygen atoms leading to the formation of heterocyclic aromatic compounds (Wilson & Jones 1993). Heterocyclic aromatic hydrocarbons are grouped together with true PAHs since they share similar chemical and physical properties (McElroy, Farrington & Teal 1989).

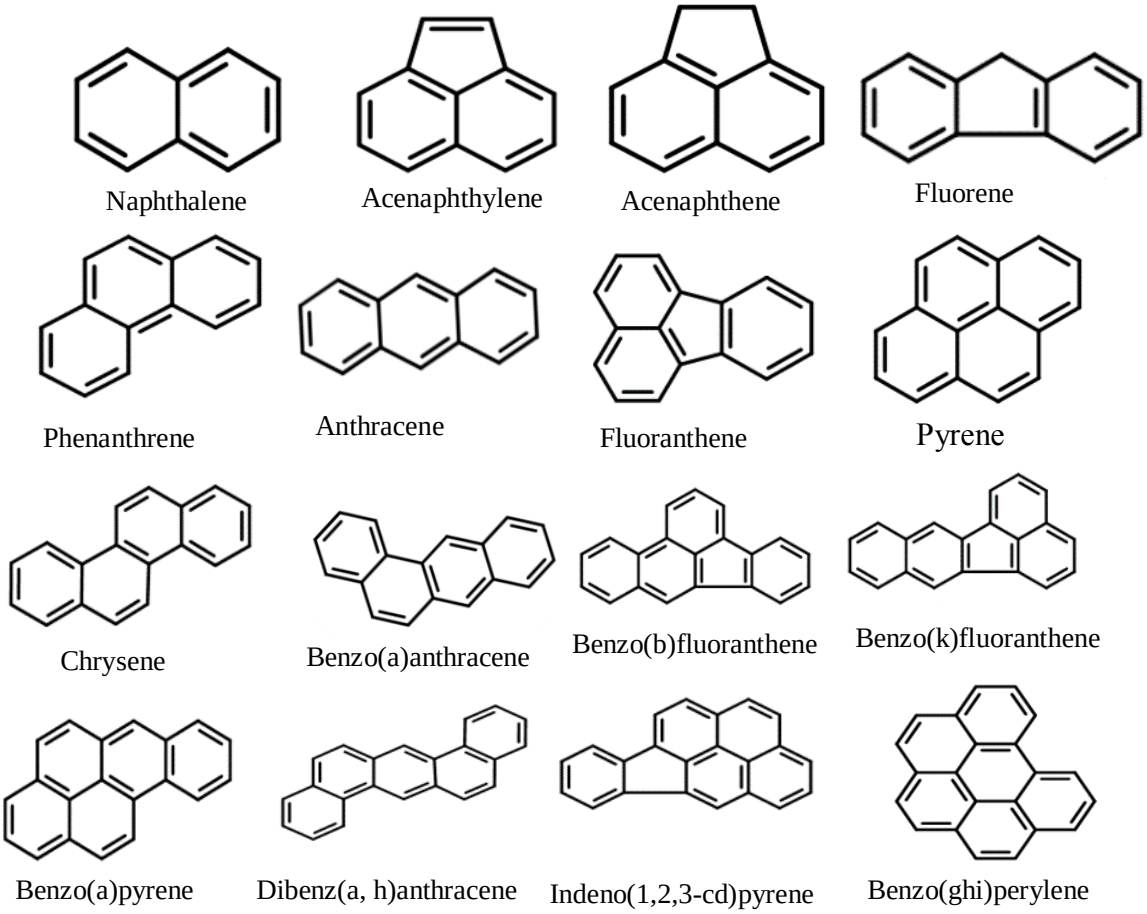

Figure 1.1. Chemical structures of the 16 PAHs identified as priority pollutants by US EPA (Wilson & Jones 1993).

1.2.2 Physio-chemical properties

PAHs are characterized by a number of physio-chemical properties (Gateuille et al. 2014; Harayama 1997; Juhasz & Naidu 2000; Mackay, Shiu & Ma 1997; McElroy, Farrington & Teal 1989; Wilson & Jones 1993). Table 1.1 lists some of these physio-chemical properties of the 16 PAHs.

PAHs exhibit relatively low solubility in water due to their hydrophobicity but are highly lipophilic (dissolve in fats, oils and lipids) (Wang et al. 2015). Some key physio-chemical

properties such as hydrophobicity, expressed as the n-octanol to water partition coefficient (K_{ow}) and boiling point increase with increasing PAH molecular size (Table 1.1). Whereas Henry Law constants, aqueous solubility and liquid vapour pressure decrease with increasing compound size. Overall, physio-chemical properties greatly influence the persistent of PAHs in the air, water, soils and sediments.

1.2.3 Occurrence/formation of PAHs

A number of mechanisms responsible for the formation of PAHs have been studied (Essumang; Essumang et al. 2009; Krauss, Wilcke & Zech 2000; Samanta, Singh & Jain 2002; Zhang et al. 2014). According to these studies, mechanisms accounting for PAHs formation can be summarized into three groups: (I) Phytogenic mechanism – a mechanism involved formation of hydrocarbons as a result of plant biomass decomposition. Elevated atmospheric pressure and temperature have been suggested to enhance the buildup of plant-driven PAHs over an extended time period (Essumang et al. 2009). (II) Petrogenic mechanism - hydrocarbon compounds formed through this mechanism are associated with petroleum products. This process may have occurred over millions of years with elevated atmospheric pressure and temperature. (III) Pyrogenic mechanism – this mechanism accounts for the formation of hydrocarbon compounds associated with incomplete combustion of organic matter such as fossil fuels, asphalt, wood, coal and oil products (Dabestani & Ivanov 1999; Khan, Ishaq & Khan 2008). PAH production is linked to our life styles, which heavily relies on energy production via fossil fuel. Different mechanisms of PAH formation yield a mixture of PAHs with variable quantities of individual PAHs. For example, coal burning (pyrogenic mechanism) produces more HMW (compound with 4 or more rings) compared to LMW (compound with 2 to 3 rings) compounds as oppose to phytogenic mechanism.

The abundance of PAHs in our environment is directly proportional to combustion processes related to electricity energy producing plants among other industrial activities (Manoli & Samara 1999). Some of the leading industrial activities connected to a significant production, usage, storage and inappropriate disposal of considerable amounts of PAH-containing substances included:

- Industrial PAH-associated producing activities
- Gasification/liquefaction of fossil fuels
- Coke production
- Carbon-black production and use

- Asphalt production and Coal-tar/coal-tar-pitch production and use
- Refining/distribution of crude oil and crude-oil-derived products
- Wood-treatment processes wood-preservative (i.e. Creo/anthracene-oil) production
- Fuel/oil storage, transportation, processing, use, and disposal
- Landfill/waste dumps
- Open burning (tyres/refuse/coal etc.)
- Incineration

A particular source of PAHs contamination could directly or indirectly be linked to one of the industrial activities listed above according to (Wilcke 2007). For instance, petrogenic hydrocarbons such as creosote could be detected in large quantities at wood preservation site, whereas pyrogenic hydrocarbons related PAHs would be found at petroleum refineries, power stations, heavy engineering-chemical plants, and paper mills plants. Large quantities of wastes generated during operational processes of these plants contain PAHs (Wilson & Jones 1993) .

1.2.4 Toxicity of PAHs

Extensive studies have been conducted in relation to PAHs toxicity, persistency and ubiquitous in the environment (Mackay et al. 2010) . Importantly, their presence in the environment poses a potential risk to organisms and humans. It has been estimated that more than 2000 priority hazardous substances were detected at contaminated sites in the United States (Johnson & DeRosa 1995). The Agency for Toxic Substances and Disease Registry (ATSDR) and the USEPA jointly listed 275 priority substances based on their toxicity. The 16 PAHs USEPA priority pollutants were developed from the list of 275 chemicals and used as a standard to monitor the occurrence of other pollutants at contaminated sites. For example, Li et al. (2014b) used the toxicity equivalency factor (TEF) / toxicity equivalency quotient (TEQ) of B(a)P to evaluate the toxicities of PAHs in wetland soil. TEF / TEQ are chemical mass balance models use to evaluate the toxicity contributed by individual compounds based on the toxicity of the most potent PAH (B[a]P). PAHs derived from different sources and compositions often present different toxicities effects because of structural and chemical dissimilarities that affect their metabolism. The chemical toxicity of each PAH correlates with its partition coefficient in a mixture of octanol and water (Table 1.1). In Table 1.1, the compounds with higher partition coefficient values are more likely to be toxic than those with lower values e.g. benzo(a)pyrene versus fluorene (Bortey-Sam et al. 2014; Wilcke 2007).

One of the critical issues in PAH toxicity is the formation of reactive metabolites. Some of the known reactive metabolites formed as a result of B(a)P metabolism include epoxides, quinones,

free radicals, reactive oxygen species, and unstable conjugates (Attia 2010) . The newly formed PAH intermediates are highly mutagenic and toxic to laboratory animals and humans compared to the parent compounds (Patri, Padmini & Babu 2010). In general, three interrelated pathways have been proposed to explore the formation of reactive metabolites from B(a)P metabolism (Figure 1.2). The initial pathway involves oxidation of B(a)P parent compound to form two epoxides namely B(a) P7,8 – epoxide and B(a)P4,5 – epoxide, a reaction catalyzed by P450 enzymes. These two reactive metabolites are further oxidized to a trans-dihydrodiols in the present of epoxide hydrolase enzymes, resulting in the formation of B(a)P-7,8-dihydrodiol, 10-epoxide (BPDE). BPDE is the primary metabolite that initiates toxicity and carcinogenicity by covalently binding to DNA bases (i.e guanine residue) leading to DNA mutation/cancer (process known as DNA-adducts). In the second pathway, one electron of B(a)P is oxidized to form 6-oxo-B(a)P- radical intermediates. This free radical intermediates attacks DNA bases leading to depurination

The third pathway is associated with an enzymatic dehydrogenation of dihydrodiol metabolites to produce quinone intermediate, with high affinity to combine with DNA to eventually form reactive oxygen species (ROS). As illustrated in Figure 1.2, oxidation of parent compounds (i.e. B(a)P) can yield a highly reactive metabolite, which may be toxic and carcinogenic to several intracellular macromolecules such as proteins, hormones and DNA. Although PAHs are known to be toxic and carcinogenic, they cannot covalently bind to macromolecules such as DNA to induce the formation of DNA-adducts without parent compounds (i.e, B(a)P) undergoing oxidation yielding reactive metabolites (Bortey-Sam et al. 2014; Nisbet & LaGoy 1992; Patri, Padmini & Babu 2010).

Exposure to elevated PAH concentrations for extended period of time has the potential of initiating adverse health issues and more likely to increase the risk of cancer (Shyr & Liu 2013). Numerous studies have reported PAH toxicity in samples obtained from different locations (Kennaway 1955; Khan, Ishaq & Khan 2008; Li, G-l et al. 2014; Li, G et al. 2014; Skupinska, Misiewicz & Kasprzycka-Guttman 2004; Yan et al. 2004). According to Li et al. (2014a), high PAH toxicity (TEQ of 95.7%) was detected in samples obtained from wetland soil with emission from vehicles as the main source of pollution. This result suggested that vehicular emissions were the major source of PAH toxicity in wetland soil compared to petrogenic sources.

Similar results showing high PAH toxicity values were reported by Khan et al. (2008) in soil sampled at road sides, where the principal source of PAH pollution was from vehicle emissions. The same method of determining toxicity can be used to quantify the carcinogenic potency of PAHs. The evaluation of carcinogenicity of PAHs conducted by the International Agency for Research on Cancer (IARC) have shown both benz(a)anthracene and B(a)P to be probably carcinogenic to human (Table 1.2). Only some members from the list of the 16 PAHs USEPA priority pollutants were classified by both IARC and USEPA as probable or possible human carcinogens.

Table 1.2. Carcinogenic classification of PAH compounds by specific agencies adapted from (Ward et al. 2010).

Agency	PAH Compound(s)	Carcinogenic Classification
U.S Department of Health and Human Service (HHS)	Benz(a)anthracene Benzo(b)fluoranthene Benzo(a)pyrene Dibenz(a, h)anthracene Indeno(1 ,2, 3-c,d)pyrene	Known animal carcinogens
International Agency for Research on Cancer (IARC)	Benzo(a)anthracene Benzo(a)pyrene	Probably carcinogenic to humans
	Benzo(a)fluoranthene Benzo(k)fluoranthene Indeno(1, 2, 3-c, d)pyrene	Possibly carcinogenic to humans
	Anthracene Benzo(g, h, i)perylene Benzo(a)pyrene Chrysene Fluoranthene Fluorene Phenanthrene Pyrene	Not classifiable as to their carcinogenicity to humans
U.S. Environmental Protection Agency (EPA)	Benzo(a)anthracene Benzo(a)pyrene Benzo(b)fluoranthene Benzo(k)fluoranthene Chrysene Diben(a, h)anthracene Indeno(1, 2, 3-c, d)pyrene	Probable human carcinogens
	Acenaphthylene Anthracene Benzo(g, h, i)perylene Fluoranthene Fluorene Phenanthrene Pyrene	Not classifiable as to human carcinogenicity

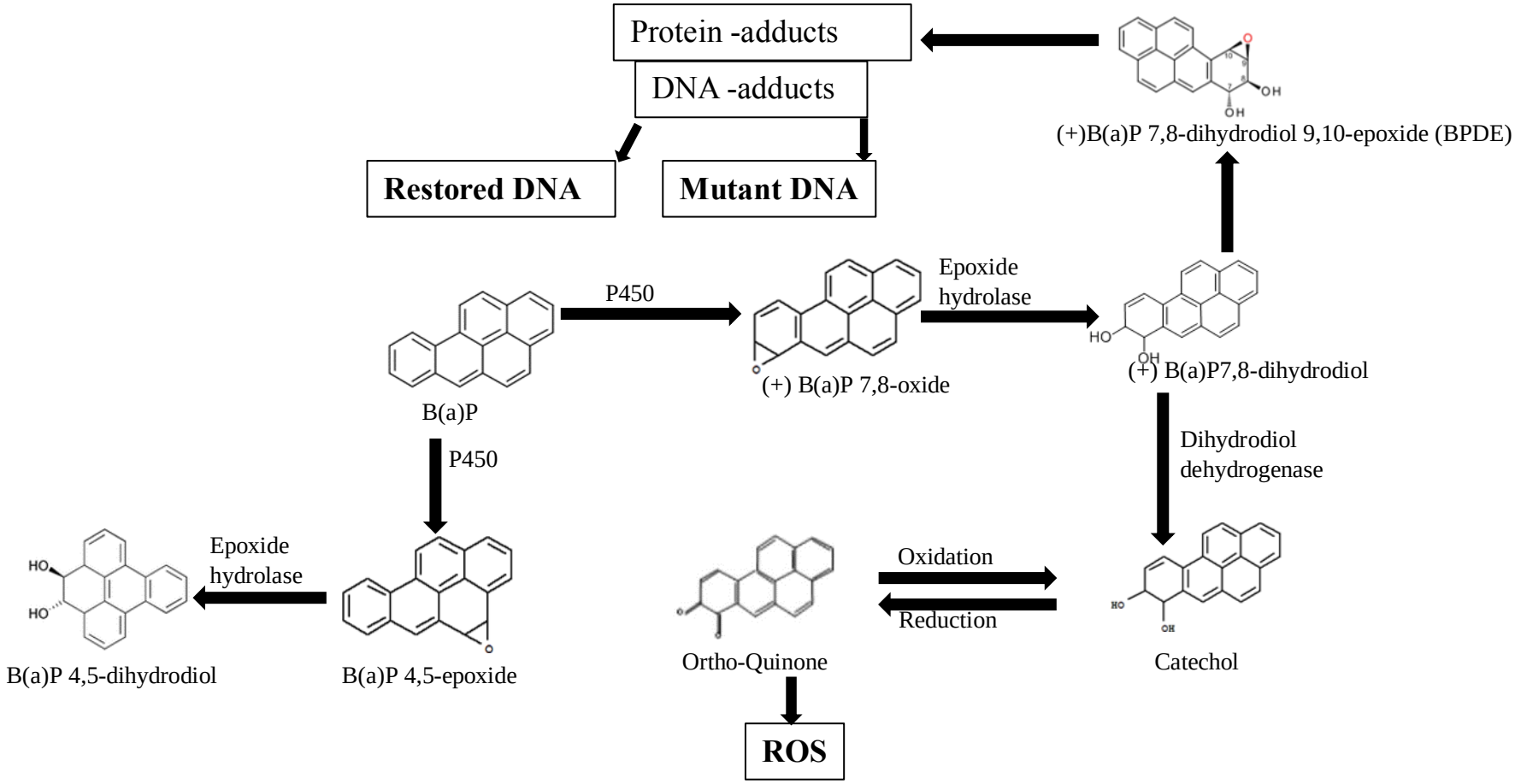

Figure 1.2. Pathways showing B(a)P activation and detoxification. A prototype representative of PAHs through which major primary and secondary reactive metabolites are formed as a results of parent compound oxidation. The cytochrome P450 enzymes are major part of this process modified from (Patri, Padmini & Babu 2010)

1.2.5 Environmental PAH contamination
1.2.5.1 Sources

PAHs may enter the environment through natural and/or anthropogenic activities (Maliszewska-Kordybach 1999; Manoli & Samara 1999; Manzetti 2013) as detailed in Table 1.3. PAHs generated by natural activities are associated with forest fires, fossil fuels and volcanic eruptions. Some biogenic reactions involving plants, bacteria and thermal geological production play a role in the generation of PAHs. The release of PAHs through anthropogenic activity is considered to be from two main routes: (1) anthropogenic sources of PAHs originating from accidental spillages, industrial and domestic wastewater discharges. PAHs originating from such sources are the major contaminants of aquatic environments, or (2) the combustion of materials for supply of industrial energy results in atmospheric discharges. The atmospheric discharge sources can be divided into stationary such as industrial waste incineration, petroleum refinery and gasification plants and the automobile sources (non-stationary) associated with vehicle emissions.

Anthropogenic sources are viewed as the most significant means through which the majority of PAHs are formed and introduced into the environment (Masih & Lal 2014; Sun, K et al. 2014). For instance, many industrial sites such as wood treatment, petroleum refinery, coke production and general manufacturer plants are heavily contaminated with high PAHs content through wastewater discharges, underground tank leaks and frequent use of oil-derivatives. Commonly, atmospheric deposition of PAHs, is widely regarded as a major route by which most volatile PAHs can reached and contaminated areas far away from industrial sites, such as terrestrial, aquatic and marine environments. This has led to wide dispersion of PAHs in places like urban and marine environments with no industrial history (Maliszewska-Kordybach 1999; Wilson & Jones 1993).

In the last few decades, most of the major sources accounting for PAHs present in the environment is believed to be related to a rapid rise in the amount of global industrial oil production, transportations, burning of refuses, gasification and plastic waste incineration. An elevated PAHs concentration may be found in the soil due to release of industrial emissions into the environment as opposed to natural sources(Manzetti 2013).

Table 1.3. Pyrogenic and Petrogenic sources of polycyclic aromatic hydrocarbons (Manzetti 2013) .

Natural Sources	Anthropogenic Sources
Fires - Forest fires, prairie fires and agricultural burning Fossil fuels – coal and crude oil Other Sources - volcanic activities and biosynthesis by bacteria and plants	**Aquatic discharge sources** – accidental spillage and/or leakage of PAH-containing fluids (e.g. waste oil, gasoline, etc.), industrial and domestic wastewaters, urban runoff, discharges originating from landfills and used of Creod pilings for docks and other shoreline structures **Atmospheric discharge source** – **Stationary source:** coal and gas-fired boilers; carbon black, coal tar pitch and asphalt production; coke-ovens, catalytic cracking towers, petroleum refineries and related activities, electrical generating plants, industrial incineration, municipal incinerators, agricultural and refuse burning and any other industry that entails the use of wood, petroleum or coal to generate heat and power. **Non-stationary (or Mobile) source**: automobiles, or other vehicles which use petroleum products as a fuel

1.2.5.2 Fate of PAH in the environment

PAHs interact with mineral and organic substances following entry into the environment. These interactions impact several distribution and transformation processes that control the fate of PAHs in the environment. There are number of processes that PAHs can undergo once deposited in the soil environments (Cerniglia 1993; Sun, L et al. 2014). Figure 1.3 shows a combination of some physical, chemical and biological processes PAHs may be subjected to in soils. PAHs are known to be associated with particulates and are likely to be adsorbed onto soil and sediment due to their hydrophobic property (Cerniglia 1993; Krauss, Wilcke & Zech 2000; Liang, C et al. 2006).

The state of being sorbed on to these substances limits the PAH fractions available for other processes including volatilisation, solubilisation, biodegradation and their mobility in the environment. PAHs may undergo degradation in soil as a result of volatilization, photo-oxidation, chemical oxidation and microbial transformation (Abulencia et al. 2006; Dell'Anno et al. 2012; Gateuille et al. 2014). Although some of these processes are known to affect the fate of PAHs in soil environment, microbial degradation/mineralisation is believed to be one of the most effective routes for PAHs removal. Microbial degradation affects the fate of PAHs in the soil since many species of bacteria and fungi are known to extensively degrade PAHs. PAHs may be utilized as a carbon and energy or fortuitous degradation may occur when alternative carbon sources are supplied.

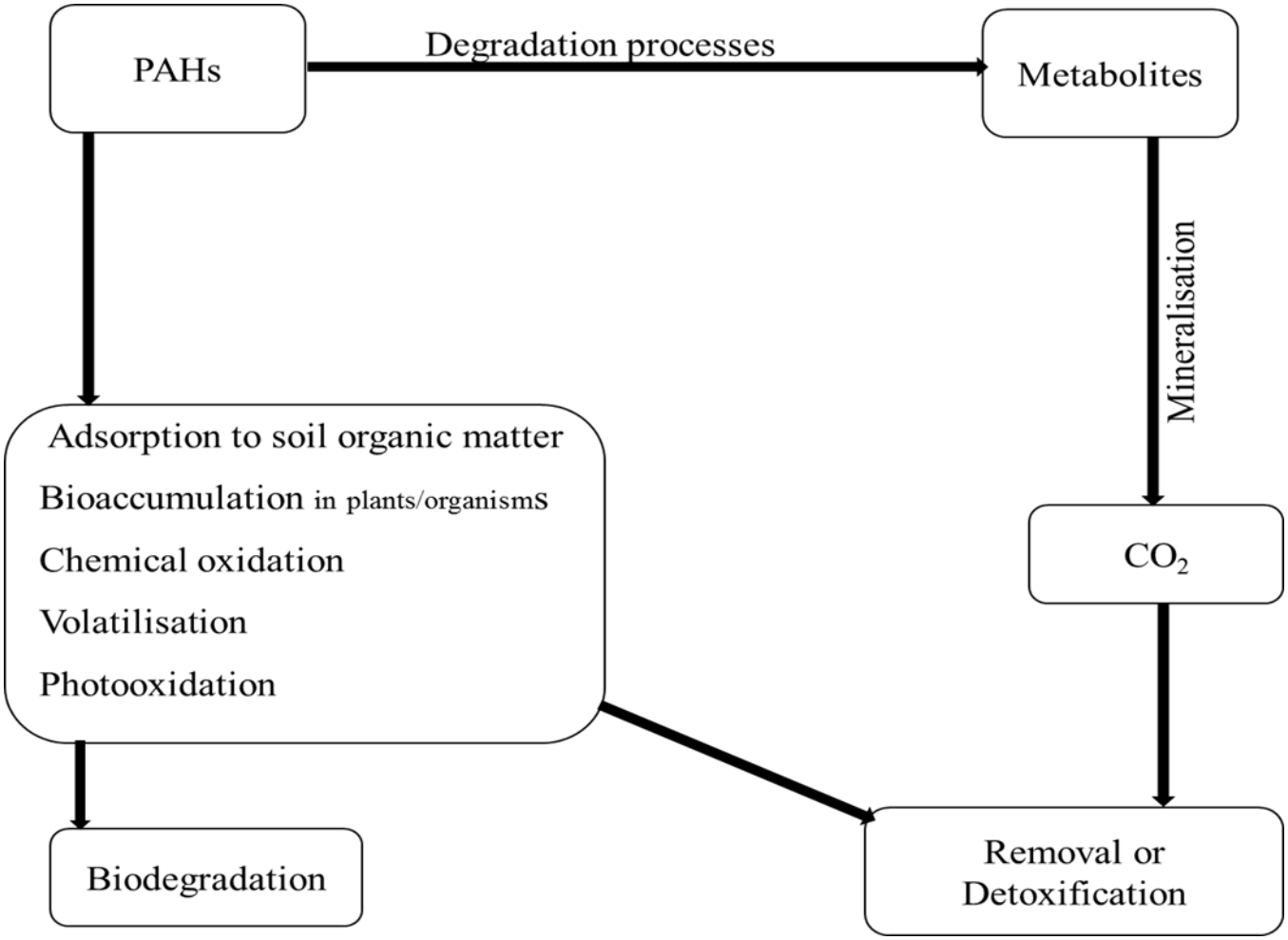

Figure 1.3. A simple schematic diagram demonstrating environmental fate of PAHs modified from (Okere & Semple 2012).

1.2.6 Biodegradation of PAH

1.2.6.1 Bacteria degradation of PAHs

Biodegradation of PAHs by aerobic bacteria encompasses a number of enzymatic reactions. A wide range of bacteria have the capacity to degrade a variety of PAHs (Table 1.4). Most of these organisms have been isolated from PAH contaminated soils. Listed in this Table, are examples of bacteria genera capable of degrading PAH compounds with three (phenanthrene), four (pyrene), and five (B(a)P) aromatic rings. These bacteria utilize PAHs as their sole carbon and energy source except HMW PAHs (compounds with 5 or more rings). The biological metabolism of PAHs by aerobic bacteria is thought to occur through the pathway presented in Figure 1.4 (Bamforth & Singleton 2005). The first step in the metabolism of PAHs is initiated by dioxygenases, in which two oxygen atoms are introduced into the aromatic ring resulting in

the formation of one or more isomeric cis-dihydrodiol metabolites (Cerniglia 1992). In this first part of metabolism, the incorporation of molecular oxygen is necessary for the initial hydroxylation of PAHs. Therefore, the initial aromatic ring oxidation is viewed as the rate-limiting step in the whole process of PAH biodegradation (Cerniglia 1992). Moreover, these dihydrodiols are dehydrogenated to produce dihydroxylated intermediate, which can eventually be metabolized through a catechol compound to carbon dioxide and water.

The oxidation of the catechol compound can occur via two pathways. Firstly, the ortho pathway, which involves the split of bond between carbon atoms of the two hydroxyl groups leading to cis, cis-muconic acid. Secondly, via the meta pathway, whereby another division of the bonds between a carbon atom with a hydroxyl group and the adjacent carbon atom with a hydroxyl group yielding 2-hydroymuconic semialdehyde (Figure. 1.4).

Several other by-products including succinic, fumaric, pyruvic, acetic acids, and aldehydes are generated as the consequence of the aromatic ring cleavage. All by-products generated via these reactions are utilised by microorganisms as synthesis materials to produce cellular constituents and energy. For example, the final by-products generated through cleavage pathways (oxidation) including the pyruvic, succinic and fumaric acids can be catabolized in the citric acid cycle (Peixoto, Vermelho & Rosado 2011). The catabolism reactions in the citric acid cycle are catalysed by another set of multicomponent enzymes such as fumarase, succinic, and pyruvate dehydrogenases to degrade hydrocarbons fully to carbon dioxide as the final end-product.

1.2.6.2 Fungal degradation of PAHs

Unlike bacteria, fungi are less diverse in nature and at the same time difficult to be cultured. However, fungi are equally important, considering their metabolic potential to degrade HMW PAHs. Numerous genera of fungi species with catabolic capacity to degrade three, four and five aromatic rings have been isolated in hydrocarbon contaminated environments (Table 1.5). Fungi do not use PAHs as sole sources of carbon and energy, but instead they use co-metabolism as an alternative route for PAH biodegradation (Bishnoi, Kumar & Bishnoi 2008; Cerniglia 1997; Das, Royer & Leff 2007; Sinha et al. 2010). There are two fundamental mechanisms whereby fungi metabolise PAHs as shown in the proposed pathway of fungi biodegradation of PAHs (Figure 1.5). These two mechanisms involve ring oxidation via (I)

lignin and manganese peroxide (lignonlytic degradation) (II) cytochrome P_{450} monoxygenase (non-lignolytic degradation) enzymes.

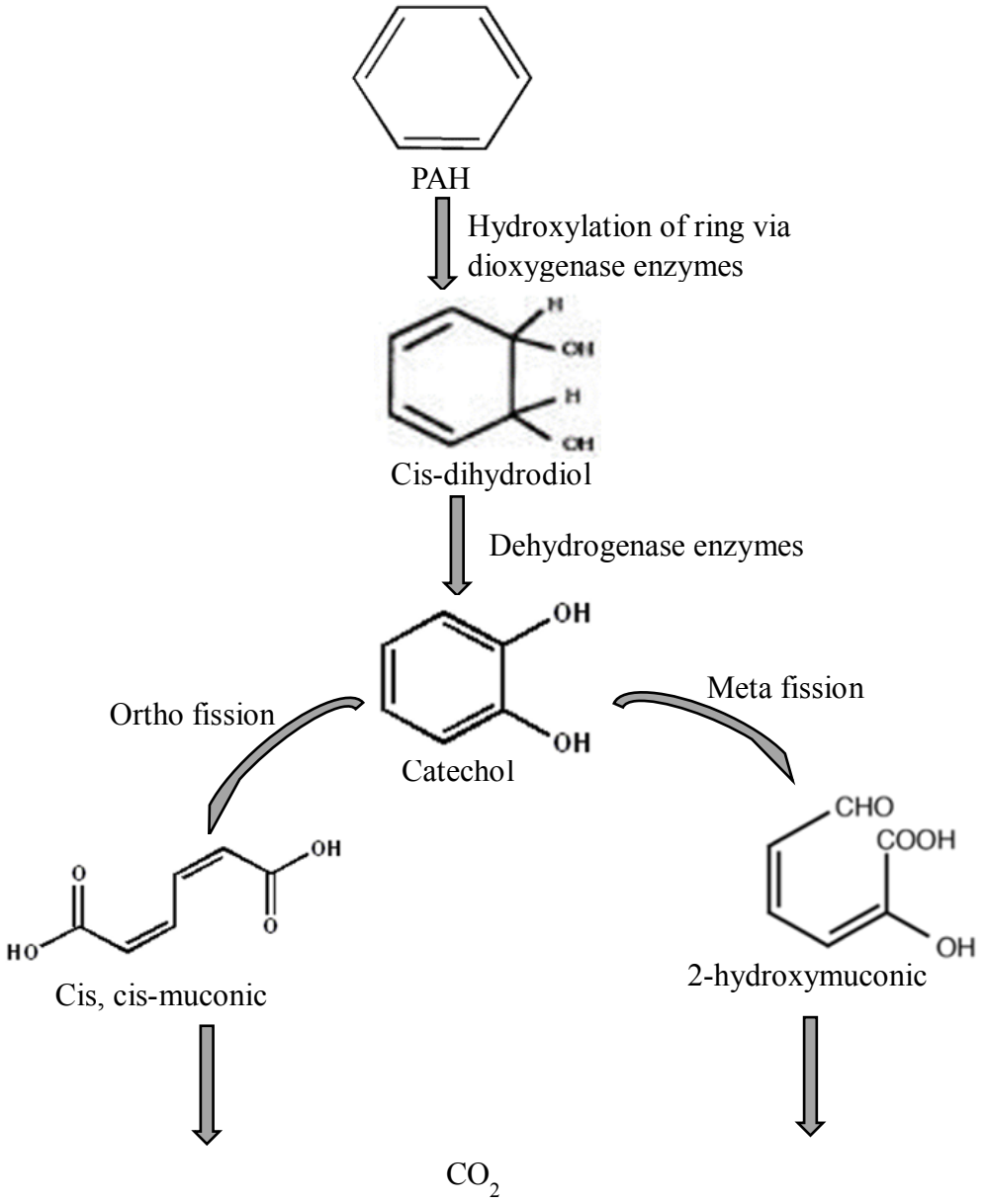

Figure 1.4. The main pathway for polycyclic aromatic hydrocarbon degradation by bacteria adapted from (Bamforth & Singleton 2005).

Table 1.4. Polycyclic aromatic hydrocarbons oxidised by difference species of bacteria adapted from Juhasz and Naidu (2000)

Compound	Ring #	Microorganisms	Reference
Phenanthrene	3	*Aeromonas sp., Alcaligenes faecalis, Alcaligenes denitrificans, Arthrobacter polychromogenes, Beijernickia sp., Micrococcus sp., Mycobacterium sp., Pseudomonas putida, Sphingomonas paucimobilis, Rhodococcus sp., Vibrio sp., Nocardia sp., Flavobacterium sp., Streptomyces sp., Streptomyces griseus, Acinetobacter sp., Pseudomonas aeruginosa, Pseudomonas stutzeri, Pseudomonas saccharophila, Stenotrophomonas maltophilia, Cycloclasticus sp., Pseudomonas uorescens, Acinetobacter, calcoaceticus, Acidovorax delafieldii, Gordona sp., Sphingomonas sp., Comamonas testosteroni, Cycloclasticus pugetii, Sphingomonas yanoikuyae, Agrobacterium sp., Bacillus sp., Burkholderia sp., Sphingomonas sp., Pseudomonas sp., Rhodotorula glutinis, Nocardioides sp., Flavobacterium gondwanense, Halomonas meridiana*	Argumedo-Delira et al., 2012, Cébron et al., 2011, Ling et al., 2011, Ruberto et al., 2006, Zhao et al., 2009b, Zhao et al., 2009a, Bamforth and Singleton, 2005, Bodour et al., 2003, Anokhina et al., 2004, Habe and Omori, 2003, Shi et al., 2001, Dagher et al., 1997, Vinas et al., 2002, Chen et al., 2008, Li et al., 2014b, Schippers et al., 2000, Kasai et al., 2005, Fischer et al., 2008, Sun et al., 2014a, Zafra et al., 2014, Sawulski et al., 2015, Hansel et al., 2008, Juhasz and Naidu, 2000, Churchill et al., 1999, Lü et al., 2003, Iwabuchi and Harayama, 1997, Andersson et al., 2000, Bell et al., 2013, Borràs et al., 2010, Dell'Anno et al., 2012, Díaz, 2010, Mao et al., 2012, Taccari et al., 2012, Tian et al., 2008, Vinas et al., 2005, Yu et al., 2005b
Pyrene	4	*Alcaligenes denitrificans, Mycobacterium sp., Rhodococcus sp., betaproteobacterium, Sphingomonas paucim obilis, Stenotrophomonas maltophilia, Acinetobacter calcoaceticus, Gordona sp., Sphingomonas sp., Pseudomonas putida, Burkholderia cepacia, Pseudomonas saccharophilia, Mycobacterium gilvum, Leclercia adecarboxylata, Mycobacterium pyrenivorans*	Argumedo-Delira et al., 2012, Cheung and Kinkle, 2001, Kotterman et al., 1998, Liang et al., 2006b, Ling et al., 2011, Sho et al., 2004, Singleton et al., 2012, Sun et al., 2014a, Borràs et al., 2010, Sawulski et al., 2015, Hansel et al., 2008, Churchill et al., 1999, Boonchan et al., 2000, Díaz, 2010
B(a)P	5	*Beijernickia sp., Mycobacterium sp., Sphingomonas paucimobilis, Burkholderia cepacia, Pseudomonas, saccharophila, Stenotrophonmonas maltophila, Rhodococcus sp.UW1, Pseudomonas sp, Agrobacterium tumefaciens, Bacillus sp.*	Argumedo-Delira et al., 2012, Samanta et al., 2002, Kanaly et al., 2000, Watanabe, 2001, Silva et al., 2009, Wu et al., 2008, Johnsen et al., 2005, Isaac et al., 2015, Waszak et al., 2015, Zhang et al., 2006, Liu et al., 2004, Bamforth and Singleton, 2005, Sawulski et al., 2015

In the first part of fungal biodegradation, PAH metabolism is mediated by lignin peroxidase, manganese peroxidase enzymes (LiP& MnP) and laccase, which can oxidize PAHs leading to the generation of PAH-quinones, the main metabolite of lignolytic oxidation for white rot fungi. The white rot fungi, among the group of organisms responsible for the production of extracellular enzymes have been extensively studied (Cerniglia 1997; Kotterman, Vis & Field 1998; Lladó, S. et al. 2013; Lundstedt 2003; Sette, de Oliveira & Rodrigues 2008). In the second mechanism of fungal biodegradation, PAH oxidation occurs via cytochrome P-450 systems and monoxygenase enzymes catalyzed reactions, producing an arene oxide as the intermediate oxidation product (Figure 1.5). The arene oxide can either be converted to phenol via non-enzyme rearrangement or subjected to hydration to form trans-didydrodiols (catalyzed by Epoxide hydrolase).

According to (Bezalel, Hadar & Cerniglia 1997), the utilisation of lignolytic fungi have demonstrated that many PAHs may be completely mineralised by combining ligninolytic enzymes, cytochrome P450 monoxygenases, and epoxide hydrolases. In such a combination, the cytochrome P450 monoxygenase system has been shown to play a crucial role in the initial oxidation of high molecular weight PAHs such as pyrene and B(a)P by *P. ostreatus.* However, one essential mechanism of fungi biodegradation is the ability of several fungi species (consortium) to co-metabolize high molecular weight PAHs (Balaji, Arulazhagan & Ebenezer 2014; Cerniglia 1997). It has been showed that the ecological interaction of a number of fungal organisms, in a form of mixed cultures or consortium function well than individual organism.

A number of research works have been dedicated towards understanding the collective roles played by microbial consortia in the degradation of HMW PAHs (Boonchan, Britz & Stanley 2000; Kotterman, Vis & Field 1998; Leštan & Lamar 1996; Qian & Chen 2012). A mixed consortia (fungi) have been reported to produce better high molecular weight PAH removal than individual isolates (Trzesicka-Mlynarz & Ward 1995).Their results suggested that the power of complimentary enzymatic ability found in the mixed consortia outweighed that of individual isolates degradability. Hence, ecological interaction of fungi is of a particular benefit in the fungal metabolism of high molecular weight PAHs.

Table 1.5. Polycyclic aromatic hydrocarbons oxidized by difference species of fungi adapted from Juhasz and Naidu (2000).

Compound	Ring #	Microorganisms	Reference
Phenanthrene	3	*Caenorhabditis elegans, Phanerochaete chrysosporium, Pomphorhynchus laevis, Pleurotus ostreatus, Tinea versicolor, Bjerkandera adjusta, Pleurotus ostreatus, Cylindrocladium simplex, Monosporium olivaceum, Curvularia lunata, Curvularia tuberculata, Laetiporus sulphureus, Daedaela quercina, Flamulina velutipes, marasmiellus sp., Penicullium sp., Kuehneromyces mutabilis, Laetiporus sulphureus, Agrocybe aegerita, Aspergillus niger, Syncephalastrum racemosum*	Andersson et al. 2000, Argumedo-Delira et al. 2012, Balaji et al.2014, Bishnoi et al.2008, Cerniglia and Yang 1984, Cerniglia et al. 1989, Morgan et al. 1991, Sutherland et al. 1991, Bumpus 1989, Hammel et al. 1992, Bezalel et al. 1996, Brodkorb and Legge 1992, Schutzendubel et al. 1999, Lisowska and Dlugonski 1999, Bogan and Lamar 1996, Sack and Gunther 1993, Collins and Dobson 1996, Casillas et al. 1996, Sutherland et al. 1993
Pyrene	4	*Caenorhabditis elegans, Phanerochaete chrysosporium, Penicillium sp., Penicillium janthinellum, Penicillium glabrum, Pleurotus ostreatus, Syncephalastrum racemosum, Bjerkandera adjusta, Pleurotus sp., Dichomitus squalens, Flammulina velutipe, Trammetes versicolor, Kuehneromyces mutabilis, Laetiporus sulphureus, Agrocybe aegerita*	Bogan et al. 1995, Cebron et al. 2013, Cobas et al. 2013, DeAngelis et al. 2011, Dixit et al. 2011, Cerniglia et al. 1986, Majcherczyk et al. 1998, Launen et al. 1995, Bezelel et al. 1996, Schutzendubel et al. 1999, Martens and Zadrazil 1998, Sack et al. 1997b, Wunder et al. 1997, Sack and Fritsche 1997, Lang et al. 1996, Stanley et al. 1999, Boonchan 1998, Mancera-Lopez et al. 2008
B(a)P	5	*Phanerochaete chrysosporium, Pycnoponus cinnabarinus, Trametes versicolor, Bjerkandera sp. strain BOS55, Nematoloma frowardii, Selenastrum capricornutum*	Duan et al. 2015, Sayara et al. 2011, Reyes-Cesar et al. 2014, Sack et al. 1997b, Sanglard et al. 1986, Rama et al. 1998, Majcherczyk et al. 1998, Kottermann et al. 1998, Qian and Chen 2012, Mancera-Lopez et al. 2008, Liu et al. 2004

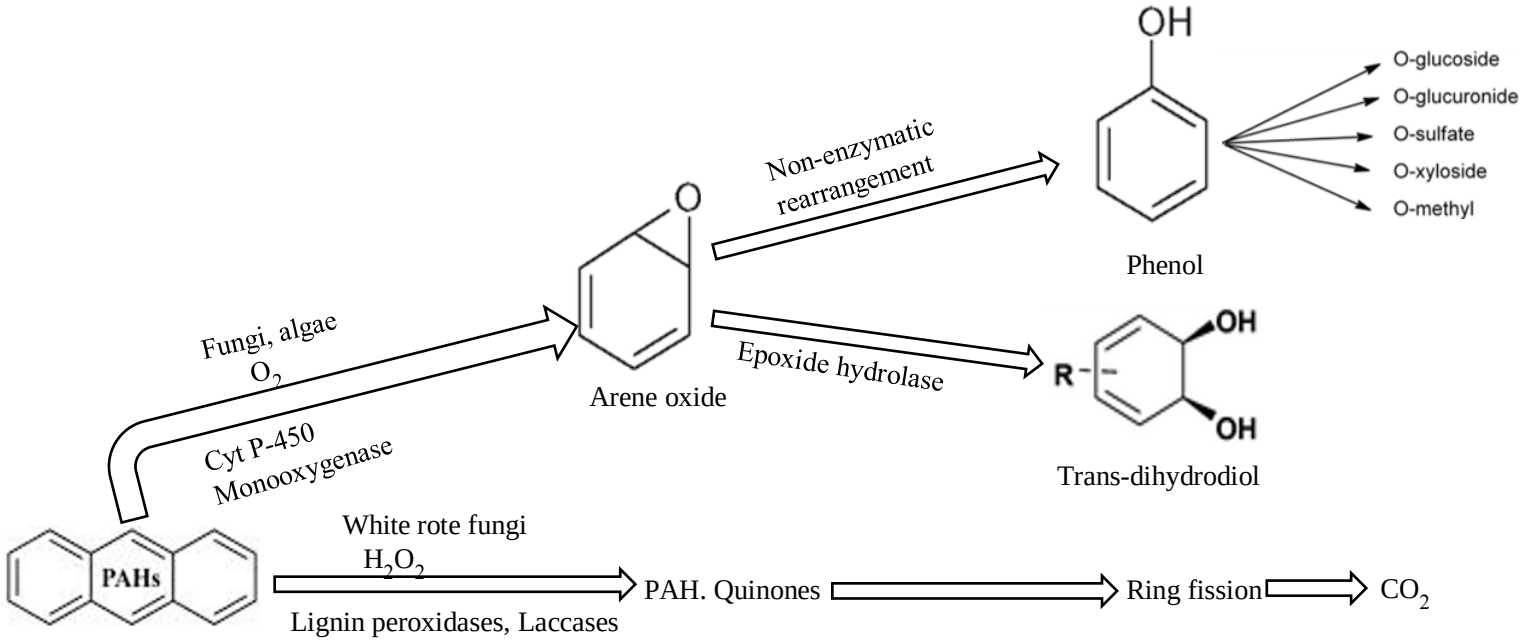

Figure 1.5. The main pathway for polycyclic aromatic hydrocarbon degradation by fungi adapted from (Bamforth & Singleton 2005).

1.2.6.3 Phenanthrene degradation

By definition, phenanthrene is one of the 16 PAH recognized priority pollutants composed of three benzene rings. It has been used in numerous studies as a model compound for LMW PAH biodegradation (Roy, Khara & Dutta 2012; Ruberto et al. 2006). Figure 1.6 describes proposed catabolic degradation pathways of phenanthrene by bacteria. Initially phenanthrene is oxidized at positions 1,2 and 3,4 to form cis-1,2-diydrox-1,2-diydrophenanthrene which is followed by meta-cleavage of phenanthrene-cis-3,4-dihydrodiol leading to the formation of 3,4-dihydroxyphenanthrene. The next step involves the oxidation of the metabolite from the previous step (meta-cleavage) resulting in the formation of hyroxy-2-naphthoic acid. Subsequently, the hydroxy-2-naphthoic acid is decarboxylated under oxidative conditions to form 1, 2-dihydroxy naphthalene which is eventually converted to salicylic acid following exposure to meta-cleavage pathway (Ruberto et al. 2006; Yu, S et al. 2005; Zhao et al. 2009). Numerous bacteria have been identified with catabolic capacity to degrade phenanthrene as listed in Table 1.5.

1.2.6.4 Pyrene degradation

Pyrene is one of the 16 PAHs defined by USEPA as a priority pollutant, composed of 4-ring polycyclic aromatic compound. It is often used as a model substrate when studying biodegradation of HMW-PAHs since its structure resembles other carcinogenic compounds. Figure 1.7 shows proposed catabolic pathways for pyrene degradation. Bacterial and fungal degradation of pyrene have been repeatedly documented by several researchers with many microorganisms identified as depicted in Tables 1.5 and 1.6 (Cheung & Kinkle 2001; Mrozik & Labuzek 2003). Other researchers have suggested that pyrene can be utilised as a carbon and energy source by PAH-degrading bacteria (Heitkamp, Franklin & Cerniglia 1988; Juhasz & Naidu 2000; Liang, Y et al. 2006).

These studies have shown pyrene degradation to be occurring predominantly via deoxygenation and monooxygenation, a reaction usually catalyzed by dioxygenase and monooxygenase at 4,5 positions yielding cis-4,5-dihydroxy-4,5-dihydropyrene and trans-4,5-dihydroxy-4,5-dihydropyrene respectively. The formation of cis- and trans-4,5-dihydroxy-4,5-dihydropyrene indicated that multiple pathways may be associated with the initial pyrene oxidative attack, in which both monooxygenase and dioxygenase are key enzymes (Figure 1.7). Subsequent metabolism of the degradation products result in ring fission products including

phenanthrene 4,5-dicarboxylic acid, 6,6'-dihydroxy-2,2'-biphenyl dicarboxylic acid, phenanthrene 4-carboxylic acid and phthalic acid.

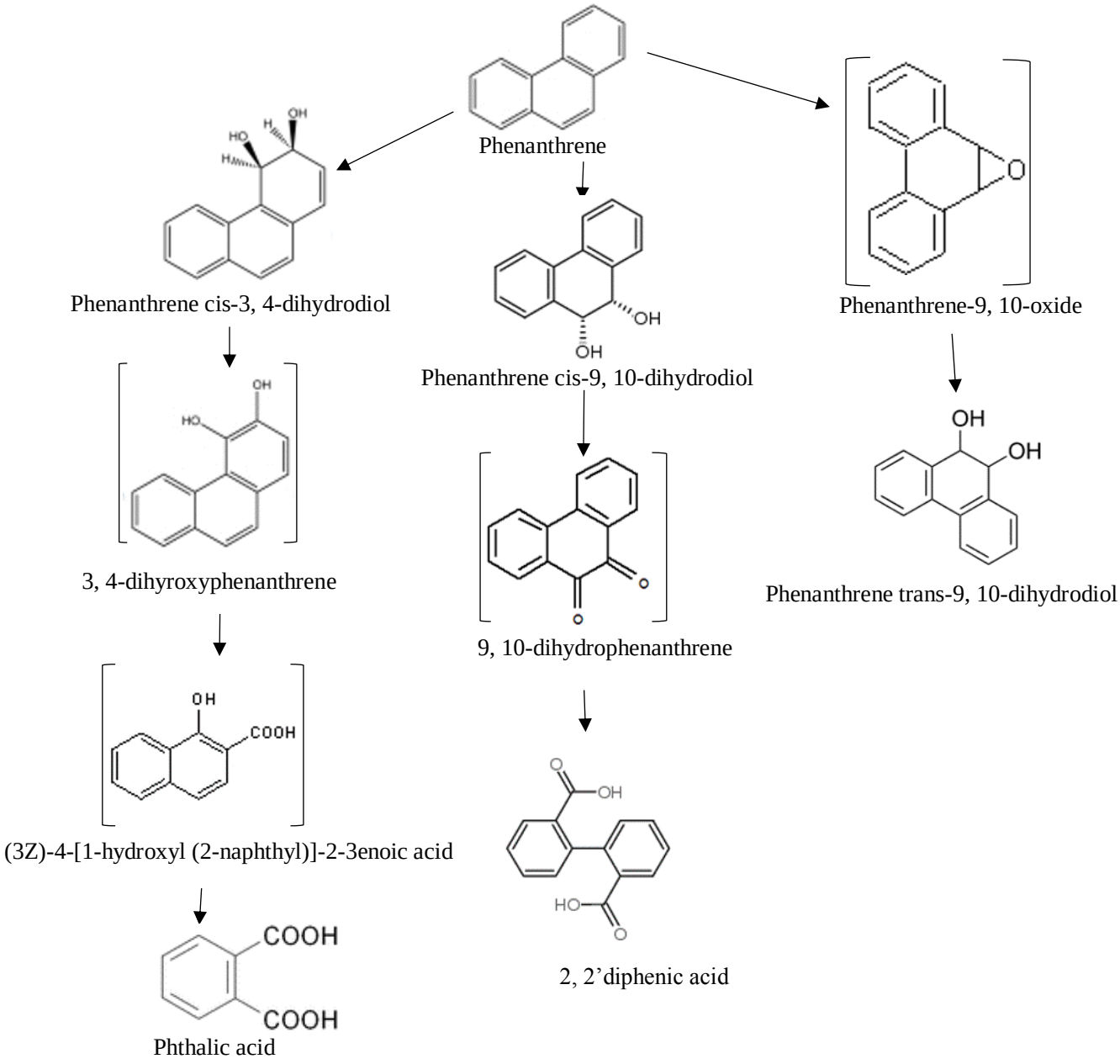

Figure 1.6. Proposed pathway for the degradation of phenanthrene by bacteria (Ghosal et al. 2010).

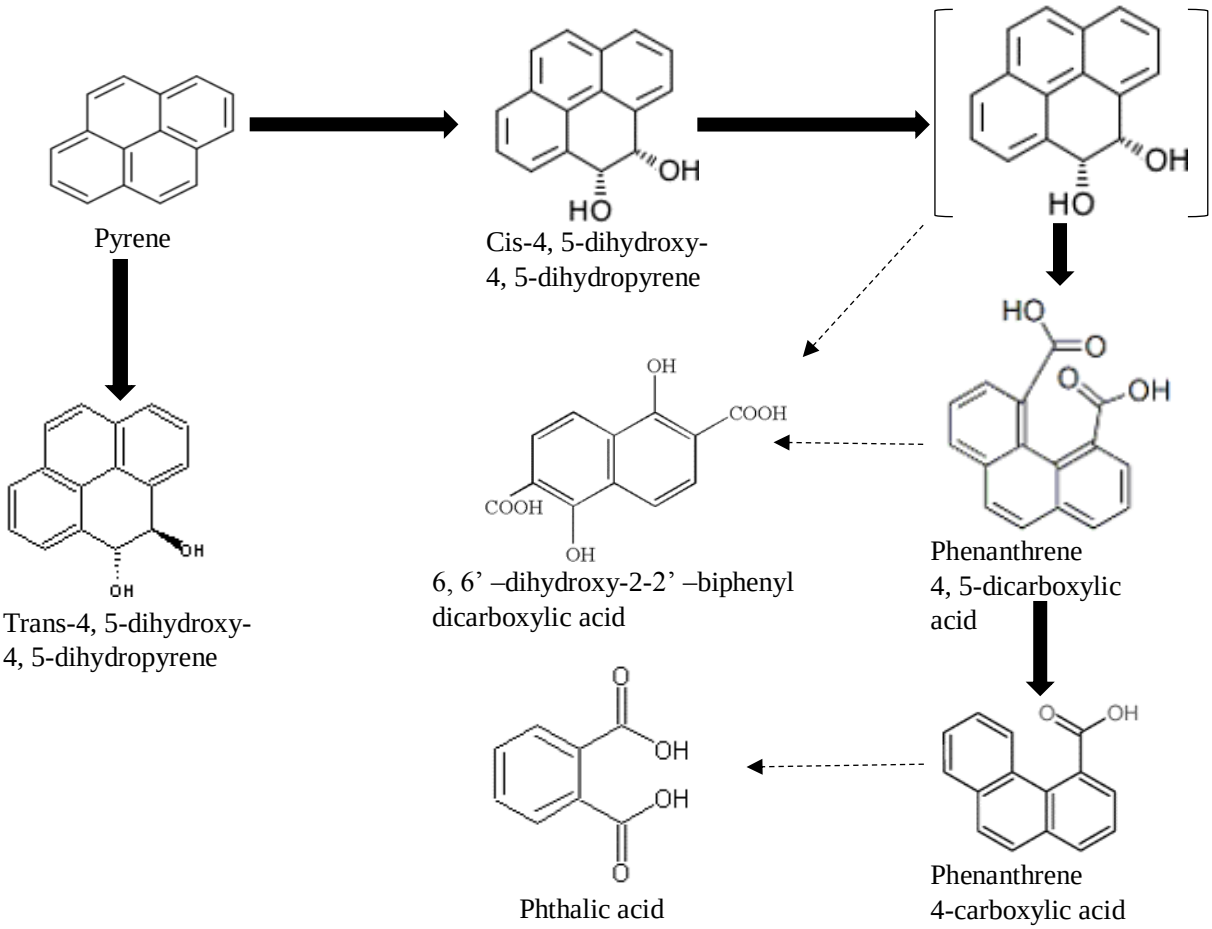

Figure 1.7. Proposed catabolic pathways of pyrene degradation by bacteria (Mrozik & Labuzek 2003).

1.2.6.5 Benzo(a)pyrene degradation

Benzo(a)pyrene is one of the 16 PAHs defined by USEPA as a priority pollutant. The compound is a 5-ring polycyclic aromatic compound (Figure 1.8 and classified as a potential carcinogenic compound to humans based on animal tests (Li, G-l et al. 2014; Manzetti 2013; Waszak et al. 2015). Similar enzymes involved in the degradation of pyrene also catalyzed metabolism of B(a)P as described in the previous section. Figure 1.8 shows proposed catabolic pathways for B(a)P metabolism. B(a)P degradation by bacteria are initiated by both mono- and di- oxygenation at 4,5-, 7,8-, and 9,10- carbon positions. The initial attack on the B(a)P molecule by the aforementioned enzymes leads to the formation of either cis-4,5-benzo(a)pyrene-dihydrdiol, cis-7,8-benzo(a)pyrne-dihydrodiol, and 9,10-benzo(a)pyrene-dihydrodiol as intermediate products. These products (dihydrodiols) undergo either dehydration or oxidative cleavage to produce 4,5-chyresene-carboxylic acid, cis-4-(8-hydroxypyrene-7-yl)-2-oxobut-3-enoic acid, cis-4-(7-hydroxypyren-8-yl)-2-oxobut-3-enoic acid, which are then decarboxylated to form polycyclic aromatic acids such as 7,8-dihydro-

pyrene-7-carboxylic and 7,8-dihydro-pyrene-8-carboxylic acids. *Mycobacterium vanbaalenii* PYR-1 had been showed to metabolise B(a)P through monooxygenase and dioxygenase mechanisms according to several studies (Jain 2014; Liu et al. 2004; Qian & Chen 2012; Waszak et al. 2015). Some studies have suggested that metabolites formed as a result of B(a)P degradation may further inhibit B(a)P metabolism (Kotterman, Vis & Field 1998; Peng et al. 2008; Silva et al. 2009).

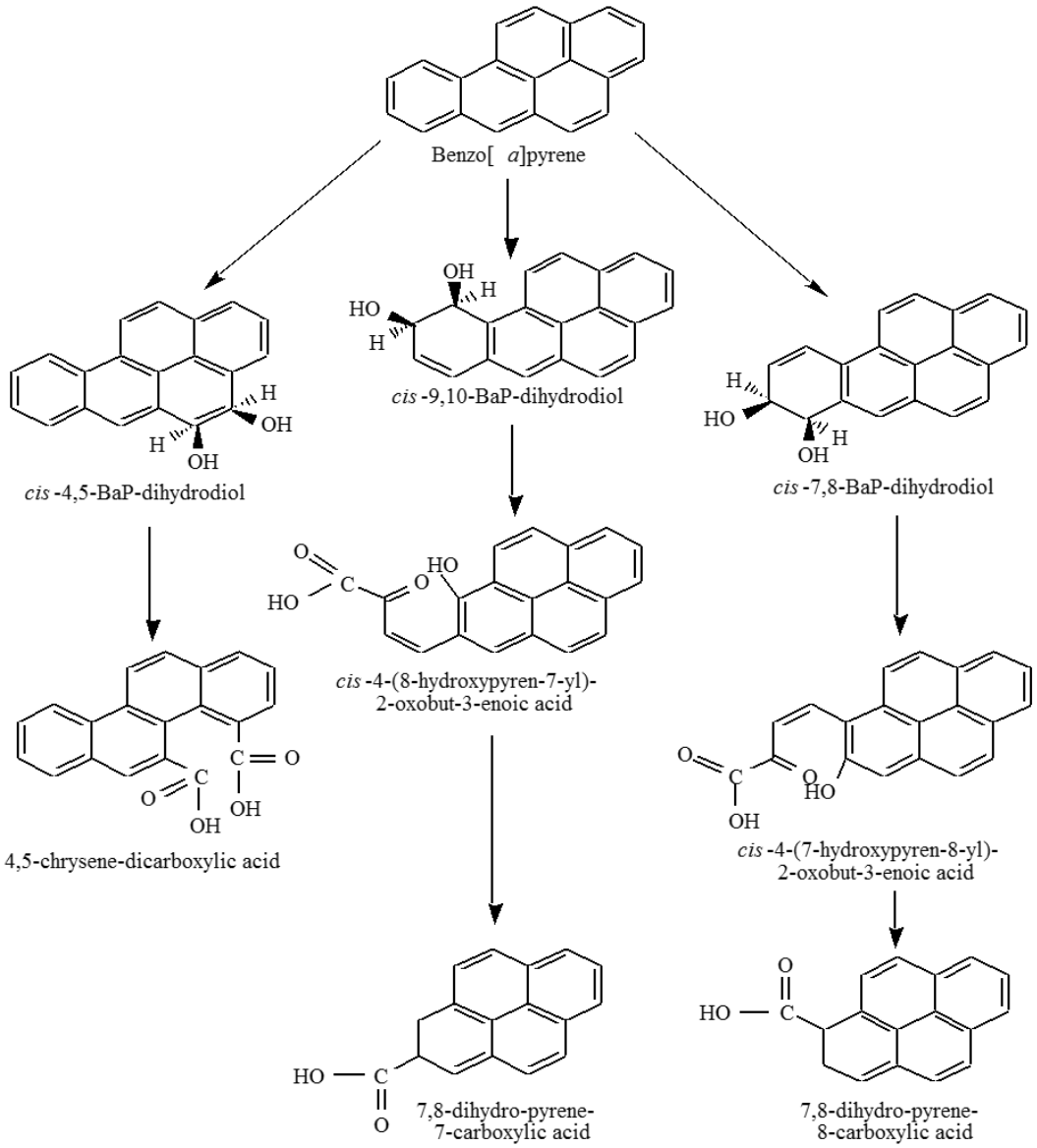

Figure 1.8. Proposed catabolic pathways of B(a)P degradation by bacteria adapted from (Juhasz & Naidu 2000).

1.3 Bioremediation of PAHs

A potential strategy for reducing the environmental impact of PAH contamination is through bioremediation; a technology which is considered cost effective and environmentally friendly (Robles-González, Fava & Poggi-Varaldo 2008). In this strategy, naturally occurring microorganisms have been shown to play a crucial role by utilizing a wide range of contaminants as a source of energy or to transform them into less toxic compounds. The success of bioremediation relies on site specific conditions, e.g. soil properties at the site and the presence of microbial consortia with catabolic potential to degrade the target contaminant (Brennerova et al. 2009). The most commonly applied bioremediation strategy is natural attenuation (NA). It is a favourable strategy because it requires limited human intervention, in terms of capital and management. However, the time it takes to reach an acceptable bioremediation endpoint may be lengthy depending on site conditions. As a consequence, other bioremediation strategies may be applied for site clean-up by stimulating native microorganisms through the addition of nutrients (enhanced natural attenuation) or alternatively, by introducing exogenous PAH degrading bacteria (bioaugmentation) to increase the rate of degradation (Singh et al., 2011*)*.

Bioremediation is currently recognized as an attractive strategy to decontaminate PAH polluted environments. To some extent, it is preferable to physical and chemical treatments *(*Margesin and Schinner, 2001*)* since its application may; (i) result in the mineralization of the contaminant, (ii) reduce the cost of cleaning up, (iii) not result in a redistribution of contaminants (iv), and result in minimal disturbance to the biosphere (Miyasaka et al., 2006 and Vidali 2001). The effectiveness of bioremediation relies on the applicability of a given clean-up technology, alongside the availability of several other factors deemed as biodegradability (carbon, nutrients, oxygen etc) limiting agents and the capacity of the microorganisms to degrade the contaminants of interest (Desai, Pathak & Madamwar 2010; Macbeth et al. 2004; Megharaj et al. 2011). Biodegradation may be performed either in situ or ex-situ, depending on the contaminated site. In situ bioremediation is a strategy where by treatments are performed on the site with a stimulation of intrinsic microbes to carry out microbial remediation. In contrast to in situ remediation, ex-situ bioremediation involves excavation of contaminated materials followed by treatments operated in a contained facility thereafter. The success of each approach is determined by the suitability of site conditions, indigenous catabolic capacity, and whether it is appropriate to use nutrients to enhance the biodegradation process (Table 1.6).

The majority of research on bioremediation has utilized three main mechanisms of bioremediation, namely: (I) natural attenuation (NA) which relies on the ability of native microorganisms to attenuate pollutants in their surroundings under natural conditions, (II) enhanced natural attenuation (ENA) is the process through which the catabolic capacity of indigenous microorganisms is stimulated by supplying nutrients, electron donors or acceptors to effectively carry out biodegradation by overcoming constrains encountered in natural attenuation and (III) bioaugmentation that involves provision of extra exogenous microbial populations with a proven catabolic ability to supplement the activities of existing populations with an intention of hastening the degradation process.

1.3.1 Natural attenuation

Natural attenuation or intrinsic biodegradation of contaminants has been in used long before engineered bioremediation. NA takes advantage of both destructive and nondestructive mechanisms. Findings from several investigations have shown NA to be the first option for low-risk fuel contaminated sites or it could be employed in the final phase after active remediation mechanisms have mitigated contaminant concentrations to moderate levels (Margesin and Schinner. 2001, Sakar et al., 2004, Katsivela et al., 2005, and Roling & Van Verserveld, 2002*)*.

Nonetheless, the success of NA is influenced by specific conditions on the site, the indigenous population of microflora, the type, magnitude, and the toxicity of pollutants (Megharaj et al. 2011; Mills et al. 2003). Wilson et al., (1993) identified that NA is publicly accepted as a realistic strategy to clean-up contaminated site due to its noninvasiveness, thereby avoiding land disruption and human exposure as a consequence of excavation and transportation.

In some cases, application of NA is considered as effective as the other bioremediation strategies. Mills et al. (2003) reported more than 95% petroleum hydrocarbon concentration removal under NA during an 11-month period of bioremediation following the 1994 San Jacinto River oil spill in Southeast Texas. The authors concluded that rapid removal of hydrocarbons from contaminated sediments was as a result of acclimation of native microorganisms due to prior hydrocarbon exposure.

Table 1.6. Summary of the advantages and disadvantages of bioremediation technologies (Vidali 2001).

Technology	Examples	Benefits	Limitations	Factors to consider
In situ	In situ bioremediation Biosparging Bioventing Bioaugmentation	Most cost efficient Noninvasive Relatively Passive Natural attenuation Processes Treats soil and water	Environmental constraint Extended treatment time Monitoring difficulties	Biodegradative abilities of indigenous microorganisms Presence of metals and other inorganics Environmental parameters Biodegradability of pollutants Chemical solubility Geological factors Distribution of pollutants
Ex situ	Land farming Composting Biopiles	Cost efficient Low cost Can be done on site	Space requirements extended treatment time Need to control abiotic loss Mass transfer problem Bioavailability limitation	See above
Bioreactors	Slurry reactors Aqueous reactors	Rapid degradation kinetic Optimized environmental parameters Enhances mass transfer Effective use of inoculants and surfactants	Soil requires excavation Relatively high cost capital Relatively high operating cost	See above. Bioaugmentation Toxicity of amendments Toxic concentrations of contaminants

In another study conducted over a period of 42 days a NA strategy achieved 17% PAH removal (from 1212 mg/kg to 1003 ± 2 mg/kg) in creosote contaminated soil (García-Delgado, Alfaro-Barta & Eymar 2015). In a recent investigation, Makadia et al. (2011) reported high reduction (>80%) in the total petroleum hydrocarbon concentration in NA microcosm conducted using previously remediated soil spiked with waste oil sludge during an 84-day incubation period. There was no significant improvement observed in the removal of TPH when ENA and BioAu or the combination of these two strategies was implemented over a similar time frame. In contrast, other researchers have reported that NA is ineffective at removing PAHs from contaminated soil.

1.3.2 Enhanced natural attenuation

Natural attenuation may be limited or fail in cases where one of the four biodegradation-limiting factors are not available(Yu, K et al. 2005). The act of accelerating NA by enhancing the activities of a microbial community through the addition of nutrients in the form of N and P and the modulation of temperature, and oxygen levels is known as ENA. The use of this strategy is accepted and supported by both regulators and the general public. Several researchers have reported supplementation of contaminated soil to increase the degradability of PAHs by indigenous microorganisms (Lladó, S. et al. 2013; Patil et al. 2014; Tyagi, da Fonseca & de Carvalho 2011; Yu, K et al. 2005). For example, addition of nutrient (mineral salts medium) to amend mangrove sediments contaminated with PAHs and additionally spiked with a mixture of PAHs, namely fluorene, phenanthrene and pyrene, achieved 98% degradation of the initial concentration (1000 mg l^{-1} each) for each compound at the end of a 4 week incubation period.

Similarly, García-Delgado et al. (2014) reported that the addition of sterile spent *Agaricus bisporus substrate* (SSAS) successfully stimulated soil bacteria to degrade 3-ring PAHs, with a statistical significant reduction observed in all tested compounds ($p < 0.05$). In this study, three lower molecular weight PAHs were significantly degraded with 75, 90 and 52% removal observed in the concentration of fluorene, phenanthrene and fluoranthene observed respectively. Contrary to these findings, the adoption of the ENA strategy did not influence degradation of hydrocarbon in one of the bioremediation experiments, conducted by Makadia et al. (2011) re-using previously remediated hydrocarbon contaminated soils but spiked with waste oil sludge.

1.3.3 Bioaugmentation

Bioremediation is often hindered by the site's biological constraints, such as the presence and activity of PAH degrading bacteria *(*Juhasz and Naidu, 2005 and Vogel, 1996). An option to overcome biological constraints (activation of indigenous microbes) is to supplement the local microbial population with known PAH degrading strains (Vogel, 1996 and Robles-Gonzalez et al., 2008*)*. This process of introducing specific strains to enhance biological activities of local microbial communities is known as bioaugmentation (Jacques et al., 2007 and Rogers et al., 2011).

Bioaugmentation, however, suffers from some difficulties including the inability of strains to adapt to their new environments, stress encountered as a result of pollutant toxicity (Vogel, 1996). Despite these disadvantages, some promising results have been achieved through the application of bioaugmentation in PAH contaminated sites (Bamforth & Singleton 2005; Bento et al. 2005; Hamdi et al. 2007; Lladó, S et al. 2013; Megharaj et al. 2011; Seo, Keum & Li 2009). For example, Hamdi et al. (2007) reported high PAH degradation rates (>96% for both anthacene and pyrene after 120 days), when a spiked soil with anthaccne, pyrene and benzo(a)pyrene (3000 mg sum of 3PAHs kg^{-1}) was bioaugmented by adding aged PAH-contaminated soil containing activated indigenous degraders (degradation rates of 33-63%).

In a recent review, Megharaj et al. (2011) reported that a failure of bioaugmentation is often encountered as a consequence of inefficiency, inadaptability and incompetent of strains. This explains why bioaugmented strains are less competitive compared to indigenous microbes. For bioaugmentation to be effective, it is wise to consider isolating naturally occurring microorganisms to be used in an inoculation from the contaminated site intended for their applications. Seeding back pure microbial cultures after enrichment to their locality of origin (contaminated site) have proven to be successful as these cultures are in the position to fit in well compare to cultures brought in from other places (Kauppi et al., 2011).

1.3.4 Factors influence bioremediation

Bioremediation of contaminated soil may be viewed as more effective and low-cost associated remedial technology to decontaminant a polluted environment with PAHs. However, the effectiveness of bioremediation depends on several factors including physio-chemical characteristics of the PAH, present of a microbial population with catabolic capacity to degrade PAHs, and environmental factors such as pH, temperature, nutrients, salinity, oxygen, and moisture contents (Mohan et al. 2006; Tyagi, da Fonseca & de Carvalho 2011; Vidali 2001). According to Vidali (2001), microbial metabolic activity and growth during bioremediation are readily influenced by a number of soil parameters including those outlined in Table 1.7.

Table 1.7. Factors influencing the bioremediation of PAHs in contaminated soils.

Factors	Influence on bioremediation	Optimum value	Reference
Moisture content	Microbial activity	40 - 60%	Vidali, 2001
pH	Microbial activity Mass transfer Metabolism rate	5.6 - 8	Sayara et al., 2011
Nutrient content	Cellular metabolism	C: N: P = 100:10:1	Cebron et al., 2013
Temperature	Microbial activity Mass transfer Contaminant solubility	20 - 30	Weiss et al., 1973
Contaminants (PAHs)	Bioavailability Mass transfer Microbial metabolism rate	5 - 10% of dry weight of soil	Krauss et al., 2000 Malish et al.,2014
Soil type	Contaminant solubility Mass transfer Microbial metabolism rate	Low clay or silt content	Manzetti et al., 2013
Electron acceptor	Mass transfer Microbial metabolism rate	10 - 40% of O_2	Thion et al., 2013 Juhasz and Naidu ,2000

1.4 Bioavailability

According to Semple et al. (2003), soil serves as an important sink for PAHs in the environment. PAHs enter the soil mostly by accidental spillage, underground tank leakage, intention application, and through atmospheric deposition. When PAHs enter the environment, they bind to minerals and organic carbon through physical and chemical interactions. In the natural environment (soil), PAHs have been thought to undergo a number of processes including leaching into groundwater(Ahangar 2010), absorption to soil organic matter (Reid, Jones & Semple 2000), sequestration (sorption & diffusion)(Peng et al. 2008), biodegradation (Reid, Jones & Semple 2000), bioaccumulation (Sijm, Kraaij & Belfroid 2000), and volatilization (McElroy, Farrington & Teal 1989) as demonstrated in Figure 1.3. The nature of

these interactions is the key factor in determining the fate and behaviour of PAHs in the soil and sediments (Ahangar 2010; Semple et al. 2004; Semple, Morriss & Paton 2003). PAH bioavailability decreases with the amount of time they remained in contact with the soil (Reid, Jones & Semple 2000).

This process has been described as 'aging'. The interactions between pollutants and soil's physiochemical properties affect solubility of the pollutants and the microbial bioavailability (Chung and Alexander, 2002 and Megharaj et al., 2011*)*. This is the critical factor to successfully bioremediate pollutants. Multiple reviews in the literature have indicated that both aging and co-contaminants to be key attributors to a pollutants microbial bioavailability (Traina and Laperche and; Straalen et al., 2005 Alexander, 2000). For example, Alexander (2000), conducted an extensive review on how aging of PAHs (ages ranging from 90-365 days) in the field is associated with lower microbial bioavailability. The author concluded that bioavailability of pollutant to microorganisms decreased over time, whereas unaged contaminant is readily available for degradation. According to Juhasz et al. (2010), the non-bioavailable PAHs residual to bioremediation may still be available to significant receptor organisms such as earthworms and plants.

1.5 Molecular tools

Soil harbors a great diversity of microorganisms. Many of these microorganisms have the potential to degrade a range of PAH compounds (Samanta, Singh & Jain 2002), either by utilizing the compound as a carbon source or via co-metabolism. As a result, microbial processes have been harnessed for the bioremediation of PAH-contaminated soil. While environmental factors may be easily measured and manipulated to ensure optimal conditions for PAH biodegradation (e.g. addition of nutrients, electron donor, electron acceptors), assessments of metabolic potential have proven to be more difficult due to the complexity of microbial population dynamics and limitations in methodologies for the assessments of population functionality. While bioremediation is an established remediation strategy, its current application is still considered a 'black box technology'. However, molecular methods targeting key functional genes-encoding for PAH-degrading enzymes may be used to assess biodegradation potential and the influence of bioremediation strategies on PAH biodegradation (Chauhan & Jain 2010; Stenuit et al. 2008). The application of both microbiology and molecular biology to assess the ability of microbial communities to degrade organic pollutants has enhanced the way researchers have attempted to restore environmental health. This would

illuminate degradative mechanisms within the 'black box' thereby providing greater certainty of degradative processes and bioremediation success.

1.5.1 Culture-dependent technique

The traditional method of isolating microorganisms through cultivation of pure cultures was the main tool used to characterize and identify microbial communities (Lovely, 2003). However, this technique has proven to account for less than 1% of microbial communities because of the inability to replicate growth conditions for the majority of microorganisms (Katsivela et al., 2005). Moreover, the traditional method of isolating, identifying, and enumerating species responsible for biodegradation has opened up ways leading to the discovery of better techniques of exploring microbial communities' potential (Goebel and Stackebrandt, 1994).

Microbial communities have great potential to remove contaminants from impacted sites when appropriate conditions are available for biodegradation. Studying isolates obtained from environmental samples has only exposed a small amount of information into the functional diversity of microorganisms (Lovely, 2003). Nonetheless, the isolation and characterization method has been the most important technique of studying organisms for a number of years, and has led to the design of a series of next-generation techniques for analyzing microbial catabolic genes. Figure 1.9 details the increasing application of newly emerging tools that are capable of predicting the physiology of microorganisms likely to be involved in controlling their activities related to bioremediation of contaminants.

1.5.2 16S rDNA/RNA strategy

As traditional methods of isolating and cultivating microorganisms became ineffective to successfully characterize microbial diversity and functionality, more advanced techniques have been developed to identify and characterize microorganisms and other species (Pontes et al., 2007 and Macrae, 2000). Traditional isolation methods lack the ability to reveal phylogenetic placement of soil microbial communities and their catabolic genes associated with biodegradation of contaminants (Wanatabe and Baker, 2000). For example, Muzyer et al. (1993) highlighted that the exploitation of 16S rDNA sequences has led to the identification of microbial communities in complex samples such as soils.

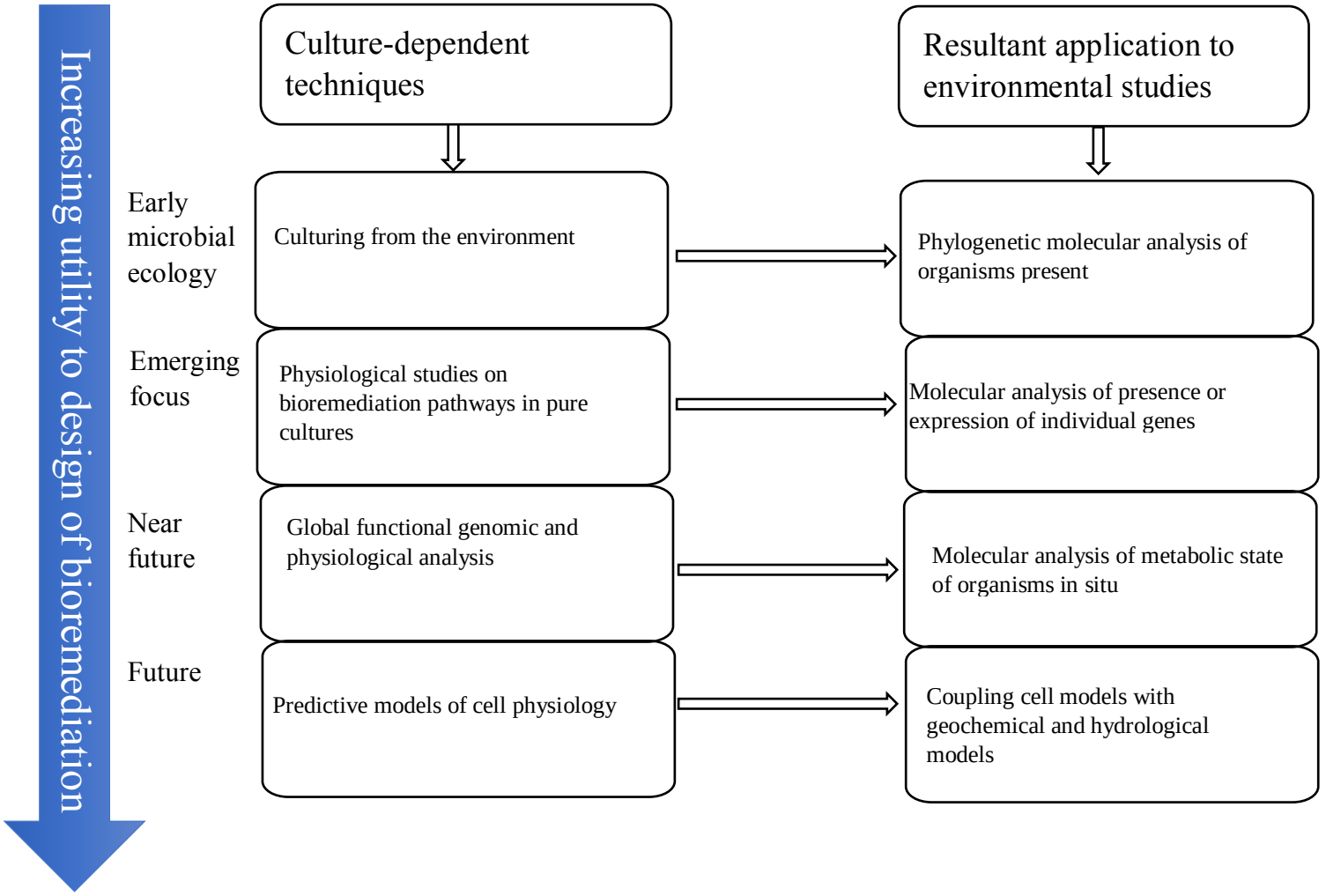

Figure 1.9. Evolution of increasingly sophisticated studies of pure cultures and their application to the study of microbial communities modified from (Lovely, 1994).

The utilization of nucleic acid sequencing has advanced our knowledge of how organisms are related and function at phylogenetic levels and has brought considerable insight in the field of microbial ecology, molecular and environmental microbiology (Olsen et al., 1986; Lovely, 2003; Roling et al., 2001and Macrae, 2000).

Moreover, molecular analyses of soil communities using 16S rDNA methods have improved ways in which we manipulate microorganisms to enhance their activities. It is more obvious from the literature that molecular sequence-based techniques are the best way of assessing the diversity and abundance of microbial populations. With the analysis of genes anticipated to be involved in bioremediation processes, there is a correlation between the abundance of degradative genes and the pollutant removal rates (Lovely, 2003). Different reports have shown that community shifts are influenced by the type and concentration of PAH, i.e. population with catabolic genes are higher and diverse at the time points, where high degradation of PAHs was observed during microcosm bioremediation (Bastiaens et al. 2000; Brezna, Khan & Cerniglia 2003; Castro-Gutiérrez, Rodriguez-Rodriguez & Vargas-Azofeifa 2012; Chadhain et al. 2006; Olsen et al. 1986). Castro-Gutierrez et al. (2012) identified 16 PAH-degrading strains with the ability to grow on 2 to 5 ring PAH compounds during preliminary PAH bioremediation studies. In this study, they found that PAH-degrading bacteria were abundance when a specific PAH was used as the source of carbon and energy. Presumably this suggests that they possess metabolic capacity to degrade a given compound. For example, out of the 16 strains, five strains were able to grow on naphthalene, six on fluorene, three on phenanthrene and two on pyrene. Most of these identified PAH-degrading bacteria belonged to related genus of *Pseudomonas, Comamonas, Sphingomonas, Stenotrophomonas* and *Delftia* based on 16S rRNA gene sequence (Castro-Gutiérrez, Rodriguez-Rodriguez & Vargas-Azofeifa 2012). In another study, conducted by Mao et al. (2012), they reported a significant increase in microbial population in the first two weeks of PAH-contaminated soil bioremediation following supplementation of bacterial consortium suspension (at 10 and 20% respectively). In addition, they also reported a decline in microbial population at the end of experiment (after 56 days of incubation period).

In contrast, Chadhain et al. (2006) reported a dynamic shift in microbial dioxygenase gene population associated with degradation of PAHs coupled with bacterial community profiling analysis. In this study, they combined the Rieske primers with bacterial community profiling to assess the diversity of Rieske gene during biodegradation of creosote contaminated soil

alongside a range of PAHs amended soils (naphthalene, phenanthrene and pyrene). Comparing the Shannon-Weaver diversity index obtained from the DGGE analysis indicated that creosote contaminated soil contained (H' = 2.41) more bacterial diversity followed by the phenanthrene enriched (H' = 2.30), pyrene enriched (H' = 1.83) and naphthalene enriched microcosm (H' = 1.14). The concept of Shannon Weaver diversity index refers to the species richness and abundances in a given sample. These results suggested that microcosms enriched with naphthalene and phenanthrene contain less bacterial diversity population stimulated by the present of these compound compared to the pyrene enriched creosote soil.

A technique such as polymerase chain reaction is capable of detecting variation in sequences leading to accurate identification of target organisms. Despite the invaluable contributions made through the use of 16S rRNA sequence analysis, this technique has its own limitations. For instance, it is difficult to design new primers to identify organisms of interest without a prior knowledge of a closely related organism's sequence available in databases (Lovely, 2003). Additionally, amplification of microbial communities residing in a certain location may be partially achieved causing underestimation of microbial diversity. Similarly, an overestimation of microbial population diversity might sometimes occur. Here a single strain could be found in a number of bands on the DGGE gel as 16S ribosomal RNAs are usually available in multiple copies in chromosomes.

A number of studies have employed molecular approaches based on 16S rDNA/RNA or traditional methods of analyses, in order to monitor changes in both the microbial diversity and various contaminants 'removal in polluted sites (Muyzer, De Waal & Uitterlinden 1993). Molecular approaches of studying microbial diversity based on PCR amplification coupled with 16S ribosomal RNA analysis of sequences allow researchers to step closer towards a new era of genomics approaches (Eyers et al. 2004). The use of these techniques to identify, characterize, and discover new species has been a great success but has fallen short of providing information in relation to microbial community functionality, genetic, evolutionary and phylogenetic diversities (Girard & Angers 2011; Liang et al. 2011; Singh et al. 2011; Yagi & Madsen 2009). The application of PCR-DGGE (16S rRNA) to characterize microbial communities has fallen short of identifying target communities because of the limited depth compare to unlimited depth generated by the NGS platforms. To put it into prospective, the PCR-DGGE is only capable of identifying a handful of species compare to hundreds generated by sequencing platforms. PCR amplification with primers yield complementary information

based on the conserved region of bacteria but may not cover everything in that environment (Handelsman et al. 1998). However, the processes of exploring microbial community potential using these molecular techniques have potentially improved from traditional methods of culturing organisms (Bertin, Médigue & Normand 2008; Kasai et al. 2005) through to molecular community fingerprinting methods and moving to the next generation sequencing technologies (NGS). The NGS is an approach based on genomics conceptual characterization of the complete genome of microorganisms direct from environmental samples. This is a powerful tool which allows characterization of microbial communities in terms of structural, diversity and functional abundance straight from their natural environments.

1.5.3 Next generation sequencing

Next generation sequencing has drawn wide attention across various scientific research communities including medicine, agriculture, life sciences, and biotechnology. Next generation sequencing is a high-throughput analytical technique that brings the power of DNA sequencing fundamental approaches together into one system, to alleviate the limitations of conventional sequencing methods. It is an approach capable of enhancing millions of sequences with high speed and accuracy (Shyr & Liu 2013). Next generation techniques have changed sequencing ability by overcoming barriers associated with the previous forms of methodologies such as the Sanger method of determining nucleotides (Sanger et al., 1997). Sanger approaches lacked power to capture uncultured organisms, inability of base-calling software and statistical analysis which may eliminate low quality sequences. Such advances have greatly improved methods to obtain genetic information from targeted biological systems such as plants, animal and microorganism (Nilsson et al. 2009).

It has become possible to sequence on a larger scale (i.e. Sanger sequencing can only do a single run based on 96 wells while next generation sequencing approaches can produce millions of sequences in parallel in one run) never seen before since the arrival of NGS platforms in 2005 (Harismendy et al. 2009). For example, the HiSeq.2000 system is cable of producing approximately 6 billon paired-end reads in an 11 day run (Egan, Schlueter & Spooner 2012). As a result of years of improvement in NGS platforms, today sequencing is more simple, rapid, accurate, flexible and cost-effective. The introduction of NGS platform has rapidly revolutionised various fields by boosting the number of discoveries (Shokralla et al. 2012). For instant, there has been significant improvement in the way various diseases are diagnosed in medicine (Roche website access on 15/4/13), re- sequencing of ancient DNA in evolutionary

biology (Knapp & Hofreiter 2010), and discovery of enormous genetic diversity in environmental microbiology (Roche website access on 15/4/13). Furthermore, there is no need to have a prior knowledge of a particular virus or pathogen with the power of NGS platforms as a proven diagnostic tool. This has improved the process of detecting cancer tumors in clinical settings. These approaches are capable of providing high-resolution data to be able to quantify and detect key alterations such as mutation, small insertions and deletions, structural variability, and DNA methylation etc. Most importantly, NGS has provided access to uncultivated microorganisms and their catabolic genes with potential application in the bioremediation of xenobiotics.

1.5.4 Sequencing technologies

Sanger technology was the dominant method of DNA sequencing for almost 28 years (Sanger, Nicklen & Coulson 1977) before the emergence of parallel sequencing technologies in 2005. The Sanger capillary concept is still in use, however NGS platforms are the technologies of choice and have progressively taken over from the former. In the 1990s, Sanger method was more rapid and accurate way of identifying most organisms than culturing techniques through bases determination (Kanavarioti et al. 2012).

The notion of developing high-throughput sequencing technologies was driven by the inevitable desire to make the cost of sequencing affordable. This desire was only achievable by developing an alternative high throughput DNA sequencing technology to the capillary sequencing based on electrophoretic separation of single strand (Kanavarioti et al. 2012). One of the advantage of this system over the Sanger method is the ability to produce millions of parallel sequences in a run (Hert, Fredlake & Barron 2008). However the concept behind NGS technology was built on the basic principles of Sanger or capillary sequencing rationale of bases determination (Quail et al. 2012). These basic principles have formed the basis of our current automated DNA sequencing method leading the way to the development of NGS technologies (Abbai et al. 2012).

Currently, there are six major platforms commercially available (Hert, Fredlake & Barron 2008). They were mostly designed and marketed by some of the leading next generation companies such as Roche /454 (Mardis 2008), Life technologies, Illumina, Applied Biosystems, and Pacific Biosciences(Hert, Fredlake & Barron 2008). The NGS technologies vary significantly in terms of strategies, application and the data generated from each platform.

Whereas their differences are seen in data output, initial starting material and the size of reads each platform generates (Table 1.9). However, their similarities are seen in the way they produced enormous number of sequences, they no longer required DNA cloning and operate on a much lower cost (Ramos et al. 2012; Varshney et al. 2009). All current NGS platforms have a standard workflow consisting of four major steps: library construction from genomic DNA, template preparation from constructed library, sequencing of template, and data analysis (Quail et al. 2012). Each platform is equipped with a simple, fast, and efficient workflow system to make it the platform of choice. Figure 1.11 is a schematic diagram of the Ion Proton workflow system explaining basic principles involved at each step from library construction to data analysis.

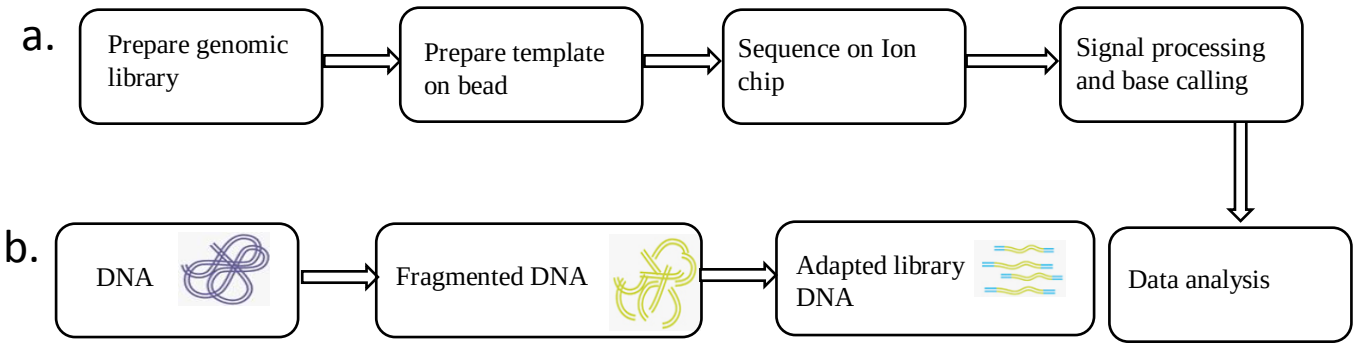

Figure 1.10. Ion Proton workflow system showing all four major steps when using Ion Express library kit. In this schematic diagram, the top section (a) is a sequential Ion Proton workflow, from genomic DNA library preparation to the data analysis. (b) Shows breakdown of two processes undertaken during library construction, genomic DNA is fragmented into selected library size (i.e 150 bp for Ion proton system) and then ligated with specific adapters.

1.5.5 Metagenomics

The study of genetic material obtained directly from environmental samples, without laboratory cultivation of microbial genomic DNA is known as metagenomics. Other related terms sometimes used to describe the same line of scientific research include: environmental; ecological and community genomics (Stenuit et al., 2008). These are integral parts of metagenomics approaches towards understanding soil microbial communities. Unlike both traditional and conventional methods, metagenomics is capable of offering collective analyses of complex microbial communities in their natural niches, by bypassing isolation and cultivation steps (Huson et al., 2008 and Handlesman et al., 1998). In a recent review, Whitehead. (2012) used comparative genomics in ecological physiology to critically evaluate

mechanisms that enable microorganisms live in variable environments. In this review, the author discussed some of the mechanisms used by various microorganisms to detect changes in their environments. Comparative genomics provided better means of understanding the mechanism by which populations and species found at different locations acclimatize to suit their new environment.

It is widely expected that species from different niches are likely to exhibit different physiological traits to suit changes in environmental conditions. For instance, Yergeau et al. (2012) compared hydrocarbon-degrading communities in uncontaminated and diesel contaminated soils obtained from the Canadian High Arctic. Here they reported an immediate incremental change in the population of several bacterial communities such as *Actinobacteria*, *Alphaproteobacteria* and *Gammaproteobacteria* immediately after contamination and excavation of soil. In contrast, a decrease in the abundance of *Acidobacteria*, *Bacteroidetes*, *Chlorobi*, *Chloroflexi*, *Cyanbacteria*, and *Firnicutes* was reported at the same time. Such findings were interesting indicators of how hydrocarbon contamination and bioremediation application may cause major shifts in microbial communities. Furthermore, a metagenomics approach may elucidate microbial community functionality through direct isolation of microbial genomic DNA in their natural environments.

1.6 Advantages and disadvantages of NGS platforms

Regardless of their potential application, each of the next generation platform comes with a number of advantages and disadvantages (Glenn 2011). Comparisons of NGS platforms have demonstrated that there are trade-offs between economics and the amount of data generated. For example, Illumina MiSeq is a low-cost Illumina platform, where its short reads length, resulted in some difficulties in read-based analyses at the assembly point.

In simple terms, the majority of NGS platform can produce massive amounts of raw data per run (up to 10 Gb for Ion Proton), but the generated data can never be appreciated until their genomic identities are specified. Great attention has been paid towards developing rapid next-generation sequencing platforms that are more efficient in throughput, affordable and with increased accuracy (Table 1.10).

Table 1.10 summarises some of the advantages and drawbacks of five selected next generation sequencing platforms alongside Sanger technology (Glenn 2011; Shokralla et al. 2012). A

common advantage possessed by all next generation sequencing technologies is the ability to generate massive data at a reduced cost (Gelderman & Contreras 2013). For example, we have witnessed a dramatic reduction in the cost of sequencing the human genome from $3 billion in 2005 down to $1000 since the Ion Proton/PGM sequencer was introduced in 2010 (Grumbt et al. 2013). Arguably, numerous studies have shown that NGS platforms are capable of multiplexing hundreds of samples in a parallel run while maintaining high yield coverage (Grumbt et al. 2013; Hert, Fredlake & Barron 2008).

Another common attribute to all next-generation platforms is the ability to offer paired end reads, where sequences can be deduced from both ends of the library fragments resulting in accurate mapping of reads compared to a single ended short reads. For example, in 2007, a team of researchers from four different countries (USA, Germany, UK and Austria) developed pair-end mapping (PEM) to detect structural variants in the human genome (Korbel et al. 2007). In this collaborative work, authors applied PEM to compare both shared and divergent structural variants in African and European individual in relation to the reference genome. Findings from this study documented more than 1000 structural variants which concluded that structural variability was much greater in humans than previously thought. Moreover, the study also touched on the formation of structural variants mechanisms in humans, which have an adverse impact on gene function.

Table 1.8. Platforms currently available in the market alongside sequencing technologies they used.

Platform	**Sanger 3730xl**	**Roche 454 FLX**	**HiSeq 2000**	**SOLiDv4**	**Ion Torrent Proton**	**PacBio RS**
Sequencing technology/chemistry	Capillary sequencing	Pyrosequencing	Synthesis-based sequencing	Ligation-based sequencing	Ion Semiconductor sequencing	Single Molecule Real Time(SMRT) sequencing
Year	1990s	2005	2006	2008	2010	2010
Market by	Applied Biostsyems	Roche (454 Life sciences)	Illumina	Applied Biosystems	Life Technologies	Pacific Bioscience
Cost per Instrument	$95,000 USD	$500,000 USD	$690,000 USD	$495,000 USD	$149,000 USD	$695,000 USD
Input material	1-3µg	0.5ng - 5 µg	50-1000 ng	10 ng to 5 µg	100 ng	2 ng ~ 1 µg
Read length	400 – 900 bp	700 bp	100 x 100 paired end	50 x 50 paired end	200 – 400 bp	5,5000 – 10,000 bp
Run time	20 mins – 3 hours	24 hours	3 -10 days	7 – 14 days	2 hours	2 – 3 hours
Data output per run	1.9 ~ 84 Kb	0.7 Gb	600 Gb	120 Gb	100 – 200 Mb	100 – 700 Mb
Amplification approach	PCR	Emulsion PCR	Bridge amplification	Emulsion PCR	Emulsion PCR	No amplification,
Cost per run	$4 USD per single read	$7,000 USD	$6,000 USD	$4,000 USD	$350 USD	$125 – 300 USD
Habitat	Microbial genome	Soil	Seawater	Soil	Medical samples	Microbial genome
Contaminant	NA	Diesel	Oil spill	Jet fuel	NA	NA
Reference	Quail et al., 2012a, Sanger et al., 1977, Sanger et al., 1992	Quail et al., 2012a, Rogers and Venter, 2005	Quail et al., 2012a, Morozova and Marra, 2008	MacLean et al., 2009, Quail et al., 2012a	Quail et al., 2012a, Ramos et al., 2012	Quail et al., 2012a, Tucker et al., 2011

NA not applicable

One major advantage of PEM is the ability to resolve the shortcoming of large structural rearrangements, arising from mechanisms such as deletions, duplications, insertions, inversions, or even the combinations of any of these mechanisms (Korbel et al. 2007). Like any other high throughput technology, PEM detection doesn't require the design and preparation of a DNA library involves a cloning process (Amend, Seifert & Bruns 2010; Sucher, Hennell & Carles 2012), hence, minimising the chance that biases could be introduced as the cloning step is bypassed. Therefore, availability of NGS tools for studying microorganisms and their catabolic genes suitable for bioremediation of PAHs is the remarkable development in the fields of microbial ecology and environmental microbiology. Many studies have used NGS platform to understand microbial community response to PAH contamination in terms of diversity, abundance and functionality (Brennerova et al. 2009; Gerlach & Stoye 2011).

1.7 Current gap in knowledge of PAH microbial biodegradation

Microbial communities living in contaminated soil have the ability to adjust their physiology in order to survive. The majority of studies, looking at microbial potential to degrade contaminants of interest, such as PAHs have used 16S rRNA sequence analysis to identify genes associated with biodegradation processes. However, this system of analysis is capable of retrieval of only single or specific genes, as it is based on the principle of the conserved region of organisms or universal PCR primers. As such, next generation molecular sequencing techniques have been developed with high throughput ability to analyses soil microorganisms in more detail than ever. In this project, one of these high throughput methods, 'metagenomics' will be used. Unlike PCR systems of detecting microorganism potential, metagenomics is capable of recovering multiple types of gene encoding for various functions that are affiliated with PAH biodegradation. There is a lack of knowledge across the scientific spectrum, explaining how bacteria function in relation to other microorganism groups (archaea, fungi and viruses), even though they have been well studied. Data generated from this study will reveal existing relationships between microorganisms through diversity and gene composition at phylogenetic level when their environment is contaminated with PAHs. Additionally, metagenomics will allow direct access to hidden novel genes associated with hydrocarbon-degrading microbial communities in PAH-impacted soils in Australia.

Table 1.9. Key advantages and drawbacks of five selected NGS platforms in comparsion to Sanger sequencer

Platform	Advantage	Disadvantage	Reference
Sanger	High quality read Long read length Low cost for small studies	High cost per large amount of data Low throughput High cost per Mb	Sanger, Nicklen and Coulson 1977,19992
Roche 454 FLX	Long read length Fast run time Good choice for de Novo assembly	High reagent cost High error rates in homopolymer Low throughput	Egan, Schlueter and Spooner 2012
Illumina/Solexa genome Analyser e.g. HiSeq 2000	High throughput High coverage Widely use platform Low cost per Mb	Short read length Less feasible for de novo assembly High capital cost	Morozova and Marra 2008, Rogers and Venter 2005
Applied Biosystems SOLiD™ sequencer	High accuracy High throughput Low cost per Gb	Short read assembly High capital cost Longest run time	MacLean, Jones and Studholme 2009
Ion Torrent/Proton	Very fast run time Cost effective Simple machine Suitable for targeted sequencing Delivers highest number of reads among NGS	Low throughput High cost per Mb Samples preparation takes long time than on the instrument	Rogers and Venter 2005, Egan, Schlueter and Spooner 2012

1.8 Summary

Characterization of microbial community diversity and functionality has been difficult to date due to limitations in traditional culture-based methodologies and molecular techniques. However, next generation high throughput pyrosequencing (metagenomics) offers direct access to uncharacterized microbial communities through bypassing limitations of both molecular and traditional methods. The use of this technique will allow for the identification of novel functional genes and enzymes affiliated with PAH-degrading microorganism which will address current knowledge gaps associated with microbial communities in PAH-contaminated soil. Accessing microbial communities directly without laboratory cultivation and isolation methods, will not only further our understanding of the mechanisms underlying the way organisms responded to contamination, but will also improve the approaches we use when assessing contaminants.

1.9 Aims and significance of this project

The general objective of this project was to explore how amendment regimes influence the pattern, diversity and metabolic capacity of microbial community dynamics in a range of PAH-contaminated soils. Identification of new genes in uncultivable species straight from environmental samples may be a valuable addition to the field of environmental microbiology. Mining genetic information by taking advantage of the unbiased high throughput shotgun pyrosequencing technique used in this project is a significant tool to assess microorganism ability previously not possible using isolation and culture techniques. Ion Proton sequencing was used to characterise the diversity of microbial populations in PAH-contaminated soils following the application of varying remediation strategies.

1.9.1 Specific aims

Specific aims for each experimental chapter include:

- **Assess PAH bioremediation performance (Chapter 3)**: PAH soil microcosm studies were undertaken to determine PAH bioremediation performance using soil amendment strategies in three distinct PAH-contaminated soils. Biodegradation performance was assessed by comparing the degradation of selected individual PAH compounds with three- (phenanthrene), four (pyrene) and five-benzene rings (B[a]P) in 3 historically-contaminated soils over a 42 weeks incubation period.

- **Evaluate the impact of bioremediation strategies on soil microbial diversity (Chapter 4).** Changes in soil microbial diversity as a consequence of bioremediation strategy was assessed through the application of DGGE coupled with PCR amplification of 16S rDNA and NidA genes. Analysis included a time series assessment of soil bacterial communities in NA, ENA and Combined treatment microcosms for the three historically PAH-contaminated soils.
- **Assess the composition and metabolic potential of microbial communities involved in biodegradation processes (Chapter 5).** Shotgun pyrosequencing (Ion Proton) was utilised to assess changes in microbial communities in NA, ENA and Combined treatment microcosms for the three historically PAH-contaminated soils (metagenomics techniques).
- **Assess PAH bioavailability (Chapter 6).** In the context of biodegradation, PAH bioavailability may be a major factor which limits PAH biodegradation perofrmance. This chapter utilised HP-β-CD extraction to investigate if a lack of PAH bioavailability was responsible for the limited PAH biodegradation observed in chapter 3. PAH bioavailability was predicted using HP-β-CD data and linear regression models from Juhasz et al. (2014), Papadopoulos et al. (2008) and Hickman et al. (2008) to determine whether prediction accuracy varied depending on model used.
- **Can alternative remediation strategies be implemented to overcome PAH bioavailability limitations (Chapter 7)?** This chapter aimed to determine whether the addition of an alternative carbon source (sodium succinate), the addition of a surfactant (Tween 20), or pre-treatment of the contaminated soil by chemical oxidation (hydrogen peroxide) increased the bioavailability of PAHs, and/or increased removal of the target compounds. This was addressed by examining the degradation of three- (phenanthrene), four- (pyrene) and five-ring (B(a)P) PAH compounds in a selected contaminated soil over a 4 week time course period. The effect of alternative treatment approaches on soil microbial diversity and functional profiles was also assessed using techniques detiled in Chapter 6.

1.10 Hypotheses

It is hypothesised that the impact of environmental pollution (i.e. PAHs) on the soil environment will result in a change in microbial population growth, adaptation and selection leading to changes in community functionality, diversity and structure. The addition of

nutrients and / or inoculation of specific-PAH degrading microorganism may enhance the biodegradation capacity of indigenous microbial communities and thus increase PAH removal. PAH degrading genes that may not be detected using library cloning and conventional molecular PCR-DGGE techniques may be detectable with the application of next generation sequencing technology (Ion proton platform).

To address the above hypothesis, this thesis examined the subject of bioremediation of PAHs in three aged contaminated soils (Creo, AP and TB) using a number of bioremediation strategies involving natural attenuation (NA), enhance natural attenuation (ENA) and bioaugmentation (BioA). This was achieved through treatability studies in the first 42 weeks (Chapter 3), coupled with detailed analyses of the microbiology via community profiling (Chapter 4) and through next generation sequencing techniques (Chapter 5). While limited biodegradation was observed, factors inhibiting biodegradation in three aged PAH contaminated soils were predicted through bioavailability experiment (Chapter 6). In addition, the final chapter detailed a series of experiments which explored the impact of applying more aggressive techniques to increase PAH degradation and their impact on bioremediation performance and micobial community diversity.

Chapter 2

Materials and Methods

2.1 Ethics statement

This study does not involve the use of any animal or restricted microorganisms or human subjects and no specific approvals were therefore required.

2.2 Chemicals and reagents

Chemicals, solvents, reagents and microbiological media were obtained from Sigma-Aldrich (Australia), Fluka, Crown Scientific (Australia), MO BIO, Laboratory Inc. (Australia), MP Biochemicals (Germany), and Life Technologies (Australia). All chemicals, solvents and reagents were of analytical grade unless otherwise specified.

2.3 Stock solutions

Ethidium bromide: Ethidium bromide (1 g) was dissolved in 95 ml Milli-Q water and the volume was made up to 100 ml. The stock solution was stored at 4oC in the dark until required.

Iodonitrotetrazolium chloride solution: Iodonitrotetrazolium chloride (p-iodotetrazolium violet 2-[4-iodophenyl]-3-[4-nitrophenyl-5-phenyltetrazolium chloride) (250 mg) was dissolved in 2 ml of dimethylformanide and made up to 25 ml using Milli-Q water. The solution was stored at 4ºC until required.

Phenanthrene solution: Phenanthrene solution was prepared by dissolving 2 mg of phenanthrene powder in 100 ml of acetone into a 100 ml Schott bottle. The phenanthrene stock solution was prepared under a fume hood and stored at 4ºC until required.

Internal standard solution: An internal standard (IS) solution was prepared by adding 0.2 g of 2.3 benzofluorene powder to 200 ml of dichloromethane to achieve a final concentration of 1 mg ml-1. The IS solution was used to monitor the recovery of PAHs during samples extraction by Accelerated solvent extraction (ASE). The solution was stored at 4ºC until needed.

Sodium hydroxide solution (0.1M NaOH): Sodium hydroxide (4 g) was dissolved in 950 ml Milli-Q water in a volumetric flask and made up to a final volume of 1000 ml. The stock was stored at room temperature.

Hydroxypropyl-β-cylodexrin solution: Hydroxypropyl-β-cylodexrin (HP-β-CD) powder (45.4 g) was dissolved in 1000 ml of water to achieve concentration of 40 mM HP-β-CD. The stock solution was stored at room temperature until required.

Buffer solution: 20 ml of buffer 50X TAE was added to 980 ml of Milli-Q water and mix thoroughly. The final concentration of 1XTAE buffer solution was 40mM acetic acid and 1mM EDTA at pH 8.3. This solution was stored at room temperature until required.

Phosphate buffer saline solution: Phosphate buffer solution was prepared in Milli-Q water by adding the required amount (g) of the following salts; NaCl (8.01 g), KCl (0.2 g), Na2HPO4 (1.78 g), and KH2PO4 (0.27 g), to 800 ml of Mill-Q water. The solution was adjusted to pH 7.4 using 0.1 M NaOH solution and made up to 1000 ml. The solution was autoclaved at 121oC for 15 mins. The phosphate buffer was made up as required and excess solution discarded after use.

Trace element solution: The trace element solution was prepared by dissolving the following: FeSO4.7H2O (0.2 g), ZnSO4.7H2O (0.01 g), MnCl2.4H2O (0.003 g), CoCl2.6H2O (0.02 g), CuSO4.2H2O (0.001 g), NiCl2.6H2O (0.002 g), Na2MoO4.2H2O (0.5 g) and H3BO3 (0.3 g) to 1000 ml of Milli-Q water. The solution was filter sterilised and stored in the dark at 4ºC until required.

Vitamins solution: The vitamins solution was prepared by dissolving the following: biotin (0.02 g), folic acid (0.02 g), thiaminse HCl (B1) (0.05 g), D-calcium pantothenate (0.05 g), vitamins B12 (0.05 g), Riboflavin (B2) (0.05 g), and Niacin (nicotinic acid) (0.2 g), pyridoxal HCL (0.03 g), and p-aminsobenzoic acid (0.02 g) into 100 ml of Milli-Q water. The solution was filter sterilised and stored at 4º C until needed.

Magnesium and calcium solution: The magnesium/calcium solution was prepared by dissolving MgSO4.7H2O (0.4 g) and CaCl2.2H2O (0.4 g) in 100 ml of Milli-Q water. The solution filter sterilised and stored at 4º C until use.

2.4 Media composition

All media was prepared using Milli-Q water. Media was sterilised by autoclaving at 121° C for 20 mins unless otherwise stated.

2.4.1 Basal salts medium (BSM)

The BSM media was prepared with the following salts; K_2HPO_4 (0.4 g), KH_2PO_4 (0.4 g), $(NH_4)_2SO_4$ (0.4 g), and NaCl (0.3 g) dissolved in 950 ml of Milli-Q water. The solution was sterilised by autoclaving before adding sterile solution of vitamins; trace element and magnesium/calcium solution (5 ml l^{-1} each).

2.4.2 Tryptone soya broth (TSB)

This medium was prepared by adding 30 g tryptone soya broth to 500 ml of Milli-Q water and make it up to 1 L before autoclaved it for 15 mins at 121º C. The prepared TSB solution was stored at 4ºC until needed.

2.4.3 Nutrient broth

This medium was prepared by adding 13 g Nutrient Broth (Oxoid) to 1000 ml of Milli-Q water. The prepared nutrient agar was stored at 4ºC until needed.

2.5 Methods

2.5.1 General laboratory equipment

There were a number of general laboratory apparatus used during this study. These apparatuses were:

- Sartorius analytical balance for weighing up to 220 g maximum with 0.01 mg resolution. Convenient for weighing small quantities of chemicals.
- For large quantities (up to 410 g) of media, soils, and chemicals, an electronic balance was used with 0.1 mg resolution.
- All stock solutions and media throughout this study were prepared using ultra-pure water produce in the lab using a Millipore Milli Q ultra-water system.
- The pH of soils, media, and stock solutions (where required) were measured using a Smart Chem-pH meter.

- Centrifugation was carried out using Multifuge 3 S-R by Heraeus, and/or a Sorvall Evolution RC 6+ centrifuge (Thermo Fisher Scientific).
- Sterilization of stock solutions and media were performed by autoclaving at 121°C and dry sterilization at 134 ^{o}C for 30 mins (glassware).
- HP-β-CD extraction were performed on a mechanical End-Over-End shaker (EQ-038) rotating at 100 rpm.
- Drying of soils was performed using a Modulyod freeze dryer (Thermo Fisher Electronic corporation).
- A Dionex ASE 200 (accelerated solvent extraction) system was used to extract and concentrate all samples.
- Molecular analyses performed with equipment such as PCR, DGGE system, vertical and horizontal electrophoresis systems (for both agarose and polyacrylamide gels), Gel Documentation system, Ion Proton (Torrent system) sequencer, High Sensitivity DNA Chip (2100 Bioanalyzer instrument by Life Technologies), Qubit® Fluorometer 2.0 (Invitrogen Life technologies) for DNA quantification and NanoDrop 2000 UV-Vis Spectrophotometer.

2.5.2 Microbiological methods

2.5.2.1 Soil processing

The soils used in this study were sourced from the CERAR-UniSA soil repository collections. Historical PAH contaminated soils were collected in 2008-2010 (by A/Prof. Albert Juhasz) from a former wood treatment plant (Adelaide, South Australia; designated Creo), a former manufacturing gas plant (Albert Park, Victoria; designated AP), and a tram barn maintenance facility (Adelaide, South Australia; designated TB). Following collection, soils were processed by drying at 40 ºC prior to sieving through a 2 mm stainless steel sieve. Processed soil samples were stored in sealable 20 L buckets at room temperature until required.

2.5.2.2 Soil physiochemical properties

The physiochemical properties of the 3 soils was determined before beginning the microcosm studies (refer to Table 3.2 in Chapter 3). The methodologies used to characterise soil physiochemical properties are described in the following sections.

2.5.2.3 Soil pH

The pH was determined in the liquid phase of the soil-water mixture as outlined by (Singh et al., 2003, Baptistsa et al., 2005). Briefly 10 g (performed in triplicate in a 1:5 dilution of soil: water) of PAH contaminated soil was placed in a 100 ml beaker containing 50 ml distilled water. The slurry was mixed for 2 mins, after which the suspension was left to settle for 15 mins. The pH values were measured by dipping pH electrode in the liquid phase.

2.5.2.4 Water holding capacity (% WHC)

In order to maintain a known soil moisture during the microcosm's incubation period, the soil water holding capacity (WHC) was measured as per the Soil Lab protocol, available from: <http://www.geocities.com/CapeCanaveral/Hall/1410/lab-Soil-contents.html> (access on 23 January 2015). Briefly, the soil WHC was determined by taking 10 g of soil dried at 105ºC for 24 h. The dried soil was saturated with water and then allowed to drain for 30 min. Soil water holding capacity was determined after drainage was completed by calculating the mass of water contained after saturation (Appendix 1).

2.5.2.5 Soil moisture content (MC %)

The soil moisture content (MC) of the soils was determined by drying 10 g (in triplicates) of wet soil for 24 h in an oven at 105°C. This was performed according to the gravimetrical method of measuring water content in the soil samples by obtaining ratio of the mass of water to dry soil, available from: <http://www.geocities.com/CapeCanaveral/Hall/1410/lab-Soil-contents.html> (access on 23 January 2015). The moisture content was obtained by dividing the difference between wet and dry mass by dry mass (Appendix 1) using the equation below;

% Moisture Content = W-D⁄D × 100%

Where

W: the wet weight of soil (g)

D: the dry weight of soil (g)

2.5.2.6 Soil organic matter (%)

Soil organic matter was determined by the combustion method (Schumacher 2002). Wet soil was dried at 80°C for 12 h until a constant weight was obtained. The dried soil was weighed into crucibles (10 g in triplicate) and placed in a muffle furnace overnight at 440°C. The crucibles were carefully removed and allowed to cool in a desiccator before the weight was

recorded. The soil organic matter was expressed as the percentage of the dry mass of the soil using the formula below (Appendix 1).

%SOM = ((MDS +MC) - (MBS+MC))/MDS*100%
Where
SOM: soil organic matter content (g)
MDS: mass of dry soil (g)
MC: mass of crucible (g)
MBS: mass of soil after burning (g)

2.6 Inoculum preparation

Mycobacterium gilvum inoculum (10 ml, provided by A/Prof. Albert Juhasz) was inoculated into 300 ml TSB (tryptone soya broth) solution in 500 ml flasks (duplicates). Inoculation procedures were performed under sterile conditions (laminar flow wiped down with 70% ethanol). All flasks were incubated at 37°C for 2 days on an orbital shaker and a shaking speed of 130 rpm.

2.6.1 Mycobacterium cells harvesting

After 2 days of incubation, *Mycobacterium* cells was harvested by centrifugation (Juan CR12) at 3500 rpm for 5 mins. The supernatant was decanted according to the modified method described by Annibale et al. (2005). The pellets were washed in an equivalent volume of phosphate buffered saline solution (600 ml). The washing step was repeated 3 times. The pellets containing the *Mycobacterium* cells (0.4 g wet weight) was resuspended in deionised water, ranging from 16.3-22.7 ml based on 60% water holding capacity of each soil and added to microcosm soil.

2.7 Bioavailability assessment

Hydrocarbon bioavailability in the Creo, TB and AP soils samples was assessed using methodologies as described by Juhasz et al. (2005). Assessments were performed on soil samples prior to set up of biodegradation microcosms. Data from the bioavailability studies were compared with values obtained from biodegradability microcosm assays. All bioavailability assays were performed in triplicate. Cyclodextrin extraction – hydroxypropyl-β-cyclodextrin (HPCD) extraction of hydrocarbon contaminated soil was performed according to the method of Reid et al. (2000). Contaminated soil (5 g wet weight) was added to glass

Schott bottles containing 100 ml of HPCD solution (40 mM). Samples were shaken end-over-end for 20 hours at room temperature. Following extraction, samples were centrifuged (3074 g for 5 mins), supernatants discarded and soils recovered for PAH extraction and analysis by GC as described in Section 2.11.2.

2.8 Soil microcosms

The propensity of indigenous soil microorganisms to degrade polycyclic aromatic hydrocarbon (PAH) under natural attenuation or enhanced natural attenuation conditions was assessed in soil microcosms. Contaminated soil (~800 g) was moistened to 60% water holding capacity and added to 5 L glass microcosms. Each treatment was set up in triplicate as shown in Table 2.1. A range of nutrient additions were added depending on the treatment being assessed. Laboratory reagents ($(NH_4)_2SO_4$, KH_2PO_4 and K_2HPO_4) were added to soils to give an approximate C: N: P ratio of 100:10:1. Microcosms were incubated at 25ºC in the dark and samples were periodically removed for chemical, microbiological and molecular analyses over a period of time. During sampling events, microcosms were mixed and moisture levels adjusted where required.

2.8.1 Summary of microcosm design

Table 2.1 summarises the experimental design for the initial microcosms study. Microcosm treatments included:

- Natural Attenuation (NA1-NA3): where the intrinsic capacities of the soil indigenous microbial community was assessed in PAH-contaminated soils without additional stimulation. Contaminated soils (800 g in each jar) moistened to 60% water holding capacity was added to 5 L glass jar (prepared in triplicate).
- Enhanced natural attenuation (ENA): microcosms were prepared in the same way as the NA microcosms but supplemented by adding nutrients ($(NH_4)_2SO_4$, KH_2PO_4 and K_2HPO_4) to achieve a C: N: P molar ratio of 100: 10:1 (ENA4-ENA6). Amount of each nutrient added per a jar was calculated based on total PAH concentration in each soil as a measure of carbon content (Table 2.2).
- Bioaugmentation (BioA): *Mycobacterium* cells (0.4 g wet weight) suspended in sterilised water ranging from 16.3-22.7 ml was added to each jar based on 60% water holding capacity of each soil (BioA7- BioA9).

- Combined strategy (Comb): Microcosms were prepared as a combination of both enhanced natural attenuation (ENA) and bioaugmentation (Comb10-Comb12). The microcosms were kept at a constant temperature (25°C) and a moisture content of 60% WHC. The moisture content of the microcosms was checked every 3 days and moisture level adjusted by adding deionised water when required.

Following the assessment of NA, ENA, BioA and Comb microcosms, additional treatability studies were undertaken using alternative treatment strategies. Soil from the initial Creo microcosm study was used to prepare treatments (200 g per a jar as in Table 2.3) for the alternative soil microcosm study as detailed in Chapter 7.

The treatments included:

- Surfactant addition (Tween 20 at 1% v/v): T_{20} was added to each microcosm at 1% loading solution based on 60% water holding capacity.
- Addition of an alternative carbon source (sodium succinate at 1% v/v): sodium succinate was added to Creo contaminated soil by dissolving 2 g of sodium succinate powder in 22.8 ml of deionised determined based on 60% water holding capacity and added to each jar(duplicate).
- Chemical oxidation (hydrogen peroxide at 20% v/v): chemical oxidation pretreatment was performed by adding 912 ml of H_2O_2 to achieve 20% aqueous solution concentration dosage based on 60% of water holding capacity. This was achieved by adding a small amount of soil until the whole amount was added (200 g in duplicate) into a 5 L beaker containing 912 ml of H_2O_2 set up under a fume hood on a stirring plate for 24 hr. Supernatant was decanted off and soil was collected into a plastic pots (2 pots). Soil was then dried in an oven at 40º C to bring moisture content to 60% water holding capacity. The experimental design is detailed as shown in Table 2.3.

Each treatment was prepared in duplicate. Microcosms were incubated at 25ºC in the dark and samples were periodically removed for chemical and molecular analyses at (Days 0, 14 and 28). During sampling events, microcosms were mixed, aerated and moisture levels adjusted by adding deionised waster when required.

2.9 Sampling

Day 0 sampling was carried out immediately after the microcosms were completed, by the removal of approximately 20 g of soil from each microcosm (glass jar) under aseptic conditions. All samples designated for molecular analysis were stored at -20°C until required. Samples designated for chemical analysis were store at 4°C. Additional sampling was carried out at three time points (weeks 6, 18, and 42) except for the second experiment, in which samples were taken at day 0, 7, 14 and 28 for chemical analysis. While molecular analysis was performed with smaples obtained at day 0, 14 and 28.

2.10 Enumeration of PAH-degrading bacteria

The microbial cells of PAH-degrading bacteria were estimated using the most probable number (MPN) method (Braddock & Catterall 1999; Yu, K et al. 2005). Phenanthrene was used as the sole hydrocarbon substrate. Phenanthrene was made up in acetone solution by adding 0.002 g (2g/ml) of phenanthrene powder to 100 ml of acetone in a 100 ml Schott bottle. Microplates were prepared by adding 10 µl of phenanthrene solution to the edge of each well in the fume hood and the acetone was allowed to evaporate. Soil samples obtained from amended and unamended microcosms at each time point (2 g) were suspended in 10 ml of MQ water. The suspensions were vortexed vigorously for 30 sec and allowed to settle for ~1 h prior to inoculating the 96-well MPN microplates.

The MPN microplates were inoculated with 180 µl of a media solution made of NB or BSM as described in Section 2.4.1. An aliquot of 20 µl of each suspension was added to the first row of each well designated for each treatment in triplicate, mixed well by pipetting and then serially diluted by a factor of 10^{0} to 10^{-8} . Plates were sealed with Parafilm prior to aerobic incubation at 25ºC for 1 week for NB plates or 2 weeks for BSM plates. Bacterial growth in each microplate was easily visible after a week of incubation (NB). The counting of positive wells was made via visual inspection of these plates. After incubation, the number of wells showing growth were examined for turbidity in the MPN plates (NB) and the patterns of growth in the wells is scored against the MPN table (Sutton 2010). Similar procedures were also performed for BSM media plates but no growth was observed after 2 weeks of incubation. The iodonitrotetrazolium violet (INT) was added to the BSM plates as an indicator of microbial activity to each well, and incubated overnight at 25ºC. The positive wells were expected to develop a red/pink pigmentation and these could be scored by visual inspection (Wrenn &

Venosa 1996). No red/pink pigmentation were observed in the BSM plates following an overnight incubation with INT solution.

Table 2.1. Experimental set up for PAH biodegradation microcosms of the amended and unamended using three historical PAH-contaminated soils (Creo, TB, and AP).

	Amendments				
Treatment	Soil (800 g)	Nutrient	Inoculums	Nutrient and Inoculums	Moisture
NA1	✓	•	•	•	✓
NA2	✓	•	•	•	✓
NA3	✓	•	•	•	✓
ENA4	✓	✓	•	•	✓
ENA5	✓	✓	•	•	✓
ENA6	✓	✓	•	•	✓
BioA7	✓	•	✓	•	✓
BioA8	✓	•	✓	•	✓
BioA9	✓	•	✓	•	✓
Comb10	✓	•	•	✓	✓
Comb11	✓	•	•	✓	✓
Comb12	✓	•	•	✓	✓

✓ Added. • Not added

Table 2.2. Amount of each nutrient (g) added per a jar calculated based on carbon content in each soil.

Constituent	Soil		
	Creo	**TB**	**AP**
Concentration. (g)	1068.0	633.0	495.9
C (mM)	87.0	50.0	39.0
N (g)	5.7	3.3	2.6
P1 (g)	0.8	0.4	0.3
P2 (g)	0.6	0.3	0.3
Total C (%)	53	36	21.0
Total amount P1 per a jar (g)	0.9	0.5	0.4
Total amount P2 per a jar (g)	0.7	0.4	0.3
Total N per a jar (g)	6.9	4.0	3.1

N is the nitrogen as in $(NH_4)_2SO_4$
P1 is first phosphorus as in KH_2PO_4
P2 is second phosphorus as in K_2HPO_4
C is carbon in contaminated

Table 2.3. Experimental set up for PAH biodegradation microcosms using Creo soil amended with sodium succinate, hydrogen peroxide and Tween 20.

Treatment	Treatment					
	Soil (200 g)	**Nutrient source**	**SS**	**H_20_2**	**T_{20}**	**Moisture**
NA-1	✓	•	•	•	•	✓
NA-2	✓	•	•	•	•	✓
ENA-3	✓	✓	•	•	•	✓
ENA-4	✓	✓	•	•	•	✓
SS-5	✓	•	✓	•	•	✓
SS-6	✓	•	✓	•	•	✓
H_20_2-7	✓	•	•	✓	•	✓
H_20_2-8	✓	•	•	✓	•	✓
T_{20}-9	✓	•	•	•	✓	✓
T_{20}-10	✓	•	•	•	✓	✓

✓ Added; • Not added

2.11 Chemical analyses

2.11.1 PAH extraction

PAH extraction was carried out on soil treatments collected from the microcosms at day 0, weeks 6, 18 and 42. Recovery of PAHs from soils was achieved using Accelerated Solvent Extraction (Dionex ASE® 200) as per manufacture Application Note 313 (Richter et al. 1996). Extraction of PAHs from the soils were performed using 11 ml stainless-steel extraction cells. Acetone-dichloromethane at 1:1 (v/v) ratio were used as extractants. Samples were loaded into the extraction cells (2 g), and the remaining volume was filled with clean sand to minimise solvent usage. A surrogate standard (2, 3 benzofluorene, 100 µl at 1 mg/ml) was added to the cells before caps were tightened. In addition, blank samples (i.e. acid washed sand) were also included for quality assurance and quality control during ASE runs. The extraction was performed at 1500 psi pressures; nitrogen was purged at 150 psi for 60 seconds according to the manufacturer protocols. The ASE extracts were concentrated under nitrogen (Solvent evaporating system SE 500) to remove excess acetone-DCM until nearly dry and then resuspended in 5 ml DCM. The final PAH extracts were stored at 4°C prior to analysis by gas chromatography analysis.

2.11.2 Gas chromatography (GC)

Gas chromatography analysis was performed using concentrated ASE extracts using Agilent Technologies 7890A gas chromatograph equipped with a flame ionisation detector (GC-FID), with a ZB-5 capillary column (30 m x 0.25 mm, Phenomenx®). One millilitre of the sample was injected into the GC equipped with FID and splitless injector. A Zebron ZB-5HT column was used for the separation of 16 PAHs priority pollutants. The following temperature ramp program was utilised; 100 º C for 5 mins, followed by increases of 10 º from 100 º to 300 º C, holding at 300 º C for 5 mins. Injector and detector temperatures were constant at 320 º C. Helium was used as the carrier gas flow at the rate of 0.5 ml min^{-1} (Juhasz, Aleer & Adetutu 2014). The quantification of GC-FID of PAH was performed according to USEPA 8100 methodology cited by Juhasz et al. (2014).

The concentration of total PAH and individual compounds was calculated using 2, 3 benzofluorene (1 mg/ml) as an internal standard (IS). Based on the concentrations of the internal standard analysed by GC-FID, the peak area ratio of each PAH to the internal standard was determined. The calibration curve was plotted using the concentration of PAHs verses the

peak area ratio and a line of best fit was obtained. The equation from the standard calibration curve (with r^2 value > 0.95) was used in conjunction with the peak area of each compound to determine total PAH concentration in the extracted samples. A blank solvent was incorporated every 12 samples to check baseline and 20% of samples were sent to external commercial lab to ensure QA/QC. The nominated external commercial lab used to ensure QA/QC was accredited Australian Laboratory Services (ALS). The mean of recovery employed during PAH quantification ranged from 87 to 102%. ALS used Laboratory Control Spike (LCS) as recoveries quality control with indicated percentages of the lower and upper detection limits for phenanthrene (69-113%), Fluroanthene (67-115%) and Pyrene (66-116%).

2.12 Molecular analyses

2.12.1 DNA extraction

Genomic DNA was extracted from samples periodically removed from three microcosms (NA, ENA & Comb all soils), at selected four sampling time points (day 0, weeks 6, 18, and 42) using a PowerSoil^{TM} DNA Kit (MoBio, Carlsbad, CA, US). The manufacturer's protocol was generally followed but modified to provide better recovery and improved DNA quality (Figure A1.1 in Appendix 1). Community genomic DNA was extracted at the selected sampling time points in order to compare how microbial communities change over time in relation to implemented soils amendments. Briefly, soil (0.5 g) was added to the powerbead tubes containing beating beads. All tubes were subjected to bead beating for 2 cycles of 45 sec each. The amount of nucleic acid was quantified using NanoDrop 2000 UV-Vis Spectrophotometer (Sambrook and Russell, 2001). The same DNA extract was used for the amplification of both bacterial 16S rDNA as well as fungal 18S rDNA using their respective primers as described in section 2.12.3.1- 2.12.3.4.

2.12.2 Agarose gel electrophoresis

The quality of DNA extracts was assessed using a 2% agarose gel in 1 X TAE buffer (Appendix 1). The agarose gel solution was prepared by heating 2 g of agarose powder in 1 X TAE buffer (2 ml) in a microwave until dissolved. The solution was allowed to cool for 15 min before pouring it into a casting tray with well combs. The combs were carefully removed from the gel to provide wells for DNA loading after the gel solidified. A 1kb (6 µl) genomic DNA ladder was used for determining the size of DNA fragments (Promega, WI USA). DNA extracts (5 µl) were added to the loading dye (4 µl) on parafilm and mixed before loading into their

respective wells. Electrophoresis was performed in a horizontal tank (BioRad, Herucles, USA) to allow DNA to migrate through the gel (positive to negative end) until the loading dyes on the gel indicated clear separation. The gel was allowed to run for 45 min at 80 V prior to staining for 35 min in $EtBr_2$ solution. DNA was then visualised using a UV transilluminsator (BioRad Laboratories Ltd) fitted with a digital camera utilising Zoombrowser Ex software.

2.12.3 Polymerase chain reaction (PCR)

2.12.3.1 Bacterial universal amplification

Primer pair 518R and 314F GC (Muyzer et al., 1993) were used to amplify the 16S DNA gene from soil-extracted DNA (Table 2.2). The purified DNA (2 µl) extract was added to the PCR master mix (48 µl). The PCR master mix contained 2 µl of forward primer 314 FGC (10 pmole μl^{-1}), 2 µl of reverse primer 518R (10 pmole μl^{-1}), 1 µl of dexoynucleotide triphosphate (dNTP 10 mM) mixture, 10 µl of Taq flexi buffer, 5 µl of magnesium chloride (2 mM of $MgCl_2$) solution, 0.25 µl of Taq polymerase enzyme (1 U), and 27.75 µl of sterilised nuclease free water to make the solution up to volume (50 µl of the PCR master mix). PCR was carried out with initial DNA denaturing step at 95°C for 5 min; followed by 10 cycles of 95°C for 30 sec, 65°C for 30 sec, and 72°C for 1 min. The annealing temperature was reduced by 1°C for every cycle until the normal annealing temperature was reached. The remaining part of PCR conditions consisting of 17 cycles were performed at 95°C for 30 sec, 55°C for 30 sec , and 72°C for 1 mins with a final extension at 72°C for 10 min.

For bacterial NidA genes PCR, the amplification reaction was carried out with forward and reverse primers (Table 2.4) without GC clamp. The purified DNA (4 µl) extract was added to the PCR master mix (48 µl). The PCR master mix contained 2 µl of forward primer NidAF (10 pmole μl^{-1}), 2 µl of reverse primer NidAR (10 pmole μl^{-1}), 1 µl of dexoynucleotide triposphate (dNTP 10 mM) mixture, 10 µl of Taq flexi buffer, 4 µl of magnesium chloride (2 mM of $MgCl_2$) solution, 0.25 µl of Taq polymerase enzyme (1 U), and 26.75 µl of sterilised nuclease free water to make the solution up to volume (50 µl of the PCR master mix). The second amplification (nested PCR) was performed with the product from the first reaction as the template and a GC primer. A similar PCR programme used for fungal amplification (Section 2.10.3.3-2.10.3.4) was used for NidA PCR reactions. PCR products were analysed on a 1.5% agarose gel electrophoresis run at 60 V for 45 mins in 1 X TAE buffer as described in Section 2.10.2.

Table 2.4. Primer pairs used for PCR amplification of bacterial genes in this study.

Primer name	Microbial target	Sequence (5' to 3')	References
341F*	Bacteria	CCTACGGGAGGCAGCAG	Muyzer et al., 1993
518R		ATTACCGCGGCTGCTGG	
NidAF*	Bacteria	ATCTTCGGGCGCGGCTGGGTGTTTCTCGG	Sho et al., 2004
NidAR		AATTGTCGGCGGCTGTCTTCCAGTTCGC	

*shows a GC clamp was attached to the 5' end of primers for DGGE analysis.
GC Clamps: CGCCCGCCGCGCGCGGCGGGCGGGGCGGGGGCACGGGGGG

2.13 Denaturing gradient gel electrophoresis (DGGE)

The PCR amplicons from both bacterial 16S rDNA and fungal 18S rDNA were analysed using a Universal Mutation Detection System (Bio-Rad, CA, USA) as outlined in Appendix 1. The DGGE plates were first assembled after cleaning them with 70% ethanol; gel setting solution was prepared from 0% and 100% denaturants, cross linking solution was added to speed up gel setting, and the denaturant solution was cast using a gradient mixing pump. The stacking gel was prepared from 0% denaturant, APS, and TEMED (10 ml). A 32 well comb was inserted into the gel and filled with 5 ml of cross linking 0% denaturant. PCR generated products of desired volume (15-18 µl) were loaded on DGGE wells depending on the intensity of each band.

2.13.1 DGGE analysis of bacterial community

For bacterial gel analysis, the desired denaturant gradient was achieved using 45% acrylamide for the lower concentration and 65% acrylamide for higher concentration (0% and 100% denaturants) respectively. The gel was run for 18 h at 60 V and at a constant temperature (60°C) in 1 X TAE buffer. The same programme used to run universal bacterial DGGE was used to run the NidA genes DGGE.

2.13.2 DGGE analysis of fungal communities

The 18S rDNA amplicons were analysed using the same protocol as described in Section 2.11 except that a different range of denaturant gradient was used. Fungal PCR-generated products were separated using a 40% acrylamide for the lower denaturant and 60% for the upper

denaturant respectively (0% and 100% denaturants). The gel was run for 16 h at 60V and with a constant temperature of 60°C in 1 X TAE buffer.

2.13.3 DGGE staining

The DGGE gel was stained by silver staining using various solutions (Appendix 1). The silver staining involved placing the gel in 400 ml of fixing solution 1, followed by shaking for 2 h. This step was followed by incubation in 200 ml of silver nitrate solution for 20 min. The gel was then placed in 200 ml of developing solution for 30-45 min. The gel was placed in 400 ml of fixing solution 2 and incubated for 10 min. Finally, the gel was preserved in 400 ml preservative solution for 10 min, after which the DGGE gel was scanned using EPSON Expression 1600 V.2.65 E software, and saved as tif files for further molecular analysis.

2.13.4 Analysis of DGGE banding patterns

DGGE bands were analysed using Total Lab-120 (TL-120) V2006 F image software. The TL-120 package was used to study the relationship between the microbial communities which were expressed as similarity coefficients. In this case, two bands were considered to be related if they migrated the same distance on the gel (Nakatsu 2007). Each sample was scored based on the presence or absence of bands at the same position on the profile (lanes) when compared to the profiles of the other samples on the gel. The UPGMA dendrograms were also generated using the Phoretix 1D advanced analysis package. This software uses a sequential clustering algorithm to produce hierarchical similarity relationships between samples based on the degree of similarities between the bands in different samples on a DGGE gel.

2.13.5 Similarity and diversity analyses

The relatedness of the microbial communities (all gels) was expressed as similarity clusters using the unweighted pair group method with mathematical averages (UPGMA). Shannon index (*H*') was calculated from DGGE profiles as described by Girvan et al. (2003) using the formula: $H' = -\sum p_i \, LN \, p_i$ where p_i; is the proportion of the community that is made of species *i* (intensity of the band *i* / total intensity of all bands in the lane). LN p_i is the natural log of p_i. Equitability index (*J*) was also calculated using the formula $J = H'/(LN \, n_i)$ where *J* is the Shannon Weaver equitability index and LN n_i is the natural log of the total number of species in a lane.

2.14 Metagenomics analyses

2.14.1 Whole genome amplification (WGA)

Following genomic DNA extraction (Section 2.11.1) using a bead beating and chemical lysis (PowerSoil™ DNA isolation Kit; MOBIO Laboratories), library construction couldn't be carried out using the original DNA extracts due to the small amount of DNA extracted. As a consequence of the low microbial DNA biomass extracted from these soils, DNA was amplified using the multiple strand displacement Phi29 DNA amplification kit (GenomiPhi v2 kit; GE Healthcare Life Sciences), in order to produce sufficient amount of DNA required for sequencing (i.e. 200 ug of starting material was needed according to Ion Xpress Plus gDNA fragment Library preparation) before proceeding to library construction (Abbai et al. 2012). The WGA was performed according to the protocol of GenomiPhi v2 amplification kit protocol. DNA quality and concentration were quantified using NanoDrop 2000 (Table A1.3 in Appendix 1) and later a Qubit® 2.0 Fluorometer (dsDNA HS Assay kit; Invitrogen Life Technologies) was used to determine the volume of input DNA for Ion Xpress library construction. Approximately, about 200 ug of high molecular weight DNA starting material was required to sequence between 100-200 base pairs on Ion Proton.

2.14.2 Preparation of sequencing libraries

Extracted DNA was amplified using a WGA kit. This product was used as the starting materials for all soil libraries according to Ion Plus Fragment Library Kit. The initial step in the library preparation is the fragmentation and purification of gDNA with Ion Shear™ Plus Reagents. During this time, the Ion Shear™ reaction is optimised to yield high quality gDNA to be adapter-compatible (Chen et al. 2014). In the second stage, ligation of adapters, nick-repair, and purification of the ligated DNA with Ion Xpress™ P1 adapter and a Barcode (16 off-the-shelf barcodes for DNA) as specified in the protocol was performed. This was followed by size-selection of the unamplified library running E-Gel® Sizeselect™ Agarose Gel (150 to 220 base pairs for Ion Proton) and amplification of the size selected DNA library through 9 cycles of PCR. All eight libraries (one soil), if possible were pooled together as one sample since each sample was assigned a unique barcode at the ligation stage. This was done by bringing all libraries to the same concentration after quantifying the concentration of each library using Qubit Fluorometer. The library size distribution was confirmed by quantifying all prepared libraries using Agilent Bioanalyzer 2100. The size (bp), concentration (pg/µl) and molarity (pmol/l) of each library is determined at this stage before moving on to template preparation.

2.14.3 Template preparation (Ion PI™ Template OT2 200 Kit V3)

A template was prepared from the pooled libraries using the Ion PI template OT2 200 kit V3 with the Ion OneTouch 2 system. Template preparation was carried out according to Ion Proton manufacturer's standard protocol with a final concentration of 100 pM of the pooled libraries. According to V3 user guide, the template positive-Ion PI™ Ion Sphere ™ particles and was run overnight (6 hours) on OneTouch ™ 2 Instrument. The template-positive Ion PI ™ Ion Sphere™ particles was recovered and the washing of template-positive Ion PI was done according the V3 user guide. The recovered template-positive was enriched using the Ion OneTouch by following steps outlined in the protocol.

2.14.4 Ion PI sequencing preparation (Sequencing 200 kit V3)

Sequencing was performed according to the Ion PI™ sequencing 200 kit V3 with 100 pM of the pooled libraries. This was done by following the workflow represented in the sequencing manual guide to perform sequencing runs with the Ion Proton™ system. The sequencing involved creation of a planned run, cleaning of sequencing template (1 M of NaOH and Milli Q water), followed by an initialisation of sequencer, and loading of the Ion PI™ Chip v2 sequencing, followed by a run sequence (2-4 h) to generate a sequence of DNA reads. The Ion Proton system is equipped with the capability to remove primer dimmers and adapters after the run.

2.14.5 Data annotation and bioinformatics analyses

Metagenomic shotgun sequence reads generated by the Ion Proton sequencer were deposited on the Metagenomics Rapid Annotation Subsystem Technology (MG-RAST) server. MG-RAST is an online annotation service that uses the SEED algorithm in a standardized pipeline analysis of metagenomic DNA sequences. Raw sequence data were uploaded onto the MG-RAST server according to MG-RAST Manual version 3.3.6 annotation pipeline (Meyer et al. 2008). All data files were submitted to the MG-RAST interface in FASTQ format as per specification defined in the manual. A total of 34 FASTQ files from two microcosms were uploaded to the server on a separate four submission events: 8 files in the first submission; another 8 in the second; and 8 more files from the microcosm studies were submitted on the third submission event; and final submission constitute all of 10 files from altenative microcosms. FASTQ reads were processed using the quality control (QC) default MG-RAST parameters according to the protocol in the MG-RAST Manual version 3.3.6. The FASTQ only

employed filtering of dynamic trimming to remove low quality sequences with a specific lower phred score that will be counted as the high-quality base (15 -5 bases) and sequences will be trimmed to contain at most this many bases below the above specified quality. The FASTQ format was used to filter low-quality regions from the 3' end with common filtering options of dereplication to remove artificial sequences produced by sequencing artifacts (Filter to remove reads whose first 50 base pairs are identical) and screening of model organisms to remove any host specific species sequences (H.sapiencs, NCBI v36 to filter plant, human or mouse sequence matching with bowtie). The MG-RAST is the public free service used to determine functional and taxonomic relationships between metagenomic sequence reads and database sequences. SEED subsystem annotations were used to identify any features annotated with metabolism of aromatics biodegradation in conjunction with other database built in the MG-RAST system.

MG-RAST also implement automated BLASTX annotation of metagenomics sequence reads generated with Ion Proton to SEED non redundant database encompassing genome sequences organised into cellular functional assignment. As per version 3.0 of MG-RAST server, SEED comprises of three hierarchical levels for metabolism and six categories for taxonomy. The head map function of the MG-RAST version 3.0 was used to generate and display a normalised abundance of sequences matching varying categories with the Euclidean distance between profiles representing metagenomes with more closely related sequences being clustered in the same dendrogram. All taxonomy and functional reconstructions generated using MG-RAST version 3.0 had an E-value cut-off of 1×10^{-5} and a 50 bp minimum alignment length were further analysed by importing them into Statistical Analysis of Metagenomic Profiles (STAMP) package. This was specifically performed to test for statistically significant abundance differences at taxonomic and functional levels. P-values were determined in STAMP using the two sided Fisher's Exact test (Boissy et al. 2014), while confidence intervals were calculated using the Newcombe-Wilson method (Newcombe 1998). The false discovery rate was corrected by using the Storey's FDR method (Storey & Tibshirani 2003).

2.15 Statistical analyses

Statistical analyses were performed using data generated with MG-RAST interface. A number of statistical analyses such including hierarchical clustering, PCA, Bray-Curtis similarities and species biodiversity measures were conducted using taxonomic and functional generated abundance data from the MG-RAST server using statistical package PRIMER V6 for Windows

(version 6.1.6). Some of the key taxa contributing to the differences in the communities were identified using similarity percentage (SIPLER) analyses (Clark, 1993*)*.

Data generated from DGGE banding patterns analysed using Total Lab image software were further analysed using IBM® SPSS statistical package version 20 to produce principal component analysis (PCA). The PCA was performed using dimension reduction factor from the SPSS interface to determine the relationship of microbial communities sampled from four microcosms (Creo, TB, & AP soils) at four sampling time points (day 0, weeks 6, 18 and 42) over the course of incubation. Microsoft Office Excel (2010) was used to graph chemical data analysis presented in this thesis (PAH concentrations). Graphed values presented are mean with standard error as the measure of statistical accuracy of replicate samples taken from each microcosm at each time point.

Chapter 3

Treatability studies to assess bioremediation performance in three PAH impacted soils

3.1. Introduction

Bioremediation has been demonstrated at times to be, an effective remediation strategy for the treatment of PAH-contaminated soil. However, bioremediation efficacy is dependent on a number of variables including the availability of nutrients and the presence of PAH degrading organisms. In addition, the role played by microorganisms during bioremediation is influenced by physical and biological parameters present at PAH-contaminated sites. For example, key strategies to improve bioremediation processes involve the addition of seeded cultures with known PAH degrading organisms (bioaugmentation), or the addition of nutrients (e.g. nitrogen and phosphorus) (ENA). These strategies have the potential to enhance bioremediation rates (Tyagi, da Fonseca & de Carvalho 2011). Yu et al. (2005) compared the performance of NA, ENA and bioaugmentation during a 4-week PAH biodegradation experiment. At the end of the incubation period, the autochthonous microorganisms were able to degrade more than 99% of fluorene and phenanthrene (340 ± 16 and 347 ± 16 mg/kg respectively) and approximately 30% of pyrene (397 ± 15 mg/kg) in NA slurry experiments (Yu, K et al. 2005). While the extent of PAH biodegradation was increased under ENA conditions, (97% removal of LMW and HMW PAHs), bioaugmentation did not improve PAH bioremediation efficacy due to the inability of the supplemented bacterial consortium to compete with the indigenous population. The authors reported inhibition of the inoculated bacterial consortium as a result of negative interactions with the indigenous microbial community (Yu, K et al. 2005). These results indicated that nutrient amendments could enhance biodegradation of both LMW and HMW PAHs provided microorganisms were present with PAH catabolic potential. A similar study was conducted by Tam and Wong (2008), in which they compared the efficacy of NA and bioaugmentation strategies to remediate mangrove sediment spiked with phenanthrene (30 mg/kg), pyrene (30 mg/kg) and B(a)P (3 mg/kg). At the end of the 154-day incubation period, Tam and Wong (2008) reported that NA microcosms achieved better contaminant removal than bioaugmented microcosms, with 80%, 68% and 32% of phenanthrene, pyrene and benzo(a)pyrene removed respectively. Bioaugmentation demonstrated little enhancement as the augmented PAH-degrading organisms could not compete with autochthonous microorganisms (Tam & Wong 2008). Tam and Wong (2008), suggested that the lack of mutual interactions between the newly

introduced and native microbial communities may have played a negative role in the bioremediation of the mangrove sediment spiked microcosms. Moreover, other studies have reported similar antagonistic effects between augmented and native soil microbiota during bioremediation of PAH-contaminated soils (Lladó, S et al. 2013; Yu, K et al. 2005; Yu, S et al. 2005). These studies found that bioaugmented microorganisms were unable to acclimatise and adapt to their new environments and had little impact on PAH removal. Another reason why bioaugmented PAH-degrading organisms had little impact on PAH removal was that mangrove sediments had a sufficient native microbial population with an intrinsic ability to biodegrade PAHs.

3.2. Assessment of PAH-contaminated soil using different bioremediation strategies

In this chapter, PAH-contaminated soil treatability studies were undertaken using different bioremediation strategies in laboratory microcosm experiments. The microcosm experiments were conducted at bench scale over a period of 42 weeks. In this chapter, changes in PAH concentration following 42 weeks of incubation are reported. Bioremediation treatability was assessed using a number of strategies including:

- Natural attenuation (NA): where the intrinsic properties of the soil were used without additional stimulation. The underlining assumption here was that there should be PAH-degrading microorganisms in the soil due to the enrichment effect of long-term PAH exposure. However, biodegradation may be limited due to the lack of nutrients.
- Enhanced natural attenuation (ENA): where nutrients were supplemented to PAH-contaminated soil to achieve a C: N: P molar ratio of 100: 10: 1. In these microcosms, the introduction of nutrients was employed to accelerate the rate and extent of PAH degradation.
- Bioaugmentaion (BioA): where specific-PAH degrading microorganisms, supplied in the form of an inoculant was augmented in PAH-contaminated soil to enhance the biodegradation capacity of the indigenous microflora. *Mycobacterium gilvum,* a known PAH degrader (Mao et al. 2012), was introduced into these microcosms.
- Bioaugmentation and ENA (Comb): a mixed microcosm was prepared by combining the inoculant and nutrients (C: N: P molar ratio of 100:10:1).

Combining nutrients with the inoculant was anticipated to be more effective than where each was added separately.

3.3. Aim of the treatability study

The overall aim of the treatability study was to determine PAH bioremediation performance using soil amendment strategies in three distinct PAH-contaminated soils.

More specific objectives were:

- To compare the degradation of three-selected individual PAH compounds with three (phenanthrene), four (pyrene) and five (B(a)P) aromatic rings in 3 soils over the incubation time course.
- To compare the overall changes in total PAH concentration in 3 soils following 42 weeks of incubation.

3.4 Hypothesis

It was hypothesised that although PAH-degrading organisms may be present in all 3 aged PAH-contaminated soils, the lack of nutrients and / or specific PAH catabolic capacity may limit the effectiveness of the NA strategy.

3.5 Soils characterisation

In this study, 3 aged PAH-contaminated soils polluted from 3 distinct sources were utilised. The 3 aged PAH-contaminated soils were characterised to determine total PAH concentration and selected physio-chemical properties. Soils used in this study were sourced from the CERAR-UniSA soil repository: previously they were collected from PAH-contaminated sites which included; a former wood preservative plant (designated 'Creo'), a former manufacturing gas plant site (designated 'AP'), and a tram maintenance facility (designate 'TB'). Soil PAHs were identified using USEPA Method 8100 (USEPA) while selected physio-chemical properties (soil texture, pH, SOM, WHC, total nitrogen and phosphorous) were determined using standard methodologies (See Material and Method Sections 2.4 - 2.7).

Table 3.1 shows the concentration of individual PAHs in Creo, AP and TB soils while Table 3.2 shows selected soil properties. Total PAH concentration ranged from 494.9 ± 31 mg/kg (AP) to 1070 ± 102 mg/kg (Creo). The concentration of individual PAHs was variable (Table 3.1). Three ring PAHs were present in all soils albeit at low concentrations. Of these compounds, phenanthrene and anthracene were detected at the highest concentration ranging from 24 ± 1.8 mg/kg in Creo (anthracene) to 94 ± 1 mg/kg in TB (phenanthrene). Three ring

compounds comprised 5.8, 19.6 and 22.2% of the total soil PAH concentration in Creo, AP and TB respectively.

In contrast, the concentration of four-ring PAHs comprised 55.4, 49.7 and 44.8% of the total PAH concentration in the Creo, AP and TB soils respectively. Of the four-ring compounds, the concentration of fluoranthene (85 ± 1 to 136.5 ± 13 mg/kg) and pyrene (74 ± 0 to 177 ± 18 mg/kg) were elevated in all 3 soils in addition to chrysene (196 ± 26 mg/kg) in the Creo. Moreover, five-ring compounds comprised 31.3, 20.5 and 22.4% of the total PAH concentration in the Creo, AP and TB soils respectively. Of the five-ring compounds, benzo(a)pyrene (48 ± 1 to 69 ± 5 mg/kg) and benzo(b)fluoranthene (41 ± 1 to 175 ± 9 mg/kg) were elevated in all 3 soils while benzo(k)fluoranthene (38 ± 6 to 77 ± 11 mg/kg) was elevated in the TB and Creo soils.

Six-ring compounds comprised 7.5, 6.5 and 10.6% of the total soil borne PAHs in the Creo, AP and TB soils respectively. The six-ring compounds, indeno (1, 2, 3-cd) pyrene and benzo (g, h, i) perylene were detected at elevated concentration ranging from 16 ± 11 mg/kg in the AP to 42 ± 3 mg/kg in the Creo soil.

Importantly, B(a)P was consistently found at concentrations exceeding the National Environmental Protection Measure for the Assessment of Site Contamination (NEPM-ASC) of human health investigation level of 3 mg/kg for residential areas (NEPM, 2013) .

Besides assessing total PAH content in all 3 soils, selected properties and physicochemical characteristics were determined as detailed in Table 3.2. Although there was variability in the proportion of sand, silt and clay in the 3 soils, all were classified as sandy loams. However, significant variability in soil organic matter was observed, with values ranging from 2.3 (TB) to 13.2 % (AP) (Table 3.2). Soils were slightly acidic with pH values ranging from 6.0 (Creo) to 6.6 (AP and TB).

The total nitrogen and phosphorus were highly variable across all soils. The Creo and AP soils exhibited higher baseline nitrogen (2850 to 3775 mg/kg) and phosphorous (746 to 731 mg kg^{-1}) concentrations compared to nitrogen (424 mg/kg) and phosphorus (159 mg/kg) in the TB soil.

Table 3.1. Individual PAH concentration in 3 contaminated soils used in this project prior to the preparation of microcosm experiments.

PAH	Soil			
		Creo	AP	TB
	# of Rings	PAH concentration (mg/kg)		
Naphthalene	2	<2.5	18.4 ± 1.1	<2.5
Acenaphthylene	3	14.4 ± 1.3	14.0± 0.2	6.1 ± 0.5
Acenaphthene	3	3.3 ± 0.2	<5.0	5.6 ± 0.1
Fluorene	3	4.5 ± 0.4	4.3 ±1.6	5.6 ± 0.3
Phenanthrene	3	7.9.3 ± 1.6	81.8 ± 11.1	71.2 ± 1.4
Anthracene	3	23.6 ± 1.8	16.9 ± 0.4	29.3 ± 1.1
Fluoranthene	4	136.5 ± 13.4	84.7 ± 1.4	99.7 ± 6.1
Pyrene	4	137.0 ± 18.4	105.3 ± 0.3	97.9 ± 5.2
Benz(a)anthracene	4	83.6 ± 7.6	46.7 ± 7.1	47.5 ± 3.3
Chrysene	4	196.0 ± 25.5	40.3 ± 3.9	44.1 ± 3.0
Benzo(b)fluoranthene	5	174.5 ± 9.2	59.0 ± 4.2	40.9 ± 0.6
Benzo(k)fluoranthene	5	77.3 ± 11.5	59.0 ± 4.2	37.9 ± 6.3
Benzo(a)pyrene	5	69.5 ± 5.7	54.8 ± 1.4	48.1 ± 4.2
Dibenz(a.h)anthracene	5	15.4 ± 1.3	7.4	13.2 ± 1.6
Indeno(1,2,3-cd) pyrene	6	41.9 ± 3.4	16.1 ± 10.5	31.4 ± 2.6
Benzo(ghi)perylene	6	38.8 ± 3.0	15.9 ± 8.9	35.8 ± 3.4
Sum of 16 PAHs		1070 ± 102	495 ± 31	633 ± 40

Table 3.2. Summary of selected soil properties for PAH-contaminated soils utilised in this study.

Soil parameter*	PAH-contaminated Soil		
	Creo	AP	TB
Sand (%)	78	88	84
Silt (%)	12	4	4
Clay (%)	10	8	12
SOM (%)	3.4	13.2	2.3
Total Nitrogen (mg/kg)	2850 ± 53	3775 ± 68	424 ± 17
Total phosphorous (mg/kg)	746 ± 12	731 ± 49	159 ± 10
WHC (%)	37.8	27.2	33.5
pH	6.0	6.6	6.6

*Values represent the mean of triplicate analyses. WHC water holding capacity. SOM soil organic matter.

3.6 Assessment of PAH biodegradation in soil microcosms

PAH biodegradation experiments were performed in order to assess the efficacy of bioremediation strategies for the degradation of PAHs in contaminated soils. Biodegradation microcosms were prepared with Creo, TB and AP soils as described in section 3.1 with changes in PAH concentration determined periodically over a 42-week incubation period. Comparison of results showing changes in total PAH concentration for all soils and 3 selected individual compounds (phenanthrene, pyrene and B(a)P are presented in Figures 3. 1 to 3.15.

3.6.1 Creo microcosms

The total PAH concentration in samples collected at each time point were calculated with average and standard error plotted as a function of time. Figure 3.1 shows changes in the total PAH concentration in unamended (NA) and amended (ENA, BioA and Comb) Creo soil microcosms following 42-weeks of incubation.

In the NA microcosms, the initial PAH concentration appears to reduce from 1018 ± 23 mg/kg (Day 0) to 904 ± 38 mg/kg over the course of experimental incubation (42 weeks). Although an 11.2% reduction in PAH concentration was observed in NA microcosms over the 42-week incubation, it appears that the degradation mostly occurred during the first 6 weeks of incubation (10.7% reduction from day 0 to week 6). Regardless of the small reduction in total PAH concentration over the 42 week incubation period, there was no statistically significant change in total PAH concentration ($P > 0.05$) in NA microcosms when initial and final concentrations were compared.

In contrast, in microcosms where nutrients were added, the initial PAH concentration decreased from 1018 ± 23 mg/kg (day 0) to 856 ± 18 mg/kg after 42-week incubation period. Unlike the other bioremediation strategies, the ENA treatment showed the highest degradation of PAH with a 16% reduction in total PAH concentration achieved at the end of 42 weeks incubation. More than half of the total PAH concentration removed from this microcosm was observed in the first 6 weeks (9.4%). The decrease was significant when compared to the NA strategy, however, this reduction was not significant in terms of overall PAH biodegradation (at $P < 0.05$).

Similar results were observed in the bioaugmented microcosms (BioA with an overall 12.2% reduction in total PAH concentration), however, the reduction in PAH concentration was

similar to the ENA treatment (16%). Statistical analysis showed no significant difference between ENA and Combined microcosms ($P > 0.05$) when the extent of PAH removal was compared at week 42. However, a significant difference was observed in total PAH degradation in ENA42, BioA42, NA42, NA6 and BioA6 microcosms ($P < 0.05$) compared to Comb6, in which no degradation was observed from day 0 to week 6 (Figure 3.1).

In comparison, PAH removal was minimal (an overall reduction of 4.9%) in the combined microcosms (ENA plus BioA) over the 42-week incubation period. Generally, there was no significant difference in the extent of PAH removal between ENA and Comb microcosms over the 42-week incubation period ($P > 0.05$).

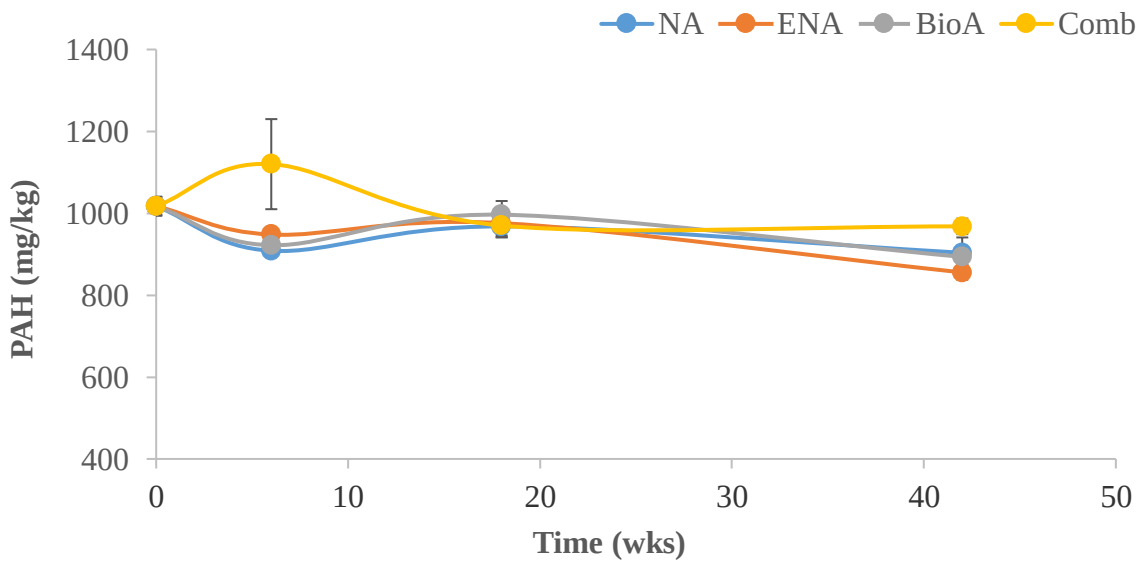

Figure 3.1. Change in total PAH concentration in Creo soil microcosms following 42 weeks incubation under natural attenuation (NA), enhanced natural attenuation (ENA), bioaugmentation (BioA), and combined treatment (Comb). The plot displays average PAH concentration (mg/kg) with standard error (± SE) in samples periodically removed from microcosms at four selected time points (Day 0, weeks 6, 18 and 42).

3.6.2 Comparison of phenanthrene, pyrene, and B(a)P degradation in Creo microcosms

Degradation of phenanthrene, pyrene and B(a)P was compared in the Creo soil microcosms over a 42-week incubation period. Changes in the concentration of individual compounds are presented in Figures 3.2 to 3.4. In all microcosms except Comb microcosm (NA, ENA, and BioA), small changes in phenanthrene concentration (Figure 3.2) were observed after 6 weeks of incubation (e.g.12%, 15.8% and 16.5% in NA, ENA and BioA). Excluding the combined

treatment, the phenanthrene concentration in the other microcosms was reduced from 8.0 ± 0 to 7.0 ± 0 mg/kg after 6 weeks incubation.

There was no significant difference between phenanthrene removal for the NA, ENA, and BioA treatments ($P > 0.05$) in this incubation period.

No further decrease in phenanthrene concentration was observed over the remaining incubation period for NA (final concentration of 7.0 ± 1 mg/kg), however, for ENA, BioA and Comb treatments phenanthrene concentration at the end of the 42-week incubation period was reduced to 4.9 ± 0, 4.8 ± 0 and 5.4 ± 0 mg/kg (ENA, BioA and Comb treatments respectively) in Creo soil (Time 0 to week 42). Although the bioremediation approach was different for these 3 strategies, there was no significant difference observed ($P > 0.05$) in phenanthrene concentration removal at the end of the incubation period.

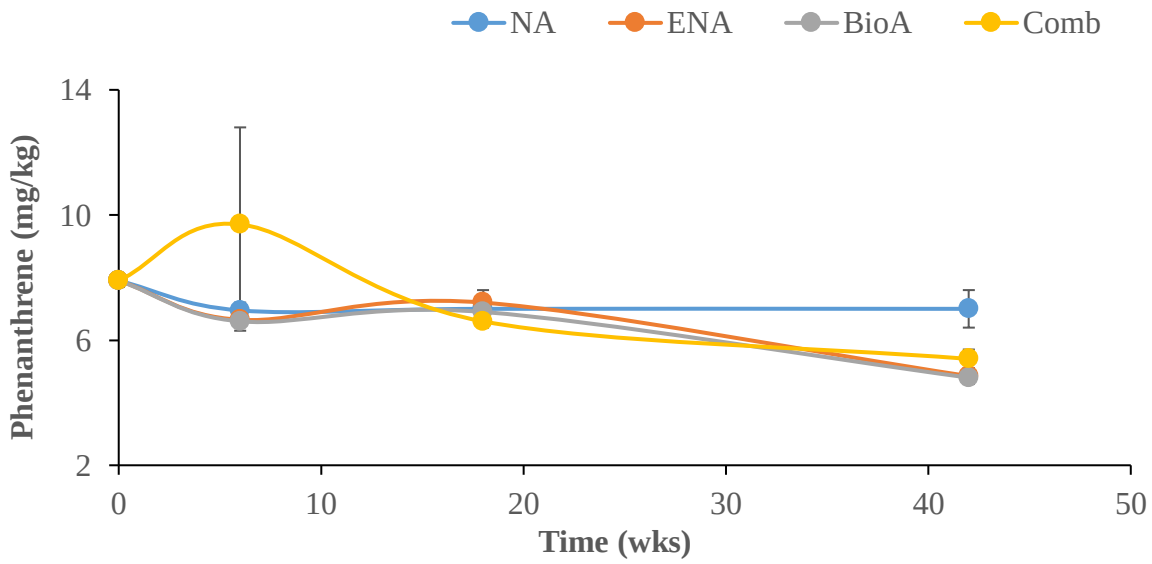

Figure 3.2. Change in phenanthrene concentration in Creo soil microcosms following 42 weeks of incubation under natural attenuation (NA), enhanced natural attenuation (ENA), bioaugmentation (BioA) and combined treatment (Comb) strategies. The plot displays average phenanthrene concentration (mg/kg) with standard error (± SE) in samples periodically removed at four selected time points (Day 0, weeks 6, 18 and 42).

Data showing pyrene degradation in Creo microcosms is presented in Figure 3.3. The initial pyrene concentration was 137 ± 7 mg/kg, however, after 6 weeks incubation period (Figure 3.3 and Table A2.1 in Appendix 2) pyrene concentration was reduced between 8 and 20% depending on the treatment strategy employed. While some variability in pyrene concentration was observed (notably at week 6 in BioA microcosms), there was no statistical different

between pyrene concentrations at time zero and week 6, for NA, ENA and Comb microcosms ($P > 0.05$).

At week 18, further decreases in pyrene concentration were observed (111 ± 3, 106 ± 2, 108 ± 3 and 106.5 ± 0 for NA, ENA, BioA, and Comb respectively) although there was no significant difference ($P > 0.05$) in pyrene concentration between treatments and samples obtained at different time points. Similarly, at week 42, pyrene concentration for NA, ENA, BioA and Comb was reduced to 99.9 ± 1, 97.6 ± 1, 100.1 ± 7 and 106 ± 2 mg/kg respectively. However, once again there was no significant difference in treatment efficacy between applied bioremediation strategies.

In comparison to the 3- and 4-ring compounds, there were small decreases in benzo(a)pyrene (5-ring compound) concentration over the 42-week incubation period (Figure 3.4), however, the final benzo(a)pyrene concentration in all microcosms was not significantly different to the initial (day 0) concentration (69.5 ± 2 mg/kg).

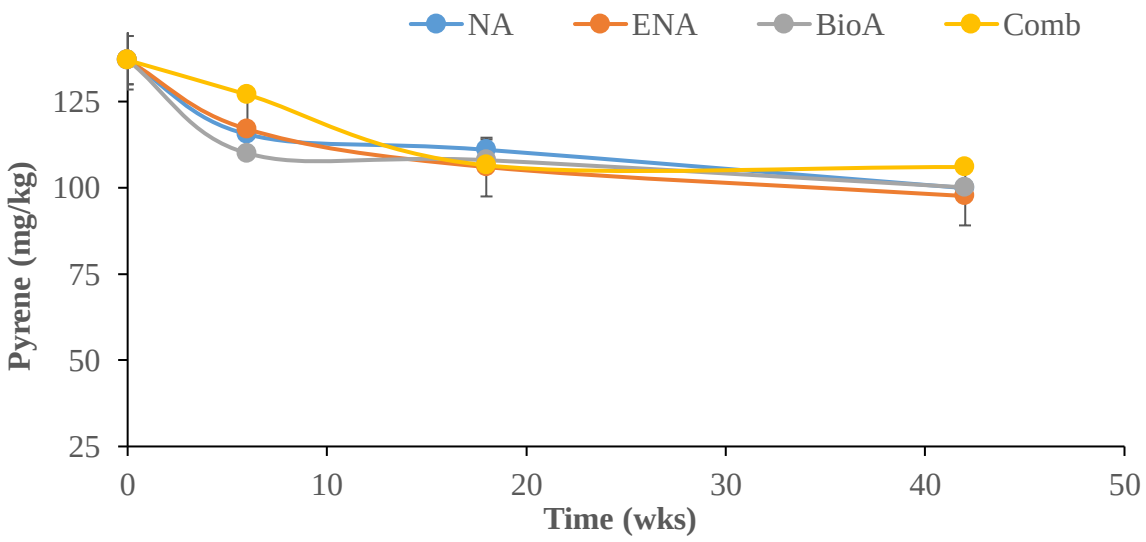

Figure 3.3. Change in pyrene concentration in Creo soil microcosms following 42 weeks of incubation under natural attenuation (NA), enhanced natural attenuation (ENA), bioaugmentation (BioA) and combined treatment (Comb) strategies. The plot displays average pyrene concentration (mg/kg) with standard error (± SE) in samples periodically removed at four selected time points (Day 0, weeks 6, 18 and 42).

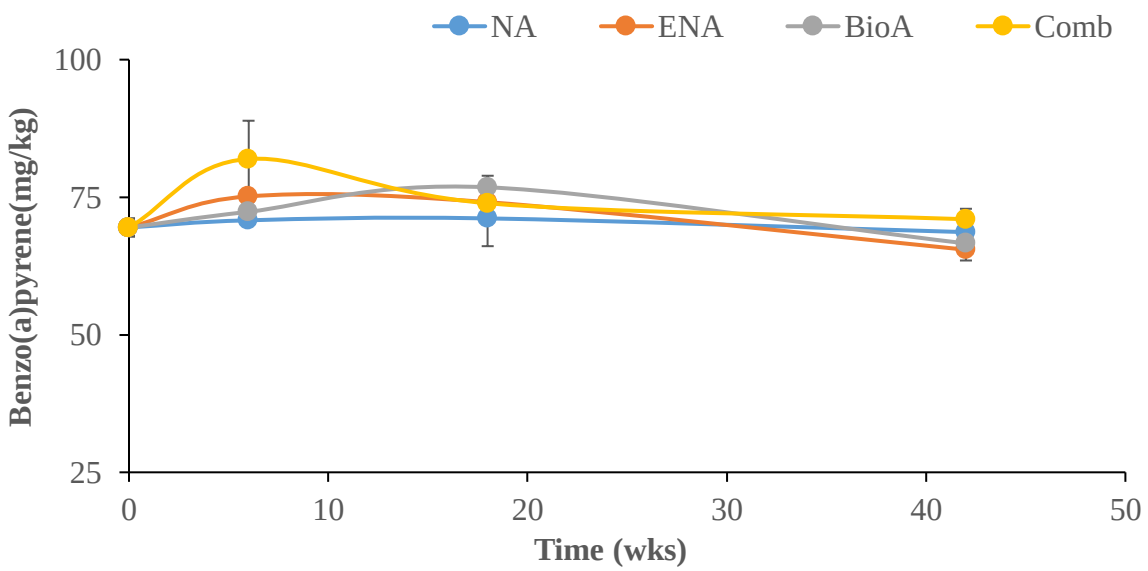

Figure 3.4. Change in B(a)P concentration in Creo soil following 42 weeks of incubation under natural attenuation (NA), enhanced natural attenuation (ENA), bioaugmentation (BioA) and combine treatment (Comb) strategies. The plot displays average B(a)P concentration (mg/kg) with standard error (± SE) in samples periodically removed at four selected time points (Day 0, weeks 6, 18 and 42).

3.6.3 Enumeration of PAH degrading population in Creo microcosms

A most probably number (MPN) method encompassing BSM and NB (Figure 3.5) media supplemented with phenanthrene as the sole carbon and energy source was employed to estimate PAH-degrading bacteria in the microcosm treatments (Yu, K et al. 2005). Similar methods of evaluating specific hydrocarbon-degrading populations have been applied elsewhere to enumerate heterotrophs (Papen & Von Berg 1998), aromatic-degrading organisms (Heitkamp & Cerniglia 1986), and ammonia-oxidizing microorganisms (Rowe, Todd & Waide 1977). The growth of PAHs degrading bacteria populations were monitored following soil microcosm amendments. Soil samples periodically removed from each of 3 amended and unamended microcosms were utilized to evaluate microbial growth during bioremediation for the first 18 weeks. While biodegradation microcosms were incubated over a period of 42 weeks, MPN results were not able to be analysed for the final sampling event (week 42) due to cross contamination issues with MPN microtitre plates (Figure 3.5).

In the NA microcosm, a decrease in microbial numbers was observed over the incubation period. From an initial population of 7.2 x 10^7 cells/g, microbial numbers decreased to 12 cells/g at week 18.

In contrast, in microcosms where an ENA treatment strategy was implemented, microbial numbers remained stable (7.2 x 10^7 cells/g) for the 13 week of incubation period. However,

further incubation resulted in a decrease in microbial numbers, resulting in a PAH degrading population of 3.0 x 10^3 cells/g at week 18. Similar results were observed for BioA and Comb microcosms (Comb), however, the decrease in microbial numbers at week 18 (4.0 x 10^4 and 5.0x 10^5 cell/g respectively) was not as severe as in the ENA microcosm treatments.

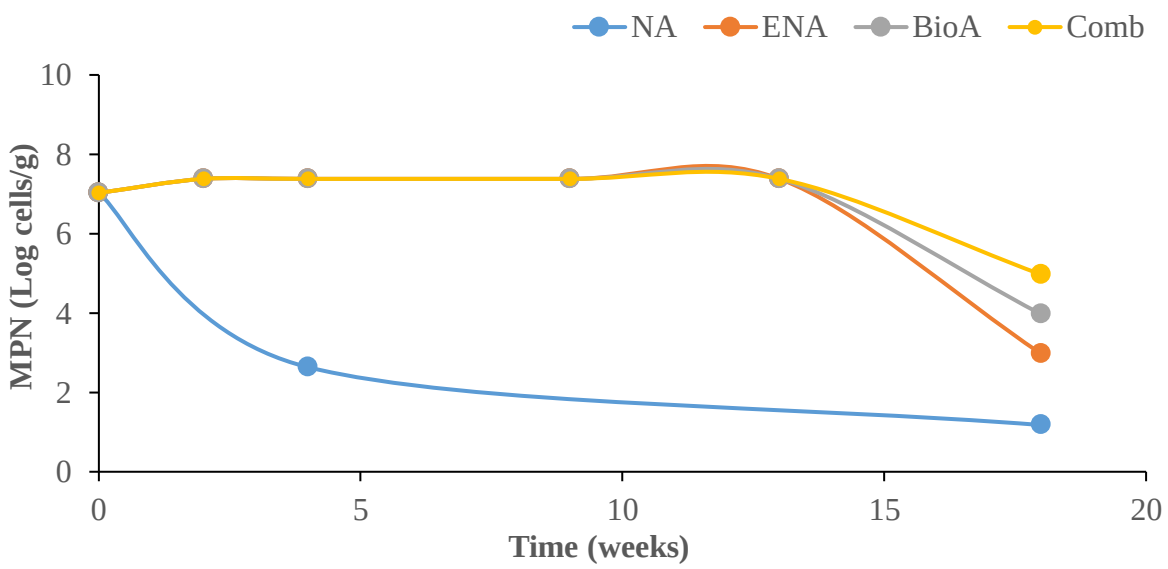

Figure 3.5. Determination of microbial populations in Creo soil microcosms using a most probable number technique (nutrient broth media). Data is presented as log MPN [Log cells/g] with coloured bars showing population from unamended (NA) and amended (ENA, BioA and Comb) microcosms.

3.6.4 TB microcosms

Total PAH concentration determined in samples taken from each time point in TB microcosms were calculated with average and standard errors plotted as a function of time. Figure 3.6 shows change in total PAH concentration from unamended (NA) and amended (ENA, BioA and Comb) TB soil microcosms following 42-weeks of incubation. In all microcosms, regardless of treatment strategy, negligible change in total PAH concentration was observed. The largest change in total PAH concentration was observed in the Comb microcosm, with a 4.4% reduction achieved at the end of the incubation period (from 569 ± 13 mg/kg to 544 ± 43 mg/kg at week42). However, there was no statistical difference between initial and final PAH concentration in unamended and amended microcosms ($P > 0.05$).

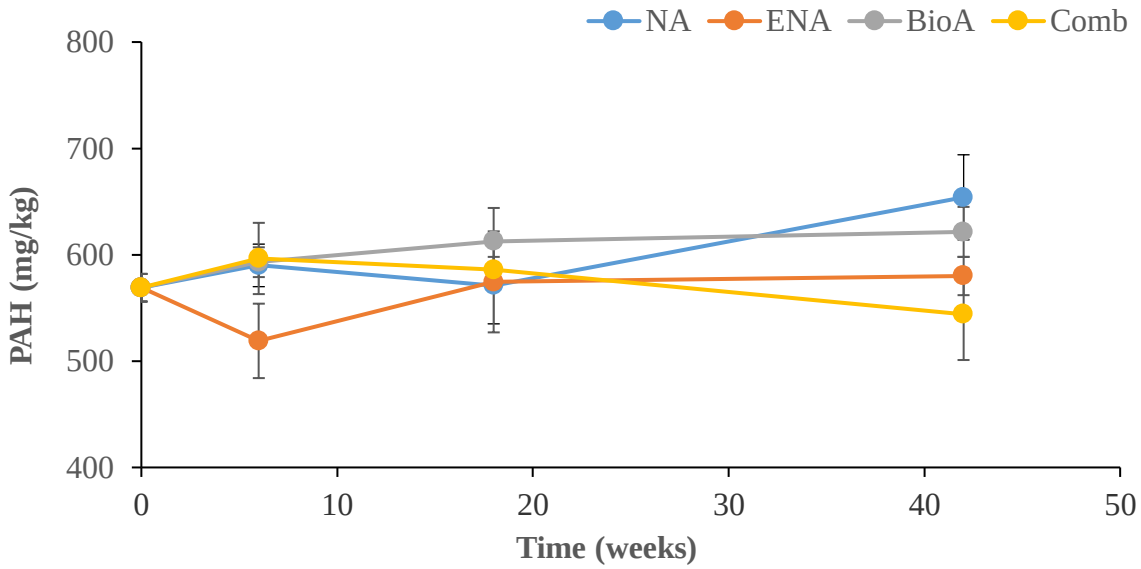

Figure 3.6. Change in total PAH concentration in TB soil microcosms following 42 weeks incubation under natural attenuation (NA), enhanced natural attenuation (ENA), bioaugmentation (BioA) and combined treatment (Comb) strategies. The plot displays average PAH concentration (mg/kg) with standard error (± SE) in samples periodically removed at four selected time points (Day 0, weeks 6, 18 and 42).

3.6.5 Comparison of phenanthrene, pyrene and B(a)P degradation in TB microcosms

Degradation of individual compound (phenanthrene, pyrene and B(a)P) was compared in TB soil microcosms over the 42-week incubation period. Changes in the concentrations of individual compounds are presented in Figures 3.7 to 3.9.

Excluding the ENA microcosm, no reduction was observed in phenanthrene concentration during the first 6 weeks of incubation in NA, BioA and Comb microcosms. However, a small reduction was observed in phenanthrene concentration over the last two sample time points (weeks 18 and 42 respectively) in all microcosms with phenanthrene concentration in ENA42 (56.9 ± 0 mg/kg) and Comb42 (50.9 ± 4 mg/kg) significantly ($P < 0.05$) lower compared to concentrations at the start of microcosms studies (71.2 ± 3 mg/kg).

There was no significant difference between phenanthrene concentration in ENA and Comb microcosms ($P > 0.05$) at the end of the incubation period (week 42). In terms of degradation, NA and BioA (67.8 ± 7 and 62.8 ± 4 mg/kg) have showed less reduction compared to ENA and Comb (56.9 ± 0 and 50.9 ± 3 mg/kg) microcosms at week 42.

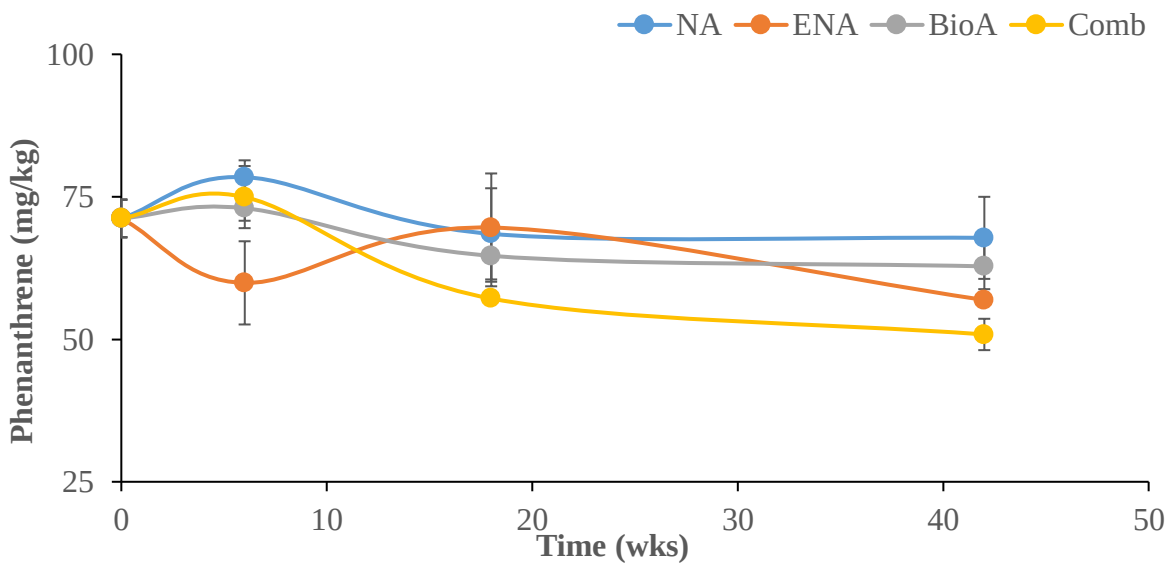

Figure 3.7. Change in phenanthrene concentration in TB soil microcosms following 42 weeks incubation under natural attenuation (NA), enhanced natural attenuation (ENA), bioaugmentation (BioA) and combined treatment (Comb) strategies. The plot displays average phenanthrene concentration (mg/kg) with standard error (± SE) in samples periodically removed at four selected time points (day 0, weeks 6, 18 and 42).

Data showing pyrene degradation is presented in Figure 3.8. No significant change ($P > 0.05$) in pyrene concentration was observed over the 42-week incubation period for both NA and BioA microcosms (final concentrations of 99.8 ± 4 and 97.7 ± 3 mg/kg), however for ENA and Comb treatments pyrene concentration at the end of the 42-week incubation period was 89.1 ± 3 and 85.4 ± 6 mg/kg respectively.

Despite the reduction in pyrene concentrations in the amended microcosms, there was no significant difference observed when values were compared to the initial pyrene concentration (97.9 ± 2 mg/kg) ($P > 0.05$). Similarly, there was no significant decrease ($P > 0.05$) in benzo(a)pyrene concentration over the 42 week incubation period in either microcosm.

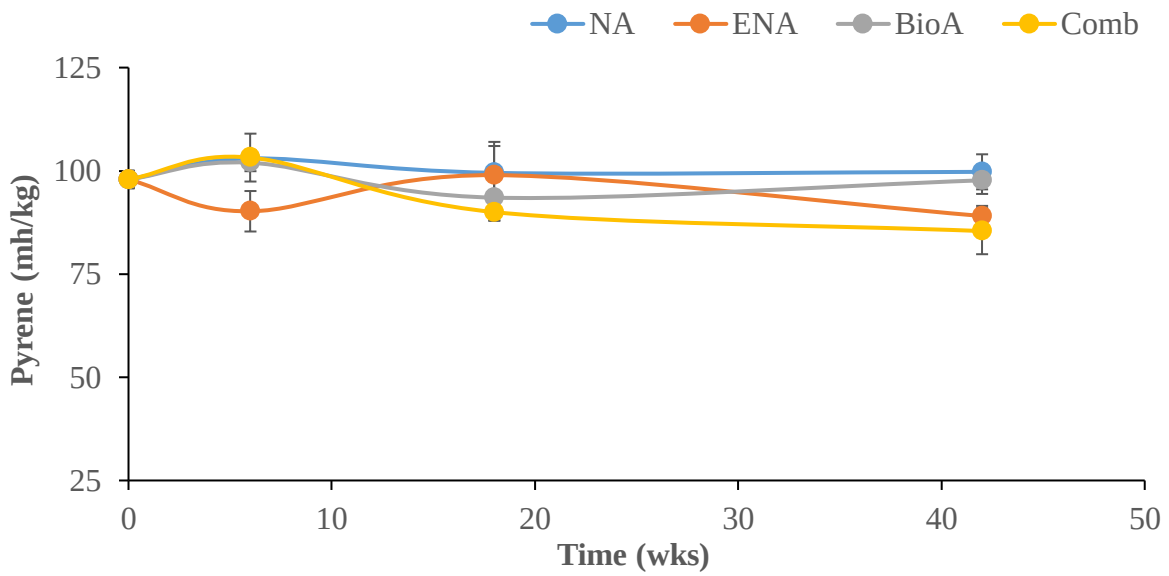

Figure 3.8. Change in pyrene concentration in TB soil microcosms following 42 weeks incubation under natural attenuation (NA), enhanced natural attenuation (ENA), bioaugmentation (BioA) and combined treatment (Comb) strategies. The plot displays average pyrene concentration (mg/kg) with standard error (± SE) in samples periodically removed at four selected time points (day 0, weeks 6, 18 and 42).

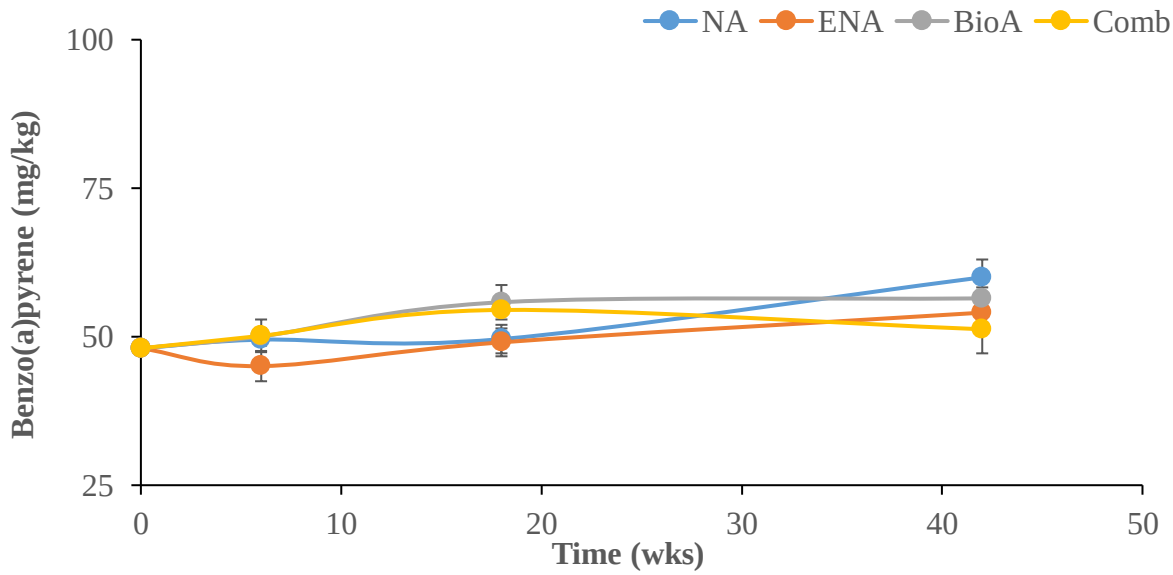

Figure 3.9. Change in B(a)P concentration in TB soil microcosms following 42 weeks incubation under natural attenuation (NA), enhanced natural attenuation (ENA), bioaugmentation (BioA) and combined treatment (Comb) strategies. The plot displays average B(a)P concentration (mg/kg) with standard error (± SE) in samples periodically removed at four selected time points (day 0, weeks 6, 18 and 42).

3.6.6 Estimation of PAH-degrading bacteria in TB soil using MPN

Evaluation of PAH-degrading organisms in samples periodically removed from each TB microcosms are presented in Figure 3.10. In the NA microcosm, a reduction in microbial numbers was observed over the incubation period from an initial microbial population size of 5.6 x 10^5 cells/g to 13 cells/g at week 18. In comparison, in the ENA treated microcosms, initial microbial numbers decreased from 7.0 x 10^7 cells/g to 5.4 x 10^5 cells/g at week 2. Nevertheless, microbial numbers remained consistent through to week 13 but then declined at week 18 (3.0 x10^3 cells/g).

In the BioA microcosm, the initial microbial population decreased from 6.0 x 10^6 cells/g to 3.6 x 10^3 cells/g at week 2. Despite an initial reduction, microbial numbers remained stable (3.6 x 10^3 cells/g) through to week 13 with an increase in population size at week 18 (5.4 x 10^4 cells/g). In microcosms where nutrients and inoculants was supplemented, a small increased in initial microbial numbers was detected. Microbial numbers increased from an initial population size of 5.0 x 10^5 cells/g to 6.0 x 10^6 cells/g at week 2. Further incubation resulted in stable microbial numbers to week 13 with a small decrease observed thereafter (5.0 x 10^5 cells/g at week 18).

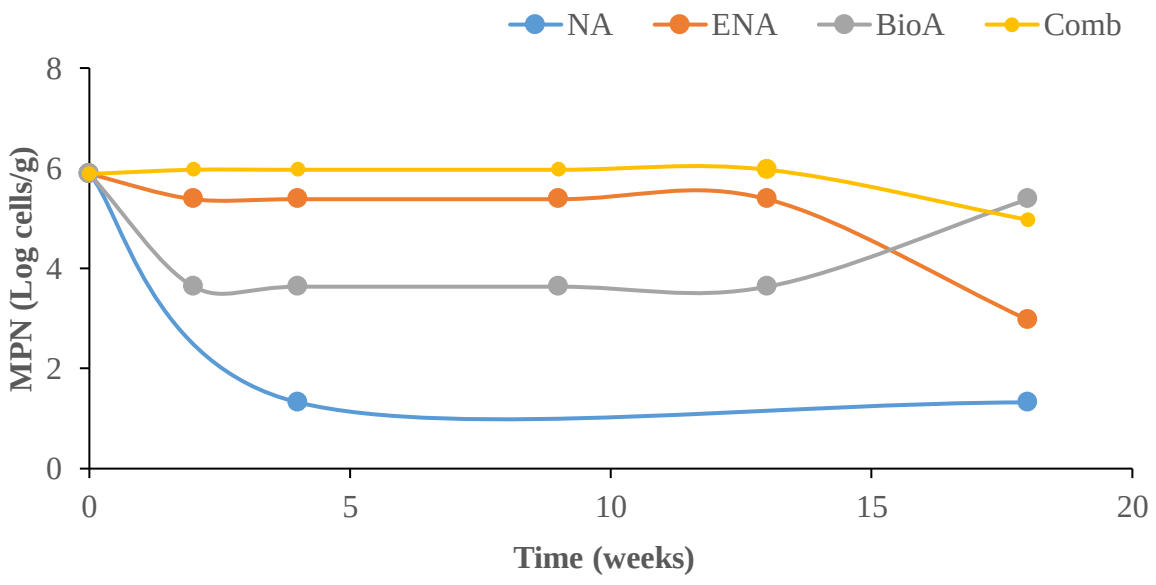

Figure 3.10. Determination of microbial populations in TB soil microcosms using most probable number technique (nutrient broth media). Data is presented as log MPN [Log cells/g] with coloured bars showing population from unamended (NA) and amended (ENA in red, BioA and Comb) microcosms.

3.6.7 AP microcosms

Figure 3.11 shows changes in total PAH concentration in unamended (NA) and amended (ENA, BioA and Comb) AP soil microcosms following 42-weeks of incubation. In all treatments, regardless of whether nutrients or microorganisms were added, no significant reduction ($P > 0.05$) in the total PAH concentration was observed over the 42-week incubation period.

3.6.8 Comparison of phenanthrene, pyrene, and B(a)P degradation in AP microcosms

In the AP microcosms, there was no significant change for either individual PAH compound over the 42-week incubation period compared to the initial concentration (Figures 3.12 to 3.14).

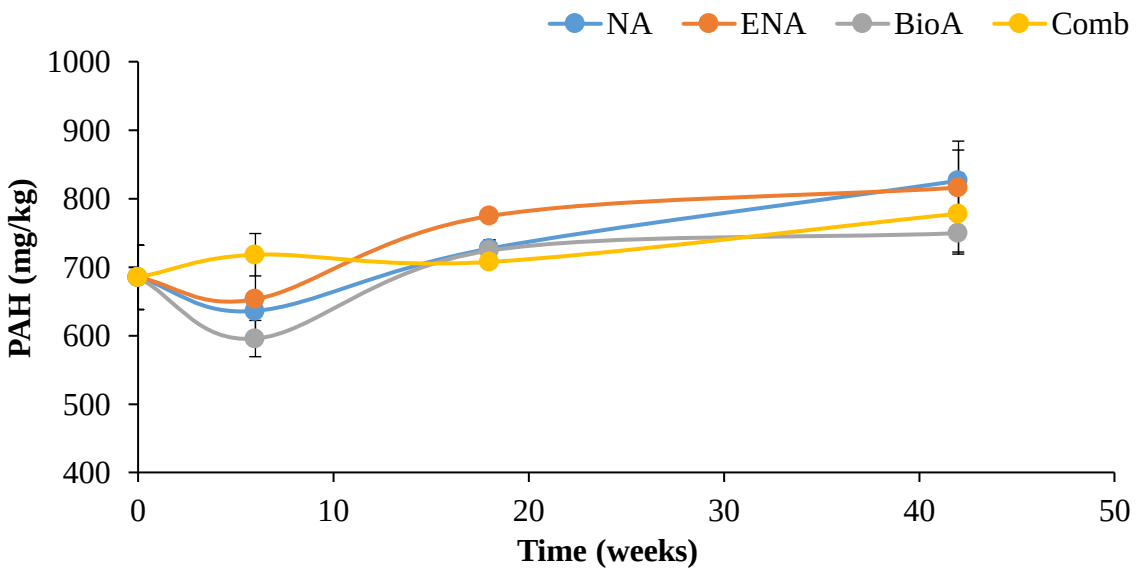

Figure 3.11. Change in total PAH concentration in AP soil microcosms following 42 weeks incubation under natural attenuation (NA), enhanced natural attenuation (ENA), bioaugmentation (BioA) and combined treatment (Comb) strategies. The plot displays average PAH concentration (mg/kg) with standard error (± SE) in samples periodically removed at four selected time points (day 0, weeks 6, 18 and 42).

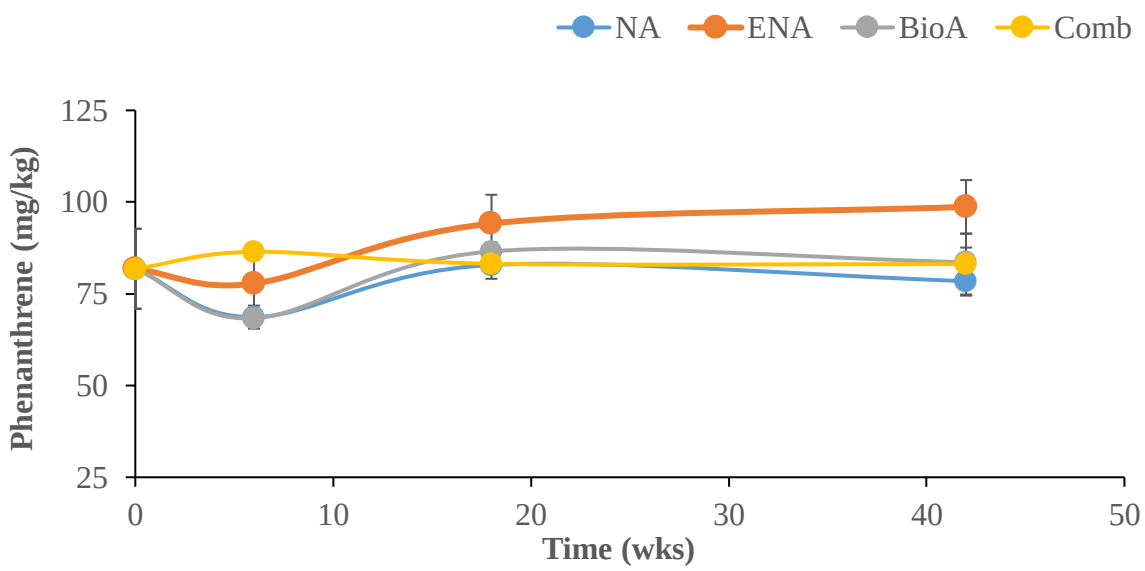

Figure 3.12. Change in phenanthrene concentration in AP soil microcosms following 42 weeks incubation under natural attenuation (NA), enhanced natural attenuation (ENA), bioaugmentation (BioA) and combined treatment (Comb) strategies. The plot displays average phenanthrene concentration (mg/kg) with standard error (± SE) in samples periodically removed at four selected time points (day 0, weeks 6, 18 and 42).

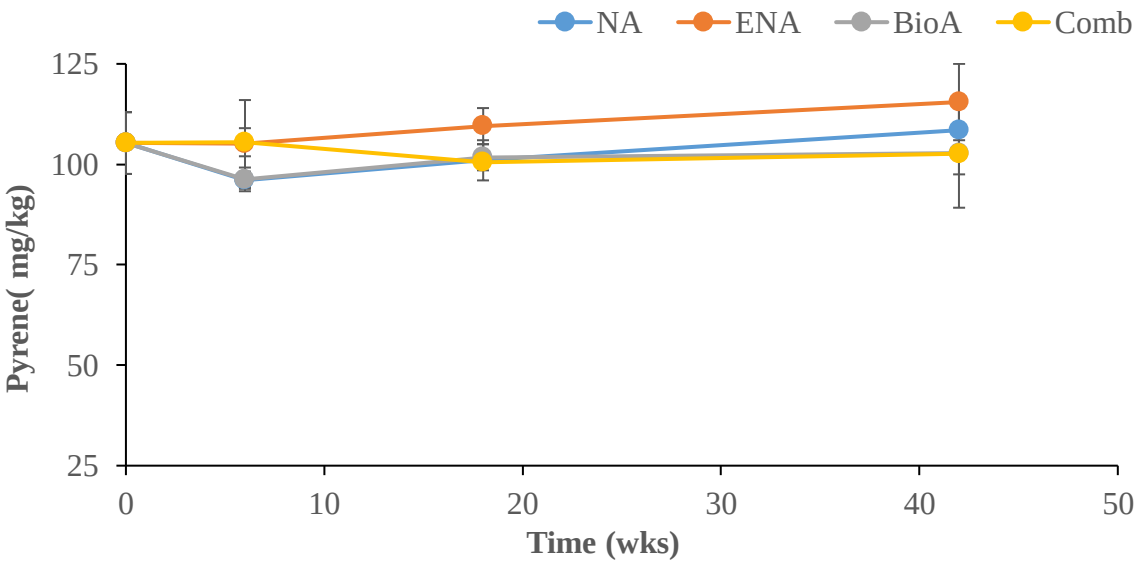

Figure 3.13. Change in pyrene concentration in AP soil microcosms following 42 weeks incubation under natural attenuation (NA), enhanced natural attenuation (ENA), bioaugmentation (BioA) and combined treatment (Comb) strategies. The plot displays average pyrene concentration (mg/kg) with standard error (± SE) in samples periodically removed at four selected time points (day 0, weeks 6, 18 and 42).

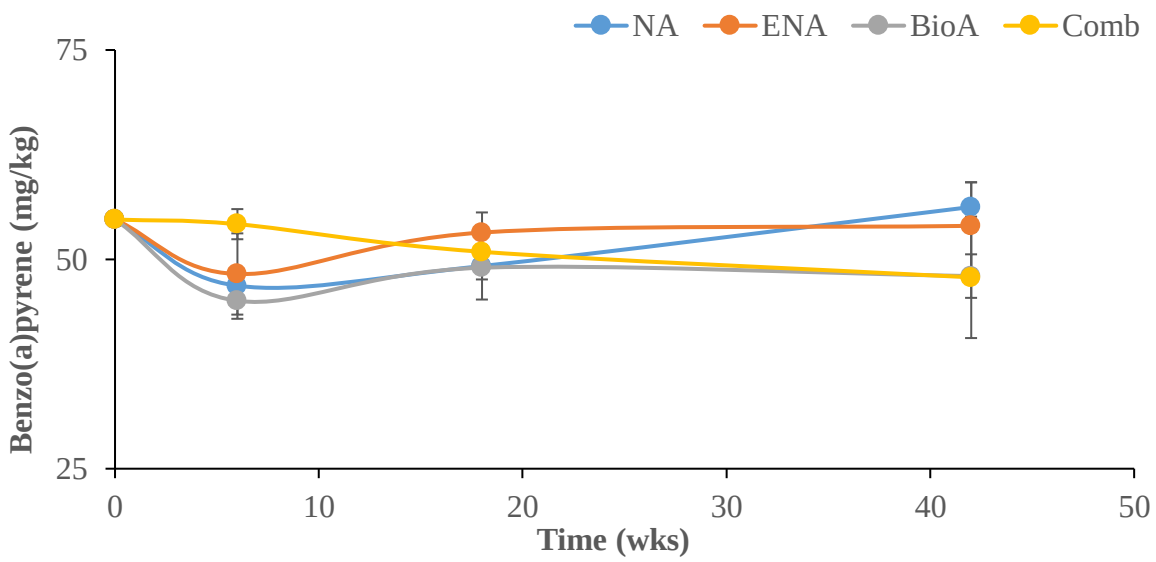

Figure 3.14. Change in B(a)P concentration in AP soil microcosms following 42 weeks incubation under natural attenuation (NA), enhanced natural attenuation (ENA), bioaugmentation (BioA) and combined treatment (Comb) strategies. The plot displays average B(a)P concentration (mg/kg) with standard error (± SE) in samples periodically removed at four selected time points (day 0, weeks 6, 18 and 42).

3.6.9 Estimation of PAH-degrading population in AP soil using MPN

Evaluation of PAH-degrading organisms in samples periodically removed from each microcosm are presented in Figure 3.15. In the NA microcosm, microbial numbers decreased over the course of incubation period. A steady reduction in microbial numbers from 3.4 x 10^3 cells/g to 0.3 cells/g was observed. In contrast, microbial numbers in ENA microcosms were stable over the initial 13 week of incubation. However, microbial numbers declined at week 18 (2.0 x 10^2 cells/g) resulting in a final population size of 4.0 x 10^4 cells/g. In contrast, in microcosms where nutrients and inoculants were implemented, microbial numbers increased from an initial microbial population size of 12 cells/g to 6.0 x 10^6 cells/g at week 2 and remained stable until week 13. However, a sharp reduction in microbial numbers was observed at week 18 resulting in a final population size of 2.6 x 10^2 cells/g.

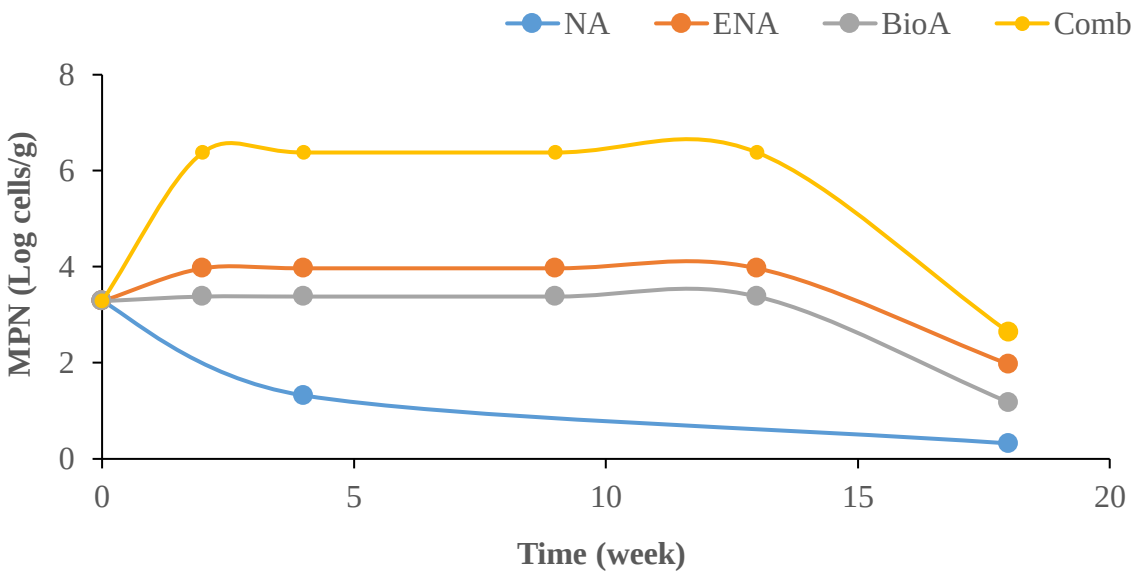

Figure 3.15. Determination of microbial populations in AP soil using a most probable number technique (nutrient broth media). Data is presented as log MPN [Log cells/g] with coloured bars showing population from unamended (NA) and amended (ENA, BioA and Comb) microcosms.

3.7 Discussion

Microbial degradation of PAHs is thought to be a major pathway leading to the reduction in PAH concentration at contaminated sites (Cerniglia 1992, 1993; Heitkamp & Cerniglia 1986). Numerous microorganisms have been identified with the capacity to utilise PAHs as carbon and energy sources and harnessing these microorganisms has provided an attractive strategy for site remediation. However, some HMW PAHs such as five - and six - ring compounds are recalcitrant to microbial biodegradation owning to their low water solubilities and resonance energy of their structures (Juhasz & Naidu 2000). In addition, the capacity of microbial communities to degrade LMW and HMW PAHs may be impaired by biological (microbial catabolic capacity), physico-chemical (desorbable or bioavailable fraction) and environmental parameters (e.g. nutrients availability, oxygen, moisture, temperature, pH and moisture). The catabolic capacity of microbial communities at contaminated sites may be enhanced by supplementation of nutrients (biostimulation) and/or inoculants (boiaugmentation) to increase the activity of microorganisms during bioremediation (Dixit et al. 2011; Mohan et al. 2006). In this chapter, the impact of amendment regimes on PAH-degradation was assessed in laboratory microcosm experiments. Soil microcosms were prepared with Creo, TB and AP soils as described in Section 3.1 with changes in PAH concentration determined over a 42-week incubation period. It was hypothesised that although PAH-degrading organisms may

be present in all three aged PAH-contaminated soils, the lack of nutrient availability would limit bioremediation effectiveness.

The initial concentration of the total 16 priority PAH compounds in three aged PAH-contaminated soils ranged from 494.9 ± 31 mg/kg (AP) to 1070 ± 102 mg/kg (Creo) while individual PAH concentrations in the soils remained (section 3.5). Despite biodegradable PAHs being present at elevated concentrations (As presented in Table 3.1), there was limited PAH removal in Creo, TB and AP soils under natural attenuation microcosms. Previous studies have reported degradation of PAHs by indigenous soil microbial communities under natural attenuation conditions (Makadia et al. 2011; Mueller, Chapman & Pritchard 1989; Mueller et al. 1991; Wang & Tam 2011; Whynot 2009). Makadia et al. (2011) reported a significant reduction in the total petroleum hydrocarbon (TPH) concentration (initial concentration of 2915 to 407.9 mg/kg) over an 84-day incubation period, observing an average removal of 86% in NA microcosms. In another study conducted by Juhasz et al. (2005) using aged Creo contaminated soil, indigenous microorganisms were able to reduce the total PAH concentration from 7767 ± 129 to 5579 ± 321 mg/kg (predominantly LMW compounds) under a natural attenuation strategy. Former industrial sites impacted with PAHs are thought to host a multitude of microorganisms that may possess the capacity to degrade these contaminants (Cébron et al. 2008). However, contrary to these studies, other researchers have reported limited PAH removal under natural attenuation similar to those reported here. Garcia-Delgado et al. (2015) reported a 17% reduction in PAH concentration after 42 days under a NA treatment in a Creo contaminated soil with an initial PAH concentration of 1212 ± 2 mg /kg.

It is known that microbial capacity to effectively utilise contaminants is affected by the soil's physio-chemical properties (including nutritional status, pH), contaminant concentration, aging, and environmental conditions such as moisture and temperature (İnceoğlu et al. 2011; Li et al. 2008; Yu, K et al. 2005). The lack of nutrient availability has been shown to limit the effectiveness of NA strategies. Analysis of soils used in this study identified that the TB soil had a lower nitrogen (N) and phosphorus (P) content compared to Creo and AP soils respectively (Table 3.2). Moreover, the limitation of N and P in the TB soil may be a contributing factor for the lack PAH degradation over the 42-week incubation period.
Number of studies have showed that biodegradation of LMW PAHs (e.g. phenanthrene) occurs more rapidly than HMW PAHs (Argumedo-Delira et al. 2012; Bezalel, Hadar & Cerniglia 1997; Johnson & Scow 1999; Kalantary et al. 2014; Ruberto et al. 2006). Yu et al. (2005)

observed that the biodegradation of phenanthrene (347 ± 2 ug/kg) after 4 weeks was slightly higher under a NA (99.7%) strategy compared to ENA (98.1%).There are several factors known to govern the process of PAH biodegradation. One of these factors is the availability of the contaminant. This affects the ability of degrading organisms as the contaminant may not be available for microbial biodegradation. The presence of microbial population with catabolic capacity to degrade PAHs, availability of nutrients, pH and other environmental conditions such as moisture, and temperature at the contaminated site are factors that influence biodegradation of PAH. In the current study, there was no significant difference observed in phenanthrene concentration at the commencement of the incubation compared to the end of the incubation period (Time 0 to week 42) in TB and AP microcosms under NA conditions ($P > 0.05$). In contrast, in the Creo soil a small (11.4%) but significant decrease in phenanthrene concentration was observed under NA conditions. Presumably, the Creo soil contained sufficient nutrients to stimulate microbial biodegradation compared to the TB and AP soils.

Similarly, a significant ($P < 0.05$) reduction in pyrene concentration was observed in the Creo soil under NA conditions at weeks 18 and 42 compared to time zero. Pyrene has been shown to be degraded by many microorganisms including *Mycobacterium sp, Rhodoccocus sp, Pseudomonas sp*, and *Bacillus vallismortis* via a well-documented metabolic pathway (Heitkamp, Franklin & Cerniglia 1988; Liang, Y et al. 2006; Ling et al. 2011; Sun, K et al. 2014). Grosser et al. (1991) reported that indigenous microbial communities were able to mineralise pyrene concentration in coal gasification plant soil, with reduction between 10 to 48% after 60 days of incubation period. The reduction in pyrene concentration under NA conditions in the Creo soil in this study illustrates the potential of this microbial community to degrade HMW PAHs. In contrast, there was no significant decrease in pyrene concentration in the TB and AP soil microcosms over the 42-week incubation period under NA conditions. The possible explanation why a reduction in pyrene concentration was observed in Creo soil may be due to lack of contaminant (pyrene) bioavailability for microbial biodegradation compared to TB and AP soils.

Presumably, the lack of PAH removal in NA TB and AP microcosms may have resulted from low microbial numbers (Figures 3.5, 3.10 and 3.15) as a consequence of low nutrient availability (N and P) (Bell et al. 2013; Kalantary et al. 2014). For effective microbial response to pollutants at a given site, microorganisms require the presence of mineral nutrients for cellular growth. As a consequence supplementation of N, P, and K have been suggested to

enhance microbial capacity to degrade hydrocarbons (Braddock et al. 1997; Juhasz, Waller & Stewart 2005). Degradation of benzo(a)pyrene was not observed in the three soils over the 42-week incubation period. This may be attributed to the aforementioned low nutrient availability, low microbial numbers and /or the recalcitrant nature of the five ring compound. Similarly, limited degradation of benzo(a)pyrene has been observed under NA conditions in other studies (Silva et al. 2009; Wu et al. 2008; Zhang et al. 2006). In general, Silva et al. (2009) observed no degradation of HMW-PAHs due to increasing contaminant-contact time with soil organic matter in microcosms over the 12-week incubation period, which is in accordance with results reported in this study (ageing effect).

Amendments are frequently used to enhance microbial biodegradation of PAHs as an alternative strategy to natural attenuation. This is usually achieved by supplementation of nutrients and/or introduction of PAH-degrading organisms to increase capacity of the indigenous population to remove contaminants (Grosser, Warshawsky & Vestal 1991; Hamdi et al. 2007; Liebeg & Cutright 1999; Nam, Rodriguez & Kukor 2001; Singh et al. 2011).
In microcosms where nutrients amendments were added, in an attempt to stimulate PAH degradation, limited PAH removal was observed above values recorded for NA treatments. This is in contrast to findings by other researchers where the addition of nutrients enhanced PAH degradation. Antizar-Ladislao et al. (2006) reported that in an aged coal-tar-contaminated soil with an initial PAH concentration (sum of 16 PAHs) of 100 mg/kg, microcosms supplemented with fresh green waste and fresh green waste compost resulted in a 75% and 62% removal in PAH concentration after 56 days of incubation. The authors demonstrated that supplementation with fresh green waste enhanced microbial activity and hence greater PAH degradation compared to compost amended with fresh green waste. This is presumably due to the fact that fresh green waste facilitated a higher oxygen transfer, which enhanced microbial activity than fresh green waste compost and this may explain why a higher reduction in PAH concentrations was observed in fresh green waste. Recently, a 91% removal in TPH concentration (20,000 to 1820 mg/kg) was observed following implementation of nutrients in an experiment incubated for 84 days to test for the possibility of remediated soil reuse for a new bioremediation strategy (Makadia et al. 2011). This study concluded that previously remediated soil possessed sufficient microbial hydrocarbon degrading capacity due to an extended exposure to the contaminant, which may only require re-harnessing by implementing the new bioremediation strategy following the addition of waste oil sludge. Compared to this

study, supplementation of nutrient did not enhance total PAH degradation in all three soils over the 42-week incubation period.

As demonstrated by PAH removal results from the ENA microcosms, the lack of available nutrients was unlikely to be the only PAH biodegradation limiting factor in the Creo, TB and AP soils. PAH persistence in the soil may be due to several factors including PAH bioavailability constraints, the lack of microorganisms with degradative capacity or the inhibition of degradative capacity (Agarry 2012; Khan et al. 2012; Peng et al. 2008).
Johnson and Scow (1999) observed that phenanthrene mineralisation rates were either depressed or remained unchanged in 4 soils following the addition of N and P. The authors observed that phenanthrene mineralisation in 1 soil did not respond to the addition of N and P due to high concentrations of inorganic nutrients in the soil. However, Johnson and Scow (1999) were unable to suggest why depression of phenanthrene mineralisation was observed in the remaining soils following N and P addition. Presumably, the bioavailability of added nutrients and the presence of alternative carbon substrates may be possible reasons affecting phenanthrene mineralisation after the ENA amendment. In the present study, Creo and AP soils had high inorganic N and P (Table 3.2) before supplementation of nutrients while TB soil had low levels of N and P. Although inorganic nutrients varied among the 3 soils in the current study, variability of nutrients was not seen as a PAH degradative limiting factor.

In order to determine whether a lack of PAH degrading capacity was responsible for limited PAH biodegradation under NA and ENA conditions, a known PAH degrader (*Mycobacterium gilvum* was added to the Creo, TB and AP microcosms. *Mycobacterium gilvum* has previously been reported to degrade a range of PAH compounds (Cheung & Kinkle 2001; Churchill, Harper & Churchill 1999; Liang, Y et al. 2006). The bioaugmentation strategy employed in this study had no impact on PAH degradation in the Creo, TB, and AP microcosms. Bioaugmentation, in some instance, has been shown to increase the rate and extent of PAH removal (Gentry, Rensing & Pepper 2004; Hamdi et al. 2007; Leštan & Lamar 1996; Mancera-López et al. 2008; Sayara et al. 2011; Singh et al. 2011; Thompson et al. 2005). Mancera-Lopez et al. (2008) reported that bioremediation of PAH was enhanced with the application of bioaugmentation, supplemented with known PAH degraders (*Rhizopus sp*., *P.funiclossum* and *A. sydowii*). After 35 days of incubation, each of the PAH degraders was able to remove 70, 64 and 51% from PAH contaminated soil (12,726 mg/kg).

Several other studies have demonstrated that combining nutrient enrichment and bioaugmentation greatly enhance PAH-contaminated soil remediation (Bento et al. 2005; García-Delgado, Alfaro-Barta & Eymar 2015; García-Delgado et al. 2015; Mohan et al. 2006; Saponaro et al. 2002; Tyagi, da Fonseca & de Carvalho 2011). In one study, Ruberto *et al.* (2006) reported that the combination of bioaugmentation (psychotolerant PAH-degrading bacterial consortium) and biostimulation significantly enhanced removal (46.6%) of phenanthrene after 56 days of incubation in a spiked (1774 ppm of phenanthrene) soil compared to biostimulation alone.

In another study, Saponaro et al. (2002) found that bioaugmentation had no effect on the bioremediation of a manufacturing gas plant PAH-contaminated soil. The authors concluded that the bioaugmented strategy was unsuccessful due to the inability of augmented organisms to adopt to their new environment or due to the low cell number in the added inoculum. In a similar experiment conducted by Yu et al. (2005), a bioaugmentation strategy did not enhance phenanthrene degradation in mangrove sediments compared to the indigenous microbial community. These findings suggest that native microbes have the capacity to outcompete supplemented PAH-degrading microorganisms and suppressed the bioaugmented population. However, the limited PAH degradation in amended microcosms does not correspond with the observed increase in MPN results. Microbial numbers appear sufficiently high (2.0×10^{-2} to 4.0×10^{-4} cells/g from time zero to week 18 in AP soil) in amended microcosms to enhance PAH degradation. However, the MPN results do not provide any information regarding the survival of *Mycobacterium gilvum* nor whether PAH degradation capacity is inhibited by other soil parameters. It was hypothesised that contaminant availability may be a controlling factor in all 3 aged PAH-contaminated soils.

3.8 Conclusion

This study demonstrated that PAH degradation was minimal in the 3 contaminated soils under the various bioremediation strategies. Results presented in this Chapter illustrated that supplementation of indigenous soil microbial communities via different soil amendment regimes, had negligible effect on the PAH concentration in PAH-contaminated soils. This may be due to several factors:

- Lack of PAH degraders
- Low microbial numbers/activity

- Inhibition of degradation
- Bioavailability of PAHs and/or added nutrients had little effect to stimulate microbial growth

The next chapter investigates if lack of microbial diversity, abundance and dynamics in amended and unamended soil microcosms, determined using community profiling analysis, was responsible for minimal PAH removal. Molecular analysis (DGGE) will be employed to assess the presence of PAH degrading capacity by monitoring changes in microbial community structure and pattern following application of the various bioremediation strategies. While other factors including low microbial numbers and lack of PAH bioavailability may be responsible for the observed hinderance of PAH biodegradation (in this chapter), these parameters will be investigated further in Chapters five and six respectively.

Chapter 4

Assessment of PAH-degrading microorganisms in three aged PAH contaminated soils using community profiling analysis

4.1 Introduction

Genetic fingerprinting analysis of soil microbial communities have been used in recent decades to assess the potential of organisms to degrade PAHs (Duarte, Pascoal & Cassio 2012; Ferris, Muyzer & Ward 1996; Muyzer, De Waal & Uitterlinden 1993; Nikolcheva, Bourque & Bärlocher 2005). One of the well-established fingerprinting techniques frequently used in microbial ecology to study the dynamics, structure and diversity of soil microorganisms is denaturing gradient gel electrophoresis (DGGE). Typically, the application of DGGE is coupled with polymerase chain reaction (PCR), where a gene of interest is amplified before its separation into a distinct community profile, has become a powerful tool for studying microbial diversity. In 1995, Muzyer et al. (1995) used DGGE analysis of PCR-amplified 16S rDNA to study the genetic diversity of microbial communities found in two different hydrothermal vents. Muzyer et al. (1995), concluded that both hydrothermal vents had a low number of dominant bacterial species as analysis of community profiles showed a single band in one sample and three bands in the other sample.

A similar study conducted by Murray et al. (1996), applied DGGE of PCR-amplified 16S rDNA fragments to compare the phylogenetic diversity of bacterioplankton assemblages in water sampled in two estuaries. In this study, the authors found that the two assemblages were different in species composition due to different types of organic substrates detected at each location. Hence, the availability of different organic substrates utilised by each population on either side of the estuary was accountable for the variability observed in their community profiles. Moreover, their findings were consistent with results found in earlier studies, in which the primary goal was to determine the fate of thymidine and the use of different carbon sources (Hollibaugh 1994). Recently, DGGE analysis of PCR-amplified 16S rDNA has been applied to monitor the population of PAH-degrading microorganisms during the bioremediation of hydrocarbon contaminated soil Shahsavari, E. et al. (2013). Shahsavari et al. (2013a) reported that in microcosms amended with pea straw, the number of PAH-degrading microorganisms increased by 13-fold compared to those found in the control microcosm. The advantage of DGGE analysis, compared to traditional microbiological methods for characterising microbial

diversity is that one can follow the succession of communities during degradation of the contaminants over a period of time (Muyzer & Smalla 1998; Shahsavari, E. et al. 2013). This means that a time series assessment of soil microbial communities can be achieved with the application of microbial ecology methods such as DGGE that does not rely on culturing.
In the previous chapter (Chapter 3), the MPN method was used to study changes in the density of PAH-degrading organisms during the first 18 weeks of bioremediation. This method enabled the estimation of bacterial density in amended and unamended microcosms using nutrient broth media supplement with phenanthrene as a carbon source. The presence of bacteria in the MPN microplates is assumed to represent PAH-degrading bacteria at specific time points. However, these findings do not provide an indication of changes within the soil community within the microcosm treatment.

In this chapter, a more advanced technique of assessing microbial diversity, abundance and dynamics in amended and unamended microcosms was adopted. In this study, genomic DNA was extracted from microcosm soil sampled over selected sampling time points (day 0, weeks 6, 18 and 42) using a MO BIO DNA Isolation kit. Following DNA extraction, two polymerase chain reactions were performed to amplify segments of 16S rDNA and NidA genes to assess bacterial and *Mycobacterium* community profiles. In the first round of PCR, the universal primer pair 314 F GC and 518 R were used to generate general bacterial amplicons (Muyzer, De Waal & Uitterlinden 1993). In the second round of PCR, a specific primer pair targeting the NidA (NidA F GC and R) gene associated with *Mycobacterium gilvum* was performed (Sho, Hamel & Greer 2004). The individual PCR products were separated by DGGE in polyacrylamide gels containing a linear gradient of DNA denaturants (combination of urea and formamide), resulting in the formation of a pattern of bands, where a single band on the DGGE is considered a single species and its intensity reflects the abundance of that species at the time of analysis.

In order to assess changes in microbial diversity over time, DGGE gels were analysed using Phoretix 1D software to generate a dendrogram using the unweighted pair group method with mathematical averages (UPGMA). The individual species richness and abundance was also performed from DGGE Phoretix generated data using Shannon Weaver diversity and Equitability Index as detailed in chapter two (Materials and Methods).

4.2 Aim

The overall aim of the work presented in this chapter was to evaluate the impact of bioremediation strategies on soil microbial density. This was achieved with the application of DGGE coupled with PCR amplification of 16S rDNA and NidA genes through time series assessment of soil bacterial communities in NA, ENA and Combined treatment microcosms (except BioA microcosms). Molecular assessments did not include samples from the bioaugmented strategy (BioA), due to the assumption that microbial communities in this microcosm may be similar to those from Comb microcosm. Specific aims include:

- Evaluation of soil amendment regime impact on bacterial population dynamics during PAH bioremediation using universal primers.
- Assessment of the survival of bioaugmented and indigenous *Mycobacterium gilvum* with the application of a specific primer targeting the NidA gene.

4.3 Hypothesis

Biostimulation of PAH-contaminated soil with nutrients will increase the soil indigenous microbial population relative to natural attenuation microcosms.

4.4 Assessment of microbial communities in Creo soil microcosms

4.4.1 Bacterial community in Creo microcosms

Bioremediation microcosms with Creo contaminated soil was performed over a period of 42 weeks. During this time period, changes in microbial communities as a result of treatment strategy (i.e. NA and ENA) were assessed using DGGE. Amplified PCR products of DNA extracted from soil samples collected on day 0, weeks 6, 18 and 42 were analysed by DGGE to generate bacterial community profiles (Figure 4.1). Based on the bacterial community DGGE profiles shown in Figure 4.1, several bands were detected in amplicons obtained from different microcosms across sampling time points, as highlighted in rectangles tagged A. Some bands with high intensity in the upper part of region A were observed in all microcosms for all sample time points. There were, however, 2-5 bands observed at the bottom of region A, where their intensity increased up to week 18 but then diminished towards the end of the incubation period. Nonetheless, in the NA microcosms, a 14.8% increase in the number of bands was observed in samples from day 0 to week 18 (increase from 27 to 31 bands) with a 6.5% reduction in band numbers for week 42 samples (bands decreased from 31 to 29). There was a shift in NA community profile as indicated by an increase in band intensity from day 0 to

week 18 (see region marked A). A similar increase in the number of bands during this time period was observed in both amended microcosms (ENA and Comb). However, in ENA microcosms, the number of bands increased by 7.1% from day 0 to week 18 (from 27 to 30 respectively). Similar to the NA microcosms, a reduction in the number of bands was observed in ENA microcosm at the end of the incubation period (from 30 to 25 bands in week 42) compared to week 18 (16.7%). The reduction in the number of bands at the end of the experimental period may be indicative of nutrient depletion in these microcosms.

In microcosms where bioaugmentation and nutrient addition was implemented (Comb), the number of bands increased by 11.1% from day 0 to week 18 (from 27 to 30 bands respectively), then decreased (20% reduction) at the end of incubation the period (42 weeks). There were some distinct bands observed from NA microcosms (at the bottom of the gel in weeks 18 and 42) that were not observed in samples from day 0 and week 6 (small rectangles tagged C). These bands may represent unique microorganisms that increase in numbers following the addition of favourable conditions. Banding profiles across all microcosms were similar, indicating that treatment strategies had little impact on microbial community profiles. Further analysis of bacterial community profiles was conducted to investigate if the shift in banding profiles was due to amendment or time influences. Shannon Weaver diversity index and equitability analysis was performed to compare the degree of similarity between microbial communities.

4.4.2 Effect of incubation time and amendments on bacterial communities

Differences in bacterial banding profiles as a result of incubation time and amendment strategy were assessed using an unweighted paired-group method with arithmetic mean (UPGMA) as showed in Figure 4.2. Cluster analysis of UPGMA demonstrated that bacterial species fell into seven clusters based on two factors: (I) time at which samples were taken from the microcosms and (II) amendment strategy. The baseline cluster (cluster I) was developed based on bacterial communities from NA microcosms in week 18. Of note, the baseline cluster was expected to contain communities from day 0 (i.e. the original population before the incubation started), but instead, communities from day 0 were in clusters located in the middle of dendrogram (Clusters IV and V respectively). Week 18 NA banding profiles were utilised as the reference point, as the bacterial population at this time point was the most diverse compared to communities from the other time points and treatments.

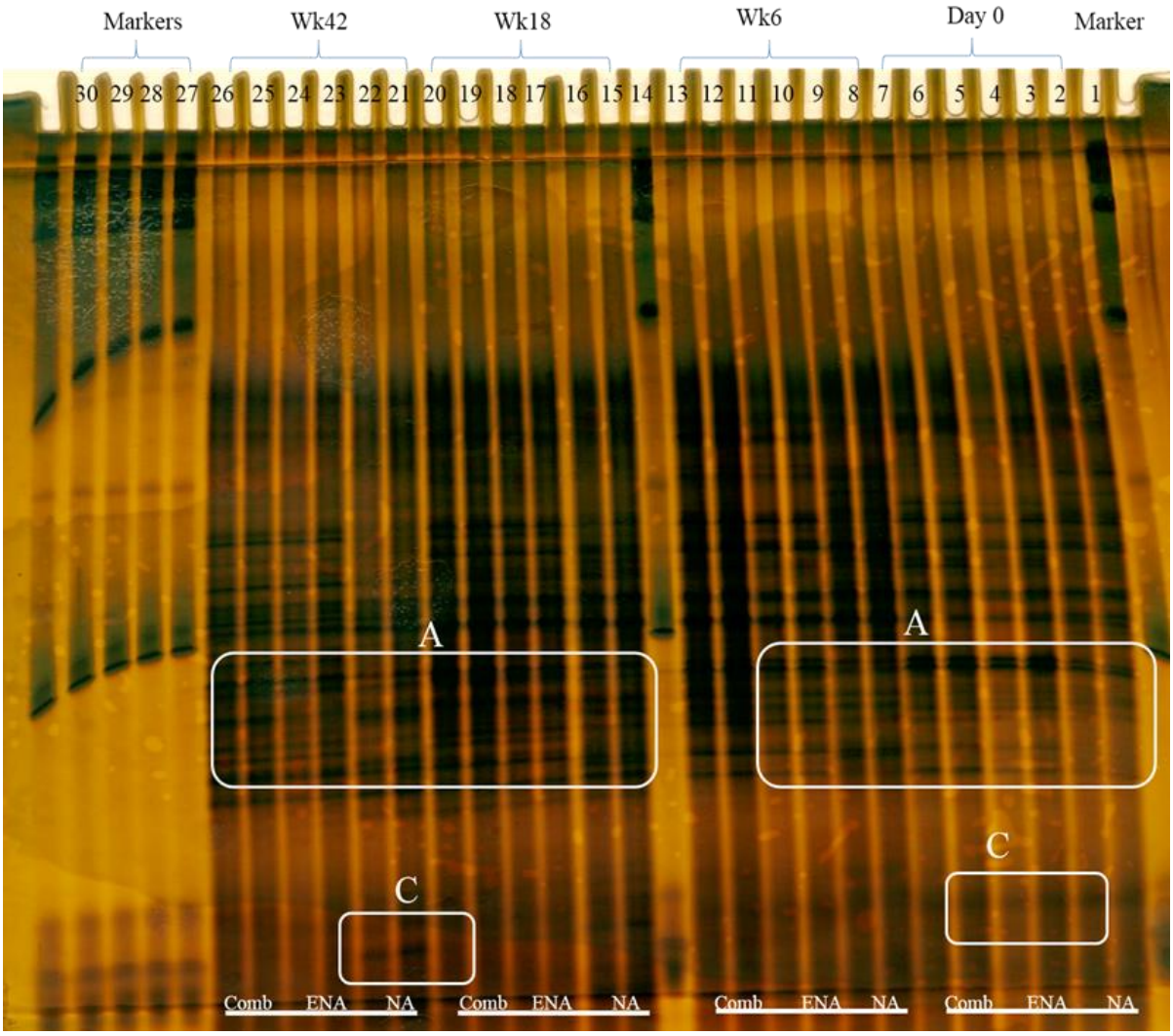

Figure 4.1. Bacterial community profiles generated using 16S rDNA from samples taken at four different time points following 42 weeks of bioremediation of Creo contaminated soil. Lane 1, 14, and 27-30 contain markers. Day 0 samples were loaded in lanes 2-7. Lanes 8-13 represent week 6 amplicons obtained from three microcosms. Lanes 15-20 contain week 18 samples. Loaded in lanes 21-26 are amplicons from samples obtained from week 42. All samples run on this gel were samples obtained from the three microcosms (NA, ENA and Comb) at the specified time points as tagged on the gel. Highlighted in rectangles tagged A, dominant bands with increasing intensity through incubation time and C, unique bands at time zero and week 42.

As showed in Figure 4.2, bacterial communities from NA microcosms were located in four clusters: including the baseline cluster (cluster I, week 18); cluster II (week 42); cluster IV (day 0) and cluster VI (week 6). As expected, the closest relationship observed from the UPGMA analysis was for sample replicates. The similarity between duplicate analysis ranged from 61% (day 0) to 95% (week 6). Bacterial species at time zero exposed to different treatments were not expected to exhibit a high degree of dissimilarity. However, this was the case in the Creo soil, in which variability in bacterial community profiles may be due to issues associated with DNA replication inefficiency (amplification stage). Bacterial profiles were closely related in samples from ENA and Comb microcosms (88% similarity) compared with NA (77% similarity to both ENA and Comb) at time zero. Generally, bacterial communities from time zero samples were more distant from communities obtained from week 18 and 42 samples (dissimilarity of 39%) compared to week 6 (similarity of 67%). This type of clustering may be due to time influences on bacterial profiling as day 0 samples clustered differently from week 42 samples. Similarly, in microcosms where amendments were added (ENA and Comb), bacterial communities were found in four different clusters based on the time at which samples were taken. The similarity between duplicate analyses in the ENA microcosms ranged from 90% (ENA in weeks 18 and 42) to 96% (ENA at day 0).

Bacterial communities in ENA samples from day 0 were clustered with day 0 samples from Comb microcosms in the middle of the dendrogram (cluster V). Similarly, ENA communities from week 6 (cluster VI) clustered with Comb communities from week 6 with similar clustering from ENA and Comb communities from week 18. In contrast, bacterial communities from ENA and Comb microcosms at week 42 formed distinct clusters (cluster III and VII respectively), indicating the dissimilarity of these communities from the previous time points. Compared to their respective day 0 samples, bacterial communities from ENA and Comb microcosms at week 42 were 60% similar to starting populations, while duplicate similarity analyses in the Comb microcosms ranged from 80% (week 6) to 94% (time zero). Overall, bacterial communities in all microcosms (NA, ENA, and Comb), at day 0 were more closely related to the bacterial community from week 6 than communities from weeks 18 and 42 with similarity of 77% and 60% respectively.

Principal component analysis (PCA) was performed using DGGE data to highlight similarities in bacterial community profiles in samples obtained from Creo microcosms (Appendix 3 Figure A3.1). Bacterial community aggregation was predominantly due to incubation and duplicate influence. For instance, communities obtained from day 0 and week 6 were grouped

together in the component 2 quadrant while those communities from weeks 18 and 42 agglomerated in a separate cluster. At the commencement of the incubation (day 0 and week 6), bacterial community profiles demonstrated a positive correlation (correlation matrix, see Appendix 3, Table A3.1) and a negative correlation to those communities from weeks 18 and 42. These data indicate that bacterial populations at the beginning of the incubation (day 0 and week 6), were distinguishable and separate from bacteria populations sampled after further incubation (weeks 18 and 42). This was driven by the high loading of positive values of these two communities being located in component 2 while low negative values were located in component 1. As a consequence, component 2 of the PCA only explained a total variance of 13% of the initial Eigenvalues. Similarly, all bacterial communities from both weeks 18 and 42 demonstrated a strong positive correlation with high loading positive values located in component 1 and a low negative loading value in component 2 (correlation matrix in Appendix 3, Table A3.1). Thus, component 1 explained a total variance of 22% of the initial Eigenvalues.

4.4.3 Bacterial community profile analysis

Two key biodiversity indices were used to evaluate microbial diversity in amended and unamended microcosms. These biodiversity indices were: (i) the number of species in a sample (species richness) and (ii) the equitability index (evenness of distribution). Microbial diversity and equitability in Creo microcosms were calculated from DGGE band intensity output based on Shannon Weaver diversity. The concept of Shannon Weaver diversity index in analysing bacterial diversity considers both species richness and abundance to allow for a statistically sound assessment of changes in diversity (Magurran & Magurran 1988).

According to Magurran (1988), the precise value to determine if Shannon's diversity is achieved where all species are similarly distributed is the diversity index. The equality of the Shannon's diversity index for environmental communities falls between 1.5 and 3.5. The equitability assumption of similar proportions of all species in a sample approaches a value of 1.0 when species are evenly distributed (Spellerberg & Fedor 2003). In theory, a single band on the DGGE is considered as a single species and its intensity is reflective of the abundance of that species at the time of analysis. Bacterial species diversity in Creo soils, determined by Shannon Weaver diversity index (H') analysis is showed in Figure 4.3 for amended and unamended microcosms.

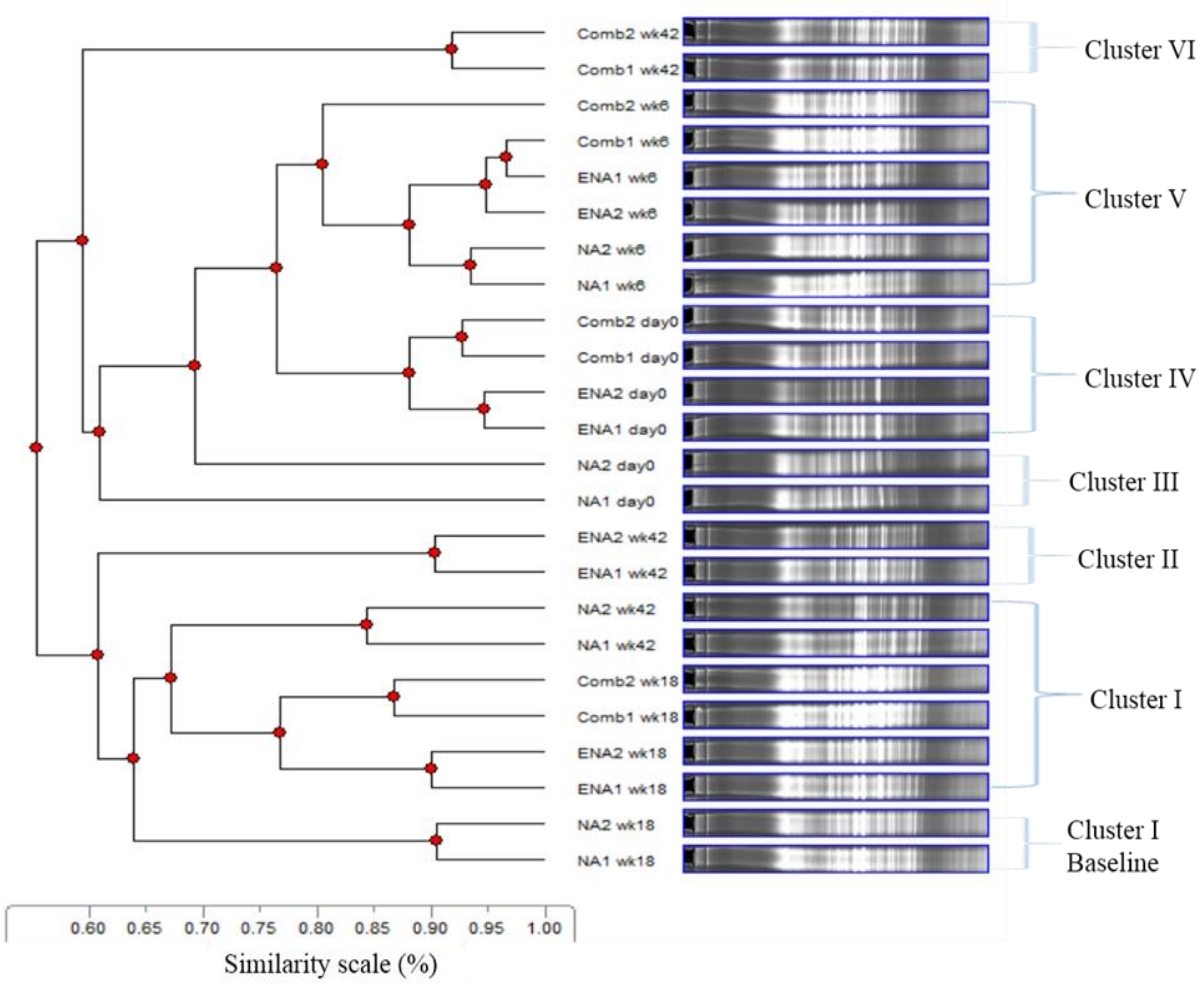

Figure 4.2. UPGMA dendrogram constructed using the similarity matching produced from Creo bacterial DGGE community profiles of the 16S rDNA fragments, amplified from all treatments across sampling time points (day 0, week 6, week 18 and week 42). The scale bar represents the level of similarity in percentage. In this dendrogram, there are seven distinct clusters associated with either (I) time of sampling; (II) treatments based grouping, and (III) replicate type clustering. These seven include; cluster I (week 18 NA), cluster II (weeks 18 and 42 comprising of NA, ENA and Comb), cluster III (week 42 ENA only), cluster IV (day 0 NA only), cluster V (day 0 composed of ENA and Comb), cluster VI (week 6 all microcosms), and cluster VII (week 42 comb only).

Bacterial diversity in NA microcosms fluctuated over the 42-week experimental time course. Although there was no significant difference ($P > 0.05$) between Shannon Weaver diversity index for day 0 (2.99 ± 0.1) and week 42 (2.78 ± 0.5) (due in part by the large standard deviation at week 42), diversity increased after the initial 6 weeks of incubation (3.22 ± 0) but then significantly decreased at week 18 (2.37 ± 0.1 at $P > 0.05$). In contrast, bacterial diversity in ENA microcosms was stable over the course of the first 6 weeks of incubation (initial diversity of 3.17 ± 0 day 0 and 3.15 ± 0 at week 6).

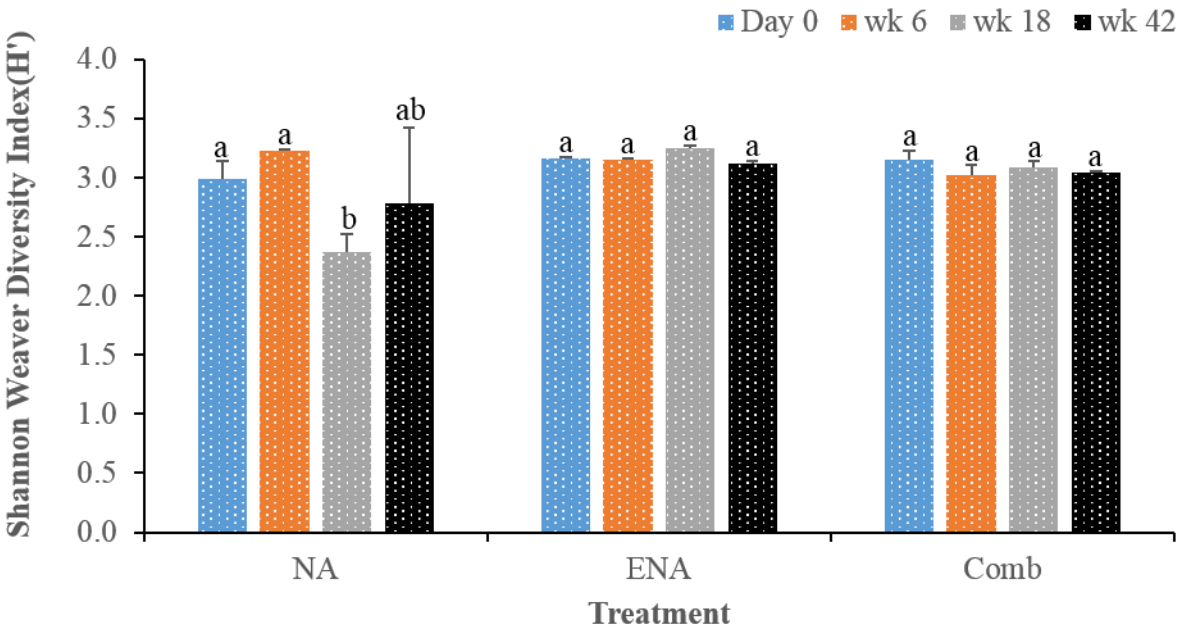

Figure 4.3. Comparison of bacterial community diversity expressed as Shannon Weaver diversity index (H') from DGGE analysis of 16S rDNA fragments in Creo soil microcosms. Samples from NA, ENA and Comb microcosms were removed at selected time points (Day 0, Weeks 6, 18 and 42) for the determination of species richness using Total Lab Software. Error bars represent the standard deviation of replicate analyses, Bars sharing the same letter for NA, ENA and Comb treatments do not differ significantly ($P > 0.05$).

Despite bacterial diversity stability at the start of the incubation period (day 0 to week 6), a small but significant increase ($p < 0.05$) in diversity was observed at week 18 (3.25 ± 0.0) which then decreased at week 42 (3.12 ± 0), whereas in microcosms where nutrients and inoculants were supplemented (Comb), the diversity varied over the incubation period. Bacterial species diversity at day 0 (3.15 ± 0.1) was similar to the diversity at week 18 (3.09 ± 0), however diversity was much lower at weeks 6 and 42 (3.03 ± 0.1 and 3.04 ± 0) respectively. Diversity was similar at day 0 and week 42 irrespective of treatment although some variabilities were observed for weeks 6 and 18.

In terms of equitability, the distribution of individual species in the whole bacterial population across four microcosms is represented in Figure 4.4. Characterisation of bacterial species distribution was performed to determine their evenness as a proportion of the total population. In NA microcosms, the distribution of individual bacterial species was quite even from day 0 (0.91 ± 0) to week 6 (0.96 ± 0). However, a decrease in equitability was observed following further incubation, from 0.96 ± 0 at week 6 to 0.69 ± 0 at week 18. Although the equitability index increased at week 42 (0.83 ± 1), significant variability was associated with this sample. In contrast, unlike NA microcosms, individual bacterial species distribution in ENA microcosms was even, with equitability diversity index ranging from 0.94 ± 0 (week 6) to 0.97 ± 0 (week 42). Similar results were observed in the Comb microcosms; however, the equitability diversity index from day 0 (0.6 ± 0) was similar to week 42 (0.96 ± 0), while that of week 6 (0.90 ± 0) was similar to week 18 (0.91 ± 0).

The variation in bacterial equitability index in NA microcosm was presumably due to the appearance of some unique (bands) species that increased in abundance as a result of incubation time. As such, the equitability index value at week 18 was < 1 indicating an unevenly distributed population (value of 1.0). Additionally, the distribution of individuals' species appeared to be equally achieved in both ENA and Comb microcosms. This is shown by the fact that the equitability index of all species was close to the Shannon's evenness value of 1.0 (Figure 4.4).

In order to determine if samples taken over the course of incubation may significantly differ, further statistical analysis was performed using repeated measures of analysis of variance (Graph Pad InStat v3). There were no statistically significant differences observed between bacterial communities sampled from NA (NA0 and NA42), ENA (all time points), and Comb (all time points) microcosms ($P > 0.05$) according to analyses performed using Graph Pad InStat version3. For NA microcosm, it was found that the bacterial communities sampled from week 18 (NA18) were statistically different from bacterial communities sampled at day 0 and week 6 (NA0 & NA6) except week 42 (NA42) ($P < 0.05$).

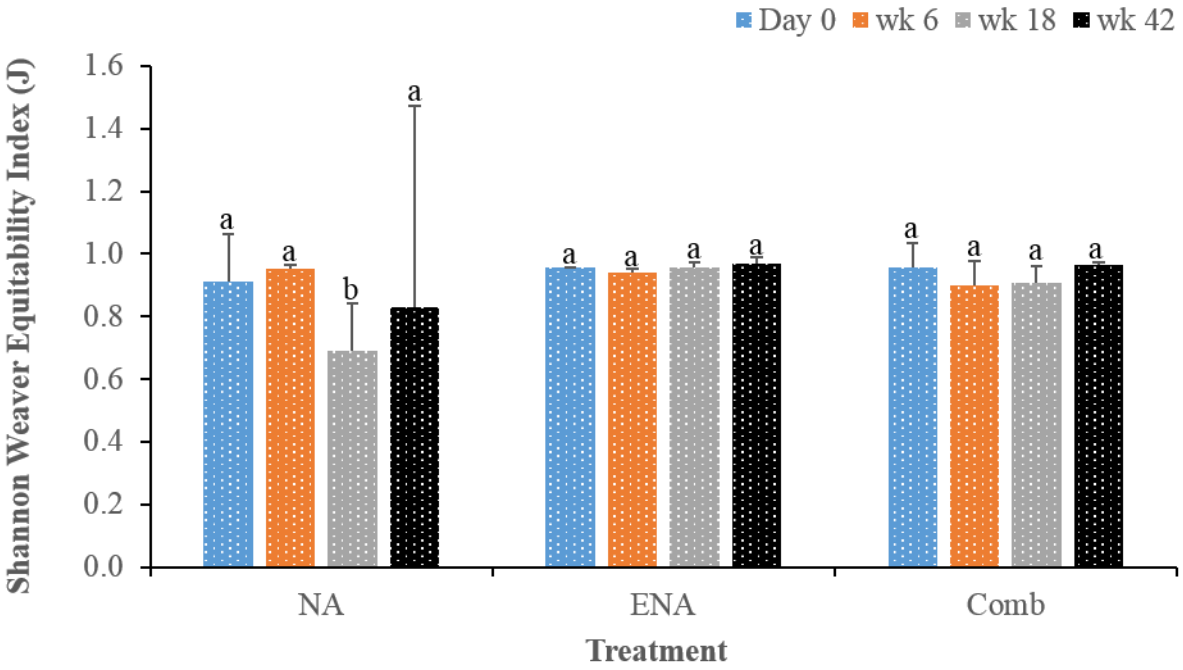

Figure 4.4. Comparison of bacterial community diversity expressed as Shannon Weaver equitability index (J) from DGGE analysis of 16S rDNA fragments in Creo soil microcosms. Samples from NA, ENA and Comb microcosms were removed at selected time points (day 0, weeks 6, 18 and 42) for the determination of species richness using Total Lab Software. Error bars represent the standard deviation of replicate analyses. Bars sharing the same letter for NA, ENA, and Comb treatments do not differ significantly ($P > 0.05$,), while bars marked with different letter were considered significantly different ($P < 0.05$).

4.4.4 Assessment of supplemented PAH-degrading organisms in Creo microcosms

In the previous section, a universal pair of primers was utilised to investigate total bacterial community diversity in amended and unamended microcosms. In this section, a specific gene probe (NidA primer pair) was employed to quantify genomic DNA, in order to assess whether the augmented PAH-degrading organisms (*Mycobacterium. gilvum*) survived the experimental conditions. The NidA primer amplifies organisms, predominantly *Mycobacterium* species that can mineralise a number of high molecular weight compounds including fluoranthene, pyrene chrysene, and B(a)P (Brezna, Khan & Cerniglia 2003; Sho, Hamel & Greer 2004).

Visual examination of *Mycobacterium* generated DGGE community profiles indicated that similar communities were amplified in all treatments across sampling time points (Figure 4.5). A consistent and stable *Mycobacterium* community was observed in all microcosms from day 0 to the end of the incubation period (week 42) as evidenced by two major banding patterns in the regions tagged M in Figure 4.5. In NA microcosms, the *Mycobacterium* population fluctuated during the 42 weeks of the incubation period. There was a 6.7% increase in the number of bands observed from day 0 to week 18 (increase from 7 to 9 bands) with a 3.3% reduction in the band numbers at the end of microcosms (decrease from 9 to 8 bands). A similar

trend in the *Mycobacterium* population was observed in ENA microcosms. In the first phase of the incubation period, band numbers increase by 6.1% from day 0 to week 18 (increase from 8 to 10 bands), however, the reduction in the ENA (6.1% reduction at week 42) was more severe in the second phase compared to NA samples. In contrast, in bioaugmented microcosms, the *Mycobacterium* population steadily increased, from day 0 to week 18 (9.6% increase from day 0 to week 18) and then decreased in the final week of incubation (3.2% reduction in week 42). Regardless of whether an amendment was implemented (ENA and BioA), the intensity of bands was consistent across all sampled time points (day 0 to week 42) in all microcosms. However, some unique (bands) were present in ENA and Comb microcosms at day 0 that were absent from NA samples (rectangles tagged A). Further analysis of *Mycobacterium* community profiles was performed to investigate if the variation in banding profiles was due to amendment or time influences. Shannon Weaver diversity index and equitability analyses were performed to compare the degree of similarity between microbial communities.

4.4.5 Effect of incubation time and amendments on Mycobacterium communities

Changes in the *Mycobacterium* community profiles due to incubation time and bioremediation strategies were assessed using an unweighted pair-group method with arithmetic mean (UPGMA). The dendrogram constructed from NidA DGGE image profiles resulted in six distinct clusters (Figure 4.6). The baseline cluster (cluster I) was developed based on *Mycobacterium* communities from ENA and Comb microcosms in week 42. Of note, the baseline cluster was expected to contain communities from day 0 (i.e. the original population before the incubation started), but instead, communities from day 0 were in the clusters located in the middle of the dendrogram (Clusters IV and V respectively).

According to this dendrogram, mixed communities from week 42 amended microcosms (ENA and Comb) were used as the reference point as the *Mycobacterium* population at these time points was the most diverse compared to populations from the other sampling time points. The clustering was associated with the time of sampling, bioremediation strategies applied or replicate based similarities. However, most of the clustering was associated with the time of sampling. For example, in NA microcosms, the clustering of the *Mycobacterium* population was predominantly due to the time of sampling (approximately 66.7% from day 0 and week 42 samples). However, only one third (33.3% from NA18 samples) of clusters formed from NA microcosms were randomly clustered and distantly located further away from each other (NA1 wk18 NA2 wk18).

The similarity observed from NA microcosms between replicate analyses ranged from 55% (week 18, duplicate clustered separately) to 100 % (day 0 and week 42, duplicate clustered together). In contrast, *Mycobacterium* communities from ENA microcosms were clustered based on time of sampling and replicate (100% time and replicate effect) although scattered in five different clusters (clusters I, II, IV, V and VI). Thus, the intra replicate similarity from ENA microcosms ranged from 35% (week 42) to 90% (day 0) whereas the overall similarity among *Mycobacterium* communities was 55%. Although the effect of incubation and replicate have been a key influential factors behind *Mycobacterium* community clustering in NA and ENA microcosms, *Mycobacterium* communities from Comb microcosms were randomly clustered (about 66.7% due to random agglomeration). The *Mycobacterium* population from week 18 and 42 samples were distantly clustered (clusters I, II, IV, V and VI). As a consequence, the similarity among the replicates ranged from 25% (week 42 samples) to 85% (day 0 samples). In the same way, the overall similarity among *Mycobacterium* communities from Comb microcosms was the lowest compared to the other microcosms (25% from baseline sample to the rest of samples).

Mycobacterium communities from day 0 were most closely related to communities from week 6 (80% similarity) compared to other time points. Similarly, *Mycobacterium* populations from weeks 18 and 42 samples exhibited a close relationship (40% similarity). There were some differences observed when comparing communities sampled from different microcosms and sampling time points. At the start of the incubation period (day 0), *Mycobacterium* communities from all the microcosms (NA, ENA and Comb) were more similar compared to the rest of sampling time points (85% similarities). However, the similarities among the communities decreased in subsequent communities sampled, following further incubation time. In comparison to day 0 communities, similarities in *Mycobacterium* populations obtained at each time point gradually decreased, with communities from week 6 showing 75%, week 18 50% and 25% similarities in week 42. Undoubtedly, the decreased in similarities of *Mycobacterium* populations at across different sampling time points may be due to incubation time.

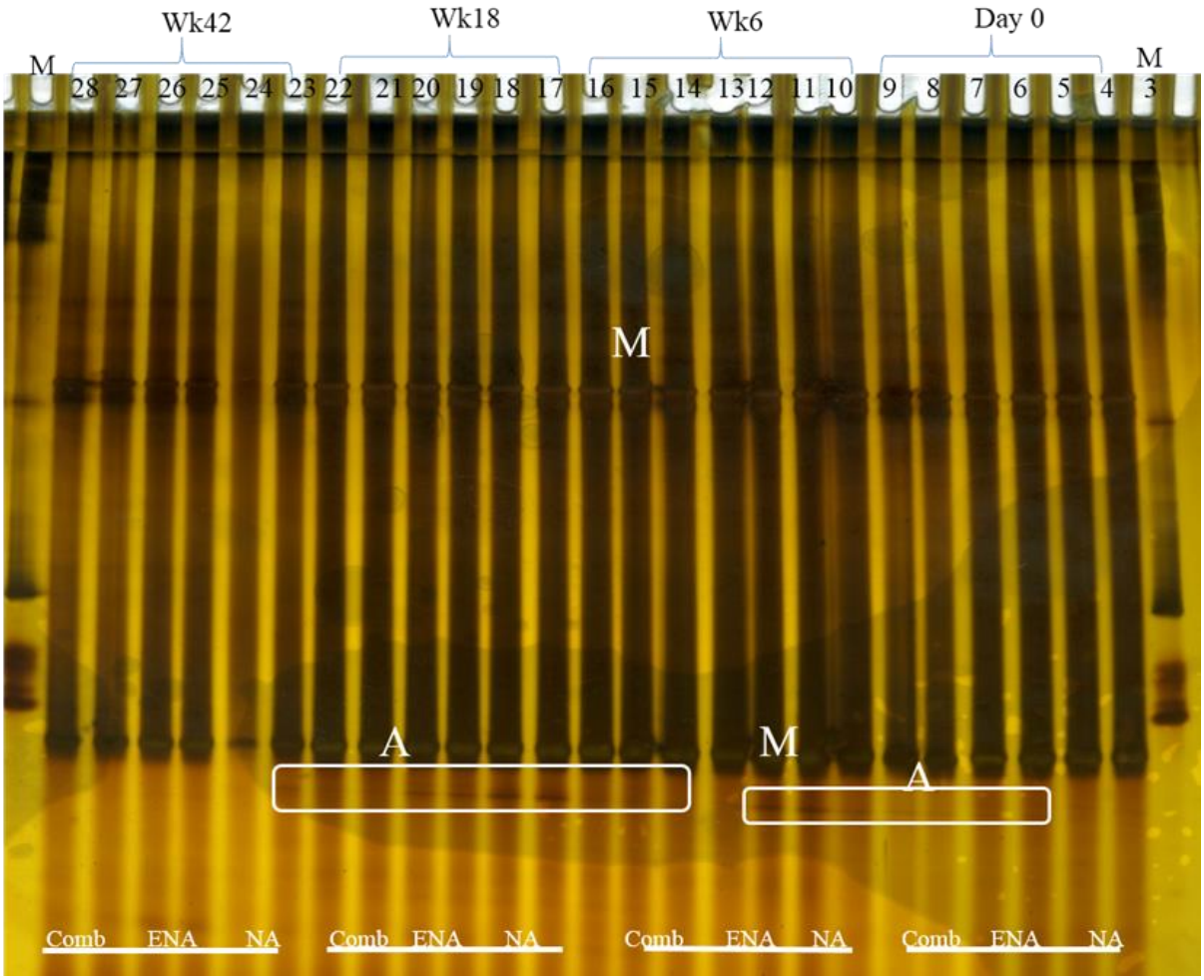

Figure 4.5. Comparison of *Mycobacterium* community profiles in Creo-contaminated soil generated using NidA genes following 42 weeks incubation. Lanes 3 and M contain markers, day 0 samples were loaded in lanes 4-9, lanes10-16 represent week 6 amplicons, lanes 17-22 contain week 18 samples, and lanes 23-28 represent samples obtained from NA, ENA and Comb at week 42. Highlighted in rectangles tagged A, unique bands at day 0 to week 18 and M, consistent bands throughout sampled time points.

4.4.6 *Mycobacterium* community profile analysis

A comparison of *Mycobacterium* community diversity and equitability was carried out using band intensity output with the Total Lab software. Ideally, the concept of Shannon Weaver diversity index refers to species richness (the number of species in the community) and abundance (the total number of individuals) in the sample. The total *Mycobacterium* community in NA microcosms demonstrated only small variability in diversity over the course of incubation (Figure 4.7). The total diversity decreased from 1.93 ± 0 (day 0) to 1.70 ± 0 (week 6), however, there was an increment in *Mycobacterium* diversity following further incubation from week 6 to week 18 (2.11 ± 0) which remained stable to the end of the incubation period (week 42). Although the diversity fluctuated throughout these microcosms, the diversity values obtained were within the range classified as moderately diverse (all values fall in a range of

1.5-3.5). However, in an amended (ENA and Comb) microcosms, total *Mycobacterium* diversity steadily increased from day 0 to week 18 of the incubation.

In ENA microcosms, *Mycobacterium* diversity increased from day 0 (1.71 ± 0) to week 18 (2.11 ± 0) and a small decrease was observed at week 42 (2.06 ± 0). However, in the microcosms where supplementation was implemented (Comb), the diversity rapidly increased from day 0 (1.69 ± 0) to week 18 (2.17 ± 0) and a small reduction in *Mycobacterium* species diversity was observed at week 42 (2.06 ± 0).

Species equitability is the measure of evenness of individuals in the community. *Mycobacterium* species equitability (J) in each microcosm was calculated from the diversity index (Figure 4.8) to determine the proportion of individual species distribution relative to the whole community. In terms of individual species abundance, there was no significant differences detected in amplicons obtained across all treatments and sampling time points (Figure 4.8).

It was found that the distribution of *Mycobacterium* species in unamended and amended microcosms was even. The equitability values obtained from all microcosms ranged from 0.99 ± 0 (day 0) to 0.97 ± 0 (week 42) in NA; 0.82 ± 0 (day 0) to 0.99 ± 0 (week 42) in ENA; and 0.99 ± 0 (day 0) to 0.98 ± 0 (week 42) in Comb. The *Mycobacterium* equitability values obtained were close to the evenness value of 1.0 in samples taken throughout the incubation (all-time points).

In order to determine if samples taken over the course of incubation may differ, further statistical analysis was performed using repeated measures of analysis of variance (Graph Pad InStat v3). There were no statistical significant differences observed within each microcosm diversity as well as comparison between the two amended communities (at $P > 0.05$) according to analyses performed using Graph Pad InStat v3 software.

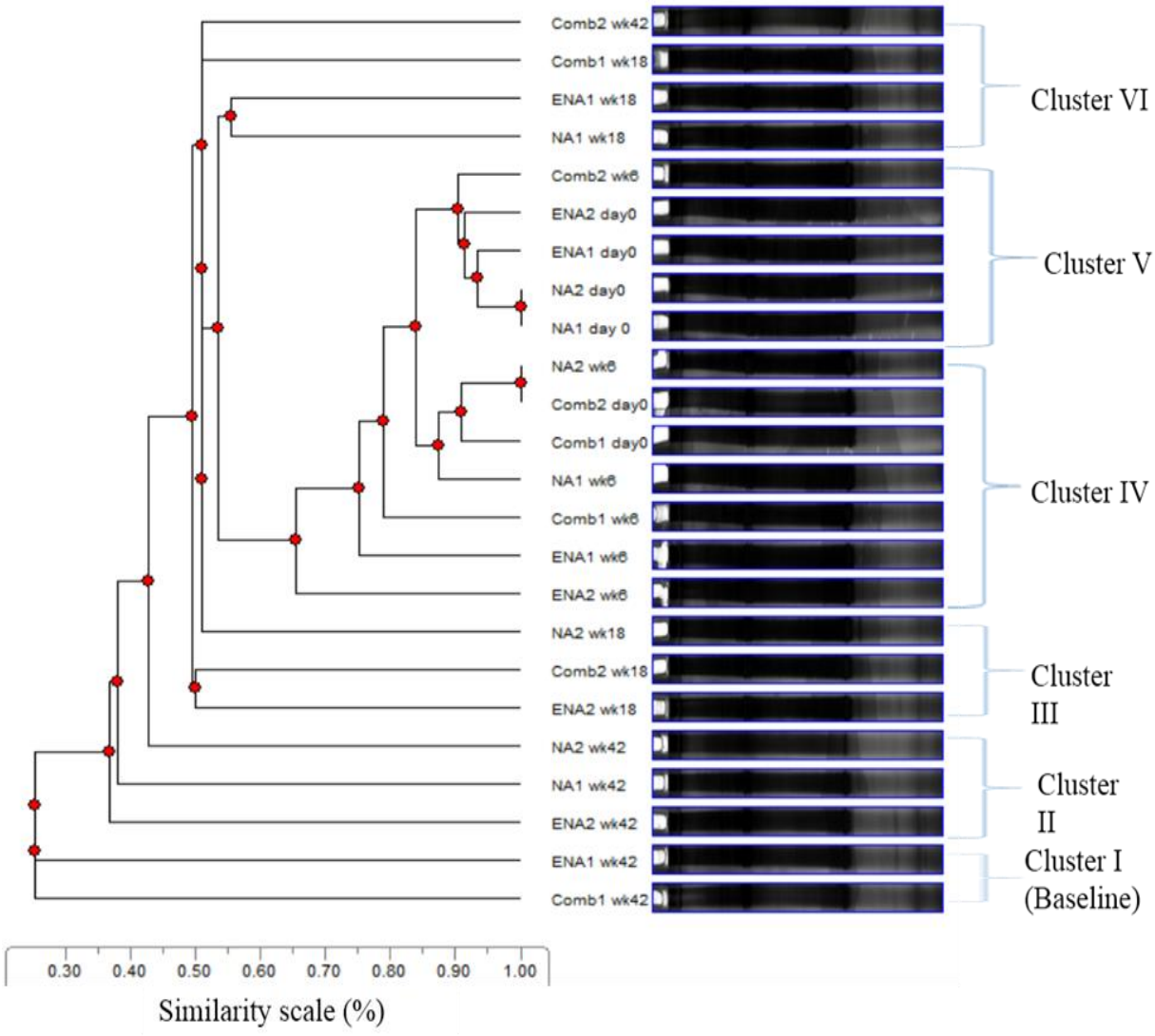

Figure 4.6. UPGMA dendrogram constructed from the similarity matching produced from Creo NidA DGGE community profiles of the 16S rDNA fragments, amplified from all treatments across sampling time point (Day 0, Weeks 6, 18 and 42). The scale bar represents the level of similarity in percentage. In this dendrogram, there are six distinct clusters associated with either (I) time of sampling; (II) treatments based grouping, and (III) replicate type clustering.

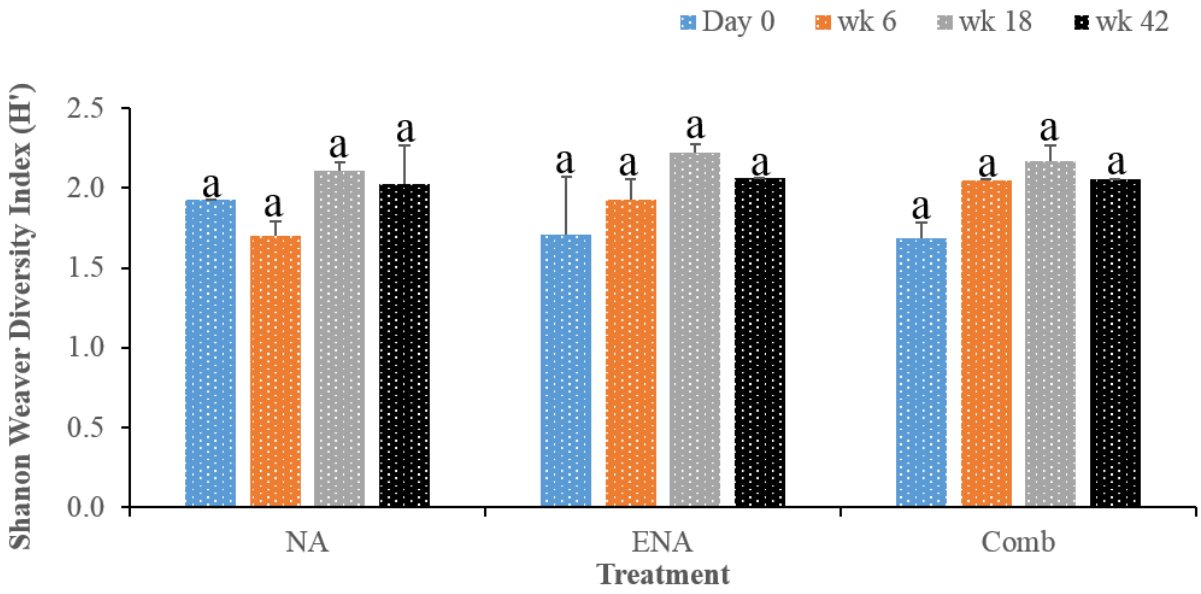

Figure 4.7. Comparison of *Mycobacterium* community expressed as Shannon Weaver diversity index (H') from DGGE analysis of 16S rDNA fragments in Creo soil microcosms incubated for 42 weeks. Comparison of *Mycobacterium* community expressed as Shannon Weaver diversity index (H') from DGGE analysis of 16S rDNA fragments in Creo soil microcosms following 42 weeks of incubation. Species richness was determined in samples from natural attenuation, enhanced natural attenuation and bioaugmentation microcosms using Total Lab Software over the course of the incubation. Bars sharing the same letter for NA, ENA and Comb treatments do not differ significantly (P > 0.05,).

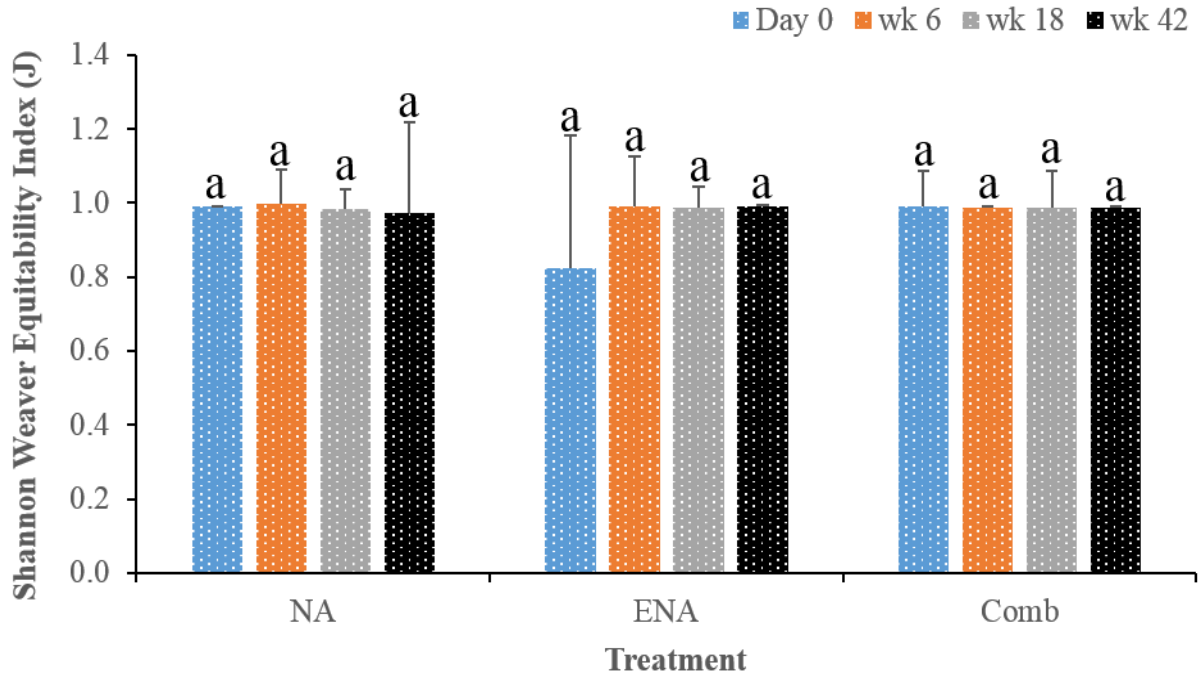

Figure 4.8. Comparison of *Mycobacterium* communities expressed as Shannon Weaver equitability index (J) from DGGE analysis of 16S rDNA fragments in Creo soil microcosms incubated for 42 weeks. Samples for molecular analysis were periodically removed during incubation time at day 0, weeks 6, 8 and 42 from each microcosm. The measure of species equitability was calculated from Shannon Weaver diversity index to determine the proportion of individual species distribution in the community. Bars sharing the same letter for NA, ENA and Comb treatments do not differ significantly (P > 0.05,).

4.5 Assessment of microbial communities in TB soil microcosms

4.5.1 Bacterial community profile analysis in TB soil microcosms

In order to assess the bacterial degradative potential in TB contaminated soils, bioremediation of the TB soil microcosms was performed over a period of 42 weeks. Changes in microbial communities due to PAH contamination, soil amendment strategy (i.e. NA, ENA and BioA) and experimental incubation time were assessed using DGGE. Amplified PCR products in DNA extracted from soil samples collected on day 0, weeks 6, 18 and 42 were analysed by DGGE to generate bacterial community profiles (Figure 4.9). According to the bacterial community DGGE profiles in Figure 4.9, a consistent group of bands were observed, from day 0 to the end of the incubation period (week 42), as highlighted in the rectangle and tagged D. Generally, these bands were present in samples obtained across sampling times but their intensities increased with incubation. For instance, similar bands were observed in samples from day 0 but with a low intensity indicating less diverse communities as compared to similar bands in samples from week 42 (ENA).

In NA microcosms, the bacterial population varied across the microcosms throughout the incubation period. There was a small increase in the number of bands present from day 0 to week 6 (2.5% increase in band numbers), which was followed by a reduction at week 18 (2.5% reduction in band numbers): these bands eventually increased by a similar percentage at week 42 (2.5% increase in band numbers). However, in the microcosms where the bacterial population was stimulated by the addition of nutrients, a small increase in the number of bands was observed, from day 0 to week 6 (2.5% increase in band numbers) but a 2-fold decrease in band numbers was observed at the last two sampling time points (5% reduction in the number of bands at week 42). This was probably at the time where a few microorganisms become dominant leading to the entire soil microbial population being less diverse as shown in the region tagged B. Clearly, these bands were present in samples collected at day 0 and week 6 but with low intensities as shown in a region highlighted with the rectangle tagged A.

In comparison to both NA and ENA, the bacterial population in microcosms supplemented with inoculant demonstrated a steady increase (5.1% increase) in the banding profiles, from day 0 (18 bands) through to week 18 (22 bands). However, a sharp reduction in the number of bands was observed at the end of the incubation (5.1% reduction at week 42) as observed in ENA microcosm (50% reduction in the population). Importantly, the increase in the number of bands was seen as indicative of the bacterial population being more diverse while the reduction

in the number of bands showed a less diverse population at a given time point. Additionally, some distinct bands were present in the area marked with a small rectangle tagged C in samples taken from week 18. These bands may represent distinct microorganisms that increase when the right conditions for microorganisms' growth are provided. No matching bands were detected on either in day 0, week 6 or at week 42. Further analysis of the bacterial community profiles was conducted to investigate if shifts in banding patterns in the microcosms was due to the amendment or time influence. Shannon Weaver diversity and equitability index were performed to compare the level of similarity.

4.5.2 Effect of incubation time and amendments on bacterial communities

Differences in bacterial banding profiles in amended and unamended microcosms was assessed using unweighted paired-group method with arithmetic mean (UPGMA) as showed in Figure 4.10. Cluster analysis of UPGMA demonstrated that bacterial species fell into six main clusters based on two factors: (I) time at which samples were taken from the microcosms and (II) the amendment strategy. These six clusters include; Cluster I or the baseline (day 0 samples), Cluster II (week 6 samples), Cluster III (week 6 samples), Cluster IV (weeks 18 samples), Cluster V (week 18 and week 42 samples), and Cluster VI (week 42 samples). As expected, the baseline cluster was formed based on bacterial communities from day 0 samples (all microcosms). As demonstrated in Figure 4.10, bacterial communities from NA microcosms were clustered based on time of sampling, with NA0 communities being located in cluster I (the original population), NA6 in cluster II, NA18 in cluster IV and NA42 in cluster V. The closest relationship observed in NA bacterial communities ranged from 95% (day 0) to 75% (week 42). The original bacterial species (day 0 samples) were highly similar to bacterial species in samples obtained at week 6 with 61% similarity, whereas bacterial populations from weeks 18-42 demonstrated a similarity value of 49% to the original populations (day 0). Overall, the bacterial communities from day 0 were more closely related to bacterial communities obtained from week 6 than the other sampling time points (weeks 18 and 42). Bacterial species at the commencement of the incubation time exhibited a high degree of similarity, however, this similarity decreased over the course of the incubation. For example, communities in samples obtained from week 42 clustered further away from communities in samples from day 0 (Figure 4.10).

In ENA microcosms, bacterial communities agglomerated into four clusters based on sampling time; bacterial populations were located in cluster I, ENA6 in cluster III, ENA18 in cluster IV,

and ENA42 in clusters V and VI. The similarity between duplicates ranged from 61% (ENA42) to 95% (ENA0). Similar to the bacterial communities from NA0, the bacterial population from ENA0 were more closely related to week 6 bacterial communities (61% similarity level) than to the bacterial communities seen in weeks 18 and 42 (49% similarity level). Similar results were observed in microcosms where both ENA and BioA strategies were implemented (Comb microcosms), however, similarity between duplicates ranged from 75% (comb 42) to 100% (comb18). Like bacterial populations from NA0 and ENA0, Comb0 bacterial communities were closely related to comb6 (61% similarity level) bacterial populations than comb18 and comb42 bacterial communities (49% similarity level).

Samples obtained at the same time point showed increased similarity compared to samples from a different time point. A similar levels of aggregation was observed when data generated from bacterial DGGE was analysed using a principle component analysis (PCA) (Appendix 3, Figure A3.2). The aggregation in this figure is largely due to the incubation and amendment strategy. For instance, communities obtained at day 0 and week 6 were grouped together in one quadrat while those communities from weeks 18 and 42 were in a separate quadrat. As demonstrated in the PCA (Appendix 3, Figure A3.2), it could be deduced that amendments had little influence on the total bacterial population compared to the impact of the incubation. According to the initial Eigenvalues, component 1 of the PCA accounted for 31% of the variance while the component 2 of the PCA was responsible for 22% of the variance in the bacterial population based on total variance analysis (Appendix 3, Table A3.2). Clearly, these analyses have shown that further incubation may be a key factor shaping bacterial community profiling of both the indigenous and supplemented microbial populations during bioremediation of PAH contaminated soils.

4.5.3 Bacterial community profile analysis

Bacterial diversity and equitability indexes were calculated using data generated from DGGE (TB microcosms) band intensities based on Shannon Weaver indexes. A brief account of Shannon Weaver diversity and equitability index concept is given in section 4.4.3 of this chapter. Bacterial species diversity in TB soil, were analysed by Shannon Weaver diversity index (H') analysis as shown in Figure 4.11 for amended and unamended microcosms.

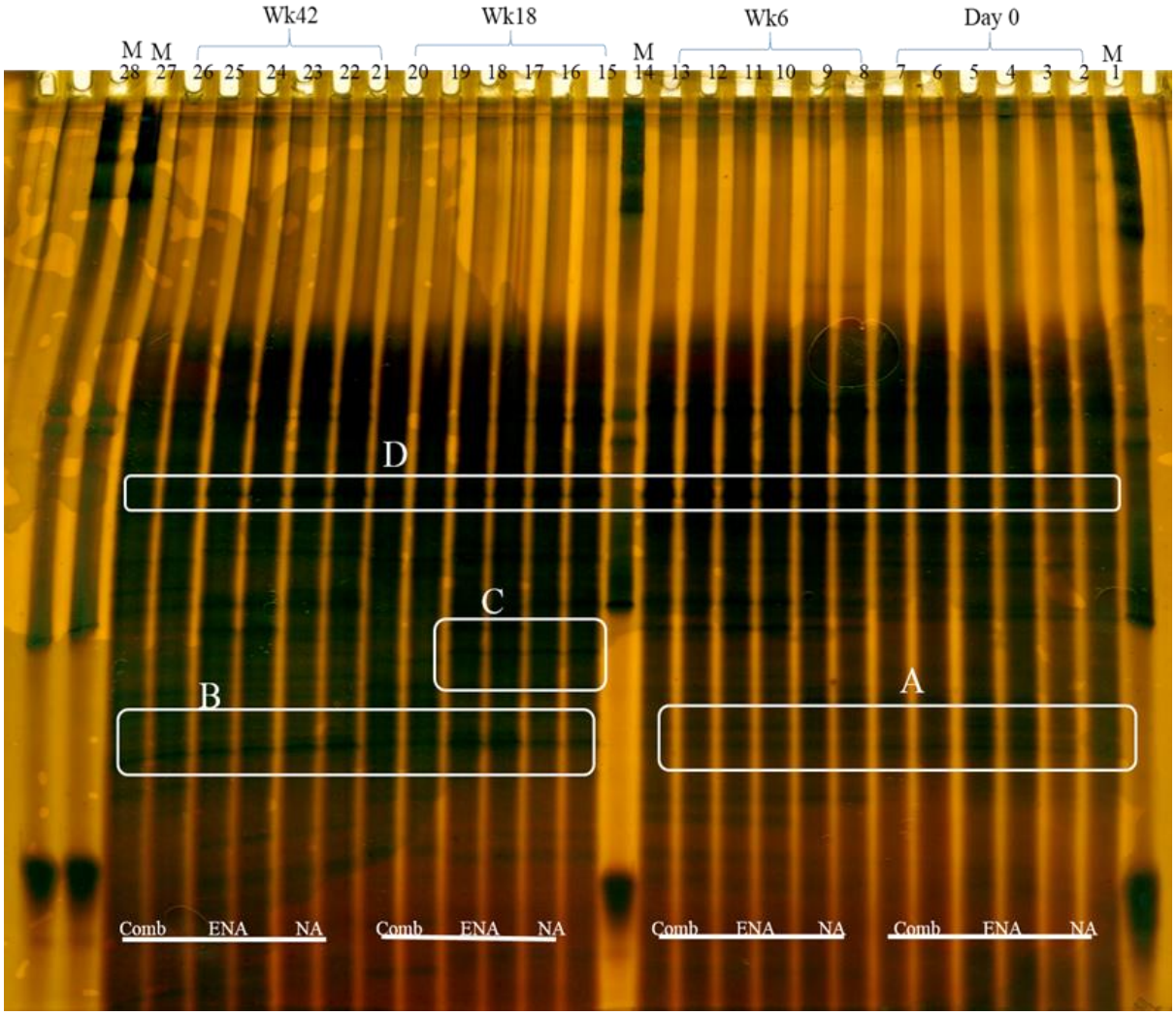

Figure 4.9. Bacterial community profiles generated using 16S rDNA from samples taken at four different time points following 42 weeks of bioremediation of TB-contaminated soil. Lane 1, 14, and 27-28 contain markers. Day 0 samples were loaded in lanes 2-7. Lanes 8-13 represent week 6 amplicons obtained from three microcosms. Lanes 15-20 contain week 18 samples. Loaded in lanes 21-26 are amplicons from samples obtained at week 42. All samples run on this gel, were samples obtained from the three microcosms (NA, ENA and Comb) at the specified time points as labelled on the gel. Highlighted in rectangles tagged A, bands common in samples at time zero and week 6 but with less intensity; B, matching bands with A but with high intensity at weeks 18 and 42, C unique bands at week 18, and D consistent and dominant bands throughout sampled time points.

In NA microcosms, bacterial species diversity was stable in the first six weeks of incubation, with Shannon Weaver diversity values range from 2.83 ± 0 (day 0) to 2.84 ± 0 (week 6) respectively. However, further incubation resulted in a significant decrease ($P > 0.05$) in bacterial species richness in samples obtained from week 18 (2.75 ± 0) and then remained stable until week 42 (2.78 ± 0).

Although small variations were observed in Shannon Weaver diversity values in samples obtained from different time points (Day 0, weeks 6,18 and 42) for NA microcosms, there was

no significant difference (P > 0.05) in bacterial species richness, regardless of when they were sampled. In contrast, bacterial species diversity in ENA microcosms gradually decreased over the course of the incubation (42 weeks). The initial bacterial diversity at day 0 was 2.87 ± 0, 2.86 ± 0 (week 6), 2.78 ± 0 (week 18) and 2.74 ± 0 (week 42). Despite a gradual decrease in bacterial diversity over the course of the incubation, no statistical differences were observed in samples obtained from ENA sampling time points (P > 0.05, all bars marked 'a').

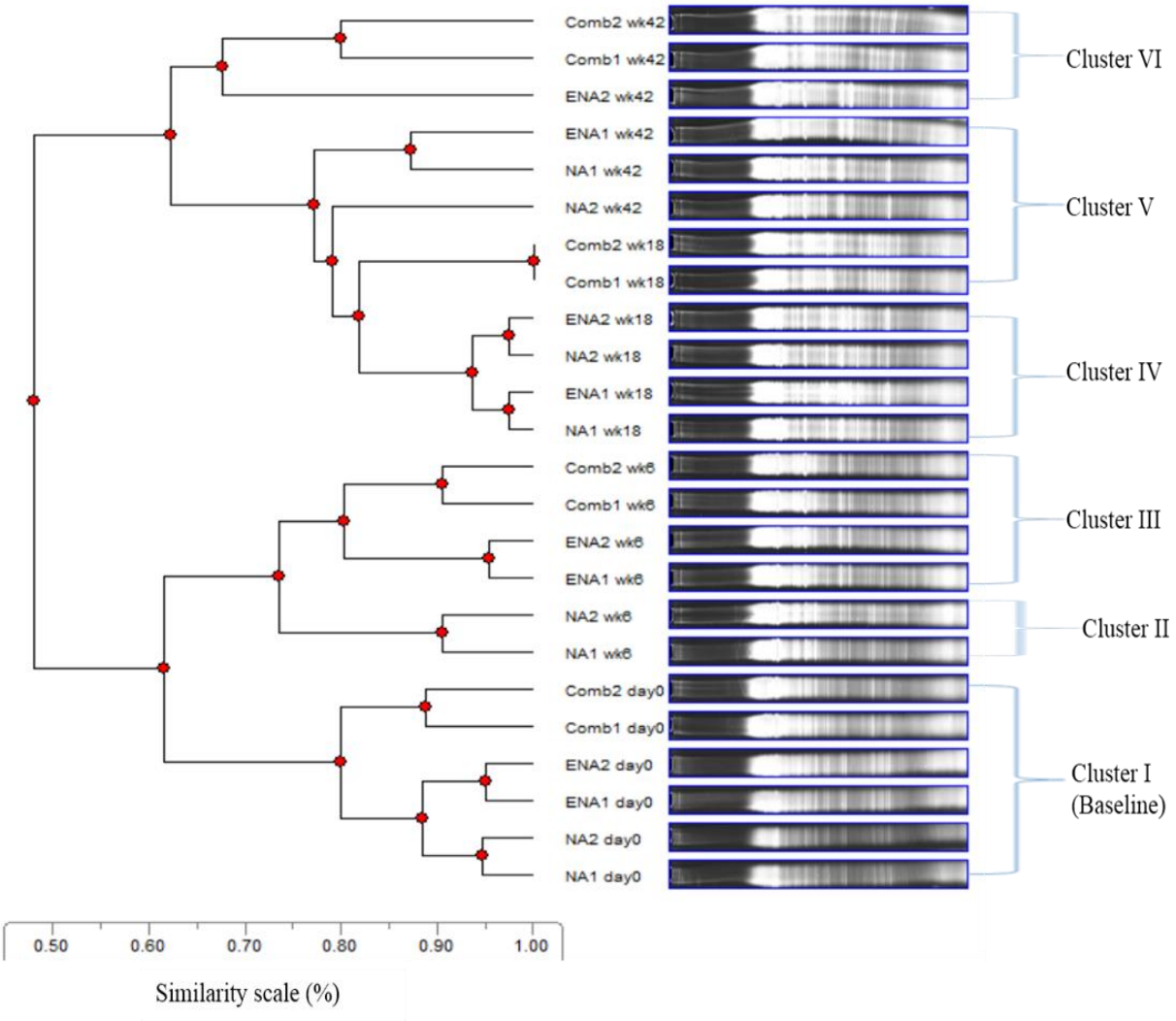

Figure 4.10. UPGMA dendrogram constructed using the similarity matching produced from TB bacterial DGGE community profiles of the 16S rDNA fragments, amplified from all treatments across sampling time point (day 0, weeks 6, 18 and 42). The scale bar represents the level of similarity in percentage. In this dendrogram, there are six distinct aggregates associated with either (I) time of sampling; (II) treatments based grouping, and (III) replicate type clustering.

In contrast, in microcosms where both ENA and BioA were implemented (Comb), bacterial species diversity steadily increased in the first 18 weeks. During these periods, Shannon Weaver diversity values ranged from 2.72 ± 0 (day 0), 2.81 ± 0 (week 6) and 2.92 ± 0 (week 18). This gradual increase was followed by a sharp reduction in bacterial diversity at the end of the incubation period (10.9% reduction at week 42). There was a statistical significant difference observed in bacterial species diversity between samples from Comb0 (bar marked 'b') and the other sampling time points (Comb6, Comb18 and Comb42) with $P < 0.05$.

Bacterial species diversity from Comb6 and Comb18 (bars marked 'a') were not significantly different from each other and the bacterial diversities from other time points (Comb0 and Comb42). Moreover, bacterial species diversity from Comb42 (bar marked 'ab') were statistically different from bacterial diversities in samples obtained from Comb0, Comb6, and Comb18 microcosms at $P < 0.05$. Regardless of small variations observed in Shannon Weaver diversity values in samples obtained from different microcosms, there were no statistical differences between NA, ENA and Comb6 and Comb18 diversities (all bars marked 'a') at $P > 0.05$. However, bacterial diversities from Comb0 and Comb42 were significantly different from bacterial diversities observed from Comb6, Comb18, NA and ENA microcosms (bars marked 'b' and 'ab').

Individual bacterial species were equally distributed across all microcosms as shown in Figure 4.12. Individual bacterial species were evenly distributed in NA microcosms, from day 0 (0.96 ± 0) to week 42 (0.92 ± 0). There were no significant differences in the distribution of individual bacterial species over the course of incubation (42 weeks) at $P < 0.05$ (all NA bars marked 'a'). Similar results were observed in ENA microcosms in samples obtained across sampling time points, with equitability index values ranging from 0.95 ± 0 (day 0) to 0.94 ± 0 (week 42).

However, characterisation of individual bacterial species in Comb microcosms showed that they were equally distributed from day 0 to week 18 (0.95 ± 0 to 0.94 ± 0) but then significantly ($P > 0.05$) decreased at week 42 (0.90 ± 0). Although equitability indexes were within the range of being evenly distributed (equitability close to value of 1.0), bacterial species from Comb42 were significantly ($P < 0.05$) different from bacterial species from the first 18 weeks (day 0, weeks 6 and 18) (bar mark 'b').

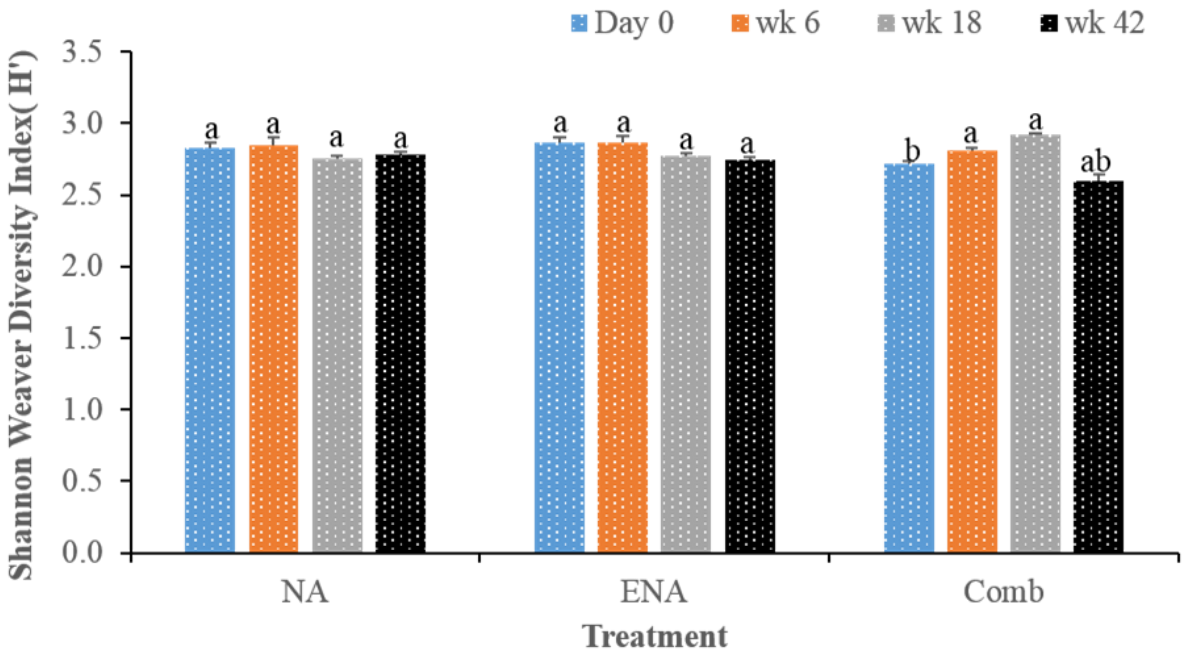

Figure 4.11. Comparison of bacterial community expressed as Shannon Weaver diversity index (H') from DGGE analysis of 16S rDNA fragments in TB soil microcosms incubated for 42 weeks over selected time points (day 0, weeks 6, 18 and 42). During these periods, species richness from natural attenuation, enhanced natural attenuation and bioagumentation were calculated using Total Lab Software over incubation time.

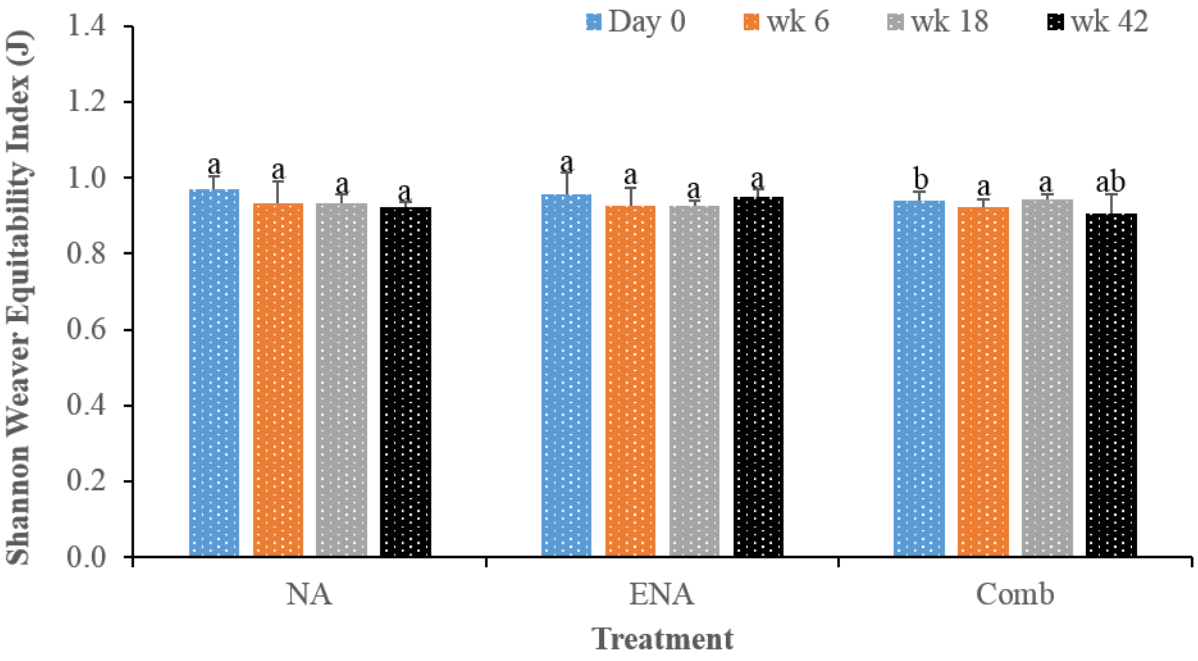

Figure 4.12. Comparison of bacterial community expressed as Shannon Weaver equitability index (J) from DGGE analysis of 16S rDNA fragments in TB soil microcosms incubated for 42 weeks. Samples for molecular analysis were periodically removed during incubation at day 0, weeks 6, 18 and 42 from each microcosm. Error bars represent the standard deviation of replicate analyses. Bars sharing the same letter for NA, ENA and Comb treatments do not differ significantly ($P > 0.05$).

4.5.4 Assessment of supplemented PAH-degrading organisms in TB microcosms

Assessment of supplemented and indigenous PAH-degrading organisms using a specific primer pair (NidA primer) in TB microcosms was performed as described in section 4.4.4. Genomic DNA extracted from samples collected over the course of 42 weeks (four selected time points) was used to generate *Mycobacterium* DGGE community profiles (Figure 4.13). Generally, there were two major banding profiles present with varying intensities, from day 0 to the end of the incubation period (42 weeks).

In NA microcosms, the *Mycobacterium* population was stable in the first 6 weeks of incubation (5 bands present at day 0 and week 6 respectively). However, there was a 4.5% increase in the number of bands from week 6 (5 bands) to week 18 (6 bands). In addition, there were no changes observed in the *Mycobacterium* population following further incubation (bands were consistent from 18 to week 42 with 6 bands each). In contrast, a 4.3% increase was observed in the *Mycobacterium* population in samples collected from ENA microcosms, following the first 6 weeks of incubation period (day 0 to week 6, from 5 to 6 bands). Regardless of further incubation, the *Mycobacterium* population in ENA microcosms remained stable in samples taken from the last two sampling time points (weeks 18 and 42 with 6 bands).

In microcosms where nutrients and inoculants were added (Comb microcosms), there was a gradual increase in the number of bands from 5 (day 0) to 6 bands (week 6) and then to 7 bands (week 18). Despite these increments, there was a 13.6% decrease in the number of bands (*Mycobacterium* population) in the final week of incubation (7 to 4 at week 42). These results suggest that both the augmented and indigenous *Mycobacterium gilvum* species survived the first 18 weeks of experimental conditions in all TB soil amended and unamended microcosms. There were some distinct bands present at the bottom of the gel in samples obtained from Comb0, NA6, ENA6, and NA42, which were not observed in samples from the other time points as shown in the circle tagged B. These unique bands may represent *Mycobacterium* species that increase in numbers as a result of favourable experimental conditions.

In comparison to NA (4.5% increase in the number of bands) and ENA (4.3% increase in the number of bands) microcosms, banding profiles of *Mycobacterium* in Comb microcosms (9.9% increase in the number of bands) increased more during the first 18 weeks of the incubation period. Further analysis of *Mycobacterium* community profiles was performed to determine if the shift in banding profiles was due to amendment or time influences. Shannon Weaver

diversity and equitability index analysis was performed to compare the degree of similarity between *Mycobacterium* species sampled over the 42-week experimental period.

4.5.5 Effect of incubation time and amendments on *Mycobacterium* communities

Shifts in the *Mycobacterium* community profiles as a consequence of incubation time and bioremediation strategies were assessed using an unweighted pair-group method with arithmetic mean (UPGMA). The dendrogram constructed from NidA DGGE image profiles resulted in five distinct clusters (Figure 4.14). These five clusters include: the baseline (cluster I), which was formed based on *Mycobacterium* communities from day 0 (NA0 and ENA0); cluster II (Comb0, ENA6, and NA6), cluster III (ENA6, NA0, ENA0, and Comb6 and NA18); cluster IV (NA18, ENA18, Comb6, Comb18, NA42, and ENA42) and cluster V (Comb42 replicate only).

The clustering in TB soil microcosms was associated with time of sampling, bioremediation strategies applied, or replicate based similarities. *Mycobacterium* communities from NA microcosms were located in four clusters based on time of sampling (Figure 4.13). Generally, the closest similarity observed among communities sampled from different time points (day 0 to week 42) from NA microcosms was 40%, while the highest similarity observed between replicates ranged from 40 % (week 18, with replicate clustered in separate clusters) to 100% (week 6, with duplicate clustered together).

Mycobacterium communities from day 0 were more closely related to communities from week 6 (64% similarity level) than communities from the latest sampling time points (weeks 18 and 42 with 40% similarity level). Similarly, *Mycobacterium* communities from ENA microcosms were based (four clusters) on time of sampling with small variations in similarities within samples.

Thus, the intra replicate similarity from ENA *Mycobacterium* communities ranged from 64% (day 0 samples) to 85% (week 42 samples) respectively, whereas the overall similarity among communities sampled over the course of incubation period was 40% (day 0 to week 42). Similarly, *Mycobacterium* communities in samples obtained from day 0 were closely related to week 6 (64% similarity level) communities than weeks 18 and 42 (59% similarity level) from ENA microcosms and were found in clusters situated next to each other (I and II).

Similar results were observed for Comb microcosms; however, similarities between duplicates ranged from 40% (week 6) to 100% (day 0 and week 42 respectively) and scattered over four clusters (cluster I-V) based on time of sampling. In addition, *Mycobacterium* communities sampled at different time points (i.e. NA0 and Comb42 samples) were distantly clustered suggesting low similarities between communities (overall 40% level).

Principle component analysis (PCA) was performed using *Mycobacterium* DGGE data to confirm the level of similarity among *Mycobacterium* communities sampled from different microcosms (NA, ENA and Comb), at four selected time points (day 0, weeks 6, 18, and 42) as demonstrated by the UPGMA dendrogram (Appendix 3, Figure A3.3).

The aggregation of *Mycobacterium* communities was predominantly due to the effect of incubation time rather than bioremediation strategies applied. For example, *Mycobacterium* population in samples obtained from day 0 and week 6 were clustered in span 1 quadrant while those communities from the latest sampling points (weeks 18 and 42) were distantly grouped in the span 2 quadrant. Moreover, the initial Eigenvalues in quadrant span 1 explained 39.2% of total variance observed while quadrant span 2 accounted for 24.1% of the total variance of *Mycobacterium* communities.

However, there were some outlying communities which clustered separately between the two main components (span 1 and 2) in samples obtained from NA18, Comb6 and Comb42 microcosms. Not surprisingly, *Mycobacterium* communities from these sampling points (NA18, Comb6 and Comb2) also clustered separately from other communities in the UPGMA dendrogram (Figure 4.20) suggesting that they were distantly related. Hence, *Mycobacterium* community profiles grouping displayed in the PCA (Appendix 3, Figure A3.4) confirmed similar clustering of communities from these microcosms (NA18, Comb6 and Comb42) demonstrated in UPGMA dendrogram (Figure 4.14).

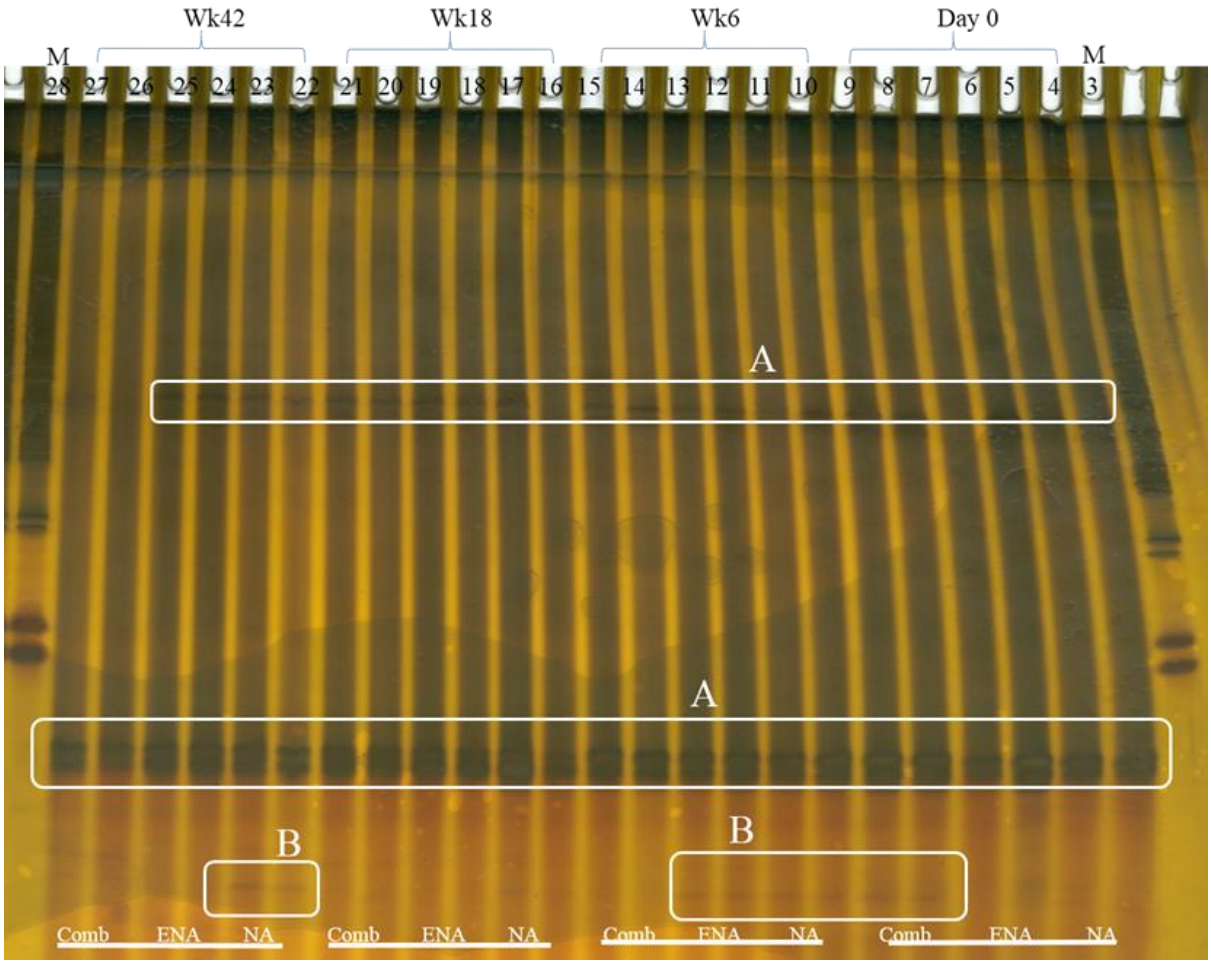

Figure 4.13. Comparison of *Mycobacterium* community profiles in TB-contaminated soil generated using NidA genes following 42 weeks incubation. Lanes 3 and 28 contain markers, day 0 samples were loaded in lanes 4-9, lanes 10-15 represent week 6 amplicons, lanes 16-21 contain week 18 samples, and loaded in lanes 22-27 represent samples obtained from week 42. (NA, ENA and Comb). Highlighted in rectangles tagged A, consistent and dominant bands throughout sampled time points and B, unique bands at day 0, weeks 6 and 42.

4.5.6 *Mycobacterium* community profile analysis

Differences in *Mycobacterium* community profiles in TB soil microcosms were assessed by Shannon Weaver diversity (H') and equitability (J) indexes as previously described in section 4.4.6. Total *Mycobacterium* species diversity in NA microcosms was not affected by either the incubation time or bioremediation strategies employed over the course of the 42-week period. Although the diversity values varied in sample obtained over the course of the incubation, these variations may be due to sampling and analytical error.

Similar results were observed in amended microcosms (ENA and Comb). *Mycobacterium* diversity indexes from these two microcosms was the same from day 0 to week 42 (ENA and Comb18, H' value of 1.67 and 1.74 respectively) as shown by bars tagged 'a' (Figure 4.15). Regardless of whether an amendment was implemented, *Mycobacterium* species richness showed similar diversity over the course of 42-week incubation period.

The individual evenness of *Mycobacterium* was also predominantly unaffected by either the incubation time or bioremediation strategies applied (Figure 4.16). *Mycobacterium* species equitability index from NA microcosms was evenly (bars tagged 'a') distributed in samples obtained across sampling points (i.e. from NA0 to NA42).

Compared to NA microcosms, *Mycobacterium* species equitability indices from ENA and Comb microcosms was not influenced by addition of nutrients/inoculums or the incubation time (all bars tagged 'a'). In addition to the Shannon Weaver diversity analyses, a stand-alone statistical analysis was employed to compare *Mycobacterium* communities in samples periodically taken over the experimental time course using repeated measures of analysis of variance (Graph Pad Instat v3).

Results from these analyses further confirmed that no statistically significant differences were observed within each microcosm. Thus, these findings suggested that addition of nutrients or inoculants didn't affect *Mycobacterium* population in TB soil.

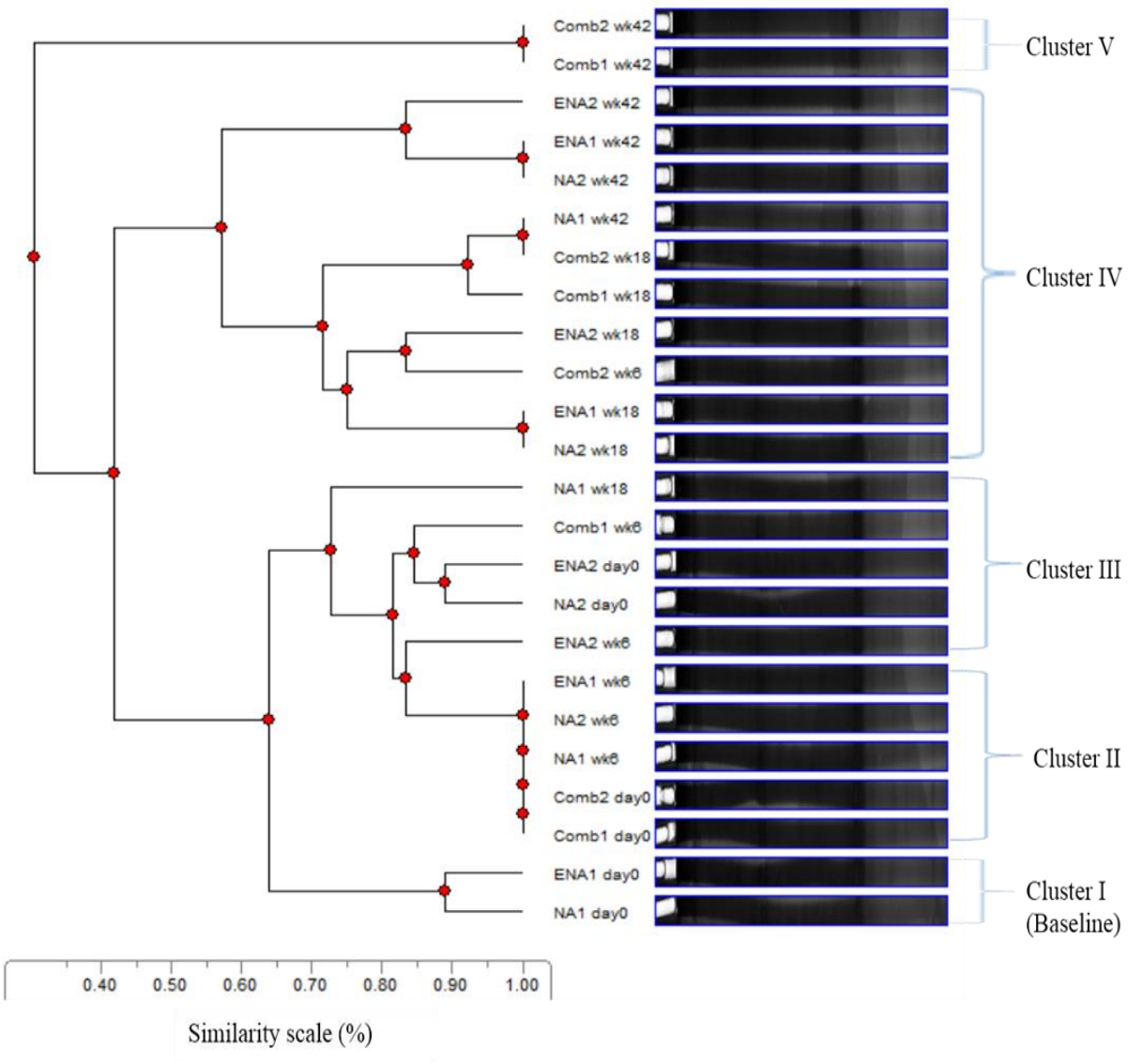

Figure 4.14. UPGMA dendrogram constructed from the similarity matching produced from TB NidA DGGE community profiles of the 16S rDNA fragments, amplified from all treatments across sampling time point (day 0, weeks 6, 18 and 42). The scale bar represents the level of similarity in percentage. In this dendrogram, there are five distinct clusters associated with either (I) time of sampling; (II) treatments based grouping, and (III) replicate type clustering.

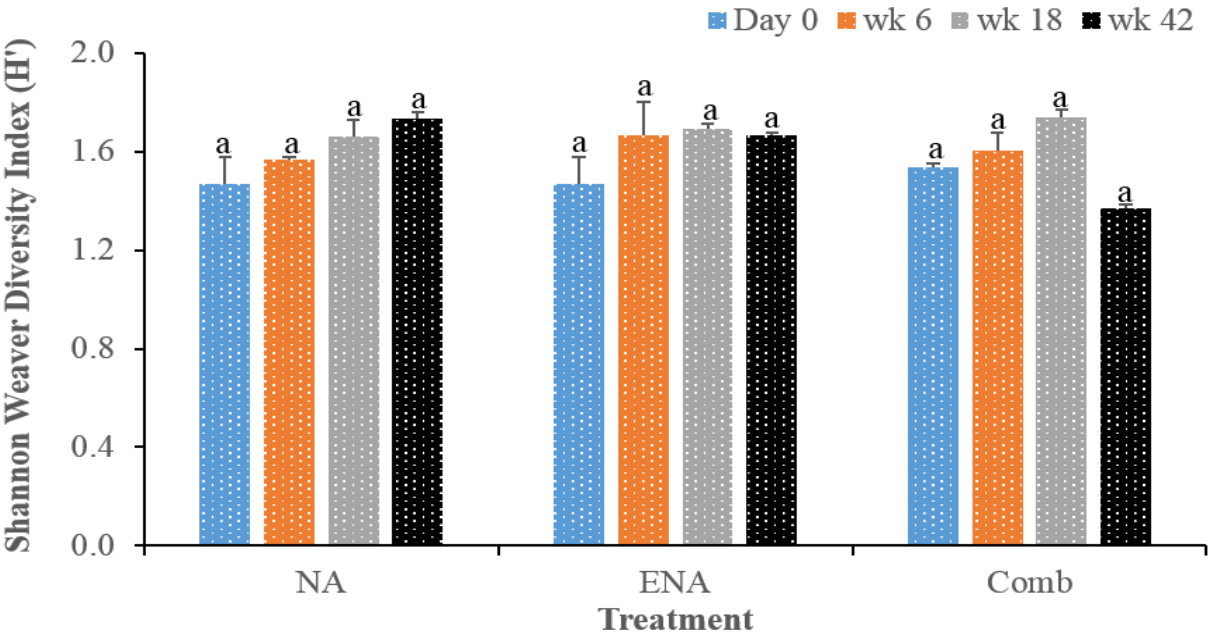

Figure 4.15. Comparison of *Mycobacterium* community expressed as Shannon Weaver diversity index (H') from DGGE analysis of 16S rDNA fragments in TB-contaminated soil microcosms incubated for 42 weeks over selected time points (day 0, weeks 6, 18 and 42). During these periods, species richness from natural attenuation, enhanced natural attenuation and bioagumentation were calculated using Total Lab Software over incubation time.

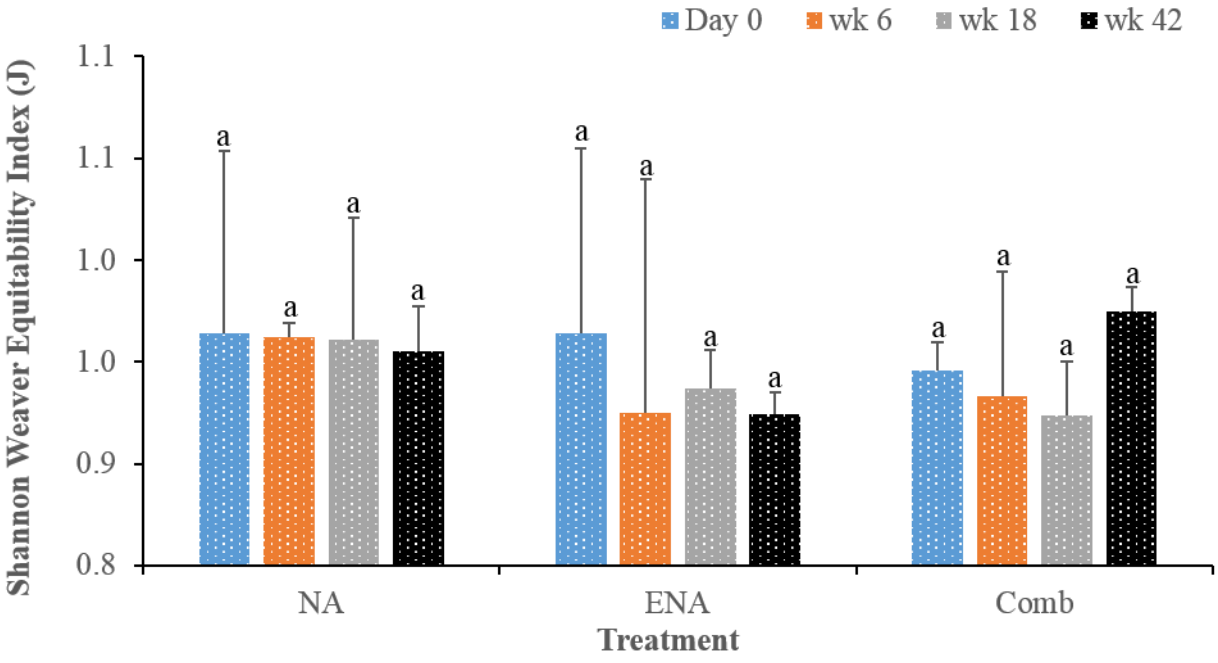

Figure 4.16. Comparison of *Mycobacterium* community expressed as Shannon Weaver equitability index (J) from DGGE analysis of 16S rDNA fragments in TB soil microcosms incubated for 42 weeks. Samples for molecular analysis were periodically removed during incubation time at day 0, weeks 6, 18 and 42 from each microcosm. The measure of species equitability was calculated from Shannon Weaver diversity index to determine the proportion of individual species distribution in the community.

4.6 Assessment of microbial communities in AP soil microcosms

4.6.1 Bacterial community in AP microcosms

Bioremediation studies using AP-contaminated soil microcosms was performed over a period of 42 weeks. During this time period, changes in microbial communities as a result of bioremediation strategy applied (i.e. NA, ENA, and BioA) were assessed using DGGE. Amplified PCR products of DNA extracted from soil samples collected on day 0, weeks 6, 18 and 42 were analysed by DGGE to generate bacterial community profiles (Figure 4.17).
Generally, based on bacterial community profiles (Figure 4.17), some dominant and unique bands were present in samples obtained across sampling time points as highlighted in rectangles tagged A, B, C, and D. In NA microcosms, the initial bacterial population decreased by 14.7% in the first 6 weeks of incubation (from 38 to 21 bands, from day 0 to week 6 respectively). Despite the initial reduction observed at the commencement of the incubation, bacterial communities increased by 7.8% following further incubation (from 21 to 30 bands at week 6 to week 42). Compared to NA microcosms, there was a small increase (1.5%) in band numbers at the commencement of incubation (from 38 to 40 bands at day 0 to week 6) in ENA microcosms. However, bacterial communities decreased by 9.9% from 40 (week 6) to 26 bands at week 18 and then remained stable at week 42 (27 bands).

In microcosms where both nutrients and inoculums were supplemented (Comb), the diversity in bacterial communities significantly decreased at the commencement of incubation (from 38 to 27 bands at day 0 to week 6), whereas an increase in the diversity of bacterial communities was observed from 27 (week 6) to 29 bands (week 42). The decrease in diversity in bacterial communities towards the end of the incubation may be indicative of nutrient depletion in amended microcosms. In addition, there were some distinct bands only present in ENA0 and Comb0 as highlighted in the rectangle tagged A and C. The bands present in rectangle tagged C have no matching bands in samples obtained from the later sampled points (weeks 6, 18 and 42), while bands in the rectangle marked A had matching bands with high intensities in samples obtained from the same time points (weeks 6, 18 and 42). Further analysis of bacterial community profiles was conducted to confirm if differences in banding profiles was due to amendment or incubation time influences. Shannon Weaver diversity and equitability analyses were performed to compare the degree of similarity between bacterial communities in amended and unamended microcosms.

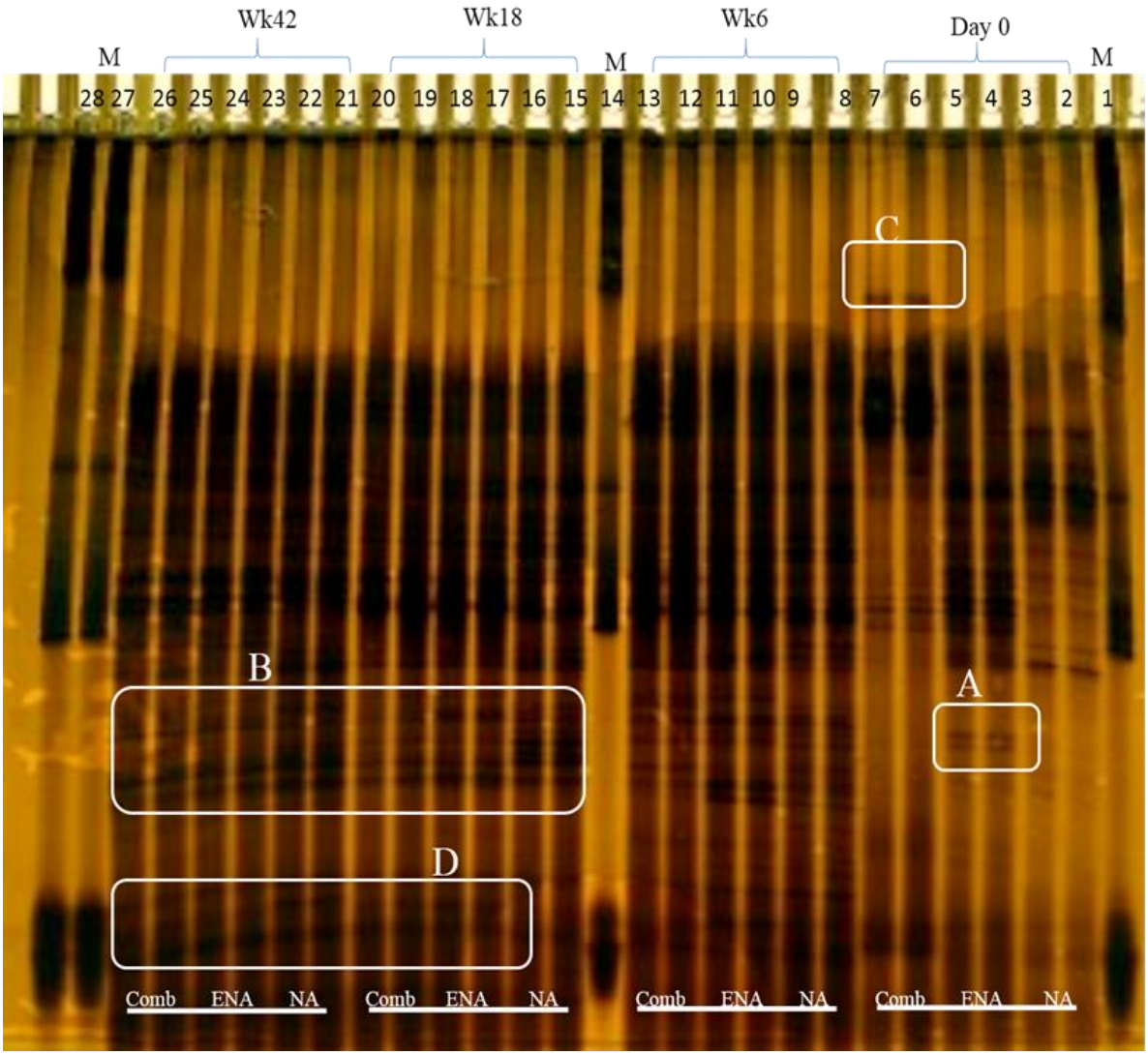

Figure 4.17. Comparison of bacterial community profiles in AP-contaminated soil generated using 16S rDNA following 42 weeks incubation. Lane 1, 14, and 27-30 contain markers, day 0 samples were loaded from lanes 2-7, lanes 8-13 represent week 6 amplicons, lanes 15-20 contain week 18 samples, and loaded in lanes 21-26 represent samples obtained at week 42. All samples run on this gel, were samples obtained from the three microcosms (NA, ENA and Comb) at the specified time points. Highlighted in rectangles tagged A, unique bands at the bottom gel day 0; B, bands with high intensity at weeks 18 and 42 and C, unique bands in the upper part of gel at day 0.

4.6.2 Effect of incubation time and amendment on bacterial communities

Similarities in bacterial community banding profiles as a result of incubation time and bioremediation strategies were assessed using an unweighted paired-group method with arithmetic mean (UPGMA) and presented in Figure 4.18. Cluster analysis of UPGMA showed that bacterial communities from AP microcosms fell into four clusters depending on the time at which each community was sampled. As expected, the baseline cluster (cluster I) was developed based on bacterial communities in samples collected on day 0 (Comb0 duplicate samples), while the remaining three clusters were developed based on bacterial communities sampled at the later sampling points. The second cluster was developed based on bacterial communities from day 0 (ENA and NA) and week 6 (all microcosms), while bacterial communities sampled at the latest time points (weeks 18 and 42) were located in clusters III (all week 18 microcosms plus NA42) and IV (ENA42 and Comb42) respectively.

In NA microcosms between 64% (NA0) to 91% (NA18) of the replicates were similar. It was shown that bacterial communities from a duplicate sampled at a given time point were present in the same cluster. For example, cluster I was developed based on Comb1 and Comb2 bacterial communities sampled on day 0. Bacterial communities from day 0 were more similar to bacterial communities from week 6 (60% similarity) than those communities sampled at weeks 18 and 42 (55% similarity). Overall, similarity among bacterial communities sampled over the course of 42 weeks incubation from NA microcosms was 45%. This was the lowest similarity observed under NA conditions compared to similarities between the duplicate samples (91% NA1 and NA2 at week18). Bacterial communities from ENA microcosms followed the same trends of clustering as observed in the NA microcosms; however, the similarity between duplicate samples ranged from 70% (ENA42) to 95% (ENA6). In contrast, in bacterial communities from microcosm where nutrients and inoculums were implemented (Comb), similarities between duplicate samples ranged from 69% (Comb42) to 93% (Comb6). The bacterial communities sampled at day 0 (Comb0 with 37% level) were less similar to the bacterial communities sampled at the later time points (weeks 6, 18 and 42). In addition, the similarity observed among bacterial communities sampled (at time points from Comb microcosms) over the course of 42 weeks incubation was the lowest (37% level) compared to overall similarity reported among bacterial communities from NA and ENA microcosms (45% similarity in both cases).

DGGE data were further analysed using principle component analysis (PCA, Appendix 3, Figure A3.4) to confirm similarities in clustering of bacterial community profiles, assessed by UPGMA analysis (Figure 4.18). Results from PCA analyses indicated that bacterial communities' aggregation (grouping of similar organisms) was predominantly driven by incubation time and duplicate similarities. For example, bacterial communities obtained on day 0 and week 6 were grouped in quadrant span 1 while those communities in samples obtained from both week 42 were clustered in quadrant span 2. As per initial Eigenvalues, the quadrant span 1 accounted for 61% of variance while quadrant span 2 only explained 9.5% of variance observed in bacterial differences (Appendix 3, Table A3.4).

Bacterial communities in samples obtained at week 18 clustered separately in between the two quadrants but closer to communities sampled on day 0 and week 6. As expected bacterial communities at the commencement of incubation were similar to each other regardless of the bioremediation strategies applied. However, there were some outlying communities that clustered separately between the two main components (span 1 and 2) in samples obtained from Comb42 microcosms. Nonetheless, the level of similarities diminished with further incubation, leading to differences in bacterial communities sampled at the end of the incubation period.

4.6.3 Bacterial community profile analysis

Changes in bacterial community profiles in the AP soil microcosms was assessed by Shannon Weaver diversity (H') and equitability (J) indexes as previously described in section 4.4.6. Total bacterial species diversity in NA microcosms was affected by incubation time over the course of 42 weeks. At the commencement of incubation, bacterial diversity decreased by 15.7% (from day 0 to week 6) and then increased by 11.9% with further incubation (week 6 to week 42). Overall, bacterial diversity varied over the course of 42 weeks incubation as shown in Figure 4.19.

In contrast, bacterial diversity in ENA microcosms was constant in the first 6 weeks of incubation (H' values of 3.46 ± 0 to 3.49 ± 0, from day 0 to week 6) as highlighted by bars marked with the same letter (a) as in Figure 4.19. However, there was a significant decrease in the bacterial diversity of 15.8% at week 18 (2.94 ± 0), which was followed by a 4.8% increase at the end of incubation (H' value of 3.08 ± 0 at week 42).

In contrast, microcosms where both nutrients and inoculums were supplemented, bacterial diversity gradually decreased over the 42-week incubation period. For example, a 10.7% decrease in bacterial diversity was observed during the first 6 weeks of incubation (H' value was reduced from 3.45 ± 0 to 3.08 ± 0), which was followed by a further 3.3% reduction in bacterial diversity at the end of the incubation (H' value of 3.01 ± 0 at week42. Bacterial diversity significantly increased from day 0 to week 42 in the microcosm where both nutrients and inoculums were supplemented ($P < 0.05$).

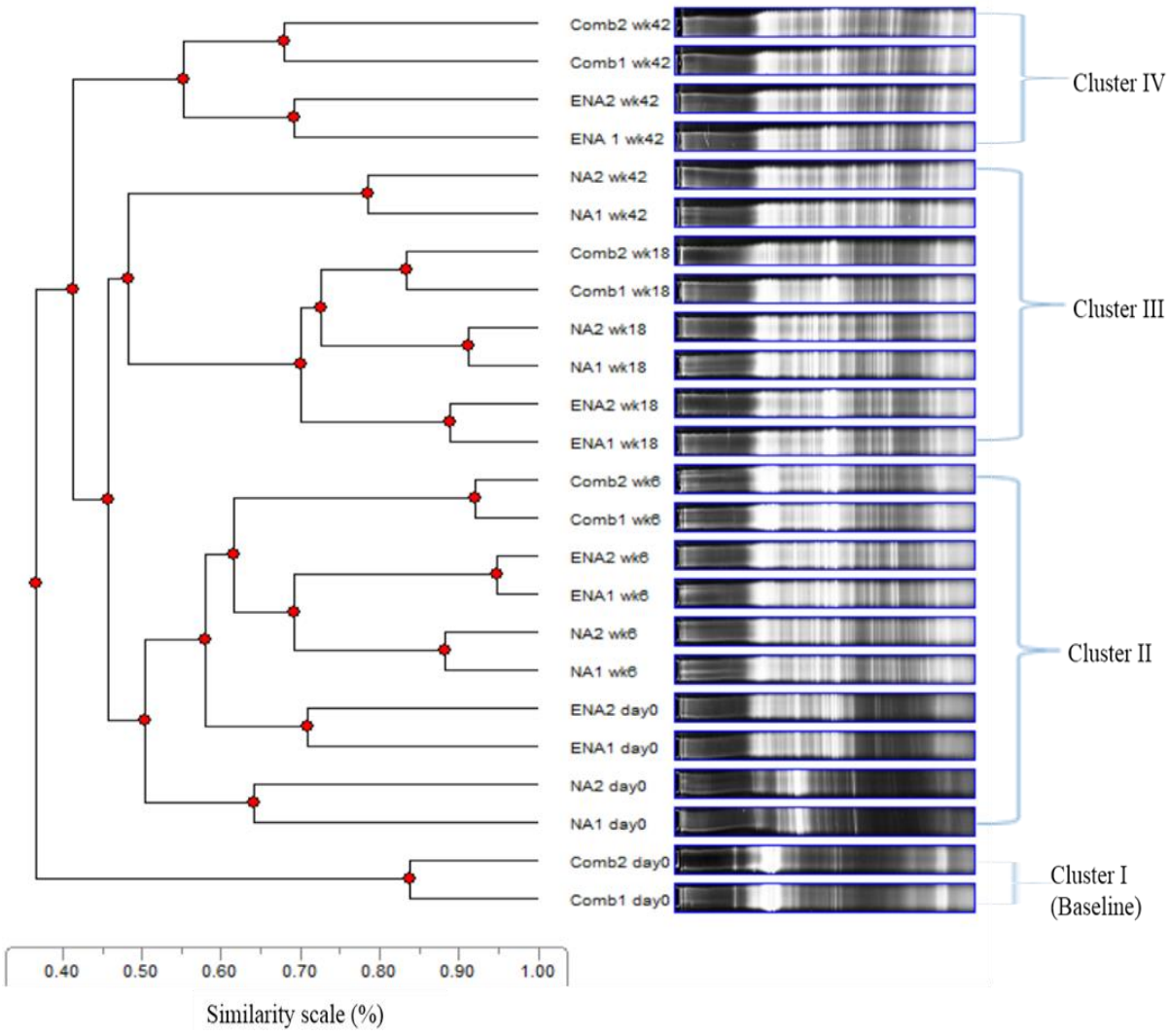

Figure 4.18. UPGMA dendrogram constructed from the similarity matching produced from AP bacterial DGGE community profiles of the 16S rDNA fragments, amplified from all treatments across sampling time points (day 0, weeks 6, 18 and 42). The scale bar represents the level of similarity in percentage. In this dendrogram, there are three distinct clusters associated with either (I) time of sampling; (II) treatments based grouping, and (III) replicate type clustering.

In addition, bacterial diversity in samples obtained from weeks 6 and 18 were similar (bars marked with c). Regardless of whether an amendment was implemented or just addition of moisture, bacterial communities in samples obtained from NA6, NA18, ENA18 and Comb42 microcosms had similar diversities (all bars marked 'a') over the course of 42 weeks incubation. In terms of equitability (J), bacterial evenness distribution relative to total the bacterial population from four microcosms (NA, ENA, and Comb) at four selected sampling events (day 0, weeks 6, 18 and 42) is presented in Figure 4.20. Bacterial equitability index from NA microcosms were evenly (bars tagged b) distributed in samples obtained from three sampling time points (i.e. from NA0, NA6 and NA42 with J values of 0.93 ± 0, 0.93 ± 0 and 0.93 ± 0 respectively), whereas the distribution of bacterial diversity in sample obtained from week 18 (0.90 ± 0) was even but less similar to the other time points. Compared to NA microcosms, individual bacterial species J values were equally distributed in the ENA microcosms, where equitability indexes of bacterial sampled on day 0 (0.95 ± 0), week 6 (0.95 ± 0) and week 42 (0.93 ± 0) showed similar distribution. The bacterial equitability index from week 18 was equally distributed but less similar to the rest of the time points. Generally, bacterial equitability distribution relative to the total bacterial population in all the treated AP microcosms was presumably influenced by incubation rather than bioremediation strategies employed. For example, bacterial equitability indices were equally distributed in samples obtained on day 0 (NA0, ENA0 and Comb0), week 6 (NA6, ENA6 and Comb6) and interestingly week 42 (NA42 and ENA42) with similarity shown by bars marked 'b'. Bacterial equitability indexes from week 18 (NA18, ENA18, Comb18) and week 42 (Comb42) were evenly and similarly distributed as represented by bars marked 'a'.

In addition to Shannon Weaver diversity analyses, a stand-alone statistical analysis was used to compare changes in bacterial population, in terms of diversity and equitability indexes in samples periodically taken over the study period using repeated measures of analysis of variance (Graph Pad Instat v3). Results from these analyses confirmed that the similarities in bacterial communities observed within each microcosm diversity as well as comparison between the two amended communities were either statistically different or not at $P < 0.05$. Table A3.4 (Appendix 3) gives overall comparisons of bacterial communities sampled from different microcosms (all sampling time points) over the course of the 42 weeks. These findings suggested that addition of either nutrients or inoculants did not affect the bacterial population in AP soil.

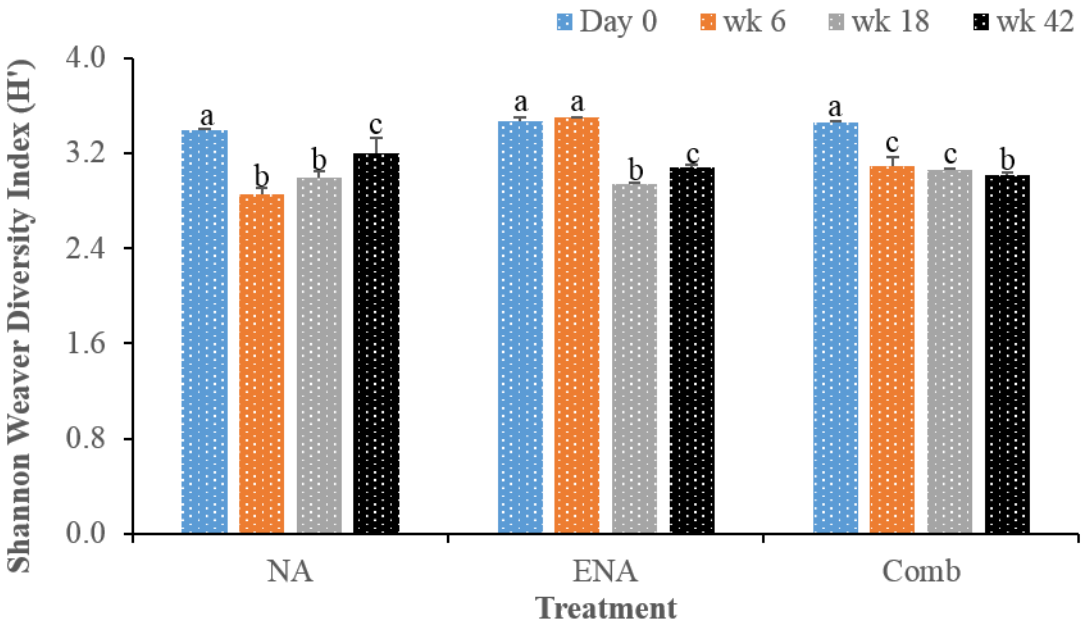

Figure 4.19. Comparison of bacterial community expressed as Shannon Weaver diversity index (H') from DGGE analysis of 16S rDNA fragments in AP soil microcosms incubated for 42 weeks over selected time points (day 0, weeks 6, 18 and 42). During these periods, species richness from natural attenuation, enhanced natural attenuation and bioaugmentation were calculated using Total Lab Software over incubation time.

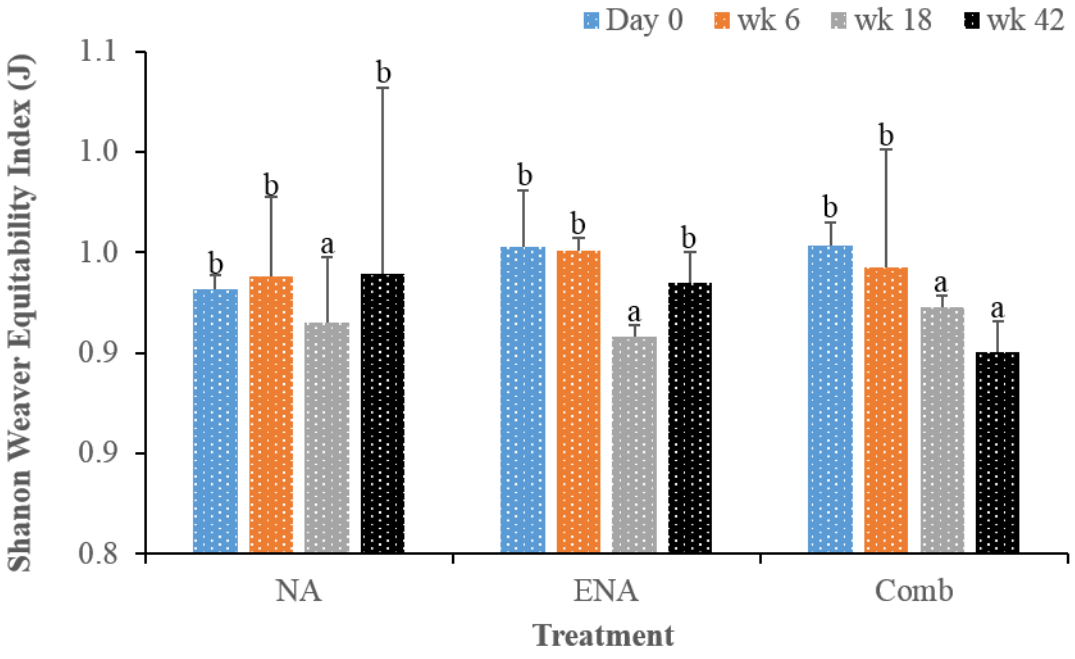

Figure 4.20. Comparison of bacterial community expressed as Shannon Weaver equitability index (J) from DGGE analysis of 16S rDNA fragments in AP soil microcosms incubated for 42 weeks. Samples for molecular analysis were periodically removed during incubation time at day 0, Weeks 6, 18 and 42 from each microcosm. The measure of species Equitability was calculated from Shannon Weaver diversity index to determine the proportion of individual species distribution in the community.

4.7 Bacterial communitity in composite gel (All three soils)

Analyses of bacterial communities in samples obtained across four time points (day 0, weeks 6, 18 and 42), performed using a DGGE composite gel resulted in the detection of 690 bands over the course of incubation (42 weeks) from the three soil microcosms (Creo, TB, and AP). In the Ap microcosms, a significant shift in total bacterial communities was observed from unamended (NA) and amended microcosms (ENA and Comb) respectively (Figure 4.21). These shifts in bacterial communty were evident by an increase in the number of bands, ranging from 63 (26.1% in NA) to 88 (36.4% in ENA) and 91 (37.6% in Comb) during the experimental period (42 weeks). Similar shifts in bacterial communties were observed in both the TB and AP microcosms (Figure 4.21). However, in the TB microcosm, a sharp increase was observed in the number of bands detected; 64 (28.3%) in NA, 83 (37.1%) in ENA and 77 (34.4%) in Comb, in the nutrients and inoculum treated microcosms. In the AP microcosms, a sharp increase in the number of bands was also observed; 61 (27.2%) in NA, 81 (36.2%) in ENA and 82 (36.6%) in Comb. The bacterial population also signifcantly ($P > 0.05$) increased with incubation time in amended microcosms (ENA and Comb) compared to the unamended microcosm (NA) in both AP and Creo microcosms.

Generally, there were some distinctive high intensity bands present in samples obtained from all microcosms (three soils) at week 6 as shown in the rectangle tagged A.These bands become less dominant in samples collected at the latter sampling events (weeks 18 and 42) in all the microcosms. Unlike those distinctive bands observed in the rectangle tagged box A, there were some dominant bands common in samples obtained from all microcosms from the commencement to the end of the incubation as highlighted in tagged box B.These bands were present in all the microcosms, regardless of biroemediation strategies applied over the course of the incubation (42 weeks).

Furthermore, distinctive bands were observed in samples obtained at week 18 in all soils and treatments (rectangle tagged box C). These bands were present at 6 weeks in all aoils but at low intensities. Highlighted in the rectangle tagged box D are a number of distinct high intensity bands found at week 18 in Creo microcosms. Based on bacterial community banding profiles (Figure 4.21), total bacterial population in Creo microcosm (237 bands) was greater compared to TB and AP microcosms (224 bands from each microcosm) respectively.

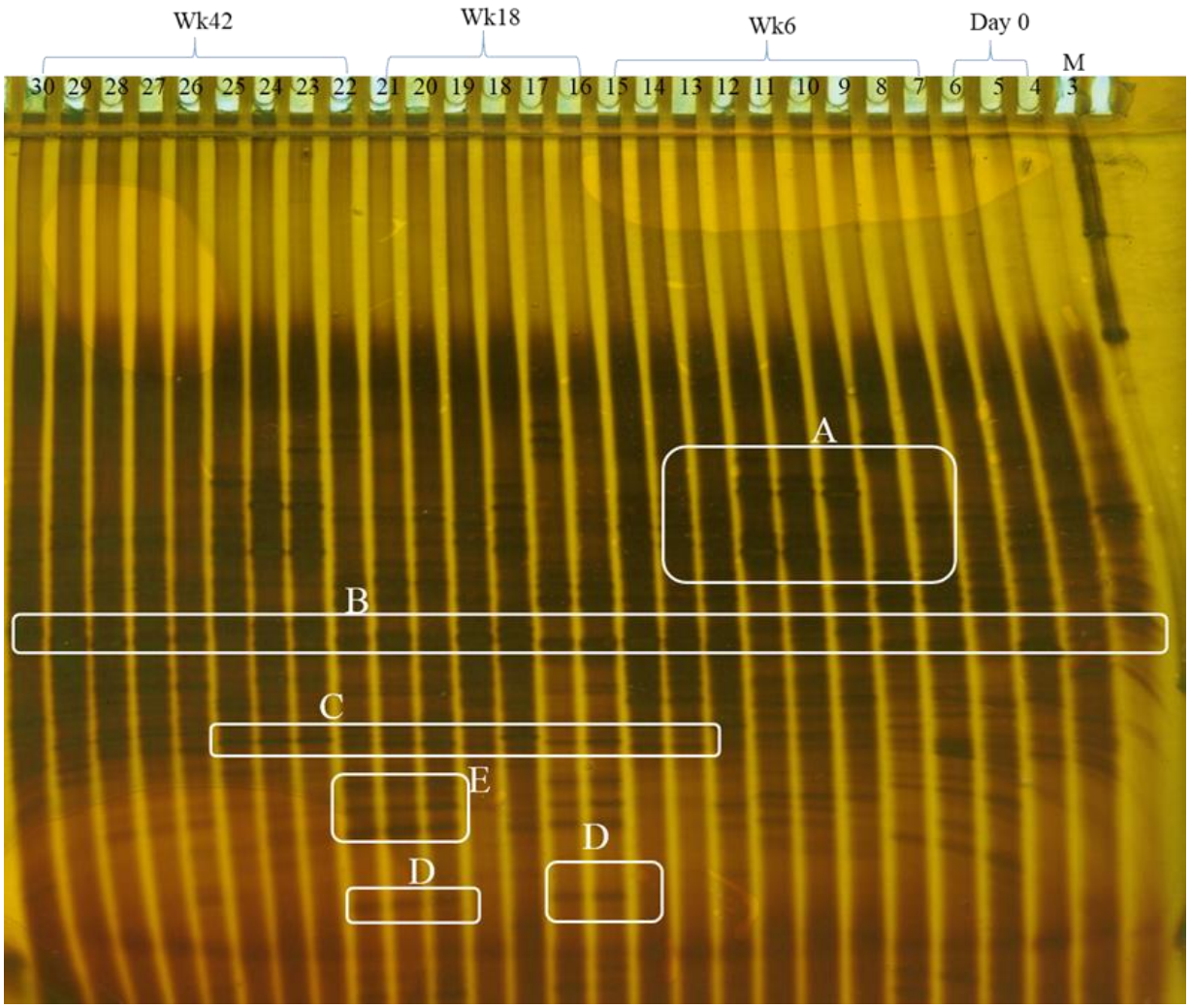

Figure 4.21. Comparison of bacterial community profiles in composite gel generated using 16S rDNA from samples taken at four different time points following 42 weeks of incubation (all soils). Lane 3 contain marker, day 0 samples were loaded in lanes 4-6, lanes 7-15 represent week 6 amplicons (all three microcosms), lanes 16-21 contain week 18 samples, and loaded in lanes 22-30 are amplicons from samples obtained at week 42. Highlighted in rectangles tagged A, dominant bands at week 6; B, consistent bands throughout sampled times; C; bands with increased dominance at weeks 18 and 42 and D, unique bands at weeks 18 and 42.

4.7.1 Effect of incubation time and amendments on bacterial communities

Differences in bacterial community banding profiles as a consequence of incubation time and bioremediation strategies were collectively assessed using unweighted pair-group method with arithmetic mean analysis (UPGMA) in samples obtained from three microcosms (AP, TB and Creo). The dendrogram constructed from bacterial DGGE image profiles eventuated in six hierarchical distinct clusters (Figure 4.22). These six clusters include: the baseline (cluster I), which was formed based on bacterial communities sampled on day 0 (Comb0 AP samples); cluster II (Comb0 TB, NA42 Creo and ENA42 Creo samples), cluster III (Comb18 AP, ENA18 AP,, ENA18 Creo, Comb18 Creo and NA42 AP samples); cluster IV (NA6 Creo, ENA6 Creo,Comb0 Creo, Comb18 and Comb42 Creo samples); cluster V (ENA6 TB, Comb6 TB, NA6 AP, ENA6 AP, NA6 TB, Comb6 AP and ENA42 AP samples); cluster VI (Comb0 Creo, ENA18, Comb42 AP, NA42 TB, ENA42 TB and Comb42 Creo samples).

The clustering observed in AP, TB and Creo microcosms was associated with the time of incubation rather than bioremediation strategies with the exception of a few bacterial communities that were randomly clustered. For example, cluster III was developed based on bacterial communities sampled at week18 and one bacterial community from week 42. The similarity between bacterial communities collected from the 3 microcosm treatments (all six hierarchical clusters) ranged from 60% (II) to 71% (III). Generally, the overall similarity observed between bacterial communities located in different clusters ranged from 55% (clusters II, III, IV) to 59% (clusters V and VI). DGGE data was analysed by principle component analysis (PCA) (Appendix 3, Figure A3.5) to confirm whether similarities in bacterial community profiles were due to incubation time or bioremediation strategy applied. Bacterial community aggregation was predominantly due to the impact of incubation time. For instance, bacterial communities sampled at day 0 and week 6 were clustered in the quadrant span 2 inclusive of all microcosms (AP, TB and Creo), while bacterial communities sampled at the latest time points (weeks 18 and 42) were found in quadrant span 1.

Overall, quadrant span 1 accounted for 24.9% of total variance while 17.5% of total variance was due to quadrant span 2 based on the initial Eigenvalues. In addition to these clusters, there was a mixed cluster developed based on bacterial communities sampled at weeks 6, 18 and 42), located adjacent to span quadrants 1 and 2. Thus the bacterial community profiles clustering in this PCA (Appendix 3, Figure A3.5) confirmed hierarchical clustering of bacterial communities shown in the UPGMA dendrogram described earlier (Figure 4.22).

4.7.2 Assessment of PAH-degrading organisms in composite gel (AP, TB and Creo) of three treated microcosms

Assessment of treated microcosm effects on PAH-degrading organisms *(Mycobacterium*) was undertaken using specific primer pair (NidA primer) as described in section 4.4.4. Genomic DNA extracted from samples collected over the course of the 42 weeks (four selected time points) incubation period was used to generate *Mycobacterium* DGGE community profiles (Figure 4.23) encompassing samples from three microcosms.

Only a limited number of samples were analysed from AP microcosms due to insufficient amount of DNA extracted. Several attempts were made to produce enough DNA by performing multiple amplifications, but only 6 samples (day 0 and week 6 samples) were successfully amplified. The results of the amplification can be seen (Figure 4.23) in lanes where these low quality amplicons (AP products) were loaded (lanes 3-8), a total of 18 bands were observed as highlighted in the rectangles tagged B.

Generally, there were two major banding profiles present with varying intensities, from time zero to the end of the incubation (42 weeks) in both TB and Creo microcosms. *Mycobacterium* communties were stable and consistently oberseved in both TB and AP microcosms. This was evident by the similar number of bands oberved ranging from day 0 (6 bands) to week 42 (6 bands) in unamended and amended microcosms as shown in the rectangles tagged A. Similarly, no differences were observed in total *Mycobacterium* communities sampled from these two microcosms over the course of 42 weeks (each with 71 bands).

However, there were some distinct high intensity bands present in Creo microcosms, which were less dominant in TB microcosms as shown in the rectangle marked C. Based on *Mycobacterium* community banding profiles (Figure 4.23), total *Mycobacterium* population in both TB and Creo microcosm were similar as demonstrated by the presence of the same number of bands (71 bands each) respectively.

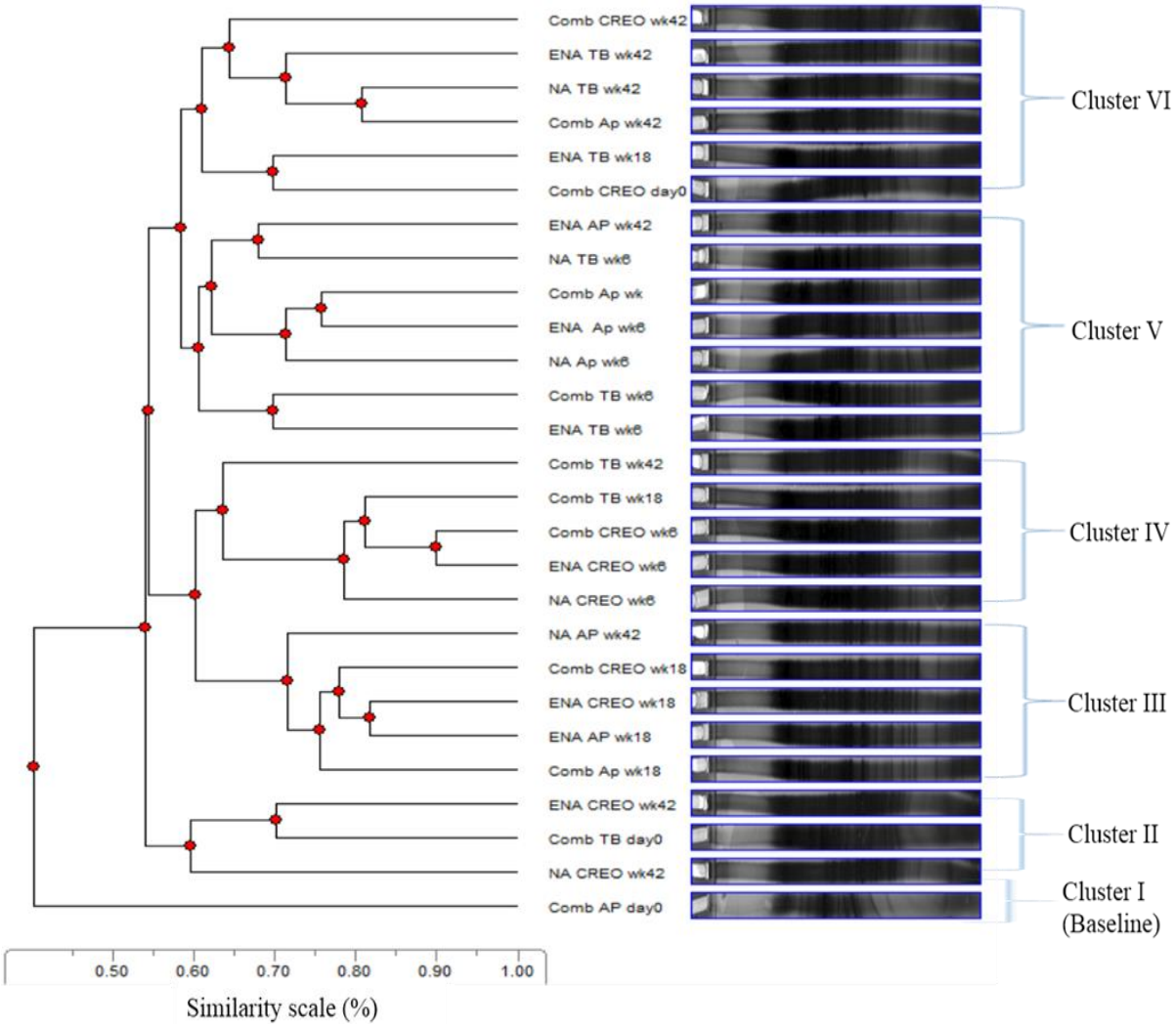

Figure 4.22. UPGMA dendrogram constructed from the similarity matching produced from composite bacterial DGGE community profiles of the 16S rDNA fragments. Amplified PCR products of DNA extracted from samples collected on day 0, weeks 6, 18 and 42 from all microcosms (AP, TB and Creo). The scale bar represents the level of similarity in percentage.

4.7.3. Effect of incubation time and amendments on Mycobacterium communities in composite gel (AP, TB and Creo)

Changes in the *Mycobacterium* community profiles as a consequence of incubation time and bioremediation strategies were collectively assessed using unweighted pair-group method with arithmetic mean analysis (UPGMA) in samples obtained from three microcosms (AP, TB and Creo). The dendrogram constructed from NidA DGGE image profiles resulted in three distinct clusters (Figure 4.24). These three clusters include: the baseline (cluster I), which was developed based on *Mycobacterium* communities from day 0 and week 6 (ENA0, Comb0 and ENA6 AP samples); cluster II (composed of 19 samples out of 24 total samples from all microcosms) contains 79.2% of total samples compared to the other two clusters and cluster III (ENA42 and Comb42 from Creo samples).

The clustering observed in all three (AP, TB and Creo) microcosms was associated with time of incubation rather than bioremediation strategies applied with the exception of a few *Mycobacterium* communities that were randomly clustered. For example, cluster II was developed based on *Mycobacterium* communities sampled on day 0 and week 6.

The similarity between *Mycobacterium* communities (all three hierarchical clusters) ranged from 91% (III) to 100% (I and II) from the three microcosms (AP, TB and Creo). Generally, the similarity observed between *Mycobacterium* communities located in different clusters ranged from 67% (between cluster I and II-II) to 84% (between cluster II and III). DGGE data from NidA composite gel was not sufficient to be analysed by principle component analysis to confirm if similarities in *Mycobacterium* community profiles were due to incubation time or bioremediation strategy applied.

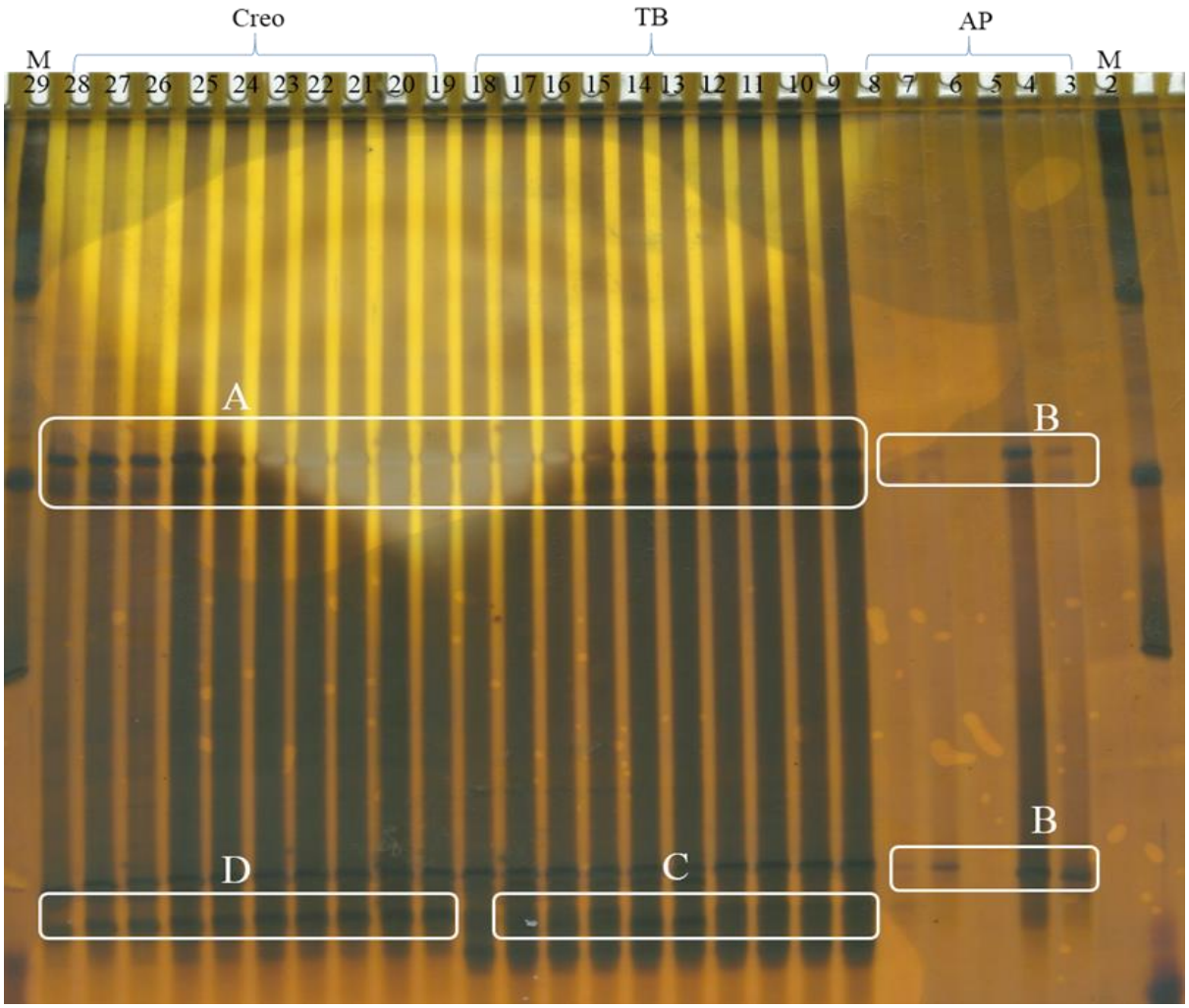

Figure 4.23. Comparison of *Mycobacterium* community profiles in three hydrocarbon-contaminated soils (AP, TB and Creo) generated using NidA genes following 42 weeks incubation. Lanes 2 and 29 contain markers. AP samples were loaded in lanes 3-8, lanes 9-18 represent TB amplicons, and lanes 19-28 contain Creo amplicons. All samples run on this gel, were sampled at four selected sampling time points (day 0, weeks 6, 18 and 42) from all microcosms. Highlighted in rectangles tagged A, are consistent bands in Creo and TB microcosms; B, matching bands with A in AP microcosms but with less intensity and C, unique bands detected in Creo microcosms.

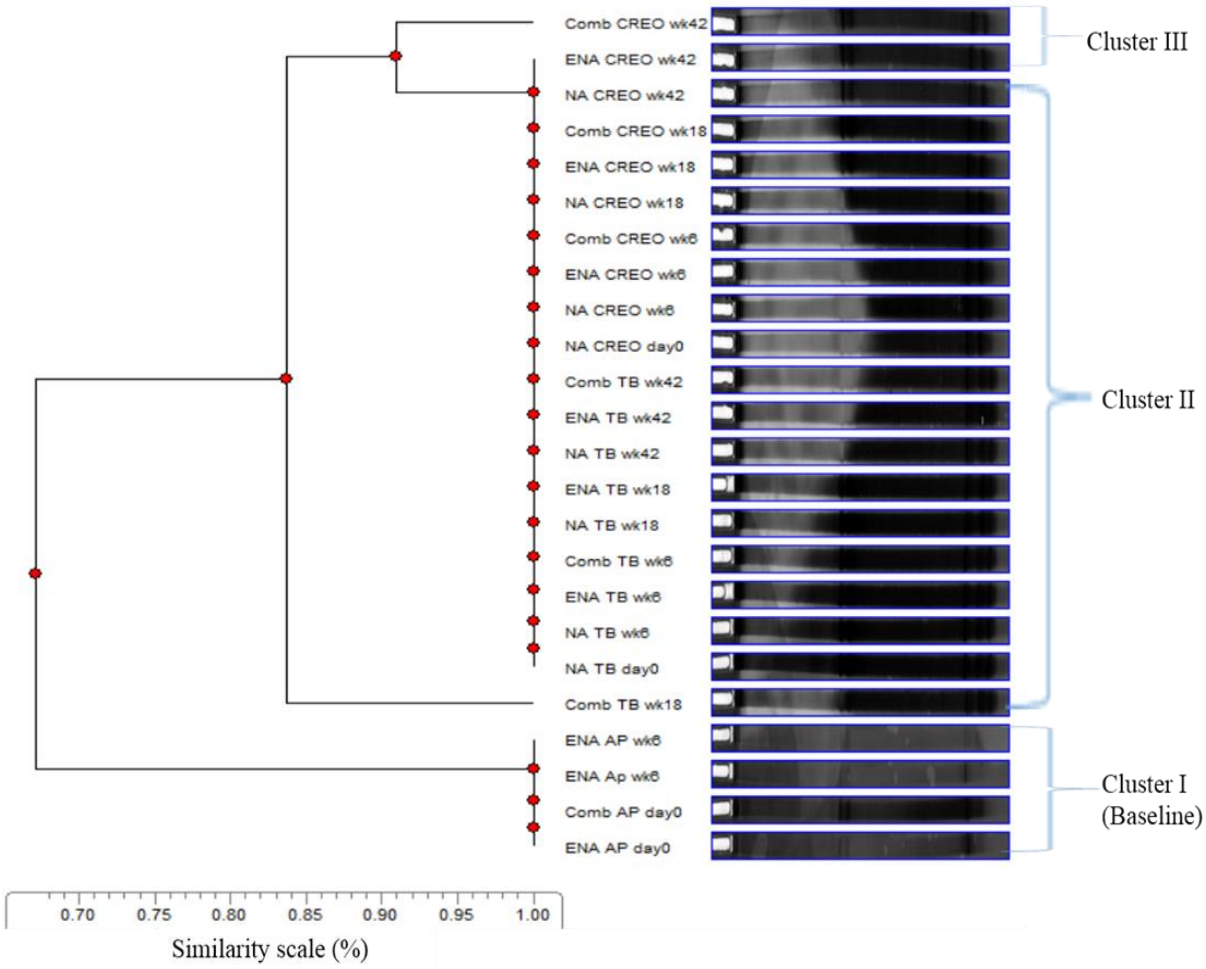

Figure 4.24. UPGMA dendrogram constructed from the similarity matching produced from composite NidA DGGE community profiles of the 16S rDNA fragments, amplified PCR products of DNA extracted from samples collected on day 0, weeks 6, 18 and 42 from all microcosms (AP, TB and Creo). The scale bar represents the level of similarity in percentage.

4.8 Discussion

Microbial bioremediation has been viewed as a cost-saving, environmental friendly, and reliable strategy for the elimination of a wide range of pollutants from the contaminated sites (Nakatsu 2007; Röling & van Verseveld 2002; Shahsavari, E. et al. 2013). Understanding the biological processes underlying this technology has gained enormous interest from scientific communities. One of the critical issues in microbial bioremediation is understanding the ecological and microbial community factors associated with the decontamination of pollutant sites. Advances in microbial ecology and molecular technologies have provided a powerful tool for assessing and monitoring microbial community diversity and dynamics during bioremediation (Duarte, Pascoal & Cassio 2012; Muyzer, De Waal & Uitterlinden 1993). Of these molecular technologies, PCR-DGGE analysis of bacterial communities was performed using three aged PAH-contaminated soils (Creo, TB and AP). This was achieved by monitoring changes in bacterial community structure and banding patterns in samples periodically removed from microcosms incubated over a period of 42 weeks. One of the aims of the research presented in this chapter was to evaluate the impact of bioremediation strategies on soil bacterial community diversity in unamended (NA) and amended (ENA and Combined) microcosms carried out under similar laboratory conditions in three aged PAH-contaminated soils. Bacterial population was assessed by the universal primer pair (314 F GC and 518 R) and a specific primer pair targeting NidA (NidA F GC and R) genes associated with *Mycobacterium* gilvum in samples taken on day 0, weeks 6, 18 and 42 from all microcosms (three soils).

4.8.1 Comparison of bacterial community profiles in unamended (NA) and amended (ENA and Combined) microcosms (Creo, TB and AP soils)

In this section, the impact of bioremediation strategies (NA, ENA and Comb) on bacterial community profiles in three aged PAH-contaminated soils (Creo, TB and AP), was assessed using DGGE analysis over the 42-week incubation period. Assessment of bacterial community in the three soils using DGGE analysis demonstrated that incubation time caused variability among communities compared to the little effect of amendments. Figures 4.2, 4.10 and 4.18 show dendrograms constructed of the similarity matching of the bacterial community profiles from Creo, TB and AP soils by DGGE analysis. Clearly bacterial populations across three soils at the commencement of incubation were in separate clusters compared to communities sampled at latter times (weeks 18 and 42). A similar phenomenon of time influences on bacterial community profiles was confirmed by PCA, in which communities obtained from day 0 and week 6 were grouped together while those from weeks 18 and 42 aggregated in the same

component following further incubation in NA microcosms (Appendix 3, Figures A3.1, A3.2 and A3.4). In microcosms where both nutrients and inoculants (ENA and Combine) were individually implemented or combined, no changes were observed in bacterial community profiles when compared to NA bacterial communities (Creo and TB soils). The addition of nutrients and inoculants in AP soil produced mixed results in ENA and Comb microcosms. The bacterial populations varied following the addition of amendments. However, the change in bacterial numbers was greater in the Comb microcosms compared to the ENA microcosms (from 38 to 27 bands at day 0 to week 6). This means that neither the application of nutrients nor inoculants enhanced PAH degradation. Another possible explanation may be that the bioaugmented organisms did not survive the experimental conditions. The purpose of adding nutrients and inoculants was purely to increase bacterial populations in order to increase contaminants removal (Bento et al. 2005; Hamdi et al. 2007; Miyasaka, Asami & Watanabe 2006). In contrast to this idea, Hamdi et al. (2005) found that the number of diesel-degrading microorganisms and heterotrophic population were not influenced by bioremediation strategies applied. Hamdi et al. (2005) concluded that dehydrogenase activities in the soil increased with increasing incubation time under natural attenuation in a Hong Kong soil (12 weeks incubation period).

In previous studies, changes in microbial population have been reported during PAH bioremediation (Mao et al. 2012; Singh et al. 2011; Yagi & Madsen 2009). Mao et al. (2012) reported that incubation of bioaugmented microcosms changed the microbial community structure during 56-day bioremediation study. In this study, bioaugmented microcosms had no effect on bacterial community structure following 42 weeks of incubation in the three soils when compared to NA microcosms. In another study, Taccari et al. (2011) observed that addition of mature compost plus a bacterial consortium caused a progressive increase in both heterotrophic and cultivatable aerobic bacteria during bioremediation of diesel contaminated soil for 120 days.

Analysis of bacterial community profiles based on Shannon Weaver index (H') indicated that total bacterial diversity was constant in most of the microcosms except in NA microcosm at 18 and 42 weeks (Figure 4.3). The bacterial diversities from these two microcosms (NA18 and NA42) were significantly different from the other microcosms ($P < 0.05$), perhaps due to a data processing error associated with DNA extraction and amplification (low quality DNA) leading to variability in bacterial diversity. However, bacterial diversity in the amended microcosms (ENA and Comb) were constant over the 42-week incubation period. Another reason to support

the suggestion that soil amendments had little effect on bacterial community profiles was the evenness of equitability index (J) determined as a proportion of the total population. The equitability indices were evenly distributed in ENA, Comb and NA0 and NA6 microcosms except NA8 and NA42 which had lower J values (Figure 4.4). Previous analyses of soil microbial community by Shahsavari et al. (2013) and Taccari et al. (2011) have reported increased in Shannon diversity index in amended contaminated soils. No significant ($P < 0.05$) changes were observed in the Shannon diversity index in this study between unamended and amended microcosms.

The lack of change in bacterial communities following addition of nutrients and inoculants may be explained by the fact that the indigenous bacteria might have already adapted to the presence of PAHs due to exposure over extended periods of time (aged soil). Consequently, trying to enhance bacterial communities in this soil (Creo), by adding nutrients did not change the compositions of bacterial populations already there. The bioaugmented organisms may have not survived following the implementation due to competition from the adapted indigenous bacterial communities resulting in no changes in bacterial community profiles.

Analysis of bacterial community profiles based on Shannon Weaver index (H') indicated that total bacterial diversity was similar in most of the microcosms except in Comb6 and Comb42 (Figure 4.11 bars marked 'b' and 'ab'). The Shannon Weaver diversity values from these two microcosms (Comb6 and Comb42) were slightly lower than the other microcosms resulting in less diverse but significant difference ($P < 0.05$) in bacterial populations. Another reason to support the lack of impact of amendments on bacterial community profiles was the evenness of the equitability index (J) distribution as a proportion of total populations. The equitability indexes were evenly distributed in NA, ENA and Comb18 microcosms except Comb6 and Comb42 which had lower J values (Figure 4.12, bars marked 'b' and 'ab'). Compared to this finding, other studies have reported increases in the bacterial Shannon diversity due to the addition of amendments (Erkelens et al. 2012; Shahsavari, Esmaeil et al. 2013; Sheppard et al. 2011). However, results from this study suggest that the initial bacterial population across treatments were not enhanced by the introduction of nutrients or inoculants. Generally, the lack of improvement in bacterial diversity following addition of nutrients may explain the negligible PAH degradation as discussed in chapter 3. In addition to this contaminant bioavailability might also have been a major contributor to low degradation as analysis of bacterial community patterns showed the presence of sufficient populations of the PAH degraders (Figure 4.9). It

is believed that the presence of a bacterial population in abundance may be potentially linked to greater metabolic activities and hence, higher removal PAH if bacteria with degradative genes are present (Nakatsu 2007; Nakatsu, Torsvik & Øvreås 2000).

Analysis of bacterial community profiles based on Shannon Weaver index (H') indicated that total bacterial diversity was similar among day 0 samples, as expected. However, there was a decrease in bacterial diversity after the initial 6 weeks of incubation from NA and Comb microcosms while diversity in ENA was constant (Figure 4.19). Further incubation resulted in an additional reduction in bacterial diversity for the remainder of the incubation time (weeks 18 and 42). Mao et al. (2012) reported that soil microbial populations increased in the early stages of incubation but decreased by the end of the experiment based on DGGE analysis of the 16S rDNA of bacterial fragments. Moreover, the ineffective of amendments was reflected in the bacterial community profiles equitability index (J). The equitability indexes were unevenly distributed in NA, ENA and Comb microcosms depending when each community was sampled (Figure 4.20, bars marked 'a' and 'b'). The effect of incubation time resulted in greater bacterial variability over the 42 weeks incubation period in AP soil compared to both Creo and TB soils.

4.8.2 Overall comparison of bacterial community profiles in composite gels (Creo, TB and AP)

A composite gel encompassing bacterial communities sampled from three aged PAH-contaminated soils is presented in Figure 4.21. At the end of the incubation period (42 weeks), a total of 690 bands were detected in the 3 soils. A significant shift in bacterial population was observed as showed by an increase in bacterial species (bands increase), from unamended microcosm (26.1% in NA) to amended microcosms (36.4 – 37.6% in ENA and Comb respectively) in samples obtained from Creo soil. Results reported in this section are in agreement with other authors (Bento et al. 2005; García-Delgado et al. 2015; Sayara et al. 2011; Sprocati et al. 2012), who report significant shifts in bacterial community diversity due to bioremediation treatments (biostimulation and bioaugmentation). In the current study, the increase in bacterial diversity may be due to both incubation time and supplementation of nutrients and inoculants. Similarly, bacterial community populations were gradually enhanced following addition of nutrients and inoculants in TB and AP microcosms over the 42 week incubation period (section 4.7.1). Surprisingly, the impact of amendments was not seen when bacterial communities in each soil were analysed separately as discussed in the previous

Sections. The impact of amendments and incubation time on bacterial communities in samples obtained from each soil was conducted separately. In the first part of DGGE analyses, bacterial communities were compared based on treatments over the 42 week incubation period for each soil. While in the second part, bacterial communities were compared in a combined gel (DGGE composite gel) for all soils. This was purposely done to understand how bacterial communities respond to amendments in three aged contaminated soils. Changes observed in bacterial populations as discussed earlier were thought to be due to the effect of incubation time solely because no increase in bacterial population was observed following the introduction of nutrients and inoculants in the three soils.

Analyses of bacterial community banding profiles indicated that Creo (237 bands) soil had a greater bacterial population compared to TB and AP soils (224 bands each). These findings also corresponded with PAH degradation discussed in Chapter three, where total PAH removal was higher in Creo compared to both TB and AP soils. Mao et al. (2012) found that microbial community profiles sampled from different time points were significant different from that of day 0 and thus clustered separately based on UPGMA dendrogram analysis.

Despite bioremediation strategies enhancing bacterial population growth over the 42-week incubation period, similarity analyses demonstrated that clustering of bacterial communities was associated with time when each community was sampled regardless from which soil (Figure 4.22).

4.8.3 Comparison of Mycobacterium community profiles in unamended (NA) and amended (ENA and Combined) microcosms (Creo, TB and AP soils)

The occurrence of *Mycobacterium* species as a result of PAH contamination have been investigated using NidA genes (Brezna, Khan & Cerniglia 2003; Leys et al. 2005; Shahsavari, E. et al. 2013; Sho, Hamel & Greer 2004). Successful amplification of microbial genera belonging to *Mycobacterium* species using specific genes suggest that PAH-degrading microorganisms were present at this site. Specific primer pairs were used to assess changes of indigenous and supplemented PAH-degrading organisms (*Mycobacterium*) in three aged PAH-contaminated soils incubated for 42 weeks. In the Creo soil, assessment of *Mycobacterium* community profiles using DGGE analysis demonstrated that incubation time resulted in a stable community over the 42-week incubation period. Figure 4.6 shows a dendrogram constructed using the similarity matching for *Mycobacterium* community profiles from Creo DGGE analysis. Based on banding profiles, *Mycobacterium* communities fluctuated throughout the sampled times in NA microcosms. Similarly, in the amended microcosms (ENA

and Comb), the *Mycobacterium* communities varied in samples obtained at different time points but were not significantly different when compared to the NA microcosm ($P > 0.05$). It has been demonstrated that *Mycobacterium* related NidA genes are prevalently detected in areas with historical PAH contamination (Cheung & Kinkle 2001).

In this study, analysis of *Mycobacterium* community profiles based on Shannon Weaver index (H') indicated that total *Mycobacterium* diversity was similar in day 0 samples, as expected.When augmentation of nutrients and inoculants was carried out, *Mycobacterium* community diversity was not enhanced, as evident by the same H' values across sampled times (Figure 4.8, all bars marked 'a'). With the effect of long time contaminant exposure, microorganisms might have already adapted to the presence of PAHs in this soil. This phenomenon would probably explain why any attempt to stimulate indigenous *Mycobacterium* populations failed in this study. The selective effect of prior exposure has been established by a number of studies (Bauer & Capone 1988; Lladó, S et al. 2013; Vinas et al. 2005).

In the current study, a similar effect of prior selectivity might have played a significant role in hampering the application of bioremediation treatments. Evaluation of *Mycobacterium* community profiles using DGGE analysis in TB soil demonstrated that incubation time resulted in a constant community over the 42 weeks incubation period. Neither addition of nutrients nor inoculants progressively increased *Mycobacterium* community diversity as showed by the detection of constant bands in samples from day 0 to week 42 when comparing NA communities. Another reason to suggest the lack of enhancement was the presence of the same bands consistently throughout the experimental time course.

Although the bioremediation strategy of enhancing indigenous *Mycobacterium* population by supplying nutrients to PAH-contaminated sites worked well in other studies (Bauer & Capone 1988; Cheung & Kinkle 2001; Leys et al. 2005), results presented in this research did not show a similar effect. It was thought that supplying nutrients to enhance the activities of indigenous microbes could be an ideal approach as they may be well suited to their environments compared to the introduction of foreign organisms. On the hand, augmented organism (*Mycobacterium*) did not increase the diversity of indigenous *Mycobacterium* in Creo and TB soils. The positive outcome of this study is that the detection of bands throughout the experiment demonstrated the presence of *Mycobacterium* population in soils. However, this population was not enhanced by nutrient supplementation as showed by the present of similar bands over the 42-week incubation period. The difficulty in amending historically contaminated soil by adding nutrients to activate preadapted microbial community have been reported previously. Garcia-

Delgado et al. (2015) found that bacterial communities in historically PAH-contaminated soil was not productive when supplemented with nutirents compared to natural attenuation stratgey.

4.8.4 Overall comparison of *Mycobacterium* community profiles in composite gels (Creo, TB and AP)

A composite gel encompassing bacterial communities sampled from three aged PAH-contaminated soils is presented in Figure 4.21. As indicated in the results section 4.7.3, only a few samples were analysed from AP microcosms due to low quality of DNA extracted from this soil. Similar bands matching bands (similar communities) from the other soils (Creo and TB) were present as shown in the *Mycobacterium* composite gel (Figure 4.23). The presence of bands with low intensity in AP may be indicative of *Mycobacterium* communities being less abundant compared to the other soils (Creo and TB) or possibly biases during sample processing through inefficiency of cell lysis and PCR amplification of different templates (Bauer & Capone 1988; Langworthy et al. 1998). Thus, this phenomenon does not explain failure of bioremediation strategies as implemented with AP contaminated soil but the paucity of targeted organisms (*Mycobacterium*). The problem with Creo and TB soils appeared to be the ineffective of the bioremediation strategies, as the *Mycobacterium* population remained unaffected following amendment.

In comparison to results represented from this study, Langworthy et al. (1998) reported the detection of PAH-degradative genes in abundance based on nucleic acid analysis in soil samples collected from PAH-impacted sites. In the same study, they reported that microbial biomass was similar at the majority of the tested sites with the exception of an increase observed at one site (Langworthy et al. 1998). Similarity in microbial biomass abundance showed that perceived changes in community structure reflects the replacement of organisms as opposed to the addition of new organisms to the community. The detection of similar bands throughout sampled time points suggested that indigenous *Mycobacterium* communities existed in these soils but could not be enhanced by amendments.

In contrast the bioaugmented organisms did not enhance PAH degradation due to inability of the organisms to adapt to their new environments in all soils. Furthermore, the effect of incubation time and the origin of each community (soil types), may be the possible cause of *Mycobacterium* communities falling into three distinctive clusters (Figure 4.24) depending when they were sampled. It could be argued that communities from one contaminated site may not be exactly similar when compared to another site in terms of community composition and diversity.

4.9 Conclusion

In this chapter, supplementation of nutrients to enhance bioremediation of PAH-contamination soil did not increase the soil microbial population relative to naturally attenuated microcosms. The data from DGGE analyses of bacterial communities do not support the hypothesis that biostimulation and bioaugmentation of PAH-contaminated soil will increase microbial population compare to the NA strategy. In unamended microcosms (NA), DGGE analysis of bacterial community profiles structures and patterns demonstrated the presence of bacterial populations throughout the experimental time course in three aged PAH-contaminated soils (Creo, TB and AP). Results represented in this study suggest that incubation time impacted bacterial community patterns and structures as bacterial banding patterns exhibited a small variability in communities sampled at different time points. An attempt to stimulate the bacterial population by supplementation of nutrients and inoculants individually or combined was less effective with some variability in the three soils in terms of bacteria distribution. In Creo, TB and AP microcosms, bacterial populations fluctuated following supplementation of nutrients and inoculants over the 42-week incubation period. Evaluation of *Mycobacterium* community profiles using specific NidA genes had shown a similar impact of incubation time compared to bioremediation strategies in the three soils. Although the identity of the bacterial communities in the three soils throughout this study could not be determined, there is evidence to suggest that potential PAH-degrading organisms may be present as a result of hydrocarbon contamination. The next chapter focuses on the identification of these organisms, diversity, abundance and functional profiles in amended and unamended microcosms in thee aged contamianated soils with the application of next generation sequencing technology (NGS).

Chapter 5

Assessment of PAH-degrading microorganisms using next generation sequencing technology (NGS)

5.1 Introduction

Microbes play a pivotal role during the removal of a wide range of environmental pollutants through microbial biodegradation processes. Broad knowledge of these processes based on understanding of their biological and ecological relationships, may provide a platform to characterise the extent of contaminant degradation from contaminated matrices. A number of studies have examined PAH-degrading microbes and their functional genes by culture-based and molecular techniques (Hugenholtz, Goebel & Pace 1998; Kanaly & Harayama 2000; Su et al. 2012; Trzesicka-Mlynarz & Ward 1995; White et al. 2011). These studies have been able to describe only a small proportion of microbial populations due to cultivation issues and the inability of 16S rDNA based methods to analyse collective microbial genomes in environmental samples (Su et al. 2012; Vartoukian, Palmer & Wade 2010; Xu et al. 2011).

The emergence of next generation sequencing technologies (NGS) have provided new opportunities to generate a wealth of information regarding microbial taxa abundance, distribution and function in diverse and complex environments (Quail et al. 2012; Shokralla et al. 2012; Tucker, Marra & Friedman 2011; Wegley et al. 2007; Xu et al. 2011). Collective analyses of microbial abundance, diversity and functionality in a range of environmental contaminated samples, including PAH-contaminated sites have been reported (Abbai et al. 2012; Adams et al. 2009; Brennerova et al. 2009; White et al. 2011; Yergeau et al. 2012; Zafra et al. 2014). Findings from these studies using NGS have suggested that generation of high sequencing depth is needed in order to acquire the desired diversity of microorganisms (taxonomy and phylogenetic) and functional genes present in soil. A significant milestone in the field of environmental microbiology, molecular biology and microbial ecology during the past decade has been the introduction of metagenomics (Bik et al. 2012; Brennerova et al. 2009; Daniel 2005; Gerlach & Stoye 2011; Hugenholtz & Tyson 2008). Metagenomics is the study of collective genetic material recovered directly from environmental samples using culture independent techniques. Complete access to microbial communities' potential in a complex environment such as soil is now achievable with the application of NGS technologies. While early metagenomic techniques encompassed a cloning step (Handelsman 2004), the later

approaches bypass cloning by using high throughput sequencing methods such as pyrosequencing (Kristiansson et al. 2011; Lee et al. 2011; Luna et al. 2007) and targeted sequencing (Myllykangas et al. 2011; Nilsson et al. 2009). In addition, pyrosequencing permits generation of high depth sequence data required to evaluate total microbial community composition in terms of structure, diversity and functional abundance in environmental samples.

In the previous chapters (three and four), microbiological (cultivation) and molecular methods of numerating and determining patterns of microorganisms were used to examine changes in the microbial populations over the 42 week incubation period. In chapter three, changes in PAH-degrading organisms using an MPN technique was described. This method allowed the estimation of bacterial density in unamended (NA) and amended (ENA and Comb) microcosms using nutrient broth media supplemented with phenanthrene as a carbon source. The presence of bacteria growth in MPN microplates was considered to represent PAH-degrading bacteria at those specific sampled time points. Nevertheless, these findings do not provide an indication of changes in other microorganisms within the soil community. Following microbiological analysis of microbial communities, more advanced techniques (molecular methods) of assessing microbial diversity and community profiles in unamended (NA) and amended (ENA and Comb) microcosms were employed (as described in chapter four). Results reported in chapter 4 suggested that implementation of nutrient or inoculants didn't have a significant influence on microbial profiles. However, small differences were observed in microbial communities between unamended (NA) and amended (ENA and Comb) soil microcosms (Creo, TB and AP) as a consequence of incubation time rather than treatments.

In this chapter (Five), high throughput sequencing (metagenomics) analysis was employed to determine the identity of PAH-degrading organisms present, diversity, proportion of each type and functional activities associated with their metabolisms. In this part of the study, genomic DNA was extracted from soil microcosms sampled over selected time point (Day 0, weeks, 18 and 42) using MO BIO DNA Isolation kits. Following DNA extraction, whole genome amplification (WGA) was performed using the multiple strand displacement Phi29 DNA polymerase (GenomiPhi v2 kit; GE Healthcare Life Sciences) as described in Sections 2.14.1 – 2.15. Sequencing was then performed using an Ion Proton^{TM} system as per Ion PI^{TM} sequencing 200 kit V3 with 100 pM of the pooled libraries to generate sequence reads. Metagenomic shotgun sequence reads generated by the Ion Proton sequencer were deposited

on the Metagenomics Rapid Annotation Subsystem Technology (MG-RAST) server. A total of 24 FASTQ (text files containing sequence data with a quality (Phed) score for each base as an ASCII character) files from microcosms study I were uploaded onto the server on three submission events. SEED (A framework that supports comparative analysis and annotation of genomes) subsystem annotations were used to identify any features annotated with Metabolism of aromatics biodegradation in conjunction with other databases built in the MG-RAST system. MG-RAST also implement automated BLASTX annotation of metagenomics sequence reads generated with Ion Proton to SEED non redundant database encompassing genome sequences organised into cellular functional assignment. All taxonomy and functional reconstructions generated using MG-RAST version 3.0 had an E-value cut-off of 1×10^{-5} and a 50 bp minimum alignment length were further analysed by importing them into Statistical Analysis of Metagenomic Profiles (STAMP) package.

Further statistical analyses were performed using data generated with the MG-RAST interface. A number of statistical analyses such as hierarchical clustering, PCA, Bray-Curtis similarities and species biodiversity measures were conducted using taxonomic and functional generated abundance data from the MG-RAST server using the statistical package PRIMER V6 for Windows (version 6.1.6).

5.2 Objective

The overarching objective of this study was to analyse the composition and metabolic potential of microbial communities that may be involved in biodegradation processes in three aged (Creo, TB and AP) PAH-contaminated soils using shotgun pyrosequencing (Ion Proton). In addition, data presented here aimed to supplement microbiological and molecular findings already reported in Chapters 3 and 4, in which changes in microbial communities were studied from the same genomic DNA using metagenomics techniques. The aims of the research component presented in this chapter were:

- Use NGS to identify PAH-degrading organisms at the domain, phyla, class, and order hierarchical levels following 42 weeks of incubation using metagenomics shotgun sequencing.
- To evaluate the prevalent of different microorganisms involved in the removal of hydrocarbons from three aged PAH-contaminated soils.

- To assess if propagation of microbial community diversity in the three microcosms was due to bioremediation strategies applied or the effect of incubation time.

5.3 Hypothesis

Ion proton permits accessibility of hydrocarbon-degrading genes propelled by individual microorganism within the microbial community sampled from PAH-contaminated soils.

5.4 Results

5.4.1 Assessment of microbial communities in Creo soil microcosms

5.4.2 Taxonomic analysis at domain level in NA Creo microcosms

The MG-RAST interface was used to annotate metagenome sequence raw data generated using the Ion Proton platform. Metagenomic samples were assessed for their taxonomic distributions at three hierarchical levels including domain, phylum, and order using the M5NR database. Taxonomic analysis of domain annotation in Creo soil microcosms demonstrated significance abundance of two taxa (Relative abundance of more than 1%), bacteria and eukaryote. A total of 8,204,163 hits were established as the number of reads with predicted protein features based on annotation source databases used by MG-RAST. The proportion representing each domain was calculated as the relative abundance of the total hits (Figure 5.1 part (i)). The majority of these reads were assigned to bacteria, from prokaryote domain (95.8% of sequences).

The remaining hits were assigned to the eukaryotic domain (3.8%) while other domains (archaeal, viruses and other sequences) constituted less than 1% of the total hits. Prokaryotes dominated domain distribution at the beginning of microcosms experiments presumably as prokaryotes have a greater propensity to survive in dry soil compared to other domains. Thus, the overrepresentation of this domain may be attributed to the fact that environmental conditions were more supportive to prokaryotes than other domains. As a consequence, more weight was placed on the most dominant domain prokaryotes compare to the other domains as detailed in the subsequent Sections.

Other metagenomic datasets (NA18 and NA42 metagenomes) were compared with day 0 (NA0) organism distribution at domain level. There was a significant reduction in the number of hits detected (943, 826) in NA18, however, the overall organism distribution in the NA18 (Figure 5.1 part (ii)) metagenome had a similar pattern to NA0 (Figure 5.1 part (i)). Similar

results were also observed in metagenomes obtained in NA42 (Figure 5.1 part (iii)) microcosms although a small decrease in bacteria was observed with a corresponding increase in eukaryotes. However, no significant difference was ($P > 0.05$) observed in NA microcosm's domain distribution over the 42 week incubation period.

5.4.3 Taxonomic analysis at domain level in ENA and Comb Creo microcosms

In microcosms where nutrient supplementation was implemented, a 1.9 to 2.1% increase in domain bacteria was observed in ENA microcosms at weeks 18 and 42 (Figure 5.1 parts (iv) and (v) respectively) when compared to abundance at day 0. Similar results were observed in Comb microcosms, with bacteria being the most abundance domain at weeks 18 (Figure 5.1 part (vi) and 42 (Figure 5.1 part (vii)) 98.0 and 97.1% respectively) when compared to Comb0. Notably, there was a small increase in the abundance of Eukaryotes and other domains at week 42 in combined microcosms (Figure 5.1 part (vii)). Moreover, bacteria distribution was similar in metagenomes obtained at weeks 18 and 42 respectively.

5.4.4 Taxonomic analysis at phylum level in NA Creo microcosms

Bacterial distribution at phylum level produced 23 distinctive phyla (Figure 5.2 part (i)) in the Creo soil at the beginning of microcosm experiments. Phyla were detected at varying proportions as shown by their relative abundances in Table 5.1. Most of these phyla (18) were individually represented at <1% of all assigned hits, while their combined relative abundance was approximately 2.9% of the total hits.

Annotation of bacterial sequences at phylum level, demonstrated that Proteobacteria were the most dominant taxon, with 82.5% of assigned hits to this phylum. The phylum Actinobacteria was the second dominant category with 5.1% relative abundance. As shown by differences in their relative abundances, phylum Proteobacteria was overrepresented by 16-fold compared to the second highest represented phylum (Actinobacteria). Other prominent phyla detected over 1% included Acidobacteria (3.8%), Firmicutes (3.3%), and Bacteroidetes (2.5%) (Table 5.1).

At weeks 18 and 42, NA microcosms demonstrated diversified taxonomic phylogenetic groups, with a total of 28 phyla at each time point, 8 phyla among the 28 detected had relative abundances greater than 1%, with Proteobacteria being the most dominant phylum at weeks 18 (53.5%) and 42 (51.4%) despite a significant reduction compared to the initial abundance (82.5% in Figure 5.2 part (i)). The decrease in abundance of Proteobacteria corresponded with

a 6-fold increase in phylum Acidobacteria abundance (3.8 to 23%). While other phyla were present at low abundance, three additional phyla were observed at weeks 18 and 42 at >1% abundance, including Verrucomicrobia, Cyanobacteria and Planctomycetes (Figure 5.2 parts (ii) and (iii)). No significant change was observed ($P > 0.05$) in the abundance of individual phylum between weeks 18 and 42 except a 2.4% increase in Actinobacteria.

Table 5.1. Taxonomic bacterial composition at phylum level in Creo soil metagenomes obtained from unamended and amended microcosms following 42 weeks incubation. Values shown are for those phyla where abundance percentages were greater than 1% of the total organisms.

Legend	Phylum	Treatment, time (weeks) and relative percentage compositions (%)								
		NA			ENA			Comb		
		0	18	42	0	18	42	0	18	42
1	Proteobacteria	82.5	53.5	51.4	82.5	63.1	64.5	82.5	69.9	47.6
2	Actinobacteria	5.1	5.3	7.7	5.1	5.0	6.3	5.1	5.1	5.4
3	Acidobacteria	3.8	23.1	23.3	3.8	8.8	19.3	3.8	10.8	29.0
4	Firmicutes	3.3	2.9	3.4	3.3	2.3	2.6	3.3	1.8	3.5
5	Bacteroidetes	2.5	2.9	2.2	2.5	16.1	2.5	2.5	8.7	2.6
6	Verrucomicrobia	*	6.4	6.1	*	1.0	1.2	*	*	6.3
7	Planctomycetes	*	1.4	1.2	*	*	*	*	*	1.1
8	Cyanobacteria	*	1.3	1.3	*	*	*	*	*	1.4
9	Others	2.9[a]	3.2[b]	3.3[c]	2.9[a]	3.7[d]	3.6[e]	2.9[a]	3.8[f]	3.4[g]

*percentages below 1% of the total organisms.
[a] 'other' represented 18 phyla each representing <1% of the total abundance.
[b] 'other' represented 20 phyla each representing <1% of the total abundance.
[c] 'other' represented 20 phyla each representing <1% of the total abundance.
[d] 'other' represented 16 phyla each representing <1% of the total abundance.
[e] 'other' represented 17 phyla each representing <1% of the total abundance.
[f] 'other' represented 18 phyla each representing <1% of the total abundance.
[g] 'other' represented 21 phyla each representing <1% of the total abundance.

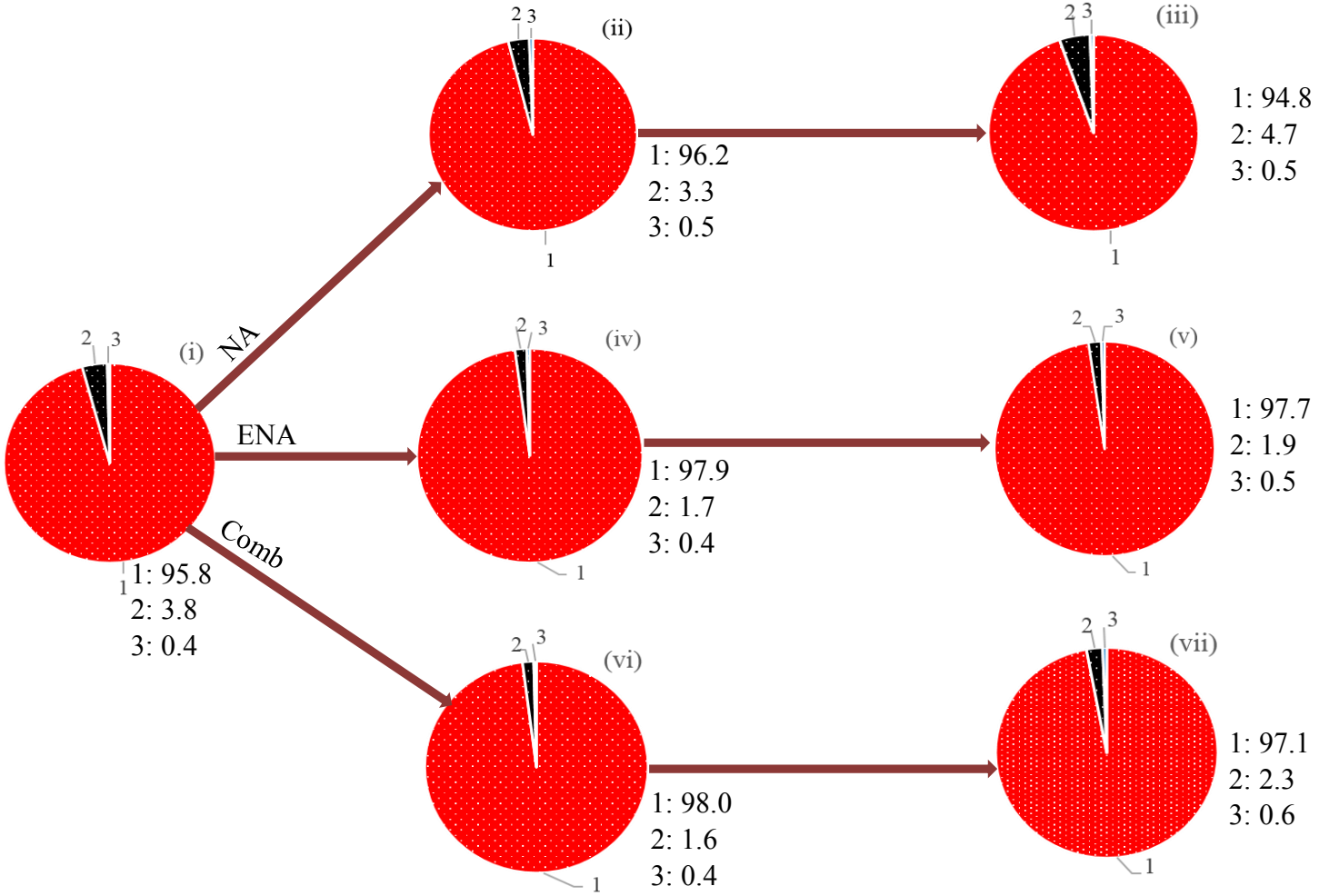

Figure 5.1. Distribution of taxonomic domain determined in sequences obtained from (i) NA0, (ii) NA18, (iii) NA42, (iv) ENA18, (v) ENA42, (vi) Comb18, and (vii) Comb42 metagenomes sampled from the Creo soil following 42 week incubation period. The proportion of each taxonomic relative abundance was calculated as a percentage of the total organisms in the metagenomic sample. Labels are shown for those domains where abundance percentages were greater than 1% of the total organisms; 1: bacteria; 2: eukaryotes; 3: others (viruses and other sequences)

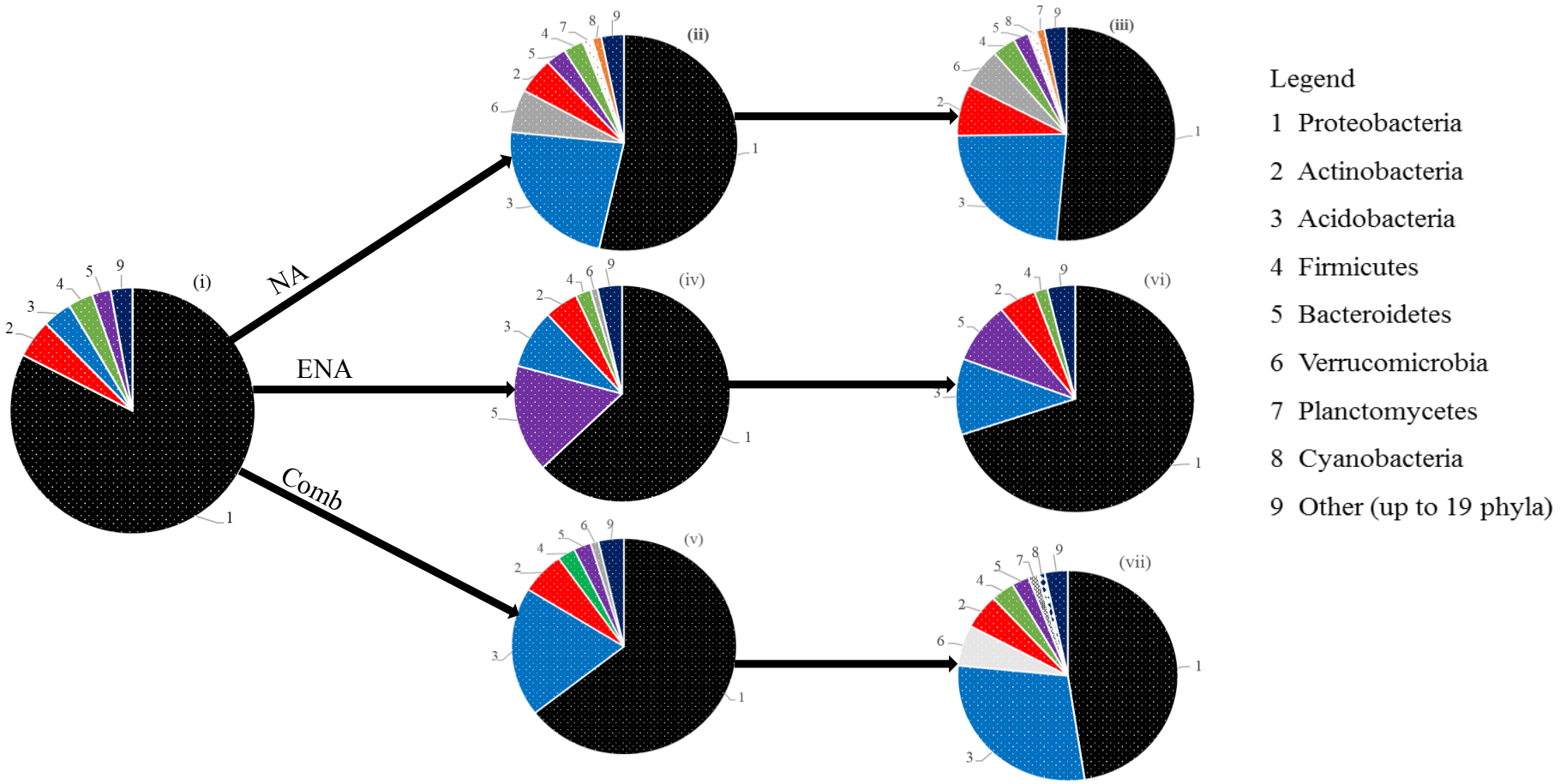

Figure 5.2. Distribution of taxonomic phylogenetic groups determined in sequences obtained from (i) NA0, (ii) NA18, (iii) NA42, (iv) ENA18, (v) ENA42, (vi) Comb18, and (vii) Comb42 metagenomes sampled from the Creo soil following 42 weeks of incubation. The proportion of each taxonomic relative abundance was calculated as a percentage of the total organisms in the metagenomic sample. Labels are shown for those phyla where abundance percentages were greater than 1% of the total organisms, while percentage abundance values are presented in Table 5.1.

5.4.5 Taxonomic analysis at phylum level in ENA and Comb Creo microcosms

In microcosms where nutrient supplementation was implemented, a small change in the number of taxonomic phylogenetic groups was observed at both sample time points (from 5 to 6 phyla at weeks 18 and 42). At week 18, 6 phyla found with over 1% abundance, with Proteobacteria being the most prevalent (63.1%). A significant reduction in Proteobacteria abundance was observed at week 18 when compared to the day 0 (82.5% to 63.1% in the in ENA microcosms) (Figure 5.2 part (i)). However, the reduction was not as significant as observed in NA microcosm treatment. Bacteroidetes showed a 5-fold increase in abundance from day 0 to week 18 (2.5 to 16.1%) following the addition of nutrients (Table 5.1), however, there was no change observed in the relative abundance of Actinobacteria at week 18. Other changes in phyla abundance were observed in the ENA42 microcosm treatment compared to week 18 (Figure 5.2, parts (iv) and (v)). Annotated data shows a significant shift in Acidobacteria abundance, with a 2-fold increase at week 42, whereas a 5-fold decreased was observed in the abundance of Bacteroidetes (16.1 to 2.5% at weeks 18 and 42 respectively).

In microcosms where both nutrients and inoculants were supplemented, a total of 24 and 29 phyla were present at weeks 18 and 42 (Figure 5.2 parts (vi) and (vii)) respectively. After 18 weeks of incubation, some changes were observed in the number of phyla abundance including a decrease in Proteobacteria (82.5 to 69.9%), and Firmicutes (3.8 to 1.8%), and an increase in Acidobacteria (3.8 to 10.8%) and Bacteroidetes (2.5 to 8.7%). At the end of the incubation period under the Comb treatment (week 42), a significant shift in the number of taxonomic phylogenetic groups (8 phyla) was observed when compared to day 0 and week 18 (Figure 5.2 part vii). Three additional phyla (Verrucomicrobia, Cyanobacteria and Planctomycetes) with relative abundance >1% emerged at week 42 although a significant decrease in the abundance of Proteobacteria from 69.9% at week 18 to 47% at week 42 and Bacteriodetes (8.7 to 2.6%) was observed. In contrast, the abundance of Acidobacteria extremely increased (3.8 to 29.0%) when compared to its abundance at day 0 (Table 5.1).

5.4.6 Taxonomic analysis at order level in NA Creo microcosms

The composition of the NA bacterial community at order level demonstrated high diversity over the 42 week incubation period. The distribution of bacteria at the order level resulted in 11 orders with over 1% relative abundance (approximately 85.9% of the overall hits) out of 121 orders detected. These findings indicated that the remaining 14.1% of total hits were attributed to 110 orders classified as others (Figure 5.3 part (i)). The majority of the combined

85.9% of hits was assigned to Enterobacteriales (55.1%), which was not surprising as this order belongs to the most abundant phylum Proteobacteria (previous section). Other prominent orders include Burkholderiales (8.9%), Actinomycetales (4.8%), Rhizobiales (4.8%) and Sphingomonadales (2.9%) as shown in Table 5.2. Significant shifts in the relative abundances of various orders were observed, when taxonomic analysis at day 0 (NA0) was compared to weeks 18 and 42. Additional orders with relative abundance over 1% were present at weeks 18 (8 orders) and 42 (7 orders) presumably due to incubation influences (Figure 5.3 parts (i) and (ii)) such as maintenance of soil moisture. These additional orders were present at a constant and low abundance in NA18 and NA42 metagenomes. Incubation of NA microcosms resulted in an increase in abundance of several orders including; Actinomycetales (4.8 to 7.4%); Rhizobiales (4.8 to 20.5%); Acidobacteriales (1.8 to 13.1%) and Solibacterales (1.2 to 4.9%) from day 0 to week 42 (Table 5.2). In contrast, incubation of Creo soil under NA conditions for 42 weeks resulted in a significant decrease in the abundance of Enterobacteriales (55.1 to < 1%), Burkholderiales (8.8 to 5.6%) and Bacillales (2.3 to 1.7%).

5.4.7 Taxonomic analysis at order level in ENA and Comb Creo microcosms

In microcosms where nutrients were supplemented, the number of orders increased by 8 (> 1% of the total abundance) at week 18 compared day 0 (Figure 5.4 parts (i) and (ii)). Among these orders, the relative abundance of Rhizobiales (4.8 - 23.2%), Burkholderiales (8.8 – 9.1%), Acidobacteriales (1.8 – 4.4%), Solibacterale (1.2 – 2.6%) and Sphingomonadales (1.1 – 7.5%) increased over the incubation period. However, a significant reduction in the relative abundance of Enterobacteriales (55.1 – 4.4%), and Bacillales (2.3 - 1.1%) was observed from day 0 to week 18 (Table 5.2 and Figure 5.4 parts (i) and (ii)). Further incubation resulted in a small change in order number and abundance. The abundance of Burkholderiales (9.1 – 13.5%) and Acidobacteriales (4.4 – 12.4%) relative abundance gradually increased from week 18 to 42, while the abundance of Enterobacteriales (4.4 – 1.4%), Rhizobiales (23.2 – 17.1%) reduced markedly.

Table 5.2. Taxonomic bacterial composition at order level in Creo soil metagenomes obtained from unamended and amended microcosms following 42 weeks of incubation. Values shown are for those phyla where abundance percentages were greater than 1% of the total organisms

Legend	Order	Treatment, time (weeks) and relative abundance percentage compositions (%)								
		NA			ENA			Comb		
		0	18	42	0	18	42	0	18	42
1	Enterobacteriales	55.1	*	*	55.1	4.4	1.4	55.1	5.5	1.1
2	Burkholderiales	8.8	6.8	5.6	8.8	9.1	13.5	8.8	10.4	7.1
3	Actinomycetales	4.8	5.0	7.4	4.8	4.8	6.1	4.8	4.8	5.0
4	Rhizobiales	4.8	19.4	20.5	4.8	23.2	17.1	4.8	27.6	14.5
5	Sphingomonadales	2.9	5.0	2.9	2.9	5.8	1.9	2.9	5.7	2.0
6	Bacillales	2.3	1.3	1.7	2.3	1.1	1.3	2.3	*	1.6
7	Acidobacteriales	1.8	12.8	13.1	1.8	4.4	12.4	1.8	5.9	17.6
8	Xanthomonadales	1.8	1.2	*	1.8	1.9	4.1	1.8	2.3	1.8
9	Pseudomonadales	1.5	1.3	1.2	1.5	1.5	1.9	1.5	1.6	1.3
10	Solibacterales	1.2	5.1	4.9	1.2	2.6	2.4	1.2	2.6	4.7
11	Sphingobacteriales	1.1	*	*	1.1	7.5	*	1.1	4.1	*
12	unclassified (Acidobacteria)	*	5.1	5.3	*	1.9	4.5	*	2.2	6.7
13	Verrucomicrobiales	*	4.2	3.9	*	*	*	*	*	4.0
14	Rhodospirillales	*	3.3	3.2	*	2.4	2.7	*	2.4	3.0
15	Rhodobacterales	*	2.8	3.2	*	2.8	3.1	*	3.0	2.7
16	Caulobacterales	*	2.0	2.8	*	1.4	1.6	*	1.3	1.8

Table 5.2 (cont.). Taxonomic bacterial composition at order level in Creo soil metagenomes obtained from unamended and amended microcosms following 42 weeks of incubation. Values shown are for those phyla where abundance percentages were greater than 1% of the total organisms

Legend	Order	Treatment, time (weeks) and relative abundance percentage compositions (%)								
		NA			ENA			Comb		
		0	18	42	0	18	42	0	18	42
17	Nitrosomonadales	*	1.3	1.2	*	*	2.1	*	*	1.5
18	Myxococcales	*	1.3	1.3	*	*	*	*	*	1.3
19	Planctomycetales	*	1.3	1.1	*	*	*	*	*	1.0
20	unclassified (Opitutae)	*	1.0	1.0	*	*	*	*	*	1.0
21	Clostridiales	*	1.0	1.1	*	*	*	*	*	1.2
22	Chromatiales	*	*	*	*	3.5	3.4	*	2.2	1.2
23	Flavobacteriales	*	*	*	*	3.0	*	*	1.5	*
24	Cytophagales	*	*	*	*	2.9	*	*	1.4	*
25	Bacteroidales	*	*	*	*	2.3	*	*	1.4	*
26	Alteromonadales	*	*	*	*	*	1.1	*	*	*
27	Rhodocyclales	*	*	*	*	*	1.5	*	*	*
28	Desulfuromonadales	*	*	*	*	*	*	*	*	1.0
29	Others	14.1[a]	18.7[b]	18.7[c]	14.1[a]	13.6[d]	17.9[e]	14.1[a]	13.7[f]	17.0[g]

*****percentages below 1% of the total organisms.
[a] 'other' represented 109 orders each representing <1% of the total abundance
[b] 'other' represented 80 orders each representing <1% of the total abundance
[c] 'other' represented 84 orders each representing <1% of the total abundance)
[d] 'other' represented 81 orders each representing <1% of the total abundance
[e] 'other' represented 84 orders each representing <1% of the total abundance
[f] 'other' represented 81 orders each representing <1% of the total abundance
[g] 'other' represented 80 orders each representing <1% of the total abundance

At the end of the incubation period (week 42), a similar number of orders were observed as found at week 18. Significant shifts in the relative abundances of various orders were observed, when taxonomic analysis at day 0 (ENA0) was compared to week 42. Incubation of ENA microcosms resulted in an increase in abundance of several orders including; Actinomycetales (4.8 to 6.1%); Burkholderiales (8.8 – 13.5%); Rhizobiales (4.8 to 17.1%); Acidobacteriales (1.8 to 12.4%) and Solibacterales (1.2 to 2.4%) from day 0 to week 42 respectively (Table 5.2). However, a significant reduction in the relative abundance of Enterobacteriales (55.1 – 1.4%), and Bacillales (2.3 - 1.3%) from day 0 to week 42 (Table 5.2 and Figure 5.4 parts (i) and (ii)) was observed. Similarly, annotation of organisms in metagenomes obtained from microcosms supplemented with inoculants and nutrients (Comb treatment) are shown in Figure 5.5. For the combined treatment, an additional 7 orders with relative abundance of greater than 1% were observed at week 18 when compared to day 0. At week 18, the relative abundance of Rhizobiales (4.5–27.6%), Burkholderiales (8.8–10.4%), Sphingomonadales (2.69-5.7%), Acidobacteriales (1.8–5.9%), and Sphingobacteriales (1.1–4.1%) increase as shown in Table 5.2.

In contrast, Enterobacteriales (55.1–5.5%) masively decreased following the implementation of both nutrients and inoculants which is similar to results from the NA and ENA microcosm treatments. However, at the end of the incubation period (week 42), a small reduction in the relative abundance of most orders were observed except Actinomycetales (4.8 to 5.0%), Acidobacteriales (4.8 to 17.6%), Unclassified from Acidobacteria (< 1 to 6.7%); and Solibacterales (1.2 to 4.7%), consistently increased when compared to day 0.
As depicted in their relative abundances (Table 5.2), there were no clear dominant orders in Comb microcosm at week 42 when compared to taxonomic analysis at day 0 and week 18 respectively.

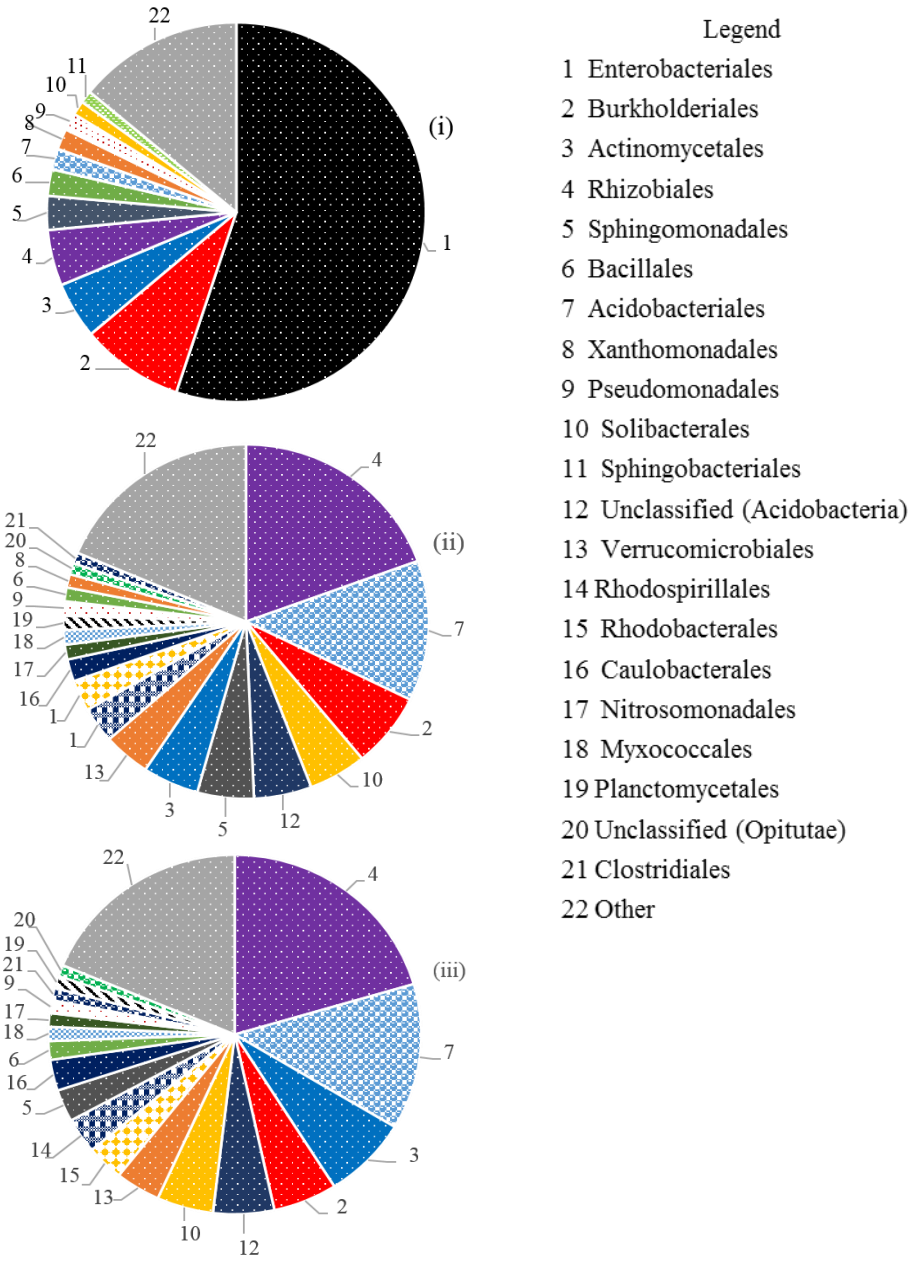

Figure 5.3. Distribution of organisms at Order level determined in sequences obtained from (i) NA0, (ii) NA18, and (iii) NA42 metagenomes sampled from the Creo soil following 42 week incubation period under natural attenuation conditions (NA). The proportion of each Order relative abundance was calculated as a percentage of the total organisms in metagenomic samples. Labels are shown for those orders where abundance percentages were greater than 1% of the total organisms, while percentage values are presented in Table 5.2.

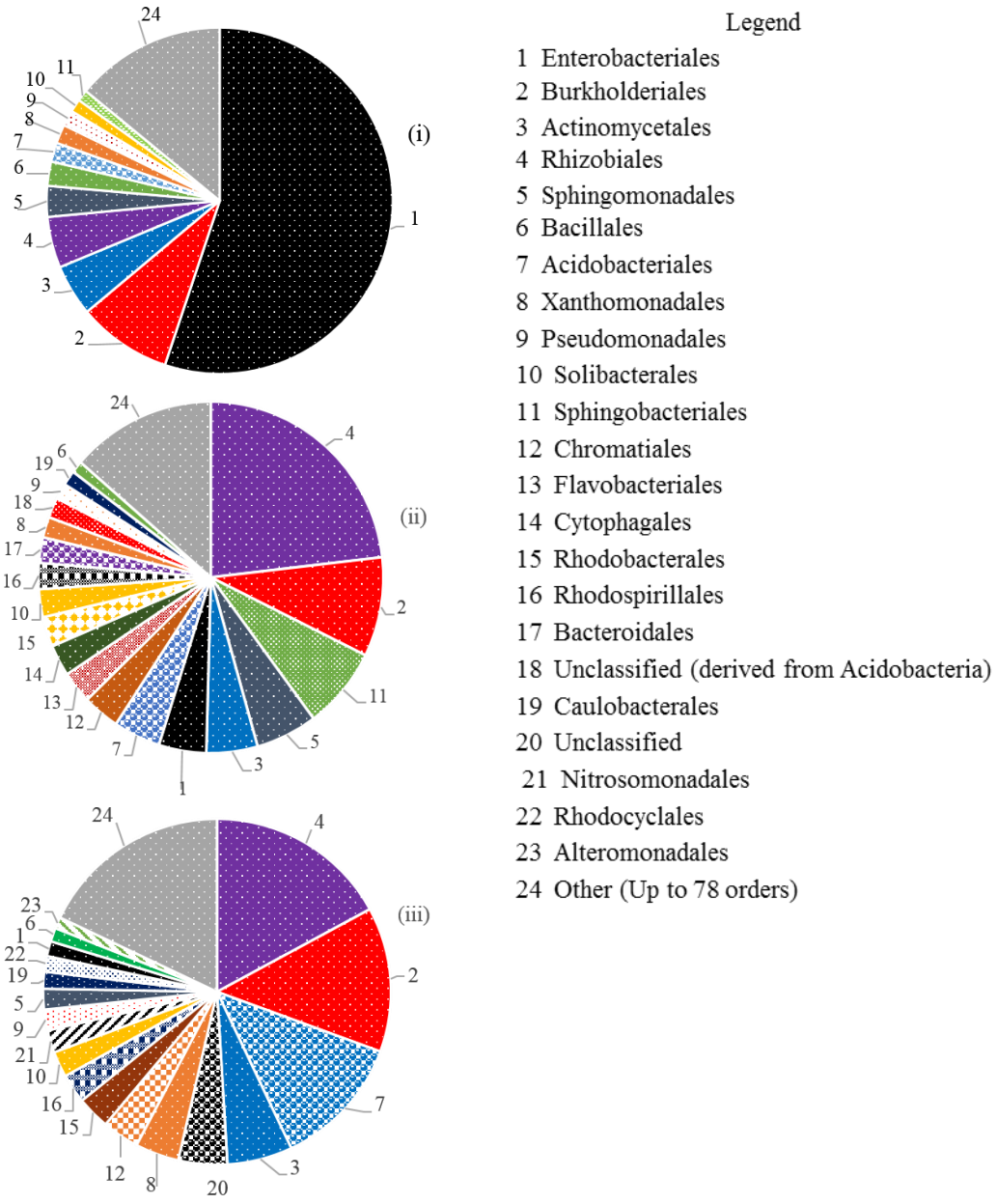

Figure 5.4. Distribution of organisms at Order level determined in sequences obtained from (i) ENA0, (ii) ENA18, and (iii) ENA42 metagenomes sampled from the Creo soil following 42 week incubation period under enhanced natural attenuation (ENA) conditions. The proportion of each Order relative abundance was calculated as a percentage of the total organisms in metagenomic samples. Labels are shown for those orders where abundance percentages were greater than 1% of the total organisms, while percentage values are presented in Table 5.2.

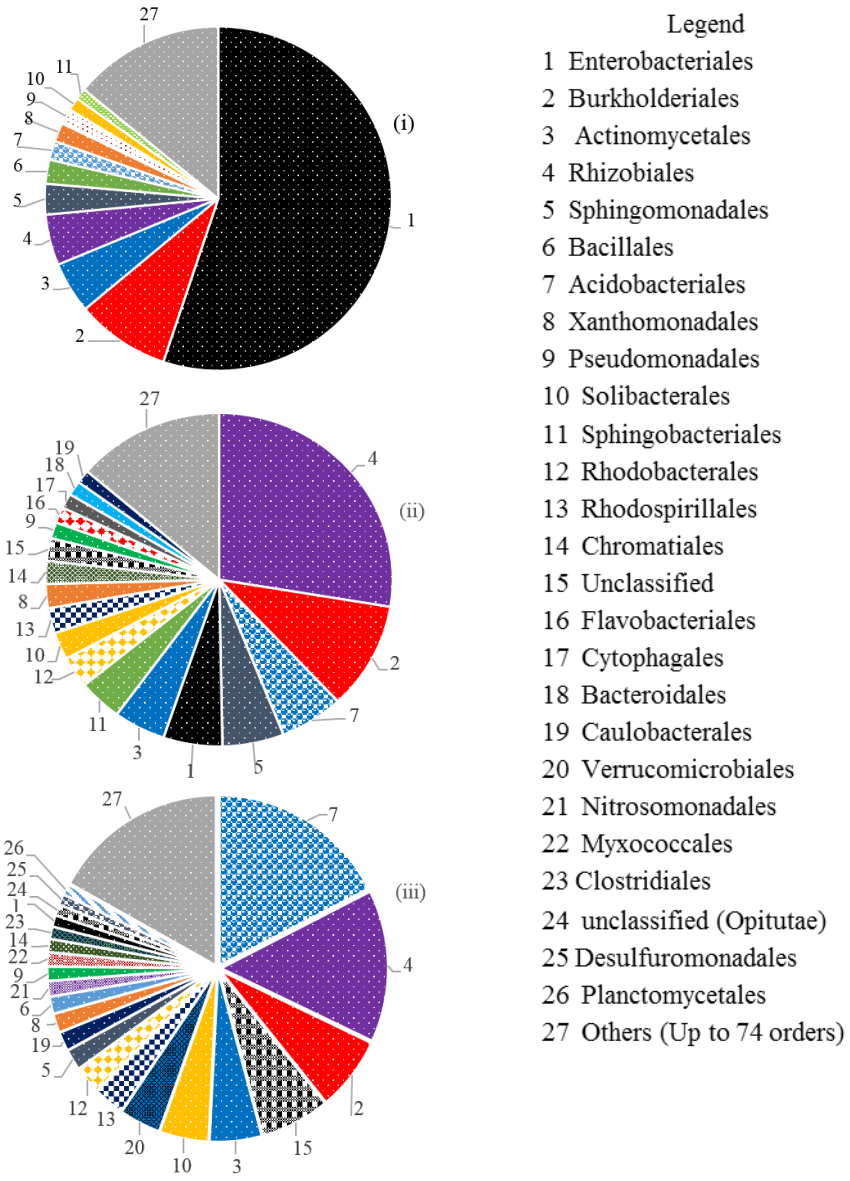

Figure 5.5. Distribution of organisms at order level determined in sequences obtained from (i) Comb0, (ii) Comb18, and (iii) Comb42 metagenomes sampled from the Creo soil following 42 week incubation period under combined (Comb) conditions. The proportion of each order relative abundance was calculated as a percentage of the total organisms in the metagenomic sample. Labels are shown for those orders where abundance percentages were greater than 1% of the total organisms, while percentage values are presented in Table 5.2.

5.5 Assessment of microbial communities in TB soil microcosms

5.5.1 Taxonomic analysis at domain level in NA TB microcosms

Similar trends in taxanomic distributions was observed in TB soil microcosms following annotation of metagenome raw sequences as described in section 5.5.1. In Tb soil microcosms, 9,562,833 hits were recorded as a number of reads with predicted protein features based on MG-RAST interface analsysis. The percentage assigned to each domain was calculated as the relative abundance of the total hits (Figure 5.6 part (i)). Large proportion of these reads were annotated to bacteria, from domain prokaryote (97.9% of sequences).

Unlike Creo soil, in TB soil, only small proportions of hits were assigned to the eukaryotic domain (1.4% of hits) and the remaining domains (archaeal, viruses and other sequences) make up less than 1% of total hits. Prokaryotes dominated the domain distribution at the commencement of microcosm experiments presumably due to prokaryotes having a greater propensity to survive in dry soil compared to other domains. Thus, the overrepresentation of this domain may be attributed to the fact that environmental conditions were more supportive to prokaryotes than other domains. As a consequence, more weight was placed on the most dominant domain prokaryotes compare to the other domains as detailed in the subsequent Sections.

Organisms distribution in samples obtained from other metagenomic datasets (NA18 and NA42 metagenomes) were compared to day 0 (NA0) at the domain level. Further incubation did not result in a greater shift in the abundance of organisms in the NA18 metagenome. The overall organism distribution in the NA18 metagenome had a similar pattern as in NA0 (Figure 5.6 part (ii)).

The same results were also observed in metagenomes smapled from NA42 microcosm, however, an increase was observed in other domains when archaea relative abundance reached 1.0% and a 2-fold increase in eukaryotes (3.8%) abundance was observed. The shifts observed in the other domains corresponded with a 3% decrease in bacteria relative abundance at the remainder of the incubation period.

5.5.2 Taxonomic analysis at domain level in ENA and Comb TB microcosms

In nutrient supplemented microcosm studies, a 1% increase in domain bacteria was observed in the ENA microcosms at week 18 when compared to the initial abundance at day 0 (97.9%, Figure5.6 part (i)). At week 18, the relative abundance of eukaryotes was reduced to below 1%

and was included in 'others' (1.3% abundance, Figure 5.6 part (ii)). By the end of the incubation period (week 42), no changes were observed in the relative abundance of bacteria, eukaryotes and others compared to initial abundances. Similar results were observed in the Comb microcosms, with bacteria being the most abundant domain at weeks 18 and 42 (99.0 and 98.0%; Figure 5.6 parts (vi) and (vii) respectively). Notably, there was a small increase in the abundance of others as eukaryotes relative abundance detected was below 1% at week 18 when compared to the initial abundance.

5.5.3 Taxonomic analysis at phylum level in NA TB microcosms

Bacterial distribution at phylum level produced 28 distinctive phyla (Figure 5.7 part (i)) in the TB microcosm at the start of experiments. Phyla detected at varying proportions are shown by their relative abundances in Table 5.3. Most of these phyla (19) were represented <1% of all assigned hits while their combined relative abundance was 3.5% of the total hits. Annotation of bacterial sequences at phylum level, showed that Proteobacteria was the most dominant taxon, with 40.9% of the total hits assigned to this phylum. According to the MG-RAST annotation systems, Actinobacteria was the second most prevalent taxon with 35.8% relative abundance. As shown by differences in their relative abundances, these two phyla were overrepresented by 3 and 2-fold compared to the third highest phylum (Firmicutes) identified. Other prominent phyla detected (>1% of the total hits) included Bacteroidetes (4.4%), Planctomycetes (1.4%), and Chloroflexi (1.3%) (Table 5.3).

At week 18, NA microcosms showed a small increase in the number of phylogenetic groups, with 9 phyla detected having a greater than 1% relative abundance. Proteobacteria was again the most prevalent phylum increasing from 40.9 at day 0 to 45.1% relative abundance at week 18 (Figure 5.7 part (ii)). Incubation resulted in the increase in relative abundance of some phyla including Bacteroidetes (4.4 to 28.3%), Plactomycetes (1.4 to 5.6%), Verrucomicrobia (<1 to 5.4%), Acidobacteria (<1 to 1.7%), and Cyanobacteria (<1 to 1.7%). In contrast, a significant decreased was observed in the relative abundance of Actinobacteria (36.8 to 3.6%), Firmicutes (12.6 to 4.3%), and Chloroflexi (1.3 to 1.0%) through the time course (Figure5.7 part (ii)).
After 42 weeks of incubation (NA42), Bacteroidetes (41.3%) were the most dominant phylum with a corresponding decrease in the relative abundance of Proteobacteria (37.3%). Other phyla were present at low relative abundance (< 5%) as depicted in Figure5.7 part iii. The proportion of sequences assigned to each phylum decreased with increasing number of phyla (8 phyla with

relative abundance greater than 1% of the total organisms) at the end of the incubation period under NA conditions.

Table 5.3. Taxonomic bacterial composition at phylum level in the TB microcosm metagenomes obtained from unamended and amended microcosms following 42 weeks of incubation. Values shown are for those phyla where abundance percentages were greater than 1% of the total organisms.

Legend	Phylum	Treatment, time (weeks) and relative percentage compositions (%)								
		NA			ENA			Comb		
		0	18	42	0	18	42	0	18	42
1	Proteobacteria	40.9	45.1	37.3	40.9	83.0	70.0	40.9	81.0	73.8
2	Actinobacteria	35.8	3.6	2.5	35.8	1.9	3.8	35.8	2.2	2.7
3	Firmicutes	12.6	4.3	4.0	12.6	1.7	4.1	12.6	3.2	2.1
4	Bacteroidetes	4.4	28.3	41.3	4.4	8.7	10.1	4.4	9.0	13.3
5	Planctomycetes	1.4	5.6	3.8	1.4	*	2.4	1.4	1.1	2.3
6	Chloroflexi	1.3	1.0	*	1.3	1.1	*	1.3	*	*
7	Verrucomicrobia	*	5.4	3.4	*	*	2.1	*	*	1.2
8	Acidobacteria	*	1.7	1.8	*	*	4.2	*	*	1.2
9	Cyanobacteria	*	1.7	1.6	*	*	*	*	*	*
10	Others	3.5[a]	3.2[b]	4.3[c]	3.5[a]	3.6[d]	3.2[e]	3.5[a]	3.5[f]	3.4[g]

*percentages <1% of the total organisms.
[a] 'other' represented 22 phyla each representing <1% of the total abundance.
[b] 'other' represented 20 phyla each representing <1% of the total abundance.
[c] 'other' represented 20 phyla each representing <1% of the total abundance.
[d] 'other' represented 23 phyla each representing <1% of the total abundance.
[e] 'other' represented 22 phyla each representing <1% of the total abundance.
[f] 'other' represented 23 phyla each representing <1% of the total abundance.
[g] 'other' represented 21 phyla each representing <1% of the total abundance.

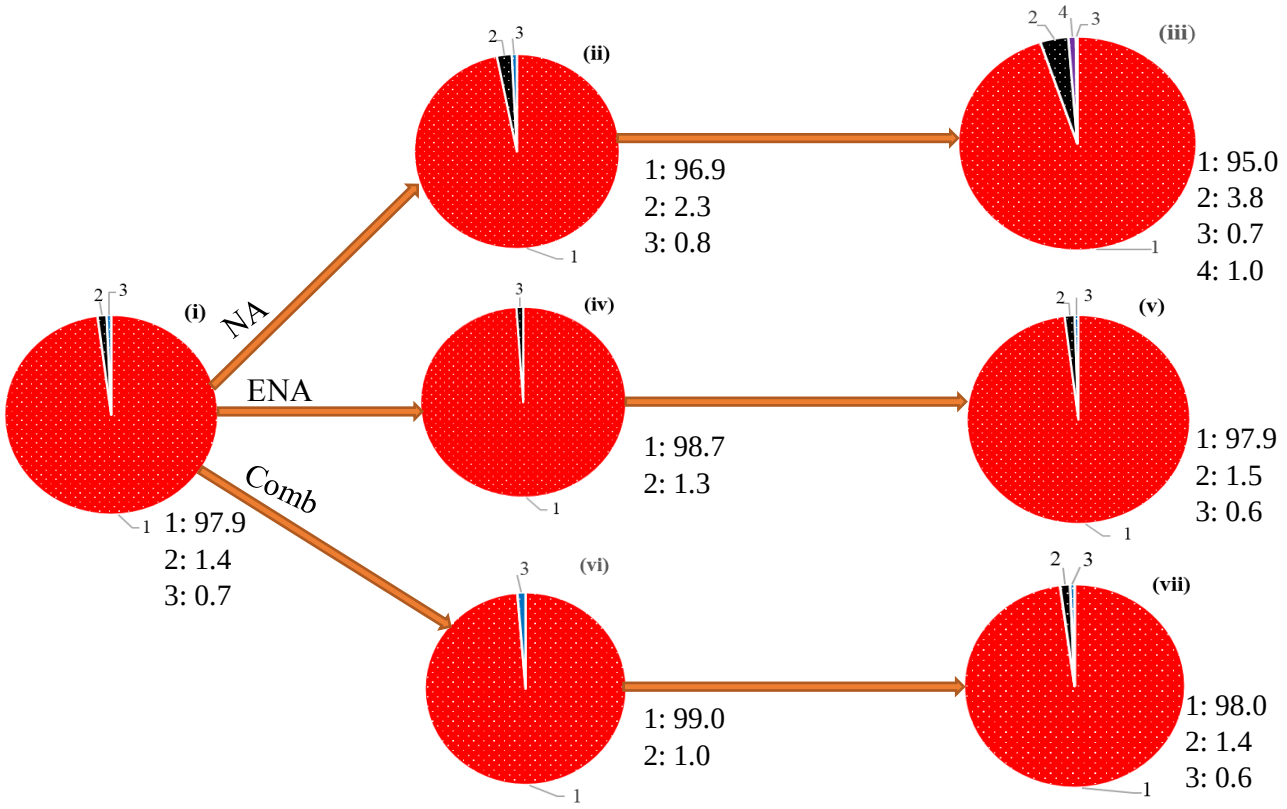

Figure 5.6. Distribution of taxonomic domain determined in sequences obtained from (i) NA0, (ii) NA18, (iii) NA42, (iv) ENA18, (v) ENA42, (vi) Comb18, and (vii) Comb42 metagenomes sampled from the TB soil following 42 week incubation period. The proportion of each taxonomic relative abundance was calculated as a percentage of the total organisms in the metagenomic sample. Labels are shown for those domains where abundance percentages were greater than 1% of the total organisms; 1: bacteria; 2: eukaryotes; 3: other (viruses and other sequenc

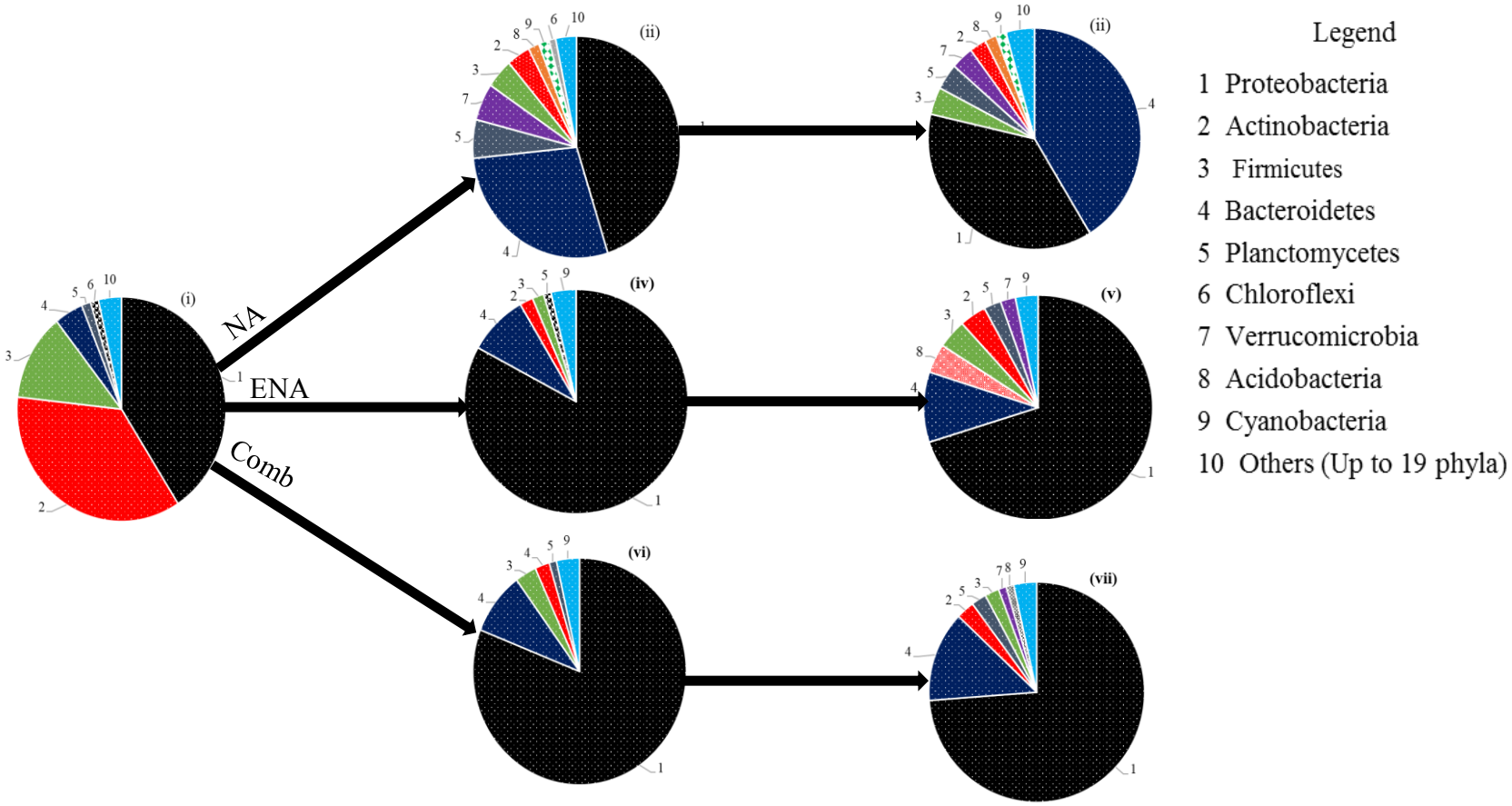

Figure 5.7. Distribution of taxonomic phylogenetic groups determined in sequences obtained from (i) NA0, (ii) NA18, (iii) NA42, (iv) ENA18, (v) ENA42, (vi) Comb18, and (vii) Comb42 metagenomes sampled from TB microcosm after 42-week incubation. The proportion of each taxonomic relative abundance was calculated as a percentage of total organism in the metagenomics sample. Labels are shown for those phyla where abundance percentages were greater than 1% of the total organisms, while percentage values are presented in Table.

5.5.4 Taxonomic analysis at phylum level in ENA and Comb TB microcosms

In nutrient supplemented microcosms, a small change in the number of taxonomic phylogenetic groups was observed from day 0 (6 phyla with relative abundance >1%) to week 18 (5 phyla with relative abundance >1%) (Figure 5.7 part (iv)). During this period, Proteobacteria (40.9 to 83.0%), and Bacteroidetes (4.4 to 8.7%) were overrepresented when compared to the initial relative abundances.

In contrast, a marked reduction in Actinobacteria (35.8 to 1.9%), Firmicutes (12.6 to 1.7%), and Chloroflexi (1.3 to 1.1%) relative abundance was observed (Table 5.3). Other phyla were present at low abundance resulting in a combined relative abundances of phyla with less than 1% of the total hits of 3.6%. At week 18, the number of phyla (5 phyla) with relative abundance greater than 1% decreased by a small margin compared to day 0 (6 phyla). However, the relative abundance of the most dominant phylum (Proteobacteria) doubled its initial abundance (40.9 to 83.0%), while the second most dominant phylum's (Bacteroidetes) relative abundance was 9-fold lower compared to Proteobacteria (Table 5.3).

At week 42, the relative abundance of Proteobacteria (70.0%) and Chloroflexi (<1%) were reduced compared to their relative abundances at week 18 (83.0 and 1.1% respectively). However, between weeks 18 and 42, a small increase in the relative of Actinobacteria (1.9 to 3.8%), Bacteroidetes (8.7 to 10.1%) and Planctomycete (<1 to 2.4%) was observed. In contrast, the relative abundance of phyla Actinobacteria (35.8 to 3.8%), and Firmicutes (12.6 to 4.1%) decreased substantially at week 42 compared to day 0. Notably, additional phyla such as Verrucomicrobia (<1 to 2.1%) and Acidobacteria (<1 to 4.2%) emerged at week 42 with relative abundance greater than 1% of the total organisms compared to their initial relative abundances at day 0 and week 18 respectively. Moreover, Actinobacteria had a 9-fold decrease in its initial relative abundance (35.8 to 3.8%) following the addition of nutrients and incubation (Table 5.3).

In microcosms where both nutrients and inoculants were supplied, a total of 28 phyla were present in metagenomic samples obtained at each time point (weeks 18 and 42, Figure 5.7 parts (vi) and (vii)). After 18 weeks of incubation, the relative abundance of Proteobacteria (40.9 to 81.0%) and Bacteroidetes (4.4 to 9.0%) were overrepresented as showed in Figure 5.7 parts (i) and (vi). In contrast, a significant decreased in the relative abundance of Actinobacteria (35.8 to 2.2%) and Firmicutes (12.6 to 3.2%) was observed.

After 42-weeks incubation, a small increase in the number of taxonomic phylogenetic groups was observed when compared to day 0 and week 18 (6 and 5 phyla at day 0 and week 18 compared to 7 phyla at week 42) respectively. Some phyla emerged with relative abundance greater than 1% of the total organisms that may have been present at day 0 and week 18 with relatively low abundances (Verrucomicrobia and Acidobacteria). (Table 5.3). Proteobacteria (73.8), Bacteroidetes (13.3%) were the dominant phyla, the relative abundance of other individual phyla was <3%.

5.5.5 Taxonomic analysis at order level in NA TB microcosms

In the TB microcosm, the composition of bacterial community at order level demonstrated high diversity over the 42-week incubation period (Up to 121 orders) under NA conditions. According to the MG-RAST data annotation, most of the classified sequences at order level were dominated by 13 genera (orders) with relative abundances greater than 1% of the total hits (Table 5.4) at the commencement of incubation.

Among these genera, Actinomycetales (34.8%) represented the highest proportion of the sequences (Figure 5.8 part (i)), which was not surprising given the order Actinomycetales belongs to the second most abundant phylum (Actinobacteria) in the TB soil. Other prominent orders include Rhizobiales (10.9%), Bacillales (10.2%), Burkholderiles (8.2%) and Sphingomonadales (4.8%) (Table 5.4).

A shift in organism diversity was observed over the initial 18-week incubation period. Additional orders with relative abundance greater than 1% were observed at week 18 (13 to 23 orders) as depicted in Table 5.4. Despite the increase in the number of orders through the incubation period, there was no clear dominant order. The relative abundance of some orders decreased, namely Actinomycetales (3.3%), Rhizobiales (7.6%), Bacillales (2.2%), Burkholderiales (4.4%), and Sphingomonadales (2.4%) while an increase in abundance of Flavobacteriales (<1 to 8.8%) and Cytophagales (<1 to 11%) was observed from day 0 to week 18.

As depicted in Table 5.4, for most orders, their relative abundances progressively declined to the end of the incubation period (week 42). A significant decrease was observed in the relative abundances of Rhizobiales (7.6 – 5.3%), Actinomycetales (3.3 – 2.3%), Bacillales (2.2 – 1.9%), Burkholderiales (4.0 – 3.3%), Sphingomonadales (2.4 – 1.5%) and Rhodobacteriales (2.2 – 1.7%). However, the decrease observed in the relative abundances of these orders corresponded

with an increase in the relative abundances of emergent orders including Flavobacteriales (8.8 to 14.3%), Cytopphagales (11.0 to 16.5%), Sphingobacteriales (4.6 to 5.6%), Bacteroidales (2.6 to 3.4%) and Nitrosomonadales (1.9 to 3.4%) at week 42 compared week 18. The relative abundance of several genera classified as others also increased throughout the time course (16.4 to 19.4%).

5.5.6 Taxonomic analysis at order level in ENA and Comb TB microcosms

In microcosms where supplementation of nutrients was implemented, the number of orders with relative abundance greater than 1% of the total hits increased by 6 at week 18 compared day 0 (Figure 5.9 part (ii)). A significant decrease in the relative abundance of Actinomycetales (34.8 to 1.9%) was observed after 18 weeks with a corresponding increase in the relative abundance of Cytophagale (<1 to 49.2%) (Table 5.4). According to the MG-RAST data annotation, the classified sequences at order level were dominated by 13 genera (orders) with relative abundance greater than 1% of the total hits (Table 5.4). Although an increase was observed in the number of orders after the initial 18 weeks of incubation, the community was dominated by Cytophagale.

Further incubation of ENA microcosms resulted in an increased in abundance of several orders including Burkholderiales (8.2 to 14.2%), Flavobacteriales (2.6 to 3.7%), Altromonadales (1.9 to 4.5%) and Nitrosomonadales (1.8 to 22.8%) from week 18 to week 42. In contrast, a significant decreased in the relative abundance of the orders including Cytophagales (49.2 to 3.1%), Sphingobacteriales (3.2 to 1.7%), Verucomicrobiales (2.9 to 1.0%), and Xanthomonadales (3.2 to 2.2%) was observed from week 18 to week 42 (Table 5.4). Interestingly, the order Cytophagales (49.2%) and Nitrosomonadales (22.8%) dominated all genera at the later times (ENA18 and ENA42), although their respective relative abundances were less than 1% of the total hits at the commencement of incubation (Figure 5.9 parts (ii) and (iii)).

In microcosms where supplementation of nutrients and inoculants were implemented (Comb), the composition of the bacterial community demonstrated high diversity at the Order level over the 42-week incubation period. The distribution of bacteria at order level resulted in 15 orders with relative abundance greater than 1% of the total hits (Figure 5.9 parts (i) and (ii)). A shift in bacterial community diversity was observed, with a significant decrease in the relative abundance of the order Actinomycetales (34.8 to 1.9%) at week 18 with a corresponded increase in the relative abundance of Nitrosomonadales (<1 to 42.6%).

Table 5.4. Taxonomic bacterial composition at order level in TB soil metagenomes obtained from unamended and amended microcosms following 42 weeks incubation. Values shown are for those phyla where abundance percentages were greater than 1% of the total organisms.

Legend	Order	Treatment, time (weeks) and relative abundance percentage compositions (%)								
		NA			ENA			Comb		
		0	18	42	0	18	42	0	18	42
1	Actinomycetales	34.8	3.3	2.3	34.8	1.7	3.5	34.8	1.9	2.5
2	Rhizobiales	10.9	7.6	5.3	10.9	4.2	6.4	10.9	5.2	4.5
3	Bacillales	10.2	2.2	1.9	10.2	*	3.1	10.2	2.4	1.0
4	Burkholderiales	8.2	4.0	3.3	8.2	8.2	14.2	8.2	9.7	6.4
5	Sphingomonadales	4.8	2.4	1.5	4.8	*	2.4	4.8	*	*
6	Rhodobacterales	2.8	2.2	1.7	2.8	*	1.4	2.8	*	1.3
7	Pseudomonadales	2.7	3.5	2.0	2.7	1.8	2.5	2.7	2.0	3.0
8	Flavobacteriales	2.6	8.8	14.3	2.6	2.6	3.7	2.6	2.3	3.6
9	Clostridiales	1.4	1.3	1.3	1.4	*	*	1.4	*	*
10	Alteromonadales	1.4	7.2	3.7	1.4	1.9	4.5	1.4	2.1	3.9
11	Planctomycetales	1.4	5.5	3.7	1.4	1.1	2.4	1.4	1.1	2.2
12	Caulobacterales	1.3	*	*	1.3	*	*	1.3	*	*
13	Rhodospirillales	1.0	1.5	1.2	1.0	*	1.3	1.0	*	1.2
14	Cytophagales	*	11.0	16.5	*	49.2	3.1	*	3.1	5.0
15	Sphingobacteriales	*	4.6	5.6	*	3.2	1.7	*	2.1	2.3

Table 5.4 (cont). Taxonomic bacterial composition at order level in TB soil metagenomes obtained from unamended and amended microcosms following 42 weeks incubation. Values shown are for those phyla where abundance percentages were greater than 1% of the total organisms.

Legend	Order	Treatment, time (weeks) and relative abundance percentage compositions (%)								
		NA			ENA			Comb		
		0	18	42	0	18	42	0	18	42
16	Verrucomicrobiales	*	3.1	1.9	*	2.9	1.0	*	*	*
17	Bacteroidales	*	2.6	3.4	*	2.0	*	*	*	1.5
18	Nitrosomonadales	*	1.9	3.4	*	1.8	22.8	*	42.6	29.2
19	Myxococcales	*	1.7	1.4	*	1.3	*	*	*	*
20	Oceanospirillales	*	1.5	1.1	*	1.0	*	*	*	1.5
21	Chromatiales	*	1.4	1.8	*	1.0	1.3	*	4.0	6.3
22	unclassified (Opitutae)	*	1.3	*	*	*	2.8	*	*	1.1
23	Enterobacteriales	*	1.2	1.1	*	*	1.4	*	1.0	1.3
24	Solibacterales	*	1.0	1.1	*	*	*	*	*	*
25	Desulfuromonadales	*	*	1.0	*	*	*	*	*	*
26	Xanthomonadales	*	*	*	*	3.2	2.2	*	2.9	2.9
27	Rhodocyclales	*	*	*	*	1.3	*	*	1.1	1.1
28	Methylophilales	*	*	*	*	1.0	*	*	*	*
29	Gallionellales	*	*	*	*	1.0	*	*	*	*
30	Others	16.4[a]	19.1[b]	19.4[c]	16.4[a]	15.9[d]	18.3[e]	16.4[a]	16.5[f]	18.3[g]

*percentages below 1% of the total organisms.

[a] 'other' represented 108 order each representing <1% of the total abundance.

[b] 'other' represented 96 order each representing <1% of the total abundance.

[c] 'other' represented 95 order each representing <1% of the total abundance.

[d] 'other' represented 100 order each representing <1% of the total abundance.

[e] 'other' represented 101 order each representing <1% of the total abundance.

[f] 'other' represented 105 order each representing <1% of the total abundance.

[g] 'other' repres ented 98 order each representing <1% of the total abundance.

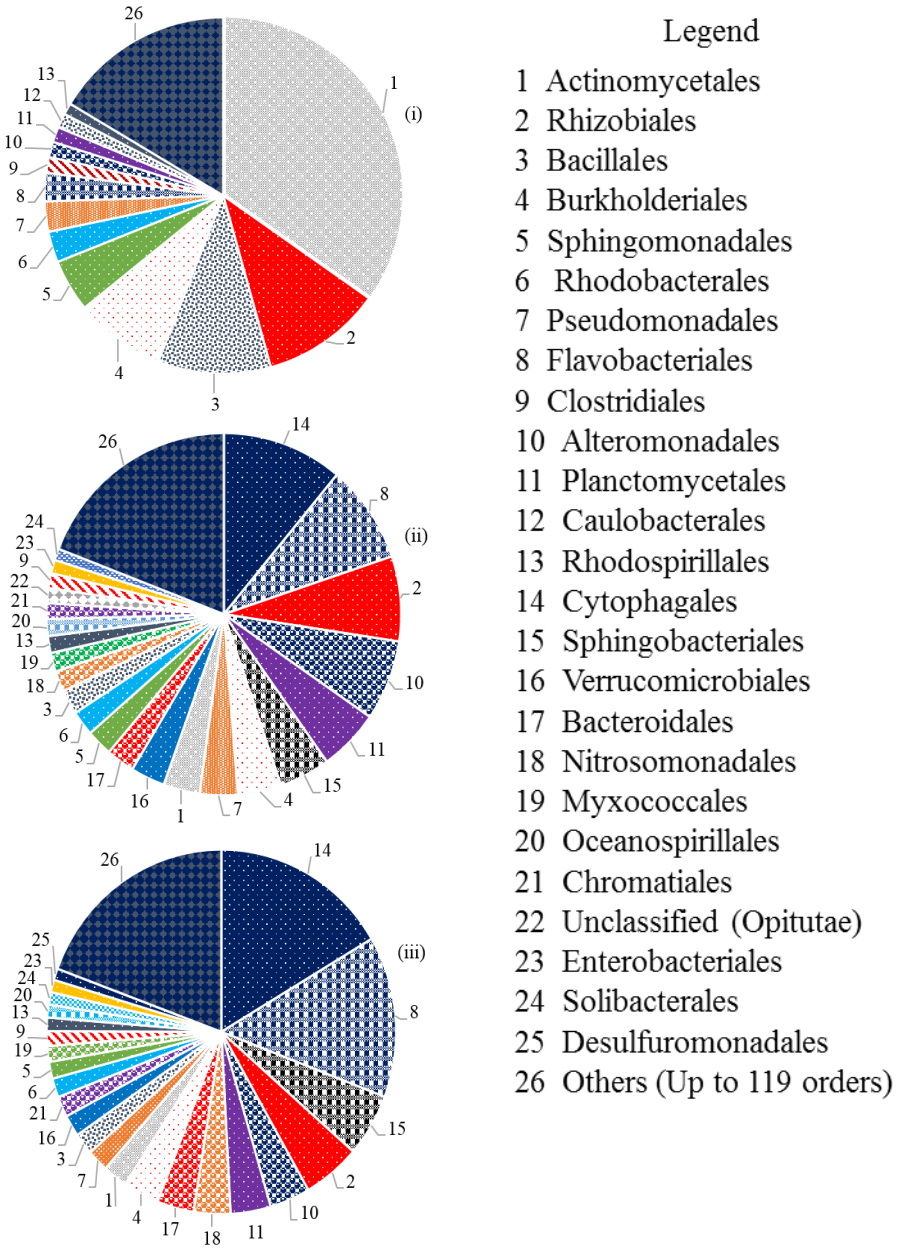

Figure 5.8. Distribution of organisms at order level determined in sequences obtained from (i) NA0, (ii) NA18, and (iii) NA42 metagenomes sampled from TB soil following 42 weeks of incubation under natural attenuation (NA) conditions. The proportion of each Order relative abundance was calculated as a percentage of total organisms in metagenomic samples. Labels are shown for those orders where abundance percentages were greater than 1% of the total organisms, while percentage values are presented in Table 5.4.

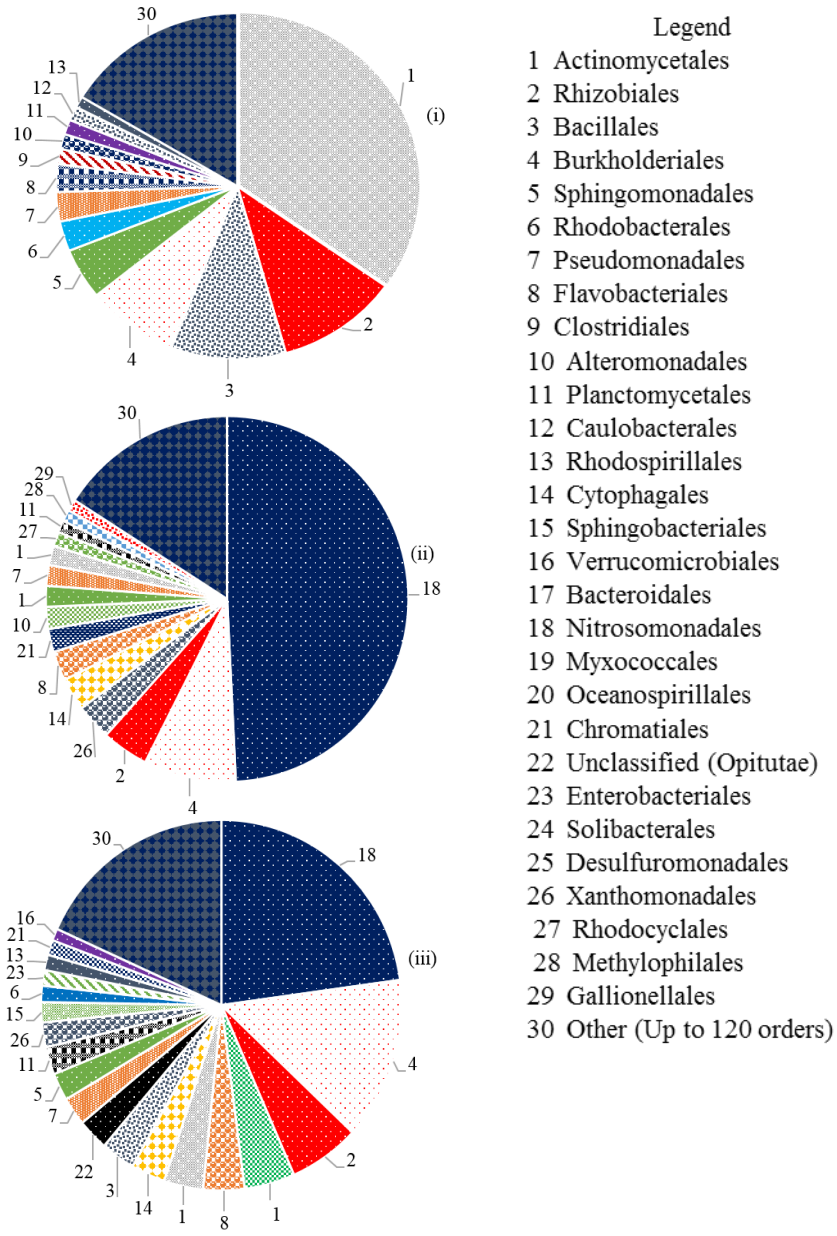

Figure 5.9. Distribution of organisms at order level determined in sequences obtained from (i) ENA0, (ii) ENA18, and (iii) ENA42 metagenomes sampled from TB soil following 42 weeks of incubation under enhanced natural attenuation (ENA) conditions. The proportion of each order relative abundance was calculated as a percentage of total organisms in the metagenomic sample. Labels are shown for those orders where abundance percentages were greater than 1% of the total organisms, while percentage values are presented in Table 5.4.

According to the MG-RAST data annotation, the classified sequences after 18 weeks of incubation (Comb18) was dominated by 15 genera (orders) with relative abundance greater than 1% of the total hits (Table 5.4).

Among these genera, Nitrosomonadales (42.6%) represented the highest proportions of the sequences obtained at week 18 (Comb1) as shown in Figure 5.10. Other orders such as Burkholderiales (8.2 to 9.7%), Cytophagale (<1 to 3.1%), and Chomatiales (<1 to 4.0%) showed small increases in their relative abundances at week 18 compared to day 0. In addition to the 13 dominant genera, other orders were present at low magnitude (Table 5.4) including up to 108 orders (>1% relative abundance) classified as others (16.5%).

At the end of the incubation period (week 42), the number of orders increased by 6 compared to week 18 (15 to 20 orders) as shown in Figure 5.9 (i) and (iii). According to the MG-RAST annotation systems, the addition of both nutrients and inoculants coupled with incubation resulted in an increase in abundance of several orders including Flavobacteriales (2.3 to 3.6%), Cytophagales (3.1 to 5.0%), and Chomatiales (4.0 to 6.3%) from week 18 to week 42. By week 42, the number of orders with relative abundance greater than 1% increased by 7 compared to day 0 (15 orders).

In contrast, incubation of microcosms under the Comb strategy resulted in a significant decrease in the relative abundance of several orders including Nitrosomonadales (42.6 to 29.2%), Bacillales (2.4 to 1.0%), and Burkholderiales (9.7 to 6.4%) at week 42 compared to week 18 (Table 5.4). Moreover, the order Nitrosomonadales (42.6 and 29.2%) dominated all genera in other treatment at weeks 18 and 42 (Comb18 and Comb42), although the initial relative abundance was less than 1% at the commencement of the incubation period (Figure 5.10 parts (i) and (iii)).

Unlike NA and ENA microcosms where high variability was observed in terms of dominance at order level, the combined microcosms (Comb) was dominated by Nitrosomonadales at the later time points (weeks 18 and 42). This is not surprising as the order Nitrosomonadales belongs to the most abundant phylum Proteobacteria at weeks 18 and 42 (section 5.54).

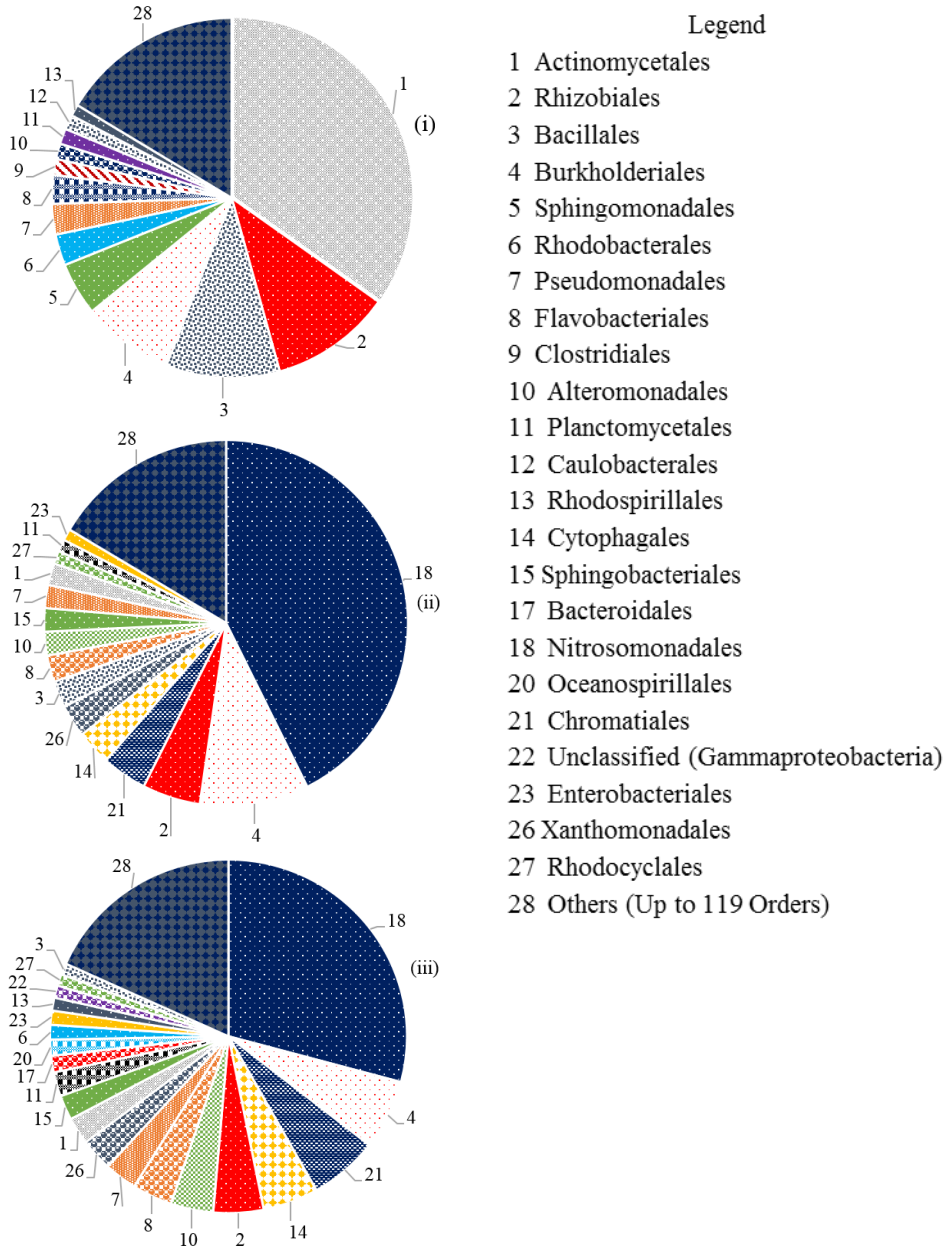

Figure 5.10. Distribution of organisms at order level determined in sequences obtained from (i) Comb0, (ii) Comb18, and (iii) Comb42 metagenomes sampled from TB soil following 42 weeks of incubation under combined conditions (Comb). The proportion of each order relative abundance was calculated as a percentage of total organisms in the metagenomic sample. Labels are shown for those orders where abundance percentages were greater than 1% of the total organisms, while percentage values are presented in Table 5.4.

5.6 Assessment of bacterial communities in the AP soil microcosms

5.6.1 Taxonomic analysis at domain level in NA AP microcosms

Annotation of metagenome sequence raw data obtained in AP soil microcosms was peformed as described in section 5.5.1. Analysis of domain distributions in the AP soil microcosms shown greater abundance of two taxa (Relative abundance of greater than 1% of the total hits), bacteria and eukaryote. Following MG-RAST data annotation in AP soil microcosms, 12,453,116 hits were found as a number of reads, with predicted protein features based on this analysis.

In the AP soil microcosms, the amount of sequences assigned to each domain was calculated as the relative abundance of the total hits (Figure 5.11 part (i)). In addition, greater of these reads were assigned as prokaryote (96. 0%).The remaining percetanges of sequences were annotated to the eukaryotic domain with 3.4% of the total hits while the rest of domains (archaeal, viruses and other sequences), classified as others constituted less than 1% of the total hits (0.5%). As observed in Creo and TB soil microcosms, Prokaryotes dominated domain distribution in AP soil microcosms at the beginning of microcosm experiments. This is due to that fact that Prokaryotes have a greater propensity to survive in dry soil compared to other domains. Thus, the dominance of this domain may be attributed to the fact that environmental conditions were more supportive to prokaryotes than other domains. As a result, more weight was placed on the most dominant domain prokaryotes compare to the other domains as detailed in the subsequent Sections.

Other metagenomic datasets (NA18 and NA42 metagenomes) were compared with organism distribution (domain level) at day 0 (NA0). The overall organism distribution in NA18 metagenome had a similar pattern to NA0 (Figure 5.11 part (i)). Similar results were obtained in metagenomes sampled in NA42 microcosm although a small decrease in bacteria (92.1%) was observed with a corresponding increase in eukaryotes (7.2%). However, no significant differences ($P < 0.05$) were observed in NA microcosm's domain distribution over the 42-week incubation period.

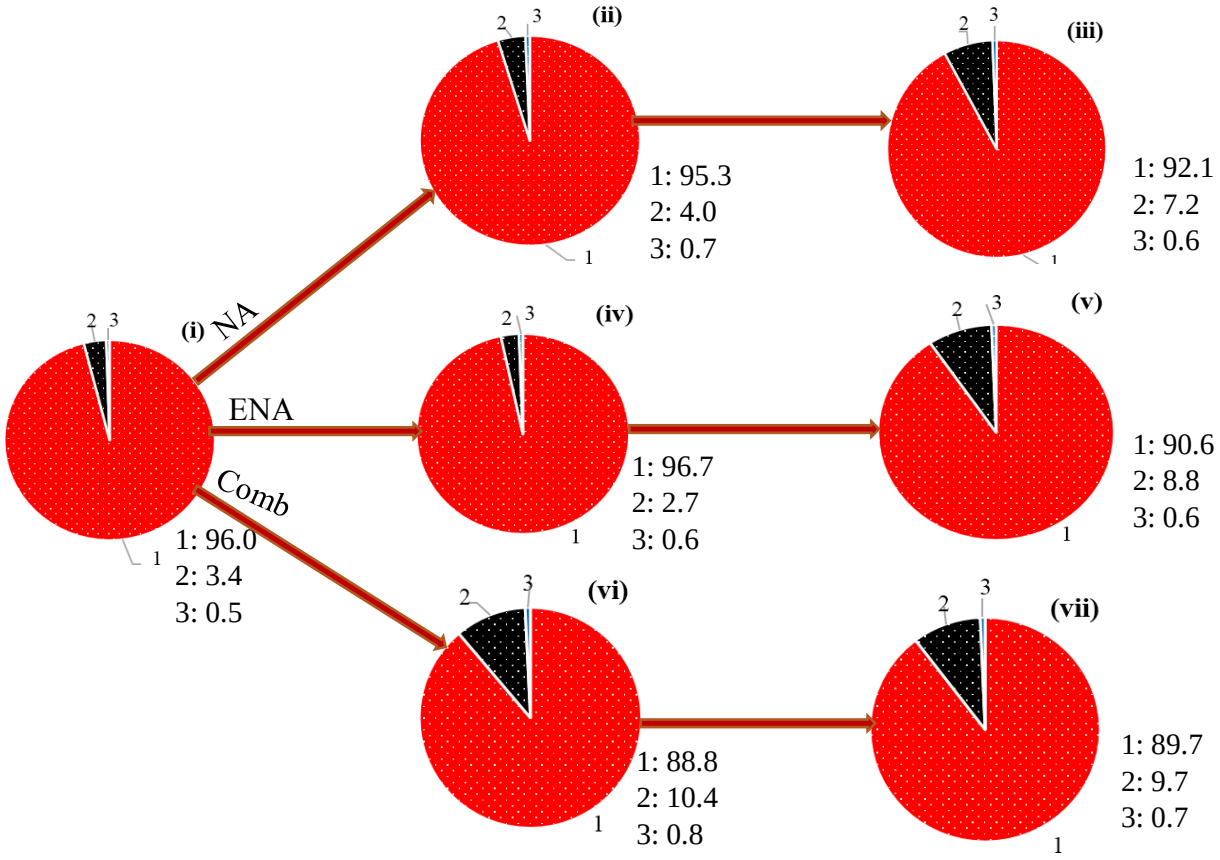

Figure 5.11. Distribution of taxonomic domain determined in sequences obtained from (i) NA0, (ii) NA18, (iii) NA42, (iv) ENA18, (v) ENA42, (vi) Comb18, and (vii) Comb42 metagenomes sampled from AP soil following 42 weeks of incubation. The proportion of each taxonomic relative abundance was calculated as a percentage of total organism in the metagenomics sample. Labels are shown for those domains where abundance percentages were greater than 1% of the total organisms; 1: bacteria; 2. Eukaryotes; 3: other (viruses and other sequence).

5.6.2 Taxonomic analysis at domain level in ENA and Comb AP microcosms

In the ENA microcosms, there was no significant change observed in domain distribution in metagenomes from day 0 and week 18 (Figure 5.11 (parts (i) and (iv)). However, a 5.4% reduction in relative abundance of bacteria was observed in metagenomes from ENA42 when compared to the initial abundance at day 0 (96.0 to 90.6%) as showed in Figure 5.11 (parts (i) and (v)). An increase in the relative abundance of eukaryotes (3.4 to 8.8%) was observed at the end of the incubation period (week 42). In contrast, in microcosms amended with nutrients and inoculants (Comb), a decrease in the relative abundance of bacteria was observed at weeks 18 and 42 (88.8 and 89.7%) (Figure 5.11 (parts (vi) and (vii) when compared to the initial relative abundance (96.0%, Figure 5.11 part (i)). Notably, there was a significant increase in the relative abundance of eukaryotes (Figure 5.11 parts (vi) and (vii)) at week 42 compared to day 0 (3.4 to 9.7%) Figure 5.11 part (i).

5.6.3 Taxonomic analysis at phylum level in NA AP microcosms

Analysis of bacterial distribution at phylum level resulted in the identification of 28 distinctive phyla (Figure 5.12 part (i)) in the AP soil at the start of microcosm experiments. Phyla were detected at varying proportions as shown by their relative abundances in Table 5.5. Most of these phyla (21 phyla) were represented by <1% of all assigned hits, while, their combined relative abundance was 3.6% of the total hits. Annotation of bacterial sequences at phylum level, demonstrated that Proteobacteria was the most dominant taxon, with 55.8% of the total hits.

According to the MG-RAST annotation systems, phylum Acidobacteria was the second most prevalent taxon with 18.1% relative abundance. Proteobacteria was overrepresented by 3- and 2-fold compared to the second and third most prevalent phyla (Acidobacteria and Bacteroidetes). Other prominent phyla detected with greater than 1% of the total hits included Bacteroidetes (11.4%), Actinobacteria (5.3%), Firmicutes (2.7%), Verrucomicrobia (2.1%), and Cyanobacteria (1.1%) as showed in Table 5.5. At week 18, NA microcosms showed a small increase in the number phylogenetic groups (28 compared to 29), with 7 phyla detected having a greater than 1% relative abundance compared to day 0 as depicted in Figure 5.12 parts (i) and (ii). After 18 weeks of incubation, an increase in the relative abundance of phylum Proteobacteria (55.8 to 65.6%), Actinobacteria (5.3 to 6.2%), and Firmicutes (2.7 to 3.1%) was observed compared to day 0. Other phyla were present at low abundance including Verrucomicrobia, Cyanobacteria and Chlamydiae (Table 5.5). During the incubation, there was

reduction in the relative abundance of some phyla, which included Acidobacteria (18.1 to 16.5%), Bacteroidetes (11.4 to 2.0%) and Verrucomicrobia (2.1 to <1%).

At the end of the incubation of period (week 42), a significant shift in the relative abundance of Actinobacteria (42.3%) was observed when compared to day 0 (18.1%) and week 18 (16.5%).The increase in the relative abundance of Actinobacteria corresponded with a decrease in the relative abundance of Proteobacteria (55.8, 65.6 to 35.4%) at day 0, weeks 18 and 42. No significant changes were observed in the abundance of individual phylum between weeks 18 and 42 except a 2-fold increase in the relative abundance of Acidobacteria at week 42. Moreover, an increase was observed in the relative abundance of Verrucomicrobia (<1 to 1.2), and Chloroflexi (<1 to 1.0%) at week 42 compared to week 18, while a corresponded decrease in the relative abundance of Chlamydia (1.1 to <1%) was also observed.

Table 5.5. Taxonomic bacterial composition at phylum level in AP soil metagenomes obtained from unamended and amended microcosms following 42 weeks incubation. Values shown are for those phyla where abundance percentages were greater than 1% of the total organisms

Legend	Phylum	Treatment, time (weeks) and relative percentage compositions (%)								
		NA			ENA			Comb		
		0	18	42	0	18	42	0	18	42
1	Proteobacteria	55.8	65.6	35.4	55.8	61.5	56.9	55.8	43.7	49.7
2	Acidobacteria	18.1	16.5	42.3	18.1	21.1	20.0	18.1	29.3	22.5
3	Bacteroidetes	11.4	2.0	2.5	11.4	1.5	3.8	11.4	2.0	3.4
4	Actinobacteria	5.3	6.2	8.4	5.3	7.7	10.9	5.3	15.8	14.4
5	Firmicutes	2.7	3.1	4.3	2.7	2.9	2.3	2.7	3.3	3.4
6	Verrucomicrobia	2.1	*	1.2	2.1	*	*	2.1	1.0	*
7	Cyanobacteria	1.1	1.3	1.4	1.1	1.2	1.5	1.1	1.3	1.3
8	Chlamydiae	*	1.1	*	*	*	1.0	*	*	1.1
9	Chloroflexi	*	*	1.0	*	*	*	*	*	*
10	Others	3.6[a]	4.2[b]	3.5[c]	3.6[a]	4.1[d]	3.7[e]	3.6[a]	3.5[f]	4.3[g]

*percentages below 1% of the total organisms.
[a] 'other' represented 21 phyla each representing <1% of the total abundance.
[b] 'other' represented 22 phyla each representing <1% of the total abundance.
[c] 'other' represented 21 phyla each representing <1% of the total abundance.
[d] 'other' represented 23 phyla each representing <1% of the total abundance.
[e] 'other' represented 21 phyla each representing <1% of the total abundance.
[f] 'other' represented 21 phyla each representing <1% of the total abundance.
[g] 'other' represented 21 phyla each representing <1% of the total abundance.

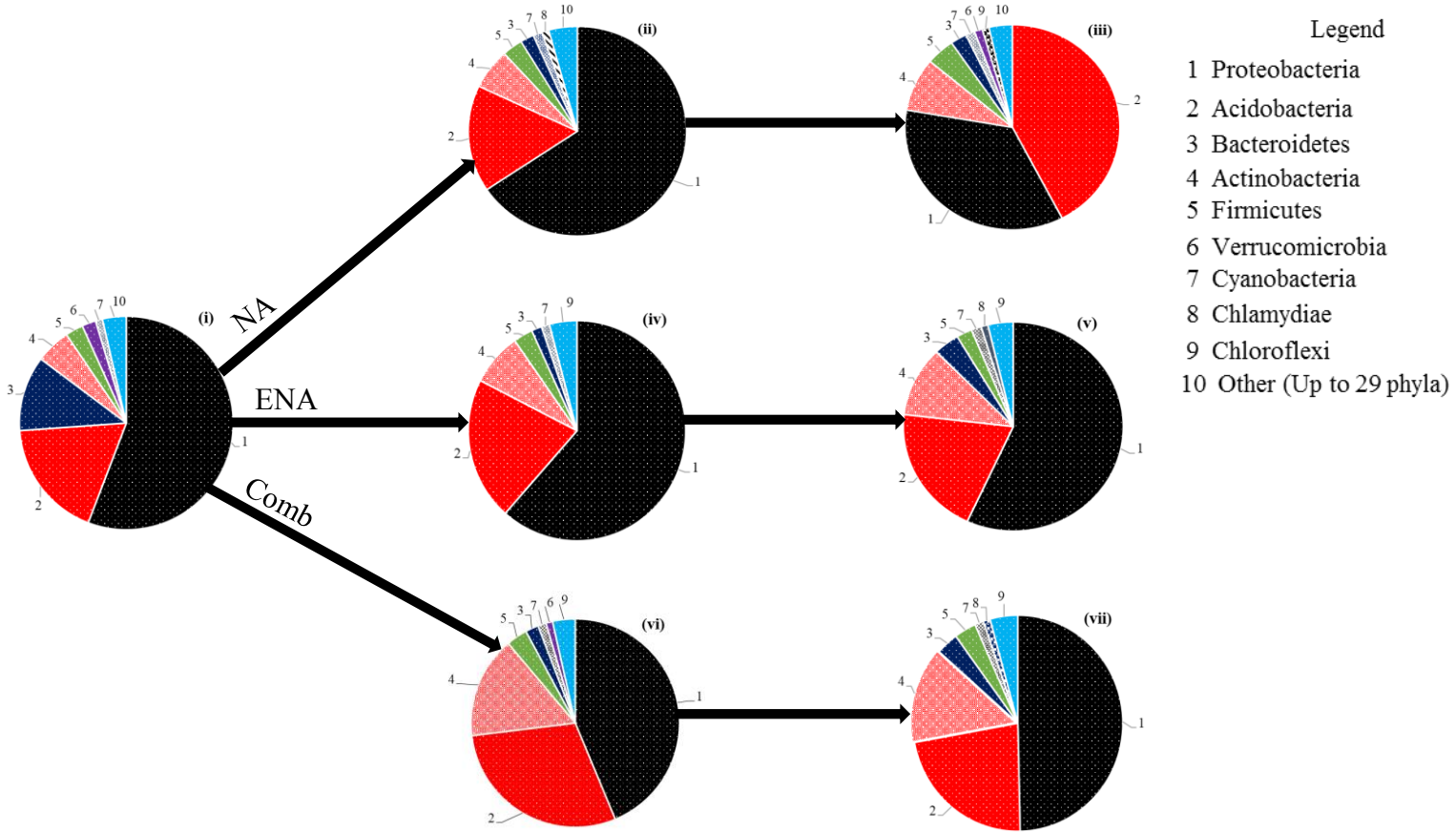

Figure 5.12. Distribution of taxonomic phylogenetic groups determined in sequences obtained from (i) NA0, (ii) NA18, (iii) NA42, (iv) ENA18, (v) ENA42, (vi) Comb18, and (vii) Comb42 metagenomes sampled from AP soil following 42 weeks of incubation. The proportion of each taxonomic relative abundance was calculated as a percentage of total organism in the metagenomics sample. Labels are shown for those phyla where abundance percentages were greater than 1% of the total organisms, while percentage values are presented in Table 5.5.

5.6.4 Taxonomic analysis at phylum level in ENA and Comb AP microcosms

In the ENA amended microcosm, a small change in the number of taxonomic phylogenetic groups was observed at sample time points, weeks 18 and 42 (from 28 to 29 phyla) compared to day 0. After 18 weeks of incubation, there were 6 phyla detected with relative abundance greater than 1% of the total hits, with Proteobacteria as the most prevalent phylum increasing from 55.8% at the start of microcosm experiment to 61.5% at week 18. An increase in the relative abundance of Acidobacteria (18.1 to 21.1%) and Actinobacteria (5.3 to 7.7%) was also observed at week 18 compared to day 0 (Figure 5.12 part (iv)). In contrast, the relative abundance of Bacteroidetes (11.4 to 1.5%) and Verrucomicrobia (2.1 to <1%) decreased. Other phyla (3 additional phyla) were also detected but at levels <1% of the total organisms (Table 5.5). Bacterial distribution at week 42 resulted in a small change in the relative abundance of several phyla compared to week 18 with Proteobacteria remaining as the most abundance phylum (56.9%).

Similar results were observed in microcosms where both nutrients and inoculants were implemented (Figure 5.12 parts (vi) and (vii)). The relative abundance of all phyla fluctuated through the time course, however, Proteobacteria was overrepresented in metagenomes from weeks 18 (43.7%) and 42 (49.7%), while Acidobacteria (29.3 and 22.5%) and Actinobacteria (15.8 and 14.4%) were the second and third most prevalent phyla at weeks 18 and 42 respectively. Overall, only small changes were observed in bacterial diversity over the 42 week incubation period (7 phyla each from day 0 to week 42) in samples incubated under combined conditions (Comb).

5.6.5 Taxonomic analysis at order level in NA AP microcosms

In the AP soil microcosms, the composition of the NA bacterial community at the order level demonstrated high diversity. According to the MG-RAST data annotation, classified sequences at order level were dominated by 21 genera (orders) with relative abundance greater than 1% of the total hits (Table 5.6). Among these orders, Burkholderiales (16.8%), Rhizobiales (11.6%) and Acidobacterialess (11.1%) were overrepresented at the commencement of incubation (Figure 5.13 part (i)). Other orders including Sphingobacteriales (6.3%), Actinomycetales (5.1%), and Sphingomonadales (4.8%) were also present at low relative abundance at day 0.

An additional 99 orders were also present at low magnitude (<1% relative abundance as in Table 5.6) with a combined relative abundance of 15.6%. A shift in the diversity of various orders was observed when a taxonomic analysis was undertaken comparing week 18 and 42 samples to day 0.Taxonomic analysis of the distribution of relative abundance in the NA microcosms found that the number of orders greater than 1% relative abundance was constant (21 orders) at week 18 compared to day 0 but decreased by 4 orders at week 42 (Figure 5.13 parts (ii) and (iii)).Taxonomic analysis also found that no single order dominated the bacterial distribution at week 18 and 42 although Burkholderiales were the dominant order present at day 0. Further incubation resulted in an increase in abundance of several orders in NA microcosms including Acidobacteriales (11.1 to 26.8%), Actinomycetales (5.9 to 8.0%), Solibacterales (2.1 to 5.6%), Unclassified derived from Acidobacteriales (3.2 to 9.9%) and Bacillales (1.8 to 2.3%) at week 18 compared to day 0. In contrast, incubation resulted in a decrease in abundance of other orders in NA microcosms including Burkholderiales (10.2 to 5.5%), Rhizobiales (11.4 to 9.5%), Rhodospirillales (2.9 to 2.0%) and Sphingomonadales (12.1 to 1.4%) between day 0 and week 18. The majority of orders were less abundant at week 42 compared to day 0 except orders including Acidobacteriales (26.8%), Actinomycetales (8.0%) and Unclassified derived from Acidobacteriales (9.9%).

Notably some additional genera were detected in metagenomes from NA18 and NA42 microcosms with relative abundances greater than 1% of the total hits (Figure 5.13 parts (ii) and (iii)). The relative abundance of several genera classified as others increased throughout the incubation time course (15.6 to 19.0%) suggesting that several bacterial communities become less abundant as the bacterial diversity increases. Moreover, orders such as Sphingobacteriales, Cytophagales, Flavobacteriales, Verrucomicrobiales, Bacteroidales, Methylophilales and Chomatiales were detected with relative abundance less than 1% of the total hits at weeks 18 and 42 compared to day 0. While Alteromonadales, Myxococales, Desulfuromonadales, Rhodocyclales, Chlamydiales and Clostridiales were found with relative abundance greater than 1% of the total hits at weeks 18 and 42.

5.6.6 Taxonomic analysis at the order level in ENA and Comb AP microcosms

In microcosms where ENA was implemented, the composition of the bacterial community at order level, ranged from 116 to 120 orders. A shift occurred following the supplementation of nutrients, with a small increase in the relative abundance of several orders including Acidobacteriales (11.1 to 14.2%), Actinomycetales (5.1 to 7.5%), Sphingomonadales 4.7 to

9.5%) after 18 weeks of incubation compared to day 0 (Figure 5.14 parts i and iii). There was no clear dominance observed in terms of relative abundances at week18, however, orders including Burkholderiales (10.4%), Rhizobiales (11.7%) and Acidobacteriales (14.2%) had the highest relative abundance.

In contrast, the addition of nutrients and incubation of ENA microcosms resulted in a significant decrease in the relative abundance of the orders such as Burkholderiales (10.4 to 7.7%) and Sphingomonadales (9.5 to3.1%) from week 18 to week 42 (Figure 5.14 parts (ii) and (iii)). Consequently, further incubation following implementation of ENA resulted in a small increase in the relative abundance of orders including Rhizobiales (11.7 to 13.7%), Actinomycetales (7.5 to 10.5%) and Chomatiales (4.0 to 5.1%) from week 18 to week 42 (Table 5.6). At weeks 18 and 42, additional orders were also detected at relative abundance less than 1% of the total hits included Cytophagales, Verrucomicrobiales, Bacteroidales, Methylophilales, Chomatiales and Clostridiales (Table 5.6).

Similarly, annotation of taxonomic phylogenetic groups in metagenomes obtained from microcosms supplemented with inoculants and nutrients are showed in Figure 5.15. The diversity at order level ranged from up to 120 orders in combined microcosms. According to the MG-RAST annotation systems, the addition of nutrients and inoculants, coupled with incubation resulted in an increased in the relative abundance of orders including Acidobacteriales (11.1 to 19.0%) and Unclassified sequences related to Acidobacteria (3.3 to 6.8%) from day 0 to week 18 (Table 5.6 and Figure 5.15 (ii) and (ii)). A corresponding decrease was observed in other orders included Burkholderiales (16.8 to 8.7%), Rhizobiales (11.6 to 8.4%), Sphingobacteriales (6.3 to <1%), and Actinomycetales (5.1 to <1%) at week 18 compared to day 0.

In contrast, the addition of nutrients and inoculants, coupled with incubation of the combined microcosms resulted in further decrease in the relative abundance of Burkholderiales (8.7 to 6.7%), Acidobacteriales (19.0 to 13.7%), Unclassified sequences derived from Acidobacteria (6.8 to 4.7%), and Sphingobacteriales (6.3 to 1.1%) from week 18 to week 42 (Table 5.4). Moreover, additional orders were detected at low relative abundance with increasing diversity in all metagenomes including the appearance of orders with relative abundances greater than 1%of the total hits (Chomatiales, Alteromonadales, Myxococcales, and Desulfuromonadales) as detailed in Table 5.6.

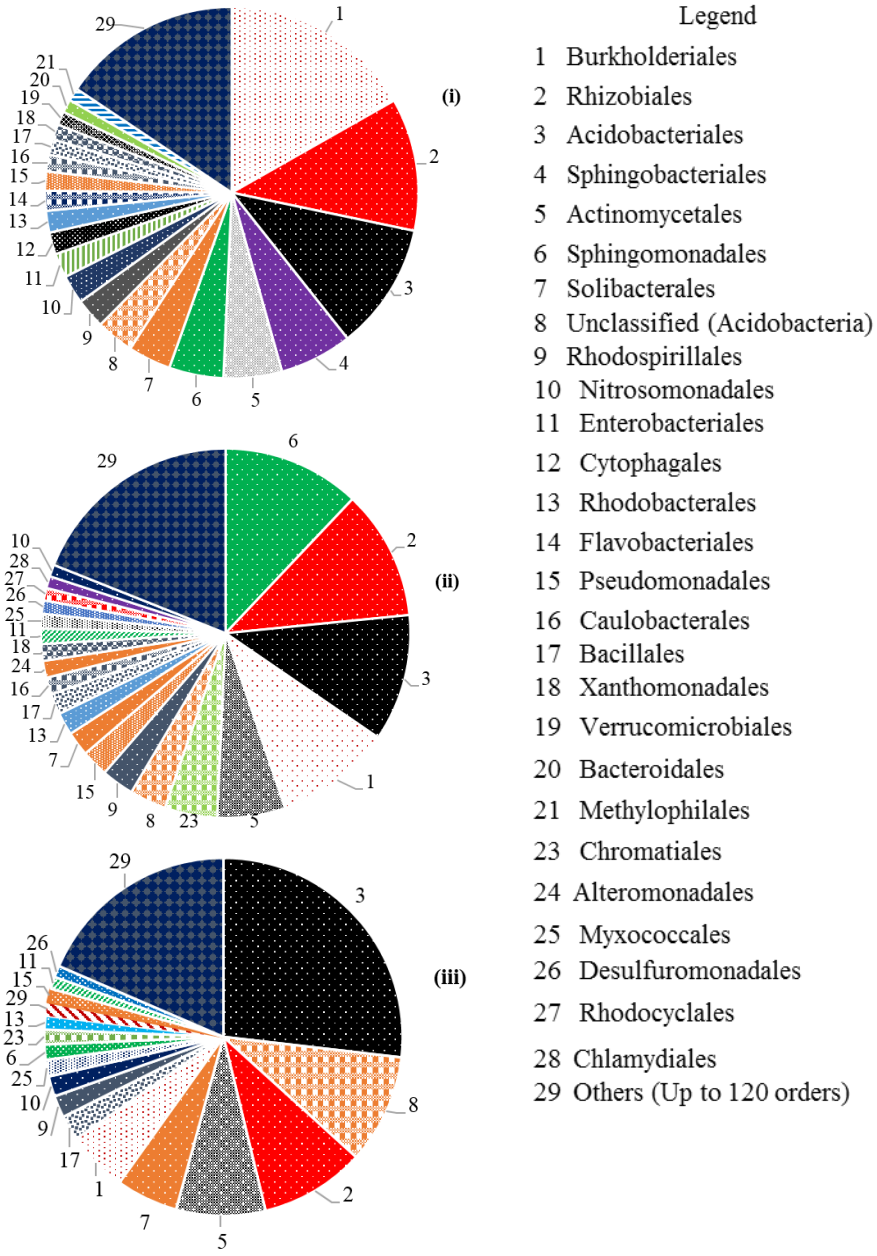

Figure 5.13. Distribution of organisms at Order level determined in sequences obtained from (i) NA0, (ii) NA18, and (iii) NA42 metagenomes sampled from AP soil following 42 weeks of incubation under natural attenuation conditions (NA). The proportion of each Order relative abundance was calculated as a percentage of total organisms in metagenomic samples. Labels are shown for those orders where abundance percentages were greater than 1% of the total organisms, while percentage values are presented in Table 5.6.

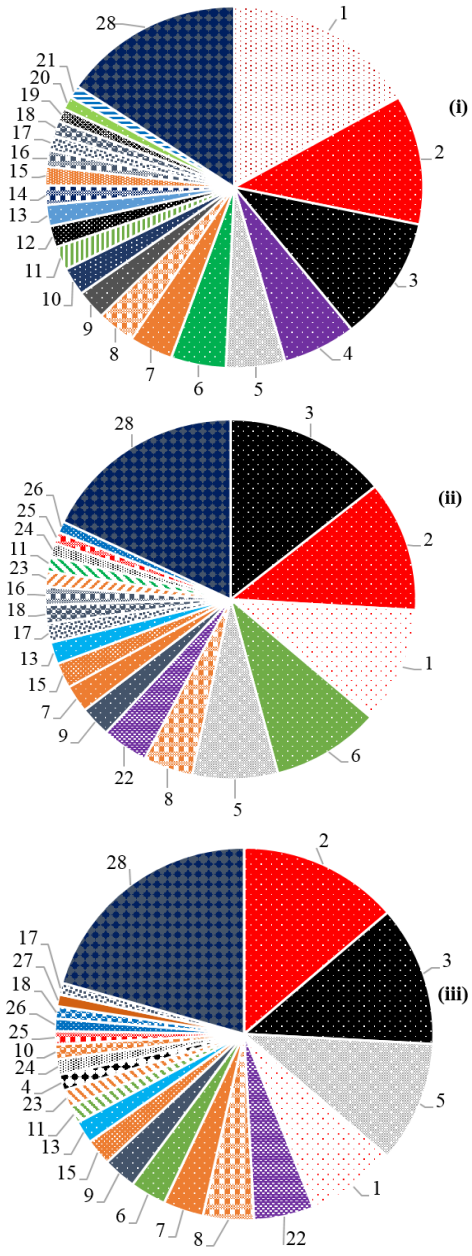

Legend

1 Burkholderiales
2 Rhizobiales
3 Acidobacteriales
4 Sphingobacteriales
5 Actinomycetales
6 Sphingomonadales
7 Solibacterales
8 Unclassified (Acidobacteria)
9 Rhodospirillales
10 Nitrosomonadales
11 Enterobacteriales
12 Cytophagales
13 Rhodobacterales
14 Flavobacteriales
15 Pseudomonadales
16 Caulobacterales
17 Bacillales
18 Xanthomonadales
19 Verrucomicrobiales
20 Bacteroidales
21 Methylophilales
22 Chromatiales
23 Alteromonadales
24 Myxococcales
25 Rhodocyclales
26 Desulfuromonadales
27 Oceanospirillales
28 Others (Up to 120 orders)

Figure 5.14. Distribution of organisms at order level determined in sequences obtained from (i) ENA0, (ii) ENA18, and (iii) ENA42 metagenomes sampled from AP soil following 42 weeks of incubation under enhanced natural attenuation conditions (ENA). The proportion of each order relative abundance was calculated as a percentage of total organisms in the metagenomic sample. Labels are shown for those orders where abundance percentages were greater than 1% of the total organisms, while percentage values are presented in Table 5.6.

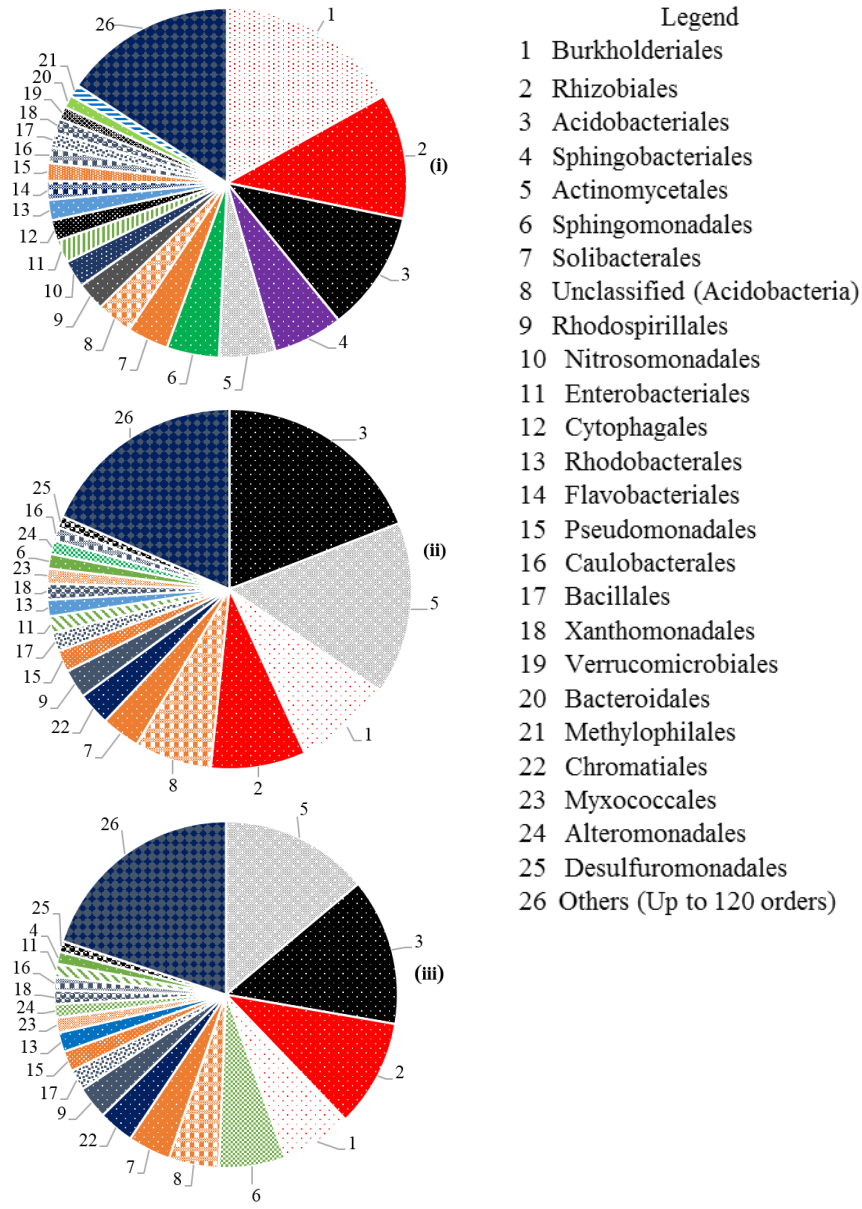

Figure 5.15. Distribution of organisms at order level determined in sequences obtained from (i) Comb0, (ii) Comb18, and (iii) Comb42 metagenomes sampled from AP soil following 42 weeks of incubation under combined conditions (Comb). The proportion of each order relative abundance was calculated as a percentage of total organisms in the metagenomic sample. Labels are shown for those orders where abundance percentages were greater than 1% of the total organisms, while percentage values are presented in Table 5.6.

5.7 MG-RAST analysis of functional profiles

Based on analysis of functional profile annotated by MG-RAST, changes in the abundance of functional categories associated with aromatic metabolism in PAH-contaminated soils were examined over the 42 week incubation period. The impact of bioremediation strategies on functional profiles was compared using the Statistical Analysis of Metagenomic Profiles (STAMP) software in metagenomes sampled on day 0, weeks 18 and 42 (Parks & Beiko 2010). High-level metabolic profiles of metagenomes sampled from unamended and amended microcosms were analysed for PAH degrading enzymes.

In order to assess biological differences between pairs of metagenomic samples, assembled sequences related to metabolic functions were imported from the MG-RAST server to the STAMP program with an E-value cut-off of 1×10^{-5} and a 50 bp minimum length. This was specifically performed to test for significant differences at functional levels. To do this, P-values were determined in STAMP using the two sided Fisher's Exact test (Boissy et al. 2014), while confidence intervals (95%) were calculated using the Newcombe-Wilson method (Newcombe 1998). False discovery rate (FDR) was corrected by using the Storey's FDR method (Storey & Tibshirani 2003). The FDR measures the balance between the true and false positives in target metabolic samples to provide an accurate measure of significance of relevant biological differences. However, a limitation of the program (STAMP) is generation of graphs to compare multiple metagenomes concurrently. As showed in Figures 5.16 – 5.33, it was possible to analyse two metagenomes simultaneously in one run resulting in a comparison figure illustrating the two metagenomic samples. As a consequence, two graphs were prepared for metagenomes obtained from each microcosm, namely comparisons of day 0 verses week 18, and week 18 verses week 42, while a comparison is described for day 0 and week 42 metagenomes.

5.7.1 Comparison of metabolic profiles in Creo metagenomes

The metabolic profiles for Creo microcosms are shown in Figures 5.16-5.21. Functional profile analysis in the Creo NA microcosm showed the occurrence of similar core metabolic functions in metagenomes sampled over the 42 week incubation period.

Table 5.6. Taxonomic bacterial composition at order level in AP soil metagenomes obtained from unamended and amended microcosms following 42 weeks of incubation. Values shown are for those phyla where abundance percentages were more than 1% of the total organisms.

Legend	Order	Treatment, time (weeks) and relative abundance percentage compositions (%)								
		NA			ENA			Comb		
		0	18	42	0	18	42	0	18	42
1	Burkholderiales	16.8	10.2	5.5	16.8	10.4	7.7	16.8	8.7	6.7
2	Rhizobiales	11.6	11.4	9.5	11.6	11.7	13.7	11.6	8.4	10.1
3	Acidobacteriales	11.1	11.1	26.8	11.1	14.2	12.2	11.1	19.0	13.7
4	Sphingobacteriales	6.3	*	*	6.3	*	1.4	6.3	*	1.1
5	Actinomycetales	5.1	5.9	8.0	5.1	7.5	10.5	5.1	*	14.0
6	Sphingomonadales	4.7	12.1	1.4	4.7	9.5	3.1	4.7	1.3	6.2
7	Solibacterales	3.7	2.1	5.6	3.7	2.5	3.4	3.7	3.4	4.0
8	unclassified (Acidobacteria)	3.3	3.2	9.9	3.3	4.4	4.3	3.3	6.8	4.7
9	Rhodospirillales	2.6	2.9	2.0	2.6	2.7	2.9	2.6	2.6	3.1
10	Nitrosomonadales	2.5	1.0	1.8	2.5	*	1.3	2.5	*	*
11	Enterobacteriales	2.1	1.3	1.1	2.1	1.4	1.5	2.1	1.5	1.2
12	Cytophagales	1.9	*	*	1.9	*	*	1.9	*	*
13	Rhodobacterales	1.9	2.0	1.2	1.9	2.0	2.0	1.9	1.5	1.8
14	Flavobacteriales	1.7	*	*	1.7	*	*	1.7	*	*
15	Pseudomonadales	1.7	2.3	1.2	1.7	2.3	2.3	1.7	1.9	1.9

Table 5.6 (cont). Taxonomic bacterial composition at order level in AP soil metagenomes obtained from unamended and amended microcosms following 42 weeks of incubation. Values shown are for those phyla where abundance percentages were more than 1% of the total organisms.

Legend	Order	Treatment, time (weeks) and relative abundance percentage compositions (%)								
		NA			ENA			Comb		
		0	18	42	0	18	42	0	18	42
16	Caulobacterales	1.4	1.5	*	1.4	1.6	*	1.4	1.2	1.2
17	Bacillales	1.4	1.8	2.3	1.4	1.7	1.0	1.4	1.7	2.0
18	Xanthomonadales	1.3	1.5	*	1.3	1.7	1.1	1.3	1.4	1.3
19	Verrucomicrobiales	1.2	*	*	1.2	*	*	1.2	*	*
20	Bacteroidales	1.1	*	*	1.1	*	*	1.1	*	*
21	Methylophilales	1.1	*	*	1.1	*	*	1.1	*	*
22	Chromatiales	*	*	*	*	4.0	5.1	*	2.9	3.3
23	Alteromonadales	*	4.6	1.3	*	1.4	1.5	*	1.3	1.4
24	Myxococcales	*	1.5	*	*	1.2	1.3	*	1.2	1.3
25	Desulfuromonadales	*	1.3	1.5	*	1.0	1.1	*	1.1	1.0
26	Rhodocyclales	*	1.2	1.0	*	1.0	1.1	*	*	*
27	Chlamydiales	*	1.1	*	*	*	1.0	*	*	*
28	Clostridiales	*	1.1	1.2	*	*	*	*	*	*
29	Others	15.6[a]	19.0[b]	18.5[c]	15.6[a]	17.9[d]	20.6[e]	15.6[a]	18.4[f]	20.0[g]

*percentages below 1% of the total organisms.

[a] 'other' represented 99 order each representing <1% of the total abundance

[b] 'other' represented 99 order each representing <1% of the total abundance

[c] 'other' represented 102 order each representing <1% of the total abundance

[d] 'other' represented 97 order each representing <1% of the total abundance

[e] 'other' represented 97 order each representing <1% of the total abundance

[f] 'other' represented 102 order each representing <1% of the total abundance

[g] 'other' represented 101 order each representing <1% of the total abundance

Comparisons of dominant core metabolic profiles in metagenomes from day 0 and week 18 using the STAMP software package (Parks & Beiko 2010), demonstrated an overrepresentation of carbohydrate metabolism, cell wall and capsule, motility and chemotaxis, and stress response at day 0 while an overrepresentation of clustering-based subsystems, protein metabolism, and respiration at week 18 (Figure 5.16).

Characterisation of genes in NA microcosms following further incubation (NA42) revealed overrepresentation of the same metabolic profiles as in NA18 (Figure 5.17). Although an overrepresentation of core metabolic functional profiles was observed when metagenomes from NA18 and NA42 were compared, there were no significant difference between the two metagenomes as demonstrated by bars with similar height and wider confidence intervals (95% CI). Other metabolic profiles were also present at low abundance including potassium metabolism (NA18) and dormancy and sporulation (NA42) as showed in Figure 5.17.

Comparison of metabolic profiles from day 0 and week 42 was also undertaken. For day 0 metagenomes, sequences related to metabolic profiles such as stress response, regulation and cell signalling, cell wall and capsule, motility and chemotaxis and carbohydrates metabolism were overrepresented. Whereas an overrepresentation of sequences assigned to respiration and protein metabolism were observed at week 42. Other metabolic functional profiles including DNA metabolism, clustering-based subsystems, and RNA metabolism were detectable at similar proportions when these two metagenomes were compared. Sequences annotated to photosynthesis, secondary metabolism and dormancy and sporulation were unaffected over the 42 week incubation period (Data not shown).

Analyses of core metabolic profiles in metagenomes obtained from amended microcosms (ENA and Comb) in the Creo soil microcosms are presented in Figures 5.18 – 5.21. In microcosms amended with nutrients (Figure 5.18), sequences assigned to metabolism of aromatic compounds, clustering-based subsystems, respiration, fatty acids, lipids, and isoprenoids, miscellaneous, cofactors, vitamins, prosthetic groups, pigments and protein metabolism were overrepresented at the start of incubation compared to week18.

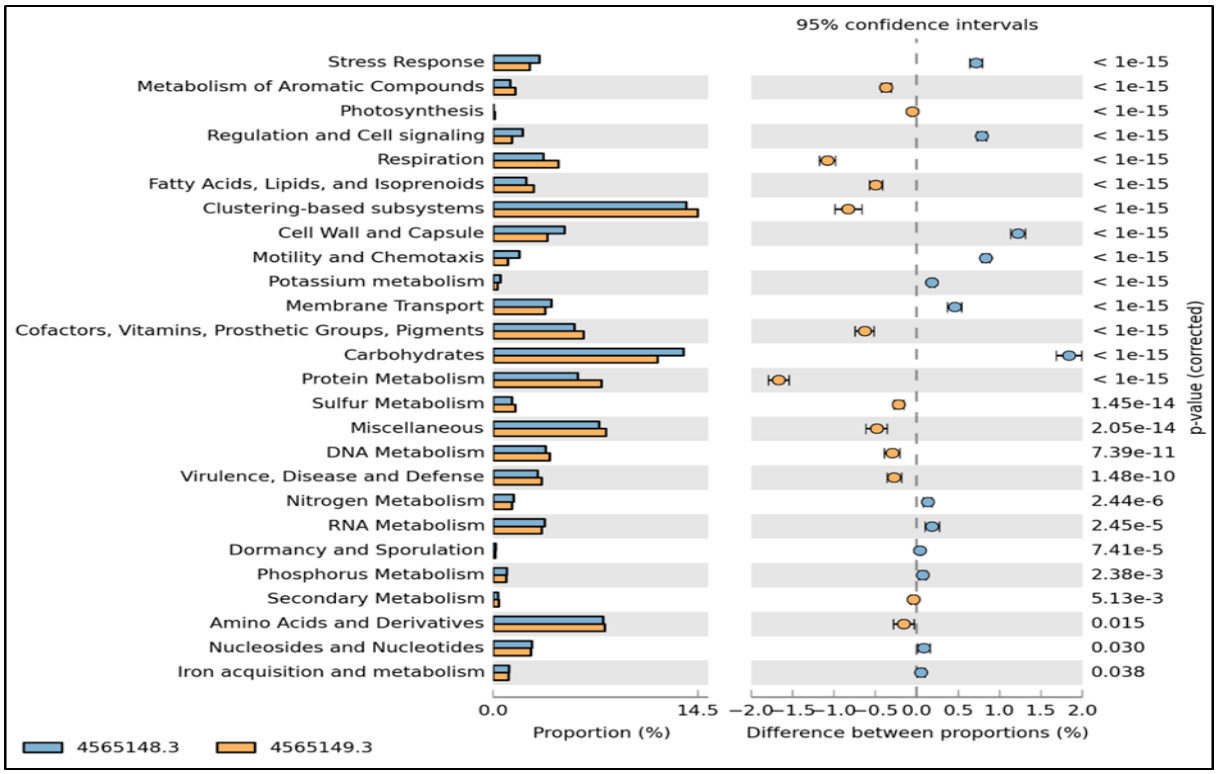

Figure 5.16. Comparison of metagenome functional profiles from Creo microcosms incubated under NA conditions. Blue bars represent (MG-RAST ID 4565148.3) metabolic functional profiles at the start of incubation while orange bars represent (MG-RAST ID 4565149.3) metabolic functional profiles at week 18. STAMP analysis of overrepresented subsystem functional profiles observed in day 0 and week 18 metagenomes with corrected q-values (95% CI) using Storey's FDR approach are also shown.

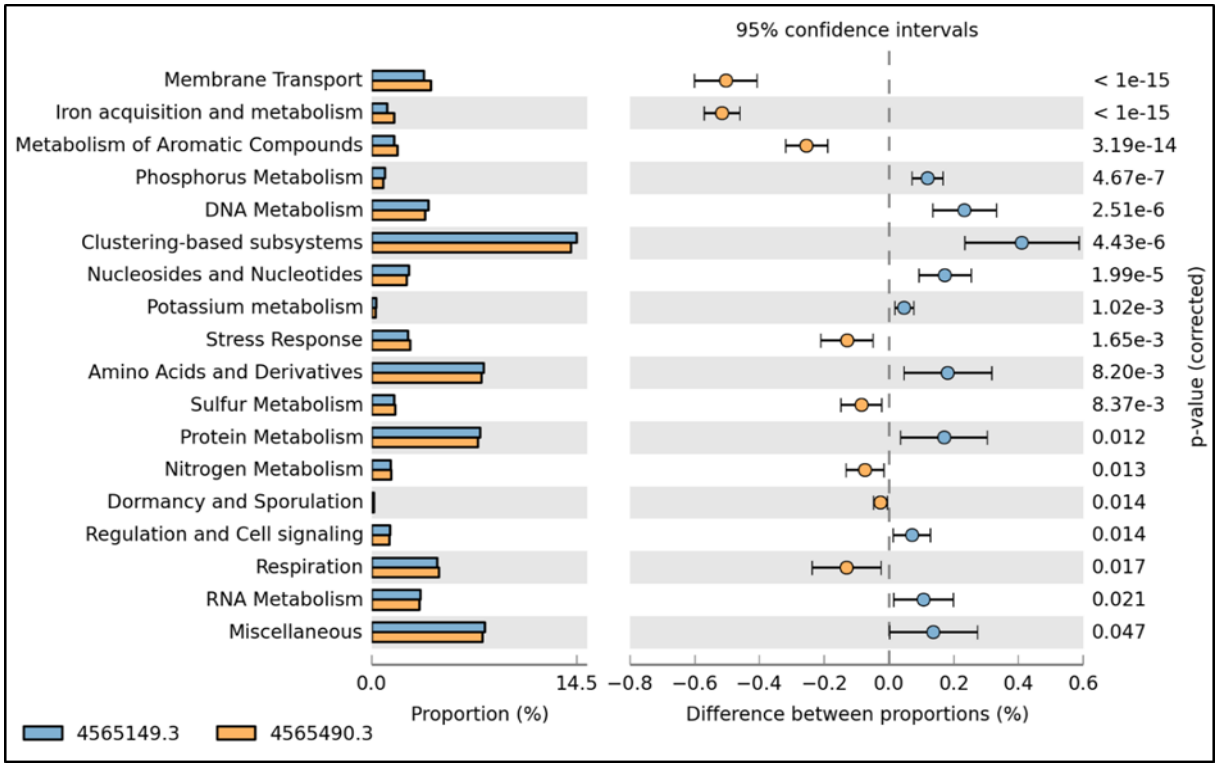

Figure 5.17. Comparison of metagenome functional profiles from Creo microcosms incubated under NA conditions. Blue bars represent (MG-RAST ID 4565149.3) metabolic functional profiles at week 18 while orange bars represent (MG-RAST ID 4565490.3) metabolic functional profiles at week 42. STAMP analysis of overrepresented subsystem functional profiles observed in weeks 18 and 42 metagenomes with corrected q-values (95% CI) using Storey's FDR approach are also shown.

After 18 weeks of incubation, core metabolic functional profiles such as stress response, regulation and cell signalling, cell wall and capsule, motility and chemotaxis, and carbohydrates metabolism increase compared to day 0. The evaluation of metabolic profiles in metagenomes sampled from ENA18 and ENA42 based subsystems, resulted in significant differences in carbohydrates utilisation and respiratory metabolic profiles (Figure 5.19).

Supplementation of nutrients didn't enhance the aforementioned metabolic profiles as shown by equal proportion (similar bars) representing each activity in the two metagenomes. Sequences annotated to secondary metabolism, dormancy and sporulation and photosynthesis were underrepresented in both two metagenomes.

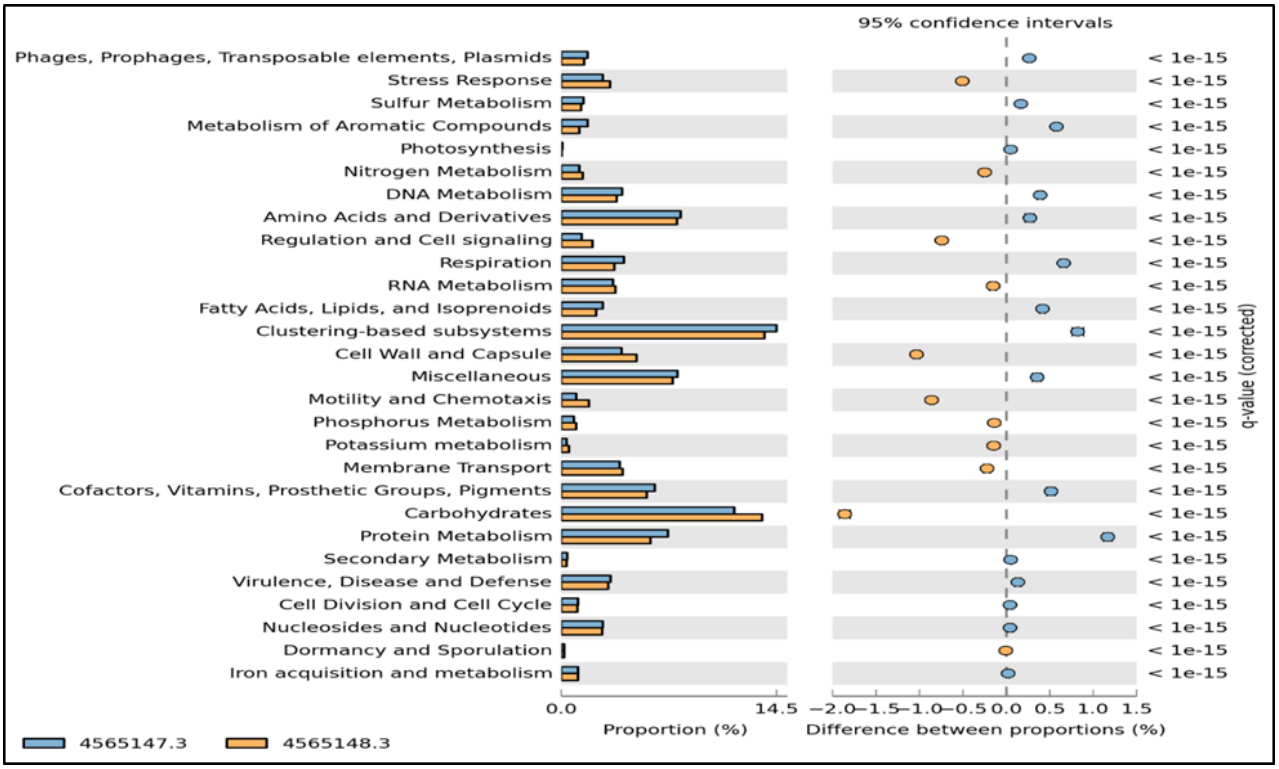

Figure 5.18. Comparison of metagenome functional profiles from Creo microcosms incubated under ENA conditions. Orange bars represent (MG-RAST ID 4565148.3) metabolic functional profiles at the start of incubation while blue bars represent (MG-RAST ID 4565147.3) metabolic functional profiles at week 18. STAMP analysis of overrepresented subsystem functional profiles observed in day 0 and week 18 metagenomes with corrected q-values (95% CI) using Storey's FDR approach are also shown.

The overrepresentation of some core metabolic profiles such as stress response, regulation and cell signalling, cell wall and capsule, motility and chemotaxis and carbohydrates metabolism were observed at the commencement of the incubation compared to week 42. In contrast, sequences related to respiration, clustering-based subsystems, cofactors, vitamins, prosthetic groups, pigments and protein metabolism were underrepresented at day 0 compared to week 42 (Data not shown).

In the combined amended treatment of the Creo microcosms, an overrepresentation of major biogeochemical processes including carbohydrates, cell wall and capsule was observed at the commencement of incubation compared to week 18. In contrast, protein metabolism, respiration and clustering-based subsystems were overrepresented at week18 (Figure 5.20). In both metagenomes, four core metabolic profiles (protein metabolism, respiration and carbohydrates, cell wall and capsule) had significant difference between mean proportion (%) values. Other metabolic profiles present at low magnitude included photosynthesis, potassium metabolism and dormancy and sporulation were observed in both two metagenomes.

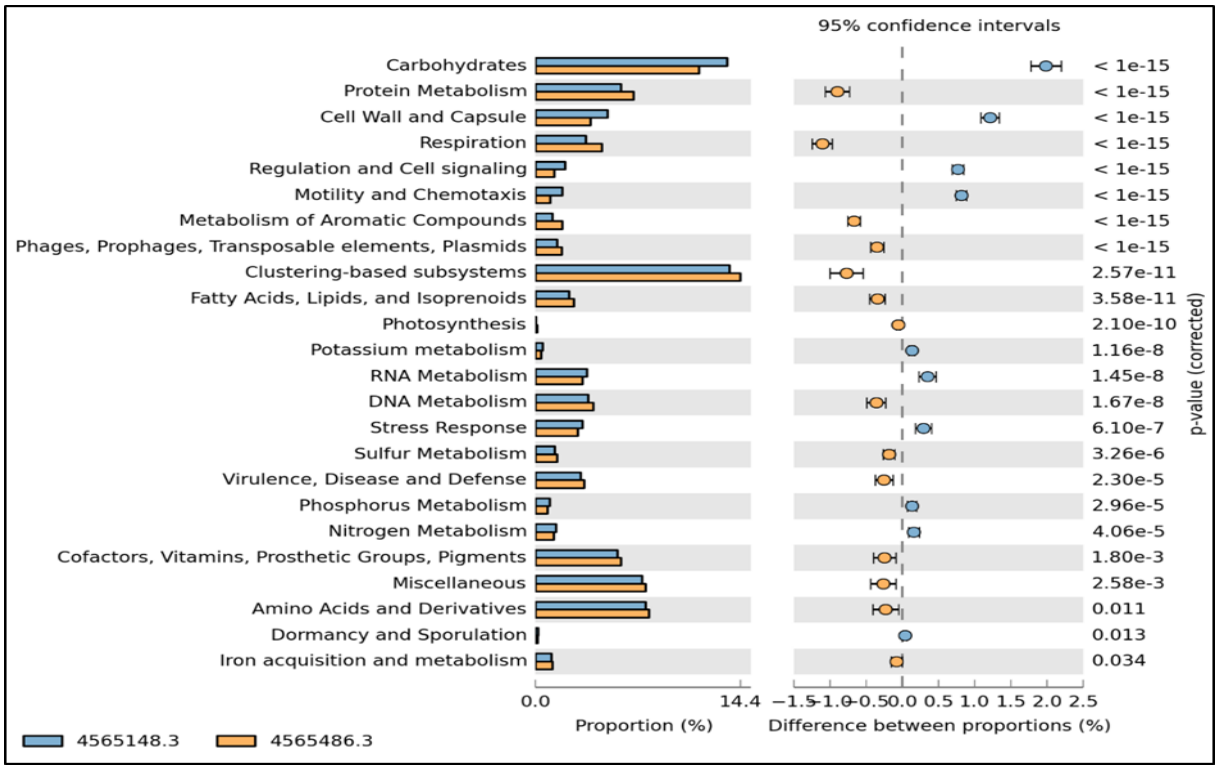

Figure 5.19. Comparison of metagenome functional profiles from Creo microcosms incubated under ENA conditions. Blue bars represent (MG-RAST ID 4565147.3) metabolic functional profiles at week 18 while orange bars represent (MG-RAST ID 4565488.3) metabolic functional profiles at week 42. STAMP analysis of overrepresented subsystem functional profiles observed weeks 18 and 42 metagenomes with corrected q-values (95% CI) using Storey's FDR approach are also shown.

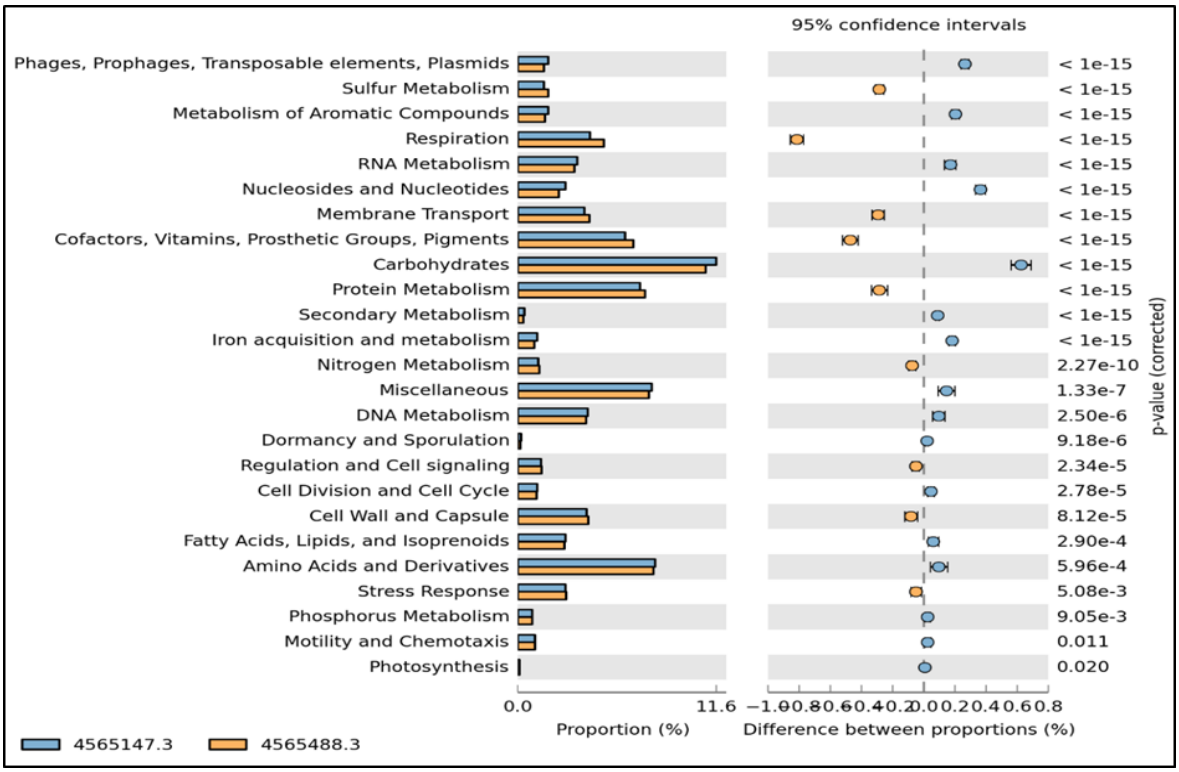

Figure 5.20. Comparison of metagenome functional profiles from Creo microcosms incubated under combined (Comb) conditions. Blue bars represent (MG-RAST ID 4565148.3) metabolic functional profiles at the start of incubation while orange bars represent (MG-RAST ID 4565486.3) metabolic functional profiles at week 18. STAMP analysis of overrepresented subsystem functional profiles observed in day 0 and week 18 metagenomes with corrected q-values (95% CI) using Storey's FDR approach are also shown.

Figure 5.21 shows a comparison between metagenomes sampled from combined microcosms at week 18 and week 42. As demonstrated, sequences related to metabolism of aromatic compounds, membrane transport, stress response, nucleosides and nucleotides and amino acids and derivatives were overrepresented at week 18. At the end of the incubation period (week 42), an overrepresentation of functional profiles including carbohydrates, protein metabolisms and cofactors, vitamins, prosthetic groups, pigments and RNA metabolism was observed compared to week 18. Moreover, metagenomes from weeks 18 and 42 treatments were statistically different at 95% confident intervals as demonstrated in Figure 5.21. Other metabolic profiles were present at low and consistent abundance including DNA, sulphur, potassium, and phosphorus metabolisms over the 42 week incubation period.

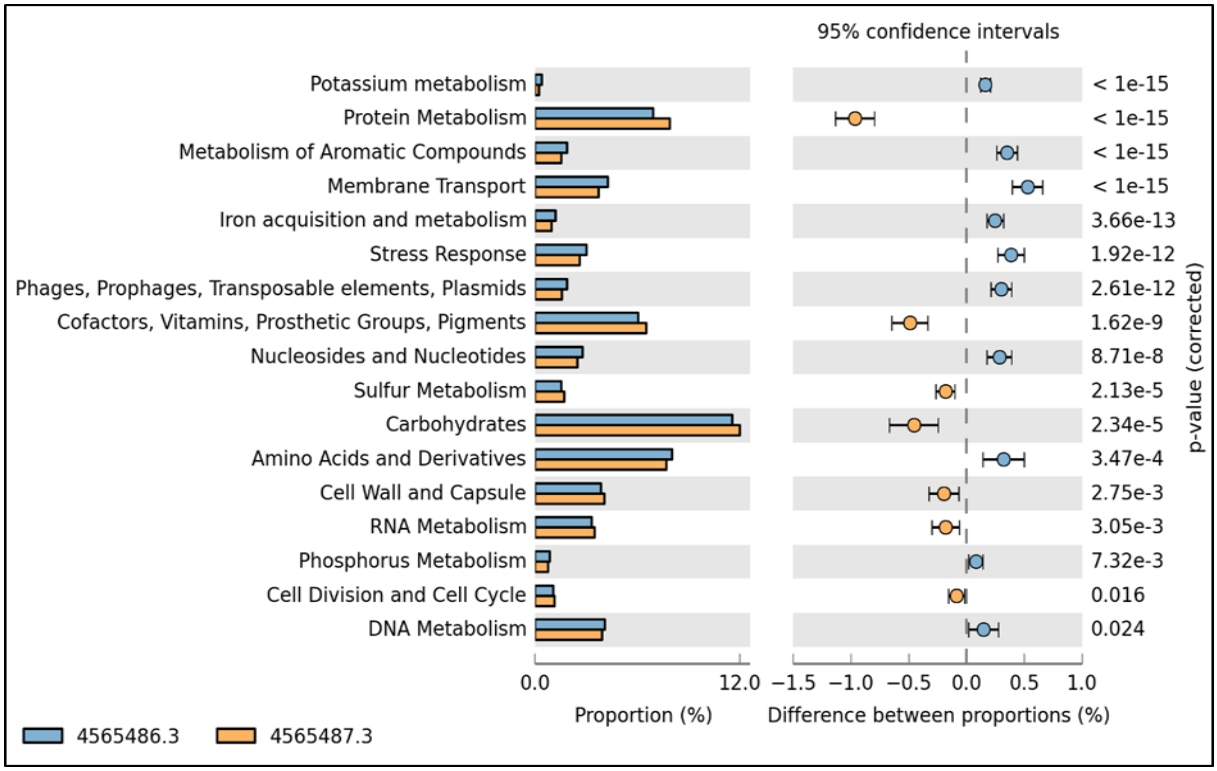

Figure 5.21. Comparison of metagenome functional profiles from Creo microcosms incubated under combined (Comb) conditions. Blue bars represent (MG-RAST ID 4565486.3) metabolic functional profiles at week 18 while orange bars represent (MG-RAST ID 4565487.3) metabolic functional profiles at week 42. STAMP analysis of overrepresented subsystem functional profiles observed at weeks 18 and 42 metagenomes with corrected q-values (95% CI) using Storey's FDR approach are also shown.

In comparison, an overrepresentation of some core metabolic profiles such as carbohydrates, regulation and cell signalling, cell wall and capsule, and motility and chemotaxis were observed at the commencement of the incubation compared to week 42. While sequences related to respiration, clustering-based subsystems, cofactors, vitamins, prosthetic groups, pigments and protein metabolism were underrepresented at day 0 compared to week 42 (Data not shown).

5.7.2 Comparison of metabolic profiles in TB metagenomes

Evaluation of functional profiles in NA microcosm showed abundance of similar core metabolic functions in metagenomes sampled over the 42 week incubation period. In metagenomes from day 0 and week 18, some core metabolic profiles were present at similar abundance including dormancy and sporulation, potassium and secondary metabolisms. Comparisons of the prevalent core metabolic functions in metagenomes using STAMP, demonstrated an overrepresentation of metabolism of aromatic compounds and membrane transport at the start of the incubation period while an overrepresentation of sequences related to protein and RNA metabolisms was observed at week18 (Figure 5.22). As depicted in Figure

5.22, other metabolic functional profiles such as carbohydrates, DNA metabolism and cell division and cell cycle were present at equal low proportions in both two the metagenomes. Characterisation of genes believed to be associated with PAH degradation following further incubation (NA18 and NA42) revealed an overrepresentation of similar metabolic profiles (Figure 5.23).

Sequences related to nitrogen, phosphorous, sulfur metabolisms, motility and chemotaxis were significantly different (95% CI) in metagenomes obtained at week 18 compared to week 42. There was no increase in the number of enzymes associated with PAH degradation observed when metagenomes from the later sampled points were compared to metagenomes obtained at day 0. Moreover, other metabolic profiles present at low and equal proportions included potassium and iron acquisition and metabolisms, and secondary metabolism in both metagenomes.

The comparison of several metabolic profiles including protein, DNA metabolisms, carbohydrates and clustering-based subsystems, and amino acids and derivative, miscellaneous and membrane transport showed the largest differences between mean values, although the results were not statistically significant due to wide confidence intervals (Figure 5.23).

Comparisons of metabolic functional profiles of metagenomics samples obtained from day 0 and week 42 was also undertaken. Incubation resulted in an underrepresentation of sequences related to membrane transport, fatty acids, lipids and isoprenoids, and metabolism of aromatic compounds at week 42 compared to day 0 while protein metabolism was overrepresented at week 42 compared to day 0. Other metabolic profiles such as respiration, nucleosides and nucleotides, and cofactors, vitamins, prosthetic groups, pigments were detectable at similar proportions over the 42 week incubation period (Data not shown).

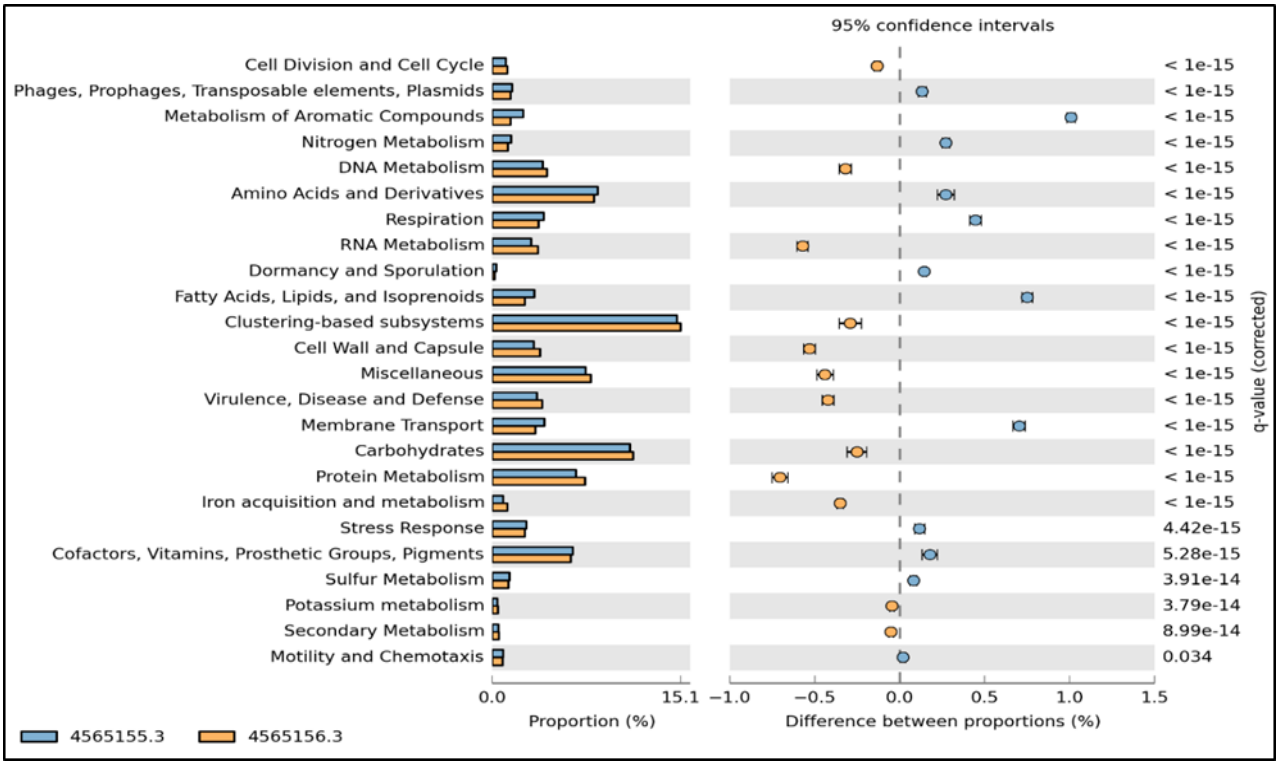

Figure 5.22. Comparison of metagenome functional profiles from TB microcosms incubated under NA conditions. Blue bars represent (MG-RAST ID 4565155.3) metabolic functional profiles at the start of incubation while orange bars represent (MG-RAST ID 4565156.3) metabolic functional profiles at week 18. STAMP analysis of overrepresented subsystem functional profiles observed in day 0 and week 18 metagenomes with corrected q-values (95% CI) using Storey's FDR approach are also shown.

Analyses of core metabolic profiles in metagenomes obtained from TB amended microcosms (ENA and Comb) are presented in Figures 5.24 – 5.27. Figure 5.24 shows the comparison of metagenome functional profiles between day 0 and week 18 incubated under ENA conditions. At week18, there was an underrepresentation of sequences related to metabolism of aromatic compounds, respiration, fatty acids, lipids, and isoprenoids and carbohydrates compared to day 0. Conversely, sequences assigned to RNA metabolism, clustering-based subsystems, cell wall and capsule, miscellaneous, virulence and disease, protein metabolism and iron acquisition and metabolism were overrepresented at week 18 compared to the commencement of the incubation.

Although an overrepresentation of sequences related to the aforementioned metabolic functional profiles was observed, other metabolic profiles such as dormancy and sporulation, secondary and potassium metabolisms were presence at low magnitude over the 18 week incubation period.

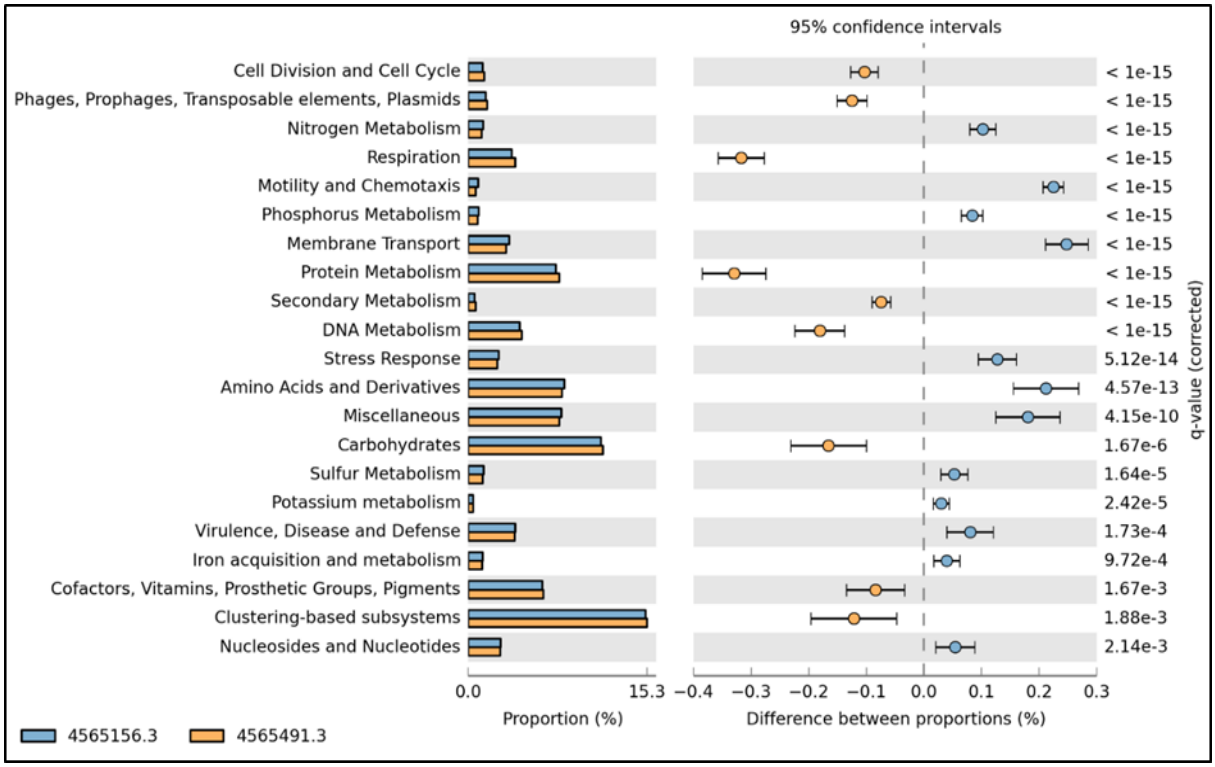

Figure 5.23. Comparison of metagenome functional profiles from TB microcosms incubated under NA conditions. Blue bars represent (MG-RAST ID 4565156.3) metabolic functional profiles at week 18 while orange bars represent (MG-RAST ID 4565491.3) metabolic functional profiles at week 42. STAMP analysis of overrepresented subsystem functional profiles observed at weeks 18 and 42 metagenomes with corrected q-values (95% CI) using Storey's FDR approach are also shown.

The evaluation of metabolic profiles in metagenomes sampled from ENA18 and ENA42 based subsystems, resulted in significant difference in sequences annotated to clustering-based subsystems at week 18 compared week 42. An overrepresentation of sequences related to carbohydrate utilisation and metabolism of aromatic of compounds was observed at week 42 compared to week 18. Moreover, other metabolic functional profiles were detected at equal proportions as demonstrated in Figure 5.25.

Comparison of metabolic profiles in metagenomes sampled from day 0 and week 42 was also undertaken. For day 0 metagenomes, sequences assigned to metabolic functional profiles including carbohydrates, nitrogen and amino acids and derivatives metabolisms, metabolism of aromatic compounds were overrepresented at the commencement of incubation (ENA0) while an overrepresentation of RNA metabolism, clustering-based subsystems, cell wall and capsule, miscellaneous and virulence, disease and defense were observed at week 42 (Data not shown).

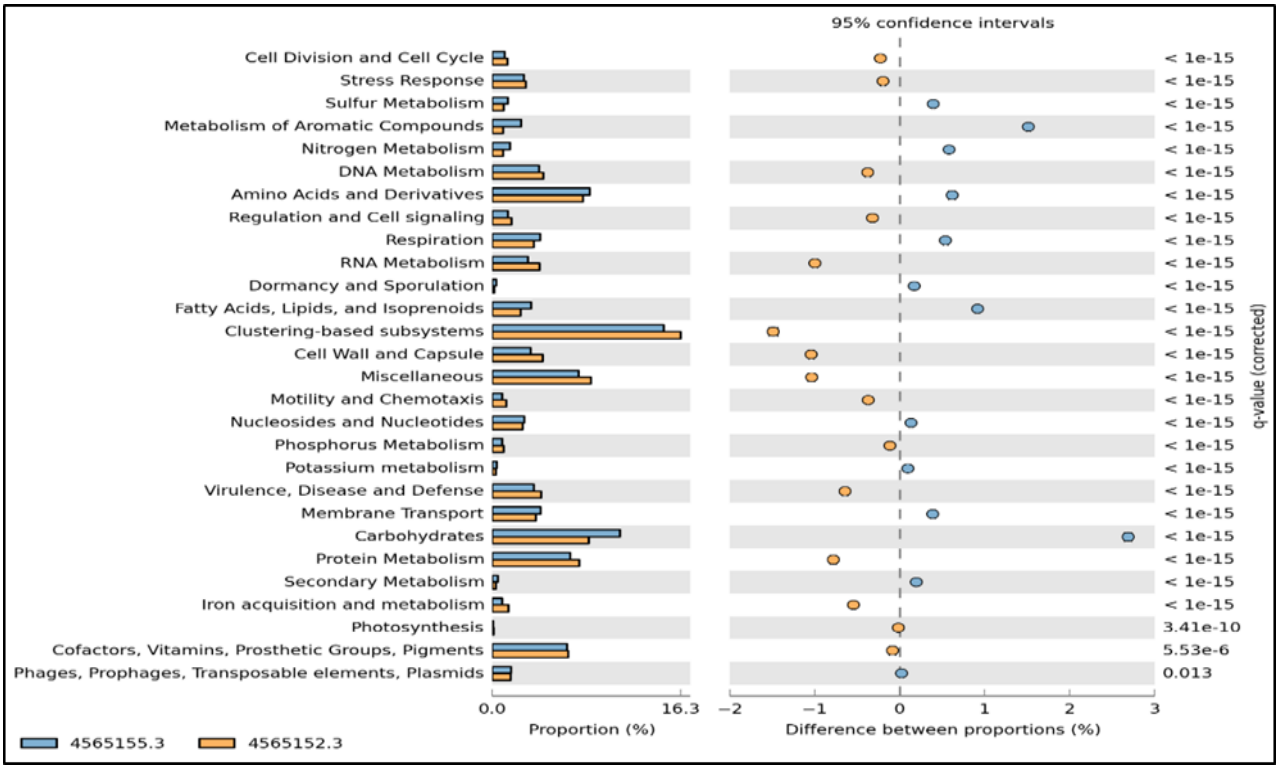

Figure 5.24. Comparison of metagenome functional profiles from TB microcosms incubated under ENA conditions. Blue bars represent (MG-RAST ID 4565155.3) metabolic functional profiles at the start of incubation while orange bars represent (MG-RAST ID 4565152.3) metabolic functional profiles at week 18. STAMP analysis of overrepresented subsystem functional profiles observed in day 0 and week 18 metagenomes with corrected q-values (95% CI) using Storey's FDR approach are also shown.

In microcosm where nutrient and inoculant supplementation was implemented, comparison of metabolic functional profiles exhibited overrepresentation of metabolism of aromatic compounds, fatty acids, lipids and isoprenoids, and carbohydrate metabolism at the start of the incubation compared to week 18 (Figure 5.26).

In addition, sequences related to some core metabolic profiles such as respiration, clustering-based subsystems, cell wall and capsule, miscellaneous, virulence, disease and defense, protein and RNA metabolisms were prevalent at week 18 compared to day 0. Such a results suggest that microbial activities increased with increasing time of incubation. Other metabolic profiles including stress response, DNA metabolism, and cofactors, vitamins, prosthetic groups, pigments were detected at similar proportions when the two metagenomes were compared (Comb0 and Comb18).

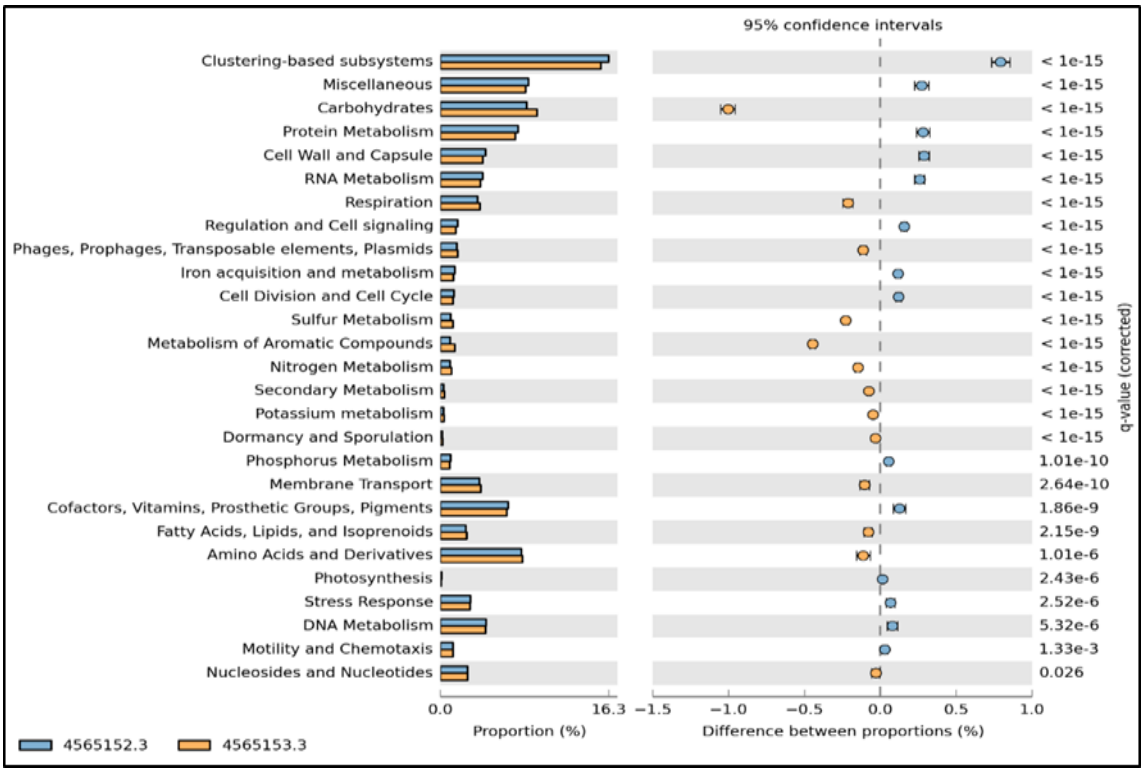

Figure 5.25. Comparison of metagenome functional profiles from TB microcosms incubated under ENA conditions. Blue bars represent (MG-RAST ID 4565152.3) metabolic functional profiles at week 18 while orange bars represent (MG-RAST ID 4565153.3) metabolic functional profiles at week 42. STAMP analysis of overrepresented subsystem functional profiles observed at weeks 18 and 42 metagenomes with corrected q-values (95% confidence intervals) using Storey's FDR approach are also shown.

Comparison of metabolic profiles in metagenomes from Comb18 and Comb42 metagenomes showed similar proportions except sequences related to clustering-based (Comb18) and carbohydrates, which were statistically different (95% CI) as depicted in Figure 5.27. In addition, sequences related to secondary metabolism, photosynthesis, dormancy and sporulation, potassium metabolism were underrepresented in the two metagenomes. In comparison, overrepresentation of major biogeochemical processes including metabolism of aromatic compounds, membrane transport, fatty acids, lipids and isoprenoids (Comb0) and RNA and protein metabolisms, cell wall and capsule and clustering-based subsystems (Comb42) was observed over the 42 week incubation period (Data not shown). This suggest that soil amendments had no effect on metabolic profiles in TB soil. In both metagenomes, assessment of functional profiles demonstrated a significant difference between mean proportion (95% CI) values of metabolism of aromatic compounds, carbohydrates, clustering-based subsystems and cell wall and capsule utilisation contributing to metabolic profiles.

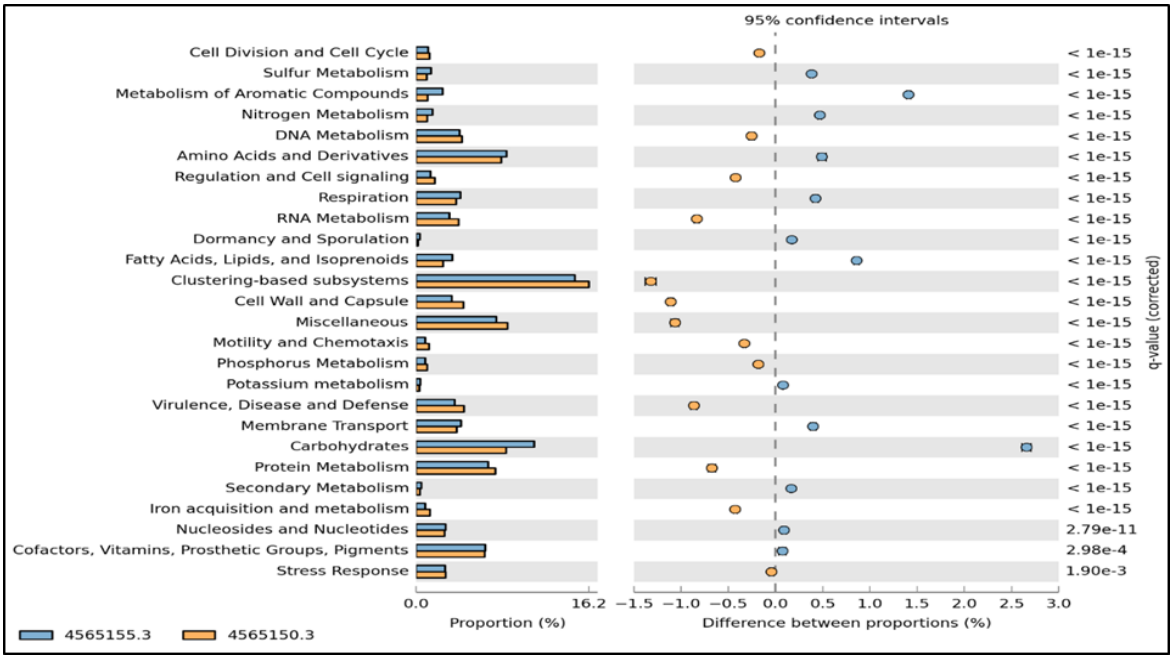

Figure 5.26. Comparison of metagenome functional profiles from TB microcosms incubated under combined (Comb) conditions. Blue bars represent (MG-RAST ID 4565155.3) metabolic functional profiles at the start of incubation while orange bars represent (MG-RAST ID 4565150.3) metabolic functional profiles at week 18. STAMP analysis of overrepresented subsystem functional profiles observed in day 0 and week 18 metagenomes with corrected q-values (95% CI) using Storey's FDR approach are also shown.

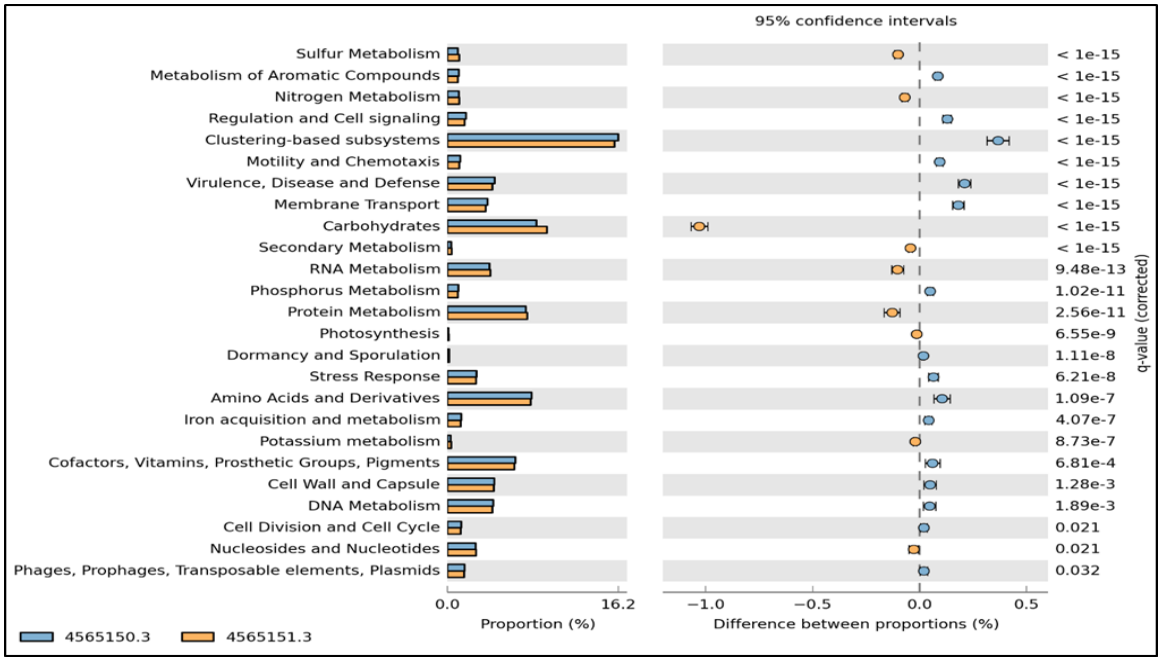

Figure 5.27. Comparison of metagenome functional profiles from TB microcosms incubated under combined (Comb) conditions. Blue bars represent (MG-RAST ID 4565150.3) metabolic functional profiles at week 18 while orange bars represent (MG-RAST ID 4565151.3) metabolic functional profiles at week 42. STAMP analysis of overrepresented subsystem functional profiles observed at week 42 metagenomes with corrected q-values (95% CI) using Storey's FDR approach are also shown.

5.7.3 Comparison of metabolic profiles in AP metagenomes

Assessment of functional profiles in the AP NA microcosm showed prevalent of similar core metabolic profiles in metagenomes sampled over the 42 week incubation period. Comparison of prevalent core metabolic functions in metagenomes from day 0 and week 18, using STAMP analysis demonstrated an overrepresentation of amino acids and derivative and carbohydrates at the commencement of incubation while an overrepresentation of clustering-based subsystems, respiration, virulence and disease and protein metabolism at week 18 (Figure 5.28).

After 18 weeks of incubation, other metabolic functional profiles such as potassium metabolism, motility and chemotaxis, cell wall and capsule, and secondary metabolism were detected at low and equal proportions in the two metagenomes.
The comparison of several metabolic profiles including protein, DNA, nitrogen metabolisms and clustering-based subsystems were underrepresented at week 42 compared to week 18 (Figure 5.29), while sequences related to amino acids and derivatives and carbohydrate utilisation were prevalent at week 42 compared to week 18. Other metabolic profiles including cell division and cell cycle, respiration, cell wall and capsule, and regulation and cell signalling were detectable at equal proportions in the two metagenomes.

Characterisation of metabolic functional profiles believed to be associated with PAH degradation following additional incubation resulted in an overrepresentation of sequences related to stress response, DNA metabolism, amino acids and derivatives, nucleosides and nucleotides, iron acquisition and metabolism and clustering-based subsystems at day 0 compared to week 42.

In contrast, sequences annotated to respiration, fatty acids, lipids and isoprenoids, protein and carbohydrates metabolisms were underrepresented at day 0 compared to week 42 (Data not shown). Moreover, other metabolic profiles detected at low magnitude included photosynthesis, dormancy and sporulation, and potassium and secondary metabolisms in both two metagenomes.

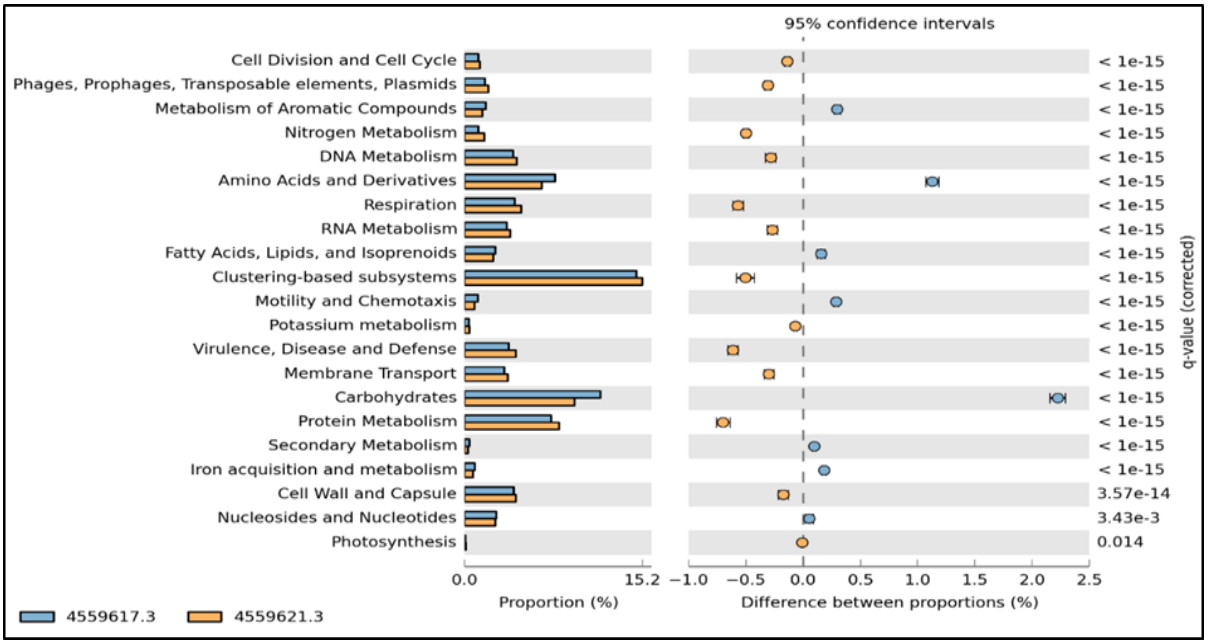

Figure 5.28. Comparison of metagenome functional profiles from AP microcosms incubated under NA conditions. Blue bars represent (MG-RAST ID 4559617.3) metabolic functional profiles at the start of incubation while orange bars represent (MG-RAST ID 455921.3) metabolic functional profiles at week 18. STAMP analysis of overrepresented subsystem functional profiles observed in day 0 and week 18 metagenomes with corrected q-values (95% CI) using Storey's FDR approach are also shown.

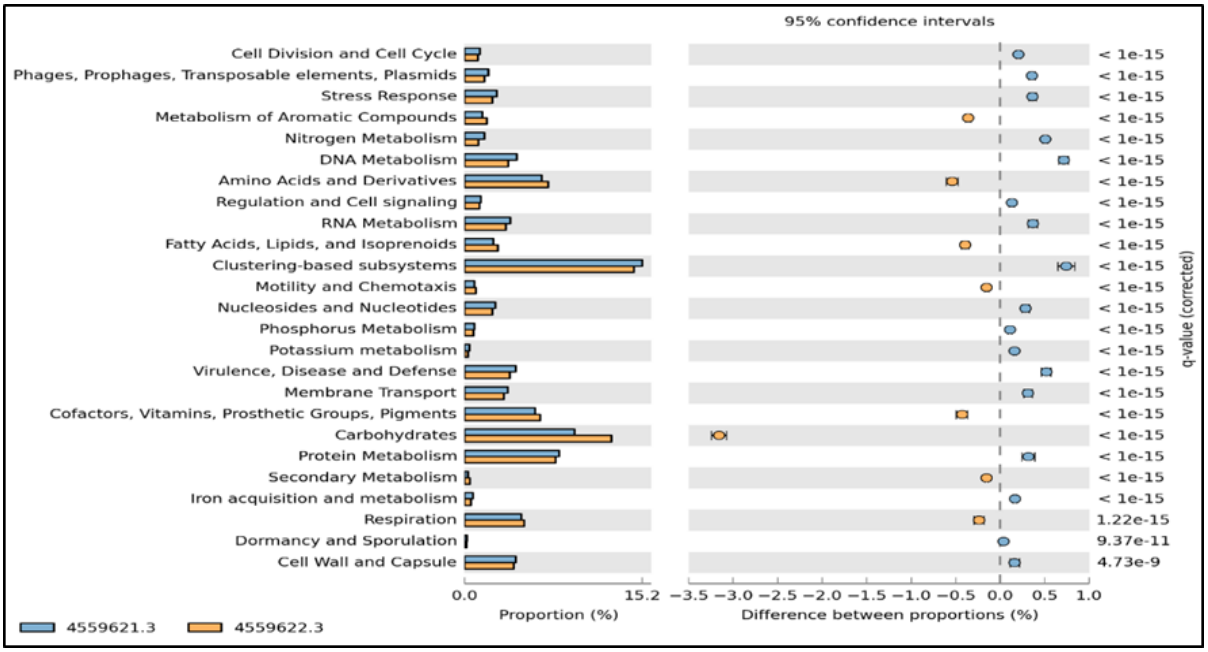

Figure 5.29. Comparison of metagenome functional profiles from AP microcosms incubated under NA conditions. Blue bars represent (MG-RAST ID 4559621.3) metabolic functional profiles at week 18 while orange bars represent (MG-RAST ID 4559622.3) metabolic functional profiles at week 42. STAMP analysis of overrepresented subsystem functional profiles observed at weeks 18 and 42 metagenomes with corrected q-values (95% CI) using Storey's FDR approach are also shown.

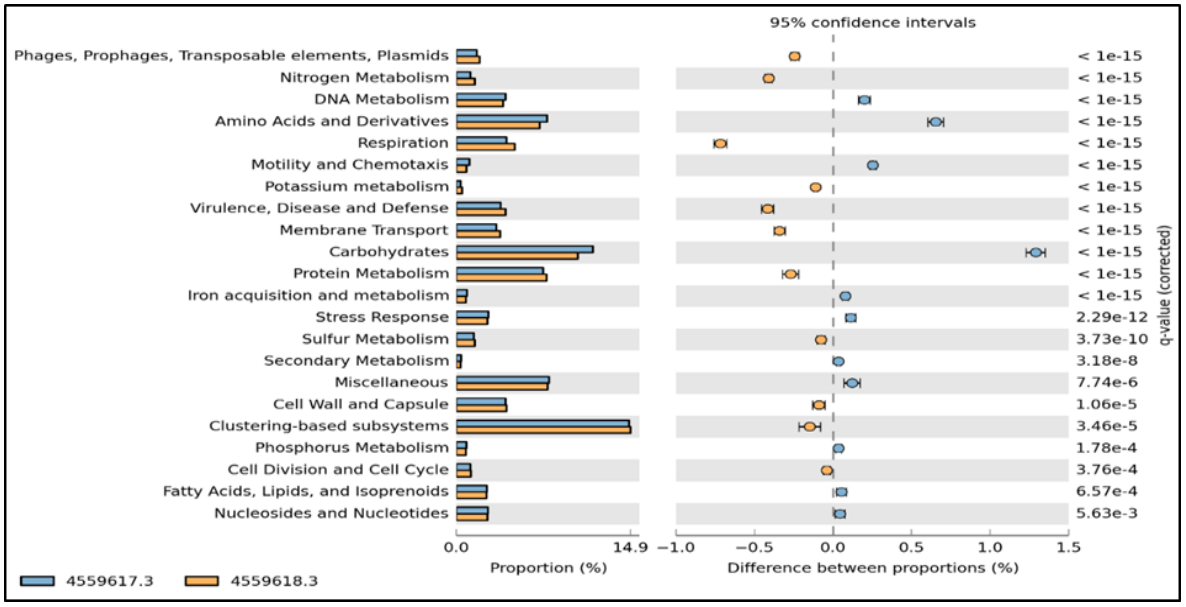

Figure 5.30. Comparison of metagenome functional profiles from AP microcosms incubated under ENA conditions. Blue bars represent (MG-RAST ID 4559617.3) metabolic functional profiles at the start of incubation while orange bars represent (MG-RAST ID 4559618.3) metabolic functional profiles at week 18. STAMP analysis of overrepresented subsystem functional profiles observed in day 0 and week 18 metagenomes with corrected q-values (95% CI) using Storey's FDR approach are also shown.

Comparisons of core metabolic profiles in metagenomes obtained from ENA and Combined microcosms are presented in Figures 5.30 – 5.33. Figure 5.30 shows the comparison of metagenome functional profiles from the commencement of incubation and week 18 incubated under ENA conditions. As demonstrated, a small but significant change (95% CI) in metabolic functional profiles was observed in sequences related to DNA metabolism, amino acids and derivatives and carbohydrate utilisation at day 0 compared to week 18 following implementation of nutrients. In contrast, sequences assigned to metabolic profiles including respiration, membrane transport, virulence and disease and protein metabolism were overrepresented at week 18 compared to day 0. Although an overrepresentation of sequences related to the aforementioned metabolic functional profiles were observed, other metabolic profiles such as secondary and potassium metabolisms were underrepresented after 18 weeks of incubation. The evaluation of metabolic profiles in metagenomes sampled from ENA18 and ENA42 based subsystems, resulted in an overrepresentation of several metabolic profiles, namely iron acquisition and metabolism, virulence, disease and defense, DNA metabolism, metabolism of aromatic compounds at week 18 compared to week 42. In contrast, sequences related to carbohydrate utilisation, nitrogen metabolism, respiration, and protein metabolism were prevalent at week 42 compared to week 18 (Figure 5.31). Other metabolic profiles such as membrane transport, stress response, phosphorous metabolism, cofactors, vitamins,

prosthetic groups, pigments and motility and chemotaxis were detected at equal proportions over the 42 week incubation period.

When metagenomes sampled from day 0 and week 42 were compared, there was an overrepresentation of carbohydrate, amino acids and derivative and DNA metabolism at the commencement of incubation. Conversely, sequences related to respiration, protein and nitrogen metabolism were underrepresented at day 0 compared to week 42. Other metabolic profiles were observed at equal proportions in the two metagenomes (Data not shown).
In microcosm where nutrient and inoculant supplementation was implemented (Figure 5.32 and 5.33), an overrepresentation of sequences related to stress response, DNA metabolism, amino acids and derivatives, miscellaneous, and clustering-based subsystems was observed at the commencement of incubation while sequences assigned to respiration, virulence, disease and defense, and metabolism of aromatic compounds were overrepresented at week 18.

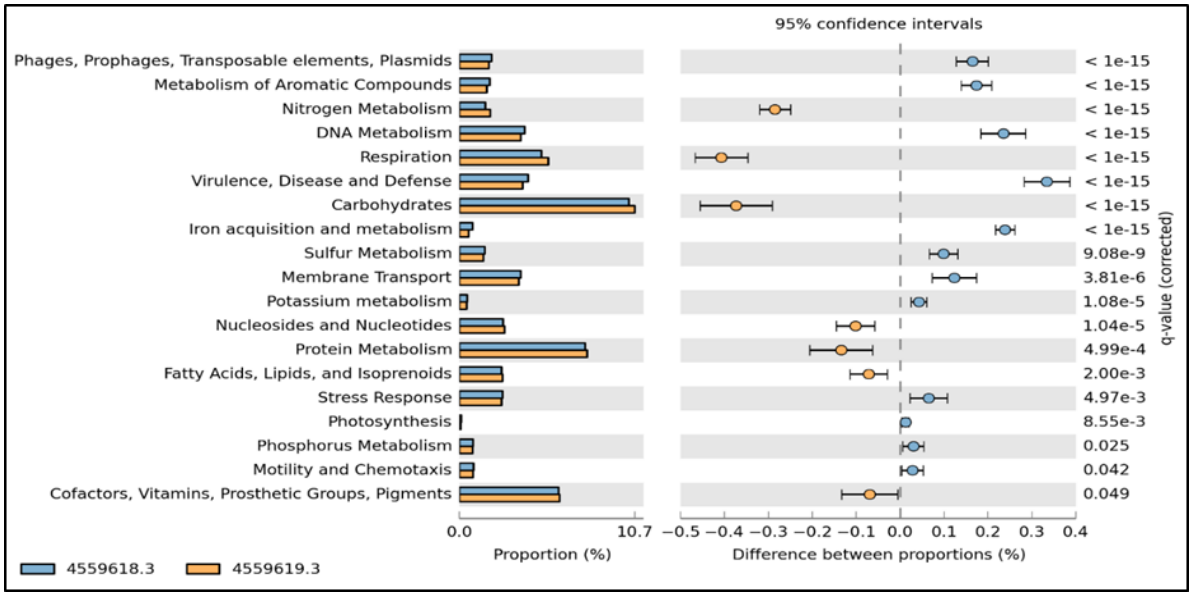

Figure 5.31. Comparison of metagenome functional profiles from AP microcosms incubated under ENA conditions. Blue bars represent (MG-RAST ID 4559618.3) metabolic functional profiles at week 18 while orange bars represent (MG-RAST ID 4559619.3) metabolic functional profiles at week 42. STAMP analysis of overrepresented subsystem functional profiles observed at weeks 18 and 42 metagenomes with corrected q-values (95% CI) using Storey's FDR approach are also shown.

Comparison of metabolic profiles in metagenomes from Comb18 and Comb42 are represented in Figure 5.33. Sequences related to carbohydrate, amino acids and derivatives, metabolism of aromatic compounds, motility and chemotaxis, and cell wall capsule were prevalent at week 18 while metabolic profiles such as clustering-based subsystems, membrane transport,

nucleosides and nucleotides were overrepresented at week 42. In addition, the remainder of metabolic functional profiles were detected at similar abundance in the two metagenomes (Comb18 and Comb42).

Comparison of metabolic profiles including phosphorus metabolism, photosynthesis and potassium metabolism were present at low magnitude in metagenomes sampled from Comb0 and Comb42. Moreover, sequences annotated to stress response, amino acids and derivatives, and carbohydrates metabolism were prevalent at the commencement of incubation while sequences related to nitrogen metabolism, respiration, virulence and disease and protein metabolism were prevalent at week42 (Data not shown).

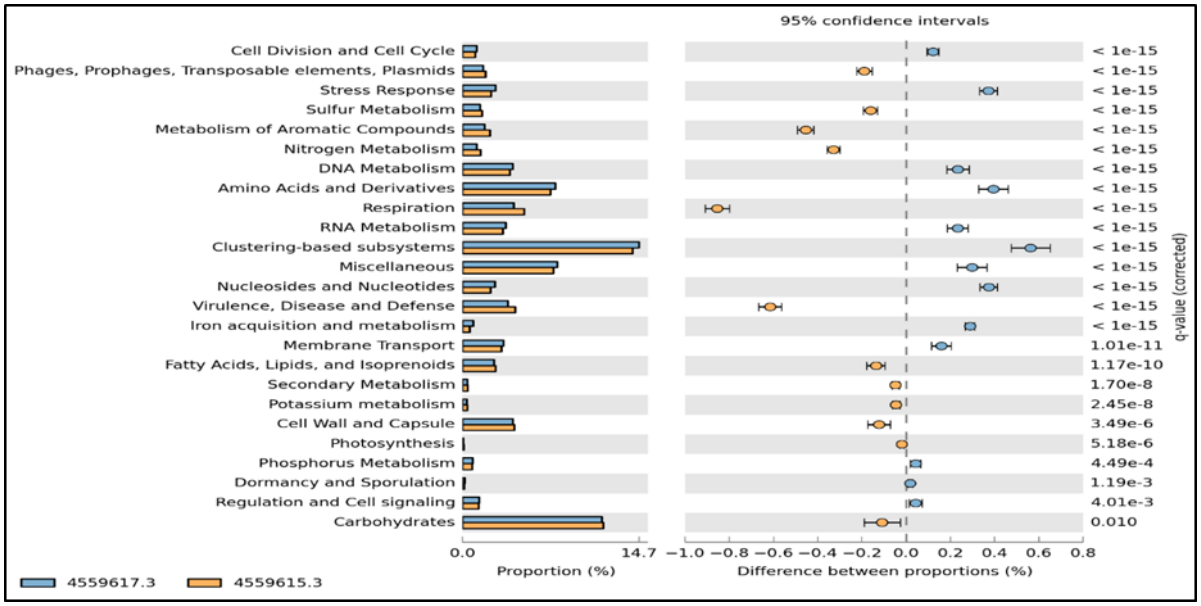

Figure 5.32. Comparison of metagenome functional profiles from AP microcosms incubated under combined (Comb) conditions. Blue bars represent (MG-RAST ID 4559617.3) metabolic functional profiles at the start of incubation while orange bars represent (MG-RAST ID 4559615.3) metabolic functional profiles at week 18. STAMP analysis of overrepresented subsystem functional profiles observed in day 0 and week 18 metagenomes with corrected q-values (95% CI) using Storey's FDR approach are also shown.

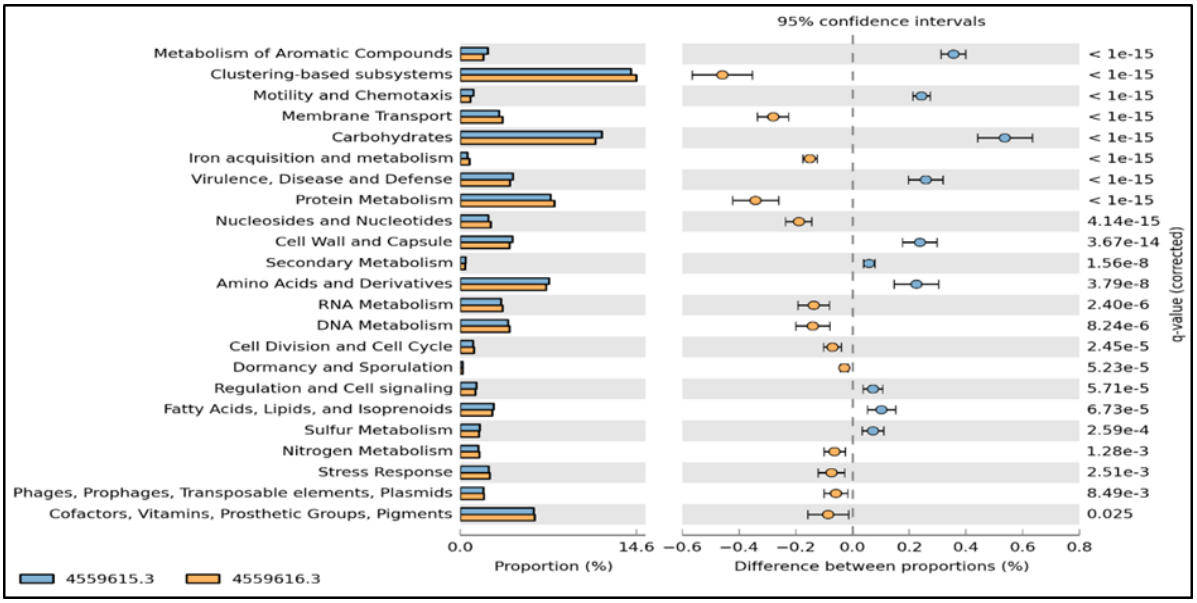

Figure 5.33. Comparison of metagenome functional profiles from AP microcosms incubated under combined (Comb) conditions. Blue bars represent (MG-RAST ID 4559615.3) metabolic functional profiles at week 18 while orange bars represent (MG-RAST ID 4559616.3) metabolic functional profiles at week 42. STAMP analysis of overrepresented subsystem functional profiles observed at weeks 18 and 42 metagenomes with corrected q-values (95% CI) using Storey's FDR approach are also shown.

5.8 Analysis of enzymes for PAH metabolism

The Kyoto Encyclopaedia of Genes and Genomes (KEGG) is a collection of several databases encompassing high-level functions and utilities related to genome annotation. KEGG mapper is one of the key built in functions in the MG-RAST interface known as a useful pathway reference tool (Kanehisa 1997). KEGG provide access to a wealth of information in terms of pathways, genes and enzymes valuable for the understanding of numerous biological processes. This database also provides useful information related to major metabolic and signalling pathways including carbohydrate, energy, PAHs, lipid and amino acid metabolism, membrane transport and signal transduction. In this section, further analysis was undertaken using KEGG analysis to specifically investigate functionality associated with PAH degradation over the course of the incubation period (42 weeks). This was performed by comparing the abundance of sequences in metagenomes related to each enzyme affiliated with PAH degradation.

The presence of several known enzymes involve in the degradation of aromatic xenobiotics was highlighted by KEGG pathway analysis. Partial or near complete pathways for naphthalene (Figure 5.34) and benzo(a)pyrene (Figure 5.35) metabolism were analysed in metagenomes sampled from NA, ENA and Combined microcosms. Shaded boxes highlight enzymes for which potential PAH-degrading genes were found in each metagenomic sample (blue = day 0

and red = week 42). On the basis of individual compound pathways, PAH-degrading genes involved in the degradation of PAHs were compared following bioremediation regimes.

In order to construct individual compound pathway, assembled metagenome data from MG-RAST interface were loaded onto the KEGG mapper database and screened against collections of high-level functional genes. Comparison was performed in pairs (two metagenomes) per analysis run using a maximum e-value of $1e^{-5}$, a minimum identify of 60%, and a minimum alignment length of 15 bp for DNA/RNA database (Meyer et al. 2008). Metagenomes sampled at the commencement of incubation were compared with metagenomes at the end of the incubation period. Changes in the number of sequences (Hits) assigned to each of the enzymes involved in the metabolism of naphthalene and benzo(a)pyrene, as representatives of the 16 PAHs priority pollutants, was monitored over the 42 week incubation period. Analyses of enzymes identified from samples collected from NA, ENA and Comb microcosms were consistent for all three PAH-contaminated soils studied over the length of the incubation period. In the following sections, data presented was limited to two pathways identified in metagenomes sampled from Creo soil microcosms, with overall an overarching summary of results from other treatments and soils provided in Table 5.7. This was purposely done to avoid repetition of information due to similarities in terms of enzymes identified regardless of soil, treatment and time point.

5.8.1 Naphthalene metabolism in unamended and amended Creo microcosms

The KEGG pathway analysis of enzymes involved in the metabolism of naphthalene in NA, ENA and Comb microcosms showed similarity in three enzymes including EC 1.14.1.1, EC 3.3.2.9 and 2.5.1.18 as illustrated in Figure 5.34. These enzymes may be involved in catalysing a wide range of reactions such as hydroxylation (Aryl hydrocarbon hydroxylase), epoxidation (epoxide hydrolase), deamination (Flavoprotein-linked monooxygenase), and reduction (Cytochome P450) of many xenobiotic compounds. However, there were many similarities in terms of enzymes encoding for unspecific monooxygenase, microsomal epoxide hydrolase, and microsomal hydrolase throughout the 42 week incubation period. This suggests that sequences related to key enzymes involved in the metabolism of aromatic hydrocarbon were repeatedly found in the microbial community from Creo microcosms as illustrated in Table 5.7.

In terms of number of hits assigned to each enzyme under natural attenuation (NA), xenobiotic monooxygenase (EC 1.14.14.1) decreased from day 0 and week 18 (18 to 0 hits), however, almost half of the initial hits was present at week 42 (8 hits). The variability in the number of

hits may suggested that the activity related to this enzyme declined due to a decrease in bacteria harbouring this capacity. In contrast, sequences assigned to glutathione transferase (2.5.1.18) extremely decreased from day 0 to week 18 (2187 to 25 hits). However, the proportions of hits annotated to this enzyme increased to approximately half the original number of hits at week 42 (25 to 1145 hits). Similarly, a reduction in the number of hits assigned to benzo(a)-4, 5-epoxide hydrolase (3.3.2.9) was also observed over the 42 week incubation period, which may reflect the declined in the microbial numbers presumably due to lack of nutrients to sustain growth.

In ENA microcosms, hits matching xenobiotic monooxygenase increased from day 0 to week 18 (18 to 29 hits) with further increases from week 18 to week 42 (29 to 60 hits). Similarly, an increase in the proportion of hits annotated to glutathione transferase (EC 2.5.1.18) was observed in ENA microcosms throughout the experimental time course. While a small reduction in the number of hits assigned to benzo(a)-4,5-epoxide hydrolase (EC 3.3.29) was observed from day 0 to week 18 (122 to 101 hits), this enzyme remained stable until the end of the incubation period.

For Comb microcosms, hits related to xenobiotic monooxygenase varied over the 42 week incubation period (Table 5.7). There was a 4-fold decreased in the initial number of hits from day 0 to week 18 (18 to 4 hits). However, further incubation resulted in a 2-fold increase from week18 to week 42 (4 to 9 hits). Sequences related to cytochome P450 enzymes (xenobiotic monooxygenase) were dominant at the commencement of the incubation (18 hits) compared to week 42 (9 hits).

In contrast, hits assigned to the other enzymes (glutathione transferase and benzo(a)-4, 5-epoxide hydrolase) followed the same pattern of fluctuation over the 42 week incubation period. In both cases, the number of hits assigned to each enzyme decreased from day 0 to week 18 (Table 5.7), with a small increase at the end of the incubation period (week 42). Supplementation of nutrients or inoculants had little effect on enzymatic activities related to naphthalene metabolism compared to NA microcosms. Among the enzymes reported in this section, the number of hits related to glutathione transferase were prevalent in metagenomes sampled from all (NA, ENA and Comb) Creo microcosms and time points. Glutathione transferase is one of the superfamily enzymes known for their role in the detoxification of contaminant such as PAHs.

5.8.2 Benzo(a)pyrene metabolism in unamended and amended Creo microcosms

On the basis of KEGG pathway analysis, functional profiles in NA, ENA and Comb metagenomes were similar in the sequences related to B(a)P metabolism (Figure 5.35 and Table 5.7). This suggested that supplementation of either nutrients or microorganisms had little effect on the enhancement of metabolic functional profiles over the 42 week incubation period. As observed from naphthalene and B(a)P pathways, no change in the diversity of the three enzymes was observed except in the proportion of hits annotated to each enzyme. An overall comparison of data from these treatments is presented in Table 5.7 while associated pathways showing metabolism of naphthalene and B(a)P from the amended microcosms are posted in Appendix 4 (Figure A4.1-A4.4).

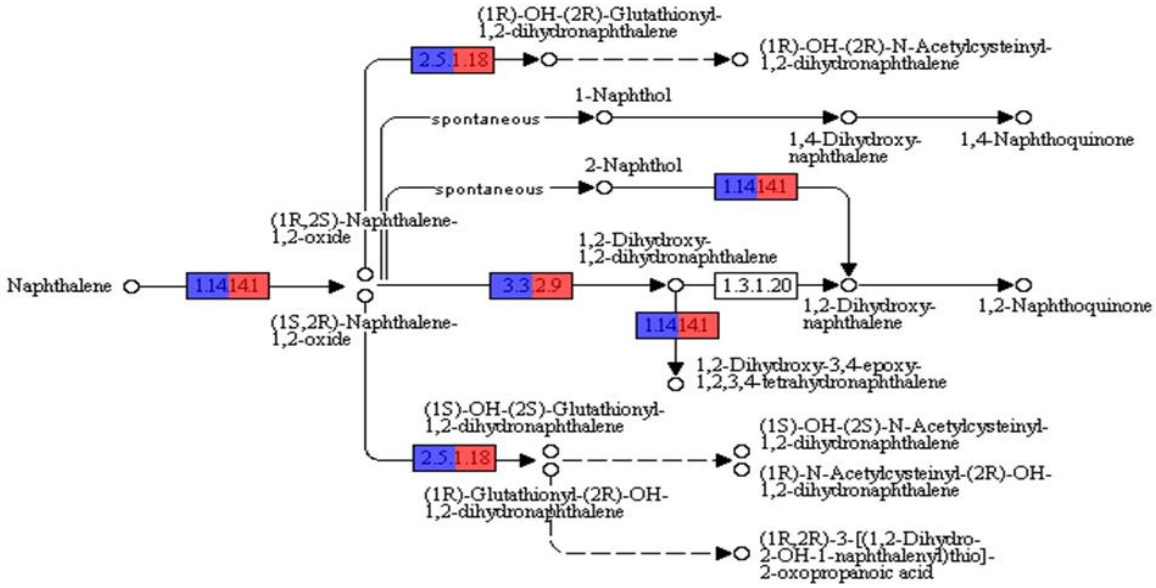

Figure 5.34. KEGG pathway analysis of metagenomes from Creo microcosms incubated under NA conditions displaying enzymes required for the metabolism of naphthalene. Enzyme profiles are showed at the start of incubation (MG-RAST ID 4565148.3 in blue) and after 42 weeks (MG-RAST ID 4565147.3 in red). Shaded boxes represent enzymes for which genes were present in each annotated metagenome.

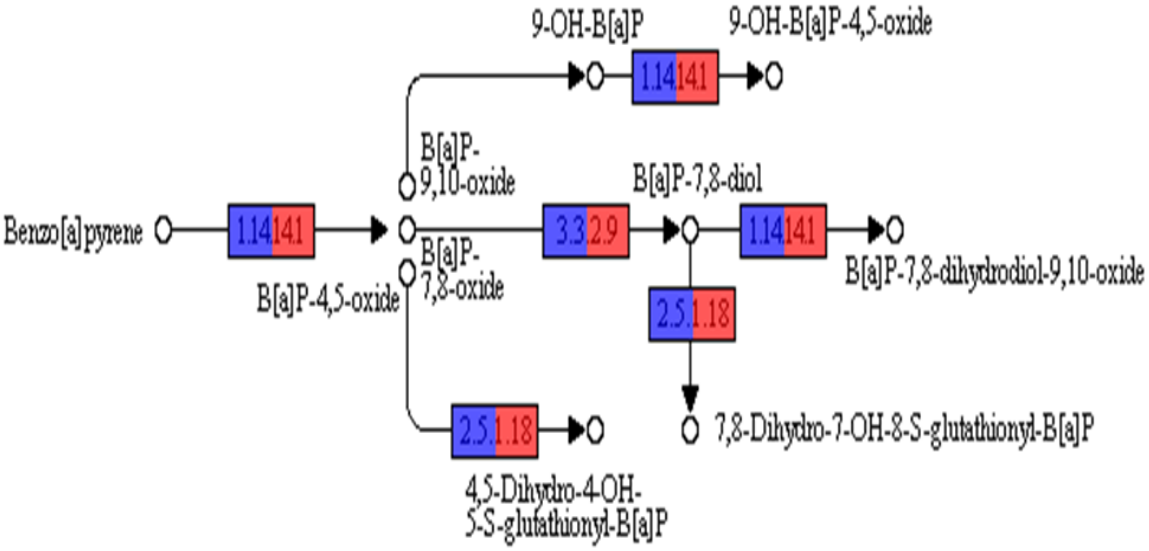

Figure 5.35. KEGG pathway analysis of metagenomes from Creo microcosms incubated under NA conditions displaying enzymes required for the metabolism of benzo(a)pyrene. Enzyme profiles are showed at the start of incubation (MG-RAST ID 4565148.3 in blue) and after 42 weeks (MG-RAST ID 4565147.3 in red). Shaded boxes represent enzymes for which genes were present in each annotated metagenome.

Table 5.7. Summary of hits matching three enzymes associated with PAH degradation specific functions in KEGG pathways analysis of metagenomes sampled from three soil microcosms (Creo, TB and AP) over the 42 week incubation period.

Treatment	Enzymes	No. of hits in Creo			No. of hits in TB			No. of hits in AP		
		Day	Weeks		Day	Weeks		Day	Weeks	
		0	**18**	**42**	**0**	**18**	**42**	**0**	**18**	**42**
NA	Xenobiotic monooxygenase (EC 1.14.14.1)	18	0	8	116	19	10	16	30	0
	Glutathione transferase (EC 2.5.1.18)	2187	25	1145	1910	1328	734	2224	1777	39
	Benzo(a)-4, 5-epoxide hydrolase (EC 3.32.9)	122	7	80	310	121	28	76	54	6
ENA	Xenobiotic monooxygenase(EC 1.14.14.1)	18	29	60	116	16	7	16	40	28
	Glutathione transferase (EC 2.5.1.18)	2187	2251	2574	1910	3297	1718	2224	2409	610
	Benzo(a)-4, 5-epoxide hydrolase (EC 3.32.9)	122	101	101	310	82	64	76	85	28
Comb	Xenobiotic monooxygenase (EC 1.14.14.1)	18	4	9	116	22	11	16	20	34
	Glutathione transferase (EC 2.5.1.18)	2187	151	1955	1910	2945	3736	2224	755	777
	Benzo(a)-4, 5-epoxide hydrolase (EC 3.32.9)	122	5	128	310	23	88	76	39	35

5.8.3 Analysis of enzymes required for metabolism of PAHs in TB microcosms

Similar analysis to the ones performed in section 5.8 was also performed with metagenomes sampled from TB soil incubated under NA, ENA and Comb conditions. Partial or near complete KEGG pathways for naphthalene (Figure 5.36) and B(a)P (Figure 5.37) metabolisms were analysed in samples obtained over the 42 week incubation period. Shaded boxes highlighted enzymes present for which potential PAH-depredating genes were found in each metagenomic sample (blue = day 0 and red = week 42). On the basis of individual compound pathway, PAH-degradation genes associated with bioremediation of PAHs were consistent with metabolic functional profiles reported in Creo metagenomes from the previous sections (5.8, 5.8.1 and 5.8.2).

5.8.4 Naphthalene metabolism in unamended and amended TB microcosms

Results from naphthalene metabolism in TB soil were similar to the results already described in Creo metagenomes in NA microcosms over the 42 week incubation period (section 5.8.1). In terms of number of hits assigned to each enzyme under NA incubation conditions, xenobiotic monooxygenase (EC 1.14.14.1) decreased from day 0 to week 18 (116 to 19 hits).

A further reduction was also observed at week 42 (10 hits). The reduction in the number of hits may suggest that the activity related to this enzyme declined due to a similar reduction in the number of bacteria community sheltering this capacity. This may also reflect on importance of nutrients for microbial growth as lack of nutrients under NA microcosm might have contributed to low microbial population. Similarly, a reduction in the number of hits assigned to glutathione transferase (2.5.1.18) and benzo(a)-4, 5-epoxide hydrolase (EC 3.3.2.9) was also observed, however, the extent of reduction was not as great as for xenobiotic monooxygenase over the 42 week incubation period (Table 5.7). At the end of the incubation period (week 42), hits were reduced from 116 to 10 for xenobiotic monooxygenase compared to glutathione transferase (1910 to 734 hits) and benzo(a)-4, 5-epoxide hydrolase (310 to 28 hits) respectively.

In the ENA microcosms, hits matching xenobiotic monooxygenase and benzo(a)-4, 5-epoxide hydrolase steadily decreased over the 42 week incubation period. Sequences matching glutathione transferase under ENA (1910 to 1718 hits) fluctuated over the 42 week incubation period but remained the most abundance enzyme compared to xenobiotic monooxygenase (116 to 7 hits) and benzo(a)-4, 5-epoxide hydrolase (310 to 64 hits). The prevalent observed in the

sequences assigned to glutathione transferase over the incubation period may be due to a tolerant (selective pressure) of bacteria groups harbouring this enzyme to toxicity of PAHs.
In the Comb microcosms, hits related to xenobiotic monooxygenase steadily decrease over the 42 week incubation period (Table 5.7). There was a 5-fold decreased in the number of hits annotated to xenobiotic monooxygenase from day 0 to week18, whereas additional 2-fold decrease was observed at week 42.

In contrast, hits assigned to glutathione transferase gradually increased through experimental time course. A 54.2% increase was observed in the number hits from day 0 to week 18. Moreover, the number hits increase by 26.9% at the end of the incubation of period (week 42). Consequently, sequences assigned to glutathione transferase increased by 95.1% at week 42 compared to day 0. While sequences related to benzo(a)-4, 5-epoxide hydrolase varied over the 42 week incubation period (Table 5.7). Supplementation of nutrients or inoculants demonstrated variable results on the enzymatic activities related to naphthalene metabolism compared to NA microcosms.

5.8.5 Benzo(a)pyrene metabolism in unamended and amended microcosms

On the basis of KEGG pathway analysis, functional profiles in NA, ENA and Comb metagenomes were similar in the sequences related to benzo(a)pyrene metabolism as described in the aforementioned Section (5.8.4 and Table 5.7). This suggested that supplementation of either nutrients or microorganisms had little effect on enhancement of metabolic functional profiles over the 42 week incubation period.

As demonstrated in figures representing the two pathways (naphthalene and B(a)P) under natural attenuation, no change in the diversity of three enzymes was observed except in the proportion of hits annotated to each enzyme in the rest of the treatments (ENA and Comb). Comparison of data from these treatments is presented in Table 5.7 while associated pathways showing metabolism of naphthalene and B(a)P from ENA and Comb microcosms are posted in Appendix 4 (Figure A4.5-A4.8).

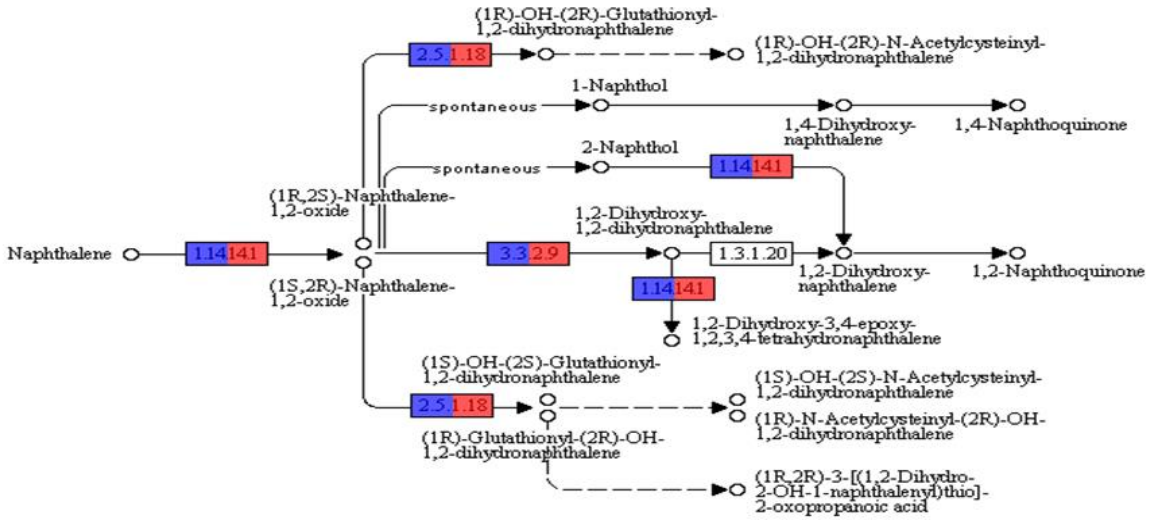

Figure 5.36. KEGG pathway analysis of metagenomes from TB microcosms incubated under NA conditions displaying enzymes required for the metabolism of naphthalene. Enzyme profiles are showed at the start of incubation (MG-RAST ID 4565155.3 in blue) and after 42 weeks (MG-RAST ID 4565491.3 in red). Shaded boxes represent enzymes for which genes were present in each annotated metagenome.

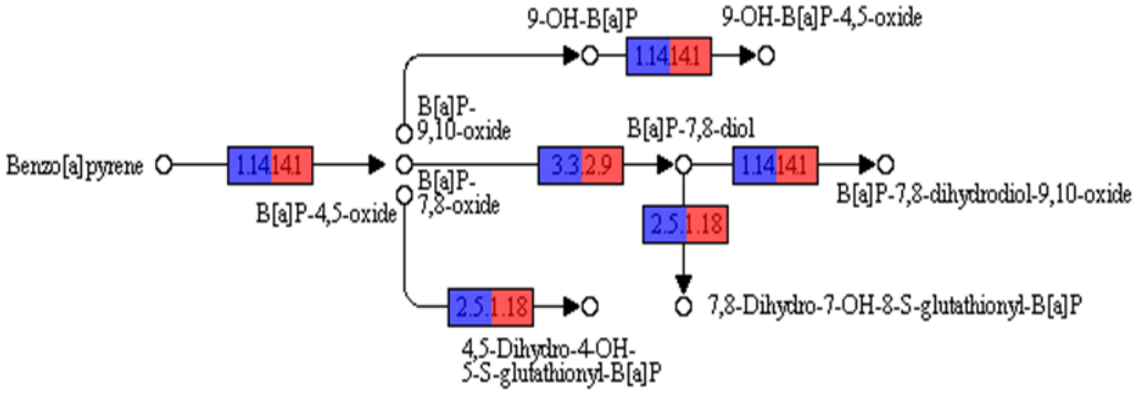

Figure 5.37. KEGG pathway analysis of metagenomes from TB microcosms incubated under NA conditions displaying enzymes required for the metabolism of benzo(a)pyrene. Enzyme profiles are showed at the start of incubation (MG-RAST ID 4565155.3 in blue) and after 42 weeks (MG-RAST ID 4565491.3 in red). Shaded boxes represent enzymes for which genes were present in each annotated metagenome.

5.8.6 Analysis of enzymes for PAHs metabolism

Similar analysis to the ones performed in Section 5.8, 5.8.1 and 5.8.2 was also performed with metagenomes sampled from AP soil incubated under NA, ENA and Comb conditions. Partial or near complete KEGG pathways for naphthalene (Figure 5.38) and benzo(a)pyrene (Figure 5.39) metabolisms were analysed in samples obtained over the 42 week incubation period. Shaded boxes highlighted enzymes present for which potential PAH-depredating genes were found in each metagenomic sample (blue = day 0 and red = week 42). On the basis of individual

compound pathway, PAH-degradation genes associated with bioremediation of PAHs were consistent with metabolic functional profiles reported in Creo metagenomes in the previous section (5.8).

Data presented in these figures showed similar metabolic profiles in NA, ENA and Comb microcosms. However, in terms of diversity and abundance of each of subfamily enzyme, EC 1.14.14.1 had the largest quantity of the annotated hits when compared to EC 3.3.2.9 and EC 2.5.1.18 respectively. Overall, the presence of a wide range of metabolic profiles in metagnomic samples obtained from NA, ENA and Comb microcosms was an indicative of microbial metabolism of PAHs.

5.8.7 Naphthalene metabolism in unamended and amended microcosms

Results from naphthalene metabolism in AP soil were similar to the results already described in Creo metagenomes in NA, ENA and Comb microcosms over the 42 week incubation period (section 5.8.1). In terms of number of hits assigned to each enzyme under NA, xenobiotic monooxygenase (EC 1.14.14.1) increased from day 0 and week 18 (16 to 30 hits), however, additional incubation resulted in no detection of sequences related to xenobiotic monooxygenase at week 42. The reduction in the number of hits may suggested that the activity related to this enzyme declined due to a decrease in the number of bacteria community sheltering this capacity. Similarly, a reduction in the number of hits annotated to glutathione transferase (2.5.1.18) and benzo(a)-4, 5-epoxide hydrolase (EC 3.3.2.9) was also observed, however, the extend of decreases was not as great as observed in xenobiotic monooxygenase over the 42 week incubation period (Table 5.7), which may largely be attributed to decline in microbial numbers presumably due to lack of nutrients to sustain growth.

In the ENA microcosms, hits matching xenobiotic monooxygenase, benzo(a)-4, 5-epoxide hydrolase and glutathione transferase fluctuated extensively over the 42 week incubation period. The number of sequences related to xenobiotic monooxygenase increase from day 0 to week 18 by 28.5% of the total hits. The increased observed at week 18 corresponded with a decreased in the number of the total hits at week 42 (14.3%). While benzo(a)-4, 5-epoxide hydrolase increase by a small margin at week 18 (3.5%), however, a 33.3% decreased was observed in the number of the total hits at week 42.

In the Comb microcosms, hits related to xenobiotic monooxygenase steadily increased over the 42 week incubation period (Table 5.7). A 26% increase in the number of total hits was

observed from day 0 to week 18. Further incubation resulted in additional 20% increase in the number of hits in samples obtained at week 42. In contrast, hits assigned to the other enzymes (glutathione transferase and) gradually decreased throughout the experimental time course. The extent of decreased was consistent with approximately 20% reduction in the number of hits at each sampled time points (weeks 18 and 42). Similar result was observed in sequences related to benzo(a)-4, 5-epoxide hydrolase under Comb microcosm over the 42 week incubation period. Supplementation of nutrients or inoculants demonstrated variable results on the enzymatic activities related to naphthalene metabolism compared to NA microcosms in AP soil.

5.8.8 Benzo(a)pyrene metabolism in unamended and amended microcosms

On the basis of KEGG pathway analysis, functional profiles in NA, ENA and Comb metagenomes were similar in the sequences related to B(a)P metabolism as described in the aforementioned Section (5.8.7 and Table 5.7). This suggested that supplementation of either nutrients or microorganisms had little effect on the enhancement of metabolic functional profiles over the 42 week incubation period. As demonstrated from naphthalene and B(a)P pathways, no change in the diversity of three enzymes was observed except in the proportion of hits annotated to each enzyme in NA, ENA and Comb microcosms. An overall comparisons of data from these treatments is presented in Table 5.7, while associated pathways showing metabolism of naphthalene and benzo(a)pyrene from ENA and Comb microcosms are posted in Appendix 4 (Figure A4-A4.12).

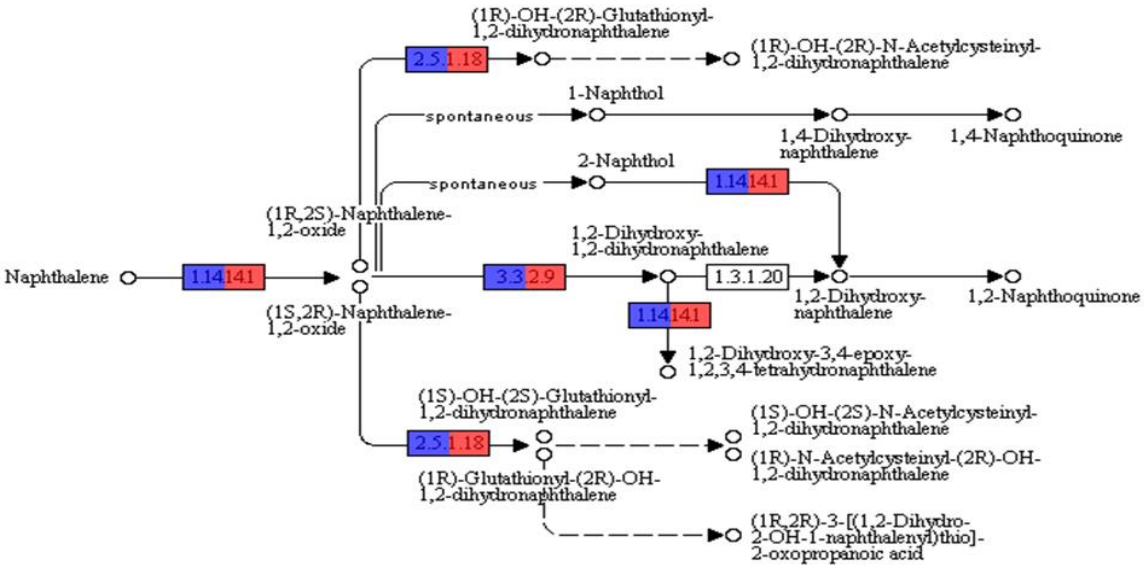

Figure 5.38. KEGG pathway analysis of metagenomes from AP microcosms incubated under NA conditions displaying enzymes required for the metabolism of naphthalene. Enzyme profiles are showed at the start of incubation (MG-RAST ID 4559617.3 in blue) and after 42 weeks (MG-RAST ID 4559622.3 in red). Shaded boxes represent enzymes for which genes were present in each annotated metagenome.

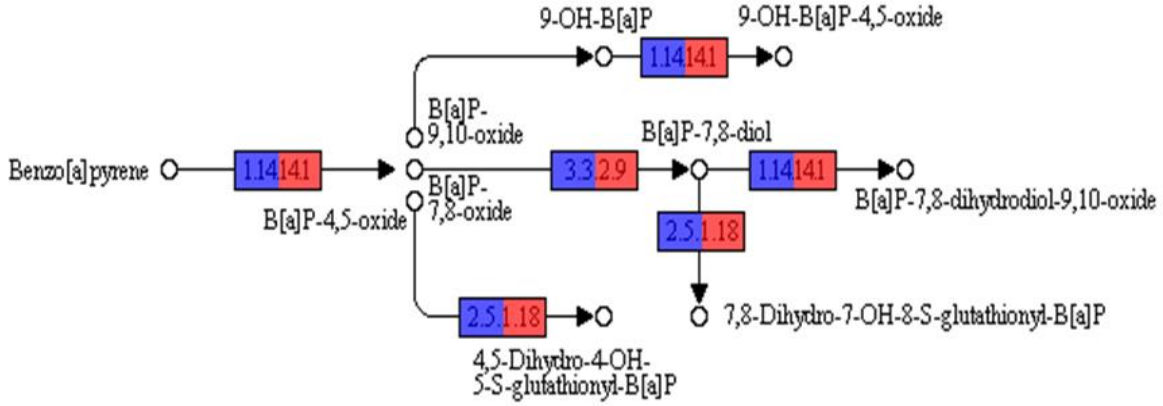

Figure 5.39. KEGG pathway analysis of metagenomes from AP microcosms incubated under NA conditions displaying enzymes required for the metabolism of benzo(a)pyrene. Enzyme profiles are showed at the start of incubation (MG-RAST ID 4559617.3 in blue) and after 42 weeks (MG-RAST ID 4559622.3 in red). Shaded boxes represent enzymes for which genes were present in each annotated metagenome**.**

5.9 Discussion

Soil is a natural dynamic environment that harbours highly complex and diverse microbial communities. These communities are active drivers of several biogeochemical cycles, including essential elements such as carbon, oxygen, sulfur, nitrogen, and phosphorus. In addition, microorganisms have evolved the capacity to degrade wide range of anthopogenic pollutants including PAHs (Abbai et al. 2012).

There have been several reports in the literature, detailing the detection, isolation and characterisation of hydrocarbon-degrading bacterial genera from hydrocarbon contaminated environments. Based on traditional (biochemical) and modern day (molecular) techniques, bacterial genera including: Acinetobacter; Alcaligenes; Bacillus; Burkholderial; Mycobacterium; Gordonia; Pseudomonas; Rolstonia; Rhodococcus; Sphingomonas have been identified with capacity to degrade PAHs (Cheung & Kinkle 2001; Chikere, Okpokwasili & Chikere 2011; Díaz 2010; Harayama 1997; Juhasz & Naidu 2000; Kanaly et al. 2000; Wilson & Jones 1993).

Generally, there are no related studies conducted so far that have monitored changes in the microbial communities in samples collected from PAH contaminated sites using shotgun pyrosequencing (Ion Proton platform) over the experimental time course. However, some studies have used other platforms such as 454 pyrosequencing (Roche) and Illumina sequencing technologies to compare bacterial diversity of activated sludge from sewage treatment plant (Yu & Zhang 2012; Zhang, Shao & Ye 2011), identification of wood-inhibiting fungi (Ovaskainen et al. 2010) and surveys of soil microbial communities (Daniel 2005; Petrosino et al. 2009).

Yu and Zhang (2012) examined microbial structure of the activated sludge community from a municipal wastewater treatment plant sequenced by Illumina Hi-seq2000. They found Proteobacteria, Actinobacteria, Bacteroidetes, Firmicutes and Verrucomicrobia were the dominant communities of the activated sludge. Based on data available from the literature, this study is one of the few studies to compare changes in microbial communities in terms of composition, diversity and abundance over the experimental time course.

In the present study, direct sequencing of environmental genomic DNA was performed to compare changes in microbial diversity, abundance and functional profiles in three aged PAH-contaminated soils using Ion Proton platform. MG-RAST pipeline was employed to compare taxonomic and functional diversity distributions in metagenome generated using Ion Proton sequencing. Data generated provides an overall comparison of taxonomic and functional

distributions, in terms of their identity (who is there), diversity (Compositions) and abundance (How many of each individual) in metagenomes sampled from Creo, TB and AP soil microcosms over the 42 week incubation period.

The primary goal of this analysis was to expand on microbiological and molecular results reported in Chapters 3, and 4, in which changes in microbial numbers (MPN) and diversity (DGGE) was determined in samples collected over a 42 week incubation period. Due to inability of both approaches (DGGE and MPN) to provide an understanding of the mechanisms adapted by microbial community in PAH contaminated soil. NGS technology was used to compare PAH-degrading communities in order to circumvent challenges associated with microbiological and molecular approaches.

In addition, it was hypothesised that Ion Proton permits accessibility of PAH-degrading genes propelled by individual microorganisms within the microbial community sampled from PAH-contaminated soil. Due to the large volume of data generated using NGS techniques, discussion of data will be restricted to genera with relative abundance greater than 4% (phylum) and 5% (order) of the total organisms with mentioning of known underrepresented PAH degraders.

Evaluation of taxonomic annotation in metagenomes generated with Ion Proton platform from aged PAH-contaminated soils, illustrated that bacteria was the most prevalent domain over the 42 week incubation period (Figures 5.1, 5.6 and 5.11). Interestingly, there was no link to suggest that the dominancy of domain bacteria in all soils resulted from nutrient or inoculants application as bacteria at proportions >90% were consistently detected regardless of remediation strategy. Domain bacteria dominancy in the three study soils was consistent with results reported from the previous studies, where the prevalence of bacteria in hydrocarbon-contaminated soils was found (Abbai et al. 2012; Hansel et al. 2008; Simon et al. 2009; Yergeau et al. 2012). Yergeau et al. (2012) argued that hydrocarbon-degrading bacteria constitute the fast-growing population in high arctic soil stimulated by hydrocarbon contamination. In another study, Simon et al. (2008) also observed the prevalence of domain bacteria as evidenced by the abundance of sequences (83% of total sequences) belonging to this phylogenetic group in Glacier Ice metagenomes using pyrosequencing. Analyses of soil bacteria communities in aged PAH-contaminated soils showed the prevalence of similar phyla in NA microcosms (Figure5.2, 5.7 and 5.12).

Bacterial communities were dominated by seven phyla including Proteobacteria, Acidobacteria, Firmicutes, Actinobacteria, Bacteroidetes, Verrucomicrobia and Planctomycete

(Relative abundance greater or equal 5% of the total organisms), which were observed with a varying relative abundances depending on the soil analysed. Throughout the NA microcosms, Proteobacteria, Bacteroidetes, Acidobacteria, and Actinobacteria were consistently found over the 42 week incubation period. In contrast, Verrucomicrobia and Planctomycetes were present in metagenomes obtained at later stages of incubation (weeks 18 and 42) in Creo and TB soils respectively. Simon et al. (2009) reported similar results as presented here, in which phylum Proteobacteria, Bacteroidetes, and Actinobacteria dominated Glacial Ice metagenomes of the Northern Schneeferner (Germany). In agreement with results reported in this study, relative abundances of Proteobacteria, Actinobacteria, Bacteroidetes, and Acidobacteria were apparent presumably due to hydrocarbon contamination according to Nemergut et al. (2008). The authors concluded that the increase in the relative abundance of these phyla may be explained by the effect of chronic nitrogen fertilisation amendment (period of N application between 1991 to 2000), which actuates significant shifts in carbon available to these communities leading to the dominancy observed in microbial communities in alpine tundra soil (uncontaminated soil).

The primary phylum consistently recovered across three soils, treatments and time points was Proteobacteria based on data generated by shotgun pyrosequencing. However, such a finding was not surprising as 44.4% of the 18 established dominant orders belong to this phylogenetic group in all soils. In addition, these results were expected as orders (belonging to phylum Proteobacteria) identified encompass known soil microbes and/or prominent orders with the capacity to degrade PAHs (Fang et al. 2013; Li et al. 2015; Nakamura, Germano & Tsai 2014; Ren et al. 2015). Members (8 orders) of the phylum Proteobacteria (Enterobacteriales, Burkholderiales, Rhizobiales, Sphingomonadales, Alteromonadales, Chomatiales, Xanthomonadales, Nitrosomonadales and Sphingobacteriales) were found in significant numbers in all soils with and without amendments (Tables 5.2, 5.4 and 5.6). The second most dominant phylum (22.2% of 18 orders with relative abundance greater than 5%) was Bacteroidetes. Orders belonging to this phylum were found with relative abundance greater than 5% of the total organisms at the later stages of incubation in Creo and TB soils (weeks 18 and 42).

In contrast, a significant decrease was observed in the relative abundance of Bacteroidetes in AP from day 0 to weeks 18 and 42 (11.4 to 2.0 and 2.5% reduction in the relative abundance), which resulted in orders belonging to this phylum being in relative abundance less than 5% of the total organisms. The decrease observed in the relative abundance of orders belonging to

Bacteroidetes corresponded with a significant increase in the relative abundance of orders belonging to Proteobacteria in AP soil. Presumably the phylum Bacteroidetes was underrepresented in AP soil as overrepresentation of Proteobacteria overshowed their existent as this phylum may have less capacity to survive on PAHs as carbon and energy source without sufficient N and P available due to limitation of both N and P in the AP soil (See Table 3.2).

In this study, it is possible to speculate that the increased orders (belonging to phylum Proteobacteria) might possess ecological competitive advantage over the decreased orders (belonging to phylum Bacteroidetes), which allowed them to perpetuate, increase and compete following the addition of moisture and aeration to the contaminated soils. The quantitative power of intra-species interaction offers Proteobacteria an ecological advantage to cooperate and function as a unit to overcome inadequate N and P content in AP soil. Apparently overrepresentation of a particular bacterial community, may impact on the rate and extent of PAH bioremediation.

Recent studies have linked bacterial community composition with removal of PAH from contaminated soil (Li et al. 2015; Nakamura, Germano & Tsai 2014). Hence, Li et al. (2015) related the abundance of the *Mycobacterium* sp. to the PAH contents, in which they estimated sequences related to indigenous *Mycobacterium* and *Trerabacter* sp. to occupy 65.9 – 100% of the total detected sequences in the soil samples collected from the urban roadside of Shanghai. Li et al. (2015) suggested that the abundance of *Mycobacterium* sp. and *Trerabacter* sp. was an indicative of parameter influencing the efficacy of bioremediation in PAH contaminated soils.

In Creo, TB and AP soil, no relationship was established linking PAH removal and the prevalence of particular bacterial orders as limited PAH degradation was observed across soils, treatments and time points. However, PAH-degrading bacteria may be abundant in soil, based on the abundance of certain orders, as a consequence of enrichment due to long-term exposure to PAH and adaptation of microorganisms to the carbon sources. There was no difference observed in terms of diversity between Creo, TB and AP soils under NA conditions. However, the only observable difference between these soils was the variability in the relative abundance of some phyla which was also reflected at the order level in metagenomic data. Vinas et al. (2005) reported the prevalence of PAH-degrading bacteria communities (Sphingomonas, Azospirillum, Ctyophaga, Xanthomonas and Alcaligenes) in a Creo (concentration of 2,724 ±

134 mg/kg of dry soil) contaminated soil with degradation (83 to 87%) occurring over the 90 day incubation period.

The abundance of these bacteria communities showed that they are likely to be involved in PAH degradation. Compared to this study, there was a limited PAH degradation in the 3 soils despite the prevalence of numerous microbial communities with degradation capacities. Potential PAH-degrading bacteria from Proteobacteria, Acidobacteria, Actinobacteria, and Bacteroidetes orders were identified in Creo, TB, and AP soils similar to reports by Tringe et al. (2005), Vinas et al. (2002), Vinas et al. (2005) and Wang and Tan (2011).

In all 3 soils, Proteobacteria occurred as the most prevalence phylum with or without soil amendment influence. It has been shown that members of this phylum (Proteobacteria) such as alphaproteobacteria may be flexible to grow in a soil with low nutrient contents (N and P), which might probably explain their abundances in samples collected from AP site with low organic N and P content (Johnson & Scow 1999; Vinas et al. 2005) (Table 3.2). Johnson and Scow (1999) observed limited phenanthrene mineralisation following the addition of N and P due to either depression or lack of response in four tested spiked soils. They author concluded that the reason for lack of phenanthrene mineralisation in the four tested soils was uncertain, however, the bioavailability of added nutrients and of PAHs as an alternative carbon and energy source might have impaired microbial capacity to metabolise phenanthrene.

In the present study, manipulation of environmental conditions by the addition of nutrients and inoculants had a minimal effect on soil microbial communities in 3 PAH contaminated soils. Clearly, analyses of soil microbial communities demonstrated a mixed response in 3 soils following the addition of different bioremediation strategies. Proteobacteria was found to be the most dominant taxon in these soils based on MG-RAST data annotation. However, a significant reduction in the relative abundance of Proteobacteria was observed in Creo soil following the addition of nutrients and inoculants. Assessment of other phyla in Creo soil after amendment regimes showed an increase in the relative abundance of Bacteroidetes and Acidobacteria with phylum Actinobacteria unaffected. In the TB soil, amendments greatly enhanced Proteobacateia as evidenced by rapid increase in its relative abundance under ENA (40.9 to 70%) and Comb (40.9 to 73.8%) conditions. In addition, phylum Bacteroidetes positively responded to the addition of nutrients and inoculants in the TB soil with 10-fold increase in its initial relative abundance.

Unlike both Creo and TB soils, a minimal response was showed by microbial communities in the AP soil following the addition of nutrients and inoculants. Characterisation of bacterial communities in 3 soils at phylum and order levels demonstrated identification of similar

microbial community. However, each microbial community was detected at a varying proportion between 3 soils. Further analysis of bacterial community at order level in 3 soils also demonstrated increase in the relative abundance of orders belonging to the aforementioned phyla (Proteobacteria, Bacteroidetes, Acidobacteria, Actinobacteria, Firmicutes, Verrrucomicrobia and Planctomycetes) with or without the addition of N and P. For examples, the prevalence orders after a 42-week incubation period included Enterobacteriales, Burkholderiales, Rhizobiales, Sphingomonadales, Alteromonadales, Sphingobacteriales, Planctomycetales, Cytophagales, Flavobacteriales, Acidobacteriales, Solibacteriales, Actinomycetales, Bacillales and Verrucomicrobiales. Thus, results from this study may suggest that these environments were inhibited by similar microbial communities although they are distant apart. Additionally, similarities observed in physio-chemical properties between 3 soils (e.g. pH, sandy loam) might have contributed to similar microbial communities being identified at these sites (Table 3.2).

A point worthwhile mentioning in this chapter is that, one of the primary aims of this study was to assess the survivability of the bioaugmented organism (*Mycobacterium* gilvum) in 3 soils over the 42 week incubation period. However, due to the complexity of data analysis beyond order level, it was difficult to drill down to the point where the identity of the inoculated organism could be confirmed to verify that the bioaugmented organism prosper soils amendment conditions. While massive data generated by shotgun pyrosequencing using 3 soils became the real challenge, characterisation of bacterial communities was limited to domain, phylum and order level in this study. Nevertheless, understanding of what happened to the *Mycobacterium* in the Comb treatments prepared using the Creo, TB and AP soils couldn't be passed on. Thus, the assessment of metagenomes sampled from bioaugmented microcosms exemplified the presence of *Mycobacterium* gilvum in both Creo (185 additional genera) and AP (202 additional genera) soils (data not shown).

In the TB soil, no *Mycobacterium* gilvum was detected but few other genera belonging to *Mycobacterium* (51 genera) were found compare to both Creo and AP soils after a 42-week incubation period. This indicates that both Creo and AP soils may have been inhibited by preadapted indigenous *Mycobacterium* communities as a consequence of long time exposure to PAH contaminated soils. *Mycobacterium* communities were unaffected by the inoculation of *Mycobacterium* gilvum in both Creo and AP soils as the diversity of indigenous was greater compared to the diversity of exogenous. Many reports (Bisht et al. 2015; Brezna, Khan & Cerniglia 2003; Cheung & Kinkle 2001; Li et al. 2015; Lladó et al. 2015; Lladó, S et al. 2013; Miller et al. 2007) have documented the presence of numerous species belonging to

Mycobacterium in PAH contaminated soils because of their catabolic potential to degrade a wide range of low and high molecular weight PAHs. Llado et al. (2015) highlighted several reasons behind the failure of bioaugmented treatment to enhance contaminants removal. In most cases, exogenous microorganisms never prospered due to the abiotic and biotic environmental stresses. These included fluctuations in temperature, water content, pH and nutrient availability in addition to the presence of potentially toxic compounds at elevated concentration at the contaminated site.

Furthermore, the added microorganisms are likely to face an inevitable competition from the indigenous bacteria. The ability of bioaugmented microorganisms to enhance PAH bioremediation under the aforementioned conditions is impaired. In another study, Llado et al. (2013) reported that the bioaugmented microcosm fall short of gradually reducing PAH contents compared to biostimulated microcosms which corresponded with low abundance of the added organisms after 60 days of incubation. In this study, the abundance of *Mycobacterium* gilvum did not increase after a 42-week incubation period because the bioaugmented organism may have not survived to enhance the indigenous population.

Annotation of sequences related to functional profiles illustrated sequences belonging to aromatic metabolism within all 3 soils, treatments and time points. Sequences annotated by the MG-RAST interface exemplified clustering-based subsystems, amino acids and derivatives, respiration, metabolism of aromatic compounds, protein metabolism, DNA metabolism and carbohydrates utilisation as the core metabolic function in the three soils studied (Figure 5.16 – 5.33). A recent survey of hydrocarbon-contaminated groundwater using pyrosequencing analysis reported the presence of genes affiliated with the metabolism of aromatic compounds (Abbai et al. 2012). Abbai et al. (2012) reported present of other functional genes such stress response, dormancy, virulence and chemotaxis expressed by microbial communities in habited polluted environment as survival strategies.

In another study, Sanapareddy et al. (2008) observed overrepresentation of functional profiles of genes encoding for the metabolism of aromatic compounds in DNA collected from the activated sludge basin of a wastewater treatment plant compared to microbial metagenomes collected from nine distinct biomes. In the wastewater treatment plant, they found no genes encoding for proteins involved in photosynthesis compared to microbial metagenomes. This was not surprising as the primary source of energy for bacteria dwelling in the wastewater treatment plant was expect to be organic materials processed by plant. While genes responsible for the degradation of aromatic compounds were expressed in a higher proportion in the

wastewater treatment plant compared to microbial metagenomes from the other distinct biomes. This observation resulted from the amount of industrial and household waste being released into the sewage on daily basis with variety of chemical compounds exerting selective pressure on degrading bacteria (Sanapareddy et al. 2009).

In the Creo, TB and AP soils, assessment of major biogeochemical processes illustrated the expression of functional profiles involved in the metabolism of aromatic compounds as a response by bacterial community to hydrocarbon contaminations. Moreover, consistent expression of the aforementioned functional metabolic profiles was anticipated in PAH-contaminated environments as some of these are essential survival strategies adapted by microbial community to overcome harsh environments.

In Creo, TB and AP soils, STAMP analysis showed consistent overrepresentation of core metabolic profiles such as carbohydrate metabolism, clustering-based subsystems and protein metabolism but were not significantly different (95% CI). This indicates that amendment regime performed using Creo, TB and AP soils did not enhance microbial community activity because the added N and P may not have been available to the indigenous microbes due to bioavailability constraint. Changes in microorganisms' niches have been shown to provoke expression of a certain stress levels (Chu et al. 2014; Patri, Padmini & Babu 2010; Zhou et al. 2011). In the current study, abundance of sequences related to genes encoding for desiccation stress detected (8.5% of total sequences) at the commencement of microcosms may explain microbial community response to dryness.

However, the expression of stress response relative to dryness was much lower (1.5% of total sequences) at the later stages of incubation following the introduction and maintenance of moisture. It has been proposed that chemotaxis may play a significant role in biodegradation and bioremediation of toxic pollutants by providing a mechanism for pollutant-degrading bacteria to come into contact with the target pollutant (Pandey et al. 2002). Exposure of microbial communities to toxic compounds induced expression of sensory systems such as motility and chemotaxis to provide the capacity to detect the pollutants. In this study, abundance of sequences related to motility and chemotaxis could be a signal to explain that these sites were contaminated with toxic compounds.

In addition, widespread presence of functional metabolic profiles involved in aromatic metabolism within soil microbial community was apparent in metagenomes obtained from the 3 soils over the 42 week incubation period. This was further supported by results of KEGG pathway analysis, with consistent detection of partial pathways involving in the biodegradation

of naphthalene, pyrene and B(a)P in three soils (Figure 5.34 – 5.39) along with three potential enzymes namely; (i) xenobiotic monooxygenase; (ii) glutathione transferase and (iii) benzo(a)-4,5-epoxide hydrolase or microsomal epoxide hydrolase (Table 5.7). The presence of these enzymes in 3 soils illustrate the catabolic potential of microbial community response to PAH contamination. In these soils, enzymes associated with aromatic metabolism were consistently detected throughout the experimental time course may have occurred as a result of longer exposure to PAHs. According to a recent review, metabolism of PAHs represent an important detoxification function of glutathione transferases as in nature (Allocati et al. 2009; Oakley 2011).

Glutathione transferase (GSTs) are widely distributed in bacteria and form a superfamily of protein with ability to catalyse a wide range of hydrophobic toxic compounds during biodegradation of xenobiotics. Allocati et al. (2009) concluded that the main mechanism of the GSTs is the conjugation of target compounds with electrophilic centres to the tripeptide glutathione, besides many other activities, including biosynthesis, peroxide degradation, and dehydroascorbate reduction. Many monooxygenases are known for their ability to incorporate one hydroxyl group into substrate in numerous metabolic pathways in the biodegradation of xenobiotics (Dixit et al. 2015; Karigar & Rao 2011; Urlacher & Girhard 2012). According to Karigar and Rao (2011), bioremediation of a polluted site depends on the power of microbial enzymatic attack. Cytochome P450 or xenobiotic monooxygenase is one of the monooxygenase subclass well characterised for its catalytic role in oxidative reactions of several substrates including alkanes, complex endogenous molecules, steroids and fatty acids (Urlacher & Girhard 2012).

There have been some reports highlighting the evolution of the microsomal epoxide hydrolase, predominantly found in all organisms (Morisseau & Hammock 2005; Newman, Morisseau & Hammock 2005; Waszak et al. 2015; Zhang et al. 2006). In recent years, the role of microsomal epoxide hydrolase was observed in the metabolism of polyaromatic compounds(benzo(a)pyrene), 1, 3-butadiene oxide and styrene oxide (Decker, Arand & Cronin 2009; Tzeng et al. 1996), with the catalytic mechanism involving the addition of water to epoxides and arene oxides to yield vicinal diol products.

While variability in the number of hits annotated to each enzyme in three soils and treatments may be due to a decrease in bacteria harbouring this capacity. Because of their relevant in the process of contaminant detoxification, glutathione transferase was the most prevalent aromatic metabolism enzyme compared to other enzymes (xenobiotic monooxygenase and benzo(a)-4,5-epoxide hydrolase) regardless of amendment regime. Evidence in the literature suggested

that GSTs have a potential application in biodegradation of xenobiotics such as PAH since they are widely distributed in prokaryotes (Allocati et al. 2009; Sheehan et al. 2001).

Even though known PAH degrading microbial communities and the relevant potential enzymes associated with partial pathways and the metabolism of PAHs were presence in 3 soils, a limited PAH degradation was observed after a 42-week incubation period. Overall, the limitation of PAHs removal observed in treated microcosms (nutrients and inoculants) by microbial biodegradation may be due to bioavailability constraints. As soils used in this study were collected from historical PAH contaminated sites, ageing may have resulted in sorption of PAH to soil matrix or minerals decreasing microbial biodegradability as contaminant may be less available to microorganisms. As a consequence, factors controlling the contaminant binding and release in these soils potentailly contributed to the failure of bioremediation strategies.

5.10 Conclusion

Shotgun pyrosequencing (Ion Proton platform) of genomic DNA can provide direct access to a wide range of microbial community inhabiting contaminated environments. Based on MG-RAST data annotation, PAHs contamination resulted in the prevalent of some known PAH-degrading bacteria including Proteobacteria, Bacteroidetes, Acidobacteria and Actinobacteria in 3 soils after a 42-week incubation period. Moreover, results reported in this Chapter indicated that soils studied here host enormous microbial community assemblages with a metabolic potential. Furthermore, consistent detection of key three enzymes associated with metabolism of naphthalene, pyrene and B(a)P based on KEGG pathway analysis indicated the degradative capacity of these soils.

Unfortunately, there was no relationship established to link the prevalent of bacterial community in the three soil microcosms with PAH degradation based on results discussed in Chapter 3 with a limited reduction in PAH concentration over the 42 week incubation period. In addition, the lack of degradation couldn't be related with amendment regimes or inadequate presence of PAH-degrading microbial communities. However, the possible explanation responsible for the lack of PAH-degradation is presumably due to contaminant bioavailability as known PAH-degraders were consistently detected in three soils over the experimental time course. The next Chapter addresses bioremediation strategies to encounter PAH bioavailability as the key bioremediation limiting factors based on the assessment of PAH-degrading microorganisms reported here.

Chapter 6

Application of bioavailability assessment tools to predict PAH bioremediation endpoints in 3 PAH-contaminated soils.

6.1 Introduction

As detailed in the previous chapter, molecular (NGS) techniques identified potential PAH degrading indigenous microflora present in Creo, TB and AP soils. However, for all soils, PAH bioremediation was limited, even in soils where nutrients were amended or PAH degrading microorganisms were augmented. It was hypothesised that the lack of PAH biodegradation may be a result of limited PAH bioavailability. In the context of biodegradation, bioavailability is dependent on a number of parameters that govern the interactions between physical properties of PAHs, soil matrix and potential microbial PAH degraders in a given environment. As detailed by Semple et al. (2003), Juhasz et al. (2005) and Mahmoudi et al. (2013), PAH bioavailability (for PAH biodegradation) may be estimated by determining the amount of PAHs that are desorbable from the soil matrix (using non-exhaustive extraction methods).

Non-exhaustive extraction methodologies using aqueous solutions of hydroxypropyl-β-cyclodextrin (HP-β-CD) have been suggested as a means of measuring the rapidly desorbable PAH fraction (i.e. PAH bioavailability) (Rhodes, McAllister & Semple 2010; Semple et al. 2007). In recent years, a number of studies have demonstrated the relationship between PAH biodegradation/mineralisation and PAH bioavailability, determined using HP-β-CD extraction, in spiked and contaminated soils (Cuypers et al. 2002; Doick et al. 2006; Doick, Dew & Semple 2005; Hickman et al. 2008; Juhasz, Waller & Stewart 2005; Mahmoudi, Slater & Juhasz 2013; Reid, Jones & Semple 2000; Rostami & Juhasz 2013; Stokes et al. 2005). For example, Allan et al. (2006), Rhodes et al. (2008), Stroud et al. (2009) and Rhodes et al. (2010) found that the relationship between phenanthrene mineralisation and bioavailability in spiked soils was approximately 1:1 (slope ranging from 0.85-1.01) with a goodness of fit ranging from 0.89-0.99.

In studies conducted with PAH-contaminated soils, a strong correlation was also observed between PAH biodegradability and bioavailability assessed using HP-β-CD by Cuypers et al. (2002), Juhasz et al. (2005), Papadopoulos et al. (2007) and Mahmoudi et al. (2013). Low molecular weight PAH biodegradation (≤ four-ring PAHs) and HP-β-CD extractability were similar (i.e. close to the 1:1 relationship), however, HP-β-CD extraction removed extensively

higher amounts of five- and six-ring PAHs compared to biodegradation (Allan et al. 2006; Cuypers et al. 2002; Juhasz, Waller & Stewart 2005; Mahmoudi, Slater & Juhasz 2013; Papadopoulos et al. 2007). For the more recalcitrant compounds, the slope of the biodegradation-bioavailability relationship may be different to that of low molecular weight PAHs as a consequence of solubility constraint.

6.2 Aim

In this chapter, HP-β-CD extraction was utilised to investigate if a lack of PAH bioavailability was responsible for the limited PAH biodegradation observed in chapter 3. PAH bioavailability was predicted using HP-β-CD data and liner regression models from Juhasz et al. (2014), Papadopoulos et al. (2008) and Hickman et al. (2008) to determine whether prediction accuracy varied depending on model used. Besides cyclodextrine extraction, some other non-exhaustive extraction methods or assays such as butanol, dichloromethane, resin extractions and persulfate oxidation have previously been used to assess bioavailability (Reid, Jones & Semple 2000). These methods or assays have been proposed and used to predict the end points of PAHs biodegradation in contaminated soils throughout the literature. In this study, HP-β-CD extraction method was chosen because cyclodextrins possess hydrophilic surface and internal hydrophobic cavity that allows the formation of a water soluble state complex between the cyclodextrin molecule and the low organic compound. As a consequence, HP-β-CD extraction method was chosen as the suitable approach over the other techniques since it can allow the mass transfer from the soil matrix to the aqueous phase.

6.3 Hypothesis

It was hypothesised that PAH biodegradation endpoints could be predicted using HP-β-CD extraction and that PAH biodegradation limitations resulted from a lack of PAH bioavailability.

6.4 Results

As detailed in section 2.7 (Material and Methods), PAH contaminated soils were extracted with 40 mM HP-β-CD for 20 h in order to quantify the residual or non-bioavailable fraction. The extent of biodegradation was then predicted using the measured residual PAH concentrations and linear regression models from Juhasz et al. (2014), Papadopoulos et al. (2007) and Hickman et al. (2008). These linear regression models were chosen because they have shown a strong relationship between the measured residual biodegradation concentrations and

predicted residual fractions (following HP-β-CD extraction) and hence, they could provide a good prediction for PAHs biodegradation endpoints (Table 6.1).

6.4.1 Three-ring compound bioavailability

In Creo soil, the endpoint of phenanthrene biodegradation (based on bioavailability) was under predicted irrespective of model used (Figure 6.1). Linear regression models 1, 2, and 3 predicted comparable residual phenanthrene concentration (10.5-11.0 mg/kg), however, when model 4 was utilised, the predicted value was in excess of the initial concentration as a consequence of the model's large y-intercept. For TB soil, there was no significant difference between predicted residual phenanthrene concentrations for models 1-4 ($P > 0.05$) and measured residual phenanthrene concentrations following 42 weeks of ENA as a result of the large variability in HP-β-CD extraction. However, in AP soil, prediction of residual phenanthrene concentration using HP-β-CD and the 4 linear regression models resulted in an over prediction of bioremediation efficacy. The residual phenanthrene concentration following 42 weeks of ENA was 98.7 ± 7 mg/kg compared to predicted residual concentrations ranging from 53.4 ± 1-61.9 ± 1 mg/kg.

6.4.2 Four-ring compound

In Creo soil, the endpoint of pyrene biodegradation (based on bioavailable fraction) was under predicted regardless of models utilised (Figure 6.2). Predicted residual pyrene concentrations (137-145 mg/kg) were comparable among 3 linear regression models, however, when linear regression model 4 was used, the predicted value (210.1 ±1 mg/kg) was greater compared to the initial pyrene concentration (137 ±7 mg/kg) as a result of the model's slope (1.38) and y-intercept (8.8).

For TB soil, there was no significant difference between predicted residual pyrene concentrations irrespective of the models (1-4) utilised ($P < 0.05$) and measured residual pyrene concentration over the 42 weeks of ENA as a consequence of high variability in HP-β-CD extractable fractions.

In contrast to Creo and TB soils, HP-β-CD extraction of AP soil resulted in much lower predicted residual pyrene concentrations using linear regression models 1, 2 and 3 (64-68 mg/kg) compared to measure residual pyrene concentration (116 mg/kg). However, when model 4 was utilised, the predicted value was greater compared to the initial pyrene concentration as a consequence of large slope (1.38) and y-intercept (8.8).

Table 6.1. Summary of linear regression models used in this study for predicting residual PAH fractions in Creo, TB and AP soils.

Assigned model #	Extraction method	Biodegradability-Bioavailability linear regression prediction models*(mg/kg)	Comments	R^2	Reference
1	HP-β -CD	$r[PHE]_{bio} = 1.07 \times r[PHE]_{\beta} - 1.01$	Linear regression models were used to predict bioavailability of individual compounds in a variety of PAH contaminated soils.	0.84	Juhasz et al. (2014)
		$r[PYR]_{bio} = 0.88 \times r[PYR]_{\beta} + 4.49$		0.95	
		$r[B(a)P]_{bio} = 1.42 \times r[B(a)P]_{\beta}$		0.95	
2	HP-β -CD	$r[PAHs]_{bio} = 0.94 \times r[PAHs]_{\beta} + 0.17$	Model was used to predict bioavailability of total PAH using manufacturing gas plant soil	0.98	Papadopoulos et al. (2007)
3	HP-β -CD	$r[PHE]_{bio} = 0.98 \times r[PHE]_{\beta} + 0.08$	Linear regression models were used to predict bioavailability of individual compound using blended contaminated soils.	0.97	Hickman et al. (2008)
		$r[PYR]_{bio} = 0.98 \times r[PYR]_{\beta} + 0.45$		0.93	
		$r[B(a)P]_{bio} = 0.78 \times r[B(a)P]_{\beta} + 0.07$		0.83	
4	HP-β -CD	$r[PHE]_{bio} = 0.75 \times r[PHE]_{\beta} + 19.4$	Linear regression models were used to predict bioavailability of individual compound using municipal gas plant soil.	0.95	Hickman et al. (2008)
		$r[PYR]_{bio} = 1.38 \times r[PYR]_{\beta} + 8.8$		0.97	
		$r[B(a)P]_{bio} = 1.8 \times r[B(a)P]_{\beta} + 2.0$		0.98	

* Residual [PAH] following biodegradation = slope x Residual [PAH] following HP-β –CD ± y intercept.

$r[PHE]_{bio}$ = residual phenanthrene concentration following biodegradation; $r(PHE]_{\beta}$ = residual phenanthrene following HP-β –CD extraction

$r[PYR]_{bio}$ = residual pyrene concentration following biodegradation; $r[PYR]_{\beta}$ = residual pyrene fraction following HP-β –CD extraction

$r[B(a)P]_{bio}$ = residual benzo(a)pyrene concentration following biodegradation; $r[B(a)P]_{\beta}$ = residual benzo(a)pyrene fraction following HP-β –CD extraction

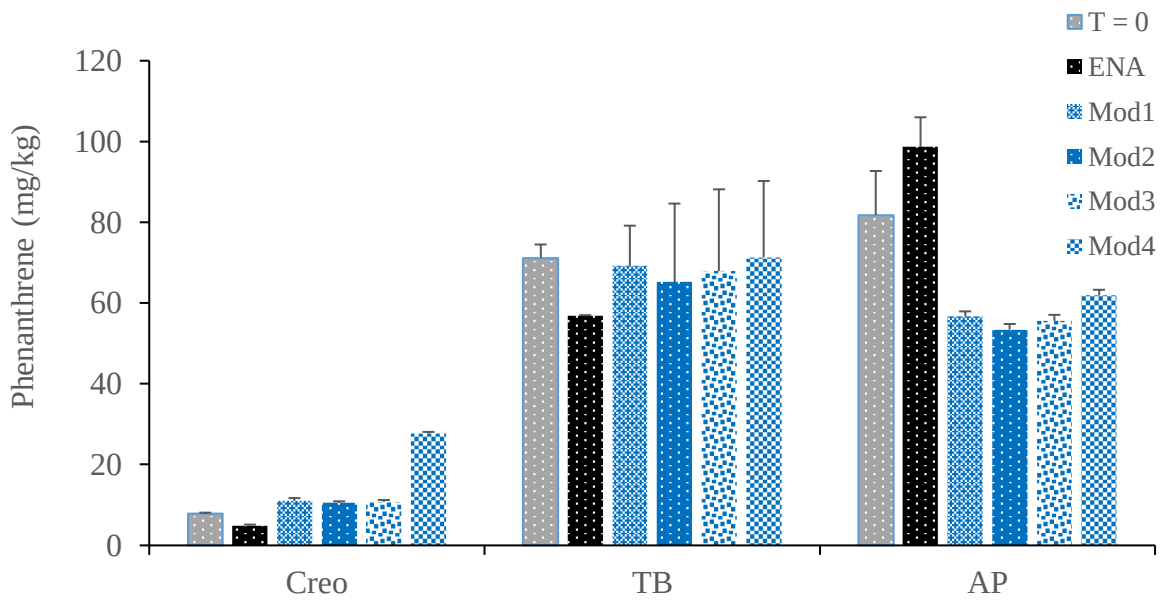

Figure 6.1. Comparison of the predicted residual phenanthrene concentration (determined using HP-β-CD extraction and Mod1 = model 1; Mod2 = model 2; Mod3 = model 3 and Mod4 = model 4) and measured residual phenanthrene concentration (following 42 weeks ENA) in Creo, TB and AP soils. The initial concentration of phenanthrene at the start of biodegradation and bioavailability analysis is also shown. Residual fractions were calculated using four linear regression models as outlined in Table 6.1. Error bars represent the standard error (SE) of duplicate analysis.

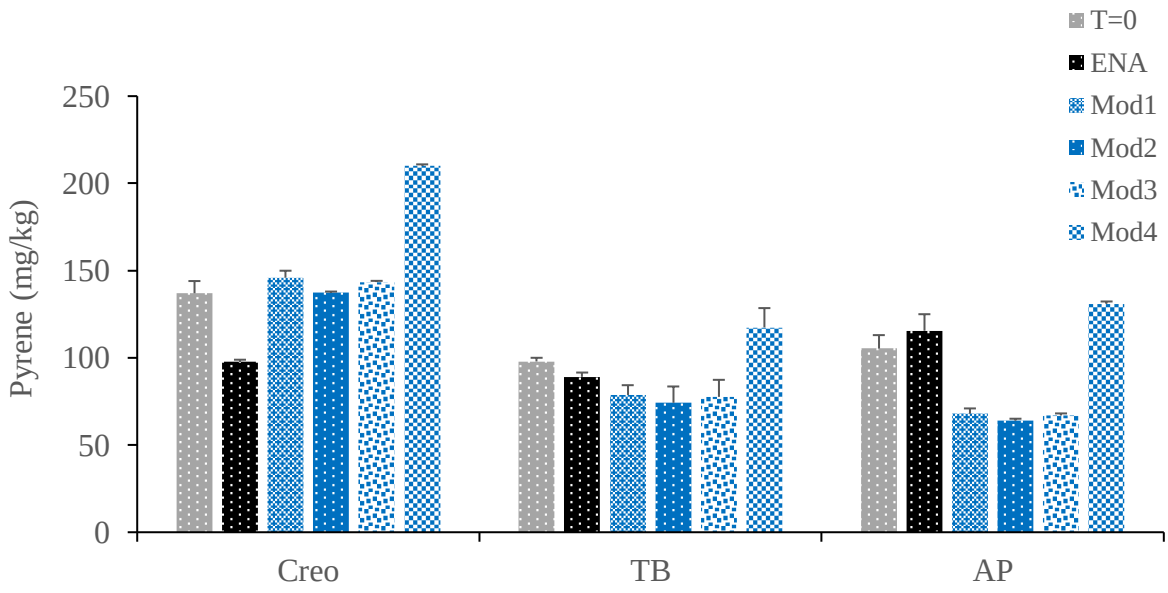

Figure 6.2. Comparison of the predicted residual pyrene concentration (determined using HP-β-CD extraction and Mod1 = model 1; Mod2 = model 2; Mod3 = model 3 and Mod4 = model 4) and measured residual pyrene concentration (following 42 weeks ENA) in Creo, TB and AP soils. The initial concentration of pyrene at the start of biodegradation and bioavailability analysis is also shown. Residual fractions were calculated using four linear regression models as outlined in Table 6.1. Error bars represent the standard error (SE) of duplicate analysis.

Table 6.2. Comparison of predicted residual PAH fractions and measured residual PAH fractions following 42-week incubation period in three aged PAH contaminated soils using four linear regression models outlined in Table 6.1.

		Initial PAH Concentration (mg/kg)	**Final PAH Concentration (mg/kg)**				**Predicted Residual PAH Concentration (mg/kg)**			
Soil	PAH	T = 0	NA	ENA	BioA	Comb	Model 1[a]	Model 2[b]	Model 3[c]	Model 4[d]
Creo	PHE	7.9 ± 0	7.0 ± 1	4.9 ± 0	4.8 ± 0	5.4 ± 0	11.0 ± 0	10.5 ± 0	10.8 ± 0	27.7 ± 0
	PYR	137 ± 7	99.9 ± 1	97.6 ± 1	100.1 ± 7	106 ± 2	145.9 ± 1	137.3 ± 1	143.4 ± 1	210.1 ± 1
	B(a)P	69.5 ±	68.7 ± 0	65.5 ± 2	66.6 ± 1	71.0 ± 2	90.4 ± 4	85.1 ± 4	70.6 ± 3	164.7 ± 7
TB	PHE	71.2 ± 3	67.8 ± 7	56.9 ± 0	62.8 ± 4	50.9 ± 3	69.2 ± 21	65.2 ± 19	67.9 ± 20	71.3 ± 16
	PYR	97.9 ± 2	99.8 ± 4	89.1 ± 3	97.7 ± 3	85.4 ± 6	78.7 ± 10	74.2 ± 9	77.6 ± 10	117.4 ± 14
	B(a)P	48.1 ± 1	60.0 ± 3	54.1 ± 2	56.5 ± 2	51.3 ± 4	100.3 ± 6	94.5 ± 5	78.3 ± 4	202.5 ± 10
AP	PHE	81.8 ± 11	78.5 ± 4	98.7 ± 7	83.1 ± 4	83.1 ± 8	56.7 ± 2	53.4 ± 1	55.6 ± 2	61.9 ± 1
	PYR	105.3 ± 8	108.5 ± 10	115.5 ± 10	102.8 ± 5	102.6 ± 13	67.9 ± 1	63.9 ±	66.9 ± 1	130.9 ± 2
	B(a)P	54.8 ± 1	56.3 ± 3	54.0 ± 5	48.0 ± 3	47.9 ± 7	70.0 ± 3	66.0 ± 3	54.7 ± 2	128.1 ± 6

[a]Model 1: developed using PAH-contaminated soils for predicting individual PAH compound (Juhasz et al., (2014)

[b]Model 2: developed using PAH-contaminated soils for predicting total PAHs residual fractions (Papadopoulos et al., (2007)

[c]Model 3: developed based on soils containing differing, but known, concentrations of diesel, lubricating oil, PAHs and cyanide for predicting individual residual fractions (Hickman et al.,(2008)

[d]Model 4: developed based on PAH-contaminated soils collected from municipal gas plant for predicting individual residual fractions (Hickman et al., (2008).

PAH nomenclature: PHE: phenanthrene, PYR: pyrene, B(a)P: benzo(a)pyrene.

6.4.3 Five-ring compound

The measured biodegradation and predicted residual B(a)P concentrations are presented in Figure 6.3. In Creo soil, the endpoint of B(a)P biodegradation was under predicted regardless of the models used. The predicted residual B(a)P concentration varied markedly (70-90 mg/kg) between models 1, 2 and 3, however, when linear regression model 4 was utilised, the predicted value was 2-fold higher compared to the initial concentration as a result of large variations in the slope of the model. Similar results were observed in TB and AP soils. Although HP-β-CD was not able to accurately predict the endpoint of PAH degradation for all target compounds and all soils, the results suggest that PAH bioavailability was the key limiting factor in Creo, TB and AP soils which contributed to limited efficacy of bioremediation, irrespective of treatment. To put it into perspective, results were similar in all three soils, regardless of bioremediation strategy and linear regression models employed to predict the bioremediation end points.

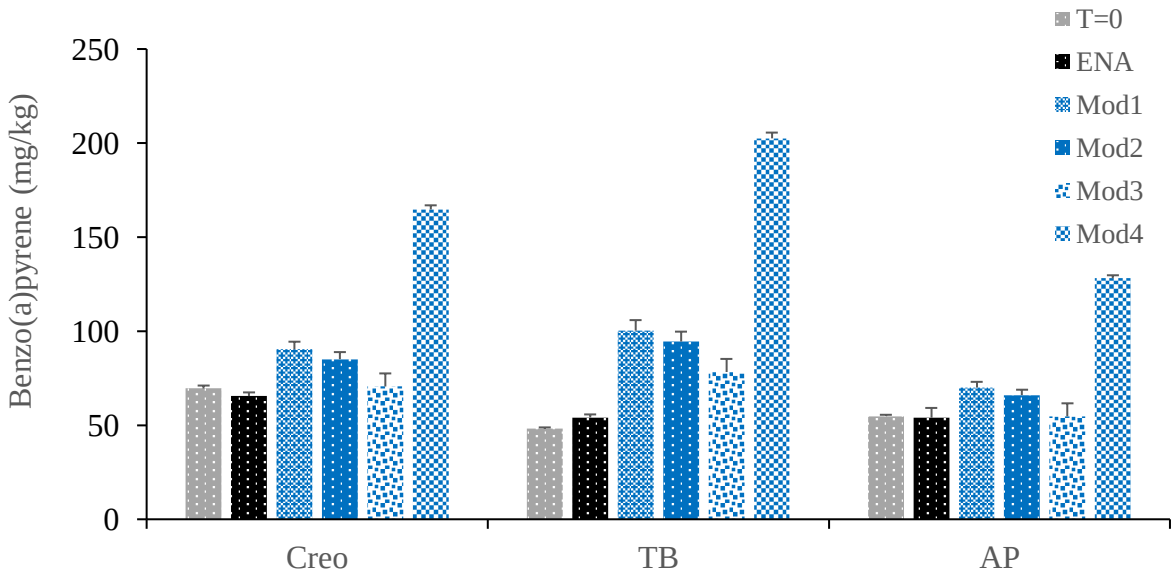

Figure 6.3. Comparison of the predicted residual B(a)P concentration (determined using HP-β-CD extraction and Mod1 = model 1; Mod2 = model 2; Mod3 = model 3 and Mod4 = model 4) and measured residual B(a)P concentration (following 42 weeks ENA) in Creo, TB and AP soils. The initial concentration of B(a)P at the start of biodegradation and bioavailability analysis is also shown. Residual fractions were calculated using four linear regression models as outlined in Table 6.1. Error bars represent the standard error (SE) of duplicate analysis.

6.5 Discussion

The extent to which PAHs are available for microbial degradation is governed by many factors including chemical nature, the PAH concentration and physicochemical properties of the soil (Joutey et al. 2013; Liste & Alexander 2002; Naidu et al. 2008; Nisbet & LaGoy 1992). In addition, HMW PAHs are resistant to microbial attack owing to their low water solubility and the resonance of their molecular structures (Couling, Towell & Semple 2010; Kanaly et al. 2000; Liu et al. 2004; Waszak et al. 2015). In this study, HP-β-CD extraction was utilised to estimate PAH residual fractions in three PAH-contaminated soils to determine whether bioavailability limitations inhibited PAH biodegradation (as observed in chapter 3). The residual fraction of key compounds (phenanthrene, pyrene and B(a)P) in Creo, TB and AP soils was calculated using four HP-β-CD linear regression models selected from the literature (Table 6.1). These linear regression prediction models were utilised to provide estimate of microbial biodegradation endpoints as they have shown strong relationships between measured residual PAH concentrations (following biodegradation) and the predicted residual fraction, determined following HP-β-CD extraction (Table 6.1). As detailed in Table 6.1, all four linear regression models were developed using different PAH contaminated soils, with some soils containing different source materials as described below.

- Linear regression model 1 (Mod1) was developed using 15 PAHs contaminated soils with sum of 16 PAHs ranging from 37.4 to 917 mg/kg. Linear regression analysis for residual PAHs after bioremediation and HP-β-CD extraction demonstrated a strong correlation as exemplified by the goodness of fit (R^2 = 0.84-0.95). These linear regression models were developed for predicting individual PAH biodegradation endpoints.
- Linear regression model 2 (Mod2) was developed using 6 PAH contaminated soils collected from manufactured gas plant sites (27.2-53.2 mg/kg). Analysis of the linear regression model show a strong relationship between PAH bioavailability and biodegradability (R^2 = 0.98). This linear regression model was developed for predicting biodegradation endpoints for all PAHs irrespective of molecular weight.
- The third linear regression model (Mod3) was developed using 4 PAH contaminated soil which were composed following blending of soils containing different concentrations of diesel, lubricating oil, PAHs and

cyanide (5.6-44 mg/kg). Analysis of linear regression models demonstrated a strong bioavailable-biodegradable relationship for these soils as shown by the goodness of fit (R2 = 0.83-0.97). These linear regression models were designed for predicting individual PAH biodegradation endpoints.

- Linear regression model 4 (Mod4) was developed using 4 highly contaminated manufactured gas plant soils (877-2620 mg/kg). Analysis of linear regression models exemplified a strong relationship between residual PAHs following biodegradation and HP-β-CD extraction as demonstrated by the goodness of fit (R2 = 0.95-0.98). These linear regression models were designed for predicting individual PAH biodegradation endpoints in MGP soil.

Although all models exhibit a strong relationship between residual PAH concentration following biodegradation and HP-β-CD extraction, differences are apparent between the slope and y-intercept for each model. As a consequence, when the endpoint of PAH biodegradation was predicted for Creo, TB and AP soil using HP-β-CD extraction and the respective linear regression models, in some cases, predicted values varied considerably (e.g. predicted endpoint for pyrene and benzo(a)pyrene using model 4 compared to models 1, 2, and 3). This may be reflective of the nature of the soils used to develop the models and the robustness of the models driven by number of soils used to derive the relationship. In addition to the effect of soils used to develop each model on residual PAH predicted values, linear regression model 4 prediction resulted in underestimation irrespective of the soils. This may be explained by the elevated concentration of PAHs (877-2620 mg/kg) in the MGP soil used in developing this model compared to models 1, 2 and 3 (5.6-917 mg/kg). Although the model developed using soils with elevanted PAH concentrations may produce larger slope and y-intercept (i.e model 4 was in this category), the undeprediction of PAH biodegradation endpoints can not be explained by such model. However, there are many factors that influence the underprediction of PAH biodegradation. One of the obviouse factors associated with underprediction of PAH is the relationship between biodegradation and bioavailability of PAH. The underprediction of PAH become increasingly refractory in soils with increasing aromatic ring size (i.e 5 and 6 ring PAHs are recalcitrant than 2 and 3 ring PAHs) as a result of high affinity to organic carbon. However, when predicted PAH bioremediation endpoints were compared to measured residual PAH concentrations following 42 weeks of ENA (as detailed in Chapter 3), in most cases, calculated values were either similar (e.g. phenanthrene and pyrene predictions in TB) or higher than biodegradation endpoints (i.e. under-predicted). The variations observed between the

calculated and the biodegradation predicted values may explain the lack of biodegradation in these soils. The lack of contaminant bioavailability would be the obvious reason why no degradation was achieved after applying bioremediation strategy to enhance microbial activity.

Previous studies have illustrated limited degradation of PAH compounds due to a lack of bioavailability as determined by HP-β-CD extraction (Mahmoudi, Slater & Juhasz 2013; Papadopoulos et al. 2007). Factors thought to influence the released of individual compound from the soil matrix included physico-chemical parameters (i.e. dissolution, desorption, diffusion, speciation etc.) and the environment where each pollutant resides. While PAHs may diffuse and be occluded in soil micropores (Northcott & Jones 2001; Semple et al. 2007; Semple, Morriss & Paton 2003), the most prominent retention mechanism for PAHs in soil is via sorption to organic carbon (OC) components with retention influenced by the nature of the OC and the octanol-water partitioning co-efficient of the individual PAH. As proposed by Pignatello and Xing (1995), the retention of PAHs to condensed (glassy) OC domains is stronger than those associated with amorphous (rubbery) domains. The association of PAHs to amorphous OC constitutes the rapid sorption phases, however, as a consequence of the amorphous nature of the OC and the mechanism of PAH-OC association (sorption), this sorbed fraction is also subject to rapid desorption processes (Rhodes, McAllister & Semple 2010; Semple, Morriss & Paton 2003). In contrast, interaction of PAHs with condensed OC domains occurs via adsorption processes (Pignatello & Xing 1995) which demonstrate slow sorption-desorption behaviour. According to Semple et al., (2003; 2007), this fraction may not be extractable following HP-β-CD treatment. In addition, some studies suggest that black carbon is a strong sorbent for PAHs and its occurrence may be responsible for low bioavailability of PAHs (Hussain & Hoque 2015; Lohmann, MacFarlane & Gschwend 2005; Rombolà et al. 2015; Thorsen, Cope & Shea 2004). Lohman et al., (2005), hypothesised that black carbon measured in Boston (0.6%) and New York harbour (0.3%) sediments was responsible for the limited release of PAHs from the sediment matrix. In this work the authors concluded that the overall partitioning was attributed to absorption into organic carbon and adsorption onto the black carbon, which influenced the mobility and bioavailability of PAHs in both harbours. PAHs may also be associated with fulvic acids, humic acids and humin fractions in soil with varying adsorption affinities (Pan et al. 2007). Tang et al.(2008) determined that pyrene associated with humic acid was more available for biodegradation than pyrene associated with humin fractions, however, the diffusion of PAHs into humin fractions may be influenced by soil organic matter (Yang et al. 2010). Even though fulvic acids, humic acids and humin

fractions were not quantified in PAH-contaminated soils used in this study, determination of condensed OC demonstrated that lower PAH bioavailability was associated with soils that contained higher proportions of condensed OC domains in organic matter (i.e.in a range of 2.3 to 13.2%, TB and Creo soils). Other researchers have shown that soot carbon-water distribution co-efficient (K_{SC}) for PAHs were in a range of 35-250 times higher than the corresponding organic carbon co-efficient predictions (k_{OC}) and thus, were closer to theoretically estimated soot-water distribution coefficients (Cornelissen et al. 2005; Thorsen, Cope & Shea 2004). This indicates a stronger association of PAHs to soot carbon compared to organic carbon. The high K_{SC} values may at least reflect the affinity of more hydrophobic PAHs for soot sorbents leading to low bioavailability particularly for HMW PAHs (Lohmann & Feichter 2005). The AP soil in this study falls into this category as it contains large amounts of soot carbon and high SOM contain (Table 3.2). This may have limited the bioavailability of the contaminants leading to negligible degradation in the AP soil following 42 week of incubation.

PAH bioremediation endpoints were over-predicted for phenanthrene and pyrene in AP soil. A number of studies have documented biodegradability of phenanthrene and pyrene by several microorganisms (Anokhina et al. 2004; Cheung & Kinkle 2001; Ghosal et al. 2010; Jain 2014; Liang, Y et al. 2006; Liu et al. 2004; Mrozik & Labuzek 2003; Schippers et al. 2000; Watanabe 2001). Soil microbial catabolic potential to degrade phenanthrene are widespread among the bacterial and fungal community at PAH contaminated sites (Peng et al. 2008). However, Macleod and Semple (2003) reported overestimation of pyrene bioavailability using HP-β-CD extraction compared to bacterial mineralisation in pyrene spiked soils over a 24 week incubation period. Juhasz et al. (2005) also observed the overestimation of the biodegradability of the four-ring compound based on the bioavailable fraction (308 ± 26 mg/kg compared to biodegradable fraction 542 ± 36 mg/kg) in a Creo-contaminated soil.

In this study, both phenanthrene and pyrene degrading orders were identified in all soils as detailed in the previous Chapter, suggesting that there was enormous metabolic potential present to degrade both LMW and HMW PAHs in all 3 soils. However, the lack of PAH biodegradation in AP may not be fully explained by the contaminant bioavailability limitations but may be related to the presence of cyanides that inhibit the biodegradation of PAH compounds. Often, PAH contamination occurs with metals at former manufactured gas plant, wood preservation and industrial plant sites whereby metals (e.g. As, Cd, Pb, Cu, Zn) may potentially inhibit microbial biodegradation (Dixit et al. 2015; Gadd 2000; Thavamani,

Megharaj & Naidu 2013; Thavamani et al. 2012). PAH biodegradation has been shown to be inhibited by metals via interactions with PAH-specific oxygenase enzymes that are involved in PAH metabolism (Thavamani, Megharaj & Naidu 2012). However, in AP soil, metals of concern were present at low concentration which should have been expected to have minimal inhibitory effect on microbial biodegradation.

While metals are frequently detected at most manufacturing gas plant (MGP) sites, there are other chemical classes (by-products/wastes) associated with the management of such site including volatile organic compounds (VOCs), phenolic compounds and complexed cyanide compounds emanating from the coal gasification (Thomas & Lester 1994).There have been some reports illustrating that microbial biodegradation of PAHs may be inhibited by phenol, at concentrations which exceed the toxicity threshold of competent bacterial species (Agarry, Audu & Solomon 2009; Dey & Mukherjee 2010; Okolo et al. 2007).

In a recent study, Dey and Mukherjee et al., (2010) observed an inhibitory effect of phenol on microbial growth at a concentration between 100-700 mg/l. There was no inhibition observed at phenol concentrations below 300 mg/l but a distinct substrate inhibition effect was reported at concentrations above 300 mg/l. This is in agreement with Baja et al (2009), who observed the inhibitory effects of phenol on a mixed microbial culture at concentrations above 300 mg/l. Characterisation of other chemical classes such as phenols and associated intermediate products was not part of the present study. Hence, these chemical classes are believed to be associated with former manufactured gas plant (MGP designated as AP in this study) site such as phenols, cyanide compounds, volatile organic compounds and their associated intermediate by-products, coupled with lack of PAH bioavailability may have impacted the capacity of microbial PAH-biodegradation in this soil. Their presence in AP soil may explain the lack of PAH removal compared to predictions. B(a)P, residual fractions following HP-β-CD extraction were higher in all soils compared to both the initial and measured ENA bioremediation endpoints irrespective of linear regression model utilised. These results suggest that B(a)P bioavailability was limited (negligible) in all soils and that the lack of B(a)P degradation may in part be due to limited bioavailability.

Several studies have reported low five-ring PAH bioavailability in soils (Cornelissen et al. 1998; Huesemann, Hausmann & Fortman 2004; Juhasz, Waller & Stewart 2005; Papadopoulos et al. 2007) determined by HP-β-CD extraction due to the strong retention of 5 ring PAHs to OC (black carbon) as a consequence of their $k_{ow.}$ In a recent study, Mahmoudi et al. (2013) observed less than 10% of the five-ring compounds for all soils tested was extractable using

HP-β-CD assays. However, the lack of degradation of B(a)P in the three soils used in this study may also be explained by the recalcitrance of HMW PAHs to microbial attack.

6.6 Conclusion

Irrespective of the variability observed in predicting the endpoints of PAH biodegradation, PAH bioavailability was low in Creo, TB and AP soil, which presumably limited PAH biodegradation. In addition, for AP soil biodegradation of phenanthrene and pyrene may have been constrained as a consequence of MGP by-products that inhibited biodegradation. As a consequence, to enhance the effectiveness of bioremediation in these soils, alternative strategies may need to be implemented. The following chapter will investigate whether the implementation of alternative bioremediation strategies may overcome the limited PAH degradation observed in chapter 3, primarily as a result of bioavailability constraints. Alternative bioremediation strategies to overcome limited bioavailability include: (1) Tween 20 (surfactant) application to enhance PAH bioavailability; (2) the addition of sodium succinate (carbon source) to prime or stimulate the growth of native microorganisms and/or to increase soil metabolic enzymatic activity and (3) pre-treatment using a chemical oxidation (H_2O_2) strategy to mitigate of recalcitrant compounds hindering biological degradation.

Chapter 7

Effect of the addition of surfactant, carbon source and chemical oxidation on the bioremediation of PAHs in contaminated soil.

7.1 Introduction

A major limitation for PAH bioremediation is the bioavailability of the contaminant to PAH degrading microorganisms. Numerous studies have shown that PAH bioremediation efficacy is reduced by factors that limit the bioavailability of the target compound. Weissenfels et al. (1992) observed no degradation of PAHs following inoculation of soil with a known PAH-degrading bacteria (*Vibrio fisheri*) in an experiment prepared using coking plant soil. Nevertheless, significant degradation of PAHs was achieved when PAHs were extracted and placed back into soil matrix. Similarly, Erickson et al. (1993) reported no degradation of PAHs after soil collected from manufacturing gas plant was bioaugmented with a known PAH-degrading bacteria presumably to enhance PAH degradation.

Strategies have been developed that enhance the bioavailability of PAHs thereby providing a mechanism for improving bioremediation efficacy. Surfactants have been demonstrated to enhance PAHs bioavailability by increasing their solubility and dissolution rates in aged PAH-contaminated soils (Cébron et al. 2013; Franzetti et al. 2010; McElroy, Farrington & Teal 1989; Peng et al. 2008; Zhang, Zhu & Li 2013). In a study by Rodrigues et al. (2013), fluoranthene (1.10 – 2.51 mg/L) and anthracene (0.19 – 0.86 mg/L) removal rates were increased following the addition of surfactant (Tween20) at a concentration of 0.08 mM (1.3 times the surfactant's critical micelle concentration) after 18 h incubation. They concluded that the application of the surfactant enhanced PAH removal efficiency by increasing their desorption from the soil. Similar results were obtained by Zhu et al. (2010) after treating PAH contaminated soil with surfactant (Brij 30 with CMC of 10 mg/L in water) at doses below (5 mg/g corresponded to 0.8 mM), slightly above (20 mg/g corresponded to 2.4 mM) or well above (50 mg/L corresponded to ~ 97 mM) the Brij 30 critical micelle concentration. Zhu et al .(2010) concluded that the addition of Brij 30 enhanced biodegradation of fluoranthene and anthracene at the two lower doses (0.8 and 2.4 mM) after 18 days primarily by increasing PAH desorption from bioreactor-treated soil (15-20%). However, surfactant addition may result in biodegradation limitations including competitive degradation of an alternative carbon source by indigenous microflora (González et al. 2011; Zhu & Aitken 2010); disruption of bacterial cell membranes due to

toxicity effects (Zhang, Zhu & Li 2013); and the affinity (Ahangar 2010) for soil sorption of surfactants leading to reduced bioavailability effects.

Other strategies may be utilised to overcome biological constrains such as pre-treatment with chemical oxidation. According to Ferrarese et al. (2008), chemical oxidation involves the application of chemical reactant to enhance the formation of highly reactive radicals with the ability to mineralise even the most recalcitrant compound (i.e compound with 5 rings and more). PAHs in contaminated soil have been shown to be rapidly oxidised through the addition of hydrogen peroxide (Agarry 2012; Ferguson et al. 2004; Goi, Trapido & Kulik 2009; Tsai et al. 2009). A combination of biodegradation and chemical oxidation strategies have resulted in fast and efficient PAH removal since chemical oxidation byproducts are potentially soluble and available for microbial biodegradation (Nam, Rodriguez & Kukor 2001). In a study conducted by Nam et al. (2001), degradation of PAHs from manufactured gas plant (MGP) soil by active bacteria enriched from the same soil was observed. Approximately, over 80% of low molecular weight degraded (LMW) and between 20-40% of high molecular weight PAHs transformed after four-week period. However, rapid removal of LMW (more than 98%) and HMW (75-85%) PAHs was observed by combining biodegradation with Fenton's treatment. For this apporach, the authors combined biodegradation with Fenton-type reaction (hydrogen peroxide oxidation) to promote bacterial degradation in a former MGP soils. Similar results were observed by Goi et al. (2009) after PAH contaminated soils were treated with hydrogen peroxide. One advantage of applying Fenton-like oxidation for contaminant oxidation is the potential release of oxygen during the decomposition of H_2O_2, which would increase oxygen concentration (Ferguson et al. 2004). Therefore, this may have a significance effect on the aerobic biodegradation of pollutants as the presence of oxygen may enhance microbial activities or may impact the organisms.

In previous chapters, the impact of PAH bioavailability on bioremediation efficacy was illustrated. The limited PAH removal in Creo, TB and AP soils was attributed to low PAH bioavailability as determined using HP-β-CD extraction (chapter 6). Analysis of PAH degradation indicated that the amendment regime such as the addition of nutrient, inoculum or combination of these treatments resulted in a negligible reduction in total PAH concentration in Creo, TB and AP soil after a 42-week period. In an attempt to overcome this bioremediation limitation, additional treatment strategies were applied to Creo soil microcosms. Creo soil was chosen over the other soils based on: (i) the initial (1017.5 ± 23 mg/kg) and the remaining

(905.1 ± 23 mg/kg) total PAH concentrations after a 42-week incubation period. There was a negligible reduction in total PAH concentration observed in Creo soil although no critical difference compared to TB and AP soils based on treatability studies (see chapter 3); (ii) the initial key individual PAH compounds (pyrene and benzo(a)pyrene) were detected at an elevated concentrations (177 ± 2 and 68 ± 6 mg/kg) in Creo soil and (ii) since PAH bioavailability was a key factor limiting efficacy of bioremediation in all soil (see chapter 6) after a 42-week incubation period. Additional treatment strategies to overcome bioremediation limitations included:

- Surfactant addition (Tween 20): a surfactant was added at 1% loading solution based on 60% water holding capacity (228 µl of Tween 20 solution). In this microcosm, the addition of Tween 20 (T_{20}) may increase the solubility of PAHs and potentially increase their bioavailability for microbial biodegradation. The choice of lower Tween 20 concentration (reported as critical micelle concentration) used in the study was based on the results of the study conducted by Rodrigues et al (2013). Rodrigues et al (20013) evaluated the effect of Tween 20 concentration on PAH biodegradation at a dose lower and above the surfactant's critical micelle concentration (i.e. to 0.04 and 0.08 mM compared to Tween 20 with CMC of 0.06mM). The authors observed increased biodegradation rate in fluoranthene and with result showing the highest biodegradation rate in anthrance with Tween 20 at concentration of 0.08 mM. This result came as a result of effective solubility of target contaminant at this concentration. The surfactant is a molecule composed of a hydrophilic head group and hydrophobic tail with the ability to increase solubility and dissolution of PAHs or by enhancing mass transfer of hydrophobic contaminants from the solid into the aqueous phase by reducing interfacial tension.
- Addition of an alternative carbon source (succinate): sodium succinate was supplied to Creo soil by dissolving 2 g of sodium succinate powder in 22.8 ml to achieve a 1% soil solution concentration based on 60% water holding capacity of field soil. Addition of sodium succinate was intended to enhance the degradation of PAHs by microbial community through selective stimulation of PAH-degrading organisms and induction of PAH metabolism. In this treatment, supplementation of sodium succinate may enhance

biodegradation of PAHs by stimulating growth of both PAH-degrading organisms and induction of soil enzymatic activity.

- Chemical oxidation pretreatment (hydrogen peroxide): addition of a strong oxidant to Creo slurry treatment soil may be an effective chemical strategy to overcome the limitation of biodegradation. Chemical oxidation was performed by adding 200 g of contaminated soil stepwise to a 5 L beaker containing 912 ml of H_2O_2 to achieve 20% aqueous solution concentration dosage based on 60% water holding capacity. The H_2O_2 aqueous solution concentration of 20% use in this study was chosen based on the findings of chemical oxidation conducted by Palmroth (2006), in which higer bacterial survival and faster regrowth was observed at 12% H_2O_2 than 30% due toxicity.
- To evaluate the effectiveness of these additional treatment strategies (T_{20}, H_2O_2 and SS) besides natural attenuation and enhanced natural attenuation microcosms, which were set up using Creo soil obtained after a 42-week incubation period (Exp 1). In the final experiment, both NA and ENA microcosms were set up with left over soil from the same treatments obtained at the end of first microcosms but moisture and nutrient were adjusted.

In addition to determining the impact of treatment strategy on PAH concentration, metagenomics analysis was undertaken to assess changes in microbial community structure and functionality as a result of the alternative treatment strategies.

7.2 Aims

The overarching aim of this study was to investigate whether the addition of an alternative carbon source (sodium succinate), the addition of a surfactant (Tween 20), or pre-treatment of the contaminated soil by chemical oxidation (hydrogen peroxide) increased the bioavailability of PAHs, and/or increased removal of the target compounds.
More specific objectives were:

- To examine the degradation of three (phenanthrene), four (pyrene) and five (B(a)P) ring PAH compounds in Creo soil over the course of the incubation period.
- To compare the overall changes in total PAH concentration in Creo soil following the addition of soil amendments.

- To monitor if supplementation of surfactant, carbon source and chemical oxidation influenced soil microbial diversity and functional profiles.

7.3 PAH remediation in Creo soil microcosms

Soil from the initial microcosm study (see chapter 3) was used to prepare microcosms using alternative treatment strategies as detailed in Section 2.16. During the 28-day incubation period, changes in PAH concentration (PHE, PYR and B(a)P) in samples obtained from unamended (NA) and amended (ENA) microcosms and alternative microcosms, treated with hydrogen peroxide (H_2O_2), sodium succinate (SS) and Tween 20 (T_{20}) was determined as presented in Figures 7.1 to 7.4. Figure 7.1 displays changes in total PAH concentration in unamended and amended microcosms over the 28-day incubation period. Although there was some variability in PAH concentration at day 14, there was no difference in total PAH concentration in NA, ENA, SS and T_{20} microcosms from day 0 to day 28. Similarly, for key individual compounds (PHE, PYR and B(a)P), there was no significant difference ($P < 0.05$) observed over the 28-day incubation period.

However, in microcosms pre-treated with hydrogen peroxide (chemical oxidation), the initial PAH concentration was rapidly reduced within 90 mins from 654 ± 5 mg/kg to 181 ± 4 mg/kg. Similarly, for key individual compounds (PHE, PYR and B(a)P), the initial concentration was reduced from 4.5-2.1, 64.5-20.9 and 52.7-6.5 mg/kg following treatment respectively (53.9, 67.6 and 87.7%). However, residual PAH concentrations remained stable over the remaining 28-day incubation period.

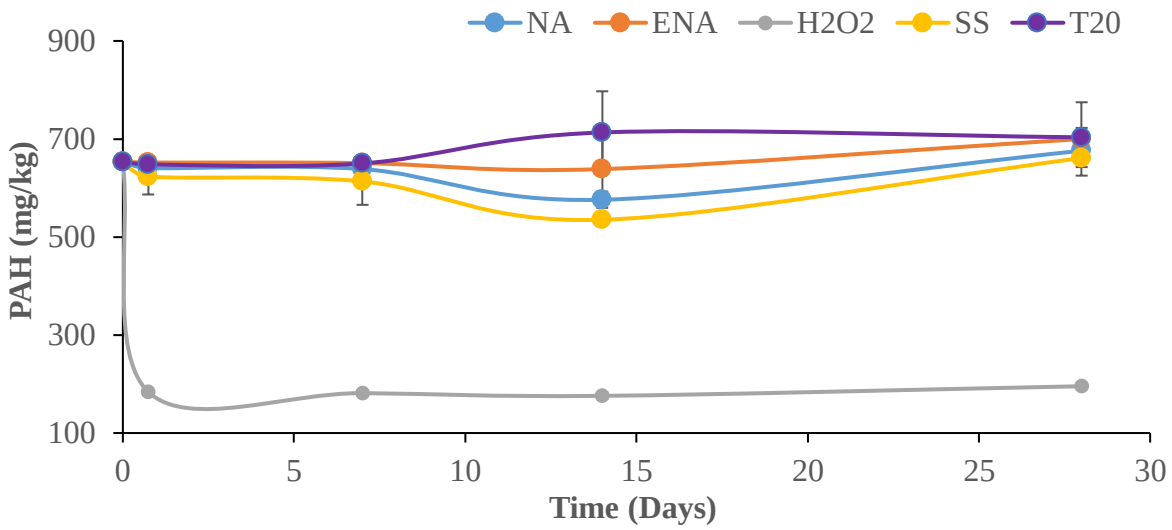

Figure 7.1. Change in total PAH concentration in Creo contaminated soil following 28 days incubation using natural attenuation (NA), enhanced natural attenuation (ENA), sodium succinate (SS), hydrogen peroxide (H_2O_2) and Tween 20 treatments (T20).

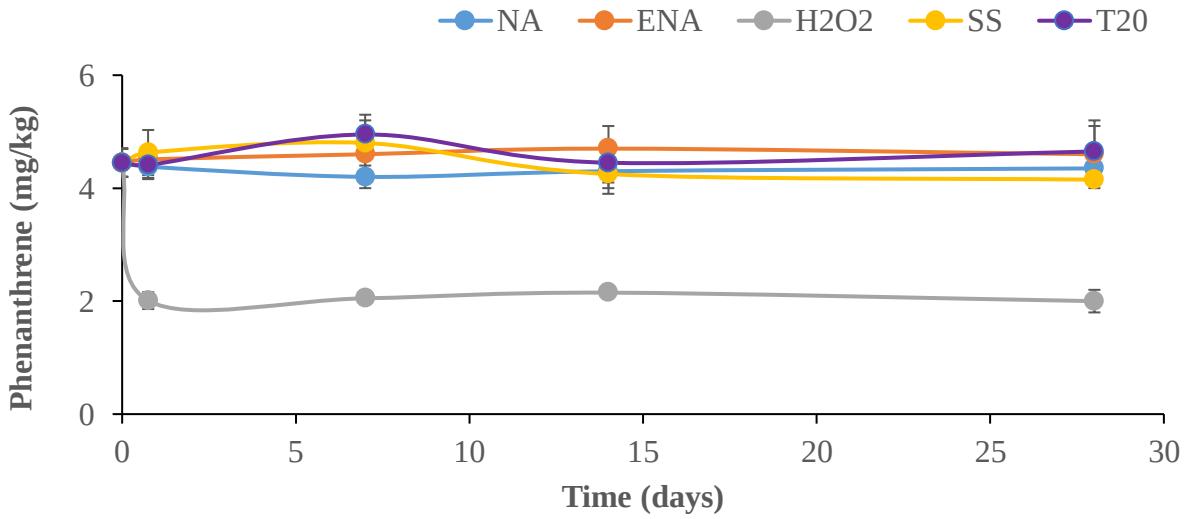

Figure 7.2. Change in phenanthrene concentration in Creo soil following 28 days incubation using natural attenuation (NA), enhanced natural attenuation (ENA), sodium succinate (SS), hydrogen peroxide (H_2O_2) and Tween 20 treatments (T20).

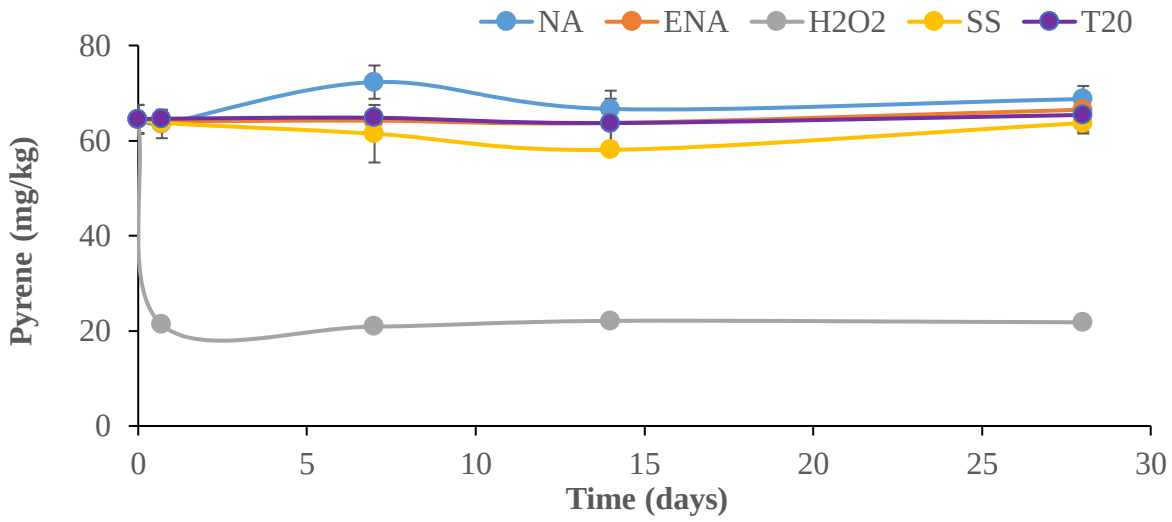

Figure 7.3. Change in pyrene concentration in Creo soil following 28 days of incubation using natural attenuation (NA), enhanced natural attenuation (ENA), sodium succinate (SS), hydrogen peroxide (H_2O_2) and Tween 20 treatments (T20).

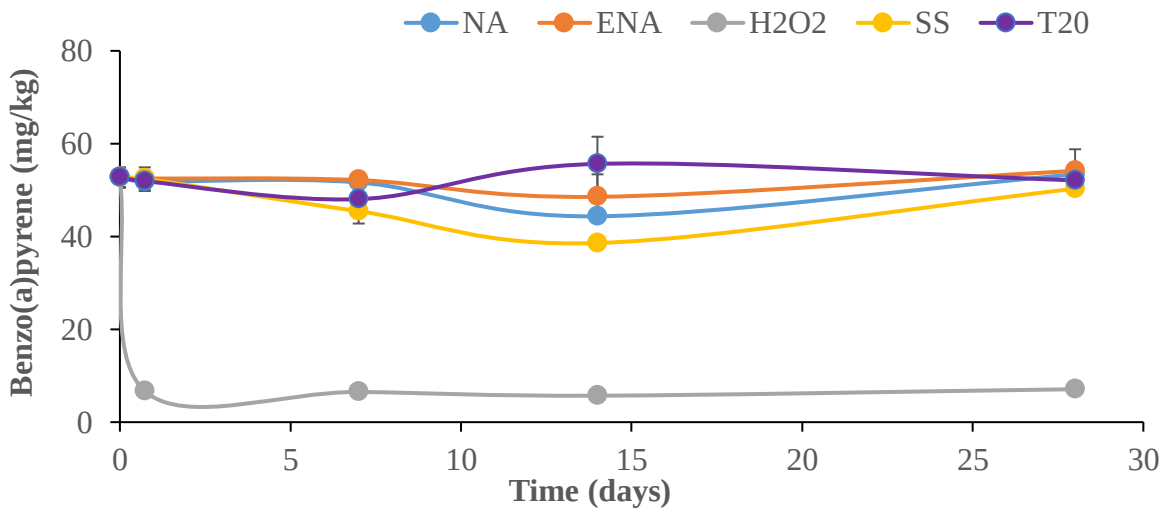

Figure 7.4. Change in benzo(a)pyrene concentration in Creo soil following 28 days incubation using natural attenuation (NA), enhanced natural attenuation (ENA), sodium succinate (SS), hydrogen peroxide (H_2O_2) and Tween 20 treatments (T20).

7.4 Assessment of PAH-degrading microorganisms using next generation sequencing technology (NGS) in alternative Creo soil microcosms

7.4.1 Taxonomic analysis at the domain level in unamended microcosms (NA)

Similar to metagenomic analysis undertaken in chapter 5, samples from alternative Creo microcosms were analysed for their taxonomic classification at three hierarchical levels including domain, phylum and order using the M5NR database. A total of 5, 922, 929 reads were established with an average read length of 168 bp based on MG-RAST annotation.

The proportion representing each domain was calculated as the relative abundance of the total hits (Figure7.5 i). Analysis of taxonomic profiles at the domain level in metagenomes sampled from alternative Creo soil microcosms demonstrated prevalence of two taxa (relative abundance > 1%) bacteria and unassigned sequences. The domain prokaryote (mainly bacteria) was assigned the majority of these reads (83.5% of sequences) in metagenomes obtained at day 0. The remaining reads were assigned to unassigned sequences (15.1%), eukaryote (1%) and other domains (archaeal, viruses and other sequences) constituted less than 1% of total hits at the beginning of the experiment.

Other metagenomics datasets (day 14 and 28 metagenomes) were compared to day 0 taxonomic organisms' distribution at the domain level. However, no significant changes were observed in the relative abundance of all domains including bacteria (79.4 and 80.1%), eukaryote (1.8 and 2.0%), unassigned sequences (18.3 and 17.4%) and other (0.5 and 0.5%) in metagenomes sampled at days 14 and 28 respectively (Figure 7.5 parts (ii) and (iii)).

The incubation of ENA microcosms, resulted in an increase in the relative abundance of the domain bacteria from 83.3-98.3% of the total organisms (from day 0 to day 14) as demonstrated in Figure 7.5 part (iv). There were no significant changes observed in the relative abundance of all domains including bacteria (98.3 and 95.1%), eukaryote (1.8 and 20%), unassigned sequences (15.1 and 17.4%) and other (0.4 and 0.4%) in metagenomes sampled at days 14 and 28 respectively (Figure 7.5 parts (iv) and (v).

Figure 7.5 (parts vi and vii) shows the proportion of each taxonomic distribution determined in sequences obtained from microcosms pre-treated with hydrogen peroxide (chemical oxidation). The relative abundance of bacteria in metagenomes sampled from microcosms pre-treated with hydrogen peroxide fluctuated over the 28-day incubation period. Notably, bacterial

relative abundance increased from day (83.5%) 0 to day 14 (97.9%), then declined at day 28 (86.3%). In contrast, a 13-fold increase was observed in sequences assigned to eukaryotes at the end of the incubation period (1.0 to 13.2%). Other domains classified as others (virus, archaeal and others) were present at constant low abundance. The relative abundance of sequences related to unassigned domains present in metagenomes sampled from day 0 (15.1%) were less than 1% of the total relative abundance at both time points (days 14 and 28).

Similarly, in microcosms where sodium succinate was supplied, the relative abundance of the domain bacteria progressively increased from day 0 to day 28 (83.5-98.2 %) as shown in Figure 7.5 parts viii and ix. Other domains were present at low abundance except the relative abundance related to unassigned sequences, which was less than 1% in metagenomes sampled at days 14 and 28 (Figure 7.5 viii and ix).

In the Tween 20 treatment, there was no analysis performed on samples obtained at day 14 due to issued surrounding genomic DNA extraction failure. Many attempts were made to isolate DNA but was unsuccessful and therefore a decision was made to compare metagenomes from day 0 and day 28 in T_{20} microcosm. Similar results were observed in microcosms amended with Tween 20 to H_2O_2 metagenomes, with bacterial relative abundance increasing from day 0 to day 28 (83.5–92.4%). At day 28, the relative abundance of eukaryotes increased 7-fold when compared to day 0 (1.0 – 7.0%)

In addition, the relative abundance of sequences annotated to other (archaeal, viruses and other) increased at day 28 (Figure 7.5 part x), however, there was no significant difference observed when compared to day 0. In contrast, a significant shift was observed in the relative abundance of sequences related to unassigned domains from day 0 to day 28 (15.1 - <1%) respectively. The reduction in the relative abundance of unassigned sequences correspond with the increase observed in the domains bacteria, eukaryotes and other over the 28 day incubation period.

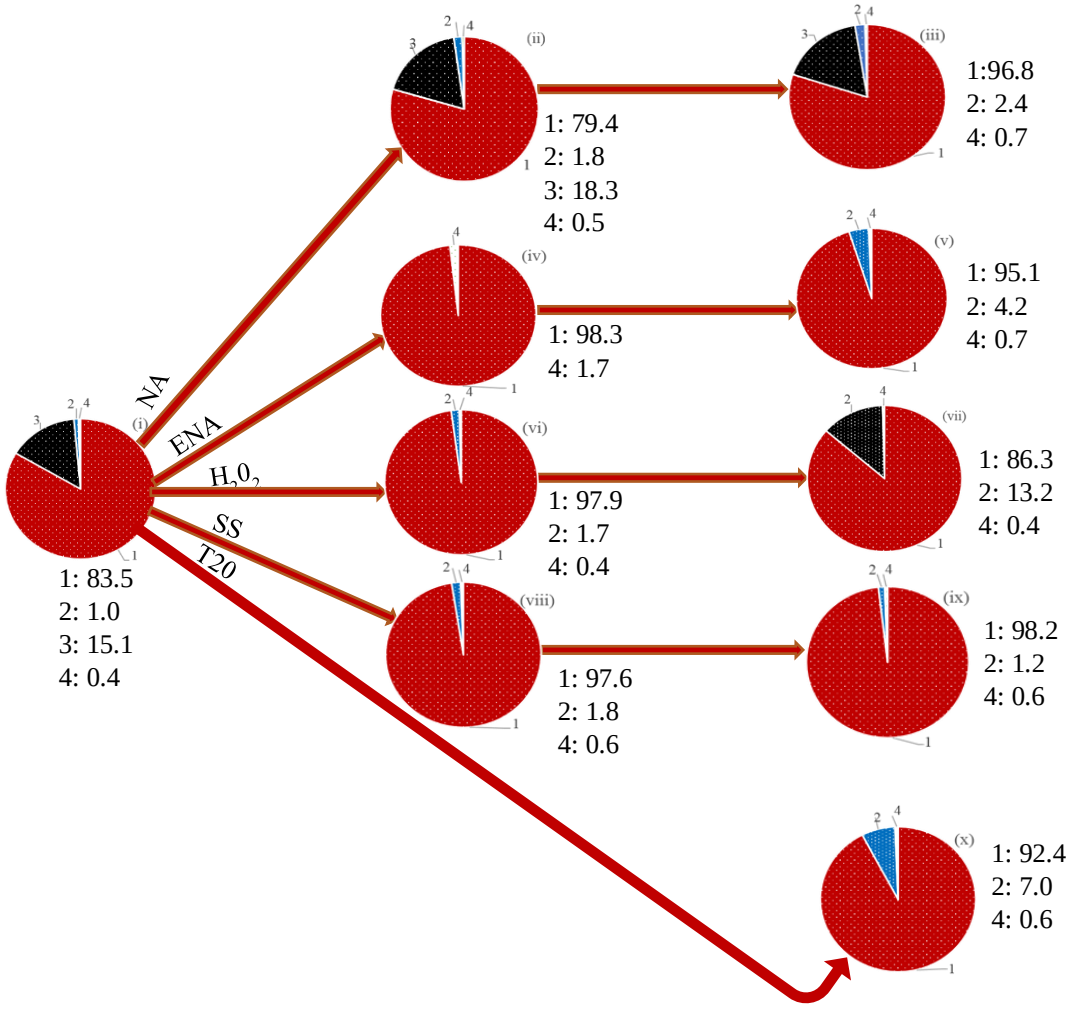

Figure 7.5. Distribution of taxonomic domain determined in sequences obtained from natural attenuation microcosms at (i) day 0, (ii) day 14), (iii) day 28), enhanced natural attenuation at (iv) day 14, (v) day 28, hydrogen peroxide at (vi) day 14, (vii) day 28), sodium succinate at (viii) day 14, (ix) day 28 and Tween 20 at (x) day 28) metagenomes sampled from Creo alternative soil microcosms. The relative abundance of each taxonomic group was calculated as a percentage of total organisms in the metagenomic sample. Labels are shown for those domains where abundance percentages were greater than 1% of total organisms; 1: bacteria; 2: eukaryote; 3: unassigned sequences; 4: other (viruses and other sequences).

7.4.2 Taxonomic analysis at the phylum level

Bacterial distribution at phylum level at the beginning of microcosm studies produced 29 distinctive phyla in unamended microcosms (Figure7.6 i). Several phyla were detected at varying proportions as demonstrated by their relative abundances in Table 7.1. The majority of these phyla (19) were individually represented by <1% of all assigned hits while their combined relative abundance was 4.1% of the total hits at day 0. At the phylum level, MG-RAST annotation of bacterial sequences demonstrated that Proteobacteria and Acidobacteria were the prevalent taxa, with 76.1% and 9.8% of assigned hits belonging to these phyla. Other prominent phyla present over 1% relative abundance included Actinobacteria (6%), Firmicutes (2.2%), and Bacteroidetes (1.7%).

At days 14 and 28, NA microcosms demonstrated diversified taxonomic phylogenetic groups, with a total of 28 phyla detected at each time point. Eight phyla had relative abundances greater than 1%, with Proteobacteria being the most abundance phylum at days 14 (51.7%) and 28 (53.7%) despite significant reduction compared to the initial abundance (Figure7.6 parts ii and iii). The decrease in abundance of Proteobacteria corresponded with a 2-fold increase in the abundance of the phylum Acidobacteria (9.8 – 22.6 and 20.7%) at days 14 and 28 respectively. While other phyla were detected at low abundance, four distinctive phyla with relative abundances over 1% were observed including Verrucomicrobia, Cyanobacteria, Planctomycetes and Chloroflexi at days 14 and 28 although the Chloroflexi was less than 1% at day 28.

In microcosms where an ENA strategy was implemented, the number of taxonomic phylogenetic groups with over 1% relative abundance at days 14 and 28 were similar to the initial diversity observed at day 0 (Figure 7.6 parts iv and v). The ENA microcosm resulted in a negligible increase in the relative abundances of Proteobacteria (76.1-84.9%), Acidobacteria (9.8-10.3%), Actinobacteria (6.0-7.6%) and Firmicutes (2.2-2.6%) from day 0 to day 14. However, extended incubation (day 14 to day 28) resulted in a 4-fold increase in the relative abundance of Firmicutes (2.6-10.2%), with a corresponding 10- and 6-fold decrease in the relative abundances of phylum Acidobacteria (9.8-1%) and Actinobacteria (6.0-<1%) respectively. Other phyla including Verrucomicrobia, Cyanobacteria, Plantctomycetes and Chloroflexi, classified as other in the ENA microcosm, had relative abundances <1% of the total hits compared to NA microcosms.

In microcosms pre-treated with H_2O_2, bacterial distribution at phylum level produced 28 distinctive phyla at days 14 and 28 compared to day 0 (29 phyla) as depicted in Figure 7.6 parts (vi) and (vii). Sequences related to Proteobacteria and Firmicutes increased by 8.8 and 7.9 % from day 0 to day 14 following treatment and incubation.

In contrast, sequences annotated to Acidobacteria (9. 8-<1%) and Actinobacteria (6.0-<1%) decreased from 0 to day 14 (Table 7.2). Overall, the relative abundances of Proteobacteria, Actinobacteria, and Firmicutes were stable over the remaining incubation period, while the relative abundance of Acidobacteria was less than 1% of the total organisms at the end of the incubation period (day 28). Notably, the reduction in the relative abundances of Acidobacteria and Actinobacteria were greater in microcosms treated with hydrogen peroxide compared to NA and ENA microcosms.

For microcosms amended with sodium succinate, analysis of phylogenetic groups determined in samples obtained at days 14 and 28 yielded 28 distinctive phyla (Figure7.7 parts iv and v). A 14.8% increase was observed in the relative abundance of Proteobacteria following the addition of sodium succinate and incubation from day 0 to day 14. Proteobacteria relative abundance decreases by approximately a similar percentage (13.6%) at day 28. An increased as observed in the relative abundance of Bacteriodetes following the addition of sodium succinate over the 28-day incubation period (1.7-15.8%).

In contrast, sequences related to Acidobacteria (9.8- <1%) and Actinobacteria (6.0-2.2%) decreased from day 0 to day 14. In addition, supplementation of sodium succinate resulted in fewer phyla (4 phyla) with relative abundance greater than 1% of total organisms compared to NA microcosms (8 phyla) at days 14 and 28. Similar results to sodium succinate supplemented microcosms were observed in microcosms amended with Tween 20 over the 28-day incubation (Figure 7.8 (vi) and Table 7.1).

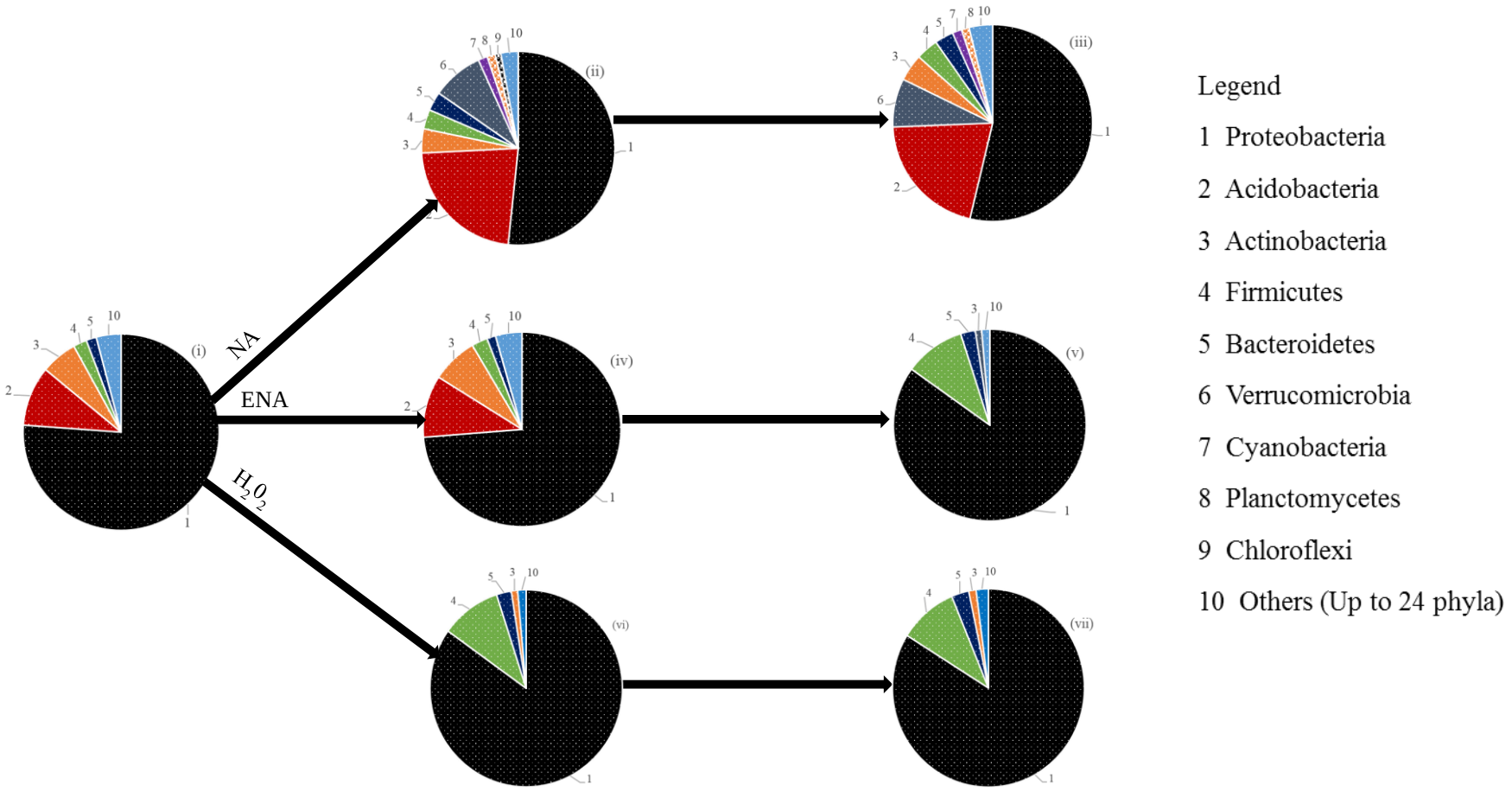

Figure 7.6. Distribution of taxonomic phylogenetic groups determined in sequences obtained from natural attenuation microcosms at (i) day 0, (ii) day 14, (iii) day 28, enhanced natural attenuation microcosms at (iv) day 14, (v) day 28, hydrogen peroxide microcosms at (vi) day 14, and (vii) day28 metagenomes sampled from the Creo soil microcosms. The relative abundance of each taxonomic group was calculated as a percentage of total organisms in the metagenomic sample. Labels are shown for those phyla where abundance percentages were greater than 1% of total organisms, while percentage abundance values are presented in Table 7.1

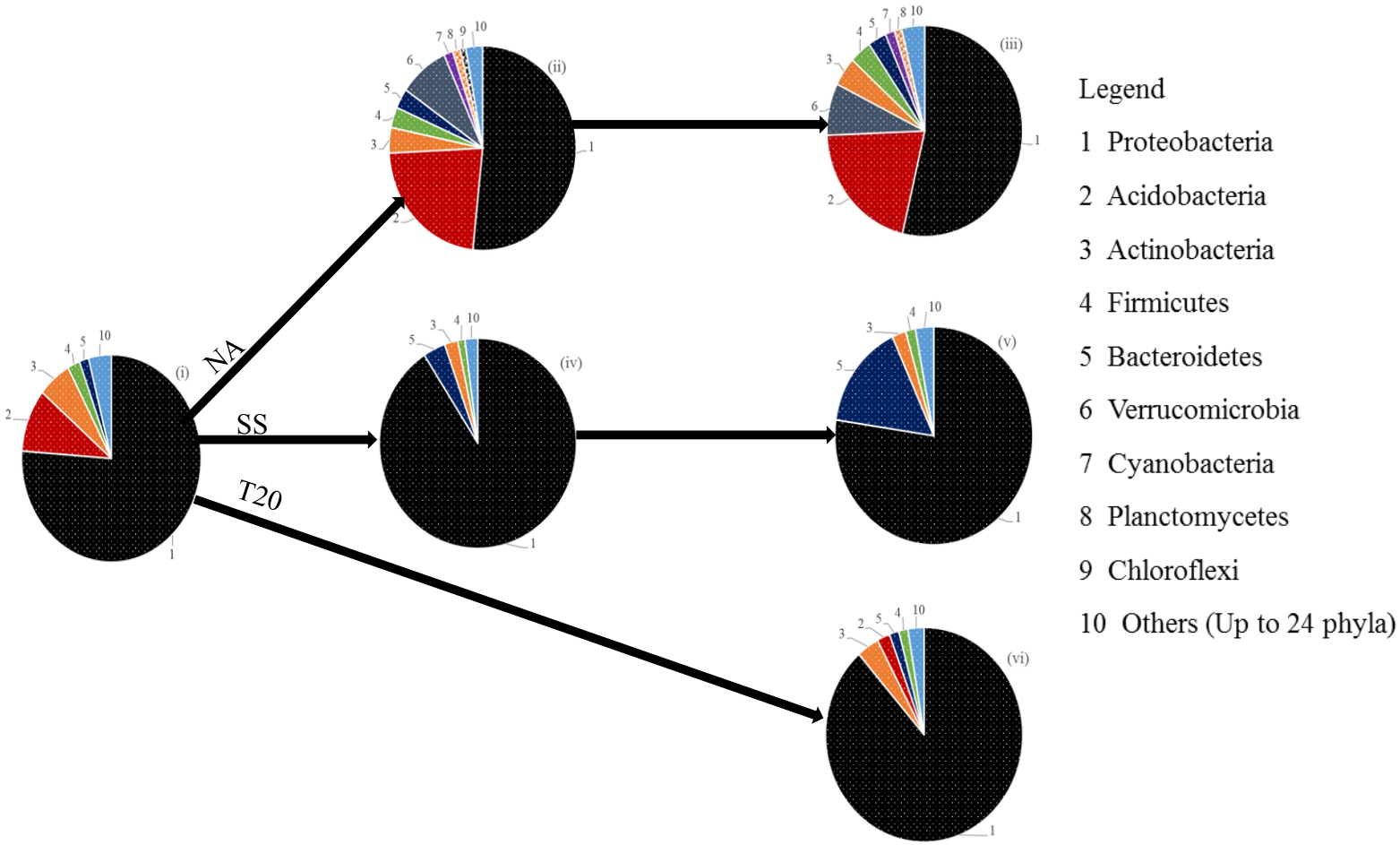

Figure 7.7. Distribution of taxonomic phylogenetic groups determined in sequences obtained from natural attenuation microcosms at (i) day 0, (ii) day 14, (iii) day 28, sodium succinate microcosms at (iv) day 14, (v) day 28 and Tween 20 microcosms at (vi) day 28 as a percentage of total organisms in the metagenomic sample. Labels are shown for those phyla where abundance percentages were greater than 1% of total organisms, while percentage abundance values are presented in Table 7.1.

Table 7.1. Taxonomic bacterial composition at the phylum level in Creo soil metagenomes obtained from microcosms incubated under natural attenuation (NA), enhanced natural attenuation (ENA), sodium succinate (SS), hydrogen peroxide (H_2O_2) and tween 20 treatments (T_{20}). Values shown are for those phyla where abundance percentages were greater than 1%.

Legend	Phylum	Treatment, time (days) and relative abundance percentage compositions (%)														
		NA			ENA			H_2O_2				SS			T_{20}	
		0	14	28	0	14	28	0	2	14	28	0	14	28	0	28
1	Proteobacteria	76.1	51.7	53.7	76.1	73.7	84.9	76.1	84.6	84.9	83.9	76.1	90.9	77.3	76.1	77.3
2	Acidobacteria	9.8	22.6	20.7	9.8	10.3	*	9.8	*	*	*	9.8	*	*	9.8	*
3	Actinobacteria	6.0	4.0	4.4	6.0	7.6	1.1	6.0	4.8	1.1	1.2	6.0	2.2	2.3	6.0	2.3
4	Firmicutes	2.2	3.2	3.6	2.2	2.6	10.2	2.2	8.5	10.1	9.9	2.2	1.2	1.6	2.2	1.6
5	Bacteroidetes	1.7	3.2	3.0	1.7	1.4	2.5	1.7	2.3	2.5	2.9	1.7	3.7	15.8	*	15.8
6	Verrucomicrobia	*	8.6	8.0	*	*	*	*	*	*	*	*	*	*	*	*
7	Cyanobacteria	*	1.5	1.5	*	*	*	*	*	*	*	*	*	*	*	*
8	Planctomycetes	*	1.4	1.3	*	*	*	*	*	*	*	*	*	*	*	*
9	Chloroflexi	*	1.0	*	*	*	*	*	*	*	*	*	*	*	*	*
10	Others	4.1[a]	2.9[b]	3.8[c]	4.1[a]	4.3[d]	1.4[e]	4.1[a]	1.3[f]	1.4[g]	2.1[h]	4.1[a]	2.1[i]	3.0[j]	4.1[a]	3.0[k]

*percentages below 1% of the total organisms.

[a] 'other' represented 24 phyla each representing <1% of the total abundance

[b] 'other' represented 19 phyla each representing <1% of the total abundance

[c] 'other' represented 20 phyla each representing <1% of the total abundance

[d] 'other' represented 24 phyla each representing <1% of the total abundance

[e] 'other' represented 28 phyla each representing <1% of the total abundance

[f] 'other' represented 24 phyla each representing <1% of the total abundance

[g] 'other' represented 24 phyla each representing <1% of the total abundance

[h] 'other' represented 24 phyla each representing <1% of the total abundance

[i] 'other' represented 24 phyla each representing <1% of the total abundance

[j] 'other' represented 24 phyla each representing <1% of the total abundance

[k] 'other' represented 24 phyla each representing <1% of the total abundance

7.4.3 Taxonomic analysis at order level

The assessment of bacteria distribution at order level in NA microcosms ranged from 117 to 121 orders (days 0 and 14). Of these orders generated, 20 genera out of 121 orders (day 0) exhibited relative abundances greater than 1% of the total hits annotated (Table 7.2). The majority of these hits were assigned to Burkholderiales (21.9%), other dominant orders include Rhizobiales (15.3%), Xanthomonadales (6.3%), and Acidobacteriales (5.7%) as shown in Table 7.2. The remaining orders with relative abundance greater than 1% were present at low magnitude (from 1.0 – 3.0%) except the combined relative abundance of orders (up to 95) classified as others (15.6%). Significant shifts in the relative abundance of various orders were observed, when taxonomic analysis at day 0 was compared to days 14 and 28 (Figure 7.8 ii and iii). The relative abundances of some orders such as Rhizobiales (15.3 to 20.9 and 22.9%), Acidobacteriales (6.0 to 12.0 and 10.9%), and Verrucomicrobiales (<1% to 5.5 and 5.1%) substantially increased by days 14 and 28 respectively. Whilst for other orders including Burkholderiales (21.9 to 5.3 and 5.5%), Xanthomonadales (6.3 to 1.2 and 1.2%), Actinomycetales (5.7 to 3.7 and 4.1%) and Pseudomonadales (3.0 to 1.3 and 1.4%) relative abundances deeply decreased through the time course. Several new orders with relative abundance greater than 1% of the total hits (Table 7.2) were observed at days 14 and 28 including Verrucomicrobiales, Planctomycetales, Desulfuromonadales Myxococcales and Clostridiales as show in Table 7.2. In addition, their relative abundance was stable between the two sampled time points (days 14 and 28).

In microcosms where an ENA strategy was implemented, there was no significant change observed in the relative abundance of Burkholderiales (21.9 and 20.3%) between days 0 and 14 (Figure 7.9). Similar results were also observed for the relative abundances of Rhizobiales (15.3 to 14.3%) and Xanthomonadales (6.3 to 6.1%) between days 0 and 14. Other orders were stable in the two metagenomes (days 0 and 14) except the emergence of Methylophilales (1%) at day 14. By day 28, there was a significant reduction in the relative abundance of several orders including Burkholderiales (21.9 to 10.2%), Rhizobiales (15.3 to 7.2%), Xanthomonadales (6.3 to 2.1%), Acidobacteriales (6.0 to < 1%), and Actinomycetales (5.7 to < 1%) compared to day 0.

In contrast, the incubation of ENA microcosms resulted in a significant increase in the relative abundance of several orders including Pseudomonadales (3.0 to 17.6%), Bacillales (1.1 to

9.5%), Oceanospirillales (1.0 to 7.7%), and Enterobacteriales (2.5 to 33.8%) when compared to day 0 (Figure 7.10 part iii).

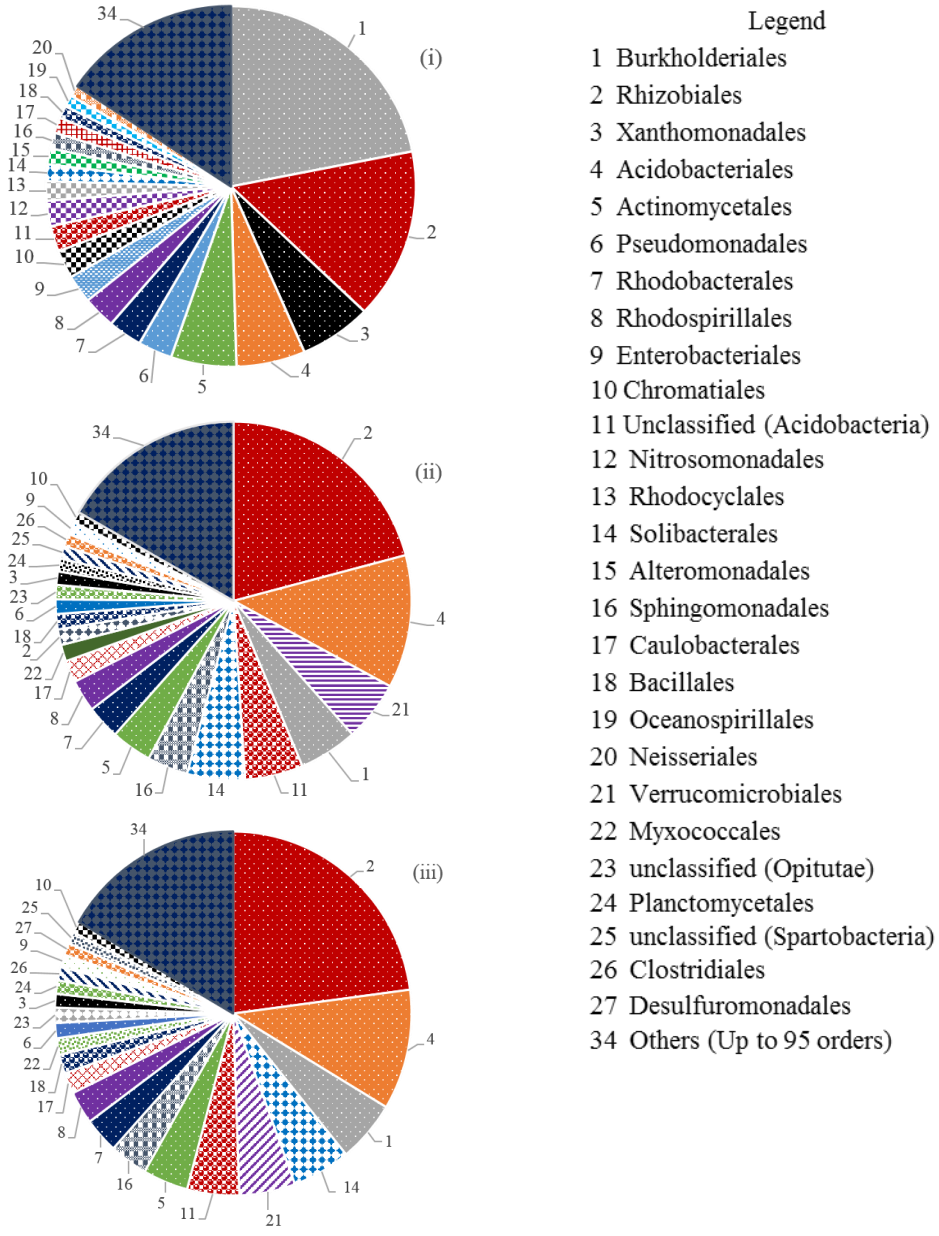

Figure 7.8. Distribution of organisms at order level determined in sequences obtained from (i) day zero, (ii) day 14 and (iii) day 28 metagenomes sampled from the Creo soil microcosms incubated under natural attenuation conditions (NA). The proportion of each taxonomic relative abundance was calculated as a percentage of total organisms in the metagenomic sample. Labels are shown for those phyla where abundance percentages were greater than 1% of total organisms

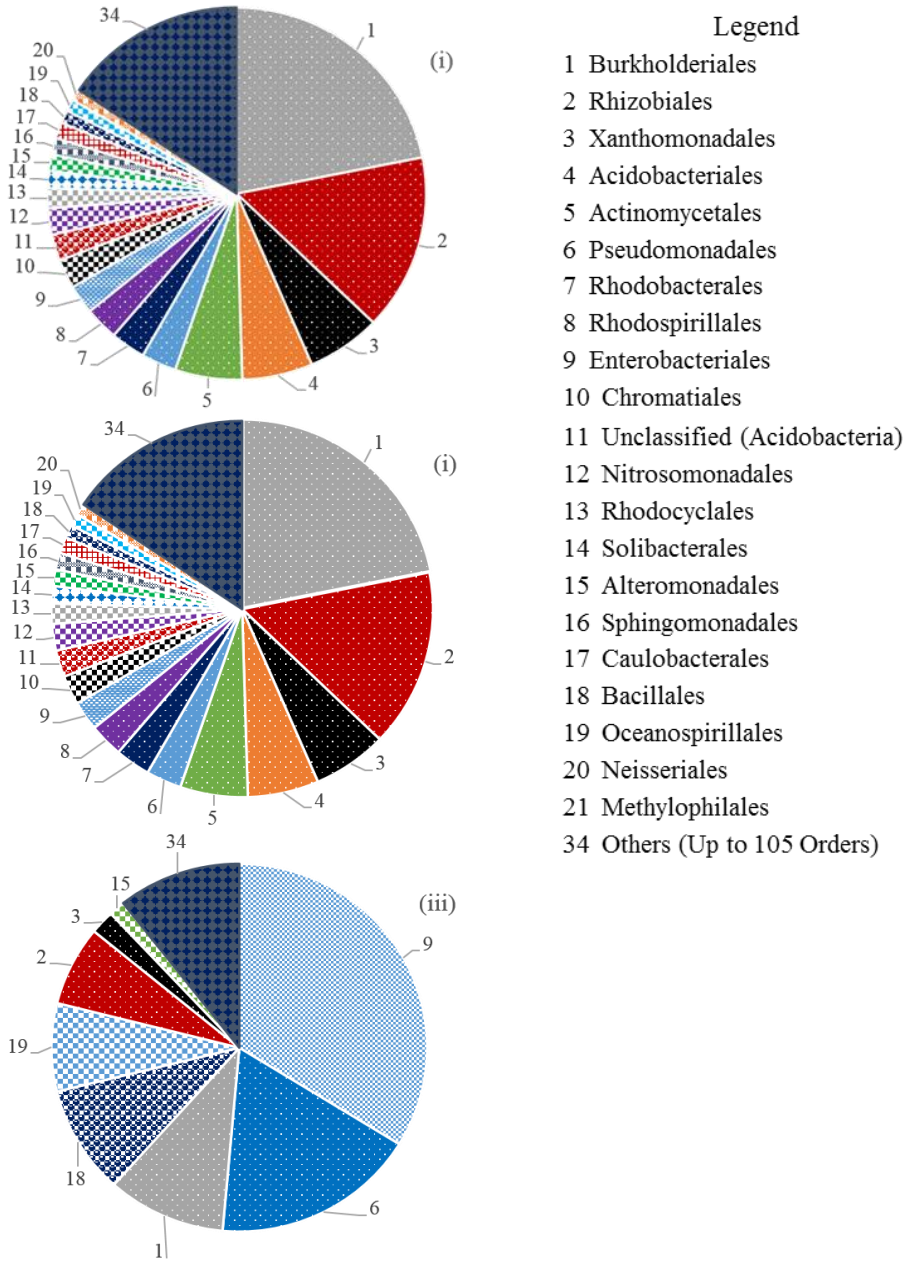

Figure 7.9. Distribution of organisms at the order level determined in sequences obtained from (i) day zero, (ii) day 14 and (iii) day 28 metagenomes sampled from the Creo soil microcosms incubated under enhanced natural attenuation conditions (ENA). The proportion of each taxonomic relative abundance was calculated as a percentage of total organisms in the metagenomic sample. Labels are shown for those phyla where abundance percentages were greater than 1% of total organisms.

As a result of these increases, Enterobacteriales and Pseudomonodales were the most prevalent order as evidenced by 13-fold and 6-fold increases in their initial relative abundances. For microcosms treated with hydrogen peroxide, a significant reduction was observed in the relative abundance of several orders (Figure 7.10). Diversity decreased following hydrogen peroxide treatment from 20 to 11 and 10 orders, when bacterial diversity from day 0 was compared to days 14 and 28 respectively. There was a shift in the top five abundance orders,

resulting in a reduction of more than half of their initial abundance following application of chemical oxidation. The most affected orders as a result of this amendment included Burkholderiales (21.9 to 10.2%), Rhizobiales (15.3 to 7%), Xanthomonadales (6.3 to 2.1%), Acidobacteriales (6.0 to < 1%), and Actinobacteriales (5.7 to < 1%). In contrast, the application of chemical oxidation resulted in a significant increase in some orders at day 14. The order Enterobacteriales was overrepresented at day 14 (13-fold) compared to the second highest represented order (Pseudomonadales) as shown in Table 7.2. Other prominent orders with a significant increase in their relative abundances include Bacillales (1.1 to 9.5%) and Oceanospirillales (1.0 to 7.9%) as depicted in Figure 7.10 (part (ii)). There was little change observed in the relative abundances of taxonomic groups for the remainder of the incubation period (day 28) as demonstrated in Figure 7.10 (parts (ii) and (iii)).

In microcosms amended with sodium succinate, the number of orders decreased over the 28-day incubation period (Figure7.11). The addition of sodium succinate resulted in a significant increase in the relative abundance of the order Burkholderiales (21.9 to 62.3%) between days 0 and 14 (Table 7.2). In contrast, the relative abundances of orders such as Rhizobiales (15.3 to 8.2%), Xanthomonadales (6.3 to 2.7%), Acidobacteriales (6.0 to < 1%), Actinomycetales (5.7 to 2.1%) and Rhodobacteriales (3.0 to 1.8%) extensively decreased at day 14 compared to day 0. Fewer orders were detected at the latter time points compared to day 0 (20 to 11 and 13 orders with >1% relative abundance) presumably due to the selective effect of sodium succinate as a carbon source.

In microcosms supplemented with Tween 20, bacterial community diversity decreased from day 0 to day 28 (20 to 17 orders with >1% relative abundance) as depicted in Figure 7.12. The most prominent order was overrepresented by 4-fold (Xanthomonadales) at day 28 when compared to day 0. Furthermore, other orders including Burkolderaiales (21.9 to 23.3%), Pseudomonadales (3.0 to 4.7%), and Alteromonadales (1.4 to 3%) also increased from day 0 to day 28. In contrast, several other orders such as Rhizobiales (15.3 to 6.6%), Acidobacteriales (6.0 to 1.3%), Actinomycetales (5.7 to 3.4%) and Rhodobacteriales (3.0 to 1.5%) massively decreased from day 0 to day 28. There was no clear dominant order in microcosms amended with Tween 20 as the relative abundances of the two prevalent orders were similar (23.3 and 26.4%). The remaining orders with relative abundances greater than 1% were present at low magnitude (from 1.0 – 3.0%) except the combined relative abundance of orders (< 1% of total hits) classified as others (14.6%) as showed in Table 7.2.

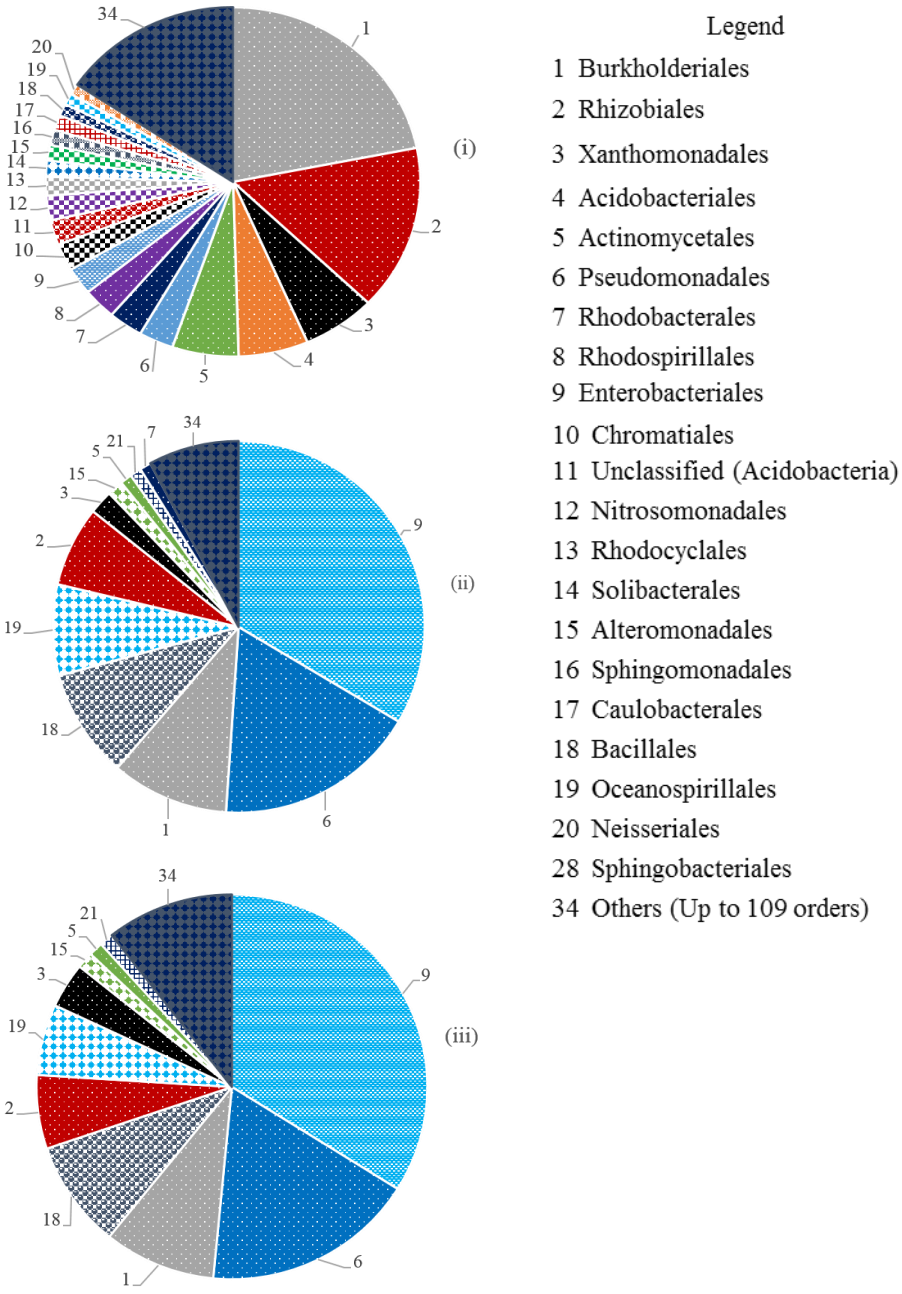

Figure 7.10. Distribution of organisms at order level determined in sequences obtained from (i) day zero metagenomes, (ii) day 14 metagenomes and (iii) day 28 metagenomes sampled from Creo soil microcosms treated with hydrogen peroxide (H_2O_2). The proportion of each taxonomic relative abundance percentage was calculated as a percentage of total organisms in the metagenomic sample. Labels are shown for those phyla where abundance percentages were more than 1% of total organisms.

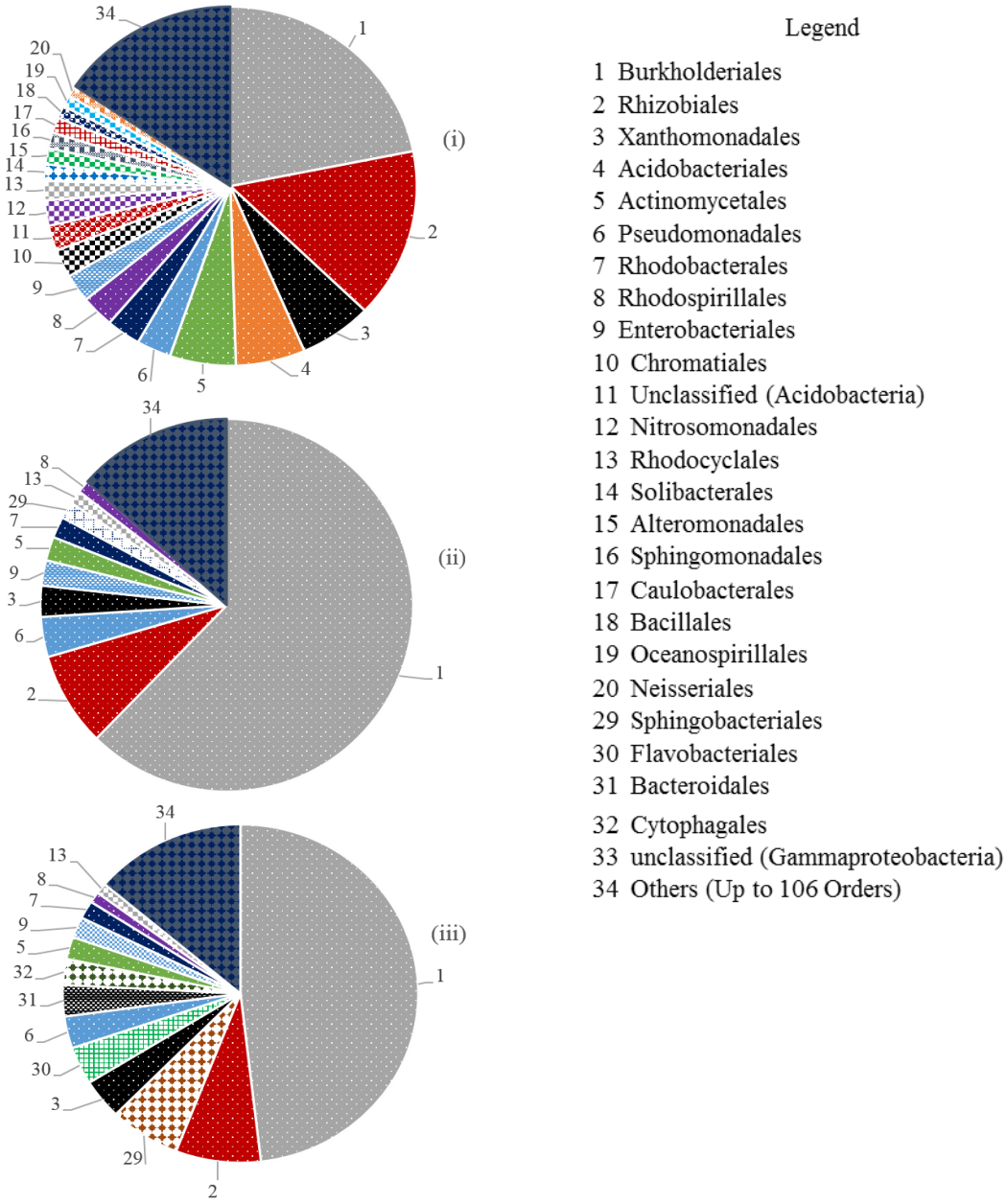

Figure 7.11. Distribution of organisms at order level determined in sequences obtained from (i) day zero, (ii) day 14 and (iii) day 28 metagenomes sampled from Creo soil microcosms amended with sodium succinate (SS). The proportion of each taxonomic relative abundance was calculated as a percentage of total organisms in the metagenomic sample. Labels are shown for those phyla where abundance percentages were greater than 1% of total organisms.

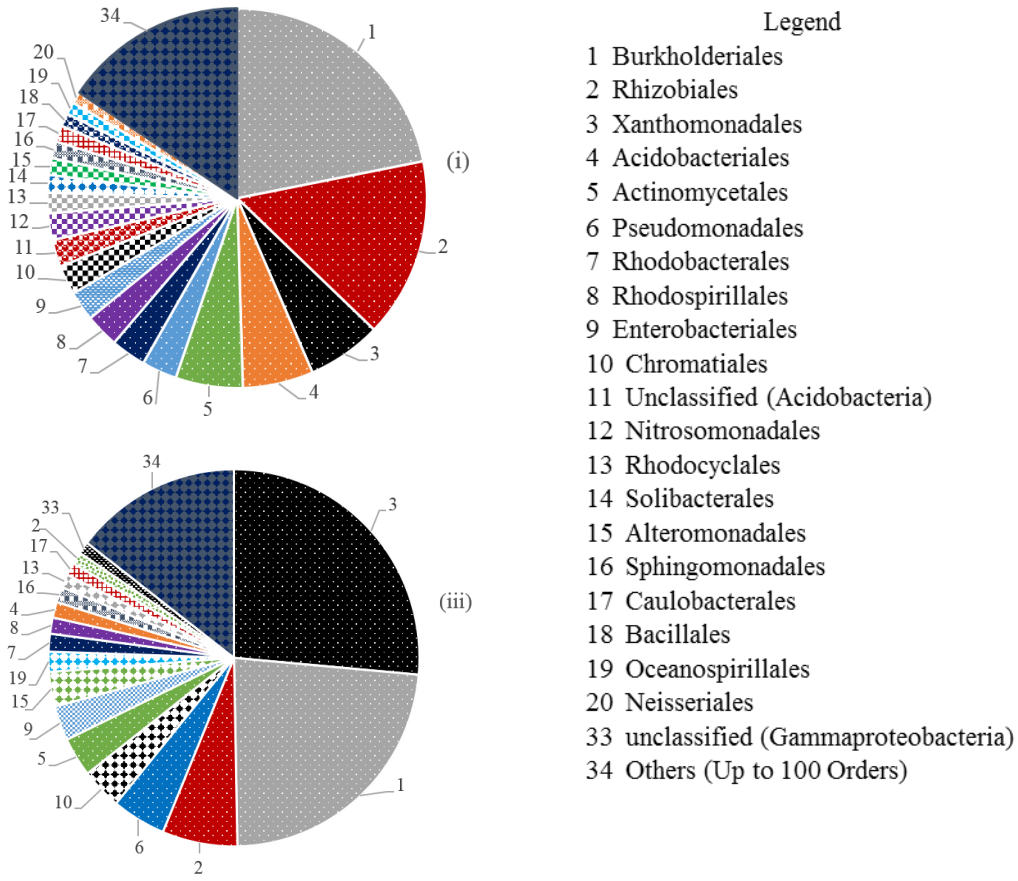

Figure 7.12. Distribution of organisms at order level determined in sequences obtained from (i) day zero and (iii) day 28 metagenomes sampled from Creo soil microcosms amended with Tween 20 (T_{20}). The proportion of each taxonomic relative abundance was calculated as a percentage of total organisms in the metagenomic sample. Labels are shown for those phyla where abundance percentages were greater than 1% of total organisms.

7.5 MG-RAST analysis of functional profiles

Based on analysis of functional profiles annotated by MG-RAST, changes in the abundance of functional categories affiliated with aromatic metabolism in PAH-contaminated soils were examined over the 28-day incubation period. The effect of bioremediation strategies on functional profiles was compared using the Statistical Analysis of Metagenomic Profiles (STAMP) software in samples taken on days 0, 14 and 28 (Parks & Beiko 2010), in which metagenomes at the commencement of incubation were compared to metagenomes obtained from the later time points. High-level metabolic profiles of metagenomes sampled from unamended and amended microcosms were analysed for generic putative PAH-degradation enzymes. Analysis of raw sequences related to metabolic functions in the current study were undertaken as described previously in chapter 5 (section 5.7).

7.5.1 Comparison of metabolic profiles in unamended and amended microcosms

Functional profile analysis in the Creo NA microcosm showed the prevalence of similar core metabolic functions in metagenomes sampled over the 28-day incubation. Comparisons of prevalent core metabolic functions in metagenomes from day 0 and day 14 using the Statistical Analysis of Metagenomic Profiles (STAMP) software package (Parks & Beiko 2010), demonstrated an overrepresentation of the membrane transport system in day 0 and an overrepresentation of carbohydrates and protein metabolism at day 14 (Appendix 5 Figure A5.1). Other core metabolic functional profiles including nitrogen, DNA, secondary and potassium metabolisms were present at low magnitude in the two metagenomes. Characterisation of genes in NA microcosms following further incubation (day 28) revealed overrepresentation of the same metabolic profiles as day 14 (Appendix 5, Figure A5.2). Other metabolic profiles were also present at low abundance including potassium (day 0), dormancy and sporulation, and photosynthesis metabolism (day 28).

Analyses of core metabolic profiles in metagenomes obtained from amended microcosms (ENA) are presented in Appendix A5 (Figure A5.3 and A5.4). In microcosms amended with nutrients (ENA), no significant change (95% CI) in metabolic functional profiles was observed in metagenomes from days 0 and 14 even though activities including membrane transport system (day 0) and carbohydrates metabolism (day 14) were overrepresented. Supplementation of nutrients did not enhance the aforementioned metabolic profiles as shown by equal proportions (%) representing each activity and wider confidence intervals (95%) in the two metagenomes (Appendix 5 Figure A5.3).

Table 7.2. Taxonomic bacterial composition at order level in Creo soil metagenomes obtained from experimental microcosms following 28 days of incubation. Values shown are for those phyla where abundance percentages were greater than 1% of the total organisms

Legend	Order	Treatment, time (days) and relative abundance percentage compositions (%)														
		NA			ENA			H_2O_2				SS			T_{20}	
		0	14	28	0	14	28	0	2	14	28	0	14	28	0	28
1	Burkholderiales	21.9	5.3	5.5	21.9	20.3	10.2	21.9	10.1	10.2	9.3	21.9	62.3	48.2	21.9	23.3
2	Rhizobiales	15.3	20.9	22.9	15.3	14.3	7.0	15.3	6.9	7.0	6.2	15.3	8.2	7.7	15.3	6.6
3	Xanthomonadales	6.3	1.2	1.2	6.3	6.1	2.1	6.3	2.3	2.1	3.8	6.3	2.7	3.8	6.3	26.4
4	Acidobacteriales	6.0	12.0	10.7	6.0	6.3	*	6.0	*	*	*	6.0	*	*	6.0	1.3
5	Actinomycetales	5.7	3.7	4.1	5.7	7.3	*	5.7	1.3	1.0	1.2	5.7	2.1	2.1	5.7	3.4
6	Pseudomonadales	3.0	1.3	1.4	3.0	3.0	17.6	3.0	17.1	17.6	17.6	3.0	3.5	3.1	3.0	4.7
7	Rhodobacterales	3.0	3.1	3.2	3.0	2.7	*	3.0	1.6	1.0	*	3.0	1.8	1.7	3.0	1.5
8	Rhodospirillales	2.9	2.9	2.9	2.9	2.8	*	2.9	*	*	*	2.9	1.1	1.0	2.9	1.4
9	Enterobacteriales	2.5	1.1	1.1	2.5	2.5	33.8	2.5	33.6	33.5	33.9	2.5	2.2	2.0	2.5	3.0
10	Chromatiales	2.5	1.0	1.0	2.5	2.8	*	2.5	*	*	*	2.5	*	*	2.5	3.5
11	Unclassified (Acidobacteria)	2.3	5.3	4.7	2.3	2.4	*	2.3	*	*	*	2.3	*	*	2.3	1.1
12	Nitrosomonadales	2.3	*	*	2.3	2.6	*	2.3	*	*	*	2.3	*	*	2.3	1.1
13	Rhodocyclales	1.7	*	*	1.7	1.8	*	1.7	*	*	*	1.7	1.2	1.0	1.7	*
14	Solibacterales	1.5	5.2	5.3	1.5	1.6	*	1.5	*	*	*	1.5	*	*	1.5	*
15	Alteromonadales	1.4	*	*	1.4	1.4	1.4	1.4	1.4	1.4	1.4	1.4	*	*	1.4	3.0
16	Sphingomonadales	1.4	3.7	3.5	1.4	1.3	*	1.4	*	*	*	1.4	*	*	1.4	1.3
17	Caulobacterales	1.4	2.0	1.9	1.4	1.2	*	1.4	*	*	*	1.4	*	*	1.4	1.1
18	Bacillales	1.1	1.4	1.7	1.1	1.4	9.5	1.1	9.2	9.5	9.0	1.1	*	*	1.1	*
19	Oceanospirillales	1.0	*	*	1.0	1.1	7.7	1.0	7.7	7.9	6.0	1.0	*	*	1.0	1.7
20	Neisseriales	1.0	*	*	1.0	1.1	*	1.0	*	*	*	1.0	*	*	1.0	*

Table 7.2 (cont). Taxonomic bacterial composition at order level in Creo soil metagenomes obtained from experimental microcosms following 28 days of incubation. Values shown are for those phyla where abundance percentages were greater than 1% of the total organisms

Legend	Order	Treatment, time (days) and relative abundance percentage compositions (%)														
		NA			ENA			H_2O_2				SS			T_{20}	
		0	14	28	0	14	28	0	2	14	28	0	14	28	0	28
21	Verrucomicrobiales	*	5.5	5.1	*	*	*	*	*	*	*	*	*	*	*	*
22	Myxococcales	*	1.5	1.5	*	*	*	*	*	*	*	*	*	*	*	*
23	unclassified (Opitutae)	*	1.4	1.4	*	*	*	*	*	*	*	*	*	*	*	*
24	Planctomycetales	*	1.3	1.2	*	*	*	*	*	*	*	*	*	*	*	*
25	unclassified (Spartobacteria)	*	1.2	1.0	*	*	*	*	*	*	*	*	*	*	*	*
26	Clostridiales	*	1.1	*	*	*	*	*	*	*	*	*	*	*	*	*
27	Desulfuromonadales	*	1.1	1.1	*	*	*	*	*	*	*	*	*	*	*	*
28	Methylophilales	*	*	*	*	1.0	*	*	1.0	1.0	1.1	*	*	*	*	*
29	Sphingobacteriales	*	*	*	*	*	*	*	*	*	*	*	1.5	6.5	*	*
30	Flavobacteriales	*	*	*	*	*	*	*	*	*	*	*	*	3.6	*	*
31	Bacteroidales	*	*	*	*	*	*	*	*	*	*	*	*	3.0	*	*
32	Cytophagales	*	*	*	*	*	*	*	*	*	*	*	*	2.5	*	*
33	unclassified (Gammaproteobacteria)	*	*	*	*	*	*	*	*	*	*	*	*	*	*	1.0
34	Others	15.6[a]	16.8[b]	16.6[c]	15.6[a]	15.0[d]	10.6[e]	15.6[a]	7.8[f]	7.9[g]	10.5[h]	15.6[a]	13.8[i]	14.6[j]	15.6[a]	14.6[k]

*percentages below 1% of the total organisms.

[a] 'others' represented 101 orders each representing <1% of the total abundance

[b] 'others' represented 95 orders each representing <1% of the total abundance

[c] 'others' represented 99 orders each representing <1% of the total abundance

[d] 'others' represented 99 orders each representing <1% of the total abundance

[e] 'others' represented 109 orders each representing <1% of the total abundance

[f] 'others' represented 106 orders each representing <1% of the total abundance

[g] 'others' represented 106 orders each representing <1% of the total abundance

[h] 'others' represented 104 orders each representing <1% of the total abundance

[i] 'others' represented 106 orders each representing <1% of the total abundance

[j] 'others' represented 105 orders each representing <1% of the total abundance

[k] 'others' represented 100 orders each representing <1% of the total abundance

The comparison of metabolic profiles in metagenomes sampled from day 0 and day 28 based subsystems, resulted in significant differences as shown in Appendix 5 (Figure A5.4). For the day 0 metagenome, sequences related to respiration, membrane transport, and virulence, disease and defence were overrepresented while an overrepresentation of metabolic profiles such as amino acids and derivatives, RNA, protein, and carbohydrate metabolisms were observed by day 28. Other metabolic profiles were detected at equal proportions (%) including clustering-based subsystems, DNA, stress response and sulphur metabolisms.

Analysis of metagenomes obtained from microcosms pre-treated with hydrogen peroxide (chemical oxidation) showed an overrepresentation of some core metabolic profiles including respiration, protein metabolism, clustering-based subsystems, cofactors, vitamins, prosthetic group and pigments were observed at the start of the incubation (Figure 7.13). By day 14, sequences related to metabolic profiles such as amino acids and derivatives, regulation and cell signalling, carbohydrates, and iron acquisition metabolisms were prevalent compared to day 0. The prevalence of these metabolic profiles reflect an increase in numerous catabolic processes accountable for metabolic pathways, through which chemical energy is generated for maintenance and growth of cells. There were no changes observed in metabolic profiles for photosynthesis, dormancy and sporulation and secondary metabolisms between days 0 and 14 metagenomes. Further incubation resulted in overrepresentation of core metabolic functional profiles including carbohydrates, amino acids and derivatives, regulation and cell signalling, iron acquisition metabolisms at day 28 (Figure 7.14).

In microcosm where sodium succinate was implemented, significant differences were observed in sequences related to amino acids and derivatives, carbohydrate metabolism at confidence intervals (95%) at day 14 (Figure 7.15). No further increase in abundances of the aforementioned metabolic profiles were observed in the remainder of the incubation (day 28) as shown in Figure 7.16.

In microcosms treated with Tween 20, an overrepresentation of metabolic functional profiles including respiration, virulence, disease, and defence, cofactors, vitamins, prosthetic groups and protein metabolisms were observed at the commencement of incubation (Figure 7.17). As depicted in Figure 7.17, sequences related to amino acids and derivatives and protein metabolism were prevalent in metagenomes obtained at day 28 compared to day 0 whereas other metabolic profiles were detected at equal proportions (%) (clustering-based subsystems, carbohydrates metabolism and stress response) over the 28-day incubation period.

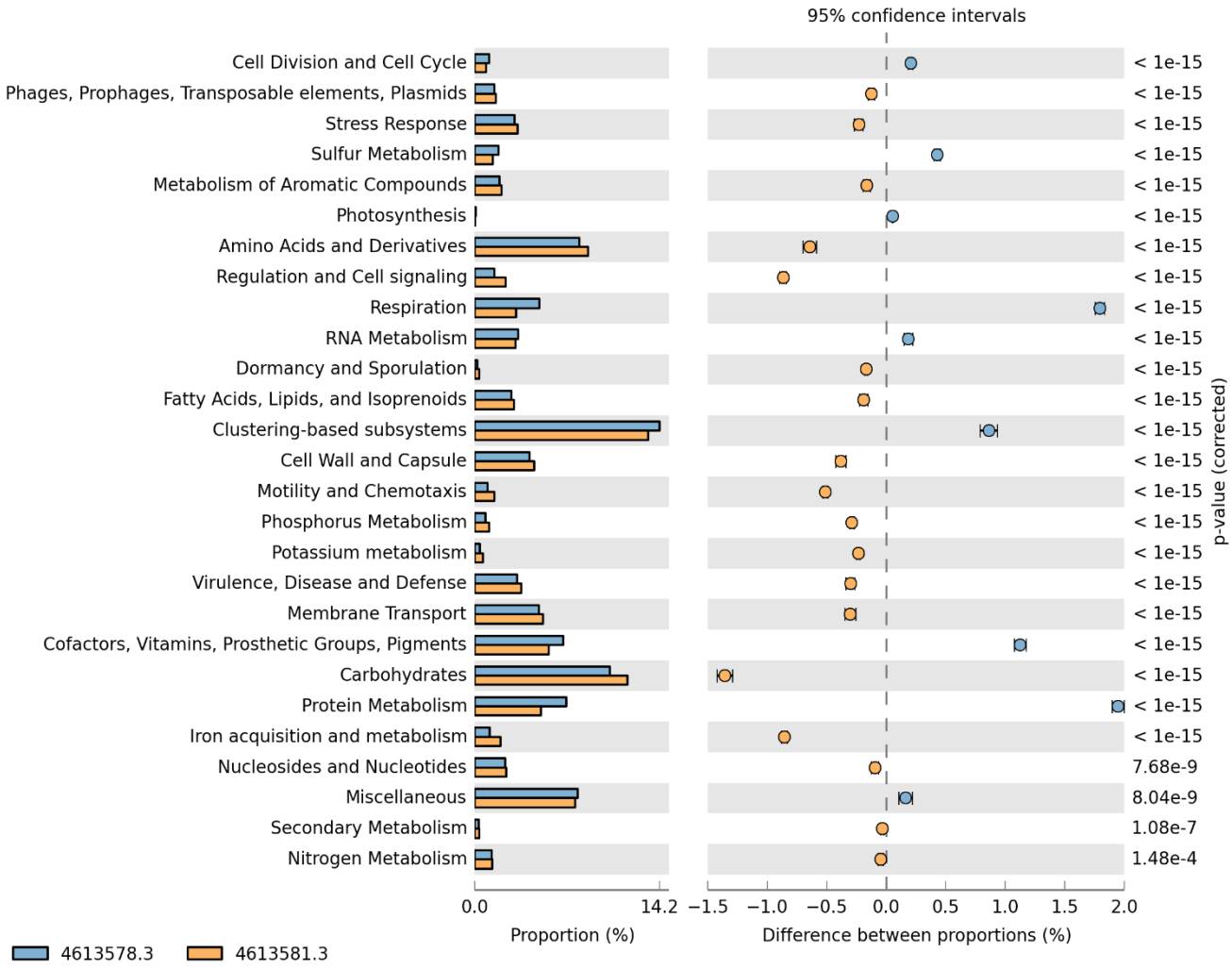

Figure 7.13. Comparison of metagenome functional profiles from Creo soil incubated under chemical oxidation (H_2O_2) conditions. Blue bars represent (MG-RAST ID 4613578.3) metabolic functional profiles at the start of incubation while orange bars represent (MG-RAST ID 4613581.3) metabolic functional profiles at day 14. STAMP analysis of overrepresented subsystem functional profiles observed in day 0 and day 14 metagenomes with corrected p-values (95% confidence intervals) calculated using Storey's FDR approach are shown**.**

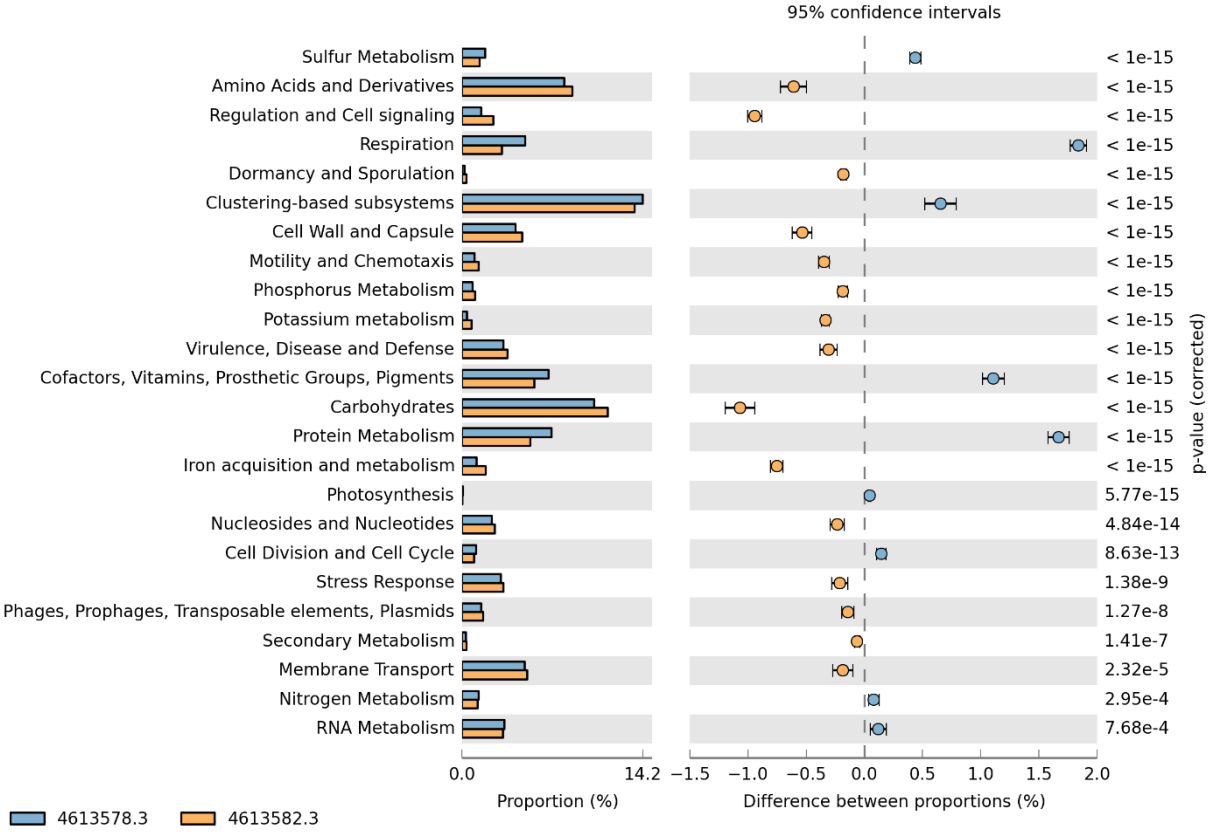

Figure 7.14. Comparison of metagenome functional profiles from Creo soil incubated under chemical oxidation (H_2O_2) conditions. Blue bars represent (MG-RAST ID 4613578.3) metabolic functional profiles at the start of incubation while orange bars represent (MG-RAST ID 4613582.3) metabolic functional profiles at day 28. STAMP analysis of overrepresented subsystem functional profiles observed in day 0 and day 28 metagenomes with corrected p-values (95% confidence intervals) calculated using Storey's FDR approach are shown.

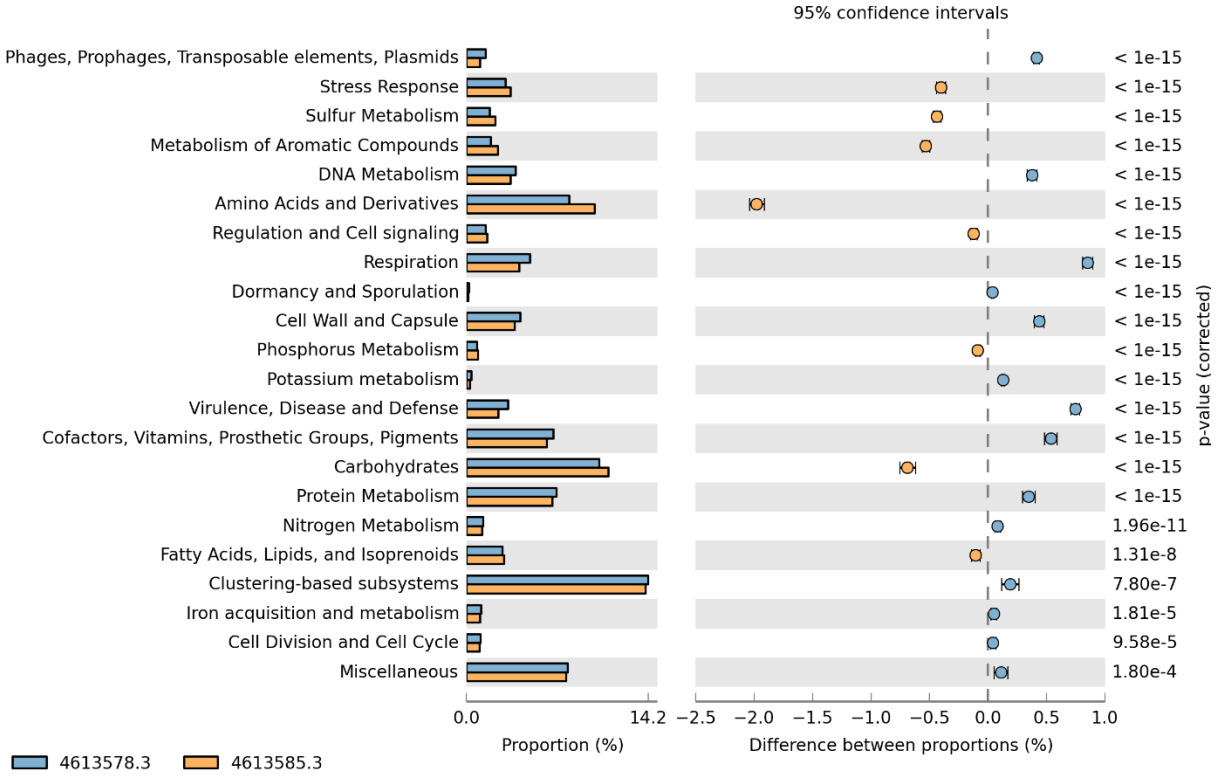

Figure 7.15. Comparison of metagenome functional profiles from Creo soil incubated in microcosms treated with sodium succinate (SS). Blue bars represent (MG-RAST ID 4613578.3) metabolic functional profiles at the start of incubation while orange bars represent (MG-RAST ID 4613585.3) metabolic functional profiles at day 14. STAMP analysis of overrepresented subsystem functional profiles observed in day 0 and day 14 metagenomes with corrected p-values (95% confidence intervals) calculated using Storey's FDR approach are shown.

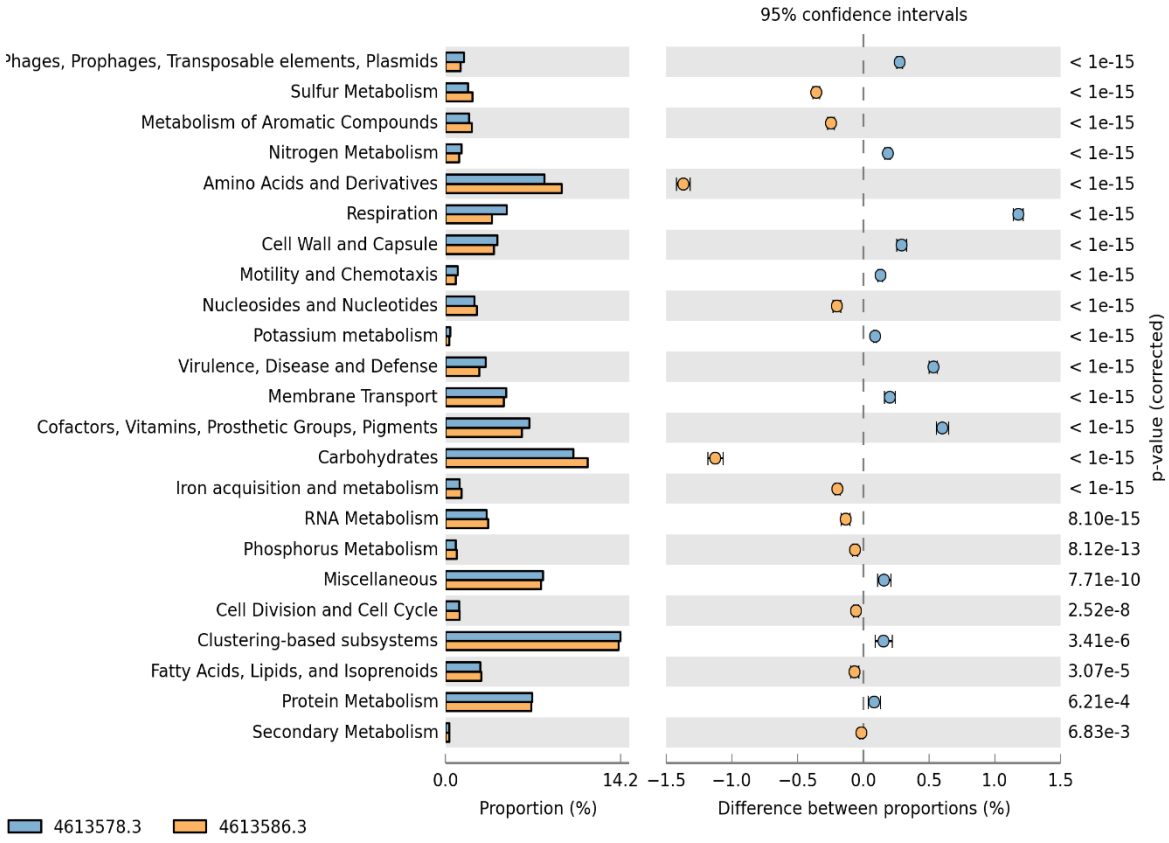

Figure 7.16. Comparison of metagenome functional profiles from Creo soil incubated in microcosms treated with sodium succinate (SS). Blue bars represent (MG-RAST ID 4613578.3) metabolic functional profiles at the start of incubation while orange bars represent (MG-RAST ID 4613586.3) metabolic functional profiles at day 28. STAMP analysis of overrepresented subsystem functional profiles observed in day 0 and day 28 metagenomes with corrected p-values (95% confidence intervals) calculated using Storey's FDR approach are shown.

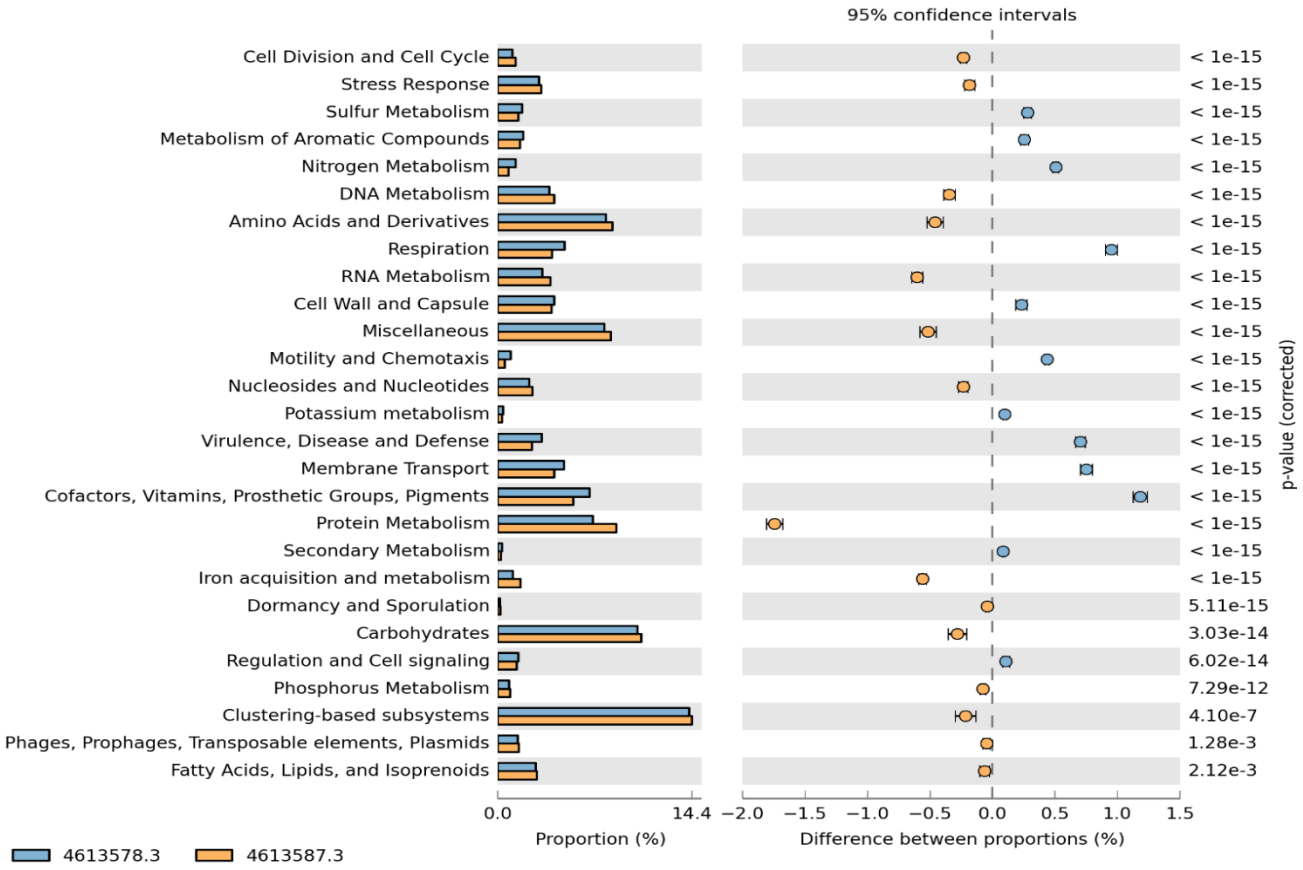

Figure 7.17. Comparison of metagenome functional profiles from Creo soil incubated in microcosms treated with Tween 20 (T_{20}). Blue bars represent (MG-RAST ID 4613578.3) metabolic functional profiles at the start of incubation while orange bars represent (MG-RAST ID 4613587.3) metabolic functional profiles at day 28. STAMP analysis of overrepresented subsystem functional profiles observed in day 0 and day 28 metagenomes with corrected p-values (95% confidence intervals) calculated using Storey's FDR approach are shown.

7.5.2 Analysis of enzymes required for metabolism of PAHs

Data generated from MG-RAST with metagenomes from alternative Creo soil microcosms were further analysed using KEGG pathway analysis as described in section 5.7.2.

7.5.3 Analysis of PAH metabolism in unamended and amended microcosms

The KEGG pathway analysis of enzymes involved in the metabolism of naphthalene and B(a)P in unamended and amended microcosms demonstrated similarities in three enzymes including EC 1.14.1.1, EC 3.3.2.9 and 2.5.1.18 (Figure 7.18 and 7.19) respectively. For example, there were many similarities in terms of enzymes encoding for unspecific monooxygenase, microsomal epoxide hydrolase, and microsomal hydrolase over the 28-day incubation period. This suggests that sequences related to key enzymes associated with the metabolism of PAHs were consistently found irrespective of treatment as demonstrated in Table 7.3.

In terms of the proportion of hits assigned to each enzyme under natural attenuation (NA), the xenobiotic monooxygenase (EC 1.14.14.1) decreased between days 0 and 14 (40 to 13 hits) but no change was observed at day 28 (Figure 7.18). The reduction in the number of hits may suggest that the activity related to this enzyme was present at the beginning of t incubation but declined at the end of incubation, presumably due to the reduction in the number of microorganisms encompassing this capacity. In contrast, sequences annotated to glutathione transferase (2.5.1.18) decreased markedly between days 0 and 14 (3666 to 1493 hits). However, the proportion of hits annotated to this enzyme increased by a small margin at day 28 (1493 to 1635 hits). A similar reduction in the number of hits assigned to benzo(a)-4, 5-epoxide hydrolase (3.3.2.9) was also observed in natural attenuation microcosms over the 28-day incubation period.

In ENA microcosms, hits matching xenobiotic monooxygenase increased from day 0 to day 14 (40 to 77 hits), however, a decline in the number of hits (54 hits) annotated to this enzyme was observed by day 28 (Appendix 5 Figure A5.5 and A5.6). In contrast, hits annotated to glutathione transferase graudally increased from day 0 to day 28 (3666 to 7805 hits) respectively. Similarly, hits associated with benzo(a)-4, 5-epoxide hydrolase also increased over the 28-day incubation period (116 to 694 hits). The increase in the number of hits observed in the three enzymes under enhanced natural attenuation, may be due to the influence of nutrient amendments on bacteria exhibiting this capacity.

In microcosms treated with hydrogen peroxide (chemical oxidation), hits related to xenobiotic monooxygenase rapidly decreased over the 28-day incubation (Table 7.3and Appendix 5 Figure A5.7 and A5.8). Similarly, a reduction in sequences related to the cytochrome P450 enzymes (xenobiotic monooxygenase) and benzo(a)-4, 5-epoxide hydrolase were observed over the 28-day incubation period.

For microcosms treated with sodium succinate, hits related to xenobiotic monooxygenase and benzo(a)-4, 5-epoxide hydrolase sharply decreased from day 0 to day 28 (40 to 5 and 116 to 83 hits, from day 0 to day 28). However, sequences annotated to glutathione transferase fluctuated over the 28-day incubation period (Table 7.3 and Appendix 5 Figure A5.9 and A5.10).

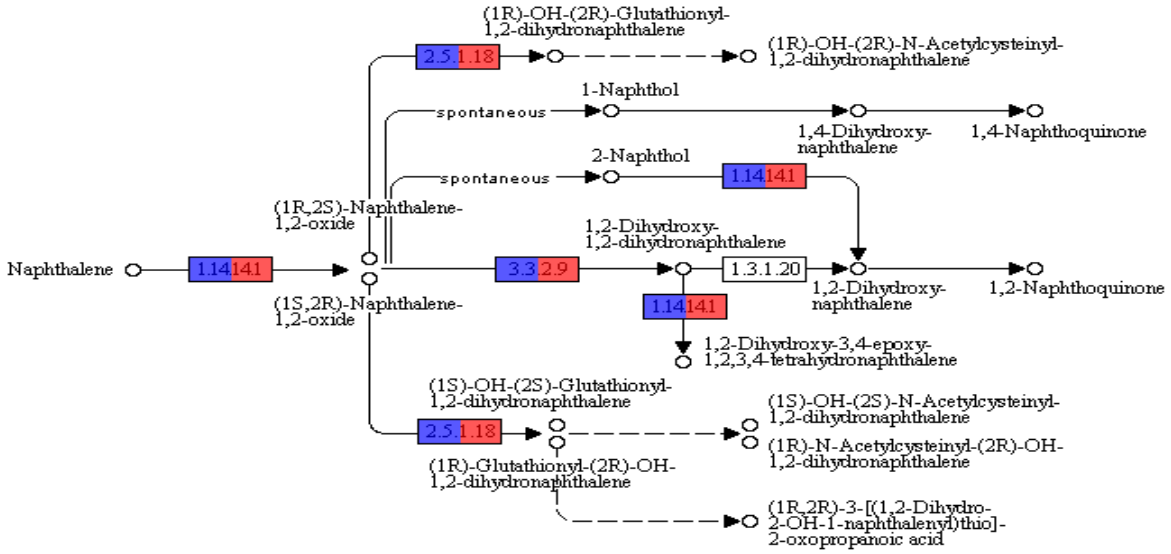

Figure 7.18. KEGG pathway analysis of metagenomes from Creo soil incubated under natural attenuation conditions (NA), displaying enzymes required for the metabolism of naphthalene. Enzyme profiles are shown at the start of the microcosm experiment (MG-RAST ID 4613578.3 in blue) and after 28 days (MG-RAST ID 4613548.3 in red). Shaded boxes represent enzymes for which genes were present in each annotated metagenome.

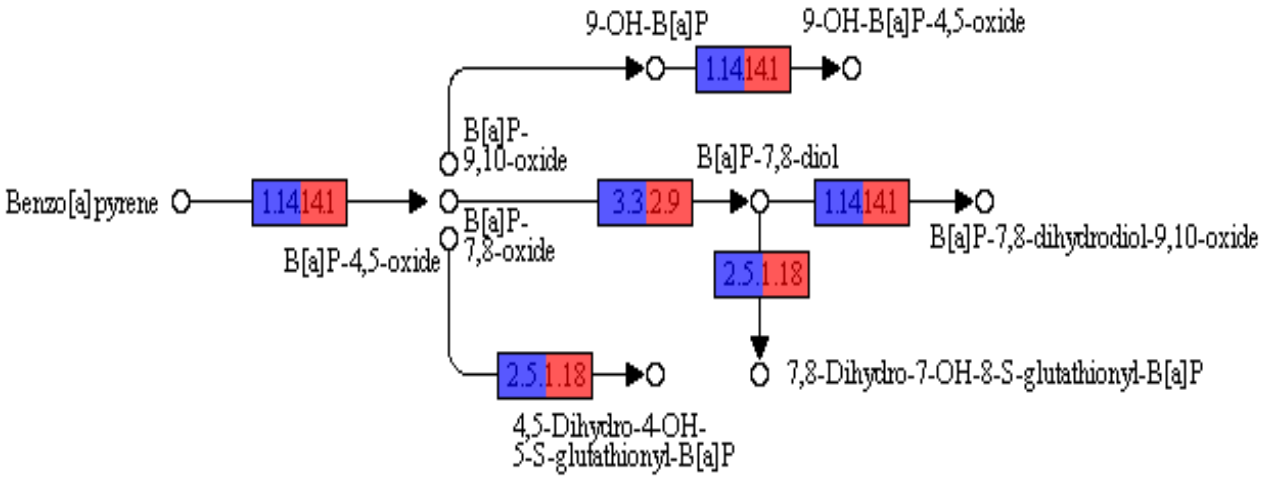

Figure 7.19. KEGG pathway analysis of metagenomes from Creo soil incubated under natural attenuation conditions (NA), displaying enzymes required for the metabolism of benzo(a)pyrene. Enzyme profiles are shown at the start of the microcosm experiment (MG-RAST ID 4613578.3 in blue) and after 28 days (MG-RAST ID 4613548.3 in red). Shaded boxes represent enzymes for which genes were present in each annotated metagenome.

In microcosms treated with Tween 20, there was a rapid reduction in the number of hits assigned to xenobiotic monooxygenase and glutathione transferase over the incubation period (28 day). It was found that hits related to benzo(a)-4, 5-epoxide hydrolase were low at the start of incubation but increased at the end of the incubation (Table 7.3 and Appendix 5 Figure

A5.11 and A5.12). Amendments involving H_2O_2, SS and T_{20} had no enhancement capacity of enzymatic activities as demonstrated by a low number of hits in metagenomes sampled from these microcosms compared to NA and ENA microcosms over the 28-day incubation period

Table 7.3. Summary of hits matching each of the three enzymes associated with PAH degradation specific functions in KEGG pathways analysis of metagenomes sampled from alternative Creo soil microcosms over the 28-day incubation period**.**

Enzyme	Number of hits					
	Time	NA	ENA	H_2O_2	SS	T20
Xenobiotic monooxygenase (EC 1.14.14.1)	0	40	-	-	-	-
	14	13	77	3	0	*
	28	14	54	2	5	14
Glutathione transferase (EC 2.5.1.18)	0	3666	-	-	-	-
	14	1635	4055	1829	2310	*
	28	1493	7805	353	3280	1877
Benzo(a)-4, 5-epoxide hydrolase (EC 3.3.2.9)	0	116	-	-	-	-
	14	89	167	37	73	*
	28	87	694	17	83	225

*No analysis performed. – Similar hits.

7.6 Discussion

Soil used to prepare microcosms described in this chapter was obtained following the completion of initial biodegradation experimental described in chapter 3. As described in the previous chapter, the lack of PAH biodegradation appeared to be as a result of bioavailability constraints. Although an attempt was made to enhance microbial biodegradation of PAHs by implementing various bioremediation strategies (ENA, BioA and Combined), there was negligible removal of PAHs in all 3 PAH-contaminated soils at the completion of the 42-week incubation period. As a consequence, the aim of this study was to investigate if the addition of an additional carbon source (sodium succinate), a surfactant (Tween 20) or pre-treatment using chemical oxidation strategies (hydrogen peroxide) may increase PAH bioavailability, hence increasing microbial degradation over the 28-day incubation period.

In addition to the overall aim of this study, pre-treatment using chemical oxidation strategy was designed to see if native microorganisms can survive the aggressiveness of H_2O_2 (Linley et al. 2012). The notion that PAH-degrading microorganisms and enzymatic activity can be induced by the addition of an alternative carbon source was investigated by supplementing Creo contaminated soil with sodium succinate. Supply of sodium succinate was expected to enhance PAH biodegradation by soil native microorganisms or to accelerate soil enzymatic activity. Since high molecular weight (HMW) PAHs may not be used as a carbon and energy source, supply of a growth substrate may initiate growth of PAH-degrading microorganisms and actuate the production of metabolic enzymes (Chen & Aitken 1999).

Thus, the addition of a growth substrate/inducer has the potential to increase the extent of PAH degradation by stimulating the lower pathway and/or catabolic enzyme production. Another possible strategy to overcome PAH bioavailability constraints is the addition of surfactants (i.e. Tween 20). The purpose of amending Creo contaminated soil with Tween 20 was to increase the rate of dissolution and desorption of PAHs by promoting the extent of contaminant transfer from solid and sorbed matrices. Because Tween 20 is an excellent dispersing agent, its application may enhance the solubility of PAHs and as a result may increase microbial PAH biodegradation(Laha, Tansel & Ussawarujikulchai 2009).

In some scenarios, the aforementioned approaches may be unsuccessful in overcoming bioavailability constraint, hence, an alternative strategy, chemical oxidation was employed. It was suggested that pretreatment of Creo contaminated soil using H_2O_2 may overcome the limitation of recalcitrant compounds to bioremediation through implementing the formation of highly reactive radicals, with the ability to mineralise even the most recalcitrant organic compounds(Goi, Trapido & Kulik 2009). In addition, this treatment has the advantage of increasing remediation efficiency of refractory compounds due to vigorous oxidation capability of hydroxyl radical, which may allow the oxidation of compound in the sorbed form. Besides this advantage, there are limitations associated with this strategy as it is unclear how the microbial community will respond to the aggressiveness of chemical oxidation treatment.

Analysis of total PAH concentration in samples incubated under continuing NA and ENA treatment had a little effect on PAH removal compared to data obtained in Chapter 3. This finding was anticipated due to bioavailability limitations as outlined in chapter 6 (Experiment 1). In a recent study, Mao et al., (2012) compared the extent of PAH removal by indigenous and bioaugmented microorganisms during a 56-day Creo soil biodegradation. By the end of

the incubation period, indigenous microorganisms were able to degrade 7.1% of the initial total PAH concentration (9362 ug/kg).

Whereas the extent of PAH degradation was approximately 3-fold and 5-fold higher in microcosms seeded with 10% and 20% bacterial consortium culture (composed of Mesorhizobium sp., Alcaligenes sp. and Bacillales sp.) after incubation for 56 days. Vinas et al. (2005) found that 87% of total PAH concentration in a highly Creo contaminated soil was degraded under NA microcosm compared to nutrient amended microcosm (83%) at the end of 200-day incubation period. In another study, Yu et al. (2005) compared the efficacy of different biodegradation strategies, by monitoring changes in the concentrations of key individual PAH compounds in mangrove sediments.

Yu et al. (2005) observed that native microorganisms were able to degrade more than 99% of fluorene and phenanthrene initial concentration (340 ± 16 and 347 ±16 mg/kg) and approximately 30% of pyrene initial concentration (397 ±15 mg/kg) at the end of 4 weeks incubation under NA strategy using spiked soil. These findings were in contrast to the results reported in the present study, where native microorganisms were unable to degrade PAHs under NA conditions, presumably due to nutrient limitation (i.e. nitrogen and phosphorus). However, the addition of nutrients did not enhance the activity of the native microbial population compared to the NA strategy.

There was no significant decrease observed in total PAH concentration ($P < 0.05$) in the continuing ENA strategy from the previous microcosm. Analysis of taxonomic assignments of metagenomes generated by shotgun pyrosequencing was dominated by bacteria under continuing NA and ENA conditions. Although there were some changes observed in bacteria composition and diversity at domain, phylum and order levels following additional incubation and moisture adjustment, the pattern of change was comparable with the previous microcosms (chapter 5). Evaluation of sequences affiliated with metabolic functional profiles in metagenomes obtained from the continuing NA and ENA microcosms, were comparable to the previous results discussed in chapter 5. This indicates that additional incubation had no benefit on microbial activities regardless of variability observed in the organisms at domain, phylum and order levels.

In the sodium succinate (SS) supplemented microcosm, some variability in total PAH concentration was observed in the early stage of incubation (18.1% after 14 days), however, further incubation resulted in no significant reduction ($P > 0.05$) in total PAH concentration at the end of the incubation period (day 28). In some cases, PAH-degrading bacteria may require

an inducer to be able to metabolise various contaminants. Chen and Aitken (1999) reported that *Psudomonas saccharophila P15* utilised the salicylate pathway to metabolise LMW and HMW PAHs with salicylate as an intermediate or inducer. The authors concluded that the addition of salicylate to PAH-contaminated soil was an attractive strategy for stimulating the biodegradation of phenanthrene due to its ability to induce expression of catabolic enzymes (PAH dioxygenase) which also enhanced the mineralisation of HMW PAHs (Chen & Aitken 1999).

However, in Creo soil, the addition of SS had little effect on microbial PAH biodegradation. This is in contrast to results from (Teng et al. 2010), in which they reported an increase in the rate of phenanthrene degradation and benzo(a)pyrene in SS supplemented microcosms maintained at 60% WHC for a 90-day period. In the study of Teng et al. (2010), the effects of SS (at concentrations of 0.2, 1.0 and 5.0 g/kg) supplementation, moisture content and aeration on the biodegradation of target compounds (phenanthrene and B(a)P) in soil was evaluated in relation to microbial population.

The primary goal of adding SS was to stimulate growth of indigenous microorganisms under natural attenuation. At the completion of the 90-day incubation period, phenanthrene degradation was enhanced in SS microcosm amended at 1.0 g/kg compared to microcosms where SS was added at 0.2 or 5.0 g/kg of dry contaminated soil. In the same work, B(a)P degradation was significantly ($P < 0.05$) enhanced when SS was added at 5.0 g/kg compared to addition at either 0.2 or 1.0 g/kg. The authors concluded that the addition of SS at concentrations of 1.0 and 5.0 g/kg had the greater influence on PAH biodegrading microbial populations.

In this study, application of SS at 0.1g/kg compare to 1.0 and 5.0 g/kg (concentration 10 and 50 times lower) may be considered as the reason for lack of PAH biodegradation but could also be due to PAH bioavailability constraints. Analysis of metagenomes sampled from the SS supplemented microcosm showed the prevalence of bacteria and eukaryotes at domain level over the 28 day incubation. In addition, the addition of SS enhanced the growth of potential PAH-degrading bacteria genera including Burkholderiales, Flavobacteriales, Bacteroidales and Sphingobacteriales at order level.

A number of studies have shown that prior exposure of bacteria to PAH contamination stimulates metabolism by induction of specific enzymes (Carmichael & Pfaender 1997; Heitkamp, Franklin & Cerniglia 1988). For example, Chen and Aitken (1999) reported that *P.saccharophila* Strain P15 grow on phenanthrene by a known pathway in which salicylate is

an intermediate. PAH dioxygenase activity was stimulated as a consequence of preincubation of *P.saccharophila* Strain P15 with phenanthrene and downstream intermediates of salicylate. This is in contrast to the results reported in the present study, in which the addition of SS had little effect on metabolic functional profiles in Creo contaminated soil.

Sequences annotated by MG-RAST server exemplified that clustering-based subsystems, amino acids and derivatives, respiration, DNA and carbohydrates metabolism were some of the generic functional profiles present throughout the incubation period without being impacted by the addition of SS. In addition, analysis of metabolic functional profiles associated with PAH metabolism was further supported by the results of KEGG pathway analysis, in which partial pathways involved in the biodegradation of naphthalene, pyrene and benzo(a) pyrene in SS amended soil (Figure A5.9–A5.10 in Appendix 5) were present.

Evaluation of metabolic functional profiles obtained from the SS supplemented microcosms demonstrated variability in the number of hits annotated to each of the 3 enzymes associated with the metabolism of PAHs throughout the incubation period (Table 7.3). This is in contrast to the results by (Teng et al. 2010), who observed an increase in the number of soil microbial biomass and enzymatic activity following the addition of SS over the 90 day period.

In addition, the authors suggested that the increase in the number of soil microbial and enzymatic activity was in line with the lowering of B(a)P concentration, which may be explained mainly by the co-metabolic role of SS.

In another study, Chen and Aitken (1999) examined the ability of *P. saccharophila* P15 to degrade B(a)P following pre-incubation with phenanthrene, salicylate or in the absence of either compound. The efficiency of B(a)P degradation was 22 and 33 times greater for salicylate and phenanthrene stimulated cells compared to unstimulated *P. saccharophila* P15 after 2 days of incubation. It was speculated that there may be a link between the mineralisation of phenanthrene and B(a)P pathway in this organism, through which both catechol 1,2-dioxygenase and catechol 2,3-dioxygenase were expressed.

Similarly, assessment of major biogeochemical processes in the SS amended Creo soil microcosms, by the Ion Proton platform showed the expression of functional profiles involved in the degradation of PAHs as a response of the microbial community to the presence of hydrocarbon contamination. However, the detection of the aforementioned functional metabolic profiles was expected in PAH-contaminated environments and presumably these were essential survival strategies adapted by the microbial community to overcome the presence of toxic substances in the environments. As a consequence of the role in the detoxification of contaminated soils, GST was the most abundant enzyme compared to other

enzymes (e.g. xenobiotic monooxygenase and benzo(a)-4,5-epoxide hydrolase) in SS amended Creo soil microcosm.

The addition of Tween 20 (T_{20}) was not effective at increasing PAH removal compared to NA. This is in contrast to (Zhu & Aitken 2010) who showed the effect of surfactant addition on PAH biodegradation. They observed that the addition of Brij 30 at two doses (5 and 20 mg/g) extensively increased biodegradation of 3- and 4-ring PAHs compared to treatments without Brij 30. Surfactant-mediated biodegradation of PAHs has been proposed as an alternative strategy to overcome contaminant bioavailability issues (Franzetti et al. 2010; González et al. 2011; Rodrigues et al. 2013).

In a recent study, Rodrigues et al. (2013) observed an improvement in fluoranthene removal (1.10 ± 0 vs 0.3 ± 0 mg/l per h) when T_{20} was applied at a concentration of 100 mg/l (0.08 mM) compared to higher concentrations (500 and 1000 mg/l) in a laboratory liquid culture batch experiment. The lack of fluoranthene degradation at higher T_{20} concentrations may be due to toxic effects to microorganisms.

The Tween 20 concentration utilised in this study was below the critical micelle concentration (CMC of 0.06 mM), which probably might have resulted in this treatment being ineffective at increasing PAH solubility. The decision to add surfactant at 1% loading solution or concentration below Tween 20 CMC was taken at the time of experimental set up based on 60% water holding capacity. This was thought to be sufficient enough for the amount of soil used in this study per a treatment but did not work as predicted. The option of using higher T_{20} concentration was an alternative but was not taken due to toxic effects on microbial activities as discussed in the previous paragraph.

In Creo soil, there are number of reasons why the addition of T_{20} was not effective at increasing PAH degradation; (1) the most likely reason being sorption to soil particle as outlined by (Laha, Tansel & Ussawarujikulchai 2009) thereby limiting the ability of T_{20} to solubilise the target contaminant; (2) another possible explanation may be due to the addition of inadequate amounts of T_{20} in (0.02 mM compared to 0.08, 0.4 and 0.8 mM (Rodrigues et al. 2013)) in this study resulting in limited solubilisation of PAHs for microbial biodegradation and (3) the possible utilisation of T_{20} as a carbon source; i.e. preferential degradation of the surfactant as a carbon source has been proposed (Tiehm 1994) to affect the degradation of the target compound.

In the T_{20} amended microcosm, there was a decrease in the relative abundance of Rhizobiales (15.3-6.6%), Acidobacteriales (6.0 1.3%) and Actinomycetales (5.7-3.4), while the relative abundance of Proteobacteria, mostly Xanthomonadales (6.3-26.4%) increased over the 28 day period (Table 7.2). The increase observed in the relative abundance of Xanthomonadales may be reflective of possible growth on T_{20}. In contrast, sequences assigned to Burkholderiales (21.9-23.3%) were stable following the addition of T_{20} whereas several other organisms at phylum and order levels were not impacted over 28 days.

In addition, analysis of metabolic functional profiles associated with PAH metabolism was supported by the results of KEGG pathway analysis, in which partial pathways involved in the biodegradation of key compounds including naphthalene, pyrene and benzo(a) pyrene in T_{20} amended soil (Figure A5.11-A5.12 in Appendix 5) were detected. Analysis of metabolic functional profiles obtained from T_{20} amended microcosms resulted in a significant reduction in the number of hits annotated to xenobiotic monooxygenase (8-fold) and glutathione transferase (2-fold) while an increase in the hits assigned to benzo(a)-4,5-epoxide hydrolase (2-fold) was observed throughout the incubation period (Table 7.3).
This is in contrast to the results by (Bautista et al. 2009), who evaluated the ability of bacteria (Entrobacteria,sp., Pseudomonas sp. and Stenotrophomonas sp.) to degrade PAHs in a spiked soil. After 15 day incubation period, their results showed highest cell density values and maximum specific growth rate when Tween-80 was applied at 1% dosage and 500 mg/l of each PAH. The highest cell density and a maximum specific bacteria growth were observed because the aforementioned bacteria were able to utilise Tween-80 as a carbon source. As such, these bacteria were able to achieve a high degree of PAH degradation (>90% of the initial spiked concentrations) in the 15 days period.

Assessment of major biogeochemical processes in the T_{20} amended Creo soil microcosms, by the Ion Proton platform showed the expression of functional profiles involved in the degradation of PAHs as a response by the microbial community to the presence of hydrocarbon contamination. Yet, the detection of the aforementioned functional metabolic profiles was expected in PAH-contaminated environments presumably as these are essential survival strategies adapted by the microbial community to overcome the presence of toxic substances in their environments.

As a result of their relevant application in the detoxification of xenobiotic contaminated soils, glutathione transferase (GSTs) was the most deteced enzyme compared to other enzymes (e.g. xenobiotic monooxygenase and benzo(a)-4,5-epoxide hydrolase) in T_{20} amended Creo soil microcosm. GSTs play a catalytic role in the biotransformation and biodegradation of xenobiotic compounds, mainly in the biodegradation of PAHs since they are commonly found in prokaryotes and eukaryotes (Allocati et al. 2009; Sheehan et al. 2001).

Although changes in microbial community structure and functionality were observed in Creo soil amended with SS and T_{20}, biodegradation may not be applicable to reduce the concentration of PAHs in this soil because of limitations governing bioavailability and the refractory nature of certain compounds, mostly HMW PAHs. Thus, chemical oxidation treatments may be an alternative strategy to overcome these limitations.

In hydrogen peroxide (H_2O_2) pre-treated microcosms, a significant decrease in PAH concentration was (72.3%) observed immediately after implementation of the treatment (90 mins), however, no further reduction was observed thereafter. These results are similar to those of (Goi, Trapido & Kulik 2009) who showed the efficacy of H_2O_2 treatment for the remediation of PAH contaminated soil. Similarly, Ferrares et al. (2008) observed that total PAH removal was effective at higher oxidant dosages (100 and 200 mmol per sample) compared to lower oxidant dosage (50 mmole per sample).

Although these three dosages were capable of removing sufficient amount of contaminant, total PAH removal varied from 91% (100 mmol) to 96% (200 mmol) compared to 52% (50 mmol) in H_2O_2 treatments with an initial concentration of 2800 mg/kg. Goi et al. (2009) concluded that PAH removal efficiency increased with oxidant dosage strength. In the present study, the application of chemical oxidation resulted in a significant reduction in total PAH concentration immediately following the treatment presumably due to the interaction of hydroxyl radicals with PAHs and soil organic matter (Ferrarese, Andreottola & Oprea 2008). However, oxidant application had an impact on microbial community structure as observed following metagenomic analysis.

Post H_2O_2 treatments, bacterial species were dominated by Proteobacteria (84.9%) and Firmicutes (10.1%) while the addition of H_2O_2 resulted in a significant reduction in the relative abundance of Acidobacteria (9.8 <1%) and Actinobacteria (6.0 <1%) respectively. The relative abundance of Firmicutes increased by 4-fold after 28-day incubation period following pre-

treatment with hydrogen peroxide (2.2-10.2 %). This finding suggests that these organisms were unable to tolerate the aggressiveness of H_2O_2 in Creo contaminated soil. Some microorganisms are known for their ability to sense and adapt to changing environmental conditions.

In a recent study, the ability of Proteobacteria, Bacteriodetes and Firmicutes to sense and adapt to high temperatures (temperatures from 35-120 ºC within different compartments of paper mill) in paper mill production process was highlighted by (Chiellini et al. 2014). Further analysis of the bacteria community at order level showed an increase in the relative abundance of some known PAH-degrading bacteria such as Pseudomonadales (5-fold), Enterobacteriales (13-fold), Bacillales (7-fold) and Oceanospirillales (8-fold) with a corresponding decreased in the relative abundance of Burkholderiales (2-fold), Rhizobiales (2-fold), Xanthomonadales (3-fold), Acidobacteriales (6-fold) and Actinobacteriales (5-fold) following H_2O_2 treatment.

The lack of further PAH degradation following post H_2O_2 addition may be due to the consumption of desorbable PAHs by hydroxyl radicals resulting in a non-bioavailable residual fraction. This may be one of the reasons for the lack of degradation observed following further incubation. Palmroth et al. (2006) observed a decrease of intact bacterial cells as a consequence of H_2O_2 treatment, which was applied at a concentration of 12% H_2O_2 (compared to 30% H_2O_2 used in this study), however, the number of viable cells increased following further incubation.The author concluded that bacteria had a better chance of surviving and regrowing at lower concentrations of H_2O_2. In a recent study, Rosik-Dulewska et al. (2015) observed similar results to those reported by Palmroth et al. (2006), in which the number of prokaryotic microorganisms initially deceased and then increased as a result of H_2O_2 treatment and subsequent incubation.

While the effect of high H_2O_2 concentrations on microbial community survival was suggested by Palmroth et al. (2006), there was no evidence to suggest that similar effects were responsible for the decrease observed in the relative abundance of some bacteria at phylum and order levels in the present study. Many studies conducted with a H_2O_2 strategy to overcome PAH bioremediation limitation have focused on decontamination of the pollutant, without considering its potential effect on bacteria diversity and metabolic functional profiles.

As a consequence, there is insufficient data currently available in the literature to which results from this study may be compared. However, results from H_2O_2 supplemented microcosm

showed little difference in the metabolic functional profiles at the completion of incubation (28 days).

Annotation of sequences from the H_2O_2 treated microcosm demonstrated an overrepresentation of some major metabolic functional profiles, including respiration, clustering-based subsystems, amino acids and derivatives, carbohydrates metabolism and iron acquisition over the 28 day period. This contrasts to the results of (Laurent et al. 2012), who assessed the impact of chemical oxidation using modified Fenton's reaction (H_2O_2, at 6 and 65 g/kg) on PAH degrading genes, cultivable heterotrophs, the 16s and 18s rDNA of industrial PAH-contaminated soil.

Laurent et al. (2012) observed a much lower number of genes in Fenton high concentration treated soil compared to the control soil. However, following additional incubation (5 weeks), the numbers of PAH-degrading genes were higher compared to the initial numbers in Fenton high concentration treated soil (initial 0 vs 1 x 10^5 gene copy/g), while there were no significant difference in the lower concentration treatment (1 x 10^5 gene copy/g) and the control soil (1 x 10^6 gene copy/g). The authors concluded that the decrease in bacterial, fungal and PAH-degrading genes could be explained by hydroxyl radicals strongly reacting with biological membranes following the treatment.

Similarly, functional metabolic profiles involved in aromatic metabolism within the soil microbial community were prevalent in metagenomes sampled from H_2O_2 treated soil over the 28-day incubation period. This was further supported by the results of KEGG pathway analysis, in which partial pathways involved in the biodegradation of naphthalene, pyrene and B(a)P were present in H_2O_2 treated soil (Figure A5.7-A5.8 in Appendix 5).

Assessment of H_2O_2 metagenomes showed a significant decrease in the number of hits annotated to each of the 3 enzymes associated with the metabolism of PAHs (Table 7.3). Contrary to this study, Laurent et al. (2012) observed a rebound in PAH-degrading genes in a modified Fenton's reaction after an additional 5 weeks of incubation. In the present study, the fact that these enzymes were detected throughout the experimental time course indicates their robustness against adverse environmental conditions. Findings from this study do not support the literature as biodegradation was negligible although GSTs were present.

7.7 Conclusion

This study showed that treatment of Creo contaminated soil with H_2O_2 resulted in a significant decrease in total PAH concentration within 90 minutes of the treatment. However, other strategies designed to increase PAH bioavailability, such as the addition of an alternative carbon source (sodium succinate) or surfactant (Tween 20) had no effect on enhancing microbial biodegradation of PAHs. Although microbial biodegradation was unable to be stimulated by these strategies, the main PAH degrading bacteria such as Proteobacteria, Acidobacteria, Actinobacteria and Bacteroidetes were prevalent in metagenomes sampled from all treatments. The lack of degradation in Creo soil may be due to several factors:

- Bioavailability limited PAH degradation
- Strategies designed to increase bioavailability were unsuccessful, however, they did show some impact on bacterial diversity
- Bioavailability limitation may be overcome by H_2O_2 treatment. Although it is an aggressive treatment, bacteria can survive. Regardless, there may be some issues with the application of H_2O_2 at large scale due to occupation health and safety issues and economic constraints.

The final chapter of this thesis represents a summary encompassing the major findings of this research with some recommendations on future research directions.

Chapter 8

Conclusions and future research work recommendations

8.1 Conclusions

This chapter provides an overall summary of major findings achieved from different research themes addressed in this thesis. The influence of various bioremediation strategies including the addition of nutrients and seeding of inoculum to enhance the activity of indigenous microbial PAH biodegradation was assessed using three soils collected from former wood preservative (Creo), manufactured gas plant (AP) and tram maintenance (TB) sites. Characterisation of microbial communities in terms of diversity and functionality was a challenging task due to limitation in traditional culture-based and molecular methodologies. However, next generation high throughput sequencing technology (metagenomics) offered direct access to uncharacterised soil microbial community structure, abundance, diversity and metabolic capacity by circumventing limitations associated with traditional and molecular methodologies.

A major focus of this thesis was to evaluate the influence of various bioremediation strategies including natural attenuation (NA), enhanced natural attenuation (ENA), bioaugmentation (BioA) and the combination of bioaugmentation and enhanced natural attenuation (Comb) conditions on microbial community diversity and metabolic capacity to decontaminate PAH contaminated soils in laboratory microcosm experiments. The degradative potential of the indigenous microbial community in the 3 aged PAH-contaminated soils was assessed by monitoring changes in PAH concentrations and microbial communities over a 42-week incubation period. Evaluation of soil indigenous microbial capacity to degrade PAHs was limited in either soils (ranging from 0-11.2% in the 3 soils) under a NA strategy. The lack of degradation under the NA strategy was initially attributed to insufficient nutrient availability to enhance microbial growth and increase PAH biodegradation. However, implementation of ENA (N and P) to accelerate microbial activity of the indigenous microbial community resulted in a small reduction in total PAH concentration in all three soils (removal ranging from 0-15.9%) over a 42-week period. Furthermore, evaluation of microcosms supplemented with *Mycobacterium gilvum* (a known PAH-degrading strain) resulted in a small increase in PAH degradation only in the Creo (4.9-12.2% in BioA and Combined) soil compared to both AP and TB soils respectively. Although previous studies have reported successful biodegradation

of PAHs by *Mycobacterium gilvum*, such ability could not be replicated in these soils; this may be due to competition from the already adapted indigenous microbial community as a consequence of long time exposure to the contaminants or PAH bioavailability limitations.. The key isuse in the three soils studied in this research is the bioavailability of the contaminants to microbial community, limiting their activities to degradation PAHs. In order to determine whether bioremediation strategies would be an ideal clean-up regime of interest to employ, bioavailability assessment of the site to be remediated should be integral part of the preliminary study before the implementation of full scale bioremediation strategies.

Analysis of microbial communities using the MPN method showed the presence of PAH-degrading microorganisms at each of the sampled time point in all soils. For instance, MPN analysis demonstrated an increase in microbial numbers from day 0 to week 18 (i.e. 2.0×10^{2} to 4.0×10^{-4} cells/g). In addition, the presence of potential PAH-degrading microorganisms was confirmed by the application of polymerase chain reaction (PCR) coupled with denaturant gradient gel electrophoresis (DGGE) analysis. Molecular analysis based on the 16s rDNA genes illustrated the presence of bacterial communities as indicated by the detection of bacterial bands over the 42 week period. As a consequence of experimental incubation time, a significance shift was observed in bacteria communities as evidenced by the changes in the banding patterns of communities obtained at different time points compared to the effect of various bioremediation strategies. Furthermore, the assessment of *Mycobacterium* gilvum using specific primers (nidA genes) resulted in the detection of bands representing this organism in all three soils. This finding supported the notion that incubation time influenced the microbial community more than the bioremediation strategies applied in all soils. Based on both the molecular and microbiological analyses, there was strong evidence to suggest that these soils harbour potential PAH-degrading microorganisms although their identities were not determined. Althe amendment strategies implemented in this study demonstrated a minimal impact on stimulating PAH degradation, the analyses of microbial communities using MPN method and molecular analysis illustrated the presence of bacterial communities in the three soils as presented in Chapters 3 and 4.

DNA pyrosequencing was used to analyse taxonomic abundance and functional profile distribution in metagenomes obtained from various bioremediation strategies. According to the MG-RAST annotation of sequences data generated using the Ion Proton platform, the bacterial domain was overrepresented, ranging from 88.8 to 99.1% in the three aged PAH-contaminated soils. Further analysis of the bacterial community in all soils confirmed that the bacteria was

dominated by phylum Proteobacteria (relative abundance ranging from 35.4-82.5%) of the total organisms over the 42 weeks incubation period. However, as a result of incubation time, the proportion of sequences annotated to Proteobacteria decreased with a corresponding increase in the relative abundance of other phyla including Acidobacteria, Actinobacteria, Firmicutes, Bacteroidetes, Verrucomicrobia and Planctomycete after incubation for 42 weeks. Evaluation of metabolic profiles demonstrated a significance prevalence of catabolic PAH degrading potential associated with PAH bioremediation in all soils. Among the different functional metabolic profiles detected, genes affiliated with activities such as metabolism of aromatic compounds, central carbohydrate metabolism and clustering-based subsystems were prevalent. In addition, three key enzymes associated with metabolism of naphthalene, pyrene and B(a)P (xenobiotic monooxygenase, glutathione transferase and benzo(a)-4,5-epoxide hydrolase) based on KGG pathway analysis were identified. The presence of these enzymes illustrates the biodegradability capacity of the microbial community present in the soils.

While abundance of bacterial community and metabolic functional profiles could not be linked with PAH removal due to limited PAH biodegradation observed in either soils, the results do signal the presence of biodegradability capacity in these soils. However, one of the major limitations for PAH biodegradation is the bioavailability of the contaminant to PAH degrading microorganisms. A number of studies have shown that there is a close link between contaminant bioavailability and biodegradable fractions. For this purpose, PAH bioavailability was assessed in the three soils using hydroxypropyl-β-cyclodextrin (HP-β-CD) non-exhaustive extraction with four linear regression models used to predict bioremediation endpoints after 42 weeks. While HP-β-CD extraction has the capacity to predict PAH bioavailability fractions, PAH bioavailability was low in Creo, TB and AP soil, resulting in limited PAH biodegradation even with attempts to enhance microbial activity. The benefit of conducting bioavailability studies such as HP-β-CD extraction is that the information generated from this analysis may be useful in making appropriate decisions in terms of remediation strategy to achieve clean up goals.

Additional biodegradation assessments were prepared using the Creo soil collected at the end of the first microcosm experiments. These additional treatments were implemented in order to increase PAH bioavailability for microbial biodegradation. The induction of an alternative carbon source (sodium succinate) and a surfactant (Tween 20) showed little impact on the indigenous microbial community as demonstrated by low PAH biodegradation after 28 days of incubation. However, microcosms pre-treated by chemical oxidation (hydrogen peroxide)

showed a significant reduction in total PAH concentration (72.3%) within the first 90 mins of the treatment. This rapid removal was due to the interaction of active oxidants such as hydroxyl radical with PAHs and other contaminants. Although variability was observed in terms of PAH-degrading potential, the diversity of the microbial community in the second biodegradation microcosms supplemented with SS, T_{20} and H_2O_2 was comparable with the microbial community in the first biodegradation microcosms.

The research themes addressed in this thesis highlighted the fact that historically contaminated sites harbour microorganisms with catabolic capacity to degrade PAHs. However bioremediation may be limited due to bioavailability constraints. The application of next generation sequencing technologies (NGS) employed in this study provided direct accessibility to a wide range of PAH-degrading microorganisms, detection of partial pathways involved in the metabolism of naphthalene, pyrene and B(a)P, with the affiliated degradative enzymes. Regardless of an attempt made to enhance microbial activity, limited PAH removal was observed in all 3 soils due to PAH bioavailability constraints. The acquisition of potential PAH degrading organisms reported in this study, through the application of NGS platform is an indicative of soil catabolic capacity to degrade PAHs. This has improved the bias of not identifying and understanding the microbial community of unknown organisms through conventional molecular technique such as DGGE.

8.2 Future research work recommendations

There are several facets of this thesis that could be pursued as themes for future investigation. Additional lines of research to be undertaken for further investigation include the following: (1) characterisation of other potential co-contaminants and assessment of their impact on biodegradation processes, (2) bioaugmentation of PAH-degrading organisms isolated from target clean-up soil and determination of their degradative capacity, (3) analysis of possible PAH metabolites or transformation products as a result of biodegradation and (4) identification of active microorganisms and specific genes involved in the metabolism of PAHs.

8.2.1 Characterisation of other potential co-contaminants and assessment of their impact on biodegradation processes.

Further characterisation needs to be undertaken including identification of other potential co-contaminants residing at contaminated sites and their impact on biodegradative processes. The information obtained from site characterisation through identification of possible co-

contaminants would be useful in the identification of potentially inhibitory substances that may impact bioremediation processes. This information could be utilised in design and decision making regarding what type of remediation strategy may be suitable to successfully achieve clean-up goals. Most often, remediation of sites contaminated with organic (i.e. PAHs), inorganic (i.e. cyanide) and other wastes such as phenolic compounds remains a major constraint for microbial biodegradation (Stoilova et al. 2006; Thomas & Lester 1994). The presence of phenolic compounds at elevated concentrations have been shown to inhibit microbial biodegradation of PAHs (Kumari et al. 2013; Okolo et al. 2007). In this study, it was speculated that the lack of PAH removal observed in either soil may not be explained only by low PAH bioavailability, but inhibition by other potential wastes/by-products may be possible. This could be overcome by characterising other co-contaminants residing at the contaminated site and assess their impact on biodegradative processes prior to bioremediation. Detailed characterisation of all constituents residing at the contaminated site may lead to a comprehensive understanding of the nature and extent of contamination of the target soil to be remediated. The chemical data reported in Chapter 3 may be used to strengthen the work of characterising potential co-contaminants in the newly proposed future investigation in these soils. Therefore, the information already gathered in relation to the soils used in this research would be the basis for additional identification of potential co-contaminants to be undertaken.

8.2.2 Bioaugmentation of PAH-degrading organisms isolated from target clean up soil and determination of their degradative capacity

Comprehensive studies of organisms selected for bioaugmentation have in some cases demonstrated that failure to achieve a clean-up target goal was due to an inability of inoculated organisms to survive in their new niche on the basis that they were outcompeted by indigenous microorganisms already adapted to the prevailing conditions at the contaminated site (Hamdi et al. 2007; Hosokawa et al. 2009; Nikolopoulou, Pasadakis & Kalogerakis 2013; Thompson et al. 2005). It is widely expected that species from different niches, released into the new niches are likely to exhibit a different set of physiological traits to suit changes in environmental conditions. Thus, the success of bioaugmentation treatments rely on appropriate identification and isolation of microbial strains, with the ability to adapt well and tolerate toxic effects associated with many contaminants once released into the soil. In the present study, inoculation of an exogenous microorganism (*Mycobacterium* gilvum) was not effective in any of the soils presumably due to the aforementioned reasons. However, a practical way to

overcome this issue would be to use microorganisms isolated from the same contaminated soil, to be decontaminated. Hence, it is critically important to consider isolation of autochthonous organisms already exposed to the contaminant rather than allochtonous ones. The application of molecular analysis would provide a powerful tool to monitor and assess their capacity to degrade PAHs and their ability to survive once reintroduced into the soil.

8.2.3 Identification of PAH metabolites

Identification of PAH metabolites originating from the biodegradation of high molecular weight. PAHs, as a result of initial ring oxidation and cleavage of pyrene, benzo(a)pyrene, and dibenz(a, h)anthracene would be beneficial to determine the partial degradative pathway found within the microbial community of soils used in this study. The primary goal of any degradation process is the complete mineralisation of target organic contaminants, with the expected by-products to be carbon dioxide, water and other inorganic compounds (Kotterman, Vis & Field 1998; Su et al. 2012). In some cases, both biological and chemical treatments may result in the production of numerous compounds that may potentially be resistant to further degradation. As a consequence, these dead-end products may then accumulate during the process of biodegradation, which may either inhibit or enhance the metabolic pathways of other species since metabolism within the microbial community involves an interactive chain of reactions. The application of high throughput metabolomics may offer a solid means of quantifying intermediates and compounds as the end products of the PAH metabolism in these soils.

The success of this recommended work would probably be built on the results PAH biodegradation presented in Chapter 3, coupled with potential pathways and associated enzymes identified through KGG pathway analysis reported in Chapters 5 and 7 in these soils.

8.2.4 Identification of active PAH-degrading organisms and specific genes involve in the metabolism of PAHs

The application of high throughput DNA sequencing employed in this study allowed the identification of microbial communities with the catabolic potential to degrade PAHs in the three soils. The application of metagenomics enable the identification of microbes are present, their abundance, diversity and the possible genomic potential they possess. However, metatranscriptomics analysis is likely to detect the active microbial community and the genes that are highly expressed as a consequence of contamination. It may be beneficial to identify active microbial community and the expression of specific genes affiliated with PAH biodegradation by the application of metatranscriptomics rather than having the identity

detected with the analysis of metagenomics as reported in this study. The new proposed line of research to identify active PAH-degrading organisms would be underpinned by massive information generated through Ion Proton sequencing platform reported in Chapters 5 and 7 in the three soils used in this study.

Reference

Abbai, NS, Govender, A, Shaik, R & Pillay, B 2012, 'Pyrosequence analysis of unamplified and whole genome amplified DNA from hydrocarbon-contaminated groundwater', *Molecular Biotechnology,* vol. 50, no. 1, pp. 39-48.

Abulencia, CB, Wyborski, DL, Garcia, JA, Podar, M, Chen, W, Chang, SH, Chang, HW, Watson, D, Brodie, EL & Hazen, TC 2006, 'Environmental whole-genome amplification to access microbial populations in contaminated sediments', *Applied and Environmental Microbiology,* vol. 72, no. 5, pp. 3291-3301.

Adams, IP, Glover, RH, Monger, WA, Mumford, R, Jackeviciene, E, Navalinskiene, M, Samuitiene, M & Boonham, N 2009, 'Next-generation sequencing and metagenomic analysis: a universal diagnostic tool in plant virology', *Molecular plant pathology,* vol. 10, no. 4, pp. 537-545.

Agarry, S, Audu, T & Solomon, B 2009, 'Substrate inhibition kinetics of phenol degradation by Pseudomonas fluorescence from steady state and wash-out data', *International Journal of Environmental Science & Technology,* vol. 6, no. 3, pp. 443-450.

Agarry, S 2012, 'Enhanced bioremediation of soil artificially contaminated with kerosene: optimization of biostimulation agents through statistical experimental design', *Journal of Petroleum & Environmental Biotechnology*.

Ahangar, AG 2010, 'Sorption of PAHs in the soil environment with emphasis on the role of soil organic matter: a review', *World Applied Sciences Journal,* vol. 11, no. 7, pp. 759-765.

Allan, IJ, Semple, KT, Hare, R & Reid, BJ 2006, 'Prediction of mono-and polycyclic aromatic hydrocarbon degradation in spiked soils using cyclodextrin extraction', *Environmental Pollution,* vol. 144, no. 2, pp. 562-571.

Allocati, N, Federici, L, Masulli, M & Di Ilio, C 2009, 'Glutathione transferases in bacteria', *Febs Journal,* vol. 276, no. 1, pp. 58-75.

Amend, AS, Seifert, KA & Bruns, TD 2010, 'Quantifying microbial communities with 454 pyrosequencing: Does read abundance count?', *Molecular Ecology,* vol. 19, no. 24, pp. 5555-5565.

Anokhina, T, Kochetkov, V, Zelenkova, N, Balakshina, V & Boronin, A 2004, 'Biodegradation of phenanthrene by Pseudomonas bacteria bearing rhizospheric plasmids in model plant–microbial associations', *Applied Biochemistry and Microbiology,* vol. 40, no. 6, pp. 568-572.

Argumedo-Delira, R, Alarcón, A, Ferrera-Cerrato, R, Almaraz, JJ & Peña-Cabriales, JJ 2012, 'Tolerance and growth of 11 Trichoderma strains to crude oil, naphthalene, phenanthrene and benzo[a]pyrene', *Journal of Environmental Management,* vol. 95, no. SUPPL., pp. S291-S299.

Attia, SM 2010, 'Deleterious effects of reactive metabolites', *Oxidative medicine and cellular longevity,* vol. 3, no. 4, pp. 238-253.

Balaji, V, Arulazhagan, P & Ebenezer, P 2014, 'Enzymatic bioremediation of polyaromatic hydrocarbons by fungal consortia enriched from petroleum contaminated soil and oil seeds', *Journal of Environmental Biology,* vol. 35, no. 3, pp. 521-529.

Bamforth, SM & Singleton, I 2005, 'Bioremediation of polycyclic aromatic hydrocarbons: current knowledge and future directions', *Journal of Chemical Technology and Biotechnology,* vol. 80, no. 7, pp. 723-736.

Bastiaens, L, Springael, D, Wattiau, P, Harms, H, Verachtert, H & Diels, L 2000, 'Isolation of adherent polycyclic aromatic hydrocarbon (PAH)-degrading bacteria using PAH-sorbing carriers', *Applied and Environmental Microbiology,* vol. 66, no. 5, pp. 1834-1843.

Bauer, JE & Capone, D 1988, 'Effects of co-occurring aromatic hydrocarbons on degradation of individual polycyclic aromatic hydrocarbons in marine sediment slurries', *Applied and Environmental Microbiology,* vol. 54, no. 7, pp. 1649-1655.

Bautista, LF, Sanz, R, Molina, MC, González, N & Sánchez, D 2009, 'Effect of different non-ionic surfactants on the biodegradation of PAHs by diverse aerobic bacteria', *International Biodeterioration & Biodegradation,* vol. 63, no. 7, pp. 913-922.

Bell, M 2003, 'From the 1870s to the 1970s: the changing face of public psychiatry in South Australia', *Australasian Psychiatry,* vol. 11, no. 1, pp. 79-86.

Bell, TH, Yergeau, E, Maynard, C, Juck, D, Whyte, LG & Greer, CW 2013, 'Predictable bacterial composition and hydrocarbon degradation in Arctic soils following diesel and nutrient disturbance', *The ISME journal,* vol. 7, no. 6, pp. 1200-1210.

Bento, FM, Camargo, FA, Okeke, BC & Frankenberger, WT 2005, 'Comparative bioremediation of soils contaminated with diesel oil by natural attenuation, biostimulation and bioaugmentation', *Bioresource Technology,* vol. 96, no. 9, pp. 1049-1055.

Bertin, PN, Médigue, C & Normand, P 2008, 'Advances in environmental genomics: towards an integrated view of micro-organisms and ecosystems', *Microbiology,* vol. 154, no. 2, pp. 347-359.

Bezalel, L, Hadar, Y & Cerniglia, CE 1997, 'Enzymatic Mechanisms Involved in Phenanthrene Degradation by the White Rot Fungus Pleurotus ostreatus', *Applied and Environmental Microbiology,* vol. 63, no. 7, pp. 2495-2501.

Bik, HM, Sung, W, De Ley, P, Baldwin, JG, Sharma, J, Rocha-Olivares, A & Thomas, WK 2012, 'Metagenetic community analysis of microbial eukaryotes illuminates biogeographic patterns in deep-sea and shallow water sediments', *Molecular Ecology,* vol. 21, no. 5, pp. 1048-1059.

Bishnoi, K, Kumar, R & Bishnoi, NR 2008, 'Biodegradation of polycyclic aromatic hydrocarbons by white rot fungi Phanerochaete chrysosporium in sterile and unsterile soil', *J Sci Ind Res,* vol. 67, pp. 538-542.

Bisht, S, Pandey, P, Bhargava, B, Sharma, S, Kumar, V & Sharma, KD 2015, 'Bioremediation of polyaromatic hydrocarbons (PAHs) using rhizosphere technology', *Brazilian Journal of Microbiology,* vol. 46, no. 1, pp. 7-21.

Boissy, RJ, Romberger, DJ, Roughead, WA, Weissenburger-Moser, L, Poole, JA & LeVan, TD 2014, 'Shotgun pyrosequencing metagenomic analyses of dusts from swine confinement and grain facilities', *PLoS ONE,* vol. 9, no. 4, p. e95578.

Boonchan, S, Britz, ML & Stanley, GA 2000, 'Degradation and mineralization of high-molecular-weight polycyclic aromatic hydrocarbons by defined fungal-bacterial cocultures', *Applied and Environmental Microbiology,* vol. 66, no. 3, pp. 1007-1019.

Bortey-Sam, N, Ikenaka, Y, Nakayama, SMM, Akoto, O, Yohannes, YB, Baidoo, E, Mizukawa, H & Ishizuka, M 2014, 'Occurrence, distribution, sources and toxic potential of polycyclic aromatic hydrocarbons (PAHs) in surface soils from the Kumasi Metropolis, Ghana', *Science of the Total Environment,* vol. 496, pp. 471-478.

Braddock, JF, Ruth, ML, Catterall, PH, Walworth, JL & McCarthy, KA 1997, 'Enhancement and inhibition of microbial activity in hydrocarbon-contaminated arctic soils: implications for nutrient-amended bioremediation', *Environmental Science & Technology,* vol. 31, no. 7, pp. 2078-2084.

Braddock, JF & Catterall, PH 1999, 'A simple method for enumerating gasoline-and diesel-degrading microorganisms', *Bioremediation Journal,* vol. 3, no. 2, pp. 81-84.

Brennerova, MV, Josefiova, J, Brenner, V, Pieper, DH & Junca, H 2009, 'Metagenomics reveals diversity and abundance of meta-cleavage pathways in microbial communities from soil highly contaminated with jet fuel under air-sparging bioremediation', *Environmental Microbiology,* vol. 11, no. 9, pp. 2216-2227.

Brezna, B, Khan, AA & Cerniglia, CE 2003, 'Molecular characterization of dioxygenases from polycyclic aromatic hydrocarbon-degrading Mycobacterium spp', *FEMS Microbiology Letters,* vol. 223, no. 2, pp. 177-183.

Cai, JJ, Song, JH, Lee, Y & Lee, DS 2014, 'Assessment of climate change impact on the fates of polycyclic aromatic hydrocarbons in the multimedia environment based on model prediction', *Science of the Total Environment,* vol. 470-471, pp. 1526-1536.

Carmichael, LM & Pfaender, FK 1997, 'Polynuclear aromatic hydrocarbon metabolism in soils: relationship to soil characteristics and preexposure', *Environmental Toxicology and Chemistry,* vol. 16, no. 4, pp. 666-675.

Castro-Gutiérrez, V, Rodriguez-Rodriguez, CE & Vargas-Azofeifa, I 2012, 'Hydrocarbon degrading microflora in a tropical fuel-contaminated aquifer: assessing the feasibility of PAH bioremediation', *International journal of environmental research,* vol. 6, no. 1, pp. 345-352.

Cébron, A, Norini, M-P, Beguiristain, T & Leyval, C 2008, 'Real-time PCR quantification of PAH-ring hydroxylating dioxygenase (PAH-RHD α) genes from Gram positive and Gram negative bacteria in soil and sediment samples', *Journal of microbiological methods,* vol. 73, no. 2, pp. 148-159.

Cébron, A, Faure, P, Lorgeoux, C, Ouvrard, S & Leyval, C 2013, 'Experimental increase in availability of a PAH complex organic contamination from an aged contaminated soil: Consequences on biodegradation', *Environmental Pollution,* vol. 177, pp. 98-105.

Cerniglia, CE 1992, 'Biodegradation of polycyclic aromatic hydrocarbons', *Biodegradation,* vol. 3, no. 2, pp. 351-368.

Cerniglia, CE 1993, 'Biodegradation of polycyclic aromatic hydrocarbons', *Microorganisms to combat pollution,* Springer, pp. 227-244.

Cerniglia, CE 1997, 'Fungal metabolism of polycyclic aromatic hydrocarbons: past, present and future applications in bioremediation', *Journal of industrial microbiology & biotechnology,* vol. 19, no. 5, pp. 324-333.

Chadhain, SMN, Norman, RS, Pesce, KV, Kukor, JJ & Zylstra, GJ 2006, 'Microbial dioxygenase gene population shifts during polycyclic aromatic hydrocarbon biodegradation', *Applied and Environmental Microbiology,* vol. 72, no. 6, pp. 4078-4087.

Chauhan, A & Jain, RK 2010, 'Biodegradation: gaining insight through proteomics', *Biodegradation,* vol. 21, no. 6, pp. 861-879.

Chemicals, BTP 2001, 'EMERGENCY PLANNING AND COMMUNITY RIGHT-TO-KNOW ACT-SECTION 313: Guidance for Reporting Toxic Chemicals: Pesticides and Other Persistent'.

Chen, S-H & Aitken, MD 1999, 'Salicylate stimulates the degradation of high-molecular weight polycyclic aromatic hydrocarbons by Pseudomonas saccharophila P15', *Environmental Science & Technology,* vol. 33, no. 3, pp. 435-439.

Chen, S, Li, S, Xie, W, Li, X, Zhang, C, Jiang, H, Zheng, J, Pan, X, Zheng, H & Liu, JS 2014, 'Performance comparison between rapid sequencing platforms for ultra-low coverage sequencing strategy', *PLoS ONE,* vol. 9, no. 3, p. e92192.

Cheung, P-Y & Kinkle, BK 2001, 'Mycobacterium diversity and pyrene mineralization in petroleum-contaminated soils', *Applied and Environmental Microbiology,* vol. 67, no. 5, pp. 2222-2229.

Chiellini, C, Iannelli, R, Lena, R, Gullo, M & Petroni, G 2014, 'Bacterial Community Characterization in Paper Mill White Water', *BioResources,* vol. 9, no. 2, pp. 2541-2559.

Chikere, CB, Okpokwasili, GC & Chikere, BO 2011, 'Monitoring of microbial hydrocarbon remediation in the soil', *3 Biotech,* vol. 1, no. 3, pp. 117-138.

Chu, H, Wang, S, Yue, H, Lin, Q, Hu, Y, Li, X, Zhou, J & Yang, Y 2014, 'Contrasting soil microbial community functional structures in two major landscapes of the Tibetan alpine meadow', *MicrobiologyOpen,* vol. 3, no. 5, pp. 585-594.

Churchill, SA, Harper, JP & Churchill, PF 1999, 'Isolation and characterization of aMycobacterium species capable of degrading three-and four-ring aromatic and aliphatic hydrocarbons', *Applied and Environmental Microbiology,* vol. 65, no. 2, pp. 549-552.

Cornelissen, G, Rigterink, H, Ferdinandy, MM & van Noort, PC 1998, 'Rapidly desorbing fractions of PAHs in contaminated sediments as a predictor of the extent of bioremediation', *Environmental Science & Technology,* vol. 32, no. 7, pp. 966-970.

Cornelissen, G, Gustafsson, Ö, Bucheli, TD, Jonker, MT, Koelmans, AA & van Noort, PC 2005, 'Extensive sorption of organic compounds to black carbon, coal, and kerogen in sediments and soils: mechanisms and consequences for distribution, bioaccumulation, and biodegradation', *Environmental Science & Technology,* vol. 39, no. 18, pp. 6881-6895.

Couling, NR, Towell, MG & Semple, KT 2010, 'Biodegradation of PAHs in soil: influence of chemical structure, concentration and multiple amendment', *Environmental Pollution,* vol. 158, no. 11, pp. 3411-3420.

Cuypers, C, Pancras, T, Grotenhuis, T & Rulkens, W 2002, 'The estimation of PAH bioavailability in contaminated sediments using hydroxypropyl-β-cyclodextrin and Triton X-100 extraction techniques', *Chemosphere,* vol. 46, no. 8, pp. 1235-1245.

Dabestani, R & Ivanov, IN 1999, 'A compilation of physical, spectroscopic and photophysical properties of polycyclic aromatic hydrocarbons', *Photochemistry and photobiology,* vol. 70, no. 1, pp. 10-34.

Daniel, R 2005, 'The metagenomics of soil', *Nature Reviews Microbiology,* vol. 3, no. 6, pp. 470-478.

Das, M, Royer, TV & Leff, LG 2007, 'Diversity of fungi, bacteria, and actinomycetes on leaves decomposing in a stream', *Applied and Environmental Microbiology,* vol. 73, no. 3, pp. 756-767.

Decker, M, Arand, M & Cronin, A 2009, 'Mammalian epoxide hydrolases in xenobiotic metabolism and signalling', *Archives of toxicology,* vol. 83, no. 4, pp. 297-318.

Dell'Anno, A, Beolchini, F, Rocchetti, L, Luna, GM & Danovaro, R 2012, 'High bacterial biodiversity increases degradation performance of hydrocarbons during bioremediation of contaminated harbor marine sediments', *Environmental Pollution,* vol. 167, pp. 85-92.

Desai, C, Pathak, H & Madamwar, D 2010, 'Advances in molecular and "-omics" technologies to gauge microbial communities and bioremediation at xenobiotic/anthropogen contaminated sites', *Bioresource Technology,* vol. 101, no. 6, pp. 1558-1569.

Dey, S & Mukherjee, S 2010, 'Performance and kinetic evaluation of phenol biodegradation by mixed microbial culture in a batch reactor', *International Journal of Water Resources and Environmental Engineering,* vol. 2, no. 3, pp. 40-49.

Díaz, E 2010, 'Bacterial degradation of aromatic pollutants: a paradigm of metabolic versatility', *International Microbiology,* vol. 7, no. 3, pp. 173-180.

Dixit, P, Mukherjee, PK, Sherkhane, PD, Kale, SP & Eapen, S 2011, 'Enhanced tolerance and remediation of anthracene by transgenic tobacco plants expressing a fungal glutathione transferase gene', *Journal of Hazardous Materials,* vol. 192, no. 1, pp. 270-276.

Dixit, R, Malaviya, D, Pandiyan, K, Singh, UB, Sahu, A, Shukla, R, Singh, BP, Rai, JP, Sharma, PK & Lade, H 2015, 'Bioremediation of Heavy Metals from Soil and Aquatic Environment: An Overview of Principles and Criteria of Fundamental Processes', *Sustainability,* vol. 7, no. 2, pp. 2189-2212.

Doick, KJ, Dew, NM & Semple, KT 2005, 'Linking catabolism to cyclodextrin extractability: determination of the microbial availability of PAHs in soil', *Environmental Science & Technology,* vol. 39, no. 22, pp. 8858-8864.

Doick, KJ, Clasper, PJ, Urmann, K & Semple, KT 2006, 'Further validation of the HPCD-technique for the evaluation of PAH microbial availability in soil', *Environmental Pollution,* vol. 144, no. 1, pp. 345-354.

Duarte, S, Pascoal, C & Cassio, F 2012, *Denaturing Gradient Gel Electrophoresis (DGGE) in Microbial Ecology-Insights from Freshwaters*, INTECH Open Access Publisher,

Egan, AN, Schlueter, J & Spooner, DM 2012, 'Applications of next-generation sequencing in plant biology', *American Journal of Botany,* vol. 99, no. 2, pp. 175-185.

EPA, U 2004, *Cleaning Up the Nation's Waste Sites: Markets and Technology Trends*, US Environmental Protection Agency Washington, DC.

Ercolini, D 2004, 'PCR-DGGE fingerprinting: novel strategies for detection of microbes in food', *Journal of microbiological methods,* vol. 56, no. 3, pp. 297-314.

Erkelens, M, Adetutu, EM, Taha, M, Tudararo-Aherobo, L, Antiabong, J, Provatas, A & Ball, AS 2012, 'Sustainable remediation–The application of bioremediated soil for use in the degradation of TNT chips', *Journal of Environmental Management,* vol. 110, pp. 69-76.

Essumang, DK, 'ENVIRONMENTAL XENOBIOTICS: PAHs IN SOIL (HEAVY METALS), INDOOR AIR AND WATER ENVIRONMENT, CASE STUDIES OF GHANA AND DENMARK', Videnbasen for Aalborg UniversitetVBN, Aalborg UniversitetAalborg University, Det Teknisk-Naturvidenskabelige FakultetThe Faculty of Engineering and Science, Sektion for KemiteknologiSection of Chemical Engineering.

Essumang, DK, ADOKOH, CK, AFRIYIE, J & Mensah, E 2009, 'Source assessment and analysis of polycyclic aromatic hydrocarbon (PAH's) in the Oblogo waste disposal sites and some water bodies in and around the Accra Metropolis of Ghana', *Journal of Water Resource and Protection,* vol. 2009.

Eyers, L, George, I, Schuler, L, Stenuit, B, Agathos, SN & El Fantroussi, S 2004, 'Environmental genomics: exploring the unmined richness of microbes to degrade xenobiotics', *Applied Microbiology and Biotechnology,* vol. 66, no. 2, pp. 123-130.

Fang, H, Cai, L, Yu, Y & Zhang, T 2013, 'Metagenomic analysis reveals the prevalence of biodegradation genes for organic pollutants in activated sludge', *Bioresource Technology,* vol. 129, pp. 209-218.

Ferguson, SH, Woinarski, AZ, Snape, I, Morris, CE & Revill, AT 2004, 'A field trial of in situ chemical oxidation to remediate long-term diesel contaminated Antarctic soil', *Cold Regions Science and Technology,* vol. 40, no. 1, pp. 47-60.

Ferrarese, E, Andreottola, G & Oprea, IA 2008, 'Remediation of PAH-contaminated sediments by chemical oxidation', *Journal of Hazardous Materials,* vol. 152, no. 1, pp. 128-139.

Ferris, M, Muyzer, G & Ward, D 1996, 'Denaturing gradient gel electrophoresis profiles of 16S rRNA-defined populations inhabiting a hot spring microbial mat community', *Applied and Environmental Microbiology,* vol. 62, no. 2, pp. 340-346.

Franzetti, A, Gandolfi, I, Bestetti, G & Banat, I 2010, '(Bio) surfactant and Bioremediation, Successes and Failures'.

Gadd, GM 2000, 'Bioremedial potential of microbial mechanisms of metal mobilization and immobilization', *Current Opinion in Biotechnology,* vol. 11, no. 3, pp. 271-279.

García-Delgado, C, Alfaro-Barta, I & Eymar, E 2015, 'Combination of biochar amendment and mycoremediation for polycyclic aromatic hydrocarbons immobilization and biodegradation in creosote-contaminated soil', *Journal of Hazardous Materials,* vol. 285, pp. 259-266.

García-Delgado, C, D'Annibale, A, Pesciaroli, L, Yunta, F, Crognale, S, Petruccioli, M & Eymar, E 2015, 'Implications of polluted soil biostimulation and bioaugmentation with spent mushroom substrate (Agaricus bisporus) on the microbial community and polycyclic aromatic hydrocarbons biodegradation', *Science of the Total Environment,* vol. 508, pp. 20-28.

Gateuille, D, Evrard, O, Lefevre, I, Moreau-Guigon, E, Alliot, F, Chevreuil, M & Mouchel, JM 2014, 'Mass balance and decontamination times of Polycyclic Aromatic Hydrocarbons in rural nested catchments of an early industrialized region (Seine River basin, France)', *Science of the Total Environment,* vol. 470-471, pp. 608-617.

Gelderman, G & Contreras, LM 2013, 'Discovery of posttranscriptional regulatory RNAs using next generation sequencing technologies', *Methods in molecular biology (Clifton, N.J.),* vol. 985, //, pp. 269-295.

Gentry, T, Rensing, C & Pepper, I 2004, 'New approaches for bioaugmentation as a remediation technology', *Critical reviews in environmental science and technology,* vol. 34, no. 5, pp. 447-494.

Gerlach, W & Stoye, J 2011, 'Taxonomic classification of metagenomic shotgun sequences with CARMA3', *Nucleic Acids Research,* vol. 39, no. 14.

Ghosal, D, Chakraborty, J, Khara, P & Dutta, TK 2010, 'Degradation of phenanthrene via meta-cleavage of 2-hydroxy-1-naphthoic acid by Ochrobactrum sp. strain PWTJD', *FEMS Microbiology Letters,* vol. 313, no. 2, pp. 103-110.

Girard, P & Angers, B 2011, 'The functional gene diversity in natural populations over postglacial areas: The shaping mechanisms behind genetic composition of longnose dace (Rhinichthys cataractae) in northeastern North America', *Journal of molecular evolution,* vol. 73, no. 1-2, pp. 45-57.

Glenn, TC 2011, 'Field guide to next-generation DNA sequencers', *Molecular Ecology Resources,* vol. 11, no. 5, pp. 759-769.

Goi, A, Trapido, M & Kulik, N 2009, 'Contaminated soil remediation with hydrogen peroxide oxidation', *World Acad. Sci. Eng. Technol,* vol. 52, pp. 185-189.

González, N, Simarro, R, Molina, M, Bautista, L, Delgado, L & Villa, J 2011, 'Effect of surfactants on PAH biodegradation by a bacterial consortium and on the dynamics of the bacterial community during the process', *Bioresource Technology,* vol. 102, no. 20, pp. 9438-9446.

Grosser, R, Warshawsky, D & Vestal, JR 1991, 'Indigenous and enhanced mineralization of pyrene, benzo [a] pyrene, and carbazole in soils', *Applied and Environmental Microbiology,* vol. 57, no. 12, pp. 3462-3469.

Grumbt, B, Eck, SH, Hinrichsen, T & Hirv, K 2013, 'Diagnostic applications of next generation sequencing in immunogenetics and molecular oncology', *Transfusion Medicine and Hemotherapy,* vol. 40, no. 3, pp. 196-206.

Hadibarata, T & Tachibana, S 2009, 'Microbial degradation of crude oil by fungi pre-grown on wood meal', *Interdisciplinary studies on environmental chemistry—environmental research in Asia,* pp. 317-332.

Hamdi, H, Benzarti, S, Manusadžianas, L, Aoyama, I & Jedidi, N 2007, 'Bioaugmentation and biostimulation effects on PAH dissipation and soil ecotoxicity under controlled conditions', *Soil Biology and Biochemistry,* vol. 39, no. 8, pp. 1926-1935.

Handelsman, J, Rondon, MR, Brady, SF, Clardy, J & Goodman, RM 1998, 'Molecular biological access to the chemistry of unknown soil microbes: a new frontier for natural products', *Chemistry & biology,* vol. 5, no. 10, pp. R245-R249.

Handelsman, J 2004, 'Metagenomics: application of genomics to uncultured microorganisms', *Microbiology and Molecular Biology Reviews,* vol. 68, no. 4, pp. 669-685.

Hansel, CM, Fendorf, S, Jardine, PM & Francis, CA 2008, 'Changes in bacterial and archaeal community structure and functional diversity along a geochemically variable soil profile', *Applied and Environmental Microbiology*, vol. 74, no. 5, pp. 1620-1633.

Harayama, S 1997, 'Polycyclic aromatic hydrocarbon bioremediation design', *Current opinion in biotechnology*, vol. 8, no. 3, pp. 268-273.

Harismendy, O, Ng, PC, Strausberg, RL, Wang, X, Stockwell, TB, Beeson, KY, Schork, NJ, Murray, SS, Topol, EJ, Levy, S & Frazer, KA 2009, 'Evaluation of next generation sequencing platforms for population targeted sequencing studies', *Genome Biology*, vol. 10, no. 3, //.

Heitkamp, MA & Cerniglia, CE 1986, 'Microbial degradation of t-butylphenyl diphenyl phosphate: A comparative microcosm study among five diverse ecosystems', *Toxicity Assessment*, vol. 1, no. 1, pp. 103-122.

Heitkamp, MA, Franklin, W & Cerniglia, CE 1988, 'Microbial metabolism of polycyclic aromatic hydrocarbons: isolation and characterization of a pyrene-degrading bacterium', *Applied and Environmental Microbiology*, vol. 54, no. 10, pp. 2549-2555.

Hert, DG, Fredlake, CP & Barron, AE 2008, 'Advantages and limitations of next-generation sequencing technologies: A comparison of electrophoresis and non-electrophoresis methods', *Electrophoresis*, vol. 29, no. 23, pp. 4618-4626.

Hickman, ZA, Swindell, AL, Allan, IJ, Rhodes, AH, Hare, R, Semple, KT & Reid, BJ 2008, 'Assessing biodegradation potential of PAHs in complex multi-contaminant matrices', *Environmental Pollution*, vol. 156, no. 3, pp. 1041-1045.

Hollibaugh, J 1994, 'Relationship between thymidine metabolism, bacterioplankton community metabolic capabilities, and sources of organic matter', *Microbial ecology*, vol. 28, no. 2, pp. 117-131.

Hosokawa, R, Nagai, M, Morikawa, M & Okuyama, H 2009, 'Autochthonous bioaugmentation and its possible application to oil spills', *World Journal of Microbiology and Biotechnology*, vol. 25, no. 9, pp. 1519-1528.

Huesemann, MH, Hausmann, TS & Fortman, TJ 2004, 'Does bioavailability limit biodegradation? A comparison of hydrocarbon biodegradation and desorption rates in aged soils', *Biodegradation*, vol. 15, no. 4, pp. 261-274.

Hugenholtz, P, Goebel, BM & Pace, NR 1998, 'Impact of culture-independent studies on the emerging phylogenetic view of bacterial diversity', *Journal of bacteriology*, vol. 180, no. 18, pp. 4765-4774.

Hugenholtz, P & Tyson, GW 2008, 'Microbiology: metagenomics', *Nature*, vol. 455, no. 7212, pp. 481-483.

Hussain, K & Hoque, RR 2015, 'Seasonal attributes of urban soil PAHs of the Brahmaputra Valley', *Chemosphere*, vol. 119, pp. 794-802.

İnceoğlu, Ö, Al-Soud, WA, Salles, JF, Semenov, AV & van Elsas, JD 2011, 'Comparative analysis of bacterial communities in a potato field as determined by pyrosequencing', *PLoS ONE*, vol. 6, no. 8, p. e23321.

Jain, PK 2014, 'Microbial biodegradation of polycyclic aromatic hydrocarbons', *Microbial Biotechnology: Progress and Trends*, p. 331.

Johnson, BL & DeRosa, CT 1995, 'Chemical mixtures released from hazardous waste sites: implications for health risk assessment', *Toxicology*, vol. 105, no. 2, pp. 145-156.

Johnson, CR & Scow, KM 1999, 'Effect of nitrogen and phosphorus addition on phenanthrene biodegradation in four soils', *Biodegradation*, vol. 10, no. 1, pp. 43-50.

Joutey, NT, Bahafid, W, Sayel, H & El Ghachtouli, N 2013, 'Biodegradation: involved microorganisms and genetically engineered microorganisms', *Biodegradation-life of science. InTech, Rijeka*, pp. 289-320.

Juhasz, AL & Naidu, R 2000, 'Bioremediation of high molecular weight polycyclic aromatic hydrocarbons: a review of the microbial degradation of benzo [< i> a</i>] pyrene', *International Biodeterioration & Biodegradation*, vol. 45, no. 1, pp. 57-88.

Juhasz, AL, Waller, N & Stewart, R 2005, 'Predicting the efficacy of polycyclic aromatic hydrocarbon bioremediation in creosote-contaminated soil using bioavailability assays', *Bioremediation Journal*, vol. 9, no. 2, pp. 99-114.

Juhasz, AL, Aleer, S & Adetutu, EM 2014, 'Predicting PAH bioremediation efficacy using bioaccessibility assessment tools: Validation of PAH biodegradation–bioaccessibility correlations', *International Biodeterioration & Biodegradation*, vol. 95, pp. 320-329.

Kalantary, RR, Mohseni-Bandpi, A, Esrafili, A, Nasseri, S, Ashmagh, FR, Jorfi, S & Ja'fari, M 2014, 'Effectiveness of biostimulation through nutrient content on the bioremediation of phenanthrene contaminated soil', *Journal of Environmental Health Science and Engineering*, vol. 12, no. 1, p. 143.

Kanaly, RA, Bartha, R, Watanabe, K & Harayama, S 2000, 'Rapid mineralization of benzo [a] pyrene by a microbial consortium growing on diesel fuel', *Applied and Environmental Microbiology*, vol. 66, no. 10, pp. 4205-4211.

Kanaly, RA & Harayama, S 2000, 'Biodegradation of high-molecular-weight polycyclic aromatic hydrocarbons by bacteria', *Journal of bacteriology,* vol. 182, no. 8, pp. 2059-2067.

Kanavarioti, A, Greenman, KL, Hamalainen, M, Jain, A, Johns, AM, Melville, CR, Kemmish, K & Andregg, W 2012, 'Capillary electrophoretic separation-based approach to determine the labeling kinetics of oligodeoxynucleotides', *Electrophoresis,* vol. 33, no. 23, //, pp. 3529-3543.

Kanehisa, M 1997, 'A database for post-genome analysis', *Trends in Genetics,* vol. 9, no. 13, pp. 375-376.

Karigar, CS & Rao, SS 2011, 'Role of microbial enzymes in the bioremediation of pollutants: a review', *Enzyme Research,* vol. 2011.

Kasai, D, Masai, E, Miyauchi, K, Katayama, Y & Fukuda, M 2005, 'Characterization of the gallate dioxygenase gene: three distinct ring cleavage dioxygenases are involved in syringate degradation by Sphingomonas paucimobilis SYK-6', *Journal of bacteriology,* vol. 187, no. 15, pp. 5067-5074.

Kennaway, E 1955, 'The identification of a carcinogenic compound in coal-tar', *British medical journal,* vol. 2, no. 4942, p. 749.

Khan, A, Ishaq, M & Khan, MA 2008, 'Effect of vehicle exhaust on the quantity of polycyclic aromatic hydrocarbons (PAHs) in soil', *Environmental monitoring and assessment,* vol. 137, no. 1-3, pp. 363-369.

Khan, MI, Cheema, SA, Shen, C, Zhang, C, Tang, X, Shi, J, Chen, X, Park, J & Chen, Y 2012, 'Assessment of phenanthrene bioavailability in aged and unaged soils by mild extraction', *Environmental monitoring and assessment,* vol. 184, no. 1, pp. 549-559.

Knapp, M & Hofreiter, M 2010, 'Next generation sequencing of ancient DNA: Requirements, strategies and perspectives', *Genes,* vol. 1, no. 2, //, pp. 227-243.

Korbel, JO, Urban, AE, Affourtit, JP, Godwin, B, Grubert, F, Simons, JF, Kim, PM, Palejev, D, Carriero, NJ & Du, L 2007, 'Paired-end mapping reveals extensive structural variation in the human genome', *Science,* vol. 318, no. 5849, pp. 420-426.

Kotterman, MJJ, Vis, EH & Field, JA 1998, 'Successive mineralization and detoxification of benzo[a]pyrene by the white rot fungus Bjerkandera sp. strain BOS55 and indigenous microflora', *Applied and Environmental Microbiology,* vol. 64, no. 8, pp. 2853-2858.

Krauss, M, Wilcke, W & Zech, W 2000, 'Polycyclic aromatic hydrocarbons and polychlorinated biphenyls in forest soils: Depth distribution as indicator of different fate', *Environmental Pollution,* vol. 110, no. 1, pp. 79-88.

Kristiansson, E, Fick, J, Janzon, A, Grabic, R, Rutgersson, C, Weijdegård, B, Söderström, H & Larsson, DJ 2011, 'Pyrosequencing of antibiotic-contaminated river sediments reveals high levels of resistance and gene transfer elements', *PLoS ONE*, vol. 6, no. 2, p. e17038.

Kumari, S, Chetty, D, Ramdhani, N & Bux, F 2013, 'Phenol degrading ability of Rhodococcus pyrinidivorans and Pseudomonas aeruginosa isolated from activated sludge plants in South Africa', *Journal of Environmental Science and Health, Part A*, vol. 48, no. 8, pp. 947-953.

Laha, S, Tansel, B & Ussawarujikulchai, A 2009, 'Surfactant–soil interactions during surfactant-amended remediation of contaminated soils by hydrophobic organic compounds: a review', *Journal of Environmental Management*, vol. 90, no. 1, pp. 95-100.

Langworthy, DE, Stapleton, RD, Sayler, GS & Findlay, RH 1998, 'Genotypic and phenotypic responses of a riverine microbial community to polycyclic aromatic hydrocarbon contamination', *Applied and Environmental Microbiology*, vol. 64, no. 9, pp. 3422-3428.

Laurent, F, Cébron, A, Schwartz, C & Leyval, C 2012, 'Oxidation of a PAH polluted soil using modified Fenton reaction in unsaturated condition affects biological and physico-chemical properties', *Chemosphere*, vol. 86, no. 6, pp. 659-664.

Lee, OO, Wang, Y, Yang, J, Lafi, FF, Al-Suwailem, A & Qian, P-Y 2011, 'Pyrosequencing reveals highly diverse and species-specific microbial communities in sponges from the Red Sea', *ISME J*, vol. 5, no. 4, 04//print, pp. 650-664.

Leštan, D & Lamar, RT 1996, 'Development of fungal inocula for bioaugmentation of contaminated soils', *Applied and Environmental Microbiology*, vol. 62, no. 6, pp. 2045-2052.

Leys, NM, Ryngaert, A, Bastiaens, L, Wattiau, P, Top, EM, Verstraete, W & Springael, D 2005, 'Occurrence and community composition of fast-growing Mycobacterium in soils contaminated with polycyclic aromatic hydrocarbons', *FEMS microbiology ecology*, vol. 51, no. 3, pp. 375-388.

Li, G-l, Lang, Y-h, Gao, M-s, Yang, W, Peng, P & Wang, X-m 2014, 'Carcinogenic and mutagenic potencies for different PAHs sources in coastal sediments of Shandong Peninsula', *Marine Pollution Bulletin*, vol. 84, no. 1, pp. 418-423.

Li, G, Lang, Y, Yang, W, Peng, P & Wang, X 2014, 'Source contributions of PAHs and toxicity in reed wetland soils of Liaohe estuary using a CMB-TEQ method', *Science of the Total Environment*, vol. 490, pp. 199-204.

Li, X, Li, P, Lin, X, Zhang, C, Li, Q & Gong, Z 2008, 'Biodegradation of aged polycyclic aromatic hydrocarbons (PAHs) by microbial consortia in soil and slurry phases', *Journal of Hazardous Materials*, vol. 150, no. 1, pp. 21-26.

Li, X, Hou, L, Liu, M, Zheng, Y, Li, Y & Lin, X 2015, 'Abundance and diversity of polycyclic aromatic hydrocarbon degradation bacteria in urban roadside soils in Shanghai', *Applied Microbiology and Biotechnology*, vol. 99, no. 8, pp. 3639-3649.

Liang, C, Dang, Z, Xiao, B, Huang, W & Liu, C 2006, 'Equilibrium sorption of phenanthrene by soil humic acids', *Chemosphere*, vol. 63, no. 11, pp. 1961-1968.

Liang, Y, Gardner, DR, Miller, CD, Chen, D, Anderson, AJ, Weimer, BC & Sims, RC 2006, 'Study of biochemical pathways and enzymes involved in pyrene degradation by Mycobacterium sp. strain KMS', *Applied and Environmental Microbiology*, vol. 72, no. 12, pp. 7821-7828.

Liang, Y, Van Nostrand, JD, Deng, Y, He, Z, Wu, L, Zhang, X, Li, G & Zhou, J 2011, 'Functional gene diversity of soil microbial communities from five oil-contaminated fields in China', *The ISME journal*, vol. 5, no. 3, pp. 403-413.

Liebeg, EW & Cutright, TJ 1999, 'The investigation of enhanced bioremediation through the addition of macro and micro nutrients in a PAH contaminated soil', *International Biodeterioration & Biodegradation*, vol. 44, no. 1, pp. 55-64.

Ling, J, Zhang, G, Sun, H, Fan, Y, Ju, J & Zhang, C 2011, 'Isolation and characterization of a novel pyrene-degrading Bacillus vallismortis strain JY3A', *Science of the Total Environment*, vol. 409, no. 10, pp. 1994-2000.

Linley, E, Denyer, SP, McDonnell, G, Simons, C & Maillard, J-Y 2012, 'Use of hydrogen peroxide as a biocide: new consideration of its mechanisms of biocidal action', *Journal of antimicrobial Chemotherapy*, vol. 67, no. 7, pp. 1589-1596.

Liste, H-H & Alexander, M 2002, 'Butanol extraction to predict bioavailability of PAHs in soil', *Chemosphere*, vol. 46, no. 7, pp. 1011-1017.

Liu, S, Luo, Y, Cao, Z, Wu, L, Ding, K & Christie, P 2004, 'Degradation of benzo [a] pyrene in soil with arbuscular mycorrhizal alfalfa', *Environmental Geochemistry and Health*, vol. 26, no. 2, pp. 285-293.

Lladó, S, Covino, S, Solanas, A, Viñas, M, Petruccioli, M & D'annibale, A 2013, 'Comparative assessment of bioremediation approaches to highly recalcitrant PAH degradation in a real industrial polluted soil', *Journal of Hazardous Materials*, vol. 248, pp. 407-414.

Lladó, S, Covino, S, Solanas, AM, Viñas, M, Petruccioli, M & D'Annibale, A 2013, 'Comparative assessment of bioremediation approaches to highly recalcitrant PAH degradation in a real industrial polluted soil', *Journal of Hazardous Materials*, vol. 248-249, no. 1, pp. 407-414.

Lladó, S, Covino, S, Solanas, A, Petruccioli, M, D'annibale, A & Vinas, M 2015, 'Pyrosequencing reveals the effect of mobilizing agents and lignocellulosic substrate amendment on microbial community composition in a real industrial PAH-polluted soil', *Journal of Hazardous Materials*, vol. 283, pp. 35-43.

Lohmann, R, MacFarlane, J & Gschwend, P 2005, 'Importance of black carbon to sorption of native PAHs, PCBs, and PCDDs in Boston and New York harbor sediments', *Environmental Science & Technology*, vol. 39, no. 1, pp. 141-148.

Luna, RA, Fasciano, LR, Jones, SC, Boyanton, BL, Ton, TT & Versalovic, J 2007, 'DNA pyrosequencing-based bacterial pathogen identification in a pediatric hospital setting', *Journal of clinical microbiology*, vol. 45, no. 9, pp. 2985-2992.

Lundstedt, S 2003, 'Analysis of PAHs and their transformations products in contaminated soil and remedial processes'.

Macbeth, TW, Cummings, DE, Spring, S, Petzke, LM & Sorenson, KS 2004, 'Molecular characterization of a dechlorinating community resulting from in situ biostimulation in a trichloroethene-contaminated deep, fractured basalt aquifer and comparison to a derivative laboratory culture', *Applied and Environmental Microbiology*, vol. 70, no. 12, pp. 7329-7341.

Mackay, D, Shiu, WY & Ma, K-C 1997, *Illustrated handbook of physical-chemical properties of environmental fate for organic chemicals*, CRC press,

Mackay, D, Shiu, W-Y, Ma, K-C & Lee, SC 2010, *Handbook of physical-chemical properties and environmental fate for organic chemicals*, CRC press,

Magurran, AE & Magurran, AE 1988, *Ecological diversity and its measurement*, Princeton university press Princeton,

Mahmoudi, N, Slater, GF & Juhasz, AL 2013, 'Assessing limitations for PAH biodegradation in long-term contaminated soils using bioaccessibility assays', *Water, Air, & Soil Pollution*, vol. 224, no. 2, pp. 1-11.

Makadia, TH, Adetutu, EM, Simons, KL, Jardine, D, Sheppard, PJ & Ball, AS 2011, 'Re-use of remediated soils for the bioremediation of waste oil sludge', *Journal of Environmental Management*, vol. 92, no. 3, pp. 866-871.

Maliszewska-Kordybach, B 1999, 'Sources, concentrations, fate and effects of polycyclic aromatic hydrocarbons (PAHs) in the environment. Part A: PAHs in air', *Polish Journal of Environmental Studies*, vol. 8, pp. 131-136.

Mancera-López, M, Esparza-Garcia, F, Chavez-Gomez, B, Rodriguez-Vazquez, R, Saucedo-Castaneda, G & Barrera-Cortes, J 2008, 'Bioremediation of an aged hydrocarbon-contaminated soil by a combined system of biostimulation–bioaugmentation with filamentous fungi', *International Biodeterioration & Biodegradation*, vol. 61, no. 2, pp. 151-160.

Manoli, E & Samara, C 1999, 'Polycyclic aromatic hydrocarbons in natural waters: sources, occurrence and analysis', *TrAC Trends in Analytical Chemistry*, vol. 18, no. 6, pp. 417-428.

Manzetti, S 2013, 'Polycyclic Aromatic Hydrocarbons in the Environment: Environmental Fate and Transformation', *Polycyclic Aromatic Compounds*, vol. 33, no. 4, pp. 311-330.

Mao, J, Luo, Y, Teng, Y & Li, Z 2012, 'Bioremediation of polycyclic aromatic hydrocarbon-contaminated soil by a bacterial consortium and associated microbial community changes', *International Biodeterioration & Biodegradation*, vol. 70, pp. 141-147.

Mardis, ER 2008, 'Next-generation DNA sequencing methods', *Annu. Rev. Genomics Hum. Genet.*, vol. 9, pp. 387-402.

Masih, A & Lal, JK 2014, 'Concentrations and carcinogenic profiles of polycyclic aromatic hydrocarbons (PAHs) in groundwater of an urban site at a terai belt of North India', *International Journal of Applied Engineering Research*, vol. 9, no. 1 SPEC.ISS., pp. 1-7.

McElroy, A, Farrington, J & Teal, J 1989, 'Bioavailability of polycyclic aromatic hydrocarbons in the aquatic environment', *Metabolism of Polycyclic Aromatic Hydrocarbons in the Aquatic Environment. CRC Press, Inc., Boca Raton Florida. 1989. p 1-39, 14 fig, 9 tab, 159 ref. NOAA Contract 83-ABD-00012.*

Megharaj, M, Ramakrishnan, B, Venkateswarlu, K, Sethunathan, N & Naidu, R 2011, 'Bioremediation approaches for organic pollutants: a critical perspective', *Environment international*, vol. 37, no. 8, pp. 1362-1375.

Meyer, F, Paarmann, D, D'Souza, M, Olson, R, Glass, EM, Kubal, M, Paczian, T, Rodriguez, A, Stevens, R & Wilke, A 2008, 'The metagenomics RAST server–a public resource for the automatic phylogenetic and functional analysis of metagenomes', *BMC Bioinformatics*, vol. 9, no. 1, p. 386.

Miller, C, Child, R, Hughes, J, Benscai, M, Der, J, Sims, R & Anderson, A 2007, 'Diversity of soil mycobacterium isolates from three sites that degrade polycyclic aromatic hydrocarbons', *Journal of applied microbiology*, vol. 102, no. 6, pp. 1612-1624.

Mills, MA, Bonner, JS, McDonald, TJ, Page, CA & Autenrieth, RL 2003, 'Intrinsic bioremediation of a petroleum-impacted wetland', *Marine Pollution Bulletin*, vol. 46, no. 7, pp. 887-899.

Miyasaka, T, Asami, H & Watanabe, K 2006, 'Impacts of bioremediation schemes on bacterial population in naphthalene-contaminated marine sediments', *Biodegradation*, vol. 17, no. 3, pp. 227-235.

Mohan, SV, Kisa, T, Ohkuma, T, Kanaly, RA & Shimizu, Y 2006, 'Bioremediation technologies for treatment of PAH-contaminated soil and strategies to enhance process efficiency', *Reviews in Environmental Science and Bio/Technology*, vol. 5, no. 4, pp. 347-374.

Morisseau, C & Hammock, BD 2005, 'Epoxide hydrolases: mechanisms, inhibitor designs, and biological roles', *Annu. Rev. Pharmacol. Toxicol.*, vol. 45, pp. 311-333.

Mrozik, A & Labuzek, S 2003, 'Bacterial degradation and bioremediation of polycyclic aromatic hydrocarbons', *Polish Journal of Environmental Studies*, vol. 1, no. 12.

Mueller, JG, Chapman, P & Pritchard, P 1989, 'Action of a fluoranthene-utilizing bacterial community on polycyclic aromatic hydrocarbon components of creosote', *Applied and Environmental Microbiology*, vol. 55, no. 12, pp. 3085-3090.

Mueller, JG, Middaugh, DP, Lantz, SE & Chapman, P 1991, 'Biodegradation of creosote and pentachlorophenol in contaminated groundwater: chemical and biological assessment', *Applied and Environmental Microbiology*, vol. 57, no. 5, pp. 1277-1285.

Muyzer, G, De Waal, EC & Uitterlinden, AG 1993, 'Profiling of complex microbial populations by denaturing gradient gel electrophoresis analysis of polymerase chain reaction-amplified genes coding for 16S rRNA', *Applied and Environmental Microbiology*, vol. 59, no. 3, pp. 695-700.

Muyzer, G & Smalla, K 1998, 'Application of denaturing gradient gel electrophoresis (DGGE) and temperature gradient gel electrophoresis (TGGE) in microbial ecology', *Antonie van Leeuwenhoek*, vol. 73, no. 1, pp. 127-141.

Myllykangas, S, Natsoulis, G, Bell, JM & Ji, HP 2011, 'Targeted sequencing library preparation by genomic DNA circularization', *BMC Biotechnology*, vol. 11.

Naidu, R, Semple, KT, Megharaj, M, Juhasz, A, Bolan, N, Gupta, S, Clothier, B, Schulin, R & Chaney, R 2008, 'Bioavailability, definition, assessment and implications for risk assessment'.

Nakamura, FM, Germano, MG & Tsai, SM 2014, 'Capacity of aromatic compound degradation by bacteria from Amazon Dark Earth', *Diversity*, vol. 6, no. 2, pp. 339-353.

Nakatsu, C 2007, 'Soil microbial community analysis using denaturing gradient gel electrophoresis', *Soil Science Society of America Journal*, vol. 71, no. 2, pp. 562-571.

Nakatsu, CH, Torsvik, V & Øvreås, L 2000, 'Soil community analysis using DGGE of 16S rDNA polymerase chain reaction products', *Soil Science Society of America Journal*, vol. 64, no. 4, pp. 1382-1388.

Nam, K, Rodriguez, W & Kukor, JJ 2001, 'Enhanced degradation of polycyclic aromatic hydrocarbons by biodegradation combined with a modified Fenton reaction', *Chemosphere*, vol. 45, no. 1, pp. 11-20.

Newcombe, RG 1998, 'Interval estimation for the difference between independent proportions: comparison of eleven methods', *Statistics in medicine*, vol. 17, no. 8, pp. 873-890.

Newman, JW, Morisseau, C & Hammock, BD 2005, 'Epoxide hydrolases: their roles and interactions with lipid metabolism', *Progress in lipid research*, vol. 44, no. 1, pp. 1-51.

Nikolcheva, LG, Bourque, T & Bärlocher, F 2005, 'Fungal diversity during initial stages of leaf decomposition in a stream', *Mycological research*, vol. 109, no. 02, pp. 246-253.

Nikolopoulou, M, Pasadakis, N & Kalogerakis, N 2013, 'Evaluation of autochthonous bioaugmentation and biostimulation during microcosm-simulated oil spills', *Marine Pollution Bulletin*, vol. 72, no. 1, pp. 165-173.

Nilsson, RH, Ryberg, M, Abarenkov, K, Sjökvist, E & Kristiansson, E 2009, 'The ITS region as a target for characterization of fungal communities using emerging sequencing technologies', *FEMS Microbiology Letters*, vol. 296, no. 1, //, pp. 97-101.

Nisbet, ICT & LaGoy, PK 1992, 'Toxic equivalency factors (TEFs) for polycyclic aromatic hydrocarbons (PAHs)', *Regulatory Toxicology and Pharmacology*, vol. 16, no. 3, pp. 290-300.

Northcott, GL & Jones, KC 2001, 'Partitioning, extractability, and formation of nonextractable PAH residues in soil. 1. Compound differences in aging and sequestration', *Environmental Science & Technology*, vol. 35, no. 6, pp. 1103-1110.

Oakley, A 2011, 'Glutathione transferases: a structural perspective', *Drug metabolism reviews*, vol. 43, no. 2, pp. 138-151.

Okere, UV & Semple, KT 2012, 'Biodegradation of PAHs in? Pristine? Soils from Different Climatic Regions', *Journal of Bioremediation & Biodegradation*, vol. 2012.

Okolo, J, Nweke, C, Nwabueze, R, Dike, C & Nwanyanwu, C 2007, 'Toxicity of phenolic compounds to oxidoreductases of Acinetobacter species isolated from a tropical soil', *Scientific Res. Essay*, vol. 2, no. 7, pp. 244-250.

Olsen, GJ, Lane, DJ, Giovannoni, SJ, Pace, NR & Stahl, DA 1986, 'Microbial ecology and evolution: a ribosomal RNA approach', *Annual Reviews in Microbiology,* vol. 40, no. 1, pp. 337-365.

Ovaskainen, O, Nokso-Koivisto, J, Hottola, J, Rajala, T, Pennanen, T, Ali-Kovero, H, Miettinen, O, Oinonen, P, Auvinen, P, Paulin, L, Larsson, KH & Mäkipää, R 2010, 'Identifying wood-inhabiting fungi with 454 sequencing - what is the probability that BLAST gives the correct species?', *Fungal Ecology,* vol. 3, no. 4, //, pp. 274-283.

Pan, B, Xing, B, Tao, S, Liu, W, Lin, X, Xiao, Y, Dai, H, Zhang, X, Zhang, Y & Yuan, H 2007, 'Effect of physical forms of soil organic matter on phenanthrene sorption', *Chemosphere,* vol. 68, no. 7, pp. 1262-1269.

Pandey, G, Chauhan, A, Samanta, SK & Jain, RK 2002, 'Chemotaxis of a Ralstonia sp. SJ98 toward co-metabolizable nitroaromatic compounds', *Biochemical and biophysical research communications,* vol. 299, no. 3, pp. 404-409.

Papadopoulos, A, Paton, GI, Reid, BJ & Semple, KT 2007, 'Prediction of PAH biodegradation in field contaminated soils using a cyclodextrin extraction technique', *Journal of Environmental Monitoring,* vol. 9, no. 6, pp. 516-522.

Papen, H & Von Berg, R 1998, 'A most probable number method (MPN) for the estimation of cell numbers of heterotrophic nitrifying bacteria in soil', *Plant and Soil,* vol. 199, no. 1, pp. 123-130.

Parks, DH & Beiko, RG 2010, 'Identifying biologically relevant differences between metagenomic communities', *Bioinformatics,* vol. 26, no. 6, pp. 715-721.

Patil, SS, Adetutu, EM, Aburto-Medina, A, Menz, IR & Ball, AS 2014, 'Biostimulation of indigenous communities for the successful dechlorination of tetrachloroethene (perchloroethylene)-contaminated groundwater', *Biotechnology letters,* vol. 36, no. 1, pp. 75-83.

Patri, M, Padmini, A & Babu, PP 2010, 'Polycyclic aromatic hydrocarbons in air and their neurotoxic potency in association with oxidative stress: a brief perspective', *Annals of Neurosciences,* vol. 16, no. 1, pp. 22-30.

Peixoto, RS, Vermelho, AB & Rosado, AS 2011, 'Petroleum-degrading enzymes: Bioremediation and new prospects', *Enzyme Research,* vol. 2011, no. 1, //.

Peng, R-H, Xiong, A-S, Xue, Y, Fu, X-Y, Gao, F, Zhao, W, Tian, Y-S & Yao, Q-H 2008, 'Microbial biodegradation of polyaromatic hydrocarbons', *FEMS microbiology reviews,* vol. 32, no. 6, pp. 927-955.

Petrosino, JF, Highlander, S, Luna, RA, Gibbs, RA & Versalovic, J 2009, 'Metagenomic pyrosequencing and microbial identification', *Clinical Chemistry*, vol. 55, no. 5, //, pp. 856-866.

Pignatello, JJ & Xing, B 1995, 'Mechanisms of slow sorption of organic chemicals to natural particles', *Environmental Science & Technology*, vol. 30, no. 1, pp. 1-11.

Qian, L & Chen, B 2012, 'Enhanced oxidation of benzo[a]pyrene by crude enzyme extracts produced during interspecific fungal interaction of Trametes versicolor and Phanerochaete chrysosporium', *Journal of Environmental Sciences (China)*, vol. 24, no. 9, pp. 1639-1646.

Quail, MA, Smith, M, Coupland, P, Otto, TD, Harris, SR, Connor, TR, Bertoni, A, Swerdlow, HP & Gu, Y 2012, 'A tale of three next generation sequencing platforms: comparison of Ion Torrent, Pacific Biosciences and Illumina MiSeq sequencers', *BMC Genomics*, vol. 13, no. 1, p. 341.

Ramos, RTJ, Carneiro, AR, Soares, SdC, Santos, ARd, Almeida, S, Guimarães, L, Figueira, F, Barbosa, E, Tauch, A & Azevedo, V 2012, 'Tips and tricks for the assembly of a Corynebacterium pseudotuberculosis genome using a semiconductor sequencer', *Microbial biotechnology*.

Reid, BJ, Jones, KC & Semple, KT 2000, 'Bioavailability of persistent organic pollutants in soils and sediments—a perspective on mechanisms, consequences and assessment', *Environmental Pollution*, vol. 108, no. 1, pp. 103-112.

Ren, G, Ren, W, Teng, Y & Li, Z 2015, 'Evident bacterial community changes but only slight degradation when polluted with pyrene in a red soil', *Frontiers in microbiology*, vol. 6.

Rhodes, AH, McAllister, LE & Semple, KT 2010, 'Linking desorption kinetics to phenanthrene biodegradation in soil', *Environmental Pollution*, vol. 158, no. 5, pp. 1348-1353.

Richter, BE, Jones, BA, Ezzell, JL, Porter, NL, Avdalovic, N & Pohl, C 1996, 'Accelerated solvent extraction: a technique for sample preparation', *Analytical chemistry*, vol. 68, no. 6, pp. 1033-1039.

Robles-González, IV, Fava, F & Poggi-Varaldo, HM 2008, 'A review on slurry bioreactors for bioremediation of soils and sediments', *Microb Cell Fact*, vol. 7, no. 5.

Rodrigues, A, Nogueira, R, Melo, LF & Brito, AG 2013, 'Effect of low concentrations of synthetic surfactants on polycyclic aromatic hydrocarbons (PAH) biodegradation', *International Biodeterioration & Biodegradation*, vol. 83, pp. 48-55.

Röling, WF & van Verseveld, HW 2002, 'Natural attenuation: What does the subsurface have in store?', *Biodegradation*, vol. 13, no. 1, pp. 53-64.

Rombolà, AG, Meredith, W, Snape, CE, Baronti, S, Genesio, L, Vaccari, FP, Miglietta, F & Fabbri, D 2015, 'Fate of soil organic carbon and polycyclic aromatic hydrocarbons in a vineyard soil treated with biochar', *Environmental Science & Technology*, vol. 49, no. 18, pp. 11037-11044.

Rostami, I & Juhasz, AL 2013, 'Bioaccessibility-based predictions for estimating PAH biodegradation efficacy–comparison of model predictions and measured endpoints', *International Biodeterioration & Biodegradation*, vol. 85, pp. 323-330.

Rowe, R, Todd, R & Waide, J 1977, 'Microtechnique for most-probable-number analysis', *Applied and Environmental Microbiology*, vol. 33, no. 3, pp. 675-680.

Roy, M, Khara, P & Dutta, TK 2012, 'meta-Cleavage of hydroxynaphthoic acids in the degradation of phenanthrene by Sphingobium sp. strain PNB', *Microbiology*, vol. 158, no. Pt 3, pp. 685-695.

Ruberto, LA, Vazquez, SC, Curtosi, A, Mestre, MC, Pelletier, E & Mac Cormack, WP 2006, 'Phenanthrene biodegradation in soils using an Antarctic bacterial consortium', *Bioremediation Journal*, vol. 10, no. 4, pp. 191-201.

Samanta, SK, Singh, OV & Jain, RK 2002, 'Polycyclic aromatic hydrocarbons: environmental pollution and bioremediation', *Trends in Biotechnology*, vol. 20, no. 6, pp. 243-248.

Sanapareddy, N, Hamp, TJ, Gonzalez, LC, Hilger, HA, Fodor, AA & Clinton, SM 2009, 'Molecular diversity of a North Carolina wastewater treatment plant as revealed by pyrosequencing', *Applied and Environmental Microbiology*, vol. 75, no. 6, pp. 1688-1696.

Sanger, F, Nicklen, S & Coulson, AR 1977, 'DNA sequencing with chain-terminating inhibitors', *Proceedings of the National Academy of Sciences of the United States of America*, vol. 74, no. 12, //, pp. 5463-5467.

Saponaro, S, Bonomo, L, Petruzzelli, G, Romele, L & Barbafieri, M 2002, 'Polycyclic aromatic hydrocarbons (PAHs) slurry phase bioremediation of a manufacturing gas plant (MGP) site aged soil', *Water, Air, and Soil Pollution*, vol. 135, no. 1-4, pp. 219-236.

Sayara, T, Borràs, E, Caminal, G, Sarrà, M & Sánchez, A 2011, 'Bioremediation of PAHs-contaminated soil through composting: Influence of bioaugmentation and biostimulation on contaminant biodegradation', *International Biodeterioration and Biodegradation*, vol. 65, no. 6, pp. 859-865.

Schippers, C, Gessner, K, Müller, T & Scheper, T 2000, 'Microbial degradation of phenanthrene by addition of a sophorolipid mixture', *Journal of Biotechnology*, vol. 83, no. 3, pp. 189-198.

Schumacher, BA 2002, 'Methods for the determination of total organic carbon (TOC) in soils and sediments', *Ecological Risk Assessment Support Center,* pp. 1-23.

Semple, KT, Morriss, A & Paton, G 2003, 'Bioavailability of hydrophobic organic contaminants in soils: fundamental concepts and techniques for analysis', *European Journal of Soil Science,* vol. 54, no. 4, pp. 809-818.

Semple, KT, Doick, KJ, Jones, KC, Burauel, P, Craven, A & Harms, H 2004, 'Peer reviewed: defining bioavailability and bioaccessibility of contaminated soil and sediment is complicated', *Environmental Science & Technology,* vol. 38, no. 12, pp. 228A-231A.

Semple, KT, Doick, KJ, Wick, LY & Harms, H 2007, 'Microbial interactions with organic contaminants in soil: definitions, processes and measurement', *Environmental Pollution,* vol. 150, no. 1, pp. 166-176.

Seo, J-S, Keum, Y-S & Li, QX 2009, 'Bacterial degradation of aromatic compounds', *International journal of environmental research and public health,* vol. 6, no. 1, pp. 278-309.

Sette, LD, de Oliveira, VM & Rodrigues, MFA 2008, 'Microbial lignocellulolytic enzymes: industrial applications and future perspectives', *Microbiology Australia,* vol. 29, no. 1, pp. 18-20.

Shahsavari, E, Adetutu, EM, Anderson, PA & Ball, AS 2013, 'Necrophytoremediation of phenanthrene and pyrene in contaminated soil', *Journal of Environmental Management,* vol. 122, pp. 105-112.

Shahsavari, E, Adetutu, EM, Anderson, PA & Ball, AS 2013, 'Plant residues—A low cost, effective bioremediation treatment for petrogenic hydrocarbon-contaminated soil', *Science of the Total Environment,* vol. 443, pp. 766-774.

Sheehan, D, MEADE, G, Foley, V & Dowd, C 2001, 'Structure, function and evolution of glutathione transferases: implications for classification of non-mammalian members of an ancient enzyme superfamily', *Biochem. J,* vol. 360, pp. 1-16.

Sheppard, PJ, Adetutu, EM, Makadia, TH & Ball, AS 2011, 'Microbial community and ecotoxicity analysis of bioremediated, weathered hydrocarbon-contaminated soil', *Soil Research,* vol. 49, no. 3, pp. 261-269.

Sho, M, Hamel, C & Greer, CW 2004, 'Two distinct gene clusters encode pyrene degradation in Mycobacterium sp. strain S65', *FEMS microbiology ecology,* vol. 48, no. 2, pp. 209-220.

Shokralla, S, Spall, JL, Gibson, JF & Hajibabaei, M 2012, 'Next-generation sequencing technologies for environmental DNA research', *Molecular Ecology*, vol. 21, no. 8, //, pp. 1794-1805.

Shyr, D & Liu, Q 2013, 'Next generation sequencing in cancer research and clinical application', *Biological Procedures Online*, vol. 15, no. 1, //.

Sijm, D, Kraaij, R & Belfroid, A 2000, 'Bioavailability in soil or sediment: exposure of different organisms and approaches to study it', *Environmental Pollution*, vol. 108, no. 1, pp. 113-119.

Silva, ÍS, dos Santos, EdC, de Menezes, CR, de Faria, AF, Franciscon, E, Grossman, M & Durrant, LR 2009, 'Bioremediation of a polyaromatic hydrocarbon contaminated soil by native soil microbiota and bioaugmentation with isolated microbial consortia', *Bioresource Technology*, vol. 100, no. 20, pp. 4669-4675.

Simon, C, Wiezer, A, Strittmatter, AW & Daniel, R 2009, 'Phylogenetic diversity and metabolic potential revealed in a glacier ice metagenome', *Applied and Environmental Microbiology*, vol. 75, no. 23, pp. 7519-7526.

Singh, A, Parmar, N, Kuhad, RC & Ward, OP 2011, 'Bioaugmentation, biostimulation, and biocontrol in soil Biology', *Bioaugmentation, Biostimulation and Biocontrol*, Springer, pp. 1-23.

Sinha, RK, Valani, D, Sinha, S, Singh, S & Herat, S 2010, 'Bioremediation of Contaminated Sites: A Low-Cost Nature's Biotechnology for Environmental Clean up by Versatile Microbes, Plants & Earthworms'.

Skupinska, K, Misiewicz, I & Kasprzycka-Guttman, T 2004, 'Polycyclic aromatic hydrocarbons: physicochemical properties, environmental appearance and impact on living organisms', *Acta Pol Pharm*, vol. 61, no. 3, pp. 233-240.

Spellerberg, IF & Fedor, PJ 2003, 'A tribute to Claude Shannon (1916–2001) and a plea for more rigorous use of species richness, species diversity and the 'Shannon–Wiener'Index', *Global ecology and biogeography*, vol. 12, no. 3, pp. 177-179.

Sprocati, AR, Alisi, C, Tasso, F, Marconi, P, Sciullo, A, Pinto, V, Chiavarini, S, Ubaldi, C & Cremisini, C 2012, 'Effectiveness of a microbial formula, as a bioaugmentation agent, tailored for bioremediation of diesel oil and heavy metal co-contaminated soil', *Process Biochemistry*, vol. 47, no. 11, pp. 1649-1655.

Stenuit, B, Eyers, L, Schuler, L, Agathos, SN & George, I 2008, 'Emerging high-throughput approaches to analyze bioremediation of sites contaminated with hazardous and/or recalcitrant wastes', *Biotechnology advances*, vol. 26, no. 6, pp. 561-575.

Stoilova, I, Krastanov, A, Stanchev, V, Daniel, D, Gerginova, M & Alexieva, Z 2006, 'Biodegradation of high amounts of phenol, catechol, 2, 4-dichlorophenol and 2, 6-dimethoxyphenol by Aspergillus awamori cells', *Enzyme and Microbial Technology,* vol. 39, no. 5, pp. 1036-1041.

Stokes, JD, Wilkinson, A, Reid, BJ, Jones, KC & Semple, KT 2005, 'Prediction of polycyclic aromatic hydrocarbon biodegradation in contaminated soils using an aqueous hydroxypropyl-β-cyclodextrin extraction technique', *Environmental Toxicology and Chemistry,* vol. 24, no. 6, pp. 1325-1330.

Storey, JD & Tibshirani, R 2003, 'Statistical significance for genomewide studies', *Proceedings of the National Academy of Sciences,* vol. 100, no. 16, pp. 9440-9445.

Su, C, Lei, L, Duan, Y, Zhang, KQ & Yang, J 2012, 'Culture-independent methods for studying environmental microorganisms: Methods, application, and perspective', *Applied Microbiology and Biotechnology,* vol. 93, no. 3, //, pp. 993-1003.

Sucher, NJ, Hennell, JR & Carles, MC 2012, *DNA fingerprinting, DNA barcoding, and next generation sequencing technology in plants*, 862, pp. 13-22.

Sun, K, Liu, J, Li, X & Ling, W 2014, 'Isolation, identification, and performance of two pyrene-degrading endophytic bacteria', *Shengtai Xuebao/ Acta Ecologica Sinica,* vol. 34, no. 4, pp. 853-861.

Sun, L, Liao, X, Yan, X, Zhu, G & Ma, D 2014, 'Evaluation of heavy metal and polycyclic aromatic hydrocarbons accumulation in plants from typical industrial sites: potential candidate in phytoremediation for co-contamination', *Environmental Science and Pollution Research*.

Sutton, S 2010, 'The most probable number method and its uses in enumeration, qualification, and validation', *Journal of Validation Technology,* vol. 16, no. 3, pp. 35-38.

Tam, N & Wong, YS 2008, 'Effectiveness of bacterial inoculum and mangrove plants on remediation of sediment contaminated with polycyclic aromatic hydrocarbons', *Marine Pollution Bulletin,* vol. 57, no. 6, pp. 716-726.

Teng, Y, Luo, Y, Ping, L, Zou, D, Li, Z & Christie, P 2010, 'Effects of soil amendment with different carbon sources and other factors on the bioremediation of an aged PAH-contaminated soil', *Biodegradation,* vol. 21, no. 2, pp. 167-178.

Thavamani, P, Megharaj, M & Naidu, R 2012, 'Bioremediation of high molecular weight polyaromatic hydrocarbons co-contaminated with metals in liquid and soil slurries by metal tolerant PAHs degrading bacterial consortium', *Biodegradation,* vol. 23, no. 6, pp. 823-835.

Thavamani, P, Megharaj, M, Venkateswarlu, K & Naidu, R 2012, 'Mixed contamination of polyaromatic hydrocarbons and metals at manufactured gas plant sites: toxicity and implications to bioremediation', *Environmental contamination—health risks, bioavailability and bioremediation. Taylor and Francis. Publs*, pp. 347-368.

Thavamani, P, Megharaj, M & Naidu, R 2013, 'Metal-tolerant PAH-degrading bacteria: development of suitable test medium and effect of cadmium and its availability on PAH biodegradation', *Environmental Science and Pollution Research*, pp. 1-12.

Thomas, A & Lester, J 1994, 'The reclamation of disused gasworks sites: New solutions to an old problem', *Science of the Total Environment*, vol. 152, no. 3, pp. 239-260.

Thompson, IP, Van Der Gast, CJ, Ciric, L & Singer, AC 2005, 'Bioaugmentation for bioremediation: the challenge of strain selection', *Environmental Microbiology*, vol. 7, no. 7, pp. 909-915.

Thorsen, WA, Cope, WG & Shea, D 2004, 'Bioavailability of PAHs: Effects of soot carbon and PAH source', *Environmental Science & Technology*, vol. 38, no. 7, pp. 2029-2037.

Tiehm, A 1994, 'Degradation of polycyclic aromatic hydrocarbons in the presence of synthetic surfactants', *Applied and Environmental Microbiology*, vol. 60, no. 1, pp. 258-263.

Trzesicka-Mlynarz, D & Ward, O 1995, 'Degradation of polycyclic aromatic hydrocarbons (PAHs) by a mixed culture and its component pure cultures, obtained from PAH-contaminated soil', *Canadian Journal of Microbiology*, vol. 41, no. 6, pp. 470-476.

Tsai, T, Kao, C, Surampalli, RY & Chien, H 2009, 'Enhanced bioremediation of fuel-oil contaminated soils: laboratory feasibility study', *Journal of Environmental Engineering*, vol. 135, no. 9, pp. 845-853.

Tucker, T, Marra, M & Friedman, JM 2011, 'Massively Parallel Sequencing', *Molecular Analysis and Genome Discovery, Second Edition*, pp. 114-134.

Tyagi, M, da Fonseca, MMR & de Carvalho, CC 2011, 'Bioaugmentation and biostimulation strategies to improve the effectiveness of bioremediation processes', *Biodegradation*, vol. 22, no. 2, pp. 231-241.

Tzeng, H-F, Laughlin, LT, Lin, S & Armstrong, RN 1996, 'The catalytic mechanism of microsomal epoxide hydrolase involves reversible formation and rate-limiting hydrolysis of the alkyl-enzyme intermediate', *Journal of the American Chemical Society*, vol. 118, no. 39, pp. 9436-9437.

Urlacher, VB & Girhard, M 2012, 'Cytochrome P450 monooxygenases: an update on perspectives for synthetic application', *Trends in Biotechnology*, vol. 30, no. 1, pp. 26-36.

USEPA, U 'Environmental Protection Agency, 1996', *Analysis of the Impacts of Control Programs on Motor Vehicle Toxic Emissions and Exposure Nationwide, Volume IUS Environmental Protection Agency, Office of Transportation and Air Quality*.

Varshney, RK, Nayak, SN, May, GD & Jackson, SA 2009, 'Next-generation sequencing technologies and their implications for crop genetics and breeding', *Trends in Biotechnology,* vol. 27, no. 9, pp. 522-530.

Vartoukian, SR, Palmer, RM & Wade, WG 2010, 'Strategies for culture of 'unculturable'bacteria', *FEMS Microbiology Letters,* vol. 309, no. 1, pp. 1-7.

Vidali, M 2001, 'Bioremediation. an overview', *Pure and Applied Chemistry,* vol. 73, no. 7, pp. 1163-1172.

Vinas, M, Sabaté, J, Espuny, MJ & Solanas, AM 2005, 'Bacterial community dynamics and polycyclic aromatic hydrocarbon degradation during bioremediation of heavily creosote-contaminated soil', *Applied and Environmental Microbiology,* vol. 71, no. 11, pp. 7008-7018.

Wang, XT, Chen, L, Wang, XK, Lei, BL, Sun, YF, Zhou, J & Wu, MH 2015, 'Occurrence, sources and health risk assessment of polycyclic aromatic hydrocarbons in urban (Pudong) and suburban soils from Shanghai in China', *Chemosphere,* vol. 119, pp. 1224-1232.

Wang, Y & Tam, N 2011, 'Microbial community dynamics and biodegradation of polycyclic aromatic hydrocarbons in polluted marine sediments in Hong Kong', *Marine Pollution Bulletin,* vol. 63, no. 5, pp. 424-430.

Ward, EM, Schulte, PA, Straif, K, Hopf, NB, Caldwell, JC, Carreón, T, DeMarini, DM, Fowler, BA, Goldstein, BD & Hemminki, K 2010, 'Research recommendations for selected IARC-classified agents', *Environ Health Perspect,* vol. 118, no. 10, pp. 1355-1362.

Waszak, DQ, da Cunha, ACB, Agarrallua, MR, Goebel, CS & Sampaio, CH 2015, 'Bioremediation of a Benzo [a] Pyrene-Contaminated Soil Using a Microbial Consortium with Pseudomonas aeruginosa, Candida albicans, Aspergillus flavus, and Fusarium sp', *Water, Air, & Soil Pollution,* vol. 226, no. 9, pp. 1-11.

Watanabe, K 2001, 'Microorganisms relevant to bioremediation', *Current opinion in biotechnology,* vol. 12, no. 3, pp. 237-241.

Wegley, L, Edwards, R, Rodriguez-Brito, B, Liu, H & Rohwer, F 2007, 'Metagenomic analysis of the microbial community associated with the coral Porites astreoides', *Environmental Microbiology,* vol. 9, no. 11, //, pp. 2707-2719.

White, J, Gilbert, J, Hill, G, Hill, E, Huse, SM, Weightman, AJ & Mahenthiralingam, E 2011, 'Culture-independent analysis of bacterial fuel contamination provides insight into the level of concordance with the standard industry practice of aerobic cultivation', *Applied and Environmental Microbiology*, vol. 77, no. 13, //, pp. 4527-4538.

Whynot, C 2009, 'The efficacy of different bioremediation strategies in removing mutagenic hazard from contaminated soil', Carleton University Ottawa, Canada 2009.

Wilcke, W 2007, 'Global patterns of polycyclic aromatic hydrocarbons (PAHs) in soil', *Geoderma*, vol. 141, no. 3, pp. 157-166.

Wilson, SC & Jones, KC 1993, 'Bioremediation of soil contaminated with polynuclear aromatic hydrocarbons (PAHs): a review', *Environmental Pollution*, vol. 81, no. 3, pp. 229-249.

Wrenn, BA & Venosa, AD 1996, 'Selective enumeration of aromatic and aliphatic hydrocarbon degrading bacteria by a most-probable-number procedure', *Canadian Journal of Microbiology*, vol. 42, no. 3, pp. 252-258.

Wu, Y, Luo, Y, Zou, D, Ni, J, Liu, W, Teng, Y & Li, Z 2008, 'Bioremediation of polycyclic aromatic hydrocarbons contaminated soil with Monilinia sp.: degradation and microbial community analysis', *Biodegradation*, vol. 19, no. 2, pp. 247-257.

Xu, X, Wang, H, Zhu, M, Sun, Y, Tao, Y, He, Q, Wang, J, Chen, L & Saffen, D 2011, 'Next-generation DNA sequencing-based assay for measuring allelic expression imbalance (AEI) of candidate neuropsychiatric disorder genes in human brain', *BMC Genomics*, vol. 12.

Yagi, JM & Madsen, EL 2009, 'Diversity, abundance, and consistency of microbial oxygenase expression and biodegradation in a shallow contaminated aquifer', *Applied and Environmental Microbiology*, vol. 75, no. 20, pp. 6478-6487.

Yan, J, Wang, L, Fu, PP & Yu, H 2004, 'Photomutagenicity of 16 polycyclic aromatic hydrocarbons from the US EPA priority pollutant list', *Mutation Research/Genetic Toxicology and Environmental Mutagenesis*, vol. 557, no. 1, pp. 99-108.

Yang, Y, Zhang, N, Xue, M & Tao, S 2010, 'Impact of soil organic matter on the distribution of polycyclic aromatic hydrocarbons (PAHs) in soils', *Environmental Pollution*, vol. 158, no. 6, pp. 2170-2174.

Yergeau, E, Sanschagrin, S, Beaumier, D & Greer, CW 2012, 'Metagenomic analysis of the bioremediation of diesel-contaminated Canadian high arctic soils', *PLoS ONE*, vol. 7, no. 1, p. e30058.

Yu, K, Wong, A, Yau, K, Wong, Y & Tam, N 2005, 'Natural attenuation, biostimulation and bioaugmentation on biodegradation of polycyclic aromatic hydrocarbons (PAHs) in mangrove sediments', *Marine Pollution Bulletin,* vol. 51, no. 8, pp. 1071-1077.

Yu, K & Zhang, T 2012, 'Metagenomic and metatranscriptomic analysis of microbial community structure and gene expression of activated sludge', *PLoS ONE,* vol. 7, no. 5, p. e38183.

Yu, S, Ke, L, Wong, Y & Tam, N 2005, 'Degradation of polycyclic aromatic hydrocarbons by a bacterial consortium enriched from mangrove sediments', *Environment international,* vol. 31, no. 2, pp. 149-154.

Zafra, G, Absalón, ÁE, Cuevas, MDC & Cortés-Espinosa, DV 2014, 'Isolation and selection of a highly tolerant microbial consortium with potential for PAH biodegradation from heavy crude oil-contaminated soils', *Water, Air, and Soil Pollution,* vol. 225, no. 2.

Zhang, D, Zhu, L & Li, F 2013, 'Influences and mechanisms of surfactants on pyrene biodegradation based on interactions of surfactant with a Klebsiella oxytoca strain', *Bioresource Technology,* vol. 142, pp. 454-461.

Zhang, T, Shao, M-F & Ye, L 2011, '454 Pyrosequencing reveals bacterial diversity of activated sludge from 14 sewage treatment plants', *The ISME journal,* vol. 6, no. 6, pp. 1137-1147.

Zhang, X-X, Cheng, S-P, Cheng-Jun, Z & Shi-Lei, S 2006, 'Microbial PAH-degradation in soil: degradation pathways and contributing factors', *Pedosphere,* vol. 16, no. 5, pp. 555-565.

Zhang, Y, Liu, M, Chen, H & Hou, G 2014, 'Source identification of polycyclic aromatic hydrocarbons in different ecological wetland components of the Qinkenpao Wetland in Northeast China', *Ecotoxicology and Environmental Safety,* vol. 102, no. 1, pp. 160-167.

Zhao, H-P, Wu, Q-S, Wang, L, Zhao, X-T & Gao, H-W 2009, 'Degradation of phenanthrene by bacterial strain isolated from soil in oil refinery fields in Shanghai China', *Journal of Hazardous Materials,* vol. 164, no. 2, pp. 863-869.

Zhou, J, He, Q, Hemme, CL, Mukhopadhyay, A, Hillesland, K, Zhou, A, He, Z, Van Nostrand, JD, Hazen, TC & Stahl, DA 2011, 'How sulphate-reducing microorganisms cope with stress: lessons from systems biology', *Nature Reviews Microbiology,* vol. 9, no. 6, pp. 452-466.

Zhu, H & Aitken, MD 2010, 'Surfactant-enhanced desorption and biodegradation of polycyclic aromatic hydrocarbons in contaminated soil', *Environmental Science & Technology,* vol. 44, no. 19, pp. 7260-7265.

Appendix

Appendix 1: Media and solutions used in this study (Chapter 2)

1.1 DGGE SOLUTIONS

Acrylamide solutions
Acrylamide 100% denaturant

- 40 ml Acrylamide (40%)
- 84 g Urea
- 80 ml 100% formamide
- 2 ml 50x TAE

Make up to 200 ml Milli-Q
Add TEMED and APS last – these are the setting agents & it can set very quickly
add 5 µl TEMED per 10 ml denaturant & 100 µl of 10% APS per 10 ml.
The solution may need to be heated up before adding TEMED and APS so that the urea dissolves – only heat at fairly low temperature for a few minutes in the hot water bath

Acrylamide 0% denaturant

- As above but replace formamide and urea with milli-Q water

50 x TAE Stock (Tris-acetic acid electrophoresis buffer)

- 242 g Tris- base
- 57.1 ml Glacial Acetic Acid
- 100 ml 0.5M EDTA
- Make to 1 l with Milli-Q water

1 x TAE Buffer (Can reuse in tank approx. 4 times)

- 20 ml 50 x TAE
- Make to 1l with Milli-Q water

10% APS stock

- 10 g APS in 100ml Milli-Q water

Store in 500 µl aliquots at -20°C or make fresh
(If the APS makes a crackling noise when adding water then it means it is good/fresh and fit to use, if fresh APS is needed, then prepare fresh one.)

1.2 **DGGE protocol**

Steps involve in preparation of DGGE (Ercolini 2004; Muyzer & Smalla 1998)
A Assembling Gel Chamber:

- Clean glass plates, spacers and combs thoroughly with 70% ethanol.
- Cut Gel bond film as per the size of small glass plate. Make sure hydrophobic side of film attaches to glass.

- Assemble the gel sandwich by placing the small glass plate on top of the large plate, being sure to correctly place a 1 mm spacer along each edge of the plate assembly. Attach the clamp tight enough to hold everything together and place the entire assembly into the rear slot of casting stand. Loose the clamps slightly and use the spacing card to assure the proper spacer alignment.
- Place the glass plates and spacers together with the sandwich clamps in the casting stand in which a rubber strip is places at the bottom to prevent leakage and check for leakage by filling it with MilliQ water.
- Place the well comb firmly in between the plates and draw a line on the glass plate where the bottom of the well is located. This will be the future reference point when pouring the gel.
- Making Acrylamide solutions- 1ml of 0% denaturant 6% Acrylamide, 10 µl of APS, 1 µl of TEMED. Use 1 ml of above solution to seal bottom of gel before adding denaturing gradient gel. Also use to form wells at the top of gel for sample loading once combs has been put in place. Allow to set for approx. 15 minutes.
- Create the proper concentrations by mixing 0% and 70% denaturant solution so that end volumes are 13 ml of acryl with highest denaturant concentration (60% for example) and 13 ml of acryl with lowest denaturant concentration (45% for example).

Denaturing conditions used: (Just as an example)

- 45-60% Denaturing gradient
- Prepare 13ml of 45%: 45/70x13ml=8.35ml of 70% D 6% A+ 4.6ml 0% D 6% A
- Prepare 13ml of 60%: 60/70x13ml= 11.14ml of 70%D 12% A+ 1.86ml of 0% D 12% A
- To each then add: 130 µl of APS (add first) + 13 µl of TEMED (after APS)
- Note - Mix all gradients well.

B Casting the gradient

- Make sure the pump is off and then the gradient maker channel is close.
- Pour the acryl-high 60%) in right leg of the gradient maker (at the pump side) and acryl-low (45%) in the left leg.
- Stirring bead on (in right leg)

- Simultaneously start the pump (5ml/min) and move the handle of gradient maker to horizontal position. (Channel open)
- Check immediately if acryl-low solution (45%) mixes with acryl- high (60%). (Most of the time air-bubble is blocking the channel, tilt the gradient maker to slightly to let it out).
- Fill the gel chamber slowly. Stop the flow when the acryl is approximately 0.5cm under the comb level.
- Allow the gel to polymerize for approx. 60 minutes. Formation of double lines indicates complete polymerization of the gel.

Stacking the gel and comb:

- Place the 24-well comb and fill up the gel chamber with a mixture of 4 ml of 0%, 4 µl of TEMED and 40 µl of APS using pasteur pipette.
- Allow the stacking gel to polymerize for at least 15 minutes.

C Running the gel:

Pre-run

- Place the core and tank into aquarium which is filled with 7 L of 1x TAE buffer. Preheat the buffer in the D-CODE BioRAD apparatus to 60° C. This takes approx. 20 – 60 minutes.
- Before loading the samples, remove the comb from the gel and flush the slots with 1X TAE buffer using syringe.
- Fill the slots with buffer.
- Loading the samples
- Load approximately 10-20µl of PCR products containing loading dye to each well. The volume loaded depends on the success of the PCR product accuracy.
- Load a marker along with samples for determination of band position and comparability of gels.
- Place the gel chamber in the cooling core and in the aquarium. Loose the clamps a quarter counters clockwise to prevent the breaking of sandwich clamps.

D Start Run

- Restart and check the circulation. (The flow into the upper compartment should be small and gentle. Make sure upper compartment fills up and overflows via holes. The flow into the tank can be more vigorous). Close the lid while paying attention to the configuration of negative and positive electrodes.
- Start power at 60 volts and run for 16-18 hrs (This may vary as per samples). Increase in voltage will reduce running time.

E Staining the gel

- When the electrophoresis is complete, take apart the apparatus and remove the glass plates. Carefully separate the plates, leaving the gel exposed on the large plate. Use the edge of small plate to trim the well wall, but be sure to leave the left most walls slightly higher than others for use as a reference.
- Follow the Silver Staining protocol for DGGE staining.

1.3 DGGE Gel Staining
Fixing Solution 1

- 50 ml ethanol 100%
- 2.5 ml Glacial Acetic Acid
- 447.5 ml MQ water

Place the gel in fixing solution 1 for at least 2hrs

Silver Nitrate Solution

- 0.2 g silver Nitrate
- 200 ml water

Add silver nitrate solution after emptying fixing solution 1 out and leave it for 20 minutes. Be sure to wash the gel 3 times with deionised water before moving on to the next stage from here.

Developing Solution

- 0.02 g Sodium borohydride
- 0.8 ml Formaldehyde
- 3 g Sodium Hydroxide
- 200 ml MQ water

Place gel in developing solution for 30 minutes.

Fixing Solution 2

- 3.75 g Sodium Carbonate
- 500 ml MQ water

Place gel in this solution for 10 minutes.

Preservative Solution

- 125 ml ethanol 100%
- 50 ml glycerol
- 325 ml of water
- Gel can stay there indefinitely.

Take the photo of gel using a scanner for analysis.

Preparation of Agarose Gel Electrophoresis

- Weigh 1g of agarose (1%) into 250 ml flask.
- Add 100ml of 1XTAE buffer and melt it in microwave for 2 minutes.
- Place conical flask in the sink to cool down.
- Insert the combe into the gel tank chamber.
- Pour agarose solution up to 1 m high and allow it to solidify for 15 minutes.

Loading and running of samples

- 4µl of loading dye was added to the parafilm.
- Add 10µl of each sample onto the loading dye on the parafilm and mix well.
- Load 10µl of this mixed volume of each sample on their respective lanes
- After loading all the samples, gel was run at 60 V for 30-45 minutes or up to 80% of the track.
- The gel was stopped and disconnects it from the power source.
- Gel was then stained with Ethidium Bromide solution for 20 minutes in foam hood.
- Took the photo of the gel.

Table A1.1 DGGE materials and solution

Plate Sandwich Materials	Gel Solutions
16 x 16 cm glass plate	70%Denaturing 6% Acrylamide Stock
16 x 14 cm glass plate	0%Denaturing 6% Acrylamide Stock
2 – 1mm glass spacers	70%Denaturing 12% Acrylamide Stock
2- Plate clamps	0%Denaturing 12% Acrylamide Stock
Pouring stand	10% Ammonium Persulfate Solution (APS)
Gradient maker and Peristaltic Pump	TEMED(N,N,N,N-teramethylenediamine)
Well combs	50 X TAE Buffer
Spacing card	Sterilized MilliQ water
Gel Bond Film	

Table A1.2 The bacterial PCR master mix for 36 reactions

Reagent	Volume for 1 reaction (µl)	Volume for 36 reactions (µl)
10 mM dNTP's	1	36
GoTaq Flexi Buffer(10x)	10	360
25 mM $MgCl_2$	5	180
GoTaq polymerase, 10 units/µl	0.25	9
Forward primer, 314F GC (10 pmol/µl)	2	72
Reverse primer, 518R (10 pmol/µl)	2	72
Sterile purified H_2O	27.75	999
Template DNA	2	72
Total volume (µl)	50	1800

Similar master mix was prepared for the other PCR amplification (NidA and ITS)

1.4 DNA extraction procedures using MoBio™ PowerSoil extraction kit

- To the **PowerBead Tubes** provided, add 0.25-0.45 grams of soil sample.
- Gently vortex to mix.
- **Check Solution C1.** If **Solution C1** is precipitated, heat solution to 60°C until dissolved before use.
- Add 60 µl of **Solution C1** and invert several times or vortex briefly.
- Secure **PowerBead Tubes** horizontally using the MO BIO Vortex Adapter tube holder for the vortex (MO BIO Catalog# 13000-V1-24) or secure tubes horizontally on a flat-bed vortex pad with tape. Vortex twice (2 x 45 seconds) for 45 seconds on bead beater.
- Make sure the PowerBead Tubes rotate freely in your centrifuge without rubbing. Centrifuge tubes at 10,000 x *g* for 30 seconds at room temperature. **CAUTION:** Be sure not to exceed 10,000 x *g* or tubes may break.
- Transfer the supernatant to a clean **2 ml Collection Tube** (provided). **Note**: Expect between 400 to 500 µl of supernatant. Supernatant may still contain some soil particles.
- Add 250 µl of **Solution C2** and vortex for 5 seconds. Incubate at 4 °C for 5 minutes.
- Centrifuge the tubes at room temperature for 1 minute at 10,000 x *g*.

- Avoiding the pellet, transfer up to, but no more than, 600 µl of supernatant to a clean **2 ml Collection Tube** (provided).
- Add 200 µl of **Solution C3** and vortex briefly. Incubate at 4 ºC for 5 minutes.
- Centrifuge the tubes at room temperature for 1 minute at 10,000 x *g*.
- Avoiding the pellet, transfer up to, but no more than, 750 µl of supernatant into a clean **2 ml Collection Tube** (provided).
- Shake to mix Solution C4 before use. Add 1200 µl of **Solution C4** to the supernatant and vortex for 5 seconds.
- Load approximately 675 µl onto a **Spin Filter** and centrifuge at 10,000 x *g* for 1 minute at room temperature. Discard the flow through and add an additional 675 µl of supernatant to the **Spin Filter** and centrifuge at 10,000 x *g* for 1 minute at room temperature. Load the remaining supernatant onto the **Spin Filter** and centrifuge at 10,000 x *g* for 1 minute at room temperature.
- **Note**: A total of three loads for each sample processed are required.
- Add 500 µl of **Solution C5** and centrifuge at room temperature for 30 seconds at 10,000 x *g*.
- Discard the flow through.
- Centrifuge again at room temperature for 1 minute at 10,000 x *g*.
- Carefully place spin filter in a clean **2 ml Collection Tube** (provided). Avoid splashing any **Solution C5** onto the **Spin Filter**.
- Add 100 µl of **Solution C6** to the center of the white filter membrane. Alternatively, sterile DNA-Free PCR Grade Water may be used for elution from the silica Spin Filter membrane at this step (MO BIO Catalog# 17000-10).
- Centrifuge at room temperature for 30 seconds at 10,000 x *g*.
- Discard the **Spin Filter**. The DNA in the tube is now ready for any downstream application. No further steps are required.

Table A1.3 Quantification of all 36 DNA extracts (all soils) using NanoDrop 2000

#	Soil	Treatment	Time point	Volume(µl)	Amount (ng)	Amount(ng/µl)	Volume(µl)	Buffer (µl)
1	Ap	NA	Day 0	2	10	8.7	1.1	8.9
2		ENA		2	10	5.1	2.0	8.0
3		COMB		2	10	6.2	1.6	8.4
4	TB	NA		2	10	6.4	1.6	8.4
5		ENA		2	10	2.9	3.4	6.6
6		COMB		2	10	0.5	20.0	-10.0
7	CREO	NA		2	10	11.9	0.8	9.2
8		ENA		2	10	12.5	0.8	9.2
9		COMB		2	10	9.4	1.1	8.9
10	Ap	NA	WK6	2	10	3	3.3	6.7
11		ENA		2	10	17.9	0.6	9.4
12		COMB		2	10	3.9	2.6	7.4
13	TB	NA		2	10	1.1	9.1	0.9
14		ENA		2	10	3.8	2.6	7.4
15		COMB		2	10	2.8	3.6	6.4
16	CREO	NA		2	10	6.4	1.6	8.4
17		ENA		2	10	17.3	0.6	9.4
18		COMB		2	10	18	0.6	9.4
19	Ap	NA	WK18	2	10	6.6	1.5	8.5
20		ENA		2	10	3.2	3.1	6.9
21		COMB		2	10	2.4	4.2	5.8
22	TB	NA		2	10	4.4	2.3	7.7
23		ENA		2	10	6.1	1.6	8.4
24		COMB		2	10	1.4	7.1	2.9
25	CREO	NA		2	10	16	0.6	9.4
26		ENA		2	10	18.3	0.5	9.5
27		COMB		2	10	5.7	1.8	8.2
28	Ap	NA	WK42	2	10	4.6	2.2	7.8
29		ENA		2	10	5.3	1.9	8.1
30		COMB		2	10	7.7	1.3	8.7
31	TB	NA		2	10	3.3	3.0	7.0
32		ENA		2	10	4.2	2.4	7.6
33		COMB		2	10	2.1	4.8	5.2
34	CREO	NA		2	10	11.6	0.9	9.1
35		ENA		2	10	10.5	1.0	9.0
36		COMB		2	10	11.1	0.9	9.1

1.5 Soil physiochemical properties

1.5.1 Soil Organic matter (SOM)

An overnight dried soil at -80°C in oven was weighed into three crucibles (10g) as described below:

Crucible A

Weight of soil before burning = 10g
Weight of crucible, lid and dried soil = 60.07g
Weight of crucible, lid and soil after burning = 55.34g
SOM = (weight of crucible + lid + soil) – (weight of crucible + lid + soil after burning)/10*100%
(60.07 – 55.34)/10 × 100% = 47.3%

Crucible B

Weight of crucible and lid = 49.72g
Weight of dry soil = 10g
Weight of crucible, lid and soil after burning = 54.99g
SOM = (weight of crucible + lid + soil) – (weight of crucible + lid + soil after burning)/10*100%
(59.72 – 54.99)/10 × 100% = 47.3%

Crucible C

Weight of dry soil = 10g
Weight of crucible and lid = 52.77g
Weight of crucible, lid and soil after burning = 57.92g
SOM = (weight of crucible + lid + soil) – (weight of crucible + lid + soil after burning)/10*100%
(62.77 – 57.92)/10 × 100% = 48.5%
Average soil organic content = (47.3% + 47.3% + 48.5%) /3 = 47.7%

1.5.2 Water Holding Capacity

To determine soil water holding capacity, 10 g of oven dried soil was weighed using balance scale into three foil bowls of a known mass and transferred into a funnel seal with filter paper placed in a measuring cylinder. Each soil sample was saturated by running through 50ml of water until the last drop of water was collected. Water holding capacity was determined after drainage was completed as below:

A

Mass of foil bowl and filter paper = 4.37 g
Mass of foil bowl, filter paper and dry soil = 14.37 g
Mass of foil bowl, filter paper, and saturated soil = 34.65 g
Mass of dry soil = 14.37 – 4.37 = 10 g
Mass of saturated soil = 34.65 – 4.37 = 30.28 g
Mass of the water contained in the saturated soil = 30.28 – 10 = 20.28 g
%WHC = (20.28/30.28) × 100% = 67%

B

Mass of foil bowl and filter paper = 4.37 g

Mass of foil bowl, filter paper and dry soil = 14.37 g
Mass of foil bowl, filter paper, and saturated soil = 28.07 g
Mass of dry soil = 14.37 – 4.37 = 10 g
Mass of saturated soil = 28.07 – 4.37 = 23.70 g
Mass of the water contained in the saturated soil = 23.70 – 10 = 13.70 g
%WHC = (13.70/23.70) × 100% = 58%

C

Mass of foil bowl and filter paper = 4.37 g
Mass of foil bowl, filter paper and dry soil = 14.37 g
Mass of foil bowl, filter paper, and saturated soil = 29.14 g
Mass of dry soil = 14.37 – 4.37 = 10 g
Mass of saturated soil = 29.14 – 4.37 = 24.77 g
Mass of the water contained in the saturated soil = 24.77 – 10 = 14.77 g
%WHC = (14.77/24.77) × 100% = 60%
Average %WHC = (60% + 58% + 67%)/3 = 61.67%
Both WHC and soil moisture content were used to work out the correct amount of water needed to keep soil at 50% moisture content. Initially this soil is intended to be at 50% WHC, meaning that 50% WHC would correspond to the soil having a water content of 30% of its water holding capacity. 30 g of water is then added to the soil already containing 20 g of water.

Appendix 2: Treatability studies to assess bioremediation performance in three PAH impacted soils (Chapter 3)

Table A2.1 Comparison of pyrene removal in Creo soil following 42 weeks on incubation under natural attenuation (NA), enhanced natural attenuation (ENA), bioaugmentation (BioA) and Combine treatment (Comb) strategies. Changes in pyrene concentrations were compared using repeated measures analysis of variance (Graph Pad InStat) to explore effect of each bioremediation strategy employed, reduction in pyrene concentration was either considered to be significantly different at p value greater or less than 0.001/0.05.

Microcosm	**Time point**	**Pyrene concentrations significant at p value < 0.05**	**Pyrene concentrations not significant at p value > 0.05**
NA	0	NA18, NA42, ENA18, ENA42, BioA6, BioA18, BioA42, Comb18, & Comb42	NA6, ENA0, ENA6, BioA0, Comb0 & Comb6
	6	None	NA0, ENA0, Comb0, NA18, NA42, ENA6, ENA18, ENA42, BioA, BioA6, BioA18, BioA42, Comb6, Comb18, & Comb42
	18	NA0, ENA0, BioA0 & Comb0	NA6, NA18, NA42, ENA6, ENA18, ENA42, BioA6, BioA18, BioA42, Comb6, Comb18, & Comb42NA42, Comb18 & ENA18
	42	NA0, ENA0, BioA0, Comb0, & Comb6	NA6, NA18, NA42, ENA6, ENA18, Comb6, Comb18 & Comb42
ENA	0	NA18, NA42, ENA18, ENA42, BioA6, BioA18, BioA42, Comb18, & Comb42	NA0, NA6, ENA6, BioA0, Comb0 & Comb6
	6	NA18, NA42, ENA18, ENA42, BioA6, BioA18, BioA42, Comb18, & Comb42	NA0, NA6, ENA0, BioA0, Comb0 & Comb6
	18	NA0, ENA0, BioA0 & Comb0	NA6, NA18, NA42, ENA6, ENA18, ENA42, BioA6, BioA18, BioA42, Comb6, Comb18, & Comb42
	42	NA0, ENA0, BioA0, Comb0, & Comb6	NA6, NA18, NA42, ENA6, ENA18, ENA42, BioA6, BioA18, BioA42, Comb18, & Comb42

Table A2.1 (cont). Comparison of pyrene removal in Creo soil following 42 weeks on incubation under natural attenuation (NA), enhanced natural attenuation (ENA), bioaugmentation (BioA) and Combine treatment (Comb) strategies. Changes in pyrene concentrations were compared using repeated measures analysis of variance (Graph Pad InStat) to explore effect of each bioremediation strategy employed, reduction in pyrene concentration was either considered to be significantly different at p value greater or less than 0.001/0.05.

Microcosm	**Time point**	**Pyrene concentrations significant at p value < 0.05**	**Pyrene concentrations not significant at p value > 0.05**
BioA	0	NA0, ENA0, BioA0, Comb0, & Comb6	NA0, NA6, ENA0, ENA6, Comb0, & Comb6
	6	NA0, ENA0, BioA0 & Comb0	NA0, NA6, ENA0, ENA6, Comb0, & Comb6
	18	NA0, ENA0, BioA0 & Comb0	NA6, NA18, NA42, ENA6, ENA18, ENA42, BioA6, BioA18, BioA42, Comb6, Comb18, & Comb42
	42	NA0, ENA0, BioA0, Comb0, & Comb6	NA6, NA18, NA42, ENA6, ENA18, ENA42, BioA6, BioA18, BioA42, Comb18, & Comb42
Comb	0	NA18, NA42, ENA18, ENA42, BioA6, BioA18, BioA42, Comb18, & Comb42	NA0, ENA0, & Comb0
	6	NA18, NA42, ENA18, ENA42, BioA6, BioA18, BioA42, Comb18, & Comb42	NA0, NA6, ENA0, ENA6, BioA0, & Comb0
	18	NA0, ENA0, BioA0 & Comb0	NA6, NA18, NA42, ENA6, ENA18, ENA42, BioA6, BioA18, BioA42, Comb6, Comb18, & Comb42
	42	NA0, ENA0, BioA0 & Comb0	NA6, NA18, NA42, ENA6, ENA18, ENA42, BioA6, BioA18, BioA42, Comb6, Comb18, & Comb42

Appendix 3: Assessment of PAH-degrading microorganisms in three aged hydrocarbons contaminated soils using community profiling analysis (Chapter 4)

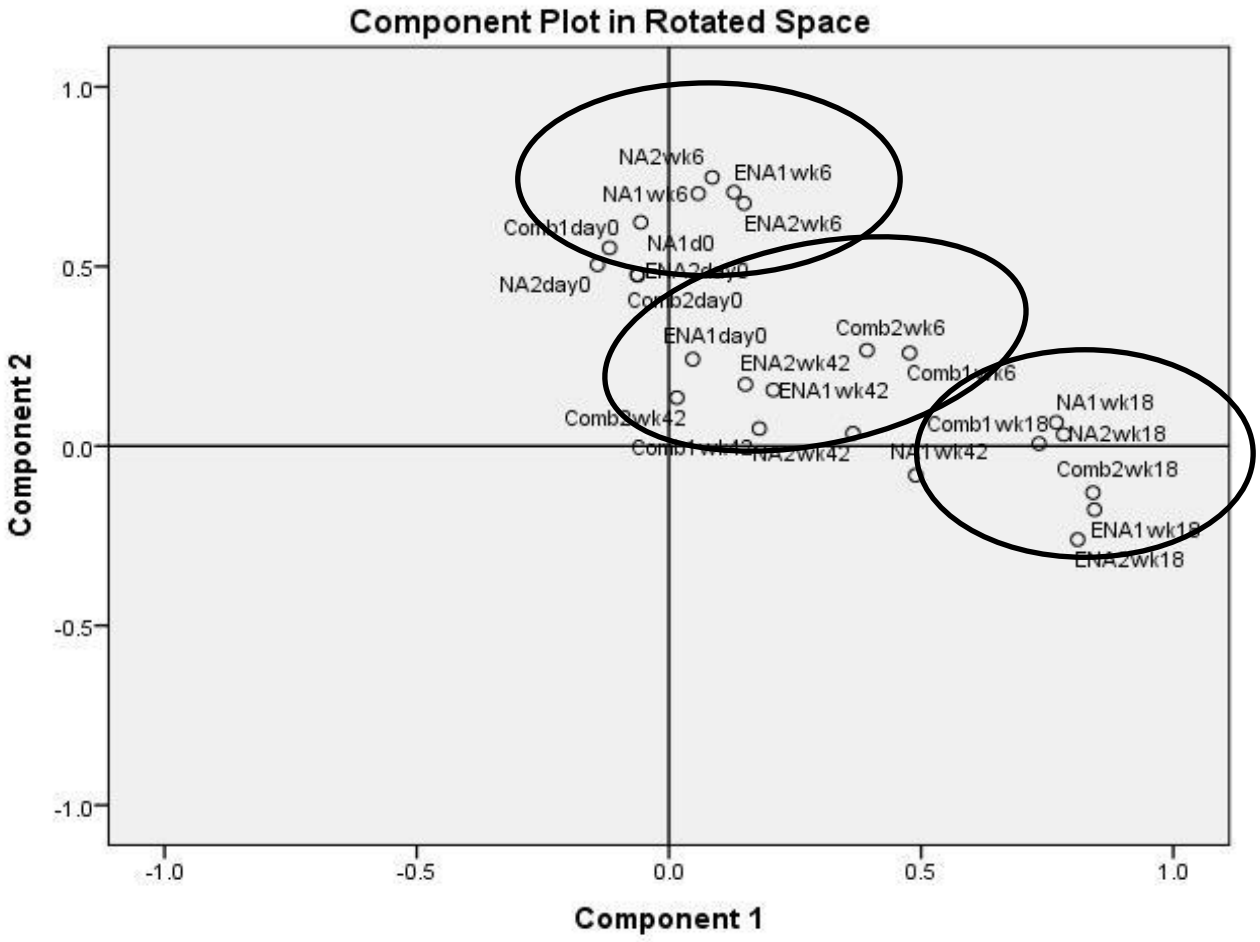

Figure A3.1 Principal component analysis of the Creo bacterial DGGE showing the variation in microbial communities sampled from four different time points (Day 0, Weeks 6, 18 & 42) in unamended and amended microcosms (NA, ENA & Comb).

Table A3.1 Comparison of individual bacterial species analysed using repeated measures analysis of variance performed using bacterial DGGE data in samples obtained from four sampling time points in Creo-contaminated soil microcosms. Individual bacterial species were either considered to be significantly different at $p < 0.05$.

Microcosm	**Time point**	**Communities significant at p value < 0.05**	**Communities not significant at p value > 0.05**
NA	0	NA18, NA42, ENA18, ENA42, Comb6, Comb18, & Comb42	NA6, ENA0, ENA6, & Comb0
	6	NA18, NA42, ENA18, ENA42, Comb6, Comb18 & Comb42	ENA6, NA0, and Comb6
	18	NA0, NA6, ENA0, ENA6, ENA42, Comb0, Comb6, & Comb42	NA42, Comb18 & ENA18
	42	NA0, NA6, ENA0, ENA6, ENA42, Comb0, Comb6, & Comb42	NA42, Comb18 & ENA18
ENA	0	NA18, NA42, ENA18, ENA42, Comb6, Comb18, & Comb42	NA6, NA0, ENA6, & Comb0
	6	NA18, NA42, ENA18, ENA42, Comb6, Comb18, & Comb42	NA6, NA0, ENA0, & Comb0
	18	NA0, NA6, ENA0, ENA6, ENA42, Comb0, Comb6, & Comb42	NA42, Comb18 & NA18
	42	NA0, NA6, NA18, NA42 ENA0, ENA6, ENA18, Comb0, Comb6 & Comb18	Comb42
Comb	0	NA18, NA42, ENA18, ENA42, Comb6, Comb18, & Comb42	NA6, NA0, ENA6, & ENA0
	6	NA0, NA6, NA18, NA42, ENA0, ENA6, ENA18, ENA42, Comb0, Comb18, & Comb42	none
	18	NA0, NA6, ENA0, ENA6, ENA42, Comb0, Comb6, & Comb42	NA42, ENA18 & NA18
	42	NA0, NA6, NA18, NA42, ENA0, ENA6, ENA18, Comb0, Comb6, & Comb18	ENA42

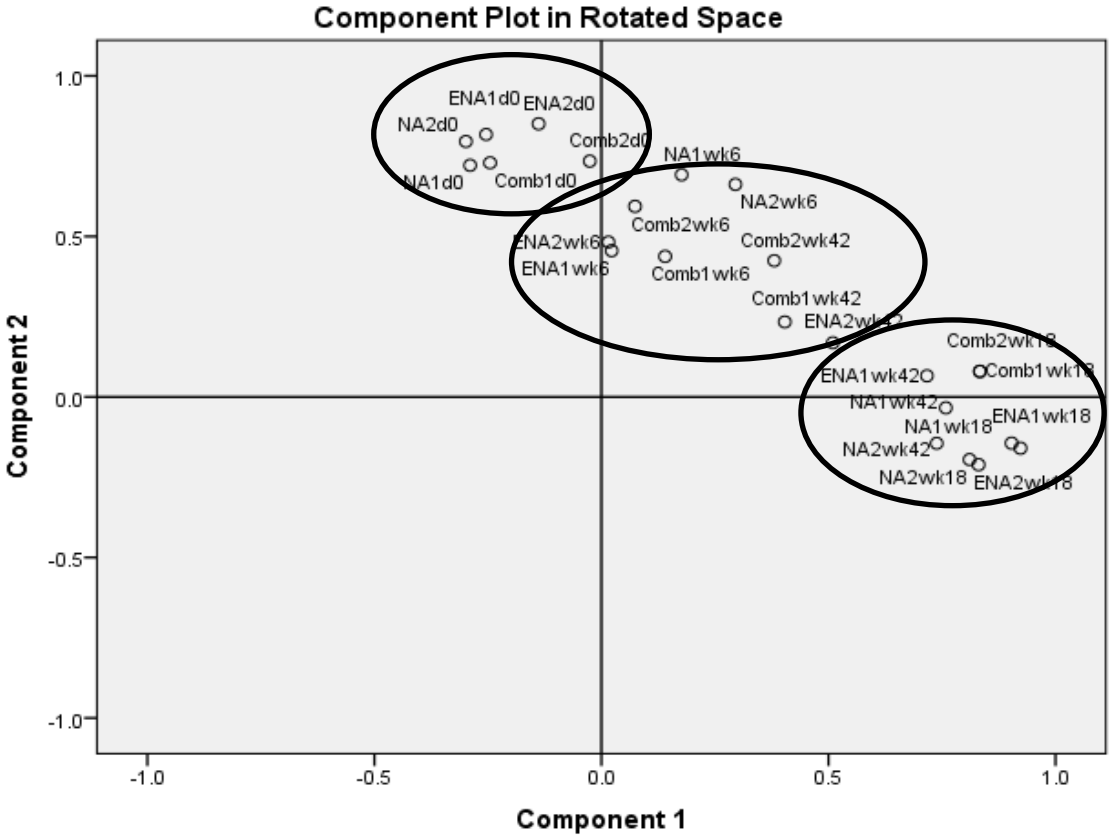

Figure A3.2 Principal component analysis of the TB bacterial DGGE showing the variations in microbial communities sampled from four different time points (Day 0, weeks 6, 18 & 42) in unamended and amended microcosm (NA, ENA, & Comb).

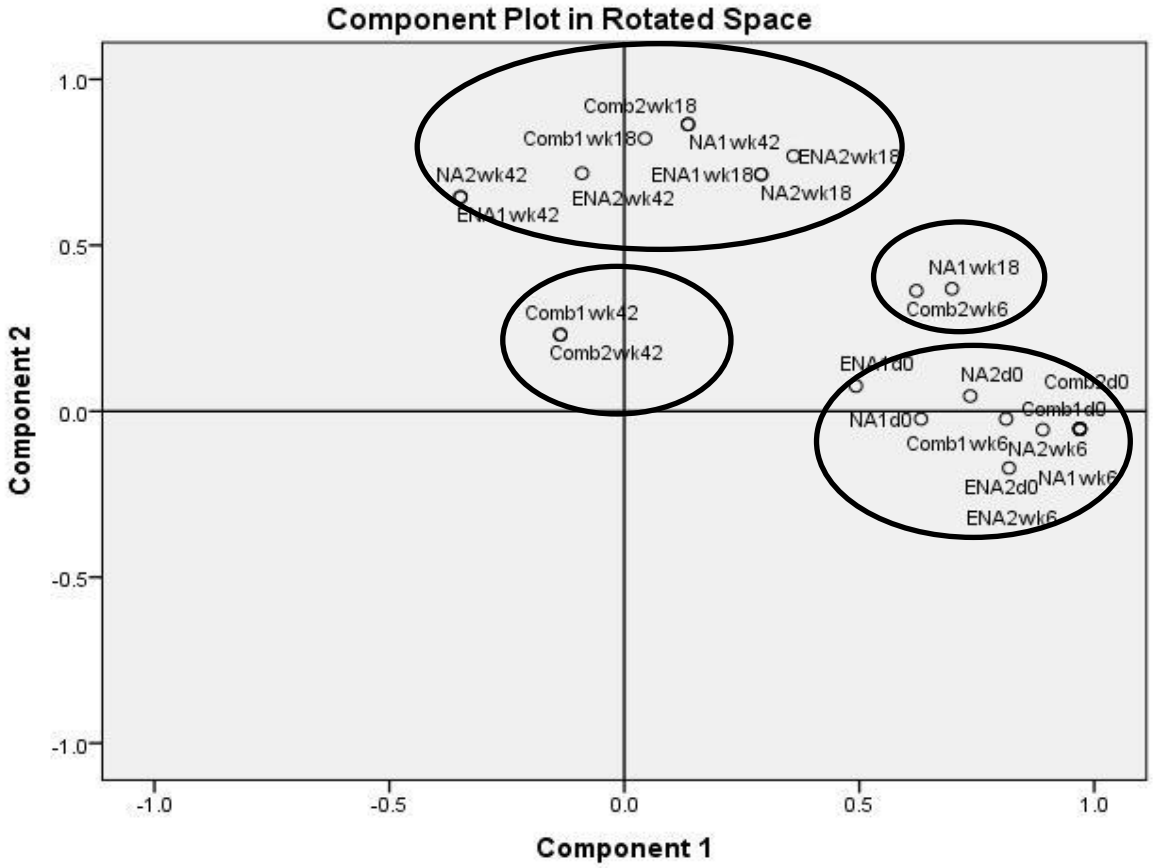

Figure A3.3 Principal component analysis of the TB NidA DGGE showing the variation in mycobacteria communities sampled from four different time points (Day 0, Weeks 6, 18 & 42) in unamended and amended microcosms (NA, ENA & Comb).

Table A3.3 Comparison of individual bacterial species analysed using repeated measures analysis of variance performed using bacterial DGGE data in samples obtained from four sampling time points in TB-contaminated soil microcosms. Individual bacterial species were either considered to be significantly different at p value less than 0.05.

Microcosm	**Time point**	**Communities significant at p value < 0.001 or 0.05**	**Communities not significant at p value > 0.001 or 0.05**
NA	0	NA42, ENA42, Comb18, & Comb42	NA6, NA18, ENA0, ENA6, ENA18, Comb0 & Comb6
	6	NA42, ENA42, Comb18, & Comb42	NA6, NA18, ENA0, ENA6, ENA18, Comb0 & Comb6
	18	NA42, ENA42, Comb18, & Comb42	NA6, NA18, ENA0, ENA6, ENA18, Comb0 & Comb6
	42	NA0, NA6, NA18, ENA0, ENA6, ENA18, Comb0, Comb6, & Comb18	ENA42, Comb18, & Comb42
ENA	0	NA42, ENA42, Comb18, & Comb42	NA6, NA18, ENA0, ENA6, ENA18, Comb0 & Comb6
	6	NA42, ENA42, Comb18, & Comb42	NA6, NA18, ENA0, ENA6, ENA18, Comb0 & Comb6
	18	NA42, ENA42, Comb18, & Comb42	NA6, NA18, ENA0, ENA6, ENA18, Comb0 & Comb6
	42	NA0, NA6, NA18, ENA0, ENA6, ENA18, Comb0, Comb6, & Comb18	ENA42, Comb18, & Comb42
Comb	0	NA42, ENA42, Comb18, & Comb42	NA6, NA18, ENA0, ENA6, ENA18, Comb0 & Comb6
	6	NA42, ENA42, Comb18, & Comb42ENA42, Comb0, Comb18, & Comb42	NA6, NA18, ENA0, ENA6, ENA18, Comb0 & Comb6
	18	NA0, NA6, NA18, NA42, ENA0, ENA6, ENA18, ENA42, Comb0, Comb6, & Comb42	None
	42	NA0, NA6, NA18, ENA0, ENA6, ENA18, Comb0, Comb6, & Comb18	ENA42, Comb18, & Comb42

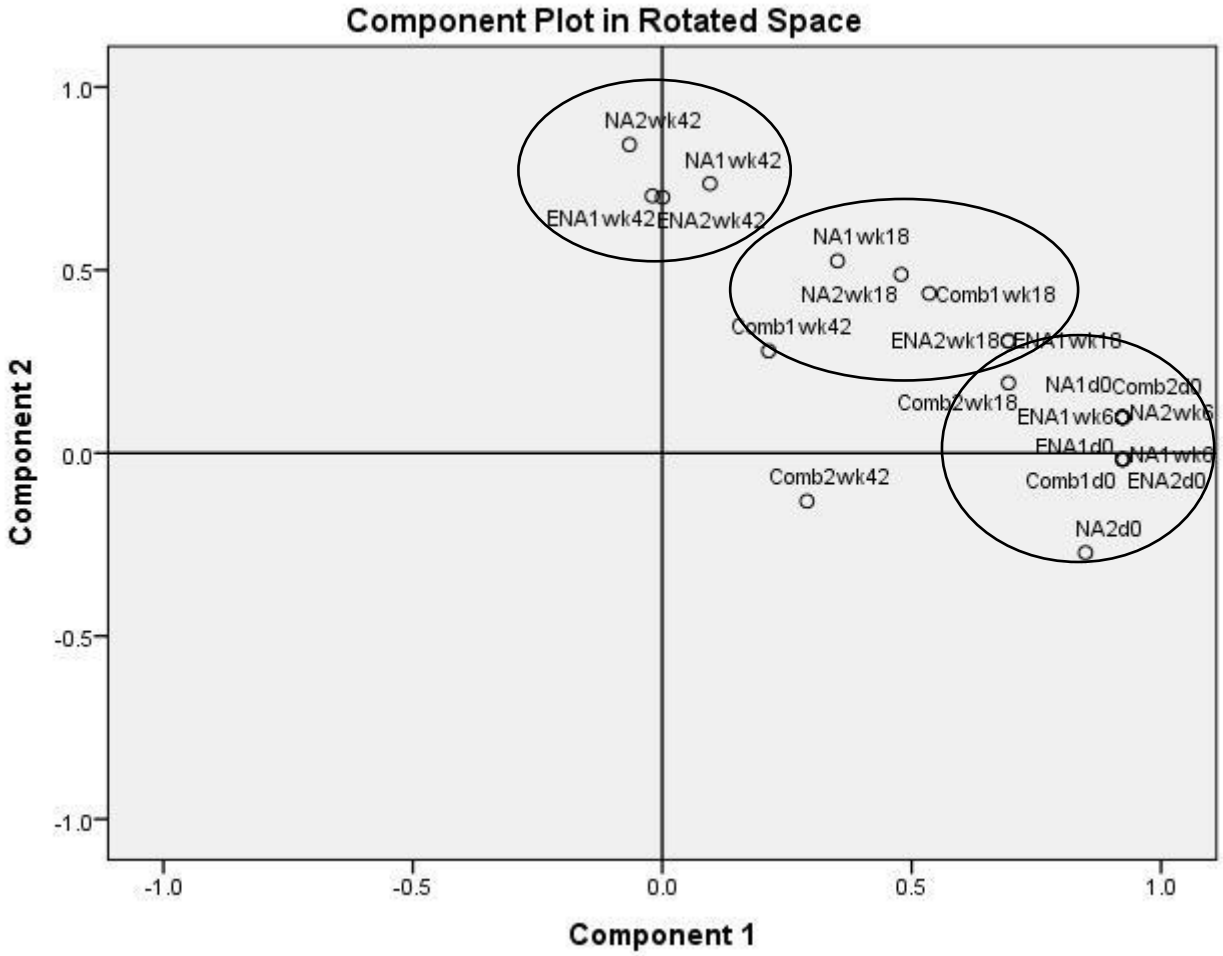

Figure A3.4 Principal component analysis of the AP DGGE showing the variation in bacterial communities of samples obtained across four different time point (Day 0, weeks 6, 18 & 42). Aggregation of communities as shown in this figure is influenced by both incubation time and types of treatments to a certain degree. Variation seen in this PCA is largely due to the incubation time related impact

Table A3.4 Comparison of individual bacterial species analysed using repeated measures analysis of variance performed using bacterial DGGE data in sample obtained from four sampling time points in AP-contaminated soil microcosms. Individual bacterial species were considered to be significantly different at p value less than 0.05.

Microcosm	**Time point**	**Communities significant at p value < 0.05**	**Communities not significant at p value > 0.05**
NA	0	NA18, NA42, NA6, ENA18, ENA42, Comb6, Comb18, & Comb42	ENA0, ENA6, & Comb0
	6	NA0, NA42, ENA0, ENA6, Comb6, Comb0, Comb6 & Comb18	ENA18, NA18, and Comb42
	18	NA0, NA42, ENA0, ENA6, ENA42, ENA18, Comb0, Comb6, & Comb18	NA6, ENA18, & Comb42
	42	NA0, NA6, NA18, ENA0, ENA6, ENA18, Comb0, & Comb42	ENA42, Comb6 & Comb18
ENA	0	NA18, NA42, NA6, ENA18, ENA42, Comb6, Comb18, & Comb42	ENA0, ENA6, & Comb0
	6	NA18, NA42, NA6, ENA18, ENA42, Comb6, Comb18, & Comb42	NA6, NA0, ENA0, & Comb0
	18	NA0, NA42, ENA0, ENA6, ENA42, ENA18, Comb0, Comb6, & Comb18	NA6, ENA18, & Comb42
	42	NA0, NA6, NA18, ENA0, ENA6, ENA18, Comb0, & Comb42	ENA42, Comb6 & Comb18
Comb	0	NA18, NA42, NA6, ENA18, ENA42, Comb6, Comb18, & Comb42	ENA0, ENA6, & Comb0
	6	NA0, NA6, NA18, ENA0, ENA6, ENA18, Comb0, & Comb42	ENA42, Comb6 & Comb18
	18	NA0, NA6, NA18, ENA0, ENA6, ENA18, Comb0, & Comb42	ENA42, Comb6 & Comb18
	42	NA0, NA42, ENA0, ENA6, ENA42, ENA18, Comb0, Comb6, & Comb18	NA6, ENA18, & Comb42

Table A3.5 Comparison of individual bacterial species analysed using repeated measures analysis of variance performed using bacterial DGGE data in sample obtained from four sampling time points in AP-contaminated soil microcosms. Individual bacterial species were either considered to be significantly different at a p value less than 0.05.

Microcosm	**Time point**	**Communities significant at p value < 0.05**	**Communities not significant at p value > 0.05**
NA	0	NA18, NA42 & Comb42	NA6, ENA0, ENA6, ENA18, ENA42, Comb0, Comb6 & Comb
	6	NA18, NA42 & Comb42	NA6, ENA0, ENA6, ENA18, ENA42, Comb0, Comb6 & Comb
	18	NA6, ENA0, ENA6, ENA18, ENA42, Comb0, Comb6 & Comb	NA42 & Comb42
	42	NA6, ENA0, ENA6, ENA18, ENA42, Comb0, Comb6 & Comb	NA18 & Comb42
ENA	0	NA18, NA42 & Comb42	NA6, ENA0, ENA6, ENA18, ENA42, Comb0, Comb6 & Comb b0
	6	NA18, NA42 & Comb42	NA6, ENA0, ENA6, ENA18, ENA42, Comb0, Comb6 & Comb
	18	NA18, NA42 & Comb42	NA6, ENA0, ENA6, ENA18, ENA42, Comb0, Comb6 & Comb
	42	NA18, NA42 & Comb42	NA6, ENA0, ENA6, ENA18, ENA42, Comb0, Comb6 & Comb
Comb	0	NA18, NA42 & Comb422	NA6, ENA0, ENA6, ENA18, ENA42, Comb0, Comb6 & Comb
	6	NA18, NA42 & Comb42	NA6, ENA0, ENA6, ENA18, ENA42, Comb0, Comb6 & Comb
	18	NA18, NA42 & Comb42	NA6, ENA0, ENA6, ENA18, ENA42, Comb0, Comb6 & Comb
	42	NA6, ENA0, ENA6, ENA18, ENA42, Comb0, Comb6 & Comb	NA18 & NA42

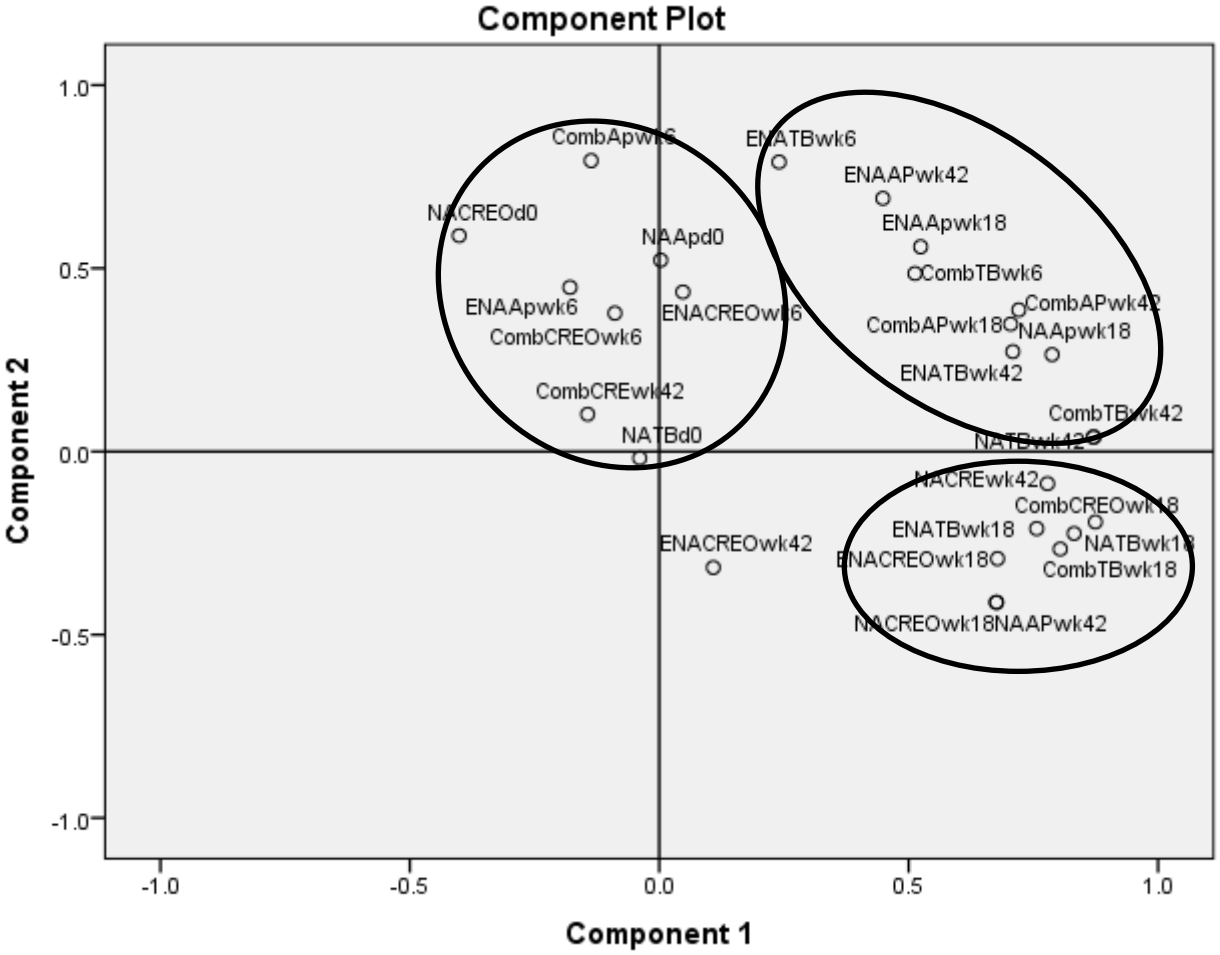

Figure A3.5 Principal component analysis of the composite DGGE showing similarities in microbial communities of samples obtained across four different time point and from all three soil types (AP, TB & Creo). Aggregation of communities as shown in this figure is influenced by incubation time rather than bioremediation strategies, whereas soil type-effect was throught to be less influential in terms of the effect on microbial communities clustering as treatments from the similar soil are found in all different quadrants.

Appendix 4: Analysis of enzymes associated with PAH metabolism (Chapter 5)

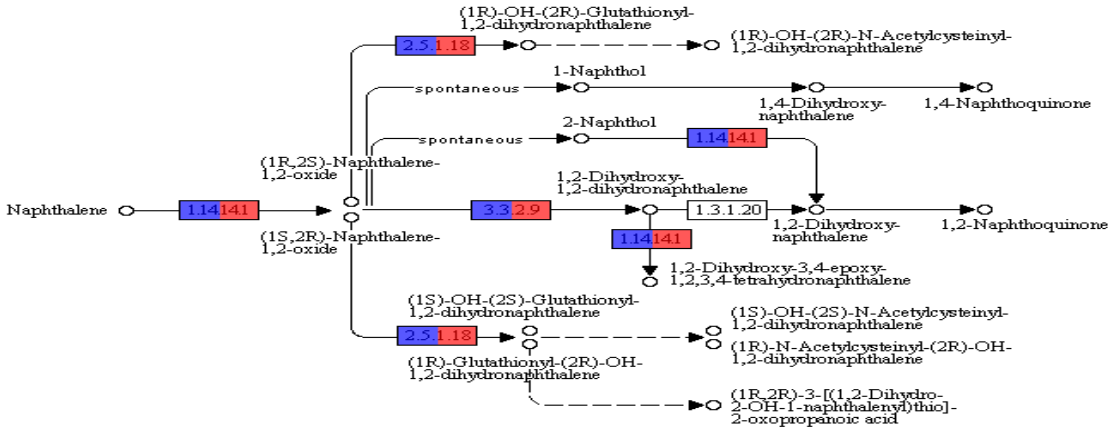

Figure A4.1 KEGG pathway analysis of metagenomes from Creo soil microcosms incubated under ENA conditions displaying enzymes required for the metabolism of naphthalene. Enzyme profile are showed at the start of incubation (MG-RAST ID 4565148.3 in blue) and after 42 weeks (MG-RAST ID 4565488.3 in red). Shaded boxes represent enzymes for which genes were present in each annotated metagenome.

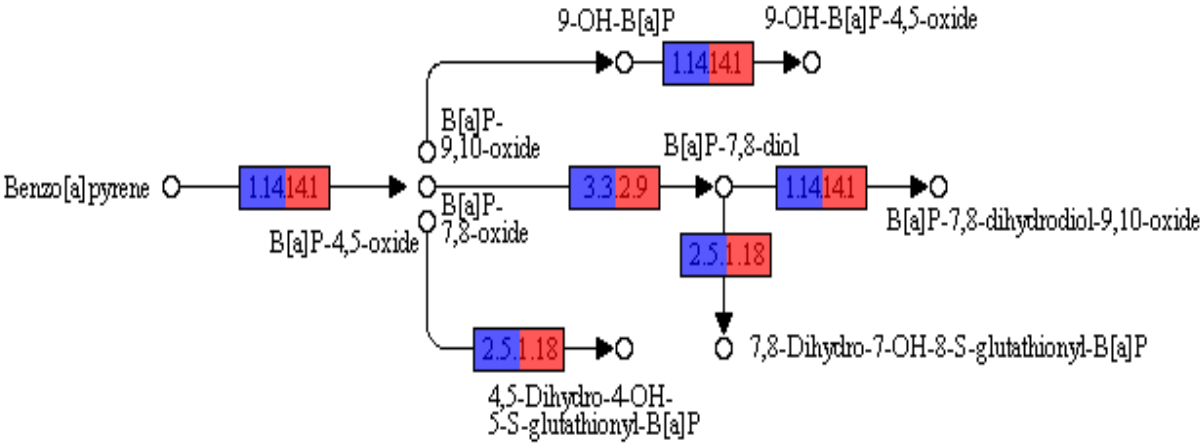

Figure A4.2 KEGG pathway analysis of metagenomes from Creo soil microcosms incubated under ENA conditions displaying enzymes required for the metabolism of benzo(a)pyrene. Enzyme profile are showed at the start of incubation (MG-RAST ID 4565148.3 in blue) and after 42 weeks (MG-RAST ID 4565488.3 in red). Shaded boxes represent enzymes for which genes were present in each annotated metagenome.

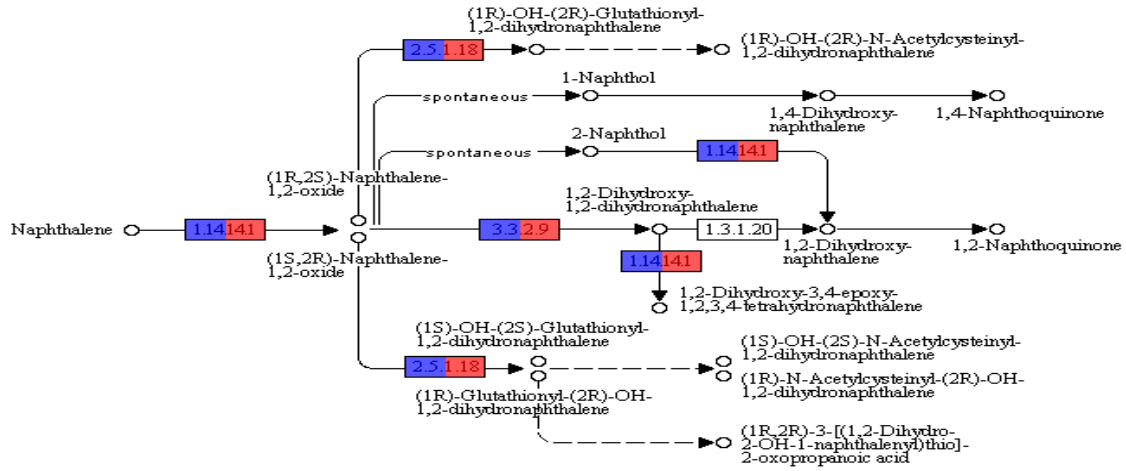

Figure A4.3 KEGG pathway analysis of metagenomes from Creo soil microcosms incubated under Comb conditions displaying enzymes required for the metabolism of naphthalene. Enzyme profile are showed at the start of incubation (MG-RAST ID 4565148.3 in blue) and after 42 weeks (MG-RAST ID 4565487.3in red). Shaded boxes represent enzymes for which genes were present in each annotated metagenome.

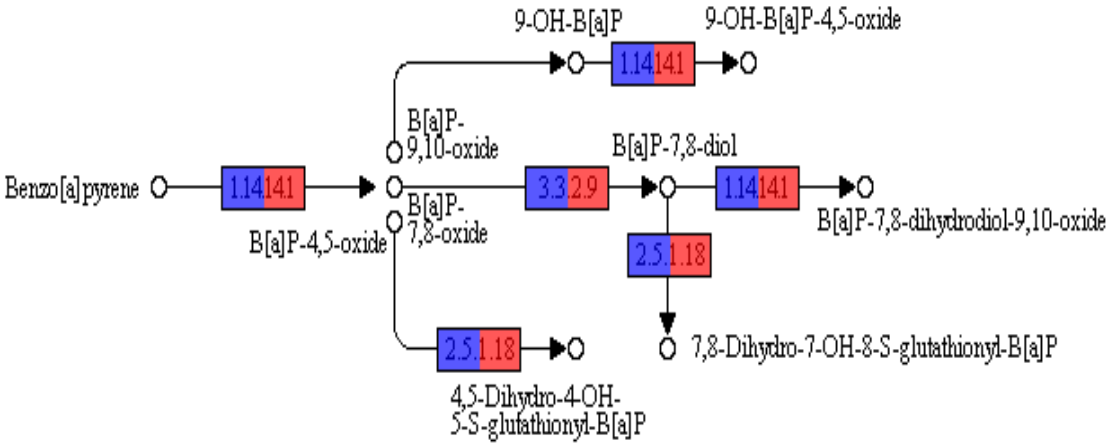

Figure A4.4 KEGG pathway analysis of metagenomes from Creo soil microcosms incubated under Comb conditions displaying enzymes required for the metabolism of benzo(a)pyrene. Enzyme profile are showed at the start of incubation (MG-RAST ID 4565148.3 in blue) and after 42 weeks (MG-RAST ID 4565487.3in red). Shaded boxes represent enzymes for which genes were present in each annotated metagenome.

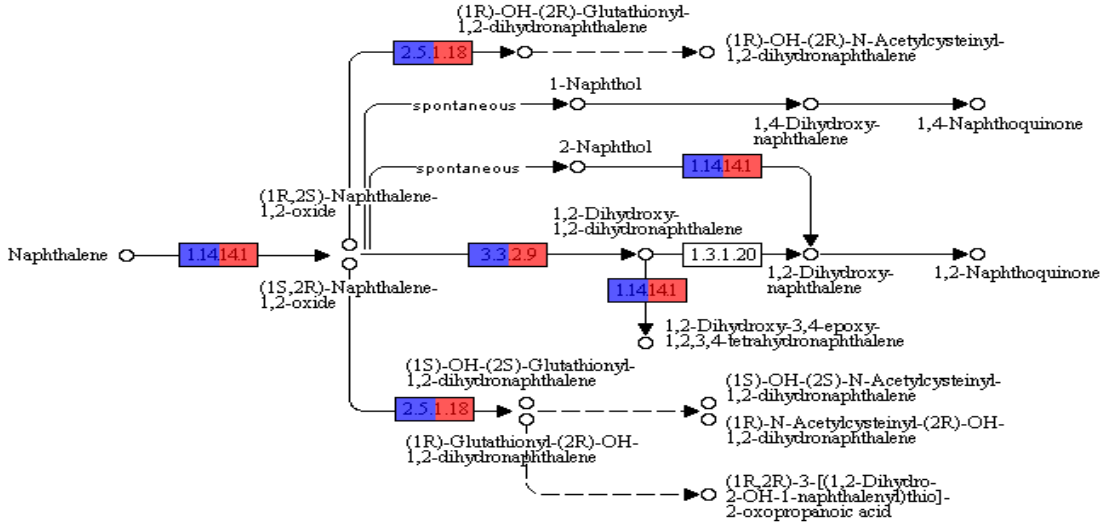

Figure A4.5 KEGG pathway analysis of metagenomes from TB soil microcosms incubated under ENA conditions displaying enzymes required for the metabolism of naphthalene. Enzyme profile are showed at the start of incubation (MG-RAST ID 4565155.3 in blue) and after 42 weeks (MG-RAST ID 4565153.3 in red). Shaded boxes represent enzymes for which genes were present in each annotated metagenome.

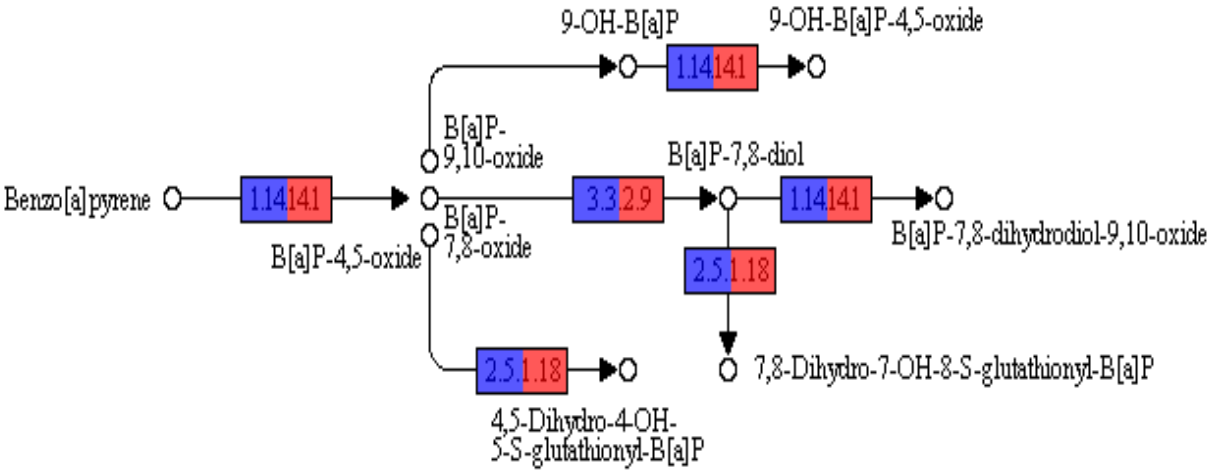

Figure A4.6 KEGG pathway analysis of metagenomes from TB soil microcosms incubated under ENA conditions displaying enzymes required for the metabolism of benzo(a)pyrene. Enzyme profile are showed at the start of incubation (MG-RAST ID 4565155.3 in blue) and after 42 weeks (MG-RAST ID 4565153.3 in red). Shaded boxes represent enzymes for which genes were present in each annotated metagenome.

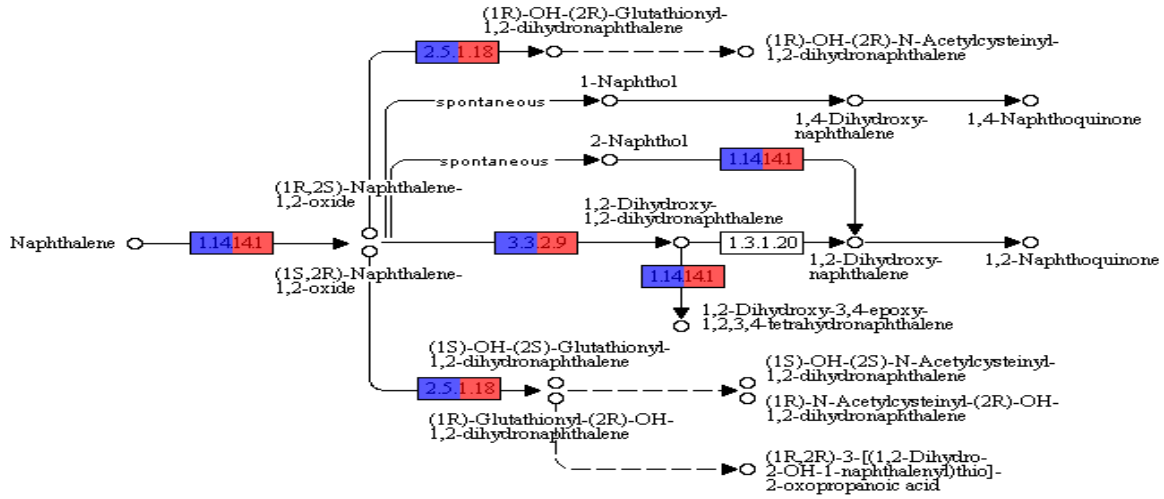

Figure A4.7 KEGG pathway analysis of metagenomes from TB soil microcosms incubated under Comb conditions displaying enzymes required for the metabolism of naphthalene. Enzyme profile are showed at the start of incubation (MG-RAST ID 4565151.3 in blue) and after 42 weeks (MG-RAST ID 4565153.3 in red). Shaded boxes represent enzymes for which genes were present in each annotated metagenome.

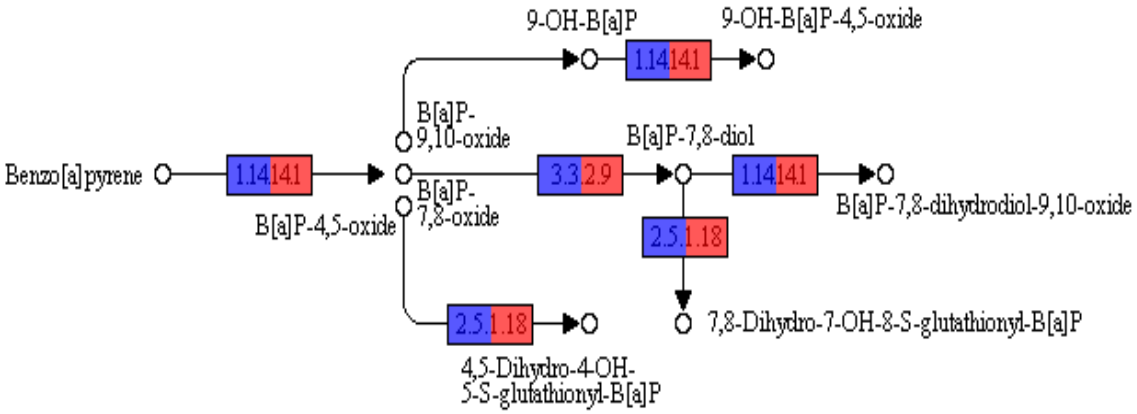

Figure A4.8 KEGG pathway analysis of metagenomes from TB soil microcosms incubated under Comb conditions displaying enzymes required for the metabolism of benzo(a)pyrene. Enzyme profile are showed at the start of incubation (MG-RAST ID 4565151.3 in blue) and after 42 weeks (MG-RAST ID 4565153.3 in red). Shaded boxes represent enzymes for which genes were present in each annotated metagenome.

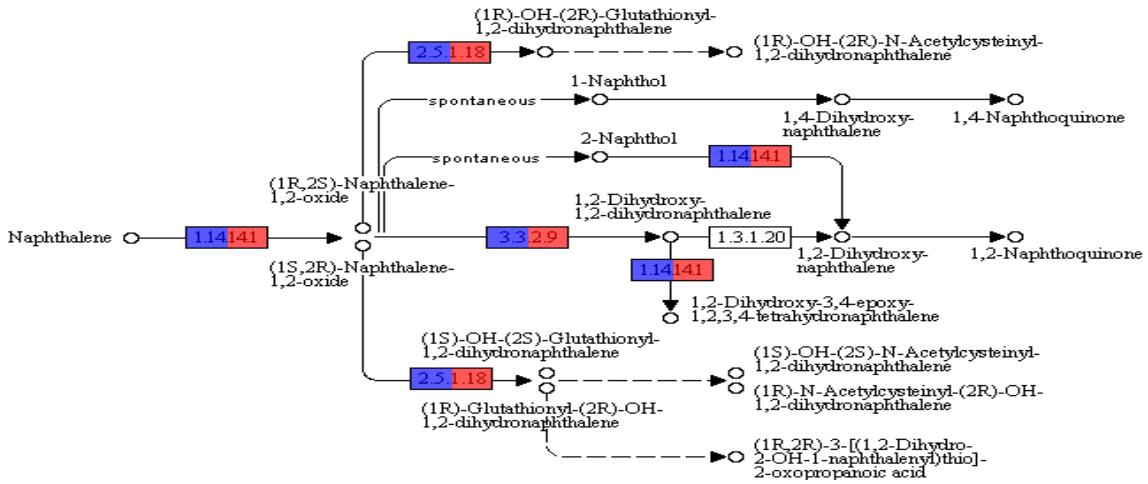

Figure A4.9 KEGG pathway analysis of metagenomes from AP soil microcosms incubated under ENA conditions displaying enzymes required for the metabolism of naphthalene. Enzyme profile are showed at the start of incubation (MG-RAST ID 4559617.3 in blue) and after 42 weeks (MG-RAST ID 4559619.3 in red). Shaded boxes represent enzymes for which genes were present in each annotated metagenome.

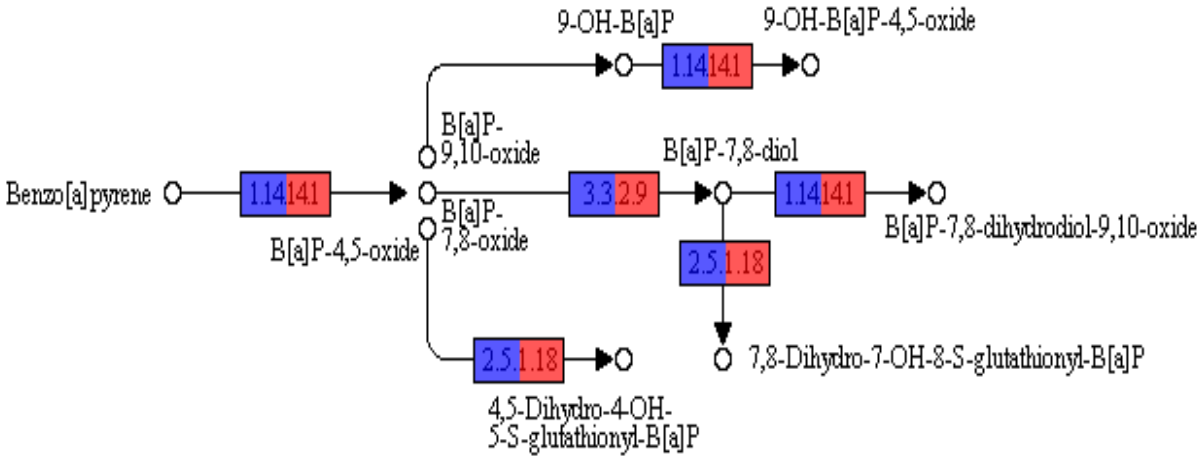

Figure A4.10 KEGG pathway analysis of metagenomes from AP soil microcosms incubated under ENA conditions displaying enzymes required for the metabolism of benzo(a)pyene. Enzyme profile are showed at the start of incubation (MG-RAST ID 4559617.3 in blue) and after 42 weeks (MG-RAST ID 4559619.3 in red). Shaded boxes represent enzymes for which genes were present in each annotated metagenome.

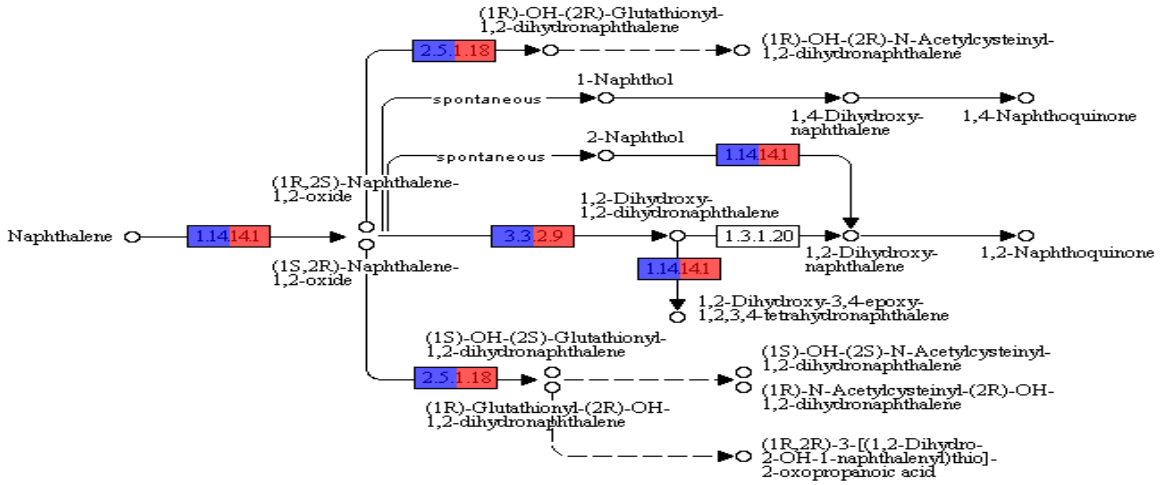

Figure A4.11 KEGG pathway analysis of metagenomes from AP soil study I incubated under Comb conditions displaying enzymes required for the metabolism of naphthalene. Enzyme profile are showed at the start of incubation (MG-RAST ID 4559617.3 in blue) and after 42 weeks (MG-RAST ID 4559616.3 in red). Shaded boxes represent enzymes for which genes were present in each annotated metagenome.

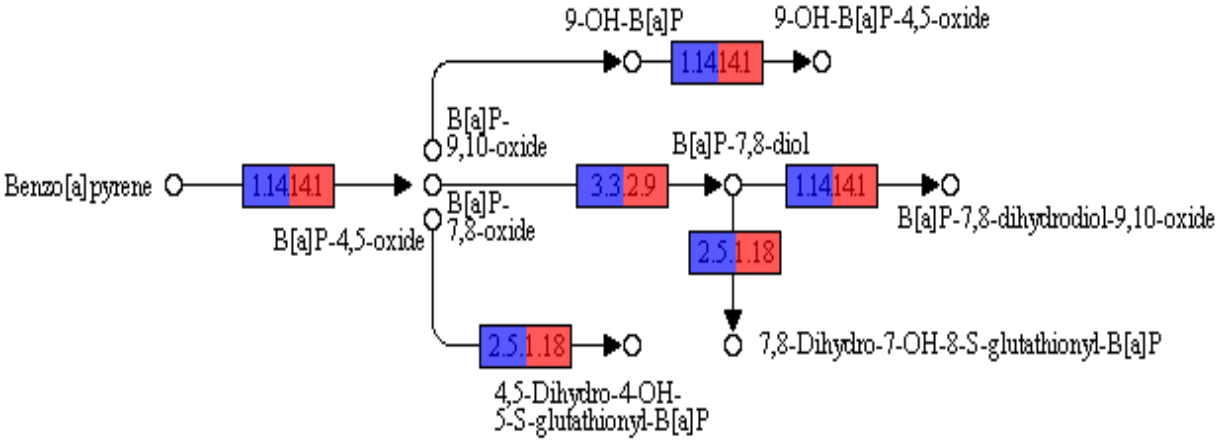

Figure A4.12 KEGG pathway analysis of metagenomes from AP soil study I incubated under Comb conditions displaying enzymes required for the metabolism of benzo(a)pyrene. Enzyme profile are showed at the start of incubation (MG-RAST ID 4559617.3 in blue) and after 42
weeks (MG-RAST ID 4559616.3 in red). Shaded boxes represent enzymes for which genes were present in each annotated metagenome.

Appendix 5: MG-RAST analysis of metabolic functional profiles (Chapter 7)

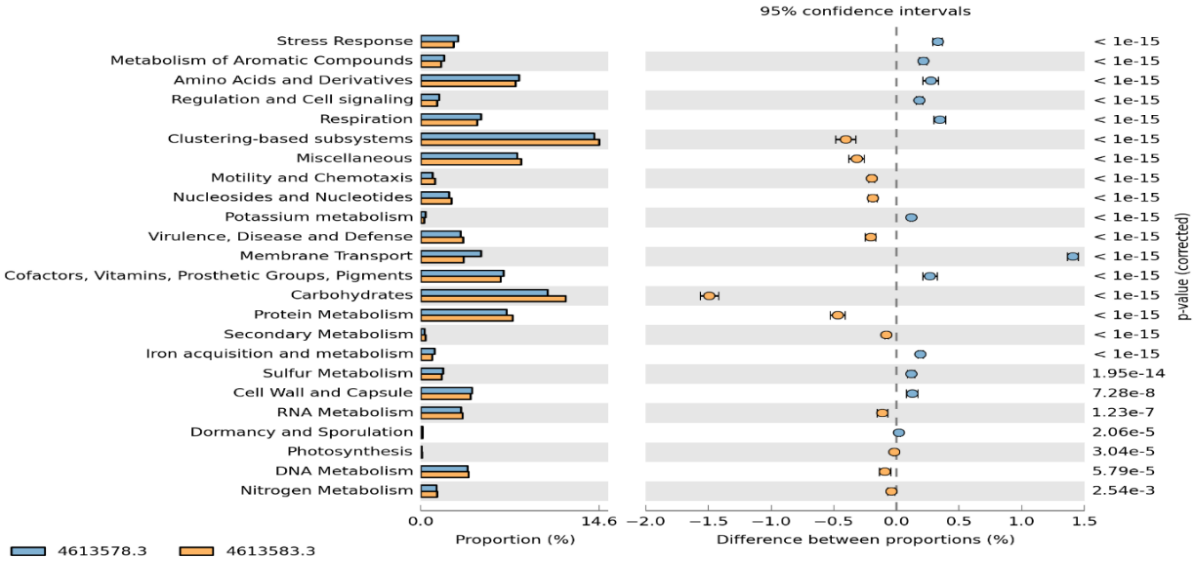

Figure A5.1 Comparison of metagenome functional profiles from Creo soil incubated under natural attenuation conditions. Blue bars represent (MG-RAST ID 4613578.3) metabolic functional profiles at the start of incubation while orange bars represent (MG-RAST ID 4613583.3) metabolic functional profiles at day 14. STAMP analysis of overrepresented subsystem functional profiles observed in day 0 and day 14 metagenomes with corrected p-values (95% confidence intervals) calculated using Storey's FDR approach are also shown.

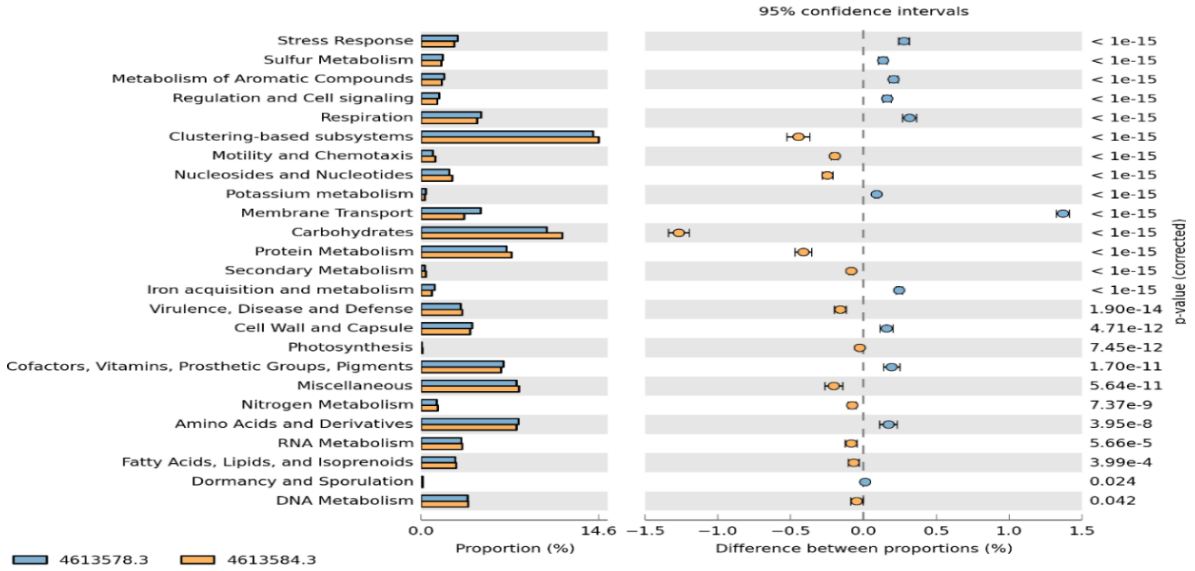

Figure A5.2 Comparison of metagenome functional profiles from Creo soil incubated under natural attenuation conditions. Blue bars represent (MG-RAST ID 4613578.3) metabolic functional profiles at the start of incubation while orange bars represent (MG-RAST ID 4613584.3) metabolic functional profiles at day 28. STAMP analysis of overrepresented subsystem functional profiles observed in day 0 and day 28 metagenomes with corrected p-values (95% confidence intervals) calculated using Storey's FDR approach are shown.

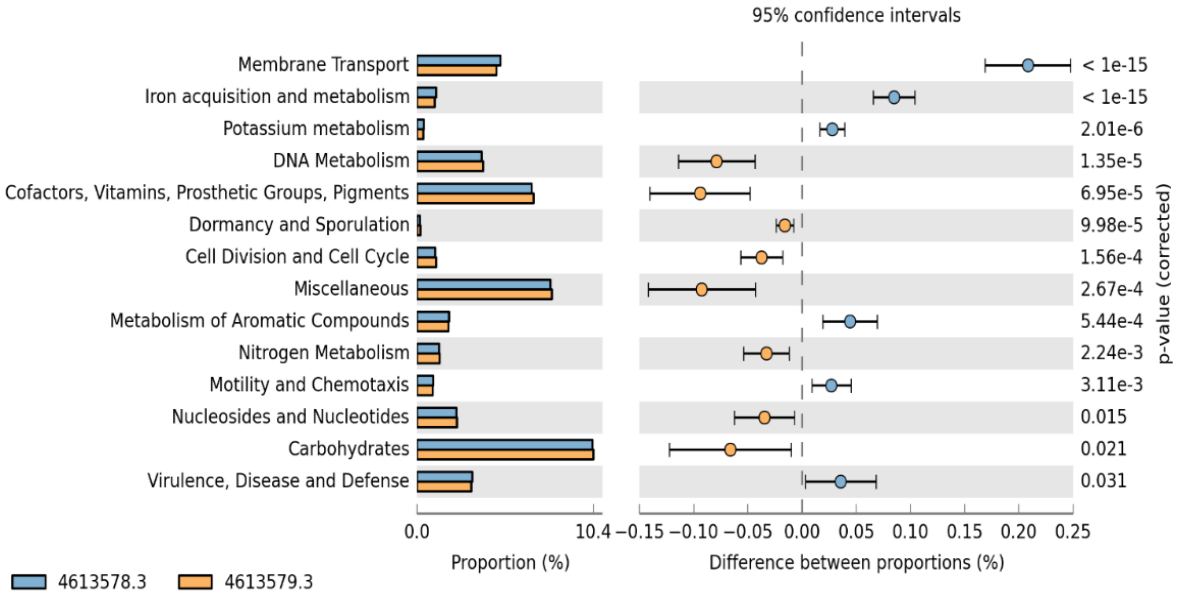

Figure A5.3 Comparison of metagenome functional profiles from Creo soil study II incubated under enhanced natural attenuation (ENA) conditions. Blue bars represent (MG-RAST ID 4613578.3) metabolic functional profiles at the start of incubation while orange bars represent (MG-RAST ID 4613579.3) metabolic functional profiles at day 14. STAMP analysis of overrepresented subsystem functional profiles observed in day 0 and day 14 metagenomes with corrected p-values (95% confidence intervals) calculated using Storey's FDR approach are shown.

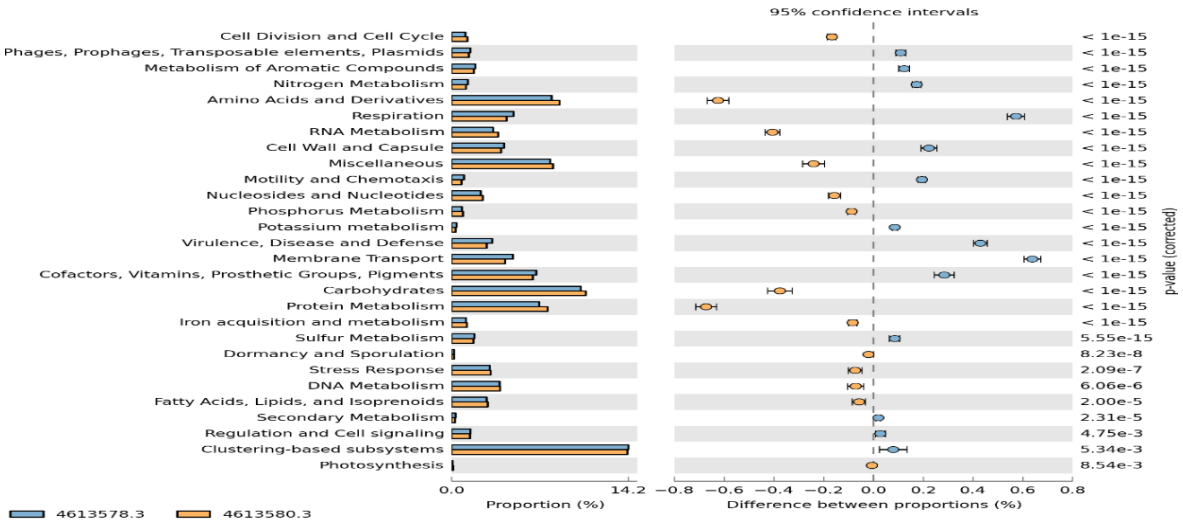

Figure A5.4 Comparison of metagenome functional profiles from Creo soil study II incubated under enhanced natural attenuation (ENA) conditions. Blue bars represent (MG-RAST ID 4613578.3) metabolic functional profiles at the start of incubation while orange bars represent (MG-RAST ID 4613580.3) metabolic functional profiles at day 28. STAMP analysis of overrepresented subsystem functional profiles observed in day 0 and day 28 metagenomes with corrected p-values (95% confidence intervals) calculated using Storey's FDR approach are shown.

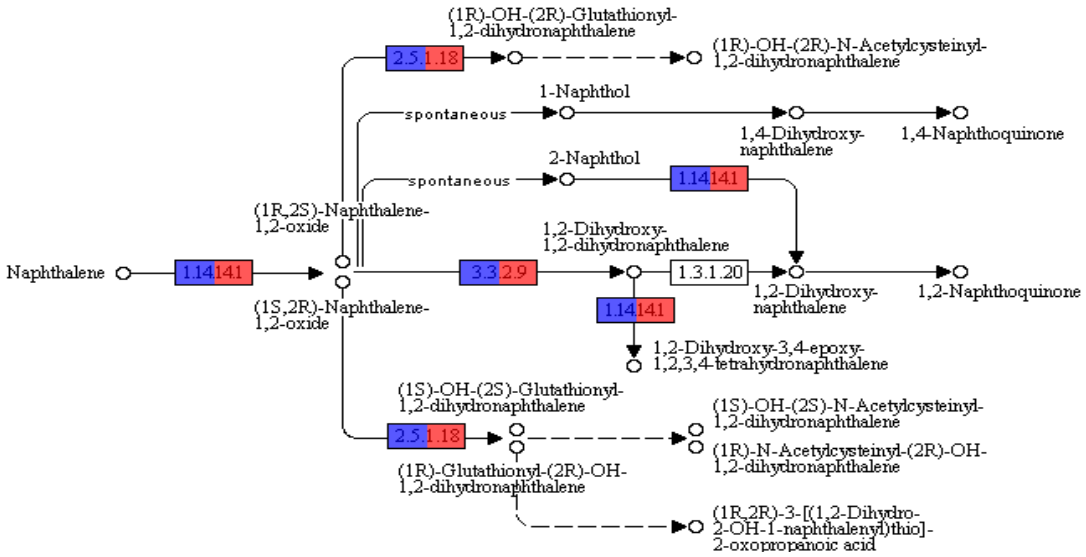

Figure A5.5 KEGG pathway analysis of metagenomes from Creo soil study incubated under enhanced natural attenuation conditions (ENA), displaying enzymes required for the metabolism of naphthalene. Enzyme profiles are shown at the start of microcosm experiment (MG-RAST ID 4613578.3 in blue) and after 28 days (MG-RAST ID 4613580.3 in red). Shaded boxes represent enzymes for which genes were present in each annotated metagenome.

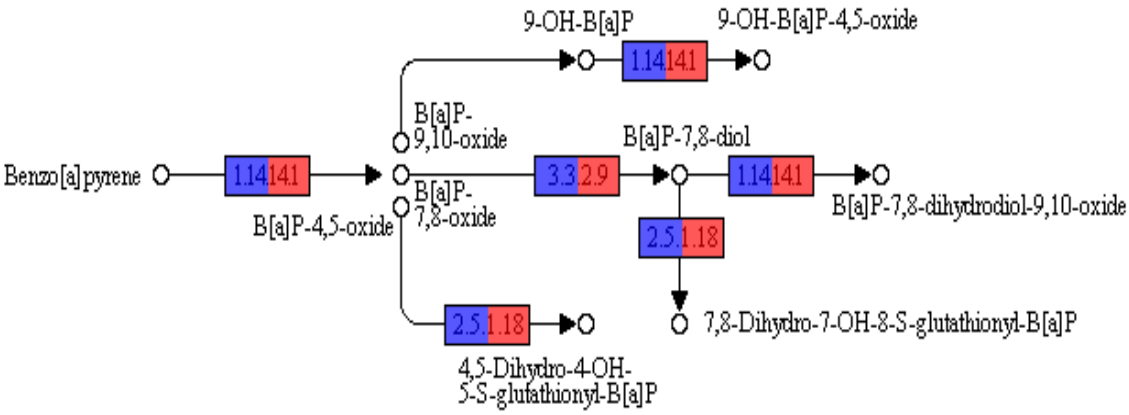

Figure A5.6 KEGG pathway analysis of metagenomes from Creo soil study incubated under enhanced natural attenuation conditions (ENA), displaying enzymes required for the metabolism of benzo(a)pyrene. Enzyme profiles are shown at the start of microcosm experiment (MG-RAST ID 4613578.3 in blue) and after 28 days (MG-RAST ID 4613580.3 in red). Shaded boxes represent enzymes for which genes were present in each annotated metagenome.

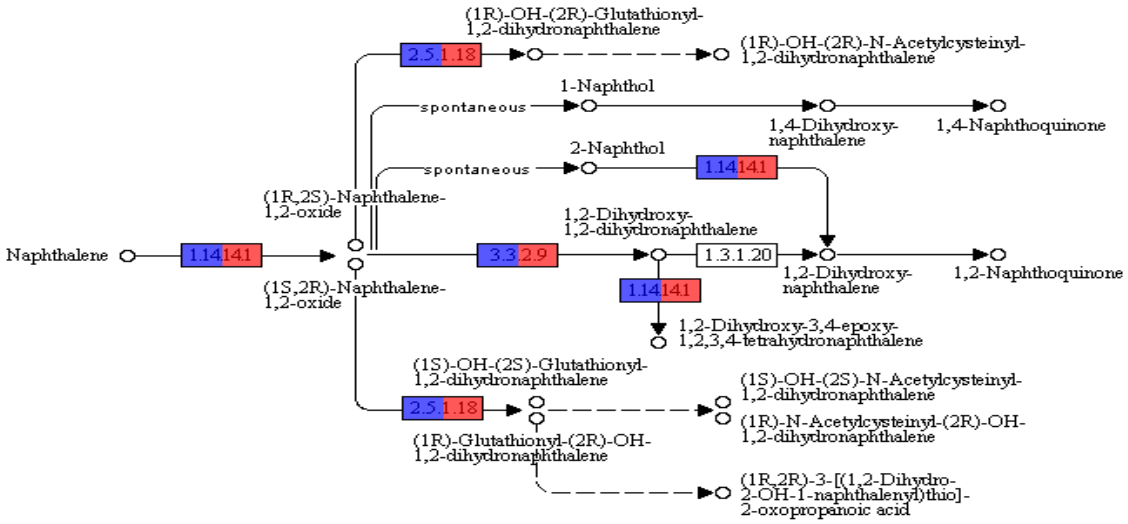

Figure A5.7 KEGG pathway analysis of metagenomes from Creo soil study incubated under chemical oxidation (H202), displaying enzymes required for the metabolism of naphthalene. Enzyme profiles are shown at the start of microcosm experiment (MG-RAST ID 4613578.3 in blue) and after 28 days (MG-RAST ID 4613582.3 in red). Shaded boxes represent enzymes for which genes were present in each annotated metagenome.

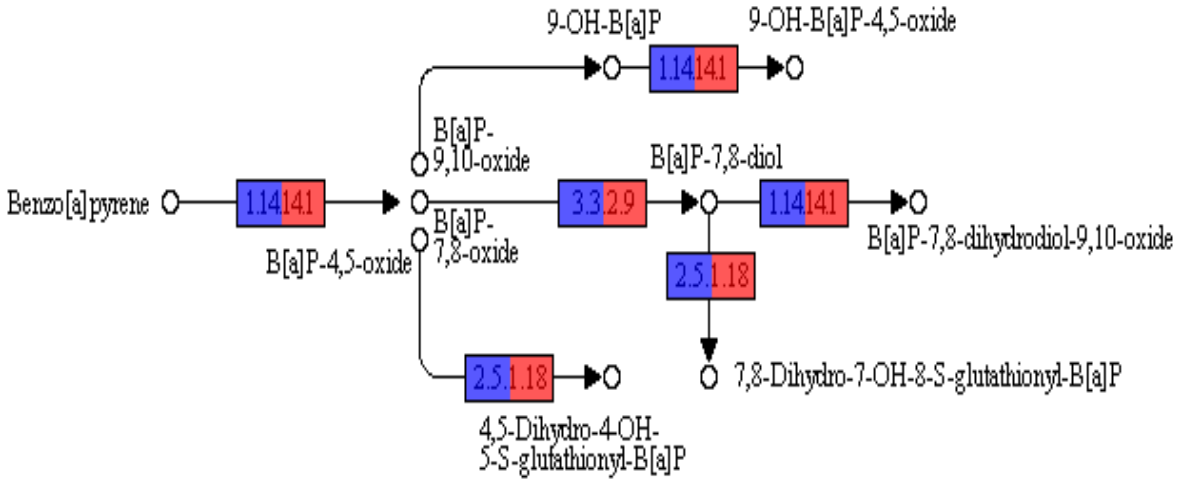

Figure A5.8 KEGG pathway analysis of metagenomes from Creo soil study incubated under chemical oxidation (H202, displaying enzymes required for the metabolism of benzo(a)pyrene. Enzyme profiles are shown at the start of microcosm experiment (MG-RAST ID 4613578.3 in blue) and after 28 days (MG-RAST ID 4613582.3 in red). Shaded boxes represent enzymes for which genes were present in each annotated metagenome.

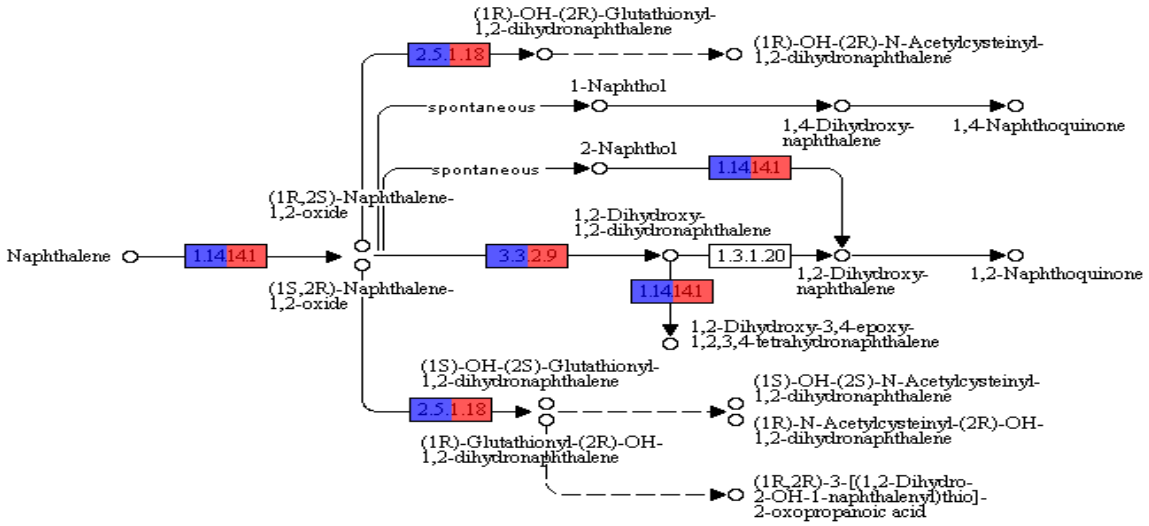

Figure A5.9 KEGG pathway analysis of metagenomes from Creo soil study incubated under microcosm treated with sodium succinate (SS), displaying enzymes required for the metabolism of naphthalene. Enzyme profiles are shown at the start of microcosm experiment (MG-RAST ID 4613578.3 in blue) and after 28 days (MG-RAST ID 4613586.3 in red). Shaded boxes represent enzymes for which genes were present in each annotated metagenome.

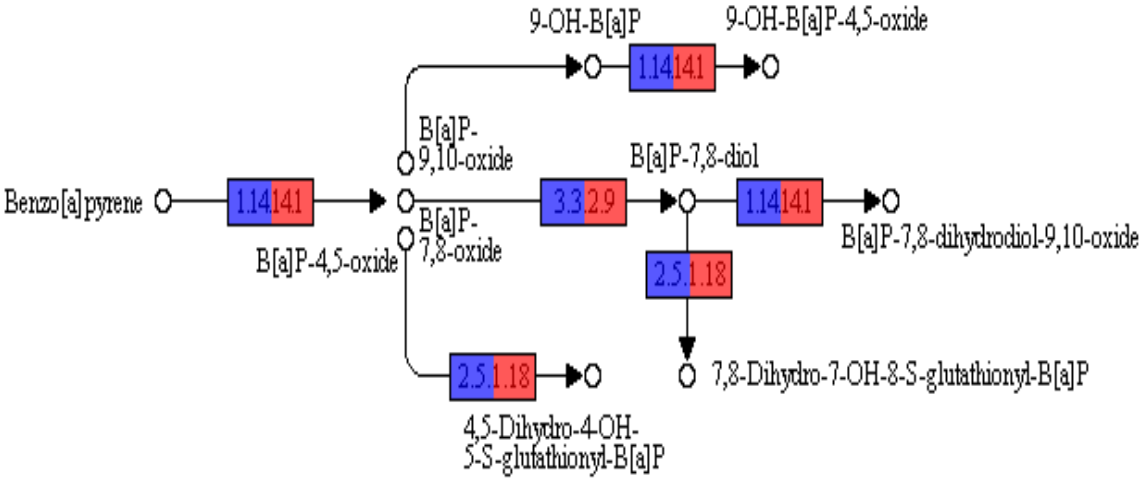

Figure A5.10 KEGG pathway analysis of metagenomes from Creo soil study incubated under microcosm treated with sodium succinate (SS), displaying enzymes required for the metabolism of benzo(a)pyrene. Enzyme profiles are shown at the start of microcosm experiment (MG-RAST ID 4613578.3 in blue) and after 28 days (MG-RAST ID 4613586.3 in red). Shaded boxes represent enzymes for which genes were present in each annotated metagenome.

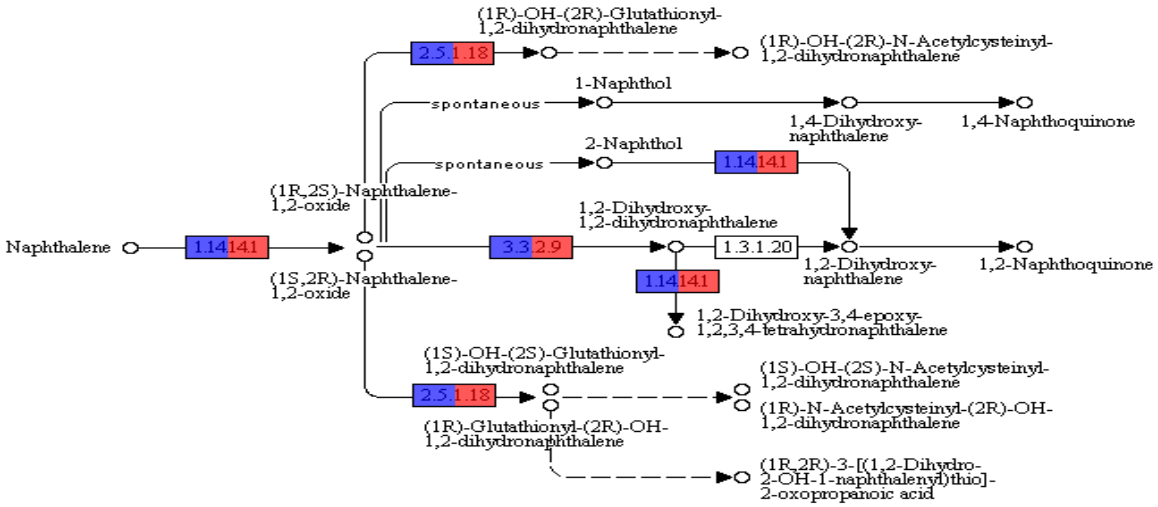

Figure A5.11 KEGG pathway analysis of metagenomes from Creo soil study II incubated under microcosm treated with Tween 20 (T20), displaying enzymes required for the metabolism of naphthalene. Enzyme profiles are shown at the start of microcosm experiment (MG-RAST ID 4613578.3 in blue) and after 28 days (MG-RAST ID 4613587.3 in red). Shaded boxes represent enzymes for which genes were present in each annotated metagenome.

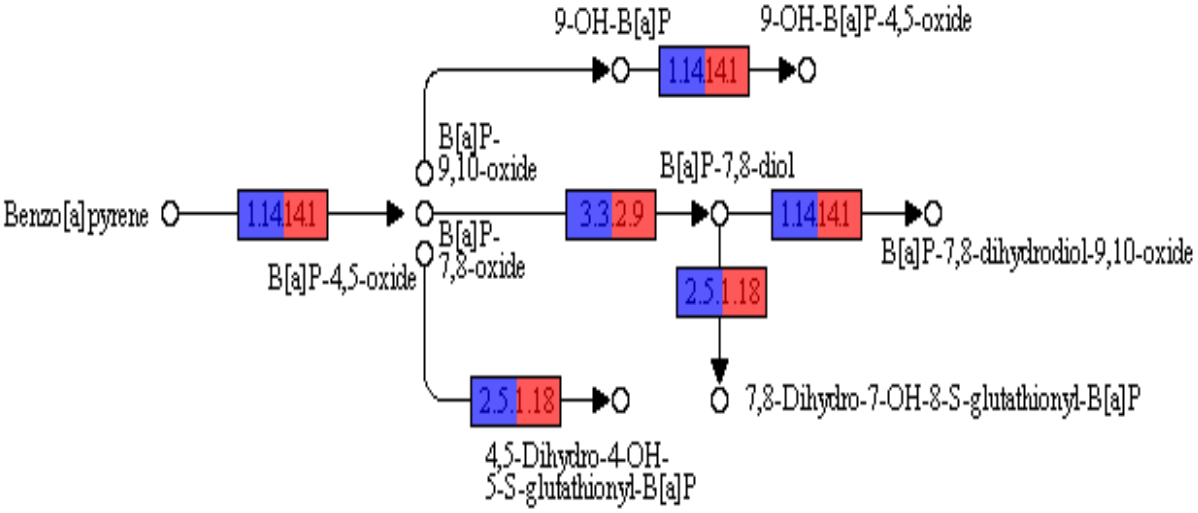

Figure A5.12 KEGG pathway analysis of metagenomes from Creo soil incubated under microcosm treated with Tween 20 (T20), displaying enzymes required for the metabolism of naphthalene. Enzyme profiles are shown at the start of microcosm experiment (MG-RAST ID 4613578.3 in blue) and after 28 days (MG-RAST ID 4613587.3 in red). Shaded boxes represent enzymes for which genes were present in each annotated metagenome.